Effects of Elevated pCO_2 on the Productivity of Marine Microbes and the Remineralisation of Nutrients in Coastal Antarctic Waters

by

Stacy Louise Deppeler

Bachelor of Science, University of Melbourne

Master of Antarctic Science, University of Tasmania

Submitted in fulfilment of the requirements for the degree of Doctor of Philosophy

University of Tasmania

April, 2018

Declaration of Originality

This thesis contains no material which has been accepted for a degree or diploma by the University or any other institution, except by way of background information and duly acknowledged in the thesis, and to the best of my knowledge and belief no material previously published or written by another person except where due acknowledgement is made in the text of the thesis, nor does the thesis contain any material that infringes copyright.

Signed: _____
Stacy Louise Deppeler

Date: 14.04.2018

Authority of Access

This thesis may be made available for loan and limited copying and communication in accordance with the *Copyright Act 1968*

Signed: _____
Stacy Louise Deppeler

Date: 14.04.2018

Statement of Co-Authorship

The following people and institutions contributed to the publication of work undertaken as part of this thesis:

Stacy Deppeler	Institute for Marine and Antarctic Studies	= **Candidate**
Andrew Davidson	Australian Antarctic Division, Supervisor	= **Author 1**
Katherina Petrou	University of Technology Sydney	= **Author 2**
Kai G. Schulz	Southern Cross University	= **Author 3**
Karen Westwood	Australian Antarctic Division	= **Author 4**
Imojen Pearce	Australian Antarctic Division	= **Author 5**
John McKinlay	Australian Antarctic Division	= **Author 5**

Author details and their roles:

Paper 1, Southern Ocean Phytoplankton in a Changing Climate:
Located in Chapter 1
Candidate was the primary author (70%) with significant input from Author 1 (30%)

Paper 2, Ocean acidification of a coastal Antarctic marine microbial community reveals a critical threshold for CO_2 tolerance in phytoplankton productivity:
Located in Chapter 2
Candidate was the primary author (70%) with contributions to the paper from Author 1 (10%), Author 2 (10%), and Author 3 (10%)
Author 1, 2, 4 conceived and designed the experiments
Author 1 led and oversaw the minicosm experiment
Candidate (60%) and Author 2 (40%) performed the experiments and data analysis
Author 3 performed the carbonate system measurements and manipulation
Author 5 performed pigment extraction and analysis
Author 6 provided statistical guidance

We the undersigned agree with the above stated "proportion of work undertaken" for each of the above published (or submitted) peer-reviewed manuscripts contributing to this thesis:

Signed: _ _____

Prof. Andrew McMinn	Prof. Craig Johnson
Primary Supervisor	Head, Ecology & Biodiversity
IMAS	IMAS
University of Tasmania	University of Tasmania
Date: 09/04/2018	12 April 2018_

ACKNOWLEDGEMENTS

None of this work would have been possible without the vision and incredible support of my supervisors Andrew Davidson (Clobbs) and Andrew McMinn. Thank you for imparting your knowledge and skills to me, entrusting me with your incredibly expensive scientific equipment, providing constructive feedback on my terrible first drafts, and not least, believing in me to do this thing. I have learnt so much and have become a more confident and passionate scientist because of you.

Completing a PhD can be tough at times and I want to give special thanks to Alyce Hancock and James Black for being on this journey with me. For the many hours spent discussing our work, helping with experimental design, giving advice, swapping R code, and learning from each other's mistakes. You've been there through the successes and the failures, the long days (and nights) in the lab, and all the ups and downs that come with being a PhD student. I'm indebted to you for the support you have given me through these last 4 1/2 years.

I want to thank everyone involved in the minicosm experiment; Katherina Petrou, Kai Schulz, Cristin Sheehan, Penny Pascoe, Karen Westwood, Imojen Pearce, Alyce Hancock, and Clobbs. After being struck down by the "A-factor" in 2013, we managed to pull it off in 2014 and our results have had a real impact on the Antarctic community. I'm grateful for the data and advice provided to me by Katherina, Kai, Penny, and Alyce that has helped shaped the content of this thesis. I also want to thank Karen Westwood for teaching me the ropes when it came to primary productivity measurements and being a constant source of advice and encouragement through my whole PhD.

I also acknowledge the assistance of Australian Antarctic Division technical support in designing and equipping the minicosms, the Helicopter Resources pilots and engineers for their assistance with logistics, and all the Davis Station expeditioners in the summer of 2013-2014 and 2014–2015 for their support and friendship while we completed this research. I want to make special mention to Stuart Shaw and Tina Donaldson, for the laughs, the shennanigans, the nights out at Watts Hutt, and for being the founding members of two of the best bands Antarctica has ever seen, the Blue Slots and Sausage Fist.

I thank the Australian Government, Department of Environment and Energy for funding our project as part of the Australian Antarctic Science Project 4026 at the Australian Antarctic Division. I also thank the Australian Antarctic Division for providing logistical support for our project at Davis Station in the summer of 2013-2014 and 2014–2015, and additional laboratory support in Kingston.

My PhD candidature was funded by an Elite Research Scholarship awarded by the Institute for Marine and Antarctic Studies, University of Tasmania. For this I am extremely grateful, along with the ongoing support from the Institute for Marine and Antarctic Studies throughout my candidature.

I would not have been able to complete my research without the incredible support from the managers and staff in the laboratories at the Australian Antarctic Division, Kingston. I thank Chris Marshall, Deb Lang, and Imojen Pearce from the Wild Laboratory for putting up with my seemingly never-ending experiments and letting me repurpose all manner of lab equipment to complete my research. I promise I will put everything away now that I am done! I am also incredibly grateful to the members of the Krill Laboratory; Rob King, Tash Waller, Blair Smith, and Ashley Cooper. Thank you for helping me find a place to perform my experiments and letting me take over a corner of your lab for many months. Thank you also for constantly providing me with assistance and encouragement throughout my successes and failures. I have become a better scientist because of the people I have worked with over these past 4 1/2 years.

I also wish to thank Philip Boyd, Kristen Karsh, Matthieu Bressac, and Christina McGraw for all the assistance in research design, training, and troubleshooting while undertaking my lab-based ocean acidification experiment. I'm glad that I got to take a great idea and see it through to fruition. There were a lot of learning experiences along the way and I thank all of you for the part you played in this project.

Last but definitely not least, I thank my family and friends for offering endless encouragement and putting up with all my levels of crazy over the last 4 1/2 years. To my mum and dad, Faye and Rowan Deppeler, my brother and sister-in-law, Bryce and Maryanne Deppeler, and my three amazing nephews, Jay, Ty, and Eli Deppeler, I thank you for the endless support and encouragement and providing me a place to get away from it all when I could. To all my friends,

both in Hobart and around the world, thank you for believing in me, cheering me on, calling me occasionally, and giving me reasons to leave the house. I haven't been the most social person while completing this thesis but I look forward to being less of an introvert now that it is done. Thanks for bearing with me. It means a lot.

One final thanks to Belinda Davis for providing me with valuable comments on the layout of my thesis. It's the little things that sometimes make all the difference. I definitely owe you one when I'm in Melbourne next.

DEDICATION

I dedicate this work to my nephews Jay, Ty, and Eli Deppeler. They are the ones who will inherit the world that we have created. I hope that I can impart a love of nature and facination with science to them so that they too will learn and discover what an incredible world we live in.

"Try today, and be less wrong tomorrow."

- Rufus Hound
The Infinite Monkey Cage, 2016

TABLE OF CONTENTS

LIST OF TABLES

LIST OF FIGURES

ABBREVIATIONS

AABW	Antarctic Bottom Water
AAIW	Antarctic Intermediate Water
α	Maximum photosynthetic efficiency
ANOVA	Analysis of variance
ASF	Antarctic Slope Front
ASL	Amundsen Sea Low
ATP	Adenosine triphosphate
AZA	Acetazolamide
β	Photoinhibition rate
C:N ratio	Carbon:nitrogen ratio
CCM	Carbon concentrating mechanism
CFC	Chlorofluorocarbon
Chl *a*	Chlorophyll *a*
CO_2	Carbon dioxide
$csBP_{^{14}C}$	^{14}C-derived cell-specific bacterial productivity
$csGCP_{O_2}$	O_2-derived Chl *a*-specific gross community production
$csGPP_{^{14}C}$	^{14}C-derived Chl *a*-specific primary productivity
CT	Colour temperature
CZ	Antarctic Continental Shelf Zone
$\Delta F/F_{m'}$	Effective quantum yield
DIC	Dissolved inorganic carbon
DMS	Dimethylsulfide
DMSP	Dimethylsulfoniopropiothetin
$DO^{14}C$	^{14}C-labelled dissolved organic carbon
DPM	Decays per minute
DPM_s	Sample DPM
E_k	Saturating irradianc
eCA	Extracellular carbonic anhydrase
ENSO	El Niño-Southern Oscillation
EZA	Ethoxzolamide
F	Light-adapted initial fluorescence
F_0	Minimum fluorescence
$F_{m'}$	Light-adapted maximum fluorescence
F_m	Maximum fluorescence
F_t	Light-adapted minimum fluorescence
F_v/F_m	Maximum quantum yield of PSII
fCO_2	fugacity of CO_2
FL1	Green fluorescence
FL2	orange fluorescence

FL3	red fluorescence
$GBP_{^{14}C}$	^{14}C-derivedgross bacterial production ($GBP_{^{14}C}$)
GCP_{O_2}	O_2-derived gross community production
$GPP_{^{14}C}$	^{14}C-derived gross primary production
H^+	Hydrogen ion
HCl	Hydrochloric acid
HCO_3^-	Bicarbonate ion
$HgCL_2$	Mercuric chloride
HNF	Heterotrophic nanoflagellates
HNLC	High nutrient, low chlorophyll
HPLC	High performance liquid chromatography
$\bar{I}$	Average minicosm light irradiance
$\bar{I}_o$	Incoming irradiance
I_a	Actinic irradiance
iCA	Intracellular carbonic anhydrase
K_d	Average vertical light attenuation
LCDW	Lower Circumpolar Deep Water
LDPE	Low-density polyethylene
mCP	m-cresol purple
MIZ	Marginal Ice Zone
NADPH	Nicotinamide adenine dinucleotide phosphate
$NaH^{14}CO_3$	^{14}C-labelled sodium bicarbonate
Nano	Nanophytoplankton
NaOH	Sodium hydroxide
NCP_{O_2}	O_2-derived net community production
ND	Neutral density
NO_3^-	Nitrate ion
NOx	Nitrate plus nitrite
NPQ	Non-photochemical quenching
NSIDC	National Snow and Ice Data Center
O_2	Oxygen
P_{max}	Light-saturated photosynthetic rate
PA	Practical alkalinity
PAR	Photosynthetically active radiation
PE	Photosynthesis versus irradiance
PF	Polar Front
pH_T	pH on the total scale
PI	Post-illumination
Pico	Picophytoplankton
PO_4^{3-}	Phosphate ion
POC	Particulate organic carbon
POM	Particulate organic matter
PON	Particulate organic nitrogen
POOZ	Permanent Open Ocean Zone
Prok	Prokaryotes
PSII	Photosystem II
$Resp_{O_2}$	O_2-derived dark PI respiration
rETR	Relative electron transport rate
$rETR_{max}$	Maximum photosynthetic rate
RuBisCO	Ribulose-1,5-bisphosphate carboxylase/oxygenase

SA	Specific activity of ^{14}C-leucine isotope
SACCF	Southern Antarctic Circumpolar Current Front
SAF	Sub-Antarctic Front
SAM	Southern Annular Mode
SAMW	Sub-Antarctic Mode Water
SAZ	Sub-Antarctic Zone
SIE	Sea ice extent
Silica	Molybdate reactive silica
SiO_3^{2-}	Silicate ion
SO	Southern Ocean
SRP	Soluble reactive phosphorus
SSC	Side scatter
SSIZ	Seasonal Sea Ice Zone
SSLC	Steady-state light curve
SST	Sea surface temperature
STF	Sub-Tropical Front
T_0	Time zero
TA	Total alkalinity
TCA	Trichloroacetic acid
$TO^{14}C$	^{14}C-labelled total organic carbon
UCDW	Upper Circumpolar Deep Water
UV	Ultraviolet radiation
WAP	West Antarctic Peninsula
WATER-PAM	Pulse-amplitude-modulated fluorometer
Z_m	Mixed depth

ABSTRACT

High-latitude oceans are anticipated to be some of the first regions affected by ocean acidification. Marine microbes are the base of the food web and support the wealth of life in Antarctica. They are also a critical link in biogeochemical processes, such as the cycling of nutrients and carbon. Despite this, the effect of ocean acidification on natural communities of Antarctic marine microbes is poorly understood. This thesis sets out to address this lack of scientific knowledge of how the base of the Antarctic food web, both as individual taxa and communities, will respond to elevated CO_2.

Much of the results of this thesis are derived from an ocean acidification study performed on an early spring, coastal marine microbial community from Prydz Bay, Antarctica. Such studies are currently rare in Antarctic waters and can provide valuable insights into how future changes in CO_2 will affect the marine microbial community. In this study, the microbial community was exposed to increasing fCO_2 levels from ambient (343 µatm) to 1641 µatm in 650 L minicosms. Measurements of abundance and primary and bacterial productivity were taken to determine the effect of CO_2 on different community groups. Photophysiological measurements were also performed to identify possible mechanisms driving changes in the phytoplankton community.

The limits for CO_2 tolerance were broad, likely due to the naturally variable environment this community inhabits. However, there were thresholds to this CO_2 tolerance that elicited responses by different community groups. An important tipping point was identified in the phytoplankton community's ability to cope with the energetic requirements of maintaining efficient productivity under high CO_2. These results highlighted the strong interplay between enrichment of CO_2 enhancing physiology and metabolic costs imposed by increased H^+. In addition, elevated CO_2 slowed the growth of heterotrophic nanoflagellates, releasing their prey (picophytoplankton and prokaryotes). Thus, increasing CO_2 has the potential to change the

composition of Antarctic microbial communities by altering interactions among trophic levels.

A diatom was isolated from the community-level study and exposed to fCO_2 levels from 276 to 1063 µatm in a unialgal culture study to determine taxon-specific CO_2 sensitivities. Comparing these results with those reported for this species in the community-level study assessed the utility of unialgal studies for predicting the sensitivity of Antarctic phytoplankton taxa to elevated fCO_2. A difference in growth response between the two studies confirmed that factors other than CO_2 affected this species when it is part of a natural community.

This research showed that ocean acidification altered microbial productivity, trophodynamics and biogeochemistry in Antarctic coastal waters. Changes in phytoplankton community production and predator-prey interactions with ocean acidification could have a significant effect on the food web and biogeochemistry in the Southern Ocean. In addition, while culture studies are useful for evaluating mechanisms of CO_2-induced tolerance and stress, such studies proved to be of limited value for predicting responses in nature as they fail to include interactions among species and trophic levels.

Chapter 1

Introduction: Southern Ocean phytoplankton in a changing climate

Stacy Deppeler[1] and Andrew Davidson[2,3]

[1]Institute for Marine and Antarctic Studies, University of Tasmania, Hobart, Tasmania, Australia
[2]Australian Antarctic Division, Department of the Environment and Energy, Kingston, Tasmania, Australia
[3]Antarctic Climate and Ecosystems Cooperative Research Centre, Hobart, Tasmania, Australia

This chapter has been published as: Deppeler, S. L., and Davidson, A. T. (2017). Southern Ocean Phytoplankton in a Changing Climate. *Frontiers in Marine Science*, 4 (40):1–18. doi:10.3389/fmars.2017.00040. A copy of the published article is provided in Appendix A.

1.1 Introduction

Iconic Antarctic wildlife from krill to whales, seals, penguins, and seabirds, ultimately depend on single-celled marine plants (phytoplankton) for their food. More than 500 species of protist have been identified in Antarctic waters, ∼350 of which are phytoplankton and ∼150 microheterotrophs (Scott and Marchant 2005, http://taxonomic.aad.gov.au). These organisms coexist with untold numbers of heterotrophic prokaryotes (bacteria and Archaea) and viruses. Together they comprise the microbial food web (Fig. 1.1), through which much of the carbon sequestered by phytoplankton is consumed, respired, and/or remineralised (Azam *et al.* 1983; Azam *et al.* 1991; Fenchel 2008; Kirchman 2008). This food web includes the microbial loop in which dissolved carbon substrates fuel the growth of bacteria and Archaea, which are subsequently consumed by protists, returning carbon to the microbial food web that is otherwise lost to the dissolved pool (Azam *et al.* 1983). Phytoplankton are the base of the Southern Ocean (SO) food web. In nutrient rich Antarctic coastal waters their blooms can reach concentrations approaching 10×10^8 cells L^{-1}. Chlorophyll *a* (Chl *a*) concentrations as high as $50\,\mu g\,L^{-1}$ have been recorded off the West Antarctic Peninsula (WAP), although maximum Chl *a* concentrations off East Antarctica are usually an order of magnitude less (Nelson *et al.* 1987; Smith and Gordon 1997; Wright and van den Enden 2000; Garibotti *et al.* 2003; Wright *et al.* 2010; Goldman *et al.* 2015). The majority of phytoplankton production in the SO is grazed by microheterotrophs or consumed and remineralised by bacteria (Lochte *et al.* 1997; Christaki *et al.* 2014). Production that escapes these fates sinks to depth, often in the form of dead cells, aggregates of biogenic material (marine snow), or faecal pellets, sequestering carbon in the deep ocean.

Some phytoplankton, such as prymnesiophytes and dinoflagellates, also synthesise substantial quantities of dimethylsulfoniopropiothetin (DMSP), which when enzymatically cleaved, forms dimethylsulfide (DMS). Oxidation of DMS in the atmosphere forms sulfate aerosols, which nucleate cloud formation and increase the reflectance of solar radiation (Charlson *et al.* 1987). The microbial food web plays a vital role in metabolizing these sulfur compounds (Kiene *et al.* 2000; Simó 2004). The active involvement of phytoplankton in the sequestration and synthesis of climate-active gases (CO_2) and biogenic sulfur compounds (DMSP and DMS), plus the

mediation of the fate of these compounds by protozoa and bacteria means that microbes are a crucial determinant of future global climate (Fig. 1.1).

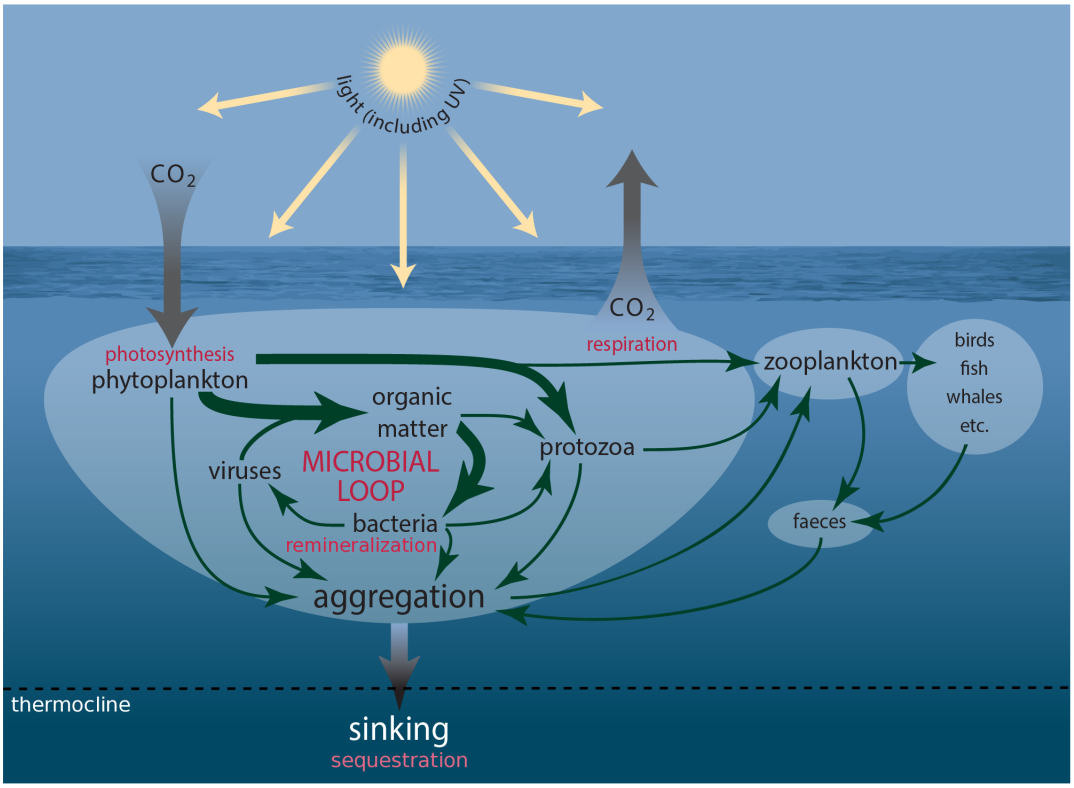

Figure 1.1: Schematic showing the connections amongst members of the microbial food web and microbial loop and the processes driving carbon transfer to higher trophic levels and flux to the deep ocean.

The SO plays a substantial role in mediating global climate. The world's oceans have taken up between 25-30% of the anthropogenic CO_2 released to the atmosphere, with ~40% of this uptake occurring in the SO (Raven and Falkowski 1999; Sabine 2004; Khatiwala *et al.* 2009; Takahashi *et al.* 2009; Frölicher *et al.* 2015). Without this, the atmospheric CO_2 concentration would be ~50% higher than it is today. Drawdown of CO_2 by phytoplankton photosynthesis and vertical transport of this biologically sequestered carbon to the deep ocean (the biological pump) is responsible for around 10% this uptake (Cox *et al.* 2000; Siegel *et al.* 2014). Any climate-induced change in the structure or function of phytoplankton communities is likely to alter the efficiency of the biological pump, with feedbacks to the rate of climate change (Matear and Hirst 1999; Le Quéré *et al.* 2007).

The SO is a region of seasonal extremes in productivity that reflect the large fluctuations in the SO

environment. In summer, the development of large blooms of phytoplankton support a profusion of Antarctic life. Their metabolic activity also affects biogeochemical cycles in the SO, which in turn can influence the global climate. Whilst their effect on global climate is substantial, their microscopic size means they are intimately exposed to changes in their environment and are also likely to be affected by climate change. Already, climate change is causing the southward migration of ocean fronts, increasing sea surface temperatures, and changes in sea ice cover (Constable *et al.* 2014). Further changes in temperature, salinity, wind strength, mixed layer depth, sea ice thickness, duration and extent, and glacial ice melt are predicted. These changes are likely to affect the composition, abundance, and productivity of phytoplankton in the SO and feed back to threaten the ecosystem services they provide, namely sustaining biodiversity, fueling the food web and fisheries, and mediating global climate (Moline *et al.* 2004).

The SO is a vast and diverse environment, and hence the effect of climate change on the phytoplankton community is likely to be complex. For the purposes of this review we define the SO as waters south of the Sub-Tropical Front, thereby comprising ∼20% of the world's ocean surface area. We subdivide these waters into five regions that group waters according to the environmental drivers of the phytoplankton community in a similar manner as Tréguer and Jacques (1992) and Sullivan *et al.* (1988), namely the Sub-Antarctic Zone (SAZ), Permanently Open Ocean Zone (POOZ), Seasonal Sea Ice Zone (SSIZ), Marginal Ice Zone (MIZ), and the Antarctic Continental Shelf Zone (CZ) (Fig. 1.2). Differences in environmental factors (physical, chemical, and biological) and processes (e.g. stratification, mixing, grazing) define the composition, abundance, and productivity of the phytoplankton community, both within and between these regions. Climate change is expected to elicit widespread changes in oceanography in each region, such as the displacement of oceanographic fronts (Sokolov and Rintoul 2009b), as well as different permutations of climate-induced stressors that may interact synergistically or antagonistically, with either beneficial or detrimental effects on the phytoplankton community (Boyd and Brown 2015; Boyd *et al.* 2016a).

Here we identify the factors and processes that critically affect phytoplankton communities in each region of the SO, consider the impacts of climate change on each of these regions, examine the likely effect of these changes on the phytoplankton inhabiting these waters, and predict the possible repercussions for the Antarctic ecosystem.

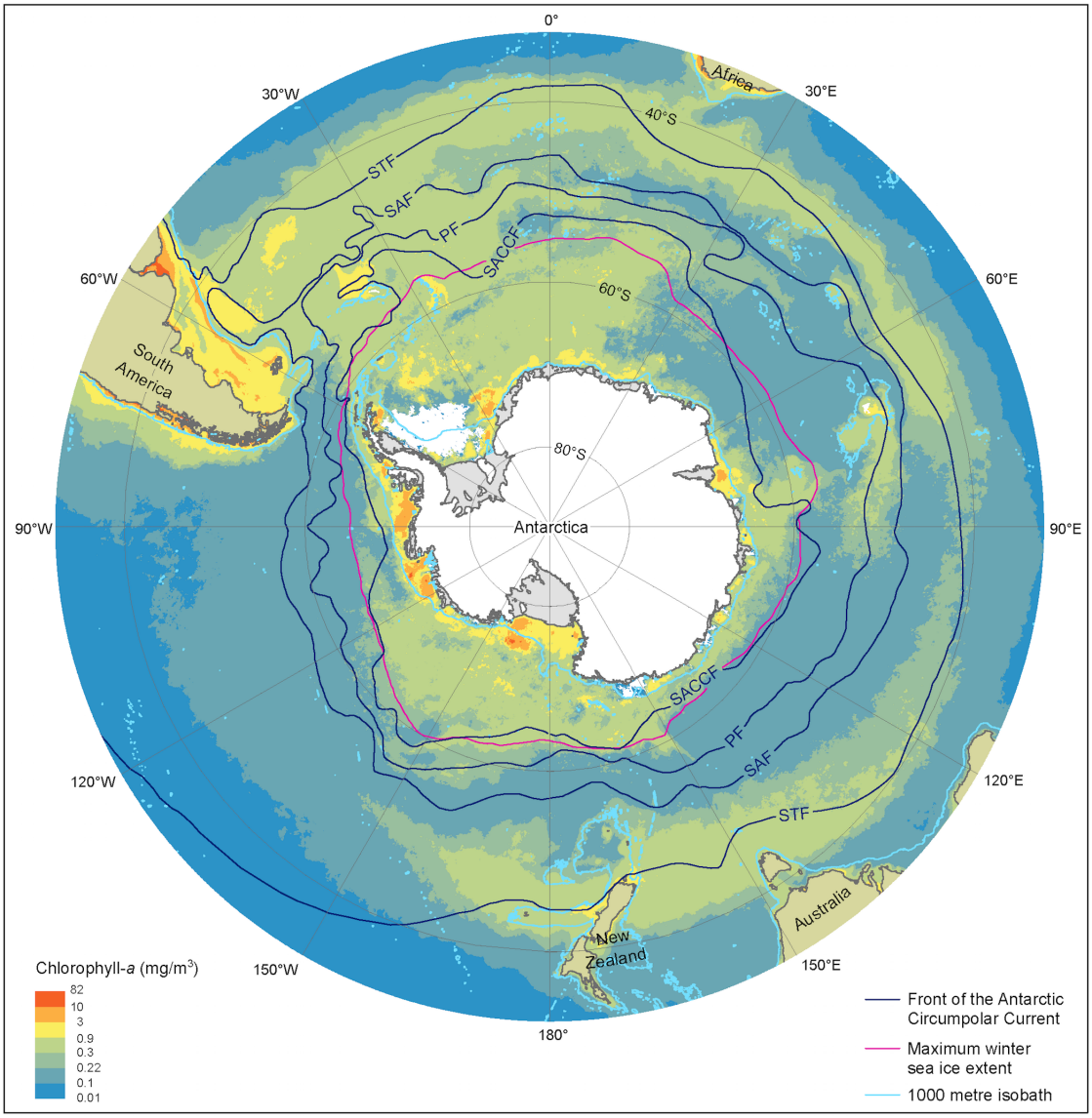

Figure 1.2: Summer near-surface Chlorophyll *a* concentration, frontal locations and sea ice extent in the Southern Ocean. Chlorophyll *a* is determined from MODerate-resolution Imaging Spectroradiometer, Aqua satellite estimates from austral summer season between 2002/03 and 2015/16 at 9 km resolution. Black lines represent, frontal positions from Orsi *et al.* (1995). The red line denotes the maximum extent of sea ice averaged over the 1979/80 to 2007/08 winter seasons, derived from Scanning Multichannel Microwave Radiometer and Special Sensor Microwave/Image satellite data. Light blue lines depict the 1000 m depth isobath, derived using the General Bathymetric Chart of the Oceans, version 20150318. Abbreviations are STF, Sub-Tropical Front; SAF, Sub-Antarctic Front; PF Polar Front; and SACCF, Southern Antarctic Circumpolar Current Front.

1.2 Sub-Antarctic zone

The Sub-Antarctic Zone (SAZ) comprises more than half the total area of the SO and incorporates three important frontal regions; the Sub-Tropical Front, the Sub-Antarctic Front, and the Polar Front (Fig. 1.2) (Orsi *et al.* 1995). Within this region, the waters between the Sub-Antarctic Front and the Polar Front are also referred to as the Polar Frontal Zone (e.g. Tréguer and Jacques 1992). This region forms an important transitional boundary within the SO between the dominance of coccolithophores that construct carbonate shells to the north and diatoms with silicate frustules to the south (Fig. 1.2, 1.3) (Trull *et al.* 2001a; Trull *et al.* 2001b; Honjo 2004). Macro- and micronutrients are more abundant at the Polar Frontal Zone where nutrients are entrained across the bottom of the mixed layer, supporting deep chlorophyll maxima at depths up to 90 m. These deep chlorophyll maxima support blooms of large diatoms, such as *Rhizosolenia* sp. and *Thalassiothrix* sp., which can grow to high abundance and contribute significantly to carbon and silica flux (Tréguer and Van Bennekom 1991; Kopczyńska *et al.* 2001; Kemp *et al.* 2006; Assmy *et al.* 2013). For the purpose of this review we are combining all waters between the Sub-Tropical Front to the north and the Polar Front to the south as the SAZ, as the physical and biological characteristics of these regions are similar.

This region of the SO is a major contributor to the uptake of CO_2 by the ocean (Metzl *et al.* 1999; Sabine 2004; Frölicher *et al.* 2015). The westerly winds that circulate Antarctica carry water from the Antarctic Slope Front north across the SAZ by Ekman transport (Fig. 1.3). This water has a partial pressure of carbon dioxide (pCO_2) below that of the atmosphere, allowing CO_2 to dissolve into the ocean (the solubility pump). North of the Sub-Antarctic Front, surface water is convected to hundreds of meters, forming Antarctic Intermediate Water and Sub-Antarctic Mode Water (Fig. 1.3) (Wong *et al.* 1999; Matear *et al.* 2000; Rintoul and Trull 2001; Lumpkin and Speer 2007). In doing so, it carries an estimated $\sim$1 Gt C yr^{-1} to the ocean's interior and connects the upper and lower components of the global overturning circulation (Metzl *et al.* 1999; Sloyan and Rintoul 2001a,b).

The SAZ is the largest high nutrient, low chlorophyll (HNLC) province in the world's ocean. Over the year phytoplankton productivity in this region is limited by a variety of bottom-up

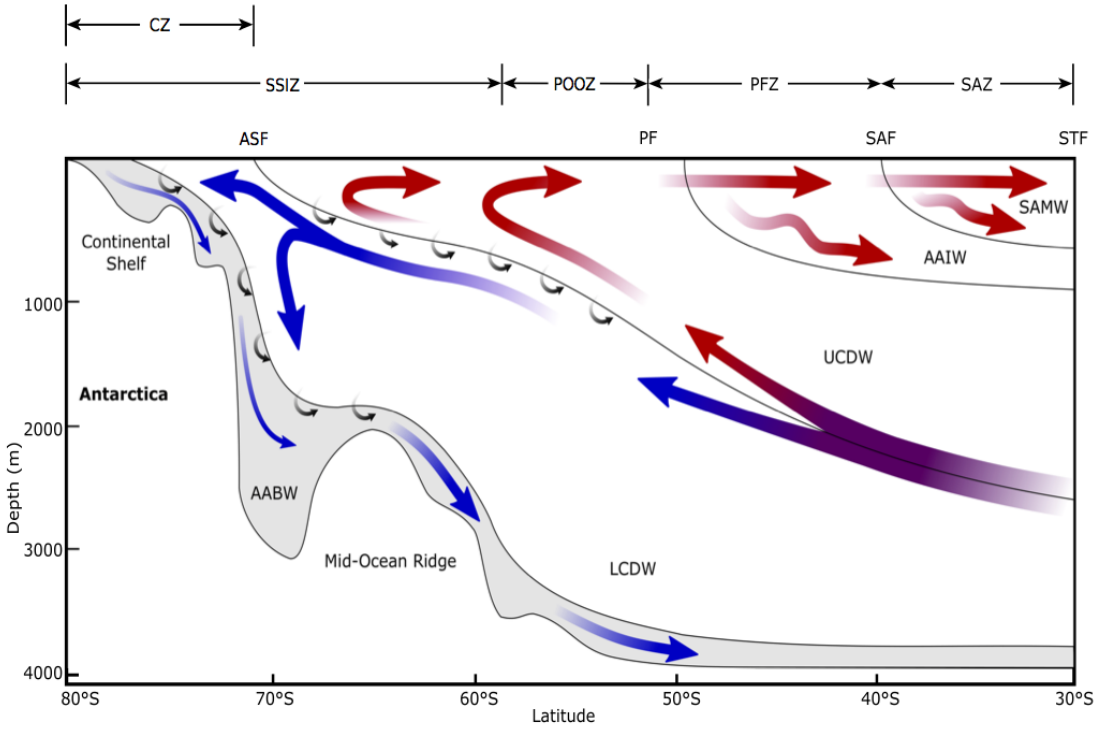

Figure 1.3: Schematic view of the meridional overturning circulation of the Southern Ocean, modified from Fig. 3 in Post *et al.* (2014). Abbreviations are: STF, Sub-Tropical Front; SAF, Sub-Antarctic Front; PF, Polar Front; ASF, Antarctic Slope Front; SAMW, Sub-Antarctic Mode Water; AAIW, Antarctic Intermediate Water; UCDW, Upper Circumpolar Deep Water; LCDW, Lower Circumpolar Deep Water; AABW, Antarctic Bottom Water; SAZ, Sub-Antarctic Zone; PFZ, Polar Frontal Zone; POOZ, Permanently Open Ocean Zone; SSIZ, Seasonal Sea Ice Zone; CZ, Continental Zone. Arrows indicate mean flow direction. Red arrows show the upper cell and blue shows the deep cell. Small arrows indicate diabatic transport due to interior mixing. Note that this is an averaged view of the emergent residual flow due to complex, time-varying, three-dimensional processes and does not reflect the current directions of any given section across the Antarctic Circumpolar Current.

(silicic acid, iron, and light) and top-down (grazing) factors (Fig. 1.4A) (e.g. Banse 1996; Boyd *et al.* 2001; Hiscock *et al.* 2003; Doblin *et al.* 2011). Iron is the main factor limiting phytoplankton growth in the SAZ, despite inputs from dust, shelf sediments, and hydrothermal vents (Boyd *et al.* 2004; Blain *et al.* 2007; Cassar *et al.* 2007; Pollard *et al.* 2009; Boyd and Ellwood 2010; Tagliabue *et al.* 2010). Silica is replete in these waters in spring but it is drawn down by silicifying plankton, such as diatoms, silicoflagellates, and radiolarians, to limiting concentrations by autumn (Trull *et al.* 2001b; Salter *et al.* 2007; Pollard *et al.* 2009). In iron-limited regions of the SAZ, Si:C ratios are high, resulting in low carbon export (Salter *et al.* 2007, 2012; Assmy *et al.* 2013). In addition, light levels experienced by phytoplankton can be very low due to cloudiness and mixed layer depths ranging from 70–100 m in summer to as deep as 600 m in winter (Bishop and Rossow 1991; Rintoul and Trull 2001). In regions of

shallow or complex bathymetry, such as sea mounts, or in waters downstream of sub-Antarctic islands, resuspension of iron-rich sediments naturally fertilises the SAZ waters creating areas of high productivity (Salter *et al.* 2007; Pollard *et al.* 2009). Large, heavily-silicified diatoms, such as *Eucampia antarctica* and *Fragilariopsis kerguelensis*, are responsible for high levels of export in these naturally fertilised regions (Salter *et al.* 2007, 2012; Assmy *et al.* 2013; Rembauville *et al.* 2016b,c). This export is aided by silica limitation, the exhaustion of which ceases diatom growth and accelerates rates of sinking. Nutrient limitation also causes a succession in the phytoplankton community to picoeukaryotes, such as *Phaeocystis* sp. and coccolithophorids (Salter *et al.* 2007; Quéguiner 2013; Balch *et al.* 2016).

Small taxa, including nanoflagellates, cyanobacteria, dinoflagellates, coccolithophores, and small or lightly silicified diatoms, dominate the protistan community in the SAZ (Odate and Fukuchi 1995; Kopczyńska *et al.* 2001, 2007; de Salas *et al.* 2011). Copepods and mesopelagic fish, particularly myctophids, are important primary and secondary consumers of the phytoplankton in these waters and form an alternative food web for squid, predatory mesopelagic fish, and penguins (Kozlov 1995; Cherel *et al.* 2010; Murphy *et al.* 2016). Measured rates of microzooplankton grazing (Jones *et al.* 1998; Griffiths *et al.* 1999; Safi *et al.* 2007; Pearce *et al.* 2011), together with high grazer biomass (Kopczyńska *et al.* 2001) suggest that grazers consume much of the primary productivity in this region. As a result of the physical and biological factors limiting primary productivity in the SAZ, phytoplankton abundance is moderately low and varies little among seasons (Banse 1996). The SAZ is more productive in the Atlantic sector and around 170°W where iron concentrations are higher due to the proximity of land (Fig. 1.2) (Comiso *et al.* 1993; de Baar *et al.* 1995; Moore and Abbott 2000). Despite the low levels of primary productivity, export efficiency is high in HNLC waters of the SAZ, suggesting that small taxa contribute to a high proportion of carbon export (Trull *et al.* 2001a; Lam and Bishop 2007; Cassar *et al.* 2015; Laurenceau-Cornec *et al.* 2015).

Climate predictions suggest that waters of the SAZ will become warmer, fresher and more acidic; the frequency of storms will increase, bringing more wind-blown dust to the region; and phytoplankton will experience increased irradiances of photosynthetically active radiation (PAR) and ultraviolet (UV) radiation (Fig. 1.4B) (Matear and Hirst 1999; Caldeira and Wickett 2003; Orr *et al.* 2005; Marinov *et al.* 2010; Boyd and Law 2011; Boyd *et al.* 2016a). Together,

these changes may have profound consequences for phytoplankton in the SAZ and the role of this region in mediating global climate.

Models suggest that global warming is likely to reduce the efficiency of both the solubility and biological pumps (Sarmiento and Le Quéré 1996; Matear and Hirst 1999). For phytoplankton, increased precipitation and warming increases the buoyancy of surface waters, enhancing stratification and reducing mixed layer depths over much of the SAZ. This reduces the delivery of nutrients to surface water, thereby reducing phytoplankton production and the vertical flux of biogenic carbon to the deep ocean via the biological pump (Matear and Hirst 1999 and refs. therein; Boyd and Law 2011; Petrou *et al.* 2016). The declining efficiency of the biological pump means it would be unable to compensate for any decline in the solubility of CO_2 as the ocean warms (Matear and Hirst 1999). Recent studies also indicate that rising temperatures cause rates of grazing to increase more rapidly than rates of phytoplankton growth (Sarmento *et al.* 2010; Evans *et al.* 2011; Caron and Hutchins 2013; Behrenfeld 2014; Biermann *et al.* 2015; Cael and Follows 2016). Thus, phytoplankton standing stocks are likely to decline and the proportion of primary production respired in near-surface waters by prokaryotes and grazers will increase. The nutritional quality of phytoplankton may also decline at higher temperatures (Finkel *et al.* 2010 and refs. therein; Hixson and Arts 2016), suggesting grazers will also need to consume more phytoplankton to obtain the nutrition they require. Together, these factors are predicted to reduce phytoplankton productivity and the uptake of CO_2 by the ocean in the SAZ region.

The absence of iron is regarded as the primary cause of HNLC waters of the SO having the world's highest inventory of unused surface macronutrients (Martin *et al.* 1990; Boyd *et al.* 2007). As the largest HNLC region in the ocean, low rates of iron supply to the SAZ restrict primary production, alter phytoplankton species composition, increase Si:C export ratios, and constrain the biological pump (Ridgwell 2002; Salter *et al.* 2012; Assmy *et al.* 2013; Salter *et al.* 2014). Aeolian dust makes a significant contribution to iron supply in the SAZ in areas downwind of landmasses and any increase in storm activity as a result of climate change may enhance delivery of iron-rich dust to these areas, enhancing productivity and carbon drawdown in this region (Cassar *et al.* 2007; Boyd and Law 2011; Boyd *et al.* 2012, 2016a). Investigations into sediment cores taken in the sub-Antarctic South Atlantic have correlated increased aeolian iron supply to the SAZ with increased

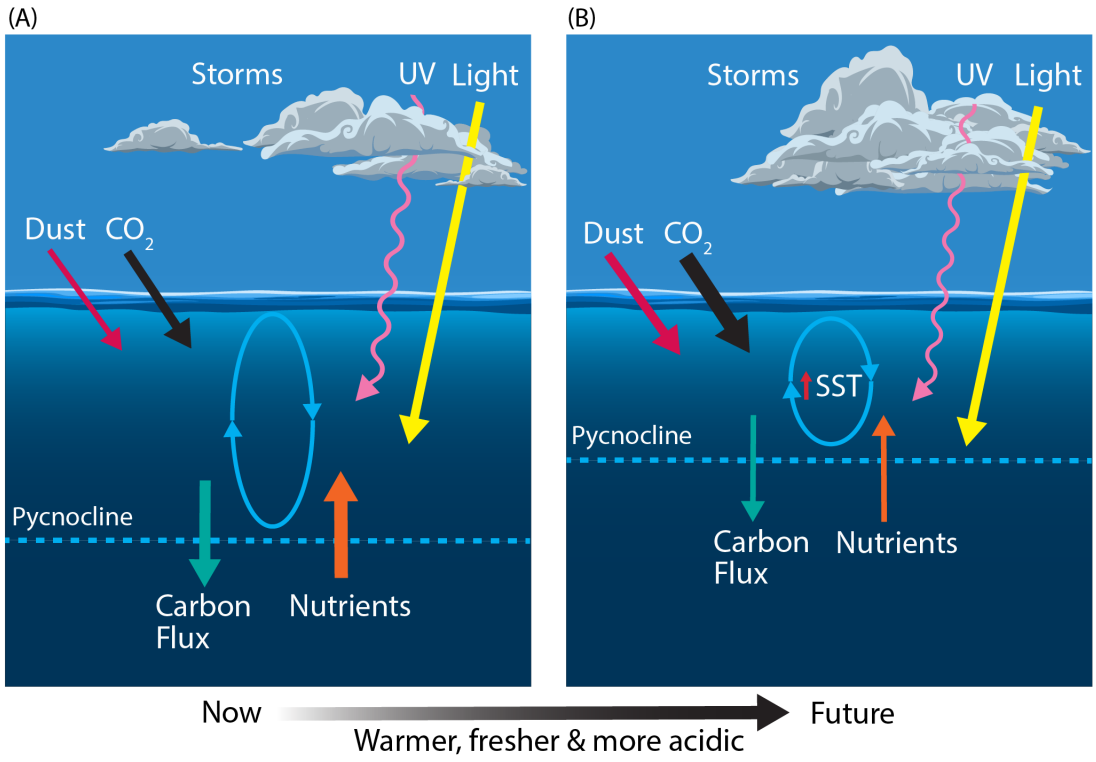

Figure 1.4: Schematic showing the primary physical constraints on phytoplankton in the Sub-Antarctic Zone (SAZ) (A) before and (B) after climate change, modified from Boyd and Law (2011). Ovals represent the depth of mixing and arrow thickness reflects relative rates of flux. SST, sea surface temperature.

productivity during ice ages, strengthening the biological pump and causing significant declines in atmospheric CO_2 (Anderson *et al.* 2014; Martínez-García *et al.* 2014). Increased desertification through climate change-related vegetation loss may result in a 10-fold increase in dust over the Southern Hemisphere (Woodward *et al.* 2005). However, the increase in dust will depend on both climate change and anthropogenic changes in land-use and re-vegetation, the net effects of which are currently uncertain (Ridgwell 2002; Hutchins and Boyd 2016).

While oceanic uptake of CO_2 ameliorates the accumulation of this gas in the atmosphere, it also alters the carbonate chemistry of the ocean. Absorption of CO_2 by the ocean reduces its pH (termed ocean acidification) and increases the solubility of calcium carbonate by reducing its saturation state (Ω) (Caldeira and Wickett 2003; Orr *et al.* 2005). Coccolithophorids are the only calcifying phytoplankton in the SO and are most abundant in naturally iron-fertilised regions in the SAZ, such as fronts and downstream of sub-Antarctic islands (Salter *et al.* 2014; Balch *et al.* 2016). Calcification releases CO_2 (the carbonate counter-pump), resulting in the elevation of pCO_2 concentrations in SAZ waters where coccolithophores are highly abundant,

particularly around the Sub-Antarctic Front (Patil *et al.* 2014; Saavedra-Pellitero *et al.* 2014; Balch *et al.* 2016). Studies of the dominant coccolithophore, *Emiliania huxleyi*, found morphological variations in calcification that closely followed the southerly decline in calcite saturation state but were strain-specific rather than caused by acidification (Cubillos *et al.* 2007; Patil *et al.* 2014; Saavedra-Pellitero *et al.* 2014; Malinverno *et al.* 2015). However, culture studies by Müller *et al.* (2015) reported that calcification by *E. huxleyi* decreased at pCO_2 concentrations $>1000\,\mu$atm. This suggests that calcifying phytoplankton in the SAZ will be vulnerable to predicted increases in pCO_2. A decrease in calcification is anticipated to have a greater negative impact on the carbonate counter-pump than cell growth, leading to greater surface water pCO_2 uptake but potentially reducing vertical carbon flux through a decline in the ballasting effect of calcification (Riebesell *et al.* 2009; Müller *et al.* 2015; Balch *et al.* 2016).

Minimal research has been performed on the effect of ocean acidification on non-calcifying phytoplankton in the SAZ. Boyd *et al.* (2016a) included ocean acidification in their multi-stressor study on a sub-Antarctic diatom and whilst their experimental design did not allow for full analysis of each individual stressor, they found that ocean acidification was not likely to be a primary controller in diatom physiology. Studies on other sub-Antarctic diatom species have reported an increase in productivity with increased CO_2 concentration, likely due to reduced energetic costs associated with the down-regulation of carbon concentrating mechanisms (CCMs) (Hopkinson *et al.* 2011; Trimborn *et al.* 2013). Most SO phytoplankton use CCMs to increase the intracellular concentration of CO_2 for fixation by RuBisCO (Hopkinson *et al.* 2011). This process requires substantial energy consumption and the down-regulation of CCMs is thought to decrease the energy cost of carbon acquisition for phytoplankton photosynthesis (e.g. Raven 1991; Rost *et al.* 2008; Hopkinson *et al.* 2011). However, iron and light limitation in these waters is likely to inhibit any positive effects of increased CO_2 supply (Hoppe *et al.* 2013; Hoppe *et al.* 2015).

Stratification of the water column is predicted to increase in the SAZ region, trapping phytoplankton in a shallowing mixed layer where they are exposed to higher irradiances of PAR and UV radiation (280–400 nm) (Davidson 2006; Gao *et al.* 2012a; Häder *et al.* 2015). Light wavelengths are differentially attenuated by sea water. Blue wavelengths ($\sim$500 nm) can reach depths exceeding 250 m in clear oceanic water but the penetration rapidly decreases as

radiation tends towards infrared (longer) and ultraviolet (shorter) wavelengths (Fig. 1.5) (Davidson 2006). Thus, red and infrared wavelengths only warm the very surface of the ocean, while damaging irradiances of UV-B penetrate to $\leq$30 m depth (Karentz and Lutze 1990; Buma *et al.* 2001; Davidson 2006). Rates of phytoplankton productivity in the SAZ are commonly limited by light availability due to cloudiness and deep mixing. Increased stratification could mitigate this limitation by keeping cells in sunlit near-surface waters. Overall, productivity would still be constrained by the availability of key nutrients (iron and silicate), which already limit phytoplankton production in the SAZ despite the low light. Thus, increased rates of productivity are unlikely to result in higher biomass or carbon export in this region without a coincident increase in nutrient supply (see above).

Exposing phytoplankton in the SAZ to higher irradiances of PAR, Ultraviolet-A (UV-A, 315–400 nm), and Ultraviolet-B (UV-B, 280–315 nm) is also likely to increase photodamage. The damage to intracellular molecules or structures become progressively less repairable as wavelengths decline below 350 nm, reducing phytoplankton productivity, growth and survival, and changing the species composition, with implications for ecosystem structure and function (e.g. Karentz 1991; Marchant and Davidson 1991; Davidson 2006). The amount of damage sustained by cells is a function of the dose and dose rate of UV exposure; the frequency and duration of exposure to low irradiances to allow repair; and species-specific differences in the UV-tolerance of component species in natural phytoplankton communities (e.g. Cullen and Lesser 1991; Davidson 2006; Häder *et al.* 2015). It is hard to assess the additional risk UV exposure may have to phytoplankton in the SAZ as such details are currently unavailable. Studies by Helbling *et al.* (1994) and Neale *et al.* (1998a,b) showed that increasing the rate of change in the light climate altered the balance between damage and repair and greatly increased the biological impact of a specific UV dose. Thus, trapping cells in a shallow mixed zone where they receive repeated exposure to high PAR and UV irradiances over short time scales (see above, Fig. 1.5) may have a far greater impact on the growth, production, and survival of phytoplankton than ozone depletion (Davidson 2006).

The SAZ region is being increasingly penetrated by both sub-tropical and polar waters. The climate-induced increase in the positive phase of the Southern Annular Mode (SAM) has caused the westerly wind belt to intensify and move south (see POOZ below). This increase in the

velocity of westerly winds to the south of the SAZ has enhanced upwelling at the Antarctic Slope Front and increased its Ekman transport into the SAZ from the south, increasing phytoplankton growth in the cool, nutrient-rich water (Lovenduski and Gruber 2005; DiFiore *et al.* 2006). A 37 year dataset of surface Chl *a* measurements south of Australia from vessels of the Japanese Antarctic Research Expeditions show as similar trend of increasing Chl *a* spreading northward from these northern limits of the POOZ (55 °S) into the Polar Frontal Zone (40 °S) (Hirawake *et al.* 2005). The southward movement of the westerly wind belt has also increased the penetration of sub-tropical waters into the SAZ; supplementing iron supply, exacerbating warming, and intensifying climate-induced stratification (Lovenduski and Gruber 2005; Poloczanska *et al.* 2007; Ridgway 2007). Warmer waters also allow the incursion of sub-tropical phytoplankton and grazers into SAZ waters, causing additional grazing competition and unknown effects on the SO food web (McLeod *et al.* 2012).

Not all of the SAZ is expected to experience shallowing mixed layer depth as a result of climate change. At the sub-Antarctic convergence, increased wind will deepen the mixed layer, causing declines in phytoplankton productivity through light limitation (Lovenduski and Gruber 2005). In addition, there are zonal differences in the effect of the increasingly positive SAM on mixed layer depth in the SAZ region, with deepening over the eastern Indian Ocean and central Pacific Ocean, and shallowing over the western Pacific Ocean (Sallée *et al.* 2010). Resulting in a mosaic of changing factors that limit phytoplankton productivity, from nutrient limitation in shallower regions to light limitation in deeply mixed waters.

Clearly, phytoplankton occupying the SAZ region are likely to experience a range of environmental stressors as a result of climate change. The net effect of these changes is uncertain. Most studies investigate the physiological effects of change on phytoplankton by imposing single stressors (e.g. Boyd *et al.* 2013; Trimborn *et al.* 2013) but research shows interaction among stressors alter their response. A multi-stressor study by Boyd *et al.* (2016a) using a sub-Antarctic diatom showed that its response to environmental change was governed by the range of stresses to which it was exposed. Negative responses to several stressors (CO_2, nutrients, and light) were offset by positive responses to others (temperature and iron). Thus, the response of an organism is determined by the interactive effect of all the stresses they experience (Boyd *et al.* 2016a). Equally, responses of single species (e.g. Boelen *et al.* 2011; Trimborn *et al.* 2014; Müller *et al.* 2015) provide valuable

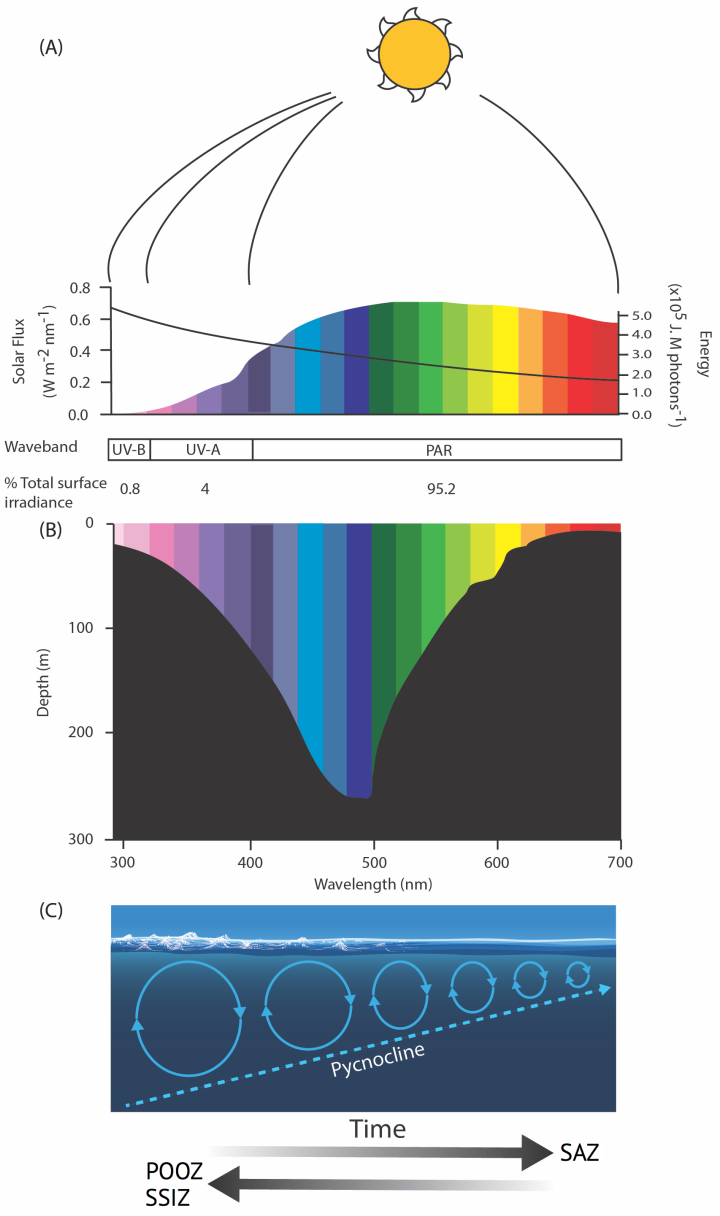

Figure 1.5: Schematic showing (A) the spectral flux (coloured bars) and molar photon energy (black line) of solar radiation, (B) the wavelength-dependent penetration of light in the ocean and (C) the role of wind in deepening the mixed layer depth, modified from Davidson (2006). Solar spectral flux was calculated from the UVSpec model for noon at the summer solstice at Davis Station, Antarctica, an albedo of 0.5 and a column Ozone of 300 Dobson units. Photon energy was calculated after Kirk (1994). SAZ, Sub-Antarctic Zone; POOZ, Permanently Open Ocean Zone; SSIZ, Seasonal Sea Ice Zone; PAR, photosynthetically active radiation.

insights into the mechanisms of sensitivity and tolerance but avoid interactions among species and trophic levels that can alter the responses or sensitivity of a community to a stressor (Davidson *et al.* 2016; Thomson *et al.* 2016). Yet gaining maximum predictive strength by simultaneously performing multi-stressor and multi-trophic level studies is often logistically so demanding as to

be impractical.

Predicted responses by phytoplankton in the SAZ to climate change differ. Many propose that the stratification-induced decline in nutrient supply to surface waters will reduce their productivity and favour small flagellates (e.g. Matear and Hirst 1999; Marinov *et al.* 2010; Petrou *et al.* 2016), heightening the role of the microbial food web and reducing carbon export. While Boyd *et al.* (2016a) indicates that increases in iron and temperature may double growth rates and favour diatoms; scenarios which have major and opposing influences on regional productivity and biogeochemistry. It is likely that the effect of climate change on phytoplankton in the SAZ is going to be determined by the timing, rate, and magnitude of change in each stressor. Stochastic inputs of iron, wind, and storms disrupt stratification; influencing productivity, species composition, and export production through changes in nutrients and light climate. Changes in community composition from diatoms to flagellates also affect particulate matter stoichiometry in this region, causing a decline in nutritional quality for grazing zooplankton (Martiny *et al.* 2013; Rembauville *et al.* 2016a) and subsequent flow on effects throughout the food web (Finkel *et al.* 2010). Ocean acidification will also cause declines in carbonate saturation, affecting coccolithophore calcification, resulting in greater surface pCO_2 uptake and decreased carbon export. Overall, our synthesis suggests that productivity will decline in the SAZ due to the net response of nutrient limitation and increased grazing, especially in silicate-limited waters.

1.3 Permanently open ocean zone

The Permanently Open Ocean Zone (POOZ) lies between the Polar Front and the northern limit of the winter sea ice, covering approximately 14 million km^{-2} (Fig. 1.2). The Polar Front at the northern extent of the POOZ forms a natural barrier between the warm SAZ water (5–10 °C) and the cold Antarctic water (<2 °C) (Pollard *et al.* 2002; Sokolov and Rintoul 2009a). These waters are predominantly HNLC with a phytoplankton community dominated by nano- and picoflagellates but characteristically contain even less Chl *a* than the SAZ (Becquevort *et al.* 2000; Moore and Abbott 2000; Kopczyńska *et al.* 2001; Olguín and Alder 2011). The exception to this is where iron concentrations in surface waters are enhanced by upwelling and/or

sediment input/resuspension from sea floor bathymetry and sub-Antarctic islands (Fig. 1.2) (e.g. Pollard *et al.* 2002; Ardelan *et al.* 2010; Rembauville *et al.* 2015b). This pattern differs from that of macronutrients, which decline northwards across the POOZ region, nitrate falling from ∼25–20 $\mu mol\,L^{-1}$ and silicate from ∼60–10 $\mu mol\,L^{-1}$. These nutrients are upwelled at the Antarctic Slope Front and are progressively drawn down by phytoplankton as they are transported northward across the POOZ by Ekman drift (Tréguer and Jacques 1992; Pollard *et al.* 2002).

The POOZ displays a strong seasonality in biological production (Abbott *et al.* 2000). Strong winds in winter deepen the mixed layer, bringing nutrient-rich water to the surface. These nutrients fuel phytoplankton growth in spring when sunlight increases, conditions are calmer, and phytoplankton are confined to shallower mixed depths by stratification (Fig. 1.6A) (Abbott *et al.* 2000; Pollard *et al.* 2002; Constable *et al.* 2014). Whilst the POOZ is considered to be an iron-limited environment, silicate limitation and grazing by micro- and metazooplankton also limit the duration of the diatom-dominated bloom in this region (Abbott *et al.* 2000; Becquevort *et al.* 2000; Timmermans *et al.* 2001; Strzepek *et al.* 2011; Christaki *et al.* 2014). Like the SAZ, large, heavily silicified diatoms contribute significantly to carbon export (Rembauville *et al.* 2015a; Rembauville *et al.* 2015b; Rigual-Hernández *et al.* 2015; Rembauville *et al.* 2016b). In regions of natural iron fertilization (e.g. the Kerguelen Plateau), phytoplankton production appears to be strongly linked to higher trophic levels rather than making a substantial contribution to carbon export (Obernosterer *et al.* 2008; Christaki *et al.* 2014; Laurenceau-Cornec *et al.* 2015; Rembauville *et al.* 2015b).

Modeling studies predict the POOZ region will experience a poleward shift and strengthening of the westerly winds; deepening of the summertime mixed layer depth; increasing cloud cover; warming and freshening of surface waters; and decreasing pH (Fig. 1.6B) (Orr *et al.* 2005; McNeil and Matear 2008; Meijers 2014; Leung *et al.* 2015; Armour *et al.* 2016; Haumann *et al.* 2016). Thus far, sea surface warming in the POOZ of only 0.02 °C per decade has been slower than the global average of 0.08 °C per decade, since 1950 (Armour *et al.* 2016). This is due to heat taken up by surface water in the POOZ being transported northward by Ekman drift into the SAZ (Fig. 1.3). Despite this, it has been proposed that rising temperatures may be contributing to an observed range extension of *E. huxleyi* below 60 °S (Cubillos *et al.* 2007; Winter *et al.* 2014).

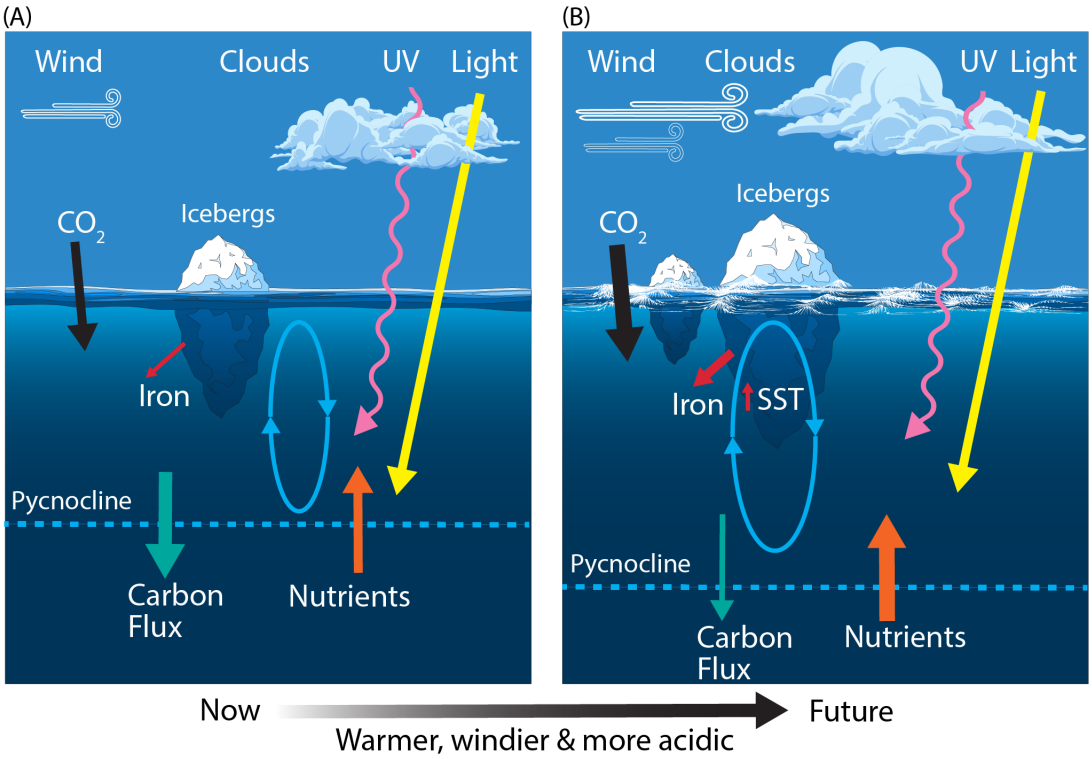

Figure 1.6: Schematic showing the primary physical constraints on phytoplankton in the Permanently Open Ocean Zone (POOZ) (A) before and (B) after climate change. Ovals represent the depth of mixing and arrow thickness reflects relative rates of flux. SST, sea surface temperature.

Whilst warming is expected to increase phytoplankton productivity (Sarmiento *et al.* 2004; Behrenfeld *et al.* 2006; Steinacher *et al.* 2010), this effect is offset against the increasingly positive phase of SAM, which is causing an intensification and southerly shift of westerly winds in summer (Lenton and Matear 2007; Lovenduski *et al.* 2007). The SAM controls the north-south shift of the circumpolar westerly winds and is the dominant climate-induced environmental change in Antarctic waters, substantially affecting SO circulation and CO_2 uptake (Thompson and Solomon 2002; Lenton and Matear 2007; Lovenduski *et al.* 2007; Swart *et al.* 2014). In the last 50 years there has been an observed increase in the positive phase of SAM, strongly related to the depletion of ozone in the atmosphere above Antarctica (Son *et al.* 2008; Polvani *et al.* 2011). Leung *et al.* (2015) predict that the positive SAM will continue to deepen the summer mixed layer and increase cloud cover in the POOZ, resulting in decreasing light availability and causing a decline in phytoplankton biomass and productivity. Observed trends in summertime mixed layer depth, cloud cover, and Chl *a* (since 1950, 1980, and 1997, respectively) correspond well to the modeled projections (Leung *et al.* 2015).

Conversely, some predict the increase in positive SAM may enhance phytoplankton productivity in the POOZ. Deepening of the mixed layer can increase the upwelling of nutrients, which some models predict will promote phytoplankton productivity and export production south of 60 °S (Lovenduski and Gruber 2005; Hauck *et al.* 2013, 2015; Laufkötter *et al.* 2015). It is hard to assess the validity of such predictions for the POOZ region as these models combine all waters south of the Polar Front, including the SSIZ. Using satellite and Argo data, Carranza and Gille (2015) reported a correlation of increased Chl *a* in the SO with increased mixed layer depth. A positive SAM also increases eddy formation and transports SAZ water across the Polar Front (Meredith and Hogg 2006; Kahru *et al.* 2007; Hogg *et al.* 2008). These cyclonic eddies trap warm water at their core, enhance stratification, and upwell nutrients and iron, creating ideal conditions for phytoplankton productivity (Kahru *et al.* 2007) and may also contribute significantly to ocean warming in the POOZ (Hogg *et al.* 2008).

Increased nutrient input from melting icebergs may also increase productivity in the POOZ. Climate warming and the breakup of Antarctic ice shelves (Scambos *et al.* 2000) could increase the number of icebergs in the POOZ (see CZ below). Melting icebergs enrich the surrounding water with iron, enhancing phytoplankton growth and productivity (Cefarelli *et al.* 2011; Lin *et al.* 2011; Shaw *et al.* 2011; Vernet *et al.* 2011; Vernet *et al.* 2012), and increasing export of carbon from surface waters (Smith *et al.* 2011). This heightened productivity also attracts large grazing populations that increase food availability to higher trophic levels and facilitates the sequestration of carbon to the deep ocean through faecal pellet production (Vernet *et al.* 2011).

Climate change is expected to change the location and area of the POOZ. The Polar Front, which denotes the northern limit of the POOZ has already shifted 60 km south since 1992 and this southward migration is expected to continue as the climate warms (Sokolov and Rintoul 2009b). To the south, the northernmost extent of sea ice coverage is also predicted to retreat with ocean warming. Overall, this would result in a net increase in the area of the POOZ in the future (Bracegirdle *et al.* 2008; McNeil and Matear 2008; Boyd *et al.* 2014). Some studies suggest that an increase in open ocean habitat will increase production in this region (Bopp *et al.* 2001; Behrenfeld *et al.* 2006). However, it is not yet understood how the multi-stressor effects of the accompanying environmental changes, such as ocean warming, decreased pH, light availability, and nutrient supply will affect the phytoplankton community.

The effect of climate change on phytoplankton productivity in the POOZ will strongly depend on the changes in light limitation and nutrient supply. Deepening of the summertime mixed layer depth due to increases in the strength of westerly winds are likely to further reduce the light available to phytoplankton, reducing their productivity over much of the POOZ (see above). However, increased nutrient concentrations as a result of increased mixing and melting icebergs, together with the incursions of warm-core eddies from the Polar Front may promote localised phytoplankton blooms when light is not limiting. Furthermore, increased nutrient concentrations might promote the growth of large diatoms (Timmermans *et al.* 2001), as well as increased abundance of phytoplankton in near surface waters rather than forming deep chlorophyll maxima. This increase in abundance is likely to increase the functioning of the microbial loop and promote grazing, as has been observed in naturally iron-fertilised regions of the POOZ (Christaki *et al.* 2014). It is also likely that with a future southward shift in SSIZ extent (see SSIZ below) the brief but substantial blooms of *Phaeocystis* sp. and large diatoms of the MIZ will be replaced by a prolonged but subdued bloom of phytoplankton over summer in waters that are now part of the POOZ (see MIZ below, Behrenfeld *et al.* 2006).

1.4 Seasonal sea ice zone

In the following sections we divide the region of the SO covered by sea ice into two distinct zones. First we consider the effects of climate change on the extent, advance and retreat of ice over the entire Seasonal Sea Ice Zone (SSIZ) and examine the implications for phytoplankton. Then we consider the processes occurring at the northern margin of the sea ice (the marginal ice zone, MIZ), and how these are predicted to respond to a changing climate.

The SSIZ encompasses the region of the SO between the winter maximum and summer minimum of sea ice cover (Fig. 1.2). The sea ice is one of the largest and most dynamic ecosystems on earth, extending to over $19\,\text{million}\,\text{km}^{-2}$ in winter and retreating to $\sim 3\,\text{million}\,\text{km}^{-2}$ over summer (Brierley and Thomas 2002; Comiso and Nishio 2008; Convey *et al.* 2009). Total productivity within the SSIZ has been estimated at $\sim$140–180 $\text{Tg}\,\text{C}\,\text{yr}^{-1}$ (Arrigo *et al.* 1997; Arrigo *et al.* 2008a). Sea ice cover plays an important role in the regulation of climate by controlling heat and gas exchange between the atmosphere and the ocean

(Massom and Stammerjohn 2010). Snow covered sea ice creates a high albedo surface that reflects most of the sun's energy back into space, thereby reducing warming of the polar oceans (Perovich 1990). Conversely, in winter the ice cover insulates the ocean from direct exposure to the cold atmosphere (Stroeve *et al.* 2016 and refs. therein). Not only is sea ice itself an important regulator of global climate, it also provides a vital environment for Antarctic life.

Sea ice supports a diverse community of algae that possess some of the most extreme adaptations to environmental stress recorded. They inhabit a range of environments throughout the ice; from surface ponds to brine channels in the sea ice interior and at the bottom ice-water interface (Knox 2007; Arrigo 2014). Here they can experience extremely low temperatures ($<-20\,^{\circ}\mathrm{C}$), light irradiances ($<1\,\mu\mathrm{mol\,m^{-2}\,s^{-1}}$), CO_2 concentrations ($<100\,\mu\mathrm{atm}$), and salinities up to $\sim$200 PSU (Thomas and Dieckmann 2002 and refs. therein). Primary production by sea ice algae contributes between 24–70 $\mathrm{Tg\,C\,yr^{-1}}$ (Legendre *et al.* 1992; Arrigo *et al.* 1997; Saenz and Arrigo 2014) and phytoplankton biomass averages between 1–100 mg Chl $a\,\mathrm{m^{-2}}$, although it can exceed 1000 mg Chl $a\,\mathrm{m^{-2}}$ in some regions (Lizotte 2001; Arrigo *et al.* 2010). Ice algal biomass and productivity varies greatly at small spatial and temporal scales, primarily due to changes in snow cover, ice thickness, surface flooding, and ice rafting (McMinn *et al.* 2007; Meiners *et al.* 2012; Arrigo 2014 and refs. within). Thus, ice algae are able to thrive in this harsh physical environment.

Ice algal productivity is essential to the nutrition of higher trophic levels in Antarctic waters. Productivity and algal biomass within the sea ice is generally low during the winter (Arrigo *et al.* 1998b). Conditions are most favourable at the ice-water interface, where warmer temperature ($-1.8\,^{\circ}\mathrm{C}$), lower salinity ($\sim$35 PSU), and high nutrients maintain higher productivity rates than the sea ice interior (Lizotte 2001). These bottom ice algal communities are an essential food source for zooplankton over winter (Brierley and Thomas 2002 and refs. therein, Jia *et al.* 2016), when phytoplankton biomass in the waters beneath the sea ice are very low due to light limitation (Perrin *et al.* 1987; Legendre *et al.* 1992; Robins *et al.* 1995). For example, the phenology of the Antarctic krill, *Euphausia superba*, a keystone organism in SO food webs, is integrally liked to sea ice and seasonality, largely due to its being a refuge and source of algal nutrition over winter (Kawaguchi and Satake 1994; Daly 1998; Atkinson *et al.* 2004; Smetacek and Nicol 2005; Quetin and Ross 2009) and is associated with the ice at all stages of its life cycle (Flores *et al.* 2012 and

refs. therein). Thus, changes in the timing and/or extent of sea ice cover are likely to have major implications for the Antarctic food web (see below, Quetin and Ross 2009).

Changes in the extent, duration, thickness, and transparency of sea ice will have major implications for the algae that inhabit the ice and processes that drive phytoplankton productivity during sea ice retreat. In stark contrast to the decline currently observed in the Arctic (Stroeve *et al.* 2012 and refs. therein), the overall sea ice extent (SIE) around Antarctica has experienced a modest increase of between 0.9 to 1.5% since 1979 (Comiso and Nishio 2008; Turner *et al.* 2009; Parkinson and Cavalieri 2012; Simmonds 2015), and modeled increases in sea ice volume of $\sim$0.4 % yr^{-1} between 1992 and 2010 due to approximately equal increases in both SIE and thickness (Holland *et al.* 2014). This culminated in the National Snow and Ice Data Center (NSIDC) reporting a maximum recorded SIE >20 million km^{-2} in September 2014, 1.54 million km^{-2} above the 1981 to 2010 average (Fetterer *et al.* 2016a). However, the SIE around Antarctica in November 2016 was only 14.54 million km^{-2}, 1.81 million km^{-2} below the 1981 to 2010 average (Fetterer *et al.* 2016b), demonstrating substantial interannual variability. Furthermore, the long term trend in increasing SIE is not uniform around Antarctica, with a significant decrease in the Amundsen and Bellingshausen Seas of between -5.1 to -6.6% per decade but a large increase in the Ross Sea of between 4.2 to 5.2% per decade due to the Amundsen Sea Low (ASL) (see below, Comiso and Nishio 2008; Massom and Stammerjohn 2010; Parkinson and Cavalieri 2012).

Dramatic changes in SIE in some regions around Antarctica have altered the timing of sea ice growth and retreat. The large changes in SIE between the Ross Sea and the WAP are driven by the combined influence of the El Niño-Southern Oscillation (ENSO), the SAM, and their interaction with the ASL, the deepest low pressure cell around Antarctica (Arrigo and Thomas 2004; Liu *et al.* 2004; Massom *et al.* 2008; Stammerjohn *et al.* 2008; Pezza *et al.* 2012; Raphael *et al.* 2016). The positive SAM phase and the La Niña phase of the ENSO have deepened the ASL. Increasing greenhouse gasses and stratospheric ozone recovery may also exacerbate the current SIE trends in these regions by further deepening the ASL (Raphael *et al.* 2016). The resultant strengthening of winds associated with the ASL lead to the compression of the sea ice in the Amundsen and Bellingshausen Seas and expansion in the Ross Sea. As a result, sea ice extent around the West Antarctic Peninsula (WAP) has declined by up to 40% over the past 26 years

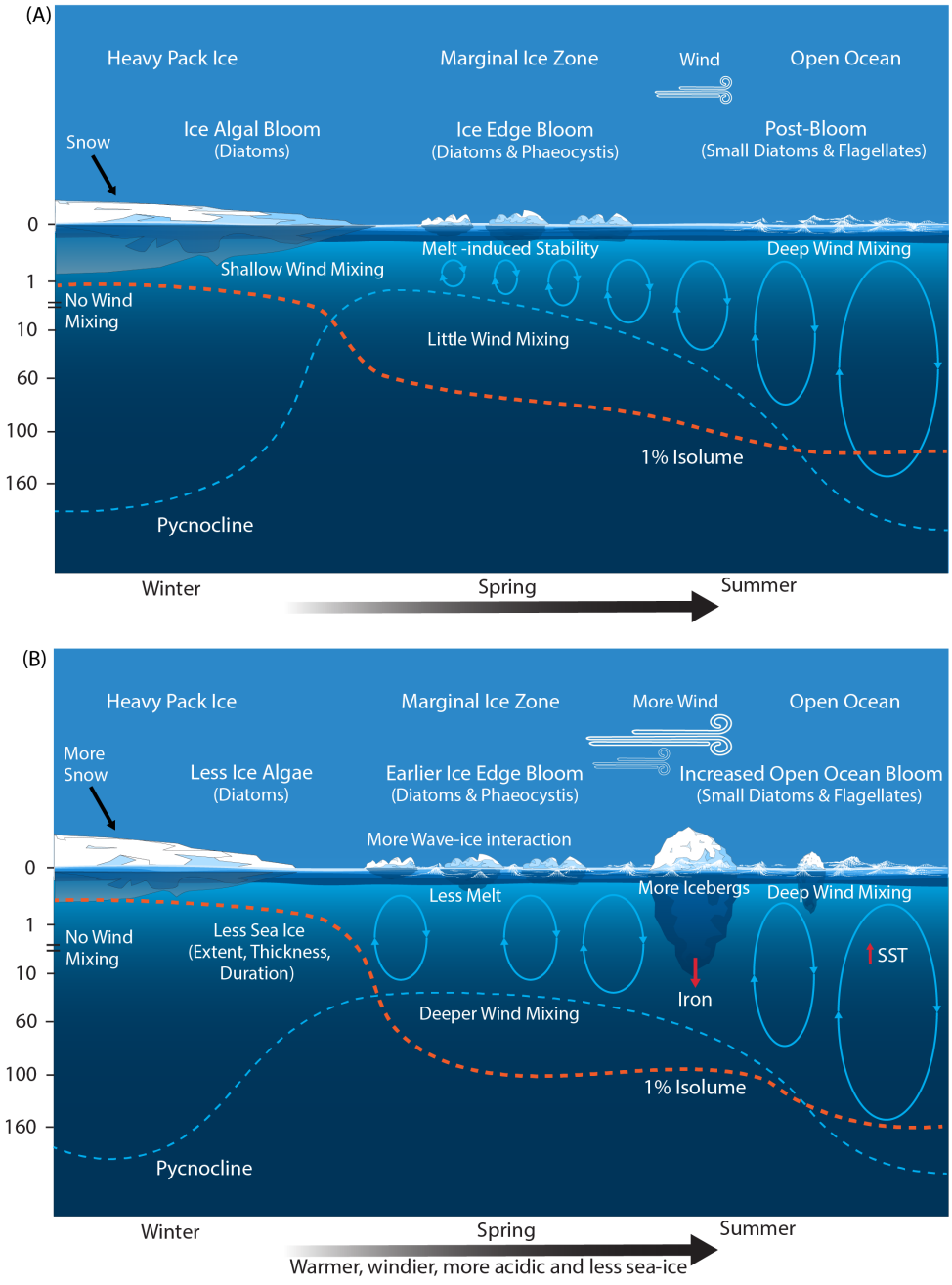

Figure 1.7: Schematic showing the primary physical constraints on phytoplankton in the Seasonal Sea Ice and Marginal Ice Zones (SSIZ and MIZ) (A) before and (B) after climate change. Modified from Sullivan *et al.* (1988) and Petrou *et al.* (2016). Ovals represent the depth of mixing and arrow thickness reflect relative rates. Blue dashed line denotes the location of the pycnocline; and the red dashed line depicts the approximated depth for 1% surface irradiance. SST, sea surface temperature.

(Smith and Stammerjohn 2001; Ducklow *et al.* 2007; Parkinson and Cavalieri 2012). Modeling studies predict that continued global warming will eventually override the SAM and ENSO effects, increasing warming to the atmosphere and ocean, and resulting in significant declines in SIE around Antarctica (Bracegirdle *et al.* 2008; Ferreira *et al.* 2015).

Changes in sea ice concentration, extent, and seasonality critically affect the timing and productivity of phytoplankton blooms. In the western Ross Sea, sea ice retreats later and advances earlier, reducing the ice-free season by ∼2.6 months (Stammerjohn *et al.* 2012). The delay in ice retreat has delayed the onset of the summer bloom and decreased its duration, thereby reducing total seasonal productivity (Arrigo and van Dijken 2004). Conversely, earlier retreat and delayed advance of sea ice has resulted in a 3 month lengthening of the summer ice-free season in the Amundsen and Bellingshausen Seas (Stammerjohn *et al.* 2012). While this extension of the ice-free period was expected to increase annual phytoplankton production and growth (Sarmiento *et al.* 2004; Moreau *et al.* 2015), no such trend has yet been observed (Montes-Hugo *et al.* 2008; Smith *et al.* 2008). This may be due to constraints imposed by nutrient and light limitation that are also key drivers of phytoplankton growth in the SSIZ (Pearce *et al.* 2010; Westwood *et al.* 2010).

The observed increase in SIE is contrary to modeling studies that predict a decline in SIE with global warming (Maksym *et al.* 2012 and refs. therein), reflecting the complex interaction of factors influencing the distribution and concentration of sea ice around Antarctica (Sen Gupta *et al.* 2009; Parkinson and Cavalieri 2012 and refs. therein, Turner *et al.* 2013). Models indicate that the continued warming of the Earth's climate will result in a 33% decline in Antarctic SIE by 2100 (Bracegirdle *et al.* 2008). Historical records (whaling records, ice charts, and direct observations) and concentrations of methane sulfonic acid in ice cores suggest SIE has declined at least 20% since the 1950s (Curran *et al.* 2003; de la Mare 2009).

The seasonal southward retreat of the sea ice initiates the phytoplankton bloom (see MIZ below) and changes in the timing of sea ice growth and retreat will alter the timing of these blooms. Such changes can impose temporal asynchronies and spatial separations between grazers and their food, reducing grazer abundance, reproductive success, and altering the distributions of higher trophic levels (Moline *et al.* 2008). SO zooplankton use the sea ice as a refuge and food

source in the winter (Daly 1998; Murphy *et al.* 2007; Jia *et al.* 2016). MIZ phytoplankton blooms supply the essential fatty acids required for reproduction and over-wintering strategies (Schnack-Schiel *et al.* 1998; Hagen 1999). It is not yet known how changes in sea ice retreat will affect higher trophic levels in SSIZ but a delay in the summer bloom may restrict the availability of an essential food source during vulnerable life-stages, resulting in significant grazer mortality and less food availability to higher trophic organisms.

A decline in SIE is likely to decrease overall ice algal abundance, reducing carbon flux to the deep ocean. Decaying sea ice releases plumes of ice algal aggregates that can sink from surface waters at rates $\leq 200\,\mathrm{m\,d^{-1}}$ (Thomas *et al.* 1998; Wright and van den Enden 2000; Wright *et al.* 2010). Given that sea ice algae contribute to ∼12% of annual productivity in the SSIZ (Saenz and Arrigo 2014); the large accumulations of algal biomass amongst the sea ice (see above); and the fact that the rate of sedimentation would largely preclude remineralization of these algal aggregates; it is likely that declining ice algal abundance would reduce this region's contribution to vertical carbon flux.

A reduction in SIE extent, and therefore sea ice algal biomass, is also likely to reduce the contribution of Antarctic sea ice algae to the global biogenic sulfur budget via synthesis of DMSP and subsequent release of DMS. Many intracellular roles have been proposed for DMSP and DMS, including cryoprotectant, antioxidant, metabolic overflow product, and even a compound that mediates grazer interactions (Kirst *et al.* 1991; Malin 2006 and refs. therein). DMS is oxidized in the atmosphere to sulfate aerosols which nucleate cloud condensation, altering global albedo (Charlson *et al.* 1987; Charlson *et al.* 1992). Estimates suggest that the Antarctic region contributes 17% of the global DMS emissions (Curran and Jones 2000), with the highest concentrations of these DMSP and DMS compounds often found amongst sea ice (e.g. Kirst *et al.* 1991; Turner *et al.* 1995; Trevena and Jones 2006; Jones *et al.* 2010; Vance *et al.* 2013). Any climate-induced decline in SIE and/or duration (see above) could reduce the magnitude of DMS production in the SSIZ, feeding back to global climate by reducing cloud-induced albedo.

Thinning of sea ice could substantially contribute to the loss of sea ice volume within the SSIZ, impacting ice algal communities. Observations of ice thickness in the SSIZ are sparse and difficult to obtain, displaying large variability within regions and among seasons (Worby *et al.* 2008). As

a result, current trends in Antarctic sea ice thickness are not well understood (Kwok 2010; Hobbs *et al.* 2016 and refs. therein) and based upon model estimates (Holland *et al.* 2014). The majority of the sea ice in the SSIZ is first-year ice, with ice thickness seldom exceeding 2 m (Worby *et al.* 2008; Meiners *et al.* 2012). Ice algal biomass is often concentrated in the bottom 20 cm of the ice (Palmisano and Sullivan 1983; McMinn *et al.* 2007; Meiners *et al.* 2012), with thicker ice (>1.0 m) supporting higher algal biomass than thin ice (<0.4 m), due to longer time for colonization and growth of the bottom ice algal community, along with development of internal communities from the rafting of ice floes (McMinn *et al.* 2007; Meiners *et al.* 2012). Thus, a decline in sea ice thickness may result in a reduction in bottom community biomass, which is an important food source for zooplankton (Brierley and Thomas 2002; Jia *et al.* 2016), thereby causing a shift in the diet of Antarctic birds and mammals toward less efficient pathways (Murphy *et al.* 2007; Moline *et al.* 2008; Flores *et al.* 2012; Ballerini *et al.* 2014).

A warming atmosphere is predicted to result in more precipitation that could cause an increase in snow deposits on the surface of the sea ice (Bracegirdle *et al.* 2008; Massom *et al.* 2008). Increased snow load depresses ice floes, flooding the ice surface and fostering phytoplankton blooms in the high light, high nutrient environment at the snow-ice interface (Arrigo *et al.* 1997; Massom *et al.* 2006). Surface communities are most often associated with thin ice (<0.4 m) (Meiners *et al.* 2012) and as such, could become more prominent in the future. Increased albedo caused by greater snow cover on the ice would also limit light transmission through the ice, reducing ice algal productivity in internal and bottom communities (Grossi *et al.* 1987; Palmisano *et al.* 1987).

Sea ice is a substantial sink for CO_2 over winter. Air-ice exchange at the ice surface over-saturates the CO_2 in sea ice brine and contributes as much as 58% of the annual atmospheric CO_2 uptake in the SO (Delille *et al.* 2014). Ice cover provides a barrier between the atmosphere and the surface water, slowing atmospheric CO_2 uptake (Boyd *et al.* 2008) and limiting predicted pCO_2 levels by 2100 to 500–580 µatm. Furthermore, it prohibits outgassing of upwelled water supersaturated in CO_2 over winter (Gibson and Trull 1999; Roden *et al.* 2013). The few studies investigating the effect of ocean acidification on sea ice algal communities suggest they can tolerate CO_2 concentrations up to 10.000 µatm (McMinn *et al.* 2014; Coad *et al.* 2016).

The increasingly positive SAM (see SAZ above) exposes the SSIZ is to stronger winds. However, future recovery of the ozone hole will reduce the SAM favouring increasing warming and stratification (see Conclusion), with consequent declines in the SIE extent, thickness and duration of ice cover. This is likely to have a strong negative effect on sea ice algal abundance, through a loss of habitat. Whilst ice algae are not major contributors to overall SO primary productivity, they are essential in the life cycles of many zooplankton species. Thus, declines in ice algal abundance will likely have a significant negative effect on critical links in the SO food web, especially krill, and promote different and less energy efficient trophic pathways such as consumption of phytoplankton by salps or via copepods to myctophids. Such changes would reduce the capacity of the SO to support the current abundance of iconic, krill-dependent Antarctic wildlife (Murphy *et al.* 2007; Murphy *et al.* 2016).

The development of the phytoplankton bloom and succession of the pelagic phytoplankton community is initiated by the seasonal retreat of the sea ice across the SSIZ. Here we consider the effects of climate-induced changes on processes in the MIZ.

1.5 Marginal ice zone

The region where the dense sea ice pack transitions to open ocean is known as the marginal ice zone (MIZ). It is an area of high productivity that accounts for the majority of the spring-summer phytoplankton blooms (Fig. 1.2) (Arrigo *et al.* 2008a). The area of the MIZ varies greatly over spring and summer, ranging from $6\,\text{million}\,\text{km}^{-2}$ in December to $\sim 0.2\,\text{million}\,\text{km}^{-2}$ by March (Fitch and Moore 2007). Sea ice formation in the winter scavenges phytoplankton cells into the ice and concentrates iron from the surface water (de Baar *et al.* 1995; Boyd 2002; Lannuzel *et al.* 2010, 2016). In the spring, low salinity, high iron melt water is released from the sea ice, creating a buoyant layer of fresher water that traps phytoplankton in an environment where conditions are ideal for growth (high light, and high macro- and micronutrients). This fosters large phytoplankton blooms (Fig. 1.7A) (Smith and Nelson 1986; Sullivan *et al.* 1988), which can reach biomasses of over $200\,\text{mg Chl}\,a\,\text{m}^{-2}$ (e.g. Smith and Nelson 1986; Nelson *et al.* 1987; Wright *et al.* 2010). The region was thought to house very high rates of productivity ($\sim 400\,\text{Tg C}\,\text{yr}^{-1}$) (Smith *et al.* 1988; Arrigo *et al.* 1998a) and

contribute 40-50% of the productivity of the entire SO (Smith and Nelson 1986; Sakshaug 1994). Advances in satellite technology and modeling algorithms provide more conservative results (Arrigo *et al.* 2008a; Taylor *et al.* 2013), suggesting the MIZ contributes $\sim$114 Tg C yr^{-1}. This equates to a total annual productivity of 54–68 g C m^{-2} yr^{-1}, which is $\sim$5 times that in the sea ice ($\sim$24 Tg C yr^{-1}) but is similar to that in the POOZ ($\sim$62 g C m^{-2} yr^{-1}) (Moore and Abbott 2000; Arrigo *et al.* 2008a; Saenz and Arrigo 2014).

A diverse array of phytoplankton inhabit the MIZ, undergoing successional change due to ice retreat, warming, nutrient depletion, and grazing (Davidson *et al.* 2010; Wright *et al.* 2010). Phytoplankton blooms in East Antarctica and the Weddell Sea, are commonly co-dominated by the colonial life-stage of *Phaeocystis* sp. and diatoms, with increasing diatom abundance over time and the appearance of dinoflagellates, silicoflagellates, and heterotrophic protists later in the season (Waters *et al.* 2000; Kang *et al.* 2001; Davidson *et al.* 2010). Once the available iron has been exhausted, the community shifts to one more typical of the POOZ, consisting of small diatoms and flagellates (Pearce *et al.* 2010; Wright *et al.* 2010). In the WAP, diatom-dominated blooms in the spring shift to flagellate communities as melting sea ice and glacial run-off reduce the salinity of surface waters (Kang *et al.* 2001). However, icebergs released by the breakup of ice shelves will increase nutrient input, as in the POOZ (see above, Duprat *et al.* 2016), promoting additional blooms of large diatoms.

Phytoplankton in the MIZ can contribute directly or indirectly to vertical flux. During large blooms phytoplankton aggregate to form marine snow, which fall rapidly through the water column, contributing to carbon sequestration into the deep ocean (Alldredge and Silver 1988). High algal biomass within decaying sea ice in summer is also a rich source of nutrition and a site of reproduction for grazers (Schnack-Schiel *et al.* 1998; Thomas *et al.* 1998). This grazing transfers carbon to higher trophic levels but can also contribute to vertical carbon flux by reparceling cells into rapidly sinking faecal pellets (Cadée *et al.* 1992; Burkill *et al.* 1995; Perissinotto and Pakhomov 1998; Pearce *et al.* 2010).

Climate change is predicted to decrease SIE, increase icebergs, and cause SAM-induced increases in wind and wave action (Fig. 1.7B). The effect of decreased SIE on total annual productivity in the SO may not be large. Reduced SIE would shift the latitudinal range of the

MIZ southward, resulting in an increase in the area of the POOZ (Smetacek and Nicol 2005). However, the restriction of intense primary productivity in the MIZ to the spring-summer season results in area-normalised annual primary production similar to that of the POOZ (see above, Moore and Abbott 2000; Arrigo *et al.* 2008a), suggesting that an increase in the size of the POOZ may not significantly affect total SO productivity (Arrigo *et al.* 2008a). Admittedly, this does not take into account other potential effects of climate change on the POOZ (see above), nor does it consider the effect of the absence of ice on the timing and magnitude of the phytoplankton bloom. It is likely that blooms would start earlier due to the higher light climate but may develop slower due to greater mixed depths (see below) and the lack of iron fertilization from the ice melt (Behrenfeld *et al.* 2006).

The most profound change in the MIZ may be caused by the increasingly positive phase of SAM. The poleward shift and intensification of wind strength and storms is predicted to deepen the mixed layer and reduce phytoplankton production in the MIZ (Fig. 1.7B) (Lovenduski and Gruber 2005; Yin 2005; Hemer *et al.* 2010; Massom and Stammerjohn 2010; Young *et al.* 2011; Dobrynin *et al.* 2012)). Phytoplankton blooms in the MIZ are patchy in space and time (Smith and Nelson 1986). They generally occur in shallow mixed layers where wind speeds are $<5\,\mathrm{m\,s^{-1}}$ (Fitch and Moore 2007). Storms, wind mixing, and waves deepen mixed depths in the MIZ, reducing the light availability and inhibiting bloom development (Fig. 1.7B) (Venables and Meredith 2014). As a result, blooms only cover 17-24% of the MIZ over summer with maximum coverage of only 0.36 million $\mathrm{km^{-2}}$ in December (Savidge *et al.* 1996; Fitch and Moore 2007). Evidence from culture studies and blooms in the Ross Sea indicate that *Phaeocystis* sp. is more tolerant of deeply mixed, low light environments than diatoms (Arrigo *et al.* 1999; Moisan and Mitchell 1999). Therefore, a more deeply mixed MIZ could cause a shift toward *Phaeocystis* sp. dominated blooms.

Large, early season blooms of *Phaeocystis* sp. can be responsible for substantial carbon export, rapidly sinking from surface waters and avoiding grazing pressure. *Phaeocystis* sp. colonies are encased in a tough outer coating, providing an effective defense against grazing protozoa and small zooplankton (Smetacek *et al.* 2004). In combination with their ability to draw down larger amounts of CO_2 than diatoms (Arrigo *et al.* 2000), it is likely that an increase in blooms dominated by *Phaeocystis* sp. may enhance carbon export in the MIZ (DiTullio *et al.* 2000). *Phaeocystis* sp. are also responsible for generating large amounts of DMSP (DiTullio and Smith 1995; Turner *et al.*

1995; Vance *et al.* 2013). If increased mixing favours *Phaeocystis* sp. growth, it may counteract some of the loss of DMSP from decreased SIE in the SSIZ (see SSIZ above).

An increase in wind and wave action could also potentially increase the area of the MIZ by increasing the breakup and dispersal of sea ice by waves (Yin 2005; Hemer *et al.* 2010; Young *et al.* 2011; Dobrynin *et al.* 2012; Stroeve *et al.* 2016). In spring and summer, large waves propagate through the sea ice up to 200 km, breaking up ice floes and accelerating ice retreat (Kohout *et al.* 2014; Horvat *et al.* 2016). Some satellite derived estimates of the MIZ region suggest a positive trend in MIZ area over time during spring (Stroeve *et al.* 2016), although not all models agree due to difficulties in accurately mapping the MIZ from satellite images (Ackley *et al.* 2003). However, changes in MIZ area are not likely to be uniform within the SSIZ, with Massom *et al.* (2006) reporting a contraction of the MIZ in the WAP due to strong northerly winds from the ASL (see SSIZ above). Interestingly, intense phytoplankton blooms still occurred amongst in the slurry of frazil ice between floes in this region (Massom *et al.* 2006), suggesting MIZ size is not necessarily a good indicator of its productivity.

Bloom formation within the MIZ is reliant on the coincidence of optimal conditions for phytoplankton growth. Increases in turbulent mixing by wind and waves would decrease light availability through a deepened mixed layer, with likely reductions in productivity and changes in the phytoplankton community structure within MIZ blooms. Additional nutrient inputs from melting icebergs are likely to cause localised increases in productivity but the extent of this effect would be felt most in the SSIZ, where growth of phytoplankton has drawn down nutrient concentrations. The net effect of future increases in MIZ area and decline in overall SIE remain uncertain.

1.6 Antarctic continental shelf zone

Antarctic Continental Shelf Zone (CZ) waters make up the smallest area of the SO ($1.28\,\text{million}\,\text{km}^{-2}$) but they are also highly productive, contributing $66.1\,\text{Tg}\,\text{C}\,\text{yr}^{-1}$ or an average of $460\,\text{mgC/m}^2\text{/d}]$ (Arrigo *et al.* 2008a). The high productivity in this region is due to high surface nutrient concentrations; iron enrichment from coastal sediments and basal shelf

melt; and upwelled upper circumpolar deep water (UCDW, Fig. 1.3) onto the continental shelf from the easterly-flowing Antarctic Slope Current, which approximately follows the 1000 m isobath (Fig. 1.2) (Jacobs 1991; Smetacek and Nicol 2005; Westwood *et al.* 2010; Williams *et al.* 2010). Blooms in CZ waters make a vital contribution to supporting the abundance and diversity of life in Antarctica. They attract large numbers of grazers that consume phytoplankton, that in turn feed higher tropic levels, while also producing faecal pellets, that are either remineralised into nutrients by heterotrophic microbes or sink rapidly into deep water, supporting the biological pump (Cadée *et al.* 1992; Turner 2002; Honjo 2004; Schnack-Schiel and Isla 2005). Open water regions over the CZ are important foraging areas for many Antarctic species, especially during the summer breeding season (Arrigo and van Dijken 2003; Smith *et al.* 2007; Stroeve *et al.* 2016). For example, DMS released from grazed phytoplankton acts as an olfactory foraging cue for white-chinned petrels (Nevitt *et al.* 1995) and Adélie penguin breeding success has been related to the proximity of colonies to open water (Ainley *et al.* 1998). The CZ is also a significant CO_2 sink over the summer as high rates of primary productivity cause surface CO_2 undersaturation (Hoppema *et al.* 1995; Gibson and Trull 1999; Ducklow *et al.* 2007; Arrigo *et al.* 2008b; Roden *et al.* 2013).

Polynyas contribute to high productivity over the CZ with average annual primary production rates up to $105.4\,\mathrm{g\,C\,m^{-2}\,yr^{-1}}$ (Arrigo and van Dijken 2003; Arrigo *et al.* 2015). Strong, cold katabatic winds freeze the surface water of the polynya, creating ice that is pushed north, adding to the seasonal sea ice extent and contributing to the generation of Antarctic Bottom Water through exclusion of high salinity brine by sea ice as it forms (Orsi *et al.* 1999). The Ross Sea polynya is the largest and the most productive polynya in Antarctica, contributing on average, $22.2\,\mathrm{Tg\,C\,yr^{-1}}$ (Arrigo *et al.* 2015), with daily production as high as $6\,\mathrm{g\,C\,m^{-2}\,d^{-1}}$ (Smith and Gordon 1997). These high productivity rates are likely due to substantial iron input from upwelling of underlying sediments and basal melt of nearby ice shelves (Arrigo *et al.* 2015). Future increases in sea surface temperature are likely to accelerate the melting of ice shelves, increasing the input of fresh, stratified, iron-rich water to polynyas. increasing productivity in these regions (Feng *et al.* 2010).

Spatial differences in the factors controlling phytoplankton production have been observed within CZ waters. Consequently, the cause and rate of climate-induced change in these waters

differs with location. Substantial differences have already been observed between East and West Antarctica (Turner *et al.* 2014 and refs. therein) and as such, we separately address the effects climate change on the phytoplankton communities in each of these two regions.

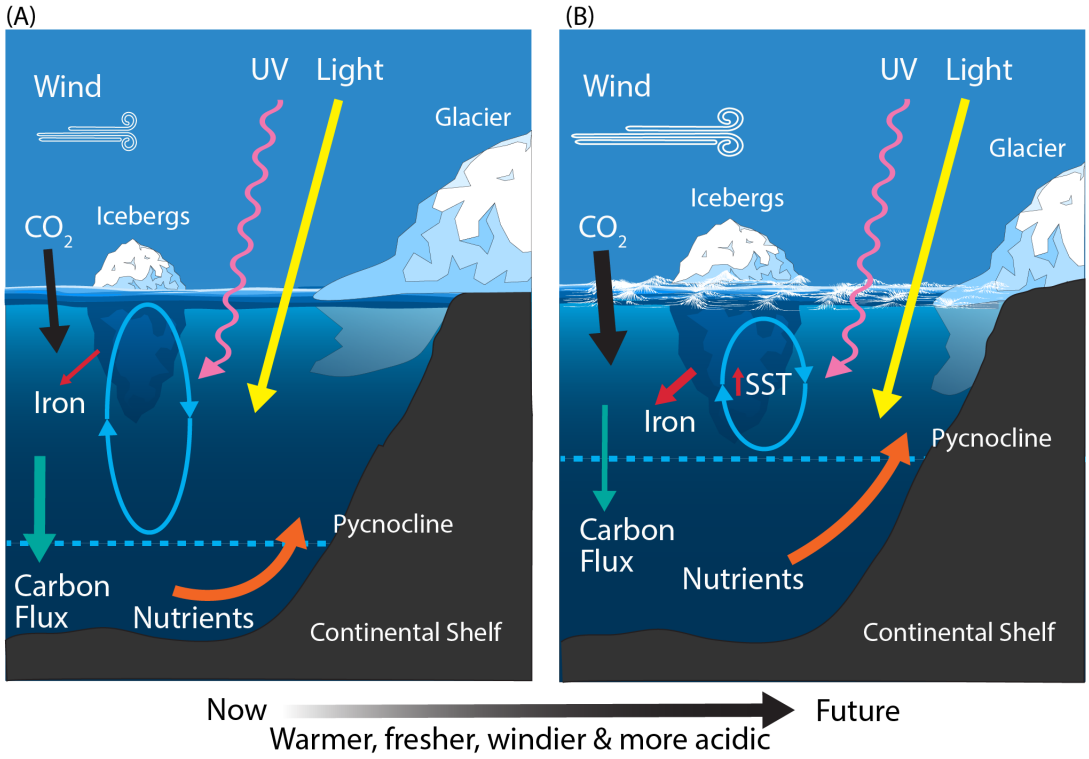

Figure 1.8: Schematic showing the primary physical constraints on phytoplankton in the Antarctic Continental Shelf Zone (CZ) (A) before and (B) after climate change. Ovals represent the depth of mixing and arrow thickness reflects relative rates of flux. SST, sea surface temperature.

1.6.1 West Antarctica

The West Antarctic CZ spans from the Amundsen and Bellingshausen Seas in the west to the Weddell Sea in the east and is dominated by the Antarctic Peninsula. Productivity is highest along the WAP and the Weddell Sea with rates of over 600 mg C m^{-2} d^{-1} during the peak of summer (El-Sayed and Taguchi 1981; Arrigo *et al.* 2008a; Vernet *et al.* 2008). The flow of warm, nutrient-rich UCDW onto the continental shelf (Fig. 1.3) in the WAP accelerates sea ice retreat and enhances phytoplankton productivity (Kavanaugh *et al.* 2015), fostering diatom blooms as in the MIZ (see above). These are replaced by small flagellate and cryptophyte communities in the fresher, more stratified surface water later in the season (Moline *et al.* 2004; Ducklow *et al.* 2007). High production in the WAP and Scotia Sea support abundant krill populations, which are

in turn food for a wealth of higher predators (Ducklow *et al.* 2007 and refs. therein).

Climate change threats to the West Antarctic CZ include warming, freshening, increased stratification, the melting and break up of glaciers and ice shelves, and ocean acidification (Fig. 1.8B). The WAP is one of the fastest warming regions on Earth with an increase in the mean atmospheric temperature of 2 °C (6 °C in the winter) since 1950 (Meredith and King 2005; Ducklow *et al.* 2007). No similar warming event has occurred on Earth in the last 1800 years (Vaughan *et al.* 2003). Along with atmospheric warming in the WAP, increased heat delivery of UCDW from the Antarctic Circumpolar Current onto the shelf has caused a 0.6 °C increase in temperature of the upper 300 m of the water column (Meredith and King 2005; Turner *et al.* 2014). This warming trend has resulted in increased glacial melt, with 87% of glaciers in the Antarctic Peninsula showing signs of retreat since 1950 (Cook *et al.* 2005; Peck *et al.* 2010). Glacial melt has resulted in an influx of fresh water to coastal regions of the WAP, freshening and increasing the stratification of surface waters over the summer. While phytoplankton productivity is expected to increase with increasing sea surface temperature (Rose *et al.* 2009a), the phytoplankton community is likely to be more affected by resultant changes in SIE and freshwater inputs to the CZ (Arrigo *et al.* 2015; Moreau *et al.* 2015).

Freshening of surface waters from glacial melt has led to a documented change in the phytoplankton community in the WAP from diatom-dominated assemblages to cryptophytes and small flagellates (Moline *et al.* 2004; Montes-Hugo *et al.* 2008). The resultant shift in size distribution from large to small phytoplankton cells has had a significant flow on effect to zooplankton grazers, particularly krill and salps (Moline *et al.* 2004). This region is historically an area of high krill abundance, which is the preferred food source for the many Antarctic birds and mammals that live in the WAP (Atkinson *et al.* 2004). Changes to the phytoplankton community structure, favouring small cells, negatively affects krill grazing as they feed most efficiently on cells >10 μm and are unable to capture particles <6 μm in size (Kawaguchi *et al.* 1999). This has caused a shift in dominance to salps, mucoid feeders that are unaffected by the particle size of their prey (Moline *et al.* 2004), and a shift toward a less efficient fish-based food web (Murphy *et al.* 2007). Reductions in the krill population in the WAP are expected have a significant negative effect on the food chain in this region (Ballerini *et al.* 2014).

Surface water freshening causes a concurrent stratification of the water column, elevating phytoplankton into shallow mixed layers with higher light intensity. Phytoplankton productivity is enhanced through increased light, however, excessive light and elevated UV-A and UV-B exposure can lead to photoinhibition and cell damage (see SAZ above, Moreau *et al.* 2015). In order to limit the damage of these conditions, phytoplankton can channel metabolic reserves into photoprotection and tolerance mechanisms (Davidson 2006). A lengthening of the open water season in the WAP, caused by earlier sea ice retreat (see SSIZ above), has increased productivity in the CZ, whilst also increasing photoinhibition rates (Moreau *et al.* 2015). Thus far, the increase in production is much greater than the loss due to photoinhibition so it is expected that increased stratification will lead to a net increase in primary productivity in the future (Moreau *et al.* 2015).

Stronger westerly winds, as a result of a positive SAM, are bringing warmer air across the Antarctic Peninsula, increasing snowfall and causing a break up of large ice shelves (e.g. Scambos *et al.* 2000; Rack and Rott 2004; Turner *et al.* 2014). The break up of the Larsen A ice shelf created new areas of high nutrient open water, stimulating phytoplankton blooms and increasing productivity in a previously ice-covered pelagic habitat (Bertolin and Schloss 2009). The continued retreat of glaciers and breaking up of ice shelves has led to the creation of new carbon sinks around the Antarctic Peninsula that have increased productivity up to $3.5\,\mathrm{Tg\,C\,m^{-2}\,yr^{-1}}$ (Peck *et al.* 2010). The continued break up of ice shelves will also lead to an increase in icebergs over the CZ. Melting icebergs have been found to provide a significant amount of iron and nutrients to surface waters, leading to increased phytoplankton productivity (Lin *et al.* 2011; Vernet *et al.* 2011; Duprat *et al.* 2016). Increased iceberg numbers will also contribute to increased productivity throughout the SSIZ and POOZ as they are propelled by ocean currents around Antarctica (see above).

Little work has investigated the effect of ocean acidification on phytoplankton in West Antarctic waters. The CO_2 concentration in waters over the West Antarctic CZ vary seasonally from ~176 to 503 µatm through to the uptake of CO_2 by phytoplankton in the summer and return to super-saturated levels in winter under the sea ice (Moreau *et al.* 2012). Coastal phytoplankton communities from the WAP (both diatom-dominated and mixed diatom-flagellate communities) displayed no significant change in community composition, cell size, or growth rate when exposed to 800 µatm CO_2 (Young *et al.* 2015). Yet, results of this study did demonstrate the

differences in physiological carbon uptake among phytoplankton species as production by diatoms may be enhanced by down-regulation of CCMs at high pCO_2, while a slight decline in production by *Phaeocystis* sp. was attributed to the alternative bicarbonate transport pathway used by this species.

1.6.2 East Antarctica

The East Antarctic CZ ranges from the Ross Sea in the east to the eastern edge of the Weddell Sea in the west. The Ross Sea is the most productive region in the CZ, contributing $\sim 24\,\mathrm{Tg\,C\,m^{-2}\,yr^{-1}}$ and accounting for ∼30% of the total annual production in shelf waters (Sweeney *et al.* 2000; Arrigo *et al.* 2008a). Iron and light availability are the dominant factors controlling growth of phytoplankton in the Ross Sea (Fig. 1.8A) (Smith *et al.* 2000b; Feng *et al.* 2010; Sedwick *et al.* 2011). In addition, the relative abundances of the dominant phytoplankton (diatoms and *Phaeocystis* sp.) are linked to mixed layer depth, with diatoms dominant in highly stratified water and *Phaeocystis* sp. where it is deeply mixed (Arrigo *et al.* 1999). These phytoplankton blooms support a unique food web in the Ross Sea, structured around the crystal krill, *Euphausia crystallorophias*, and the Antarctic silverfish, *Pleuragramma antarcticum* (Smith *et al.* 2007). Elsewhere around East Antarctica the CZ is relatively narrow and contributes $\sim 12\,\mathrm{Tg\,C\,m^{-2}\,yr^{-1}}$ (Arrigo *et al.* 2008a) and like the West Antarctic CZ, the Antarctic krill, *E. superba*, is a keystone species (Nicol *et al.* 2000; Nicol *et al.* 2010). Here the phytoplankton community is dominated by blooms of diatoms and *Phaeocystis* sp. during the summer and shifts to small flagellates once nutrients have been exhausted (Waters *et al.* 2000; Wright and van den Enden 2000; Davidson *et al.* 2010).

The East Antarctic CZ is expected to experience increased freshening, stratification, the melting and break up of glaciers and ice shelves, ocean acidification, and modest warming (Fig. 1.8B). In contrast to the warming trend around West Antarctica, there has been a measured cooling over East Antarctica for the same period (1969-2000) (Thompson and Solomon 2002). Despite this, most recent model projections for the Ross Sea by the end of the century predict a 0.15–0.4 °C increase in SST, with decreases in the mixed layer depth (∼50–70 m), sea ice concentration (2-11%), and macronutrient concentrations (Rickard and Behrens 2016).

Freshening has already been reported in the Ross Sea and has been attributed to changes in precipitation, sea ice production, and melting of the West Antarctic ice sheet (Jacobs *et al.* 2002). Projected changes to the remaining area of East Antarctica are not well understood but similar trends are anticipated (Watanabe *et al.* 2003; Convey *et al.* 2009; Gutt *et al.* 2015).

Ocean acidification is anticipated to affect polar waters sooner than the rest of the world, due to the increased solubility of CO_2 in cold water (Orr *et al.* 2005; McNeil and Matear 2008). Phytoplankton communities in Antarctic shelf waters are already exposed to strong annual variations in pCO_2 (Gibson and Trull 1999; Sweeney *et al.* 2000; Roden *et al.* 2013; Shadwick *et al.* 2013; Kapsenberg *et al.* 2015). Sea ice cover during the winter restricts air-sea gas transfer, allowing for CO_2 oversaturation of the water column (up to 450 µatm) through upwelling of high CO_2 UCDW water from the Antarctic Slope Current (Fig. 1.3). Photosynthetic drawdown over the summer can result in CO_2 levels falling below 100 µatm. This large seasonal variation seems to favour species that tolerate large fluctuations in pH. Phytoplankton communities have been observed to show little change in composition when grown at CO_2 concentrations similar to those already experienced in coastal environments (84–643 µatm) (Davidson *et al.* 2016). However, superimposing anthropogenic pCO_2 increase upon the large natural fluctuation already occurring in the natural environment may push some species past their limit sooner than anticipated (McNeil and Matear 2008), causing changes in phytoplankton productivity, growth and community composition. Concentrations of CO_2 exceeding 1000 µatm induced a change in phytoplankton community composition in Prydz Bay, increasing the abundance of small phytoplankton species (Davidson *et al.* 2016; Thomson *et al.* 2016). Studies on Ross Sea phytoplankton communities also suggest that high CO_2 concentrations (760–800 µatm) may cause a shift in dominance in this region from *Phaeocystis* sp. to large chain-forming diatom communities (Tortell *et al.* 2008a; Feng *et al.* 2010). Investigation into the physiological reasons for changes in growth rates link increased growth and carbon fixation to the energy saved through the down-regulation of CCMs (Rost *et al.* 2008; Tortell *et al.* 2008a), while inhibition of growth and productivity may be related to the metabolic costs of proton pumps to exclude hydrogen ions (Gao *et al.* 2012a; McMinn *et al.* 2014).

A change in phytoplankton community composition will likely have significant effects on carbon export in the CZ. A shift toward smaller cell communities will allow for increased remineralization

of cells through the microbial consumption, decreasing the downward flux of carbon into the deep ocean (Finkel *et al.* 2010 and refs. therein). These cells are also likely to be less efficiently grazed by zooplankton, resulting in less carbon transfer to higher trophic organisms. Any CO_2-induced increase in the dominance of diatoms in the Ross Sea may cause a decline in net carbon export as blooms of *Phaeocystis* sp. are capable of exporting more carbon than diatoms (Arrigo *et al.* 2000). However, diatom-dominated communities are likely to be grazed more than *Phaeocystis* sp., providing better nutrition for the Antarctic food web and also producing negatively buoyant faeces that can assist in the sinking of diatoms (Schnack-Schiel and Isla 2005).

Whilst most studies have focused on individual factors predicted to alter as a result of climate change, phytoplankton in the SO will be simultaneously exposed to multiple climate change stressors (Gutt *et al.* 2015). Recent work has focused on the interaction of multiple stressors on phytoplankton growth in the Ross Sea, highlighting the complex interaction between environmental changes and the phytoplankton community (Rose *et al.* 2009a; Feng *et al.* 2010; Xu *et al.* 2014; Zhu *et al.* 2016). Iron promotes phytoplankton growth, whereas interactive effects between iron, warming, increased CO_2, and light favour the dominance of diatoms over *Phaeocystis* sp. (Rose *et al.* 2009a; Xu *et al.* 2014; Zhu *et al.* 2016). In contrast, high pCO_2 only affected diatoms, favouring the growth of large centric species (Feng *et al.* 2010). As well as causing shifts in phytoplankton taxa, changes in temperature and iron supply caused modifications to microzooplankton abundance, suggesting possible changes in predator/prey interactions (Rose *et al.* 2009a). No multi-stressor experiments have yet been performed on other East Antarctic phytoplankton communities, though it appears likely that climate-induced change will alter the competitive interactions among dominant phytoplankton taxa and change trophodynamics throughout continental waters.

Freshening, increased stratification, ocean acidification, and the melting and break up of glaciers and ice shelves are all occurring across the Antarctic CZ due to climate change. Phytoplankton growth is promoted by freshening, increased stratification, and the break-up of ice shelves by establishing conditions that are optimal for growth, most notably an increase in iron supply and light availability. However, freshening and ocean acidification also appear to be responsible for shifts in community composition that could result in a decrease in food quality and availability for grazers. This could have a significant negative effect on the structure and function of the Antarctic

food web as well as reducing carbon export. In contrast, the proposed CO_2-induced increase in abundance of large diatoms in the Ross Sea may benefit the food web in this region but may still result in a decline in carbon export.

Temperature trends currently differ between East and West Antarctica, with significant warming in West Antarctica and a slight cooling trend over East Antarctica. Increases in temperature appear to promote phytoplankton growth and may accelerate sea ice retreat, changing the timing and magnitude of bloom onset in this highly productive region. However, the interactive effects that this combination of climate stressors will have on phytoplankton communities in this region is not well understood. Further work will be required before we can fully understand how phytoplankton over the CZ will be affected by a changing climate.

1.7 Conclusion

The SO comprises a vast expanse of ocean containing a diverse array of environments, each of which exposing phytoplankton to environmental factors that limit their production, growth, survival, and composition. Despite these stressors, phytoplankton thrive in some of the most extreme conditions on earth. Climate-induced changes in the physical characteristics of the SO and the responses by phytoplankton differ substantially among environments. No long-term trends in satellite-derived Chl *a* or primary productivity are yet detectable due to the large background of interannual/decadal variability (Henson *et al.* 2010; Gregg and Rousseaux 2014). It is unlikely that unambiguous trends due to climate change will be seen until approximately 2055 (Henson *et al.* 2010). However, some longer time series of underway Chl *a* measurements exist that could indicate climate-induced trends (see below).

Given the competing influences on phytoplankton within each region of the SO, predictions are bound to be tentative and contentious. Our assessment of the available information suggest the responses of phytoplankton in various regions of the SO are:

- In the SAZ, the stratification-induced decline in nutrient supply to surface waters (Fig. 1.4) will reduce productivity and favour small flagellates (e.g. Matear and Hirst 1999; Marinov *et al.* 2010; Petrou *et al.* 2016). Boyd *et al.* (2016a) indicates that increases in iron and

temperature may double growth rates and favour diatoms but such events depend on the frequency and magnitude of storms to deposit dust in the SAZ and the proximity to land.

- In the POOZ, productivity may increase due to enhanced mixing, eddy activity, and nutrient supply from upwelling and melting icebergs (Fig. 1.6). Yet, light limitation imposed by a deepened mixed layer and increased cloud cover may limit this potential increase (Armour *et al.* 2016).

- In the SSIZ, ice algal abundance is likely to decrease through a decline in SIE, thickness, and duration (Fig. 1.7). The absence of sea ice will preclude ice algae providing an essential food source over winter for some zooplankton species. This has the potential to cause significant changes throughout the Antarctic food web. The decline of sea ice as a result of ocean warming may not markedly alter the annual SO productivity but the expansion of the POOZ into the SSIZ is likely to alter the timing, magnitude, and duration of the phytoplankton blooms in these waters.

- In the MIZ, increased wind and wave action is likely to accelerate sea ice retreat, increasing the mixed layer depth and destabilizing the seasonal progression of phytoplankton blooms (Fig. 1.7). Such changes would reduce the frequency of ice edge blooms and cause taxonomic shifts in the phytoplankton community toward small diatoms and flagellates.

- In the CZ, the few available studies suggest that warming, freshening, and ocean acidification are likely to elicit changes to community composition (Fig. 1.8), with reports of a shift towards communities composed of smaller cells and flagellates (Moline *et al.* 2004; Davidson *et al.* 2016). Increased nutrients and stratification from melting glaciers and icebergs are likely to increase productivity (Fig. 1.8). Localised shifts in community composition in the Ross Sea toward diatom-dominated communities will potentially decrease carbon export but may provide better nutrition for higher trophic levels.

These changes are likely to have a significant effect on the biogeochemical processes in the SO, affecting the biological pump, microbial loop, and nutrition for higher trophic levels. It is likely that the effect of climate change on phytoplankton in each of these regions is going to be

determined by the timing, rate, and magnitude of change in each stressor; as well as the sequence in which these stressors are imposed. Climate change models of the SO still contain large uncertainties, in part due to knowledge gaps in biogeochemical processes and carbon uptake (Frölicher *et al.* 2016). The vast majority of phytoplankton research in the SO have been observational studies, providing essential data on phytoplankton communities, seasonal community succession, nutrient utilization, primary and export production, and food web interactions (e.g. El-Sayed 1994; Nicol *et al.* 2000; Smith *et al.* 2000a; Nicol *et al.* 2010; Olguín and Alder 2011; Quéguiner 2013). These studies are essential for our understanding of the current and potential future state of SO phytoplankton. Relatively few studies have focused on the manipulation of climate stressors on SO phytoplankton species/communities (e.g. Tortell *et al.* 2008a; Rose *et al.* 2009a; Hoppe *et al.* 2013; Müller *et al.* 2015; Boyd *et al.* 2016a; Coad *et al.* 2016; Davidson *et al.* 2016). More of these studies are necessary in all of the regions of the SO to determine the thresholds for climate-induced stressors on phytoplankton communities. It is also important to perform multi-stressor experiments, incorporating a range of environmental factors affected by climate change, if we are to understand the interactive effects (from synergistic to antagonistic) of future stressors on phytoplankton species and communities (e.g. Feng *et al.* 2010; Xu *et al.* 2014; Boyd *et al.* 2016a; Zhu *et al.* 2016).

The vastness and environmental diversity of the SO; the inherent spatial and temporal variability in phytoplankton communities; and the logistical costs and difficulty in obtaining data from the SO, especially year-round observations, means the effect of climate change on phytoplankton in this region is poorly understood. In some instances, advances in remote sensing technology and computer modeling have allowed access to data sets that can assist in understanding trends. However, they are still limited in their ability to detect some physical changes, such as sea ice thickness and Chl *a* concentration in waters covered by ice (Massom *et al.* 2006; Hobbs *et al.* 2016). There are very few places that have long-term monitoring programs to detect changes in the physical and biological environment (such as the Palmer-Long Term Ecological Research program, Smith *et al.* 1995) and few of these have collected data for a sufficient duration to detect trends in phytoplankton against the background of natural variation. Decades long monitoring programs should be established as a matter of urgency to detect changes in SO phytoplankton abundance, production, and composition.

Stratospheric ozone concentrations exert a pervasive effect on atmospheric circulation in the Southern Hemisphere and recovery of the ozone hole will change the trajectory of climate. Concern over ozone depletion and the consequent rise in short wave UV radiation reaching the Earth's surface, galvanised the international community, culminating in the Montreal protocol, which banned the use of ozone depleting substances, such as chlorofluorocarbons (CFCs) and halons. Unrecognised at the time, ozone depletion was also the primary cause of increases in the positive phase of the SAM, resulting in the acceleration and poleward shift of westerly winds over the SO (see POOZ above, Polvani *et al.* 2011; Thompson *et al.* 2011). This proved to be the most obvious and persistent characteristic of Southern Hemisphere climate change in the last half century (Thompson and Wallace 2000; Polvani *et al.* 2011). Modeling studies indicate that recovery of the ozone hole will decelerate the westerly winds (Son *et al.* 2008) and result in a more rapid rise in Antarctic temperatures than elsewhere in the Southern Hemisphere (Shindell and Schmidt 2004). Nearly 30 years after the Montreal protocol came into effect, the first signs are emerging that the ozone hole is beginning to heal (Solomon *et al.* 2016). Projections suggest that ozone concentrations in the stratosphere are likely to return to pre-ozone hole values around 2065 (Son *et al.* 2008; Schiermeier 2009). Thus, the main factor presently driving climate change and phytoplankton responses over much of the SO will decline over the next half century. Ozone depletion and positive SAM cause increases in wind and wave action, deeper mixing, and increased nutrient entrainment into surface waters (see POOZ, SSIZ, MIZ above). Replenishment of ozone is likely to reverse these climate-induced drivers of phytoplankton dynamics in Antarctic waters, moving to a scenario reminiscent of the SAZ region and dominated by increased warming, stratification, and declining nutrient availability in surface waters. The effect of this reversal in climate fortunes is unknown but the rate of change ($\sim$50 years) may prove too fast for some species to adapt and/or evolve to the changing environment.

The response of phytoplankton to anticipated future environmental conditions in the SO will eventually depend upon their capacity to adapt and evolve (Boyd *et al.* 2016a and refs. therein). Phytoplankton communities have short generation times and high genetic diversity, which allow for adaptation to changing environmental conditions through natural selection (Collins *et al.* 2014). Some SO phytoplankton communities are already exposed to large variations in their environment, such as sea ice and coastal communities. Phytoplankton that are already exposed

to large variations in their environment are considered inherently more tolerant and capable of adapting to future changes (Sackett *et al.* 2013; Schaum and Collins 2014). Davidson *et al.* (2016) showed that exposing natural microbial communities to the large range in CO_2 concentrations they encounter in nature over a year had little effect. Concentrations above this reduced productivity and changed the composition of the phytoplankton community, suggesting that their tolerance to variability outside of those normally encountered was low. Furthermore current experiments, which determine the tolerance limits of phytoplankton over short time scales, may not be a good indicator of long-term resilience as the metabolic costs of climate-induced stress may not be sustainable over numerous generations (Schaum and Collins 2014; Torstensson *et al.* 2015). It is currently unknown whether the rate of environmental change will outpace the ability of SO phytoplankton to adapt and/or evolve. It is, however, inevitable that changes at the base of the SO will influence trophodynamics, biogeochemistry, and climate change.

Chapter 2

Ocean acidification of a coastal Antarctic marine microbial community reveals a critical threshold for CO_2 tolerance in phytoplankton productivity

Stacy Deppeler[1], Katherina Petrou[2], Kai G. Schulz[3], Karen Westwood[4,5], Imojen Pearce[4], John McKinlay[4] and Andrew Davidson[4,5]

[1]Institute for Marine and Antarctic Studies, University of Tasmania, Hobart, Tasmania, Australia
[2]School of Life Sciences, University of Technology Sydney, Ultimo, New South Wales, Australia
[3]Centre for Coastal Biogeochemistry, Southern Cross University, East Lismore, New South Wales, Australia
[4]Australian Antarctic Division, Department of the Environment and Energy, Kingston, Tasmania, Australia
[5]Antarctic Climate and Ecosystems Cooperative Research Centre, Hobart, Tasmania, Australia

This chapter has been published as: Deppeler, S., Petrou, K., Schulz, K. G., Westwood, K., Pearce, I., McKinlay, J., and Davidson, A. (2018). Ocean acidification of a coastal Antarctic marine microbial community reveals a critical threshold for CO_2 tolerance in phytoplankton productivity. *Biogeosciences*, 15 (1):209–231. doi:10.5194/bg-15-209-2018. A copy of the published article is provided in Appendix B.

2.1 Introduction

The Southern Ocean (SO) is a significant sink for anthropogenic CO_2 (Metzl *et al.* 1999; Sabine 2004; Frölicher *et al.* 2015). Approximately 30% of anthropogenic CO_2 emissions have been absorbed by the world's oceans, of which 40% has been via the SO (Raven and Falkowski 1999; Sabine 2004; Khatiwala *et al.* 2009; Takahashi *et al.* 2009, 2012; Frölicher *et al.* 2015). While ameliorating CO_2 accumulation in the atmosphere, increasing oceanic CO_2 uptake alters the chemical balance of surface waters, with the average pH having already decreased by 0.1 units since pre-industrial times (Sabine 2004; Raven *et al.* 2005). If anthropogenic emissions continue unabated, future concentrations of CO_2 in the atmosphere are projected to reach ∼930 µatm by 2100 and peak at ∼2000 µatm by 2250 (Meinshausen *et al.* 2011; IPCC 2013). This will result in a further reduction of the surface ocean pH by up to 0.6 pH units, with unknown consequences for the marine microbial community (Caldeira and Wickett 2003). High-latitude oceans have been identified as amongst the first regions to experience the negative effects of ocean acidification, causing potentially harmful reductions in the aragonite saturation state and a decline in the ocean's capacity for future CO_2 uptake (Sabine 2004; Orr *et al.* 2005; McNeil and Matear 2008; Fabry *et al.* 2009; Hauck and Völker 2015). Marine microbes play a pivotal role in the uptake and storage of CO_2 in the ocean through phytoplankton photosynthesis and the vertical transport of biological carbon to the deep ocean (Longhurst 1991; Honjo 2004). As the buffering capacity of the SO decreases over time, the biological contribution to total CO_2 uptake is expected to increase in importance (Hauck and Völker 2015; Hauck *et al.* 2015). Thus, it is necessary to understand the effects of high CO_2 on the productivity of the marine microbial community if we are to predict how they may affect ocean biogeochemistry in the future.

Phytoplankton primary production provides the food source for higher trophic levels and plays a critical role in the sequestration of carbon from the atmosphere into the deep ocean (Azam *et al.* 1983; Azam *et al.* 1991; Longhurst 1991; Honjo 2004; Fenchel 2008; Kirchman 2008). In Antarctic waters it is restricted to a short summer season and is characterised by intense phytoplankton blooms that can reach over 200 mg Chl $a\,m^{-2}$ (Smith and Nelson 1986; Nelson *et al.* 1987; Wright *et al.* 2010). Relative to elsewhere in the SO, the continental shelf around Antarctica accounts for a disproportionately high percentage of annual primary productivity

(Arrigo *et al.* 2008a). In coastal Antarctic waters, seasonal CO_2 variability can be up to 450 µatm over a year (Gibson and Trull 1999; Boyd *et al.* 2008; Moreau *et al.* 2012; Roden *et al.* 2013; Tortell *et al.* 2014). Sea ice forms a barrier to the outgassing of CO_2 in winter, causing supersaturation of the surface water to ∼500 µatm. Intense primary productivity in summer rapidly draws down CO_2 to <100 µatm, making this region a significant CO_2 sink during summer months (Hoppema *et al.* 1995; Ducklow *et al.* 2007; Arrigo *et al.* 2008b).

Ocean acidification studies on individual phytoplankton species have reported differing trends in primary productivity and growth rates. Increased CO_2 enhanced rates of primary productivity (Wu *et al.* 2010; Trimborn *et al.* 2013) and growth (Sobrino *et al.* 2008; Tew *et al.* 2014; Baragi *et al.* 2015; Chen *et al.* 2015; King *et al.* 2015) in some diatom species, while others were unaffected (Chen and Durbin 1994; Sobrino *et al.* 2008; Berge *et al.* 2010; Trimborn *et al.* 2013; Chen *et al.* 2015; Hoppe *et al.* 2015; King *et al.* 2015; Bi *et al.* 2017). In contrast, CO_2-related declines in primary productivity and growth rate have also been observed (Barcelos e Ramos *et al.* 2014; Hoppe *et al.* 2015; King *et al.* 2015; Shi *et al.* 2017), suggesting that responses to ocean acidification are largely species specific. These differing responses among phytoplankton species may also cause changes in the composition of phytoplankton communities (Trimborn *et al.* 2013). It is difficult to extrapolate the response of individual species to natural communities, as monospecific studies exclude interactions among species and trophic levels. Estimates of CO_2 tolerance under laboratory conditions may also be influenced by experimental acclimation periods (Trimborn *et al.* 2014; Hennon *et al.* 2015; Torstensson *et al.* 2015; Li *et al.* 2017a), differences in experimental conditions (e.g. nutrients, light climate) (Hoppe *et al.* 2015; Hong *et al.* 2017; Li *et al.* 2017b), methods of CO_2 manipulation (Shi *et al.* 2009; Gattuso *et al.* 2010), and region-specific environmental adaptations (Schaum *et al.* 2012). Thus, investigations on natural communities are essential in order to better understand the outcome of these complex interactions.

The effects of ocean acidification on natural Antarctic phytoplankton communities is currently not well understood (Petrou *et al.* 2016; Deppeler and Davidson 2017). Tolerance to CO_2 levels up to ∼800 µatm have been reported for natural coastal communities in the West Antarctic Peninsula and Prydz Bay, East Antarctica (Young *et al.* 2015; Davidson *et al.* 2016). Although in Prydz Bay, when CO_2 levels exceeded 780 µatm, primary productivity declined and community

composition shifted toward smaller, picoeukaryotes (Davidson *et al.* 2016; Thomson *et al.* 2016; Westwood *et al.* 2018). In contrast, Ross Sea phytoplankton communities responded to CO_2 levels $\geq$750 µatm with an increase in primary productivity and abundance of large chain-forming diatoms, suggesting that as CO_2 increases in this region, diatoms may increase in dominance over the prymnesiophyte *Phaeocystis antarctica* (Tortell *et al.* 2008a; Feng *et al.* 2010). The paucity of information regarding the ocean acidification response of these Antarctic coastal phytoplankton communities highlights the need for further research to determine region-specific tolerances and potential tipping points in community productivity and composition in Antarctica.

Bacteria play an essential role in the microbial food web through the remineralisation of nutrients from sinking particles (Azam *et al.* 1991) and as a food source for heterotrophic nanoflagellates (Pearce *et al.* 2010). Bacterial populations respond to increases in phytoplankton primary productivity by increasing their productivity and abundance, with maximum abundance often occurring after the peak of the phytoplankton bloom (Pearce *et al.* 2007). High CO_2 levels have been observed to have either no effect on abundance and productivity (Grossart *et al.* 2006; Allgaier *et al.* 2008; Paulino *et al.* 2008; Baragi *et al.* 2015; Wang *et al.* 2016) or increase growth rate and production only during the post-bloom phase of an experiment (Grossart *et al.* 2006; Sperling *et al.* 2013; Westwood *et al.* 2018). Thus, bacterial communities appear to be relatively tolerant to ocean acidification, with bacterial growth indirectly affected by the ocean acidification responses of the phytoplankton community (Grossart *et al.* 2006; Allgaier *et al.* 2008; Engel *et al.* 2013; Piontek *et al.* 2013; Sperling *et al.* 2013; Bergen *et al.* 2016).

Mesocosm experiments are an effective way of monitoring the community response of microbial assemblages to environmental changes. Experiments examining multiple species and trophic levels can provide responses that differ significantly from monospecific studies. Numerous mesocosm studies have now been performed to assess the effect of ocean acidification on natural marine microbial communities around the world (e.g. Kim *et al.* 2006; Hopkinson *et al.* 2010; Riebesell *et al.* 2013; Paul *et al.* 2015; Bach *et al.* 2016; Bunse *et al.* 2016). Studies in the Arctic reported increases in phytoplankton primary productivity, growth, and organic matter concentration at CO_2 levels $\geq$800 µatm under nutrient-replete conditions (Bellerby *et al.* 2008;

Egge *et al.* 2009; Engel *et al.* 2013; Schulz *et al.* 2013), whilst the bacterial community was unaffected (Grossart *et al.* 2006; Allgaier *et al.* 2008; Paulino *et al.* 2008; Baragi *et al.* 2015). These studies also highlight the importance of nutrient availability in the community response to elevated CO_2, with substantial differences in primary and bacterial productivity, chlorophyll *a* (Chl *a*), and elemental stoichiometry observed between nutrient-replete and nutrient-limited conditions (Riebesell *et al.* 2013; Schulz *et al.* 2013; Sperling *et al.* 2013; Bach *et al.* 2016).

Previous community-level studies investigating the effects of ocean acidification on natural coastal marine microbial communities in East Antarctica reported declines in primary and bacterial productivity when CO_2 levels exceeded 780 µatm (Westwood *et al.* 2018). To build upon the results of Westwood *et al.* (2018), a similar experimental design was utilised, with a natural marine microbial community from the same region exposed to CO_2 levels ranging from 343 to 1641 µatm in 650 L minicosms. The methods were refined in our study to include an acclimation period to the CO_2 treatment under low light. Rates of primary productivity, bacterial productivity, and the accumulation of particulate organic matter (POM) were examined to ascertain whether the threshold for tolerance to CO_2 was similar to that reported by Westwood *et al.* (2018) or if acclimation affected the community response to high CO_2. Photophysiological measurements were also undertaken to assess underlying mechanisms that caused shifts in phytoplankton community productivity.

2.2 Methods

2.2.1 Minicosm set-up

Natural microbial assemblages were incubated in six 650 L polythene tanks (minicosms) housed in a temperature-controlled shipping container (Fig. 2.1). All minicosms were acid washed with 10% vol:vol AR HCl, thoroughly rinsed with MilliQ water, and given a final rinse with seawater from the sampling site before use. The minicosms were filled with seawater taken amongst decomposing fast ice in Prydz Bay, at Davis Station, Antarctica (68° 35′S 77° 58′E) on 19th November, 2014. Water was transferred by helicopter in multiple collections using a 720 L Bambi Bucket to fill a 7000 L polypropylene holding tank. Seawater was gravity fed into the

minicosm tanks through Teflon-lined hosing fitted with an in-line 200 µmol Arkal filter to exclude metazooplankton. All minicosms were filled simultaneously to ensure uniform distribution of microbes in all tanks.

Figure 2.1: Minicosm tanks filled with seawater in temperature-controlled shipping container.

The ambient water temperature at the time of sampling in Prydz Bay was −1.0 °C. Tanks were temperature controlled to an average temperature of 0.0 °C, with a maximum range of ±0.5 °C, through cooling of the shipping container and warming with two 300 W aquarium heaters (Fluval) that were connected to a temperature control program via Carel temperature controllers. The contents of each tank were gently mixed by a shielded high-density polyethylene auger, rotating at 15 rpm, and each tank was covered with a sealed acrylic lid.

Each tank was illuminated on a 19:5 h light:dark cycle by two 150 W HQI-TS/NDL (Osram) metal halide lamps (transmission spectra: Deppeler *et al.* 2018a). The light output was filtered by a light-scattering filter and a one-quarter colour temperature (CT) blue filter (Arri) to convert the tungsten lighting to a daylight spectral distribution; attenuating wavelengths <500 nm by ∼20% and >550 nm by ∼40% (Davidson *et al.* 2016).

Similar to Schulz *et al.* (2017) the fugacity of carbon dioxide (fCO_2) in each tank was raised to the target concentration in a stepwise manner over the first 5 days of the incubation (Fig. 2.2, see below). During this acclimation, phytoplankton growth in the tanks was slowed by attenuating the light intensity to 0.9 ± 0.2 µmol photons m^{-2} s^{-1} using two 90% neutral density (ND) filters (Arri).

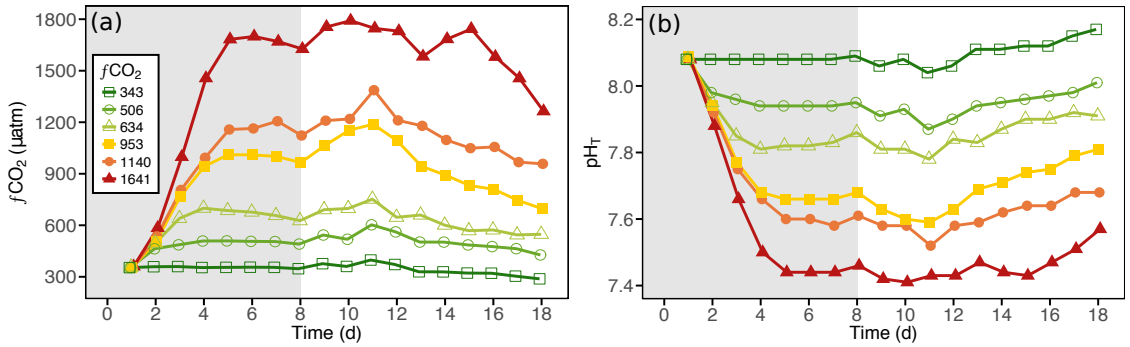

Figure 2.2: The (a) fugacity of CO_2 ($f\,CO_2$) and (b) pH on the total scale (pH_T) carbonate chemistry conditions in each of the minicosm treatments over time. Grey shading indicates CO_2 and light acclimation period.

At the conclusion of this CO_2 acclimation period, the light intensity was increased for 24 h through the replacement of the two 90% ND filters with one 60% ND filter. The final light intensity was achieved on day 7 with a one-quarter CT blue and a light-scattering filter, which proved to be saturating for photosynthesis (see below).

Unless otherwise specified, samples were taken for analyses on days 1, 3, and 5 during the CO_2 acclimation period and every 2 days from day 8 to 18.

2.2.2 Carbonate chemistry measurements and calculations

Samples for carbonate chemistry measurements were collected daily from each minicosm in 500 mL glass-stoppered bottles (Schott Duran) following the guidelines of Dickson *et al.* (2007). Subsamples for dissolved inorganic carbon (DIC; 50 mL glass-stoppered bottles) and pH on the total scale (pH_T; 100 mL glass-stoppered bottles) measurements were gently pressure filtered (0.2 µm) with a peristaltic pump at a flow rate of ~30 mL min^{-1}, similar to Bockmon and Dickson (2014).

DIC was measured by infrared absorption on an Apollo SciTech AS-C3 analyser equipped with a Li-cor LI-7000 detector using triplicate 1.5 mL samples. The instrument was calibrated (and checked for linearity) within the expected DIC concentration range with five sodium carbonate standards (Merck Suprapur) that were dried for 2 h at 230 °C and prepared gravimetrically in MilliQ water (18.2 MΩ cm^{-1}) at 25 °C. Furthermore, daily measurements of certified reference material batch

CRM127 (Dickson 2010) were used for improved accuracy. Volumetrically measured DIC was converted to $\mu mol\,kg^{-1}$ using calculated density derived from known temperature and salinity. The typical precision among triplicate measurements was $<2\,\mu mol\,kg^{-1}$.

The pH_T was measured spectrophotometrically (GBC UV-vis 916) in a ten centimetre thermostated (25 °C) cuvette using the pH indicator dye m-cresol purple (Acros Organics, 62625-31-4, lot A0321770) following the approach described in Dickson *et al.* (2007), which included changes in sample pH due to dye addition. Contact with air was minimised by sample delivery, dye addition, and mixing via a syringe pump (Tecan; Cavro XLP 6000). Dye impurities and instrument performance were accounted for by applying a constant off-set (+0.003 pH units), determined by the comparison of the measured and calculated pH_T (from known DIC and total alkalinity (TA), including silicate and phosphate) of CRM127. Typical measurement precision for triplicates was 0.001 for higher and 0.003 for lower pH treatments. For further details see Schulz *et al.* (2017).

Carbonate chemistry speciation was calculated from measured DIC and pH_T. In a first step, at salinities measured in situ (WTW197 conductivity meter), practical alkalinity (PA) was calculated at 25 °C using the dissociation constants for carbonic acid determined by Mehrbach *et al.* (1973) as refitted by Lueker *et al.* (2000). Then, total carbonate chemistry speciation was calculated from measured DIC and calculated PA for in situ temperature conditions.

2.2.3 Carbonate chemistry manipulation

The fCO_2 in the minicosms was adjusted by additions of 0.22 µm filtered natural seawater that was saturated by bubbling with AR-grade CO_2 for ≥30 min. In order to keep fCO_2 as constant as possible throughout the experiment, pH in each minicosm was measured with a portable NBS-calibrated probe (Mettler Toledo) in the morning before sampling and in the afternoon, to estimate the necessary amount of DIC to be added. The required volume of CO_2-enriched seawater was then transferred into 1000 mL infusion bags and added to the individual minicosms at a rate of about $50\,mL\,min^{-1}$. After reaching target levels, the mean fCO_2 levels in the minicosms were 343, 506, 634, 953, 1140, and 1641 µatm (Table A3.1).

2.2.4 Light irradiance

The average light intensity in each minicosm tank was calculated by measuring light intensity in the empty tanks at three depths (top, middle, and near-bottom) and across each tank (left, middle, and right) using a Biospherical Instruments' Laboratory Quantum Scalar Irradiance Meter (QSL-101). The average light irradiance received by the phytoplankton within each tank was calculated following the equation of Riley (1957) (Table 2.1). Incoming irradiance ($\bar{I}_o$) was calculated as the average light intensity across the top of the tank. The average vertical light attenuation (K_d) was calculated as the slope from the regression of the natural log of light intensity at all three depths, and mixed depth (Z_m) was the depth of the minicosm tanks (1.14 m).

Changes in vertical light attenuation due to increases in Chl *a* concentration throughout the experimental period were calculated from the equation in Westwood *et al.* (2018); $K_{d(biomass)} = 0.0451157 \times$ Chl *a* (mg m^{-3}). Total light attenuation $K_{d(total)}$ in each tank at each sampling day was calculated by addition of K_d and $K_{d(biomass)}$.

2.2.5 Nutrient analysis

No nutrients were added to the minicosms during the experiment. Macronutrient samples were obtained from each minicosm following the protocol of Davidson *et al.* (2016). Seawater was filtered through 0.45 μm Sartorius filters into 50 mL Falcon tubes and frozen at −20 °C for analysis in Australia. Concentrations of ammonia, nitrate plus nitrite (NOx), soluble reactive phosphorus (SRP), and molybdate reactive silica (Silica) were determined using flow injection analysis by Analytical Services Tasmania following Davidson *et al.* (2016).

2.2.6 Elemental analysis

Samples for POM analysis, particulate organic carbon (POC) and particulate organic nitrogen (PON), were collected following the method of Pearce *et al.* (2007). Equipment for sample preparation was soaked in Decon 90 (Decon Laboratories) for >2 days and thoroughly rinsed in MilliQ water before use. Forceps and cutting blades were rinsed in 100% acetone between

Table 2.1: Definitions, measurements and calculations for productivity data

Name	Definition	Units	Measurements and calculations
Primary Productivity			
Carbon incorporation	Total ^{14}C-sodium bicarbonate incorporation	mg C (mg Chl a)$^{-1}$ L^{-1} h^{-1}	Equation from Steemann Nielsen (1952) $= \frac{(DPM_s - DPM_{T_0})}{DPM_{100\%}} \times$ DIC $\times$ 1.05 / time / Chl a
α	Maximum photosynthetic efficiency	mg C (mg Chl a)$^{-1}$ (μmol photons m^{-2} s^{-1})$^{-1}$ h^{-1}	Modelled from PE curve of 21 light intensities 0–1411 μmol photons m^{-2} s^{-1}
β	Photoinhibition rate	mg C (mg Chl a)$^{-1}$ (μmol photons m^{-2} s^{-1})$^{-1}$ h^{-1}	Modelled from PE curve of 21 light intensities 0–1411 μmol photons m^{-2} s^{-1}
P_{max}	Maximum photosynthetic rate	mg C (mg Chl a)$^{-1}$ h^{-1}	Equation from Platt *et al.* (1980) $= P_s \times \frac{\alpha}{(\alpha+\beta)} \times \frac{\beta}{(\alpha+\beta)}^{\frac{\beta}{\alpha}}$
E_k	Saturating irradiance	μmol photons m^{-2} s^{-1}	Equation from Platt *et al.* (1980) $= P_{max}$ / α
$\bar{I}$	Average irradiance received by phytoplankton cells	μmol photons m^{-2} s^{-1}	Equation from Riley (1957) $= \bar{I}_o \times (1\text{-}e^{(-K_d \times Z_m)})$ / ($K_d \times Z_m$)
$csGPP_{^{14}C}$	^{14}C Chl a-specific primary productivity	mg C (mg Chl a)$^{-1}$ h^{-1}	Equation from Platt *et al.* (1980) $= P_s \times e^{\frac{-\alpha\bar{I}}{P_s}} \times e^{\frac{-\beta\bar{I}}{P_s}}$
$GPP_{^{14}C}$	^{14}C gross primary production	μg C L^{-1} h^{-1}	= $csGPP_{^{14}C} \times$ Chl a
$csGCP_{O_2}$	O_2 Chl a-specific gross community productivity	mg O_2 (mg Chl a)$^{-1}$ h^{-1}	= $NCP_{O_2} + Resp_{O_2}$ / Chl a
GCP_{O_2}	O_2 gross community production	mg O_2 L^{-1} h^{-1}	= $csGCP_{O_2} \times$ Chl a
Photophysiology			
F_v/F_m	Maximum quantum yield of PSII	(arbitrary units)	= (F_m - F_O) / F_m
$\Delta F/F_{m'}$	Effective quantum yield of PSII	(arbitrary units)	= ($F_{m'}$-F) / $F_{m'}$
rETR	Relative electron transport rate	(arbitrary units)	= ΔF_v / $F_{m'} \times I_a$
NPQ	Non-photochemical quenching	(arbitrary units)	= (F_m - $F_{m'}$) / $F_{m'}$
Bacterial Productivity			
nmol $Leucine_{inc}$	Moles of exogenous ^{14}C-leucine incorporated	nmol L^{-1} h^{-1}	Equation from Kirchman (2001) = (DPM_s - DPM_{t_0}) / time / 2.22 $\times 10^6 \times$ SA (nmol μCi^{-1}) / sample vol (L)
$GBP_{^{14}C}$	^{14}C gross bacterial production	μg C L^{-1} h^{-1}	Equation from Simon and Azam (1989) = (nmol $Leucine_{inc}$ / 10^3) $\times$ 131.2 / 0.073 $\times$ 0.86 $\times$ 2
$csBP_{^{14}C}$	^{14}C cell-specific bacterial productivity	fg C cell^{-1} L^{-1} h^{-1}	= $GBP_{^{14}C}$ / cells L^{-1}

P_s: maximum photosynthetic output with no photoinhibition, from Platt *et al.* (1980), DPM_s: sample DPM, SA: specific activity of ^{14}C-leucine isotope
All other abbreviations defined in Methods Section

samples. Seawater was filtered through muffled 25 mm Sartorius quartz microfibre filters until clogged. The filters were folded in half and frozen at −80 °C for analysis in Australia. Filters were thawed and opposite 1/8 subsamples were cut and transferred into a silver POC cup (Elemental Analysis Ltd). Inorganic carbon was removed from each sample through the addition of 20 µL of 2 N HCl to each cup and drying at 60 °C for 36 h. When dry, each cup was folded shut, compressed into a pellet, and stored in desiccant until analysed at the Central Science Laboratory, University of Tasmania using a Thermo Finnigan EA 1112 Series Flash Elemental Analyser.

2.2.7 Chlorophyll *a*

Seawater was collected from each minicosm and a measured volume was filtered through 13 mm Whatman GF/F filters (maximum filtration time of 20 min). Filters were folded in half, blotted dry, and immediately frozen in liquid nitrogen for analysis in Australia. Chlorophyll *a* (Chl *a*) pigments were extracted, analysed by HPLC, and quantified following the methods of Wright *et al.* (2010). Chl *a* was extracted from filters with 300 µL of dimethylformamide plus 50 µL of methanol, containing 140 ng apo-8'-carotenal (Fluka) internal standard, followed by bead beating and centrifugation to separate the extract from particulate matter. Extracts (125 µL) were diluted to 80% with water and analysed on a Waters HPLC using a Waters Symmetry C8 column and a Waters 996 photodiode array detector. Chl *a* was identified by its retention time and absorption spectra compared to a mixed standard sample from known cultures (Jeffrey and Wright 1997), which was run daily before samples. Peak integrations were performed using Waters Empower software, checked manually for corrections, and quantified using the internal standard method (Mantoura and Repeta 1997).

2.2.8 ^{14}C primary productivity

Primary productivity incubations were performed following the method of Westwood *et al.* (2010) based on the technique of Lewis and Smith (1983). This method incubated phytoplankton for 1 h, minimising respiratory losses of photo-assimilated ^{14}C so that the uptake nearly approximated gross primary productivity (e.g. Dring and Jewson 1982; González *et al.* 2008; Regaudie-de-gioux

et al. 2014). Samples were analysed for total organic carbon ($TO^{14}C$) content, thereby including any ^{14}C-labelled photosynthate leaked to the dissolved organic carbon ($DO^{14}C$) pool (Regaudie-de-gioux *et al.* 2014).

For all samples, 5.92 MBq (0.16 mCi) of ^{14}C-sodium bicarbonate ($NaH^{14}CO_3$; PerkinElmer) was added to 162 mL of seawater from each minicosm, creating a working solution of 37 kBq ml^{-1}. Aliquots of this working solution (7 mL) were then added to glass scintillation vials and incubated for 1 h at 21 light intensities ranging from 0–1412 µmol photons m^{-2} s^{-1}. The temperature within each of the vials was maintained at -1.0 ± 0.3 °C through water cooling of the incubation chamber. The reaction was terminated with the addition of 250 µL of 6 N HCl and the vials were shaken for 3 h at 200 rpm to remove dissolved inorganic carbon. Duplicate time zero (T_0) samples were set up in a similar manner to determine background radiation, with 250 µL of 6 N HCl added immediately to quench the reaction without exposure to light. Duplicate 100% samples were also performed to determine the activity of the working solution for each minicosm. For each 100% sample, 100 µL of working solution was added to 7 mL 0.1 M NaOH in filtered seawater to bind all ^{14}C. For radioactive counts, 10 mL of Ultima Gold LLT scintillation cocktail (PerkinElmer) was added to each scintillation vial, shaken, and decays per minute (DPM) were counted in a PerkinElmer Tri-Carb 2910TR Low Activity Liquid Scintillation Analyzer with a maximum counting time set at 3 min.

DPM counts were converted into primary productivity following the equation of Steemann Nielsen (1952) (Table 2.1), using measured DIC concentrations (varying between ~2075 and 2400 µmol kg^{-1}) and normalised to Chl *a* using minicosm Chl *a* concentration (see above). Photosynthesis versus irradiance (PE) curves were modelled for each treatment following the equation of Platt *et al.* (1980) using the *Phytotools* package in R (Silsbe and Malkin 2015; R Core Team 2016). Photosynthetic parameter estimates included the light-saturated photosynthetic rate (P_{max}), maximum photosynthetic efficiency (α), photoinhibition rate (β), and saturating irradiance (E_k).

Chl *a*-specific primary productivity ($csGPP_{^{14}C}$) was calculated following the equation of Platt *et al.* (1980) using average minicosm light irradiance ($\bar{I}$). Gross primary production rates ($GPP_{^{14}C}$) in each tank were calculated from modelled $csGPP_{^{14}C}$ and Chl *a* concentration (see

above). Calculations and units for each parameter are presented in Table 2.1.

2.2.9 Gross community productivity

Community photosynthesis and respiration rates were measured using custom-made mini-chambers. The system consisted of four 5.1 mL glass vials with oxygen sensor spots (Pyro Science) attached on the inside of the vials with non-toxic silicon glue. The vials were sealed, ensuring that any oxygen bubbles were omitted, and all vials were stirred continuously using small Teflon magnetic fleas to allow homogenous mixing of gases within the system during measurements. To improve the signal-to-noise ratio, seawater from each minicosm was concentrated above a 0.8 μm, 47 mm diameter polycarbonate membrane filter (Poretics) with gentle vacuum filtration and resuspended in seawater from each minicosm CO_2 treatment. Each chamber was filled with the cell suspension and placed in a temperature-controlled incubator (0.0 ± 0.5 °C). Light was supplied via fluorescent bulbs above each chamber and light intensity was calibrated using a 4π sensor. Oxygen optode spots were connected to a FireSting O_2 logger and data was acquired using FireSting software (Pyro Science). The optode was calibrated according to the manufacturer protocol immediately prior to measurements using a freshly prepared sodium thiosulfate solution (10% w/w) and agitated filtered seawater (0.2 μm) at experimental temperature for 0% and 100% air saturation values, respectively. Oxygen concentration was recorded until a linear change in rate was established for each pseudoreplicate (n = 4).

Measurements were first recorded in the light (188 $\mu mol\,photons\,m^{-2}\,s^{-1}$) and subsequently in the dark, with the initial steeper portion of the slope used for a linear regression analysis to determine the post-illumination (PI) respiration rate. Gross community production (GCP_{O_2}) was then calculated from dark PI respiration ($Resp_{O_2}$) and net community production (NCP_{O_2}) rates and normalised to Chl *a* concentration ($csGCP_{O_2}$, Table 2.1). Chl *a* content for each concentrated sample was determined by extracting pigments in 90% chilled acetone and incubating in the dark at 4 °C for 24 h. Chl *a* concentrations were determined using a spectrophotometer (Cary 50; Varian) and calculated according to the equations of Jeffrey and Humphrey (1975), modified by Ritchie (2006).

2.2.10 Chlorophyll *a* fluorescence

The photosynthetic efficiency of the microalgal community was measured via Chl *a* fluorescence using a pulse-amplitude-modulated fluorometer (WATER-PAM; Walz). A 3 mL aliquot from each minicosm was transferred into a quartz cuvette with continuous stirring to prevent cells from settling. To establish an appropriate dark adaptation period, several replicates were measured after 5, 10, 15, 20, and 30 min of dark adaptation, with the latter having the highest maximum quantum yield of PSII (F_v/F_m). Following dark adaptation, minimum fluorescence (F_0) was recorded before the application of a high-intensity saturating pulse of light (saturating pulse width = 0.8 s; saturating pulse intensity >3.000 µmol photons m^{-2} s^{-1}) and maximum fluorescence (F_m) was determined. The maximum quantum yield of PSII was calculated from these two parameters (Schreiber 2004). Following F_v/F_m, a five-step steady-state light curve (SSLC) was conducted with each light level (130, 307, 600, 973, 1450 µmol photons m^{-2} s^{-1}) applied for 5 min before recording the light-adapted minimum (F_t) and maximum fluorescence ($F_{m'}$) values. Each light step was spaced by a 30 s dark 'recovery' period before the next light level was applied. Three pseudoreplicate measurements were conducted on each minicosm sample at 0.1 °C. Non-photochemical quenching (NPQ) of Chl *a* fluorescence was calculated from F_m and $F_{m'}$ measurements. Relative electron transport rates (rETRs) were calculated as the product of effective quantum yield ($\Delta F/F_{m'}$) and actinic irradiance (I_a). Calculations and units for each parameter are presented in Table 2.1.

2.2.11 Community carbon concentrating mechanism activity

To investigate the effects of CO_2 on carbon uptake, two inhibitors for carbonic anhydrase (CA) were applied to the 343 and 1641 µatm treatments on day 15: ethoxzolamide (EZA; Sigma), which inhibits both intracellular carbonic anhydrase (iCA) and extracellular carbonic anhydrase (eCA), and acetazolamide (AZA; Sigma), which blocks eCA only. Stock solutions of EZA (20 mM) and AZA (5 mM) were prepared in MilliQ water, and the pH was adjusted using NaOH to minimise pH changes when added to the samples. Before fluorometric measurements were made, water samples from the 343 and 1641 µatm CO_2 treatments were filtered into ≥10 and <10 µm fractions and aliquots were inoculated either with 50 µL of MilliQ water adjusted with

NaOH (control) or a 50 μM final concentration of chemical inhibitor (EZA and AZA). Fluorescence measurements of size-fractionated control- and inhibitor-exposed cells were performed using the WATER-PAM. A 3 mL aliquot of sample was transferred into a quartz cuvette with stirring and left in the dark for 30 min before the maximum quantum yield of PSII (F_v/F_m) was determined (as described above). Actinic light was then applied at 1450 μmol photons m^{-2} s^{-1} for 5 min before the effective quantum yield of PSII ($\Delta F/F_{m'}$) was recorded. Three pseudoreplicate measurements were conducted on each minicosm sample at 0.1 °C.

2.2.12 Bacterial abundance

Bacterial abundance was determined daily using a Becton Dickinson FACScan or FACSCalibur flow cytometer fitted with a 488 nm laser following the protocol of Thomson *et al.* (2016). Samples were pre-filtered through a 50 μm mesh (Nitex), stored at 4 °C in the dark, and analysed within 6 h of collection. Samples were stained for 20 min with 1:10,000 dilution SYBR Green I (Invitrogen) (Marie *et al.* 2005) and PeakFlow Green 2.5 μm beads (Invitrogen) were added to the sample as an internal fluorescence standard. Three pseudoreplicate samples were prepared from each minicosm seawater sample. Samples were run for 3 min at a low flow rate (∼12 μL min^{-1}) and bacterial abundance was determined from side scatter (SSC) versus green (FL1) fluorescence bivariate scatter plots. The analysed volume was calibrated to the sample run time and each sample was run for precisely 3 min, resulting in an analysed volume of 0.0491 and 0.026 04 mL on the FACSCalibur and FACScan, respectively. The volume analysed was then used to calculate final cell concentrations.

2.2.13 Bacterial productivity

Bacterial productivity measurements were performed following the leucine incorporation by microcentrifuge method of Kirchman (2001). Briefly, 70 nM ^{14}C-leucine (PerkinElmer) was added to 1.7 mL of seawater from each minicosm in 2 mL polyethylene Eppendorf tubes and incubated for 2 h in the dark at 4 °C. Three pseudoreplicate samples were prepared from each minicosm seawater sample. The reaction was terminated by the addition of 90 μL 100%

trichloroacetic acid (TCA; Sigma) to each tube. Duplicate background controls were also performed following the same method, with 100% TCA added immediately before incubation. After incubation, samples were spun for 15 min at 12.500 rpm and the supernatant was removed. The cell pellet was resuspended into 1.7 mL of ice-cold 5% TCA and spun again for 15 min at 12.500 rpm and the supernatant was removed. The cell pellet was then resuspended into 1.7 mL of ice-cold 80% ethanol, spun for a further 15 min at 12.500 rpm and the supernatant was removed. The cell pellet was allowed to dry completely before addition of 1 mL of Ultima Gold scintillation cocktail (PerkinElmer). The Eppendorf tubes were placed into glass scintillation vials and DPMs were counted in a PerkinElmer Tri-Carb 2910TR Low Activity Liquid Scintillation Analyzer with a maximum counting time of 3 min.

DPM counts were converted to ^{14}C-leucine incorporation rates following the equation in Kirchman (2001) and used to calculate gross bacterial production ($GBP_{^{14}C}$) following Simon and Azam (1989). Bacterial production was divided by total bacterial abundance to determine the cell-specific bacterial productivity within each treatment ($csBP_{^{14}C}$). Calculations and units for each parameter are presented in Table 2.1.

2.2.14 Statistical analysis

The minicosm experimental design measured the microbial community growth in six unreplicated $f\,CO_2$ treatments. Therefore, subsamples from each minicosm were within-treatment pseudoreplicates and thus, only provide a measure of the variability of the within-treatment sampling and measurement procedures. We use pseudoreplicates as true replicates in order to provide an informal assessment of differences among treatments, noting that results must be treated as indicative and interpreted conservatively.

For all analyses, a linear or curved (quadratic) regression model was fitted to each CO_2 treatment over time using the *stats* package in R (R Core Team 2016) and an omnibus test of differences between the trends among CO_2 treatments over time was assessed by ANOVA. This analysis ignored the repeated measures nature of the data set, which could not be modelled due to the low number of time points and an absence of replication at each time. For the CCM activity measurements, differences between treatments were tested by one-way ANOVA,

followed by a post-hoc Tukey's test to determine which treatments differed. The significance level for all tests was set at <0.05.

2.3 Results

2.3.1 Carbonate chemistry

The fCO_2 of each treatment was modified in a stepwise fashion over 5 days to allow for acclimation of the microbial community to the changed conditions. Target treatment conditions were reached in all tanks by day 5 and ranged from 343 to 1641 µatm, equating to an average pH_T of 8.10 to 7.45 (Fig. 2.2, Table A3.1), respectively. The initial seawater was calculated to have an fCO_2 of 356 µatm and a PA of 2317 $\mu mol\,kg^{-1}$, from a measured pH_T of 8.08 and DIC of 2187 $\mu mol\,kg^{-1}$ (Fig. A3.1, Table A3.2). One minicosm was maintained close to these conditions (343 µatm) throughout the experiment as a control treatment.

2.3.2 Light climate

The average light irradiance for all CO_2 treatments is presented in Table A3.3. During the CO_2 acclimation period (days 1-5) the average light irradiance was $0.9 \pm 0.2\,\mu mol\,photons\,m^{-2}\,s^{-1}$ and was increased to $90.5 \pm 21.5\,\mu mol\,photons\,m^{-2}\,s^{-1}$ by day 8. The average vertical light attenuation (K_d) across all minicosm tanks was 0.92 ± 0.20 Increasing Chl *a* concentration over time in all CO_2 treatments increased $K_{d(total)}$ from 0.96 ± 0.01 on day 1 to 3.53 ± 0.28 on day 18, resulting in a decline in average light irradiance within the minicosms from 86.61 ± 20.50 to $35.97 \pm 9.30\,\mu mol\,photons\,m^{-2}\,s^{-1}$ between days 8 and 18.

2.3.3 Nutrients

Nutrient concentrations were similar across all treatments at the beginning of the experiment (Table A3.2) and did not change during the acclimation period (days 1-5). Ammonia concentrations were initially low ($0.95 \pm 0.18\,\mu M$) and fell rapidly to concentrations below the

limits of detection beyond day 12 in all treatments (Fig. A3.2). No differences in drawdown between CO_2 treatments were observed, and thus it was excluded from further analysis. NOx fell from $26.20 \pm 0.74\,\mu M$ on day 8 to concentrations below detection limits on day 18 (Fig. 2.3a), with the slowest drawdown in the 1641 µatm treatment. SRP concentrations were initially $1.74 \pm 0.02\,\mu M$ and all CO_2 treatments followed a similar drawdown sequence to NOx, reaching very low concentrations ($0.13 \pm 0.03\,\mu M$) on day 18 in all treatments (Fig. 2.3b). In contrast, silica was replete in all treatments throughout the experiment falling from $60.00 \pm 0.91\,\mu M$ to $43.60 \pm 2.45\,\mu M$ (Fig. 2.3c). The drawdown of silica was exponential from day 8 onwards and followed a similar pattern to NOx and SRP, with the highest silica drawdown in the 634 µatm and the least in the 1641 µatm treatment.

2.3.4 Particulate organic matter

Particulate organic carbon (POC) and nitrogen (PON) concentrations were initially low at 4.70 ± 0.15 and $0.50 \pm 0.98\,\mu M$ respectively, and increased after day 8 in all treatments (Fig. 2.4a, b). The accumulation of POC and PON was effectively the reciprocal of the drawdown of nutrients (see above), being lowest in the high CO_2 treatments ($\geq$1140 µatm) and highest in the 343 and 634 µatm treatments. Rates of POC and PON accumulation were both affected by nutrient exhaustion, with declines in the 343 and 634 µatm treatments between days 16 and 18. POC and PON concentrations on day 18 were highest in the 953 µatm treatment. The ratio of POC to PON (C:N) was similar for all treatments, declining from 8.00 ± 0.38 on day 8 to 5.70 ± 0.28 on day 16 (Fig. 2.4c). The slowest initial decline in the C:N ratio occurred in the 1641 µatm treatment, displaying a prolonged lag until day 10, after which it decreased to values similar to all other treatments. Nutrient exhaustion on day 18 coincided with an increase in the C:N ratio in all treatments, with C:N ratios >10 in the 343, 634, and 953 µatm treatments and lower C:N ratios (8.6–6.7) in the 506, 1140, and 1641 µatm treatments.

2.3.5 Chlorophyll *a*

Chl *a* concentrations were low at the beginning of the experiment at $0.91 \pm 0.16\,\mu g\,L^{-1}$ and increased in all treatments after day 8 (Fig. 2.5a). Chl *a* accumulation rates were similar

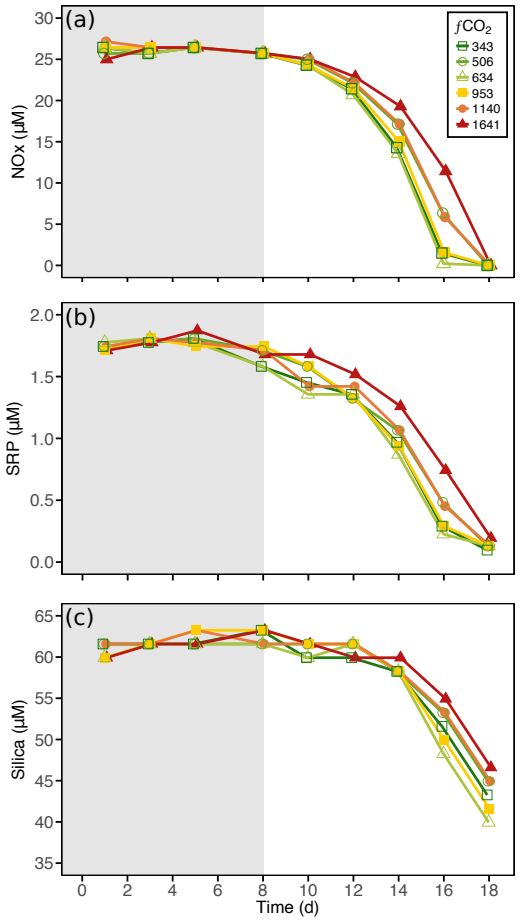

Figure 2.3: Nutrient concentration in each of the minicosm treatments over time. (a) Nitrate + nitrite (NOx), (b) soluble reactive phosphorus (SRP), and (c) molybdate reactive silica (Silica). Grey shading indicates CO_2 and light acclimation period.

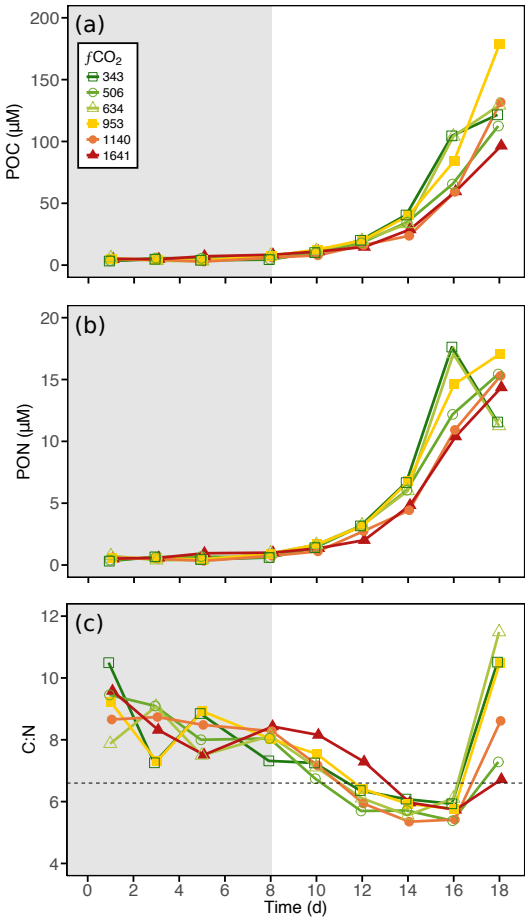

Figure 2.4: Particulate organic matter concentration and C:N ratio of each of the minicosm treatments over time. (a) Particulate organic carbon (POC), (b) particulate organic nitrogen (PON), and (c) carbon:nitrogen (C:N) ratio. The dashed line indicates the C:N Redfield ratio of 6.6. Grey shading indicates CO_2 and light acclimation period.

amongst treatments ≤634 µatm until day 14, with a slightly higher Chl *a* concentration in the 506 and 634 µatm treatments on day 16 compared to the control treatment. By day 18, only the 506 µatm treatment remained higher than the control. Chl *a* accumulation rates in the 953 and 1140 µatm treatments were initially slow but increased after day 14, with Chl *a* concentrations similar to the control on days 16-18. The highest CO_2 treatment (1641 µatm) had the slowest rates of Chl *a* accumulation, displaying a lag in growth between days 8 and 12, after which the Chl *a* concentration increased but remained lower than the control. Rates of Chl *a* accumulation slowed between days 16 and 18 in all treatments except 1641 µatm, coinciding with nutrient limitation. At day 18, the highest Chl *a* concentration was in the 506 µatm exposed treatment and lowest at 1641 µatm.

The omnibus test among CO_2 treatments of trends in Chl *a* over time indicated that the accumulation of Chl *a* in at least one treatment differed significantly from that of the control ($F_{5,23} = 5.5$, $p = 0.002$; Table A3.4). Examination of individual coefficients from the model revealed that only the highest CO_2 treatment, 1641 µatm, was significantly different from the control at the 5% level.

2.3.6 ^{14}C primary productivity

During the CO_2 and light acclimation phase of the experiment (days 1-8), all treatments displayed a steady decline in the maximum photosynthetic rate (P_{max}) and the maximum photosynthetic efficiency (α) until the levels on day 8 were approximately half of those at the beginning of the experiment, suggesting cellular acclimation to the light conditions (Fig. A3.3a, b). Thereafter, relative to the control, P_{max} and α were lowest in CO_2 levels ≥953 µatm and ≥634 µatm, respectively. Rates of photoinhibition (β) and saturating irradiance (E_k) were variable and did not differ among treatments (Fig. A3.3c, d). The average E_k across all treatments was 28.7 ± 8.6 µmol photons m^{-2} s^{-1}, indicating that the light intensity in the minicosms was saturating for photosynthesis (see above) and not inhibiting ($\beta < 0.002$ mg C (mg Chl *a*)$^{-1}$ (µmol photons m^{-2} s^{-1})$^{-1}$ h^{-1}.

Chl *a*-specific primary productivity ($csGPP_{^{14}C}$) and gross primary production ($GPP_{^{14}C}$) were low during the CO_2 acclimation (days 1-5) and increased with increasing light climate after day 5.

Rates of $csGPP_{^{14}C}$ in treatments ≥634 µatm CO_2 were consistently lower than the control between days 8 and 16, with the lowest rates in the highest CO_2 treatment (1641 µatm; Fig. 2.6a). Rates of $GPP_{^{14}C}$ in treatments ≤953 were similar between days 8 and 16, with the 343 (control), 506, and 953 µatm treatments increasing to $46.70 \pm 0.34\,\mu g\,C\,L^{-1}\,h^{-1}$ by day 18 (Fig. 2.5b). Compared to these treatments, $GPP_{^{14}C}$ in the 634 µatm treatment was lower on day 18, only reaching $39.7\,\mu g\,C\,L^{-1}\,h^{-1}$, possibly due to the concurrent limitation of NOx in this treatment on day 16 (see above).

The omnibus test among tanks of the trends in CO_2 treatments over time indicated that $GPP_{^{14}C}$ in at least one treatment differed significantly from the control ($F_{5,23} = 4.9$, $p = 0.003$; Table A3.5). Examination of the significance of individual curve terms revealed that this manifested as differences between the 1140 and 1641 µatm treatments and the control group at the 5% level. No other curves were different from the control. In particular, $GPP_{^{14}C}$ in the 1641 µatm treatment was much lower until day 12, after which it increased steadily until day 16. Between days 16 and 18, a substantial increase in $GPP_{^{14}C}$ was observed in this treatment, subsequently resulting in a rate on day 18 that was similar to the 1140 µatm treatment ($36.30 \pm 0.08\,\mu g\,C\,L^{-1}\,h^{-1}$), although these treatments never reached rates of $GPP_{^{14}C}$ as high as the control.

2.3.7 Gross community productivity

The productivity of the phytoplankton community increased over time in all CO_2 treatments; however, there were clear differences in the timing and magnitude of this increase between treatments (Fig. 2.6b). A CO_2 effect was evident on day 12 when Chl *a*-normalised gross O_2 productivity rates ($csGCP_{O_2}$) increased with increasing CO_2 level, ranging from 19.5–248 $mg\,O_2\,(mg\ Chl\ a)^{-1}\,h^{-1}$. After day 12, the communities in CO_2 treatments ≤634 µatm continued to increase their rates of $csGCP_{O_2}$ until day 18 ($97.7 \pm 17.0\,mg\,O_2\,(mg\ Chl\ a)^{-1}\,h^{-1}$). The 953 and 1140 µatm CO_2 treatments peaked on day 12 (90.4 and $126\,mg\,O_2\,(mg\ Chl\ a)^{-1}\,h^{-1}$, respectively) and then declined on day 14 to rates similar to the control treatment. In contrast, the 1641 µatm treatment maintained high rates of $csGCP_{O_2}$ from days 12-14 ($258.0 \pm 13.8\,mg\,O_2\,(mg\ Chl\ a)^{-1}\,h^{-1}$), coinciding with the recovery of photosynthetic health (F_v/F_m; see below) and the initiation of growth in this treatment (see

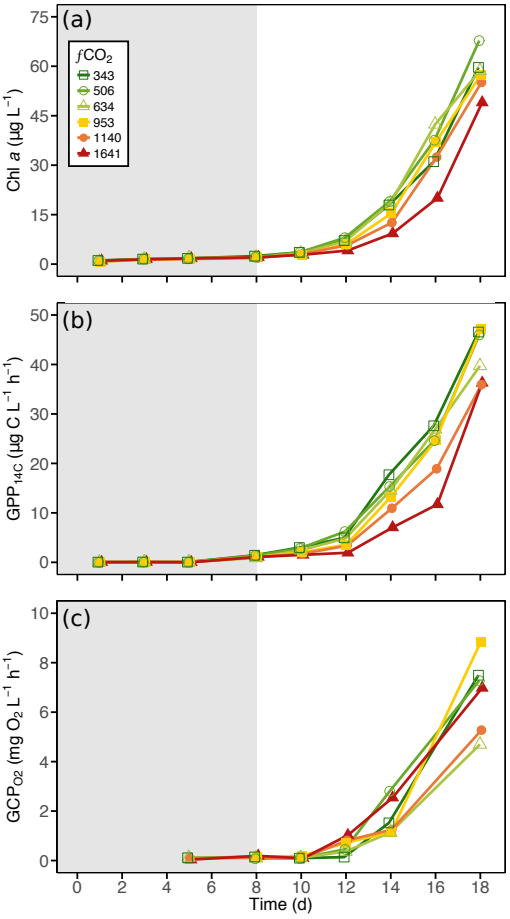

Figure 2.5: Phytoplankton biomass accumulation and community primary production in each of the minicosm treatments over time. (a) Chlorophyll *a* (Chl *a*) concentration, (b) ^{14}C-derived gross primary production ($GPP_{^{14}C}$), and (c) O_2-derived gross community production (GCP_{O_2}). Grey shading indicates CO_2 and light acclimation period.

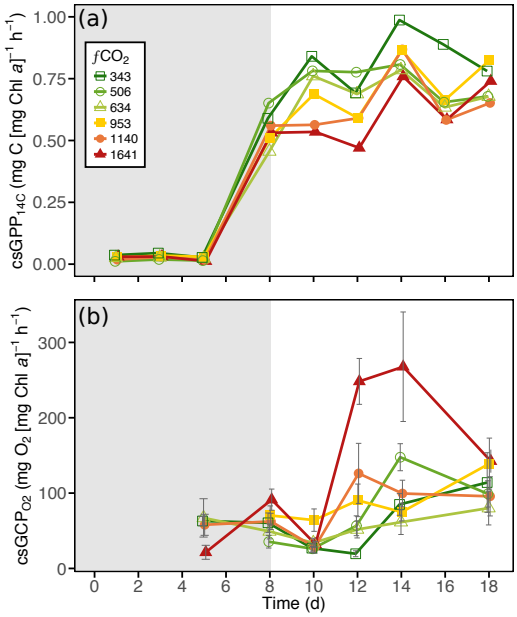

Figure 2.6: (a) ^{14}C-derived Chl *a*-specific primary productivity ($csGPP_{^{14}C}$) and (b) O_2-derived Chl *a*-specific community productivity ($csGCP_{O_2}$) in each of the minicosm treatments over time. Error bars display one standard deviation of pseudoreplicate samples. Grey shading indicates CO_2 and light acclimation period.

above). After this time, rates of $csGCP_{O_2}$ declined in this treatment to rates similar to the control. Despite these differences in $csGCP_{O_2}$, there was no significant difference in the gross community production (GCP_{O_2}) among CO_2 treatments (Fig. 2.5c).

2.3.8 Community photosynthetic efficiency

The community maximum quantum yield of PSII (F_v/F_m) showed a dynamic response over the duration of the experiment (Fig. 2.7). Values initially increased during the low-light CO_2 adjustment period but declined by day 8 when irradiance levels had increased. Between days 8 and 14, differences were evident in the photosynthetic health of the phytoplankton community across the CO_2 treatments, although by day 16 these differences had disappeared. Steady-state light curves revealed that the community photosynthetic response did not change with increasing CO_2. The effective quantum yield of PSII ($\Delta F/F_{m'}$) and NPQ showed no variability with CO_2 treatment (Fig. A3.5, A3.6). There was, however, a notable decline in overall NPQ in all tanks with time, indicating an adjustment to the higher light conditions. Relative electron transport rates (rETR) showed differentiation with respect to CO_2 at high light ($1450\,\mu mol\,photons\,m^{-2}\,s^{-1}$) on days 10-12. However, as seen with the F_v/F_m response, this difference was diminished by day 18 (Fig. A3.6).

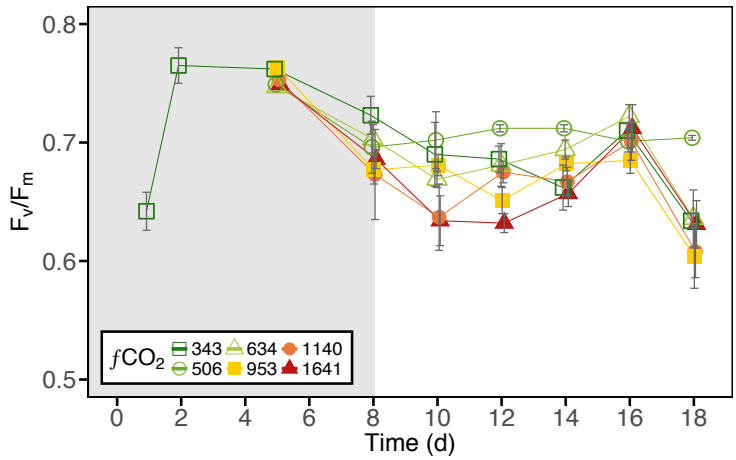

Figure 2.7: Maximum quantum yield of PSII (F_v/F_m) in each of the minicosm treatments over time. Error bars display one standard deviation of pseudoreplicate samples. Grey shading indicates CO_2 and light acclimation period.

2.3.9 Community CCM activity

There was a significant decline in the effective quantum yield of PSII ($\Delta F/F_{m'}$) with the addition of the iCA and eCA inhibitor EZA to both the large (≥10 µm, $p = 0.02$) and small (<10 µm, $p < 0.001$) size fractions of the phytoplankton community exposed to the control (343 µatm) CO_2 treatment (Fig. 2.8). The addition of EZA to cells under high CO_2 (1641 µatm) had no effect on $\Delta F/F_{m'}$ for either size fraction. However, in the case of the small cells under high CO_2 (Fig. 2.8b), $\Delta F/F_{m'}$ was the same as that measured in the control CO_2 in the presence of EZA. The addition of AZA, which inhibits eCA only, had no effect for either CO_2 treatment in the large-celled community. In contrast, there was a significant decline in $\Delta F/F_{m'}$ in the smaller fraction in the control CO_2 treatment ($p < 0.001$), but no effect of AZA addition under high CO_2. Again, the high CO_2 cells exhibited the same $\Delta F/F_{m'}$ as those measured under the control CO_2 in the presence of AZA.

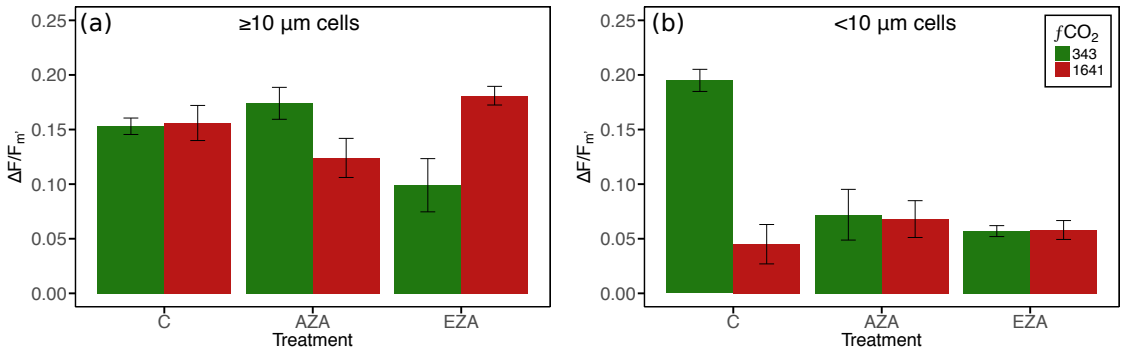

Figure 2.8: Effective quantum yield of PSII ($\Delta F/F_{m'}$) of (a) large (≥10 µm) and (b) small (<10 µm) phytoplankton in the control (343 µatm) and high (1641 µatm) CO_2 treatments treated with carbonic anhydrase (CA) inhibitors. A decline in $\Delta F/F_{m'}$ with the application of inhibitor indicates CCM activity. C denotes the control treatment, which received no CA inhibitor; AZA is the acetazolamide treatment, which blocks extracellular carbonic anhydrase; EZA is the ethoxzolamide treatment, which blocks intracellular and extracellular carbonic anhydrase. Error bars display one standard deviation of pseudoreplicate samples.

2.3.10 Bacterial abundance

During the 8-day acclimation period, bacterial abundance in treatments ≥634 µatm increased with increasing CO_2, reaching $26.0–32.4 \times 10^7$ cells L^{-1} and remaining high until day 13 (Fig. 2.9a). Between days 7 and 13, bacterial abundances in CO_2 treatments ≥953 were higher than the control. In contrast, abundance remained constant in treatments ≤506 µatm

($20.6 \pm 1.4 \times 10^7$ cells L^{-1}) until day 11. Cell numbers rapidly declined in all treatments after day 12, finally stabilising at $0.5 \pm 0.2 \times 10^7$ cells L^{-1}. An omnibus test among CO_2 treatments of the trends in bacterial abundance over time showed that changes in abundance in at least one treatment differed significantly from the control ($F_{5,185} = 9.8$, $p < 0.001$; Table A3.6). Examination of individual coefficients from the model revealed that CO_2 treatments ≥953 µatm were significantly different from the control at the 5% level.

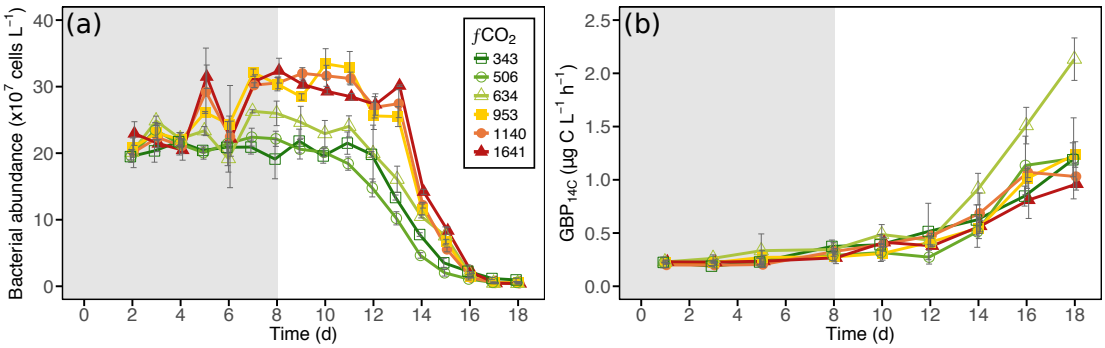

Figure 2.9: Bacterial abundance and community production in each of the minicosm treatments over time. (a) Bacterial cell abundance and (b) ^{14}C-derived gross bacterial production ($GBP_{^{14}C}$). Error bars display one standard deviation of pseudoreplicate samples. Grey shading indicates CO_2 and light acclimation period.

2.3.11 Bacterial productivity

Gross bacterial production ($GBP_{^{14}C}$) was low in all CO_2 treatments (0.20 ± 0.03 µg C L^{-1} h^{-1}) and changed little during the first 5 days of incubation (Fig. 2.9b). Thereafter it increased, coinciding with exponential growth in the phytoplankton community. The most rapid increase in $GBP_{^{14}C}$ was observed in the 634 µatm treatment, resulting in a rate twice that of all other treatments by day 18 (2.1 µg C L^{-1} h^{-1}). No difference was observed among other treatments, all of which increased to an average rate of 1.1 ± 0.1 µg C L^{-1} h^{-1} by day 18. Cell-specific bacterial productivity ($csBP_{^{14}C}$) was low in all treatments (1.2 ± 0.5 fg C L^{-1} h^{-1}) until day 14, with slower rates in treatments ≥953 µatm, likely due to high cell abundances observed in these treatments (Fig. A3.8). It then increased from day 14, coinciding with a decline in bacterial abundance. Rates of $csBP_{^{14}C}$ did not differ among treatments until day 18, when the rate in the 634 µatm treatment was higher than all other treatments (0.5 pg C L^{-1} h^{-1}).

2.4 Discussion

Our study of a natural Antarctic phytoplankton community identified a critical threshold for tolerance of CO_2 between 953 and 1140 µatm, above which photosynthetic health was negatively affected and rates of carbon fixation and Chl *a* accumulation declined. Low rates of primary productivity also led to declines in nutrient uptake rates and POM production, although there was no effect of CO_2 on C:N ratios, indicating that ocean acidification effects on the phytoplankton community did not modify POM stoichiometry. Assessing the temporal trends of Chl *a*, $GPP_{^{14}C}$, and PON against CO_2 treatment revealed that the downturn in these parameters occurred between 634 and 953 µatm fCO_2 and could be discerned following ≥12 days incubation (Fig. 2.10). On the final day of the experiment (day 18), this CO_2 threshold was less clear and likely confounded by the effects of nutrient limitation (Westwood *et al.* 2018). In contrast, bacterial productivity was unaffected by increased CO_2. Instead, production coincided with increased organic matter supply from phytoplankton primary productivity. In the following sections these effects will be investigated further, with suggestions for possible mechanisms that may be driving the responses observed.

2.4.1 Ocean acidification effects on phytoplankton productivity

The results of this study suggest that exposing phytoplankton to high CO_2 levels can decouple the two stages of photosynthesis (see also the discussion below). At CO_2 levels ≥1140 µatm, Chl *a*-specific oxygen production ($csGCP_{O_2}$) increased strongly yet displayed the lowest rates of Chl *a*-specific carbon fixation ($csGPP_{^{14}C}$; Fig. 2.6). This mismatch in oxygen production and carbon fixation is likely due to the two-stage process in the photosynthetic fixation of carbon (reviewed in Behrenfeld *et al.* 2004). In the first stage, light-dependent reactions occur within the chloroplast, converting light energy (photons) into the cellular energy products, adenosine triphosphate (ATP) and nicotinamide adenine dinucleotide phosphate (NADPH), producing O_2 as a by-product. This cellular energy is then utilised in a second, light-independent pathway, which uses the carbon-fixing enzyme RuBisCO to convert CO_2 into sugars through the Calvin cycle. However, under certain circumstances the relative pool of energy may also be consumed

in alternative pathways, such as respiration and photoprotection (Behrenfeld *et al.* 2004; Gao and Campbell 2014). Increases in energy requirements for these alternate pathways have been demonstrated, where measurements of maximum photosynthetic rates (P_{max}) and photosynthetic efficiency (α) display changes that result in no change to saturating irradiance levels (E_k) (Behrenfeld *et al.* 2004; Behrenfeld *et al.* 2008; Halsey *et al.* 2010). This "E_k-independent variability" was evident in our study, in which decreases in P_{max} and α were observed in the high CO_2 treatments, while E_k remained unaffected (Fig. A3.3).

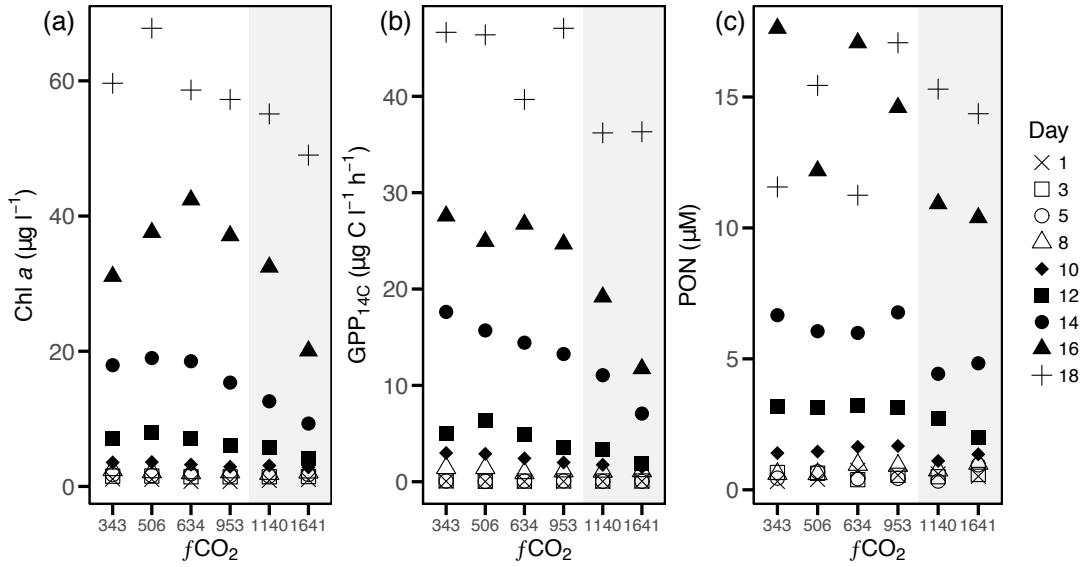

Figure 2.10: Temporal trends of (a) Chl *a*, (b) ^{14}C-derived gross primary production ($GPP_{^{14}C}$), and (c) particulate organic nitrogen (PON) against CO_2 treatment. Grey shading indicates CO_2 treatments $\geq$1140 µatm.

This highlights an important tipping point in the phytoplankton community's ability to cope with the energetic requirements of maintaining efficient productivity under high CO_2. While studies on individual phytoplankton species have reported decoupling of the photosynthetic pathway under conditions of stress, no studies to date on natural phytoplankton communities have reported this response. Under laboratory conditions, stresses such as nutrient limitation (Halsey *et al.* 2010) or a combination of high CO_2 and light climate (Hoppe *et al.* 2015; Liu *et al.* 2017) have been shown to induce such a response, in which isolated phytoplankton species possess higher energy requirements for carbon fixation. In our study, the phytoplankton community experienced a dynamic light climate due to continuous gentle mixing of the minicosm contents, and although nutrients weren't limiting, the phytoplankton in the higher

CO_2 treatments did show lower $csGPP_{^{14}C}$ rates (Fig. 2.6a), which could be linked to higher energy demand for light-independent processes. Since nutrients were replete and not a likely source of stress, it follows that CO_2 and light were likely the only sources of stress on this community.

Increased respiration rates could account for the decreased carbon fixation rates measured. Thus far, respiration rates are commonly reported as either unaffected or lower under increasing CO_2 (Hennon *et al.* 2014; Trimborn *et al.* 2014; Spilling *et al.* 2016). This effect is generally attributed to declines in cellular energy requirements via processes such as the down-regulation of CCMs, which can result in observed increased rates of production (Spilling *et al.* 2016). Despite this, decreased growth rates have been linked to enhanced respiratory carbon loss at high CO_2 levels (800–1000 µatm) (Gao *et al.* 2012b). The contribution of community respiration rates to $csGCP_{O_2}$ was high and increased with increasing CO_2 (Fig. A3.4). However, respiration rates were generally proportional to the increase in O_2 production (i.e. the ratio of production to respiration remained constant across CO_2 conditions), making it unlikely to be a significant contributor to the decline in carbon fixation. Instead, high respiration rates were possibly a result of heterotrophic activity.

It has been suggested that the negative effects of ocean acidification are predominantly due to the decline in pH and not the increase in CO_2 concentration (e.g. McMinn *et al.* 2014; Coad *et al.* 2016). A decline in pH with ocean acidification increases the hydrogen ion (H^+) concentration in the seawater and is likely to make it increasingly difficult for phytoplankton cells to maintain cellular homeostasis. Metabolic processes, such as photosynthesis and respiration, impact cellular H^+ fluxes between compartments, making it necessary to temporarily balance internal H^+ concentrations through H^+ channels (Taylor *et al.* 2012). Under normal oceanic conditions (pH ∼8.1), when the extracellular environment is above pH 7.8, excess H^+ ions generated within the cell are able to passively diffuse out of the cell through these H^+ channels. However, a lowering of the oceanic pH below 7.8 is likely to halt this passive removal of internal H^+, requiring the utilisation of energy-intensive proton pumps (Taylor *et al.* 2012) and thus potentially reducing the energy pool available for carbon fixation. While not well understood, these H^+ channels may also perform important cellular functions, such as nutrient uptake, cellular signalling, and defense (Taylor *et al.* 2012). Our results are consistent with this idea of a critical pH threshold, as significant declines in $GPP_{^{14}C}$ were observed in

treatments ≥1140 µatm (Fig. 2.10), which are the CO_2 treatments for which the pH ranged from 7.69-7.45 (Fig. 2.2).

Despite the initial stress of high CO_2 between days 8 and 12, the phytoplankton community displayed a strong ability to adapt to these conditions. The CO_2-induced reduction in F_v/F_m showed a steady recovery between days 12 and 16, with all treatments displaying similarly high F_v/F_m at day 16 (0.68-0.71; Fig. 2.7). This recovery in photosynthetic health suggests that the phytoplankton community was able to acclimate to the high CO_2 conditions, possibly through cellular acclimation, changes in community structure, or most likely, a combination of both. Cellular acclimations were observed in our study. A lowering of NPQ and a minimisation of the CO_2-related response to photoinhibition (rETR) at high light intensity suggested that PSII was being down-regulated to adjust to a higher light climate (Fig. A3.6, A3.6). Decreased energy requirements for carbon fixation were also observed in the photosynthetic pathway, resulting in increases in $GPP_{^{14}C}$ and Chl *a* accumulation rates (Fig. 2.5). Acclimation to increased CO_2 has been reported in a number of studies, resulting in shifts in carbon and energy utilisation (Sobrino *et al.* 2008; Hopkinson *et al.* 2010; Hennon *et al.* 2014; Trimborn *et al.* 2014; Zheng *et al.* 2015). Numerous photophysiological investigations on individual phytoplankton species also report species-specific tolerances to increased CO_2 (Gao *et al.* 2012a; Trimborn *et al.* 2013; Gao and Campbell 2014; Trimborn *et al.* 2014), and a general trend toward smaller-celled communities with increased CO_2 has been reported in ocean acidification studies globally (Schulz *et al.* 2017). Changes in community structure were observed with increasing CO_2, with taxon-specific thresholds of CO_2 tolerance (Hancock *et al.* 2018). Within the diatom community, the response was also related to size, leading to an increase in abundance of small (<20 µm) diatoms in the higher CO_2 treatments (≥953 µatm). Therefore, the community acclimation observed is likely driven by an increase in the growth of more tolerant species.

It is often suggested that the down-regulation of CCMs helps to moderate the sensitivity of phytoplankton communities to increasing CO_2. The carbon-fixing enzyme RuBisCO has a low affinity for CO_2 that is compensated for through CCMs that actively increase the intracellular CO_2 (Raven 1991; Badger 1994; Badger *et al.* 1998; Hopkinson *et al.* 2011). This process requires additional cellular energy (Raven 1991) and numerous studies have suggested that the energy savings from down-regulation of CCMs in phytoplankton could explain increases in rates

of primary productivity at elevated CO_2 levels (e.g. Cassar *et al.* 2004; Tortell *et al.* 2008a, 2010; Trimborn *et al.* 2013; Young *et al.* 2015). In Antarctic phytoplankton communities, Young *et al.* (2015) showed that the energetic costs of CCMs are low and any down-regulation at increased CO_2 would provide little benefit. We found that the CCM component carbonic anhydrase (CA) was utilised by the phytoplankton community at our control CO_2 level (343 µatm) and was down-regulated at high CO_2 (1641 µatm; Fig. 2.8). Yet we saw no promotion of primary productivity that coincided with this down-regulation. Thus, our data support the previous studies showing that increased CO_2 may alleviate energy supply constraints but does not necessarily lead to increased rates of carbon fixation (Rost *et al.* 2003; Cassar *et al.* 2004; Riebesell 2004).

Furthermore, size-specific differences in phytoplankton CCM utilisation were observed. The absence of eCA activity in the large phytoplankton (≥10 µm; Fig. 2.8a) suggests that bicarbonate (HCO_3^-) was the dominant carbon source used by this fraction of the phytoplankton community (Burkhardt *et al.* 2001; Tortell *et al.* 2008b). This is not surprising as direct HCO_3^- uptake has been commonly reported among Antarctic phytoplankton communities (Cassar *et al.* 2004; Tortell *et al.* 2008b, 2010). On the other hand, the small phytoplankton (<10 µm; Fig. 2.8b) seem to have used both iCA and eCA, implying that carbon for photosynthesis was sourced through both the extracellular conversion of HCO_3^- to CO_2 and direct HCO_3^- uptake (Rost *et al.* 2003). Despite these patterns, CCM activity in this study was only determined via Chl *a* fluorescence and therefore direct measurement of light-dependent reactions in photosynthesis. This imposes limitations to the interpretability of this particular data set, as CA is involved primarily in carbon acquisition, which occurs during photosynthetic reactions that are independent of light.

The presence of iCA has also been proposed as a possible mechanism for increased sensitivity of phytoplankton to decreased pH conditions. Satoh *et al.* (2001) found that the presence of iCA caused strong intracellular acidification and inhibition of carbon fixation when a CO_2-tolerant iCA-expressing algal species was transferred from ambient conditions to very high CO_2 (40%). Down-regulation of iCA through acclimation in a 5% CO_2 treatment eliminated this response, with similar tolerance observed in an algal species with low ambient iCA activity. Thus, the down-regulation of iCA activity at high CO_2, as was seen in our study, may not only decrease cellular

energy demands but may also be operating as a cellular protection mechanism, allowing the cell to maintain intracellular homeostasis.

Contrary to the high CO_2 treatments, the phytoplankton community appeared to tolerate CO_2 levels up to 953 µatm, which identified a CO_2 threshold. Between days 8 and 14 we observed a small and insignificant CO_2-related decline in F_v/F_m, $GPP_{^{14}C}$, and Chl *a* accumulation among the 343-953 µatm treatments (Fig. 2.7, 2.10). Tolerance of CO_2 levels up to ∼1000 µatm has often been observed in natural phytoplankton communities in regions exposed to fluctuating CO_2 levels. In these communities, increasing CO_2 often had no effect on primary productivity (Tortell *et al.* 2000; Tortell and Morel 2002; Tortell *et al.* 2008a; Hopkinson *et al.* 2010; Tanaka *et al.* 2013; Sommer *et al.* 2015; Young *et al.* 2015; Spilling *et al.* 2016) or growth (Tortell *et al.* 2008a; Schulz *et al.* 2013), although an increase in primary production has been observed in some instances (Riebesell 2004; Tortell *et al.* 2008a; Egge *et al.* 2009; Tortell *et al.* 2010; Hoppe *et al.* 2013; Holding *et al.* 2015). These differing responses may be due to differences in community composition, nutrient supply, or ecological adaptations of the phytoplankton community in the region studied. They may also be due to differences in the experimental methods, especially the range of CO_2 concentrations employed (Hancock *et al.* 2018), the mechanism used to manipulate CO_2 concentrations, the duration of the acclimation and incubation, the nature and volume of the mesocosms used, and the extent to which higher trophic levels are screened from the mesocosm contents (see Davidson *et al.* 2016).

Previous studies in Prydz Bay report a tolerance of the phytoplankton community to CO_2 levels up to 750 µatm (Davidson *et al.* 2016; Thomson *et al.* 2016; Westwood *et al.* 2018). Although these experiments differed in nutrient concentration, community composition, and CO_2 manipulation from ours, when taken together, these studies demonstrate consistent CO_2 effects throughout the Antarctic summer season and across years in this location. The most likely reason for this high tolerance is that these communities are already exposed to highly variable CO_2 conditions. CO_2 naturally builds beneath the sea ice in winter, when primary productivity is low (Perrin *et al.* 1987; Legendre *et al.* 1992), and is rapidly depleted during spring and summer by phytoplankton blooms, resulting in annual fCO_2 fluctuations between ∼50 and 500 µatm (Gibson and Trull 1999; Roden *et al.* 2013). Thus, variable CO_2 environments appear to promote adaptations within the phytoplankton community to manage the stress imposed by fluctuating CO_2.

Changes in POM production and the C:N ratio in phytoplankton communities can have significant effects on carbon sequestration and change their nutritional value for higher trophic levels (Finkel *et al.* 2010; van de Waal *et al.* 2010; Polimene *et al.* 2016). We observed a decline in POM at CO_2 levels $\geq$1140 µatm (Fig. 2.10), while changes in organic matter stoichiometry (C:N ratio) appeared to be predominantly controlled by nutrient consumption (Fig. 2.4). Increases in POM production were similar to Chl *a* accumulation, with declines in high CO_2 treatments ($\geq$1140 µatm) due to low rates of primary productivity. Carbon overconsumption has been reported in some natural phytoplankton communities exposed to increased CO_2, resulting in observed or inferred increases in the particulate C:N ratio (Riebesell *et al.* 2007; Engel *et al.* 2014). While in our study the C:N ratio did decline to below the Redfield ratio during exponential growth, it remained within previously reported C:N ratios of coastal phytoplankton communities in this region (Gibson and Trull 1999; Pasquer *et al.* 2010). However, as we did not analyse the elemental composition of dissolved inorganic matter, carbon overconsumption cannot be completely ruled out (Kähler and Koeve 2001). Therefore, it is difficult to say whether or not changes in primary productivity will affect organic matter stoichiometry in this region, particularly as any resultant long-term changes in community composition to more CO_2-tolerant taxa may also have an effect (Finkel *et al.* 2010).

2.4.2 Ocean acidification effects on bacterial productivity

In contrast to the phytoplankton community, bacteria were tolerant of high CO_2 levels. The low bacterial productivity and abundance of the initial community is characteristic of the post-winter bacterial community in Prydz Bay where growth is limited by organic nutrient availability (Pearce *et al.* 2007). Whilst an increase in cell abundance was observed at CO_2 levels $\geq$634 µatm (Fig. 2.9a), it was possible that this response was driven by a decline in grazing by heterotrophs (Thomson *et al.* 2016; Westwood *et al.* 2018) instead of a direct CO_2-related promotion of bacterial growth. The subsequent decline in abundance was likely due to top-down control from the heterotrophic nanoflagellate community, which displayed an increase in abundance at this time (Hancock *et al.* 2018). Bacterial tolerance to high CO_2 has been reported previously in this region (Thomson *et al.* 2016; Westwood *et al.* 2018) and has also been reported in numerous studies in the Arctic (Grossart *et al.* 2006; Allgaier *et al.* 2008;

Paulino *et al.* 2008; Baragi *et al.* 2015; Wang *et al.* 2016), suggesting that the marine bacterial community will be resilient to increasing CO_2.

While we detected an increase in bacterial productivity, this response appeared to be correlated with an increase in Chl *a* concentration and available POM rather than CO_2. Bacterial productivity was similar among all CO_2 treatments, except for a final promotion of productivity at 634 µatm on day 18 (Fig. 2.9b). This promotion of growth may be linked to an increase in diatom abundance observed in this treatment (Hancock *et al.* 2018). The coupling of bacterial growth with phytoplankton productivity has been reported by numerous studies on natural marine microbial communities (Grossart *et al.* 2006; Allgaier *et al.* 2008; Engel *et al.* 2013; Piontek *et al.* 2013; Sperling *et al.* 2013; Bergen *et al.* 2016). Thus, it is likely that the bacterial community was controlled more by grazing and nutrient availability than by CO_2 level.

2.5 Conclusions

These results support the identification of a tipping point in the marine microbial community response to CO_2 between 953 and 1140 µatm. When exposed to CO_2 $\geq$634 µatm, declines in growth rates, primary productivity, and organic matter production were observed in the phytoplankton community and became significantly different at $\geq$1140 µatm. Despite this, the community displayed the ability to adapt to these high CO_2 conditions by down-regulating CCMs and likely adjusting other intracellular mechanisms to cope with the added stress of low pH. However, the lag in growth and subsequent acclimation to high CO_2 conditions allowed for more tolerant species to thrive (Hancock *et al.* 2018).

Conditions in Antarctic coastal regions fluctuate throughout the seasons and the marine microbial community is already tolerant to changes in CO_2 level, light availability, and nutrients (Gibson and Trull 1999; Roden *et al.* 2013). It is possible that phytoplankton communities already exposed to highly variable conditions will be more capable of adapting to the projected changes in CO_2 (Schaum and Collins 2014; Boyd *et al.* 2016b). This will likely also include adaptation at the community level, causing a shift in dominance to more tolerant species. This has been observed in numerous ocean acidification experiments, with a trend in community

composition favouring picophytoplankton and away from large diatoms (Davidson *et al.* 2016; Reviewed in Schulz *et al.* 2017). Such a change in phytoplankton community composition may have flow-on effects to higher trophic levels that feed on Antarctic phytoplankton blooms. It could also have a significant effect on the biological pump, with decreased carbon drawdown at high CO_2, causing a negative feedback on anthropogenic CO_2 uptake. Coincident increases in bacterial abundance under high CO_2 conditions may also increase the efficiency of the microbial loop, resulting in increased organic matter remineralisation and further declines in carbon sequestration.

Chapter 3

Ocean acidification reduces growth and grazing of Antarctic heterotrophic nanoflagellates

3.1 Introduction

Oceanic uptake of anthropogenic CO_2 has resulted in a ∼0.1 unit decline in pH in the oceans since pre-industrial times (Sabine 2004; Raven *et al.* 2005), with ∼40% of this uptake occurring in the Southern Ocean (Takahashi *et al.* 2012; Frölicher *et al.* 2015). In addition, the low overall water temperature and naturally low $CaCO_3$ saturation state make the Southern Ocean particularly vulnerable to ocean acidification (Orr *et al.* 2005; McNeil and Matear 2008). Coastal Antarctic waters are regions of high productivity, that provide an essential food source for the abundance of life in Antarctica (Arrigo *et al.* 2008a). While large phytoplankton, such as diatoms and dinoflagellates, are often believed to be responsible for most of the energy transfer to higher trophic levels in this region, picophytoplankton, prokaryotes, mixotrophic phytoflagellates, microheterotrophs, and heterotrophic nanoflagellates (HNF) also play important roles in grazing and the carbon cycle (Azam *et al.* 1991; Sherr and Sherr 2002; Smetacek *et al.* 2004).

Marine microbes are an essential part of the marine food web and are a critical link in biogeochemical processes, such as the cycling of nutrients and carbon (Azam and Malfatti 2007). Globally, it is estimated that ∼80-100% of daily primary production is either consumed by grazers or lost via processes such as cell lysis and sinking (Behrenfeld 2014). Grazing can profoundly affect phytoplankton abundance in marine ecosystems, with microzooplankton consuming on average 60-75% of daily primary production (Landry and Calbet 2004) and HNF grazing between 20-100% of daily bacterial production (Safi *et al.* 2007; Pearce *et al.* 2010). Prokaryotes salvage dissolved organic matter released from phytoplankton primary production, whish is returned to the food web upon grazing by HNF (Pearce *et al.* 2010; Buchan *et al.* 2014). Prokaryotes also produce essential micronutrients and vitamins required for phytoplankton growth (Azam and Malfatti 2007; Buchan *et al.* 2014; Bertrand *et al.* 2015) and are important in the supply of nutrients to microzooplankton in Antarctic waters over winter, when primary productivity is low (Azam *et al.* 1991). This transfer of organic matter between primary producers, prokaryotes (bacteria and Archaea), and protozoa forms the microbial loop, upon which all life in the ocean relies (Azam *et al.* 1983; Fenchel 2008).

In Antarctic waters, heterotrophic flagellates make a significant contribution to the top-down control of phytoplankton and prokaryote productivity. They can achieve growth rates that exceed that of their phytoplanktonic prey and their grazing can significantly alter the microbial community composition (Bjørnsen and Kuparinen 1991; Archer *et al.* 1996; Pearce *et al.* 2010). Heterotrophic flagellates, microzooplankton, and ciliates of all sizes (2–>200 μm) have been observed grazing on picophytoplankton 0.2–2 μm and prokaryotes 0.1–5 μm (Safi *et al.* 2007). Despite their importance in marine ecosystems, they remain relatively unstudied (Caron and Hutchins 2013). Difficulties in identification of HNF in natural seawater samples has no doubt contributed to the scarcity of published studies (Rose *et al.* 2004). Of the few studies that have included heterotrophic flagellates, most studies have focused on the larger microzooplankton community (20–200 μm), reporting no changes in abundance or grazing rates with elevated CO_2 (Suffrian *et al.* 2008; Aberle *et al.* 2013; Davidson *et al.* 2016). However, ocean acidification effects on microzooplankton grazers may also be indirect, due to changes in the abundance and composition of their prey (Rose *et al.* 2009a). Thomson *et al.* (2016), in their Antarctic minicosm study, reported a negative effect of ocean acidification on HNF abundance when CO_2 concentrations were $\geq$750 μatm. Species-specific responses to ocean acidification have also been observed amongst choanoflagellates in the present study (Hancock *et al.* 2018), exposing a hitherto unrecognised layer of complexity to predicting the effects of ocean acidification on microbial communities.

When assessing ocean acidification studies globally, Schulz *et al.* (2017) reported a general trend toward increased abundance of picophytoplankton with declining ocean pH. The cyanobacterium *Synechococcus* and picoeukaryotes in the prasinophyte class were identified as the key beneficiaries of increased CO_2 levels, potentially through increased CO_2 concentration in the relatively small diffusive boundary layer of these small cells, allowing for down regulation of energetically costly CO_2 and HCO_3^- transporters into the cell (Beardall and Giordano 2002). Unlike temperate oligotrophic ecosystems, cyanobacteria are rare in Antarctic waters (Wright *et al.* 2009; Lin *et al.* 2012; Flombaum *et al.* 2013; Liang *et al.* 2016) meaning the picophytoplankton in waters south of the Polar Front are composed largely of eukaryotes. This group can comprise up to 33% of total phytoplankton biomass (Wright *et al.* 2009; Lin *et al.* 2012). A minicosm study on natural communities of coastal Antarctic marine microbes

observed an increase in picoeukaryote abundance at CO_2 levels above 750 µatm, although their results suggested that this may have been due to a reduction in top-down control of the HNF community, as opposed to a direct promotion of picoeukaryote growth (Thomson *et al.* 2016).

In natural marine microbial communities, prokaryotes have been shown to have a high tolerance to ocean acidification, with little effect on abundance or productivity (Grossart *et al.* 2006; Allgaier *et al.* 2008; Paulino *et al.* 2008; Wang *et al.* 2016). Prokaryote abundance and production is generally linked to increased primary production, with peaks in abundance often occurring immediately after the peak of a phytoplankton bloom (Pearce *et al.* 2007; Buchan *et al.* 2014). This is likely due to increased availability of dissolved organic matter, released by phytoplankton during growth, viral lysis, or bacterial degradation of dead cells (Azam and Malfatti 2007). A CO_2-induced increase in the production of organic matter and the formation of transparent exopolymer particles has been reported in a natural community Endres *et al.* (2014). This promoted bacterial abundance and stimulated enzyme production for organic matter degradation, suggesting that ocean acidification may increase the flow of carbon through the microbial loop in surface waters Endres *et al.* (2014). Shifts in prokaryote community composition have also been reported, although with no significant effect on total prokaryote abundance (Roy *et al.* 2013; Zhang *et al.* 2013; Bergen *et al.* 2016). Instead, the composition and abundance of prokaryote communities appear to be indirectly affected by ocean acidification by altering biotic factors that influence their growth and mortality.

In our study, a natural community of marine microbes from Prydz Bay, East Antarctica was exposed to increasing levels of CO_2, up to 1641 µatm, in 650 L minicosms. The abundance of HNF, nano- and picophytoplankton, and prokaryotes was measured and the results used to assess whether interactions between these communities could be inferred. A previous community-level study in the Antarctic reported a decline in HNF abundance and an increase in picophytoplankton and prokaryotic abundance when CO_2 concentrations were $\geq$750 µatm (Davidson *et al.* 2016; Thomson *et al.* 2016; Westwood *et al.* 2018). We used a similar experimental design to Thomson *et al.* (2016) but added an initial CO_2 acclimation period at low light to determine whether this acclimation would alter the response previously reported.

3.2 Methods

3.2.1 Minicosm

A natural microbial assemblage from Prydz Bay, Antarctica was incubated in six 650 L polythene tanks (minicosms) and exposed to six CO_2 treatments; ambient (343 µatm), 506, 634, 953, 1140, and 1641 µatm. Before commencement of the experiment, all minicosms were acid washed with 10% vol:vol AR HCl, rinsed thoroughly with MilliQ water, and finally rinsed with seawater from the sampling site. Seawater to fill the minicosms was collected from amongst the decomposing fast ice in Prydz Bay at Davis Station, Antarctica (68° 35′ S 77° 58′ E) on 19th November, 2014. A 7000 L polypropylene reservoir tank was filled by helicopter, using multiple collections in a thoroughly rinsed 720 L Bambi bucket. The seawater was then gravity fed from the reservoir to the minicosms through Teflon-lined hose, fitted with a 200 µm pore size Arkal filter to exclude metazooplankton that would significantly graze the microbial community. Microscopic analysis showed that very few metazooplankton and nauplii passed through the pre-filter and they were seldom observed throughout the experiment (see Hancock *et al.* 2018). Thus, it is unlikely that their grazing effected the CO_2-induced trends in community composition in our study. All minicosms were filled simultaneously to ensure uniform distribution of microbes.

The six minicosms were housed in a temperature-controlled shipping container, with the water temperature in each minicosm maintained at 0.0 ± 0.5 °C. The temperature in each minicosm was maintained by offsetting the cooling of the shipping container against warming of the tank water with two 300 W Fluval aquarium heaters connected via Carel temperature controllers and a temperature control program. Each minicosm was sealed with an acrylic lid and the water was gently mixed by a shielded high-density polyethylene auger, rotating at 15 rpm.

Minicosms were illuminated by two 150 W HQI-TS (Osram) metal halide lamps on a 19:5 h light:dark cycle. Low intensity light (0.90 ± 0.22 µmol photons m^{-2} s^{-1}) was provided for the first 5 d to slow phytoplankton growth while the CO_2 levels were gradually raised to the target concentration for each minicosm (see below). Following this 5 d CO_2 acclimation period, light

was progressively increased over 2 d to a final light intensity of $90.5 \pm 21.5\,\mu mol\,photons\,m^{-2}\,s^{-1}$. The microbial assemblages were then incubated for 10 d with samples taken at regular intervals (see below) and no further addition of seawater or nutrients. For further details on minicosm setup see Deppeler *et al.* (2018b).

3.2.2 Carbonate chemistry calculation and manipulation

Carbonate chemistry was measured throughout the experiment, allowing the fugacity of CO_2 (fCO_2) to be manipulated to the desired values over the first 5 d of acclimation and then maintained for the remainder of the experiment. Samples were taken daily from each minicosm in 500 mL glass-stoppered bottles (Schott Duran) following the guidelines of Dickson *et al.* (2007), with sub-samples for dissolved inorganic carbon (DIC, 50 mL glass-stoppered bottles) and pH on the total scale (pH_T, 100 mL glass stoppered bottles) gently pressure filtered (0.2 µm) following Bockmon and Dickson (2014). For each minicosm, DIC was measured in triplicate by infrared absorption on an Apollo SciTech AS-C3 analyser equipped with a Li-cor LI-7000 detector calibrated with five prepared sodium carbonate standards (Merck Suprapur) and daily measurements of a certified reference material batch CRM127 (Dickson 2010). DIC measurements were converted to $\mu mol\,kg^{-1}$ using calculated density from known sample temperature and salinity.

Measurements of pH_T were performed using the pH indicator dye m-cresol purple (Acros Organics) following Dickson *et al.* (2007) and measured by a GBC UV-vis 916 spectrophotometer at 25 °C in a 10 cm thermostated cuvette. A syringe pump (Tecan Cavro XLP 6000) was used for sample delivery, dye addition, and mixing to minimise contact with air. An offset for dye impurities and instrument performance (+0.003 pH units) was determined through measurement of pH_T of CRM127 and comparison with the calculated pH_T from known DIC and total alkalinity (TA), including silicate and phosphate. Salinity was measured in situ using a WTW197 conductivity meter and used with measured DIC and pH_T to calculate practical alkalinity (PA) at 25 °C, using the dissociation constants for carbonic acid determined by Mehrbach *et al.* (1973) and Lueker *et al.* (2000). Total carbonate chemistry speciation was then calculated for in situ temperature conditions from measured DIC and calculated PA.

During the acclimation period, the fCO_2 in each minicosm was adjusted daily in increments until the target level was reached, after which fCO_2 was kept as constant as possible for the remainder of the experiment. Twice-daily measurements of pH were performed in the morning (before sampling) and the afternoon using a portable, NBS-calibrated probe (Mettler Toledo) to determine the amount of DIC to be added to the minicosm. Adjustment of the fCO_2 in each minicosm was performed by addition of a calculated volume of 0.2 µm filtered CO_2-saturated natural seawater to 1000 mL infusion bags and drip-fed into the minicosms at ∼50 mL min^{-1}. One minicosm was maintained close to the fCO_2 of the initial (ambient) sea water (343 µatm) and was used as the control treatment, against which the effects of elevated fCO_2 were measured. The mean fCO_2 levels in the other five minicosms were 506, 634, 953, 1140, and 1641 µatm. For further details of the carbonate chemistry sampling methods, calculations, and manipulation see Deppeler *et al.* (2018b).

3.2.3 Nutrient analysis

Concentrations of the macronutrients nitrate plus nitrite (NOx), soluble reactive phosphorus (SRP), and molybdate reactive silica (silicate) were measured in each minicosm during the experiment. Samples were taken on days 1, 3, and 5 during the CO_2 acclimation period and every 2 days for the remainder of the experiment (days 8-18). Samples were obtained following the protocol of Davidson *et al.* (2016). Briefly, seawater samples were filtered through 0.45 µm Sartorius filters into 50 mL Falcon tubes and frozen at −80 °C for analysis in Australia. Determination of the concentration of NOx, SRP, and silicate were performed by Analytical Services Tasmania, using flow injection analysis.

3.2.4 Flow cytometry

Flow cytometric analyses were performed daily to determine the abundance of small protists (HNF, pico- and nanophytoplankton, and prokaryotes) in each minicosm during the experiment. Samples were pre-filtered through a 50 µm mesh (Nitex), stored in the dark at 4 °C, and analysed within 6 h of collection, following Thomson *et al.* (2016). Samples were analysed using a Becton Dickinson FACScan or FACSCalibur flow cytometer fitted with a 488 nm laser. MilliQ water was

used as sheath fluid for all analysis. The analysed volume for each flow cytometer was calibrated to the sample run time and flow rate and was used to calculate final cell concentrations from event counts on bivariate scatter plots. PeakFlow Green 2.5 µm beads (Invitrogen) were added to samples as an internal fluorescence and size standard.

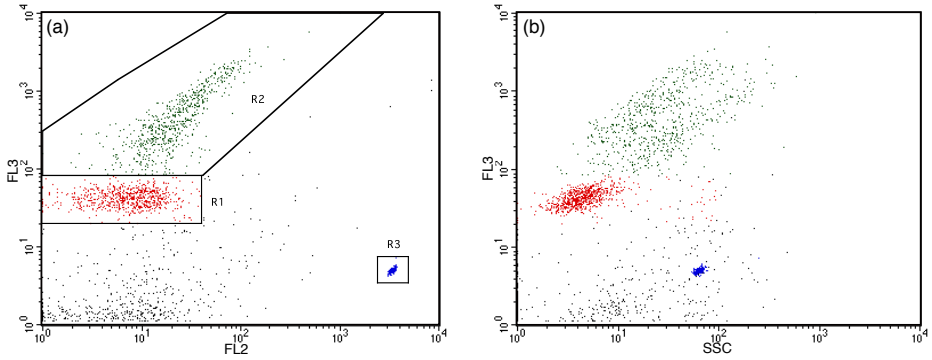

Figure 3.1: Nano- and picophytoplankton regions identified by flow cytometry. (a) Two separate regions identified based on red (FL3) versus orange (FL2) fluorescence scatter plot. (b) Picophytoplankton (R1) and nanophytoplankton (R2) communities determined from side scatter (SSC) versus FL3 fluorescence scatter plot. PeakFlow Green 2.5 µm beads (R3) used as fluorescence and size standard.

Pico- and nanophytoplankton abundance

Three pseudoreplicate 1 mL samples for pico- and nanophytoplankton abundance were prepared from each minicosm seawater sample. Each sample was placed in a beaker of ice and run for 3 min at a high flow rate of $\sim$40 µL min^{-1} for FACScan and $\sim$70 µL min^{-1} for FACSCalibur, resulting in an analysed volume of 0.1172 and 0.2093 mL, respectively. Phytoplankton populations were separated into regions based on their chlorophyll autofluorescence in bivariate scatter plots of red (FL3) versus orange fluorescence (FL2) (Fig. 3.1a). The pico- and nanophytoplankton communities were determined from relative cell size in side scatter (SSC) versus FL3 fluorescence bivariate scatter plots (Fig. 3.1b). Final cell counts in cells L^{-1} were calculated from event counts in the phytoplankton regions and analysed volume.

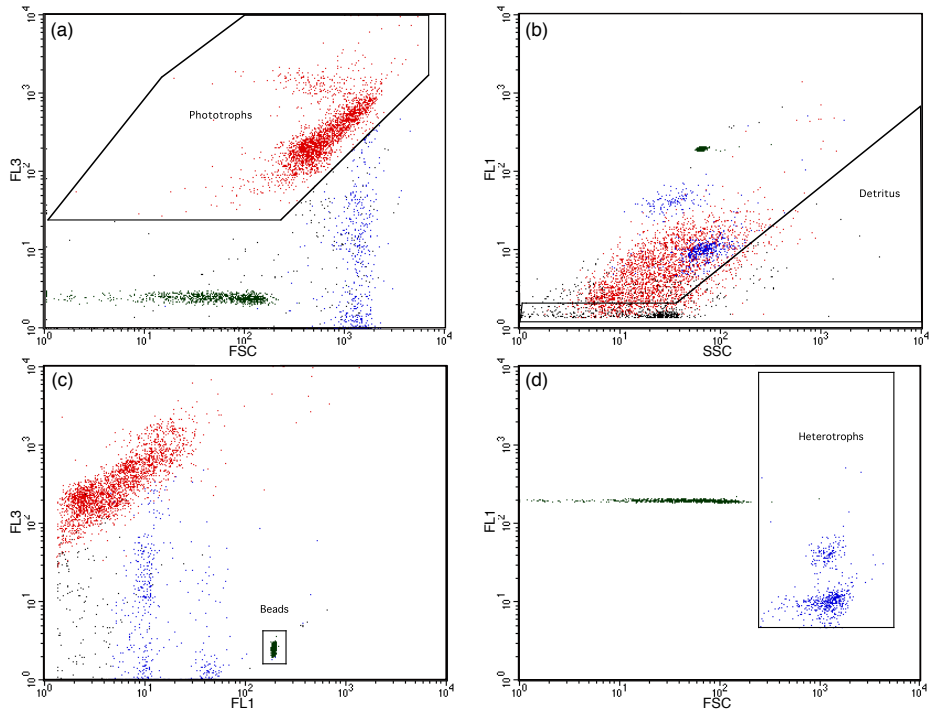

Figure 3.2: LysoTracker Green-stained heterotrophic nanoflagellates identified by flow cytometry. (a) Phytoplankton identified based on red (FL3) versus orange (FL2) fluorescence scatter plots. (b) Detritus particles identified from high side scatter (SSC) versus LysoTracker Green fluorescence (FL1). (c) PeakFlow Green 2.5 µm beads identified from high FL1 versus low red (FL3) fluorescence. (d) Phytoplankton and detritus from (a) and (b) removed from FL1 and forward scatter (FSC) plot and remaining LysoTracker Green-stained particles >2.5 µm were counted as heterotrophic nanoflagellates.

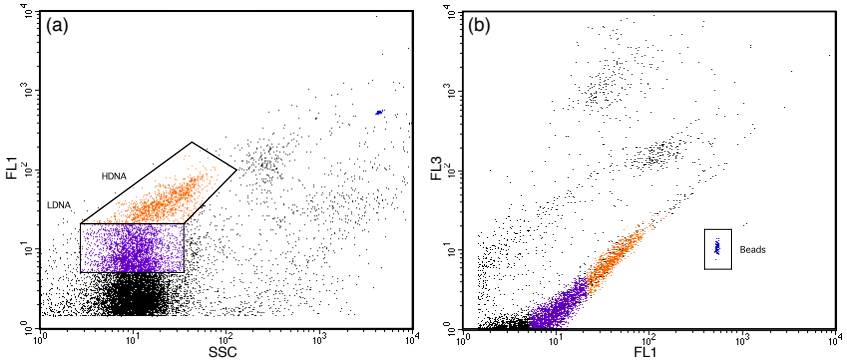

Figure 3.3: Prokaryote regions identified by flow cytometry. (a) SYBR-Green I-stained high DNA (HDNA) and low DNA (LDNA) prokaryote regions identified from side scatter (SSC) versus green fluorescence (FL1) scatter plots. (b) Prokaryote cells determined from high FL1 versus low red (FL3) fluorescence. PeakFlow Green 2.5 µm beads used as fluorescence and size standard.

Heterotrophic nanoflagellate abundance

Heterotrophic nanoflagellate (HNF) abundance was determined using LysoTracker Green (Invitrogen) staining following the protocol of Thomson *et al.* (2016). A 1:10 working solution of LysoTracker Green was prepared daily by diluting the commercial stock into 0.22 μm filtered seawater. For each minicosm sample, 10 mL of seawater was stained with 7.5 mL of working solution to a final stain concentration of 75 nM. Stained samples were then incubated in the dark on ice for 10 min. Triplicate 1 mL sub-samples were taken from the stained sample and run for 10 min at a high flow rate of $\sim$40 μL min^{-1} for FACScan and $\sim$70 μL min^{-1} for FACSCalibur, resulting in an analysed volume of 0.4153 and 0.7203 mL, respectively.

LysoTracker Green stained HNF abundances were determined in green fluorescence (FL1) versus forward scatter (FSC) plots after removal of phytoplankton and detritus particles following Rose *et al.* (2004) and Thomson *et al.* (2016) and shown in Fig. 3.2. Phytoplankton were identified by high chlorophyll autofluorescence in bivariate scatter plots of FL3 versus FL2 fluorescence (Fig. 3.2a) and detritus was identified by high SSC in FL1 fluorescence versus SSC plots (Fig. 3.2b). HNF abundance was then determined in a bivariate plot of FL1 fluorescence versus FSC with phytoplankton and detritus particles removed. Remaining particles larger than the 2.5 μm PeakFlow Green beads were counted as HNF (Fig. 3.2c). Final cell counts in cells L^{-1} were calculated from event counts and analysed volume.

Prokaryote abundance

Samples for prokaryote abundance were stained for 20 min with 1:10,000 dilution SYBR Green I (Invitrogen) following Marie *et al.* (2005). Three pseudoreplicate 1 mL samples were prepared from each minicosm seawater sample and were run for 3 min at a low flow rate ($\sim$12 μL min^{-1}), resulting in an analysed volume of 0.0260 and 0.0491 mL on the FACScan and FACSCalibur, respectively. Prokaryote abundance was determined from SSC versus FL1 fluorescence bivariate scatter plots (Fig. 3.3). Final cell counts in cells L^{-1} were calculated from event counts and analysed volume.

3.2.5 Statistical analysis

Microbial community growth in the minicosms was measured in six unreplicated fCO_2 treatments and thus, sub-samples from individual minicosms represent within-treatment pseudoreplicates. Therefore, means and standard error of these pseudoreplicate samples only provide the within-treatment sampling variability for each procedure. For the purpose of analysis, we treated pseudoreplicates as independent to provide an informal assessment of the difference among treatments. A curved (quadratic) regression model was fitted to each CO_2 treatment over time for all analyses using the *Stats* package in R (R Core Team 2016), with an omnibus test of differences between the trends in CO_2 treatments over time assessed by ANOVA. Growth rates were calculated from linear regression on the region that marked steady-state logarithmic growth and the differences between the trends in CO_2 treatments over time was assessed by ANOVA. For peak abundance measurements, differences between treatments were tested by one-way ANOVA, followed by a post-hoc Tukey test to determine which treatments differed. The lack of replication in our study and limited number of time points at which each minicosm was sampled means that the trends within treatments are indicative and the statistical differences among treatments should be interpreted conservatively. The significance level for all tests was set at <0.05.

3.3 Results

3.3.1 Carbonate chemistry

The carbonate chemistry of the initial seawater was measured as a pH_T and DIC of 8.08 and 2187 $\mu mol\,kg^{-1}$, respectively, resulting in a calculated fCO_2 of 356 μatm and a PA of 2317 $\mu mol\,kg^{-1}$ (Fig. 3.4, A4.1; Table A4.1). Measurements of carbonate chemistry during the acclimation period showed a stepwise increase in fCO_2, after which the CO_2 level remained largely constant, with treatments ranging from 343 to 1641 μatm and a pH_T range from 8.1 to 7.45 (Fig. 3.4; Table 3.1). Some decline in fCO_2 was observed in the high CO_2 treatments towards to the end of the experiment indicating that the addition of CO_2-saturated seawater

was insufficient to fully compensate for its out-gassing into the headspace and drawdown by phytoplankton photosynthesis.

3.3.2 Nutrients

There was little variance in nutrient concentrations among all treatments at the start of the experiment (Table A4.1). Concentrations of NOx fell from $26.20 \pm 0.74\,\mu M$ on day 8 to below detection limits on day 18 (Fig. 3.5a), with the 1641 µatm treatment being drawn down the slowest. SRP concentrations were drawn down in a similar manner as NOx, falling from $1.74 \pm 0.02\,\mu M$ to $0.13 \pm 0.03\,\mu M$ on day 18 in all treatments (Fig. 3.5b). Silicate was replete throughout the experiment in all treatments, with initial concentrations of $60.00 \pm 0.91\,\mu M$ falling to $43.60 \pm 2.45\,\mu M$ (Fig. 3.5c). Silicate draw-down was highest in the 634 µatm and lowest in the 1641 µatm treatment.

3.3.3 Picophytoplankton abundance

Picophytoplankton abundance did not change during the CO_2 acclimation period and remained at $\sim 2.00 \pm 0.02 \times 10^6\,cells\,L^{-1}$. Cell abundance increased in all treatments from day 8, with a significantly enhanced growth rate in the 953 µatm treatment when compared with the control (Table 3.2, 3.3). Abundance peaked on day 12 in treatments $\leq$506 µatm at $5.50 \pm 0.61 \times 10^6\,cells\,L^{-1}$ but continued to rise in treatments $\geq$634 µatm until day 13 (Fig. 3.6a). Despite a faster growth rate in the 953 µatm treatment, peak abundance in this treatment was similar to the 1641 µatm treatment ($7.80 \pm 0.05 \times 10^6\,cells\,L^{-1}$), while the 634 and 1140 µatm treatments peaked at a slightly lower abundance of $6.90 \pm 0.02 \times 10^6\,cells\,L^{-1}$ (Fig. 3.6a). After reaching their peak, cell numbers rapidly declined in all treatments until day 18, falling to $0.80 \pm 0.03 \times 10^6\,cells\,L^{-1}$. The 506 µatm treatment was excluded from analysis on day 18 due to very high background noise on the flow cytometer, resulting in artificially elevated event counts.

Table 3.1: Mean carbonate chemistry conditions in minicosms

Tank	fCO_2 (μatm)	pH_T	DIC (μmol kg^{-1})	PA (μmol kg^{-1})
1	343 ± 30	8.10 ± 0.04	2188 ± 6	2324 ± 11
2	506 ± 43	7.94 ± 0.03	2243 ± 8	2325 ± 10
3	634 ± 63	7.85 ± 0.04	2270 ± 5	2325 ± 12
4	953 ± 148	7.69 ± 0.07	2314 ± 11	2321 ± 11
5	1140 ± 112	7.61 ± 0.04	2337 ± 5	2320 ± 10
6	1641 ± 140	7.45 ± 0.04	2377 ± 8	2312 ± 10

Data are mean ± one standard deviation of triplicate pseudoreplicate measurements

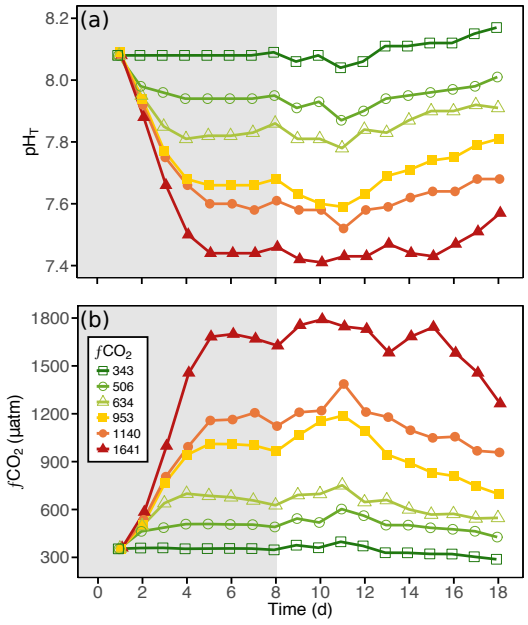

Figure 3.4: The (a) pH on the total scale (pH_T) and (b) fugacity of CO_2 (fCO_2) carbonate chemistry conditions in each of the minicosm treatments over time. Grey shading indicates CO_2 and light acclimation period.

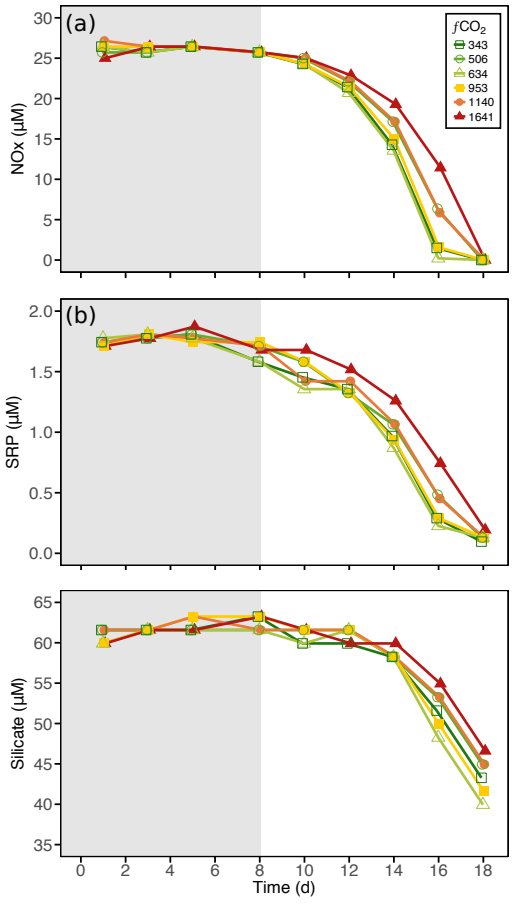

Figure 3.5: Nutrient concentration in each of the minicosm treatments over time. (a) Nitrate + nitrite (NOx), (b) soluble reactive phosphorus (SRP), and (c) molybdate reactive silica (Silicate). Grey shading indicates CO_2 and light acclimation period.

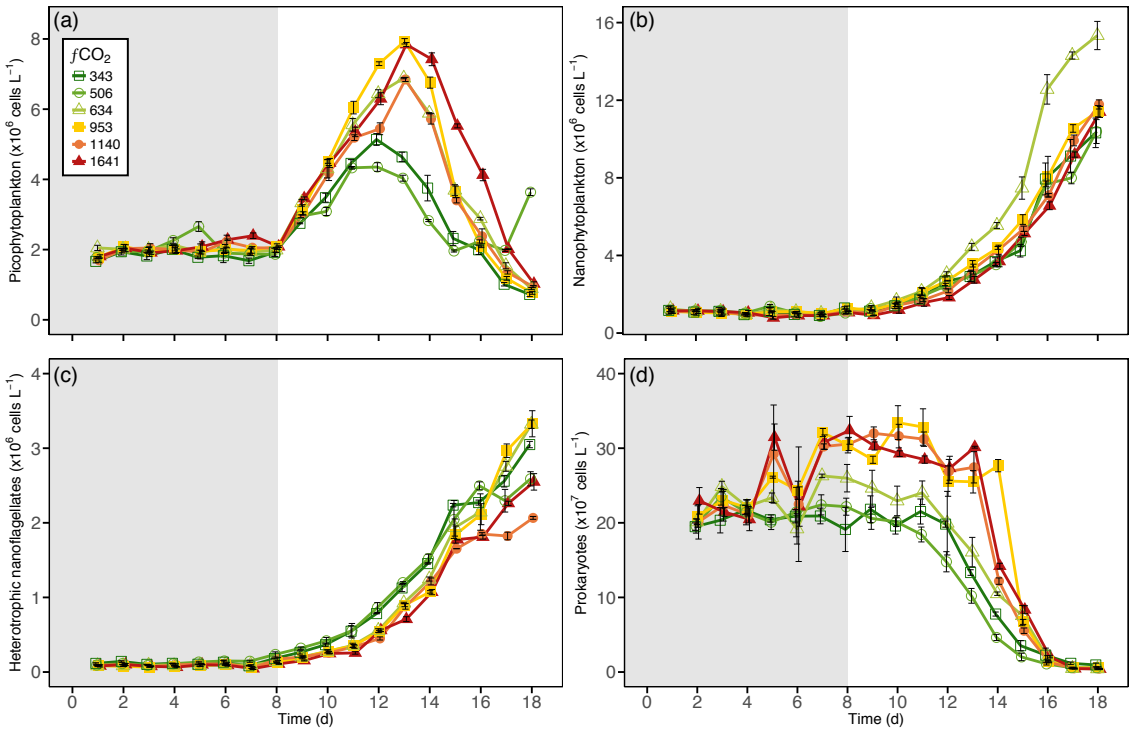

Figure 3.6: Abundance of (a) picophytoplankton, (b) nanophytoplankton, (c) heterotrophic nanoflagellates, and (d) prokaryotes in each of the minicosm treatments over time. Error bars display standard error of pseudoreplicate samples. Grey shading indicates CO_2 and light acclimation period.

Abundance curves for each CO_2 treatment were modelled from days 8 to 18, excluding the acclimation period when no growth occurred. The omnibus test of trends in picophytoplankton abundance among CO_2 treatments over time indicated there was no significant difference among treatments (Table 3.2, A4.2). However, examination of the model fits showed that whilst there was a reasonable fit to the data set (Adjusted $R^2 = 0.82$; Table 3.2), the constraints of limited data meant that the high abundance values between days 12-14 in the treatments $\geq$634 µatm were not well fitted (Fig. A4.2). Despite this, the models did show the general trend of increased abundance in treatments $\geq$634 µatm. Analysis of the differences between peak abundances revealed that CO_2 treatments $\geq$634 µatm reached significantly higher maximum abundances than the control, while the 506 µatm treatment was significantly lower (Fig. 3.7a).

Table 3.2: ANOVA results comparing trends in each CO_2 treatment over time against the control

	F	Adjusted R^2	Day:506 p-value	Day:634 p-value	Day:953 p-value	Day:1140 p-value	Day:1641 p-value
Modelled growth curves							
Pico	$F_{12,182} = 74.6$	0.82	0.38	0.80	0.57	0.76	0.08
Nano	$F_{12,311} = 478.8$	0.95	0.47	**<0.01**	**0.01**	0.10	0.78
HNF	$F_{12,307} = 634.3$	0.96	0.15	0.88	0.99	**<0.01**	**<0.01**
Prok	$F_{12,256} = 131.5$	0.85	0.39	0.49	**<0.05**	**0.04**	0.08
Steady-state growth rate							
Pico	$F_{11,81} = 144.7$	0.95	0.71	0.12	**<0.01**	0.48	0.98
Nano	$F_{11,132} = 611.1$	0.98	0.34	**<0.01**	0.29	**<0.05**	**0.01**
HNF	$F_{11,131} = 518.6$	0.98	**0.02**	0.30	0.32	0.39	**0.02**
Prok	$F_{11,113} = 12.94$	0.51	0.52	0.17	**<0.01**	**<0.01**	**<0.01**

Bold text denotes significant p-values (<0.05). Pico; picophytoplankton, Nano; nanophytoplankton, HNF; heterotrophic nanoflagellates, Prok; prokaryotes.

Table 3.3: Steady-state logarithmic growth rates in CO_2 treatments

	343 µatm	506 µatm	634 µatm	953 µatm	1140 µatm	1641 µatm
Pico	0.25	0.26	0.29	**0.32**	0.23	0.25
Nano	0.26	0.25	**0.32**	0.27	**0.28**	**0.29**
HNF	0.36	**0.32**	0.38	0.37	0.34	**0.40**
Prok	0.00	0.01	0.02	**0.07**	**0.07**	**0.07**

Bold text denotes growth rates significantly different to the control (343 µatm, p <0.05). Pico; picophytoplankton, Nano; nanophytoplankton, HNF; heterotrophic nanoflagellates, Prok; prokaryotes.

3.3.4 Nanophytoplankton abundance

Nanophytoplankton abundance declined during the CO_2 acclimation period in all treatments, falling from a mean initial abundance of $1.20 \pm 0.03 \times 10^6$ cells L^{-1} to $0.90 \pm 0.02 \times 10^6$ cells L^{-1} on day 7. Following acclimation, nanophytoplankton abundance increased in treatments ≤953 µatm until day 18, while treatments ≥1140 µatm remained low through to day 9 before increasing (Fig. 3.6b, A4.3). Analysis of steady-state logarithmic growth rates revealed that growth rates in the 634, 1140, and 1641 µatm treatments were significantly higher than the control (Table 3.2, 3.3). In spite of this, comparison of the trends between modelled abundance curves for each CO_2 treatment indicated that the 634 and 953 µatm treatments were significantly enhanced compared to the control (Table 3.2, A4.3). In the

634 µatm CO_2 treatment, elevated nanophytoplankton abundance was observed from day 12 through to day 18, reaching a final abundance of $15.0 \pm 0.4 \times 10^6$ cells L^{-1} (Fig. 3.6b). Despite lower abundance on days 8-9, enhanced growth rates in treatments ≥1140 µatm led to final abundances similar to the 953 µatm treatment on day 18, reaching $12.0 \pm 0.5 \times 10^6$ cells L^{-1} (Fig. 3.6b, A4.3). The lowest nanophytoplankton abundance on day 18 was in the CO_2 treatments ≤506 µatm, which were $10.0 \pm 0.3 \times 10^6$ cells L^{-1}.

3.3.5 Heterotrophic nanoflagellate abundance

HNF abundance was initially low ($0.90 \pm 0.04 \times 10^5$ cells L^{-1}) and remained at a similar abundance throughout the CO_2 acclimation period. Abundance increased from day 8 in all treatments, but by day 9 was lower in CO_2 treatments ≥634 µatm than ≤506 µatm treatments, at $1.90 \pm 0.08 \times 10^5$ cells L^{-1} and $2.90 \pm 0.18 \times 10^5$ cells L^{-1}, respectively and remained lower until day 15 (Fig. 3.6c). Growth rate analysis between days 8 and 15 revealed that growth rates were significantly slower in the 506 µatm treatment and significantly faster in the 1641 µatm treatment, when compared with the control treatment (Table 3.2, 3.3). From day 15 to 18, the control, 634, and 953 µatm treatments continued to rise, reaching $3.20 \pm 0.07 \times 10^6$ cells L^{-1}, while abundance in the 506 µatm treatment stabilised between days 16 and 18, reaching $2.60 \pm 0.95 \times 10^6$ cells L^{-1}. HNF abundance remained lower than the control in the 1140 and 1641 µatm, reaching abundances on day 18 of $2.10 \pm 0.02 \times 10^6$ and $2.50 \pm 0.11 \times 10^6$ cells L^{-1}, respectively (Fig. 3.6c). The omnibus test among modelled abundance curves for each CO_2 treatment over time indicated that HNF abundance in at least one treatment differed significantly from the control (Table 3.2, A4.4). Examination of the significance of individual curve terms revealed that this reflected the significantly lower abundance of HNF in these two highest CO_2 treatments (1140 and 1641 µatm; Table 3.2).

3.3.6 Prokaryote abundance

Prokaryote abundance increased in CO_2 treatments ≥634 µatm during the acclimation period, with growth rates in treatments ≥953 µatm significantly higher than the control between days 4 and 8 (Table 3.2, 3.3). In contrast, abundance in treatments treatments ≤506 µatm remained

unchanged (Fig. 3.6d). Between days 7 and 11, prokaryote abundance remained steady in all treatments, with abundances in treatments ≥634 significantly higher than the control (Fig. 3.7). During this time, the mean abundance was $3.09 \pm 0.02 \times 10^8$ cells L^{-1} for treatments ≥953 µatm, $2.47 \pm 0.02 \times 10^8$ cells L^{-1} in the 634 µatm treatment, and $2.07 \pm 0.03 \times 10^8$ cells L^{-1} in treatments ≤506 µatm (Fig. 3.6d). After day 12, prokaryote abundance declined in all treatments, falling to $0.60 \pm 0.06 \times 10^7$ cells L^{-1} by day 17.

Prokaryote abundance curves were modelled for each CO_2 treatment from days 4 to 18, excluding days 2 and 3 when no growth occurred. There was no significant difference between CO_2 treatments in the omnibus test among modelled abundance curves (Table A4.5) but curves for the 953 and 1140 µatm treatments differed significantly from the control (Table 3.2). In a similar manner to the picophytoplankton data, the models did not well represent the high values in the treatments ≥953 µatm (Fig. A4.2). Whilst no significant differences were reported for the 634 and 1641 µatm treatments, the general trend in the modelled curves did follow that of the analysis, with increased abundance in all treatments ≥634 µatm.

3.3.7 Microbial community interaction

Although grazing experiments were not performed, the co-occurrence of slowed HNF growth with increased picophytoplankton and prokaryote abundance in CO_2 treatments ≥634 µatm suggests that the picophytoplankton and prokaryote communities were released from grazing pressure. Growth rates of prokaryotes and picophytoplankton were compared with HNF abundance on day 8 and 13, respectively, to examine whether trophic interactions could be inferred. Picophytoplankton had a negative but non-significant trend (Fig. 3.8a; Table A4.6), while prokaryotes displayed a significant negative trend with HNF abundance (Fig. 3.8b; Table A4.7). This suggests that reduced HNF abundance reduced grazing mortality of the picoplankton community. This hypothesis was further supported by the observation that above a threshold HNF abundance there was a rapid decline in both the picophytoplankton and prokaryote abundance, irrespective of treatment and the duration of incubation. For picophytoplankton, this decline occurred when HNF abundance reached $0.84 \pm 0.02 \times 10^6$ cells L^{-1} (Fig. 3.9a) and for prokaryotes it occurred after HNF abundance

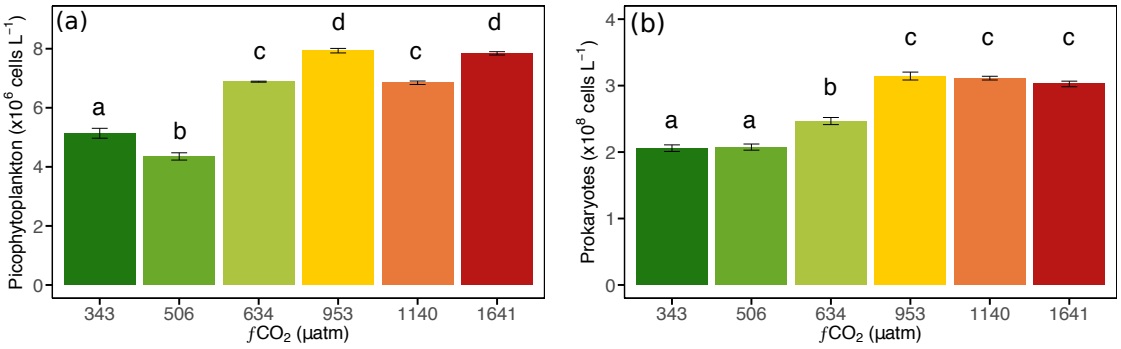

Figure 3.7: Peak abundances of (a) picophytoplankton and (b) prokryotes in each of the minicosm treatments. Letters indicate significantly different groupings assigned by post-hoc Tukey test. Error bars display standard error of pseudoreplicate samples.

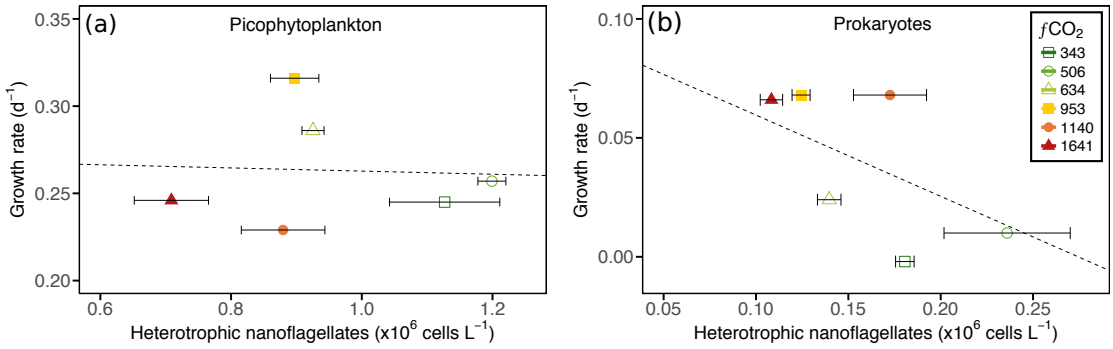

Figure 3.8: Comparison of (a) picophytoplankton (day 13) and (b) prokaryote (day 8) steady-state growth rates against heterotrophic nanoflagellate abundance. Error bars display standard error of pseudoreplicate samples of heterotrophic nanoflagellates. Dotted line indicates linear regression trend (Data in Table A4.6, A4.7).

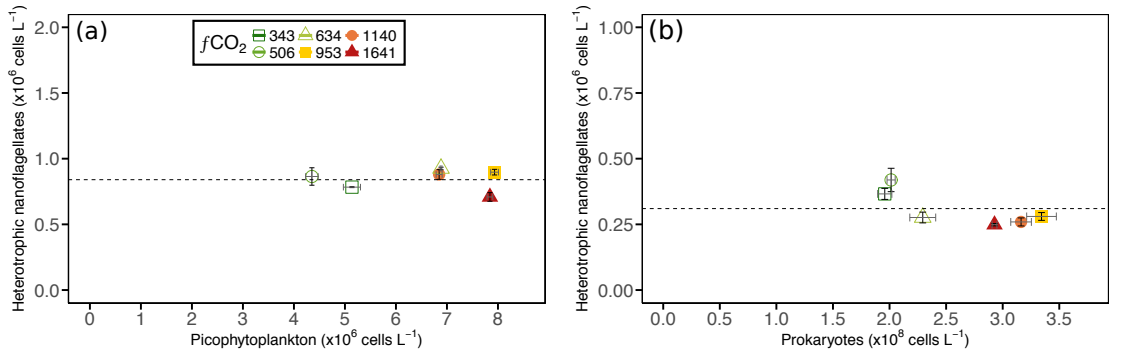

Figure 3.9: Heterotrophic nanoflagellate abundance on the day before (a) picophytoplankton and (b) prokaryote abundance declined in each of the minicosm treatments. Error bars display standard error of pseudoreplicate samples of heterotrophic nanoflagellates (grey) and picophytoplankton/prokaryotes (black). Dotted line indicates threshold of heterotrophic nanoflagellate abundance of (a) $0.84 \pm 0.02 \times 10^6$ cells L^{-1} and (b) $0.31 \pm 0.02 \times 10^6$ cells L^{-1}.

reached $0.31 \pm 0.02 \times 10^6$ cells L^{-1} (Fig. 3.9b). Interestingly, the decline in picophytoplankton and prokaryote abundances in the CO_2 treatments $\geq$634 µatm was greater than the control and 506 µatm treatments. However, this provided no benefit to HNF abundance in these treatments, which never surpassed that of the control (Fig. 3.6c).

3.4 Discussion

Mesocosm experiments are useful in assessing the effects of environmental perturbations on multiple trophic levels of a marine ecosystem (Riebesell *et al.* 2008). Our results suggest that there are both direct effects of elevated CO_2 on nanophytoplankton and indirect effects of trophic interactions occurring between HNF and their picoplanktonic prey that can significantly alter the composition and abundance of organisms at the base of the food web.

Exposing cells to a gradual change in CO_2 during an acclimation period allows cells an opportunity to adjust their physiology to environmental change and may alleviate some of the stress experienced when changes are imposed rapidly (Dason and Colman 2004). However, little is known about the time scales required for the changes in physiology necessary to optimise cellular tolerance of CO_2-induced stress. In addition, acclimating cells over the years to decades anticipated for anthropogenic ocean acidification is unachievable in most experimental designs. Acknowledging these limitations, a gradual increase in fCO_2 over 5 days was included in this study to assess whether acclimation would moderate the previously observed response of Antarctic microbial communities exposed to rapid changes in CO_2 (Davidson *et al.* 2016; Thomson *et al.* 2016; Westwood *et al.* 2018).

The results of the current study were similar to those reported previously (Davidson *et al.* 2016; Thomson *et al.* 2016; Westwood *et al.* 2018) that lacked acclimation. Thus, it appears that an acclimation period had no discernible effect on the response of the community to enhanced CO_2. Hancock *et al.* (2018) did observe a significant change in microbial community composition in all treatments between days 1 and 3 but no further change in community composition was found between any of the treatments during the acclimation. Therefore, they attributed this initial change to acclimation of the community to the minicosm tanks and not a

response to increasing CO_2. This lack of acclimation may be due to ineffectiveness of the acclimation we used or to the highly variable CO_2 experienced by the marine microbial community at the study site. Here, CO_2 levels have been measured to vary by ∼450 µatm throughout the year, with highest CO_2 levels experienced at the end of winter and strong CO_2 draw-down occurring in the Austral summer (Gibson and Trull 1999; Roden *et al.* 2013). Marine organisms exposed to highly variable environments have been shown to be more tolerant of changes in CO_2 (Boyd *et al.* 2016b) and have also been demonstrated in this region (e.g Thomson *et al.* 2016; Deppeler *et al.* 2018b).

It is also possible that the acclimation under low light conditions did not allow the cells to adjust their physiology effectively and that much of the acclimation occurred after the light levels were increased. Indeed, phytoplankton cell health (measured by photochemical quantum yield; F_v/F_m) was high during the low light acclimation period and a CO_2-induced decline in health was only observed when light intensity was increased between days 5 and 8 (see Deppeler *et al.* 2018b). Synergistic effects of CO_2 and light stress have been observed in a number of phytoplankton studies, with declines in growth, productivity, and cell health (F_v/F_m) reported under a combined high CO_2 and light intensity (Gao *et al.* 2012a,b; Li *et al.* 2015; Trimborn *et al.* 2017, e.g.). In our study, the phytoplankton community did appear to acclimate to this light and CO_2 stress, with F_v/F_m increasing in all treatments after day 12 (Deppeler *et al.* 2018b). Consequently, it is likely that the acclimation was either incomplete or ineffective. Despite this, the similarity of our results with those previously reported does allow us to gain a more comprehensive understanding of the seasonal and temporal effects of ocean acidification on the marine microbial community in this region.

3.4.1 Heterotrophic nanoflagellates

Our study indicates that HNF abundance is negatively affected by elevated CO_2. This contrasts with the study by Moustaka-Gouni *et al.* (2016), who found no effect of CO_2 on the HNF community when exposed to levels up to 1040 ppm. As HNF cells are difficult to identify by microscopy in fixed samples (Sherr *et al.* 1993; Sherr and Sherr 1993), we were unable to determine whether the reduction in HNF abundance and differences in growth rates among

treatments were due to CO_2-induced effects on the entire HNF community or if species-specific sensitivities changed the community composition. Hancock *et al.* (2018) reported a CO_2-related change in the relative abundances of two choanoflagellate species at CO_2 levels $\geq$634 µatm (see 4.4 below) and thus, it is possible that other CO_2-induced changes to HNF community composition may have occurred. Previous experiments in Prydz Bay, Antarctica also reported a reduction in HNF abundance when CO_2 was $\geq$750 µatm in both high and low nutrient conditions (Thomson *et al.* 2016). The consistency of these results over the Austral summer and between years suggests that if CO_2 emissions continue to increase at rates similar to the IPCC RCP8.5 projections, the abundance and composition of HNF communities may change around 2050 (IPCC 2013).

Increased top-down control by heterotrophic dinoflagellates and ciliates on the HNF community may have led to the lower abundance of HNF in the high CO_2 treatments. However, this was unlikely as Hancock *et al.* (2018) saw no effect of CO_2 on the composition or abundance of the microheterotrophic community in our study. Few other studies have investigated the effect of ocean acidification on heterotrophic protists and as yet there are no reports of direct effects of elevated CO_2 on microheterotrophic grazing rates, abundance, or taxonomic composition (Suffrian *et al.* 2008; Aberle *et al.* 2013). One study by Rose *et al.* (2009b) did report an increase in microzooplankton abundance when a natural North Atlantic microbial community was exposed to high CO_2 (690 ppm). However, this increased abundance was thought to be an indirect effect of CO_2-induced promotion of phytoplankton abundance and a change in the phytoplankton community composition, as opposed to a direct effect of ocean acidification on microzooplankton physiology.

It is difficult to evaluate the potential reasons for reduced abundance in the HNF community in high CO_2 treatments as the mechanism(s) responsible for CO_2 sensitivity in HNFs are unstudied (Caron and Hutchins 2013). Heterotrophs do not require CO_2 for growth, thus pH is likely the dominant driver of the effects observed (Sommer *et al.* 2015). The CO_2 sensitivity of heterotrophic flagellates may be governed by the effectiveness of the mechanism(s) they possesses to regulate intracellular pH (Pörtner 2008). However, little is known about the pH sensitivities of heterotrophic flagellates. Among the few studies on flagellates, a decline in pH influenced the swimming behaviour of a harmful algal bloom causing raphidophyte (Kim *et al.*

2013) and an inability to control intracellular pH disrupted the growth of the autotrophic dinoflagellates *Amphidinium carterae* and *Heterocapsa oceanica* (Dason and Colman 2004). Disruption of flagella motility has also been observed in marine invertebrate sperm, due to inhibition of the internal pH gradients required to activate signalling pathways (Nakajima 2005; Morita *et al.* 2010; Nakamura and Morita 2012). Whilst these examples do not provide evidence for direct inhibition of HNF growth, they do highlight the diverse sensitivities of flagellates to changes in pH that require further investigation. Size may also play a part in CO_2 sensitivity, with size-related declines in the external pH boundary layer meaning small cells are likely to be more affected by lower ocean pH (Flynn *et al.* 2012). As heterotrophs respire CO_2 and do not photosynthesise, it is likely that pH would be even lower at the cell surface than for autotrophs. This may explain why HNFs showed reduced growth rates in our study while the larger microheterotrophs were unaffected (see Hancock *et al.* 2018).

This study highlights the need for additional research on the nanoflagellate community. There is an increasing understanding of the prevalence of mixotrophy in the marine microbial community (Mitra *et al.* 2014; Stoecker *et al.* 2017; Gast *et al.* 2018). Mixotrophs are able to utilise both autotrophic and heterotrophic methods of energy production and consumption, although the methods employed can be diverse (Stoecker *et al.* 2017). It is currently unknown how mixotrophic phytoflagellates will respond to ocean acidification. Caron and Hutchins (2013) speculated that with an increasing concentration of DIC at increasing levels of CO_2, autotrophic energy production may be more efficient. However, the simultaneous increase in H^+ may have negative effects on both heterotrophic and autotrophic cellular mechanisms, causing multiple stresses to mixotrophic physiology. As molecular methods are allowing for better identification of mixotrophic species (Gast *et al.* 2018), further research into how these species respond to increasing CO_2 may now be possible. Whilst iron was not a limiting factor for phytoplankton in the coastal region studied (Davidson *et al.* 2016), it is a significant driver on the ecology of the marine microbial community in a majority of the Southern Ocean (Martin *et al.* 1990). Iron limitation has been found to lessen the impact of CO_2 on some diatom species, especially in combination with other stressors (Hoppe *et al.* 2013). No studies to date have investigated the effect of ocean acidification on HNF in the iron-limited Southern Ocean, despite their dominance in the microbial community this region (Safi *et al.* 2007). Thus, it is imperative that further study be done.

3.4.2 Nano- and picophytoplankton

A significant increase in picophytoplankton abundance was observed in our study when CO_2 levels were $\geq$634 µatm (Fig. 3.6a). Increased abundance of picophytoplankton has been reported in ocean acidification studies on natural communities around the world (e.g. Brussaard *et al.* 2013; Schulz *et al.* 2013; Biswas *et al.* 2015; Crawfurd *et al.* 2017). In contrast, Antarctic community studies report varying responses to elevated CO_2. Shifts toward larger diatom species have been reported in coastal waters of the Ross Sea (Tortell *et al.* 2008a; Feng *et al.* 2010), while there was no CO_2-induced change to growth or community composition at a site on the Antarctic Peninsula (Young *et al.* 2015). This variability in response among sites in Antarctic waters may be due to factors such as differences in microbial composition or study methods. Picophytoplankton were either not counted (Tortell *et al.* 2008a; Feng *et al.* 2010) or were considered negligible (Young *et al.* 2015) in these studies. The significant increase in picophytoplankton abundance at CO_2 levels $\geq$634 µatm that we report is similar to the findings of Thomson *et al.* (2016) at the same site and using similar methods, indicating that this response is consistent across different seasonal and temporal environments. It has been suggested that increased abundance of picophytoplankton may be due to increases in productivity derived from more readily-available CO_2 at the cell surface, allowing more passive diffusion of CO_2 into the cell, and thus, reduced requirements for energy-intensive carbon concentration mechanisms (CCMs) (Riebesell *et al.* 1993; Paulino *et al.* 2008; Schulz *et al.* 2013; Calbet *et al.* 2014). CCMs were down-regulated in the high CO_2 (1641 µatm) treatment in both small (<10 µm) and large ($\geq$10 µm) cells in our study (Deppeler *et al.* 2018b). We did not observe any increase in primary productivity from CCM down-regulation in this treatment (Deppeler *et al.* 2018b) although, small changes in exponential growth get amplified over time and are difficult to pick up in primary productivity measurements, which are representative for the entire community.

Larger cell surface to volume ratios in small cells, allowing increased nutrient utilisation in nutrient-limited environments, has also been invoked to explain the increased abundance of picophytoplankton with elevated CO_2 (Schulz *et al.* 2013). Size-related differences in growth rates may allow picophytoplankton to establish a bloom faster than larger phytoplankton

species (e.g. Newbold *et al.* 2012). However, this is not seen in nutrient-replete Antarctic waters, where early summer blooms are dominated by large diatoms and *Phaeocystis antarctica* in its colonial life-stage (Davidson *et al.* 2010). It was also not observed in this study, where only the 953 µatm treatment displayed a significantly enhanced growth rate (Table 3.2). Increased rates of nutrient draw-down were observed in the 634–953 µatm CO_2 treatments (Fig. 3.5), suggesting that moderate increases in CO_2 may stimulate phytoplankton growth, but further increases in CO_2 led to significant reductions in primary productivity (Deppeler *et al.* 2018b).

Nanophytoplankton abundance was significantly higher in the 643 and 953 µatm treatments, with significantly increased growth rates in the 634, 1140, and 1641 µatm treatments (Fig. 3.6b; Table 3.2). This was likely due to favourable conditions, including the inhibition of growth of larger phytoplankton species, that allowed nano-sized phytoplankton to thrive at higher CO_2 levels (Hancock *et al.* 2018). The initial decline in nanophytoplankton abundance in all treatments between days 1 and 7 may have been due to acclimation of the community to the mesocosms or grazing by microzooplankton. Increasing light intensity had a temporary inhibitory effect on growth at CO_2 levels $\geq$1140 µatm between days 8 and 9 (Fig. 3.6b), suggesting that the significantly enhanced growth rates in these treatments between days 9 and 15 may have been caused by an increase in relative abundance of more tolerant species. The most abundant nanophytoplankton species present in the minicosms were *Fragilariopsis* spp. and *Phaeocystis antarctica* in it's colonial form (Hancock *et al.* 2018). These species displayed a CO_2-related threshold in dominance around 634 µatm, with a shift from *P. antarctica* to *Fragilariopsis* spp. in the high CO_2 treatments (Hancock *et al.* 2018). Thus, it is likely that relative fitness of both of these species is increased with a moderate increase in CO_2 level, explaining the higher abundance observed at 643 and 953 µatm CO_2. Interestingly, whilst no negative effect of CO_2 was observed on the overall nanophytoplankton abundance, there were very strong species-specific responses to increasing CO_2, resulting in a significant change in community structure (Hancock *et al.* 2018). Increased abundance of *Fragilariopsis* spp. with elevated CO_2 has also been observed in other ocean acidification studies on natural Antarctic microbial communities (Hoppe *et al.* 2013; Davidson *et al.* 2016). Therefore, it is likely that increasing CO_2 will cause the phytoplankton community to shift from a summer community that is currently dominated by large diatoms to one composed of smaller species or

morphotypes of nano- and picophytoplankton.

3.4.3 Prokaryotes

There was a significant increase in abundance of prokaryotes at CO_2 levels $\geq$634 µatm (Fig. 3.6d; Table 3.2). Increases prokaryote abundance with elevated CO_2 was also observed in previous studies at Prydz Bay (Thomson *et al.* 2016), as well as in Arctic mesocosms (Endres *et al.* 2014; Engel *et al.* 2014). Other studies have reported no influence of CO_2 on the prokaryote community (Grossart *et al.* 2006; Allgaier *et al.* 2008; Paulino *et al.* 2008; Newbold *et al.* 2012), suggesting that the prokaryote community will tolerate increasing CO_2 levels (Reviewed in Hutchins and Fu 2017). Like HNF, prokaryotes do not require CO_2 for growth, although it appears they are more resistant to large variations in pH. However, there is evidence that CO_2 may affect prokaryotes by inducing changes in community composition, selecting for more tolerant species or allowing rare species to emerge (Krause *et al.* 2012; Roy *et al.* 2013; Zhang *et al.* 2013; Bergen *et al.* 2016). This may be related to differential responses of phylogenetic groups to maintaining pH homeostasis in either acid and alkaline conditions (Padan *et al.* 2005; Bunse *et al.* 2016). The mechanisms for transporting hydrogen ions (H^+) out of the cell are energetically demanding and may reduce the energy available for growth. Whether these energy demands are increased or decreased with ocean acidification depends upon the different strategies for pH homeostasis employed by individual prokaryote species (Teira *et al.* 2012). In their study, Teira *et al.* (2012) observed a significant increase in growth efficiency with elevated CO_2 in one bacterial strain, although no increase in productivity or abundance resulted. Instead, these changes may affect dissolved organic carbon consumption (Endres *et al.* 2014), with potential impacts on organic matter cycles.

3.4.4 Community interactions

The coincidence of the increase in picophytoplankton and prokaryote abundances with reduced abundance of HNF suggests that these communities were being released from grazing pressure at CO_2 levels $\geq$634 µatm. Grazing rates in East Antarctica are on average, 62% of primary production per day, up to a maximum of 220% (Pearce *et al.* 2010). In addition, >100% of

prokaryote production can be removed by micro- and nanoheterotrophs when Chl *a* concentration and prokaryote abundance is high (Pearce *et al.* 2010). The rapid decline in abundance we observed in picophytoplankton and prokaryotes after 12 days incubation is entirely consistent with the rapid rates of grazing observed in other Antarctic marine microbial communities in this region. In relation to fCO_2, it is reasonable to hypothesise that the lower abundances of these prey sizes in the control and 506 µatm treatments may have been due to stronger top-down control on the community as opposed to a reduction in growth rate. Grazing control of the picophytoplankton community has been proposed in other mesocosm studies to explain both positive (Paulino *et al.* 2008; Rose *et al.* 2009b) and negative (Meakin and Wyman 2011; Newbold *et al.* 2012) changes in picophytoplankton abundance, although they were not confirmed by HNF counts. In our study, the rapid decline in prokaryote abundance coincided with a dramatic increase in choanoflagellate abundance, bactivorous eukaryotes, between days 14 and 16 (Hancock *et al.* 2018). Furthermore, picophytoplankton and prokaryotes in all CO_2 treatments both declined after HNF abundance reached a critical threshold (Fig. 3.9), suggesting that at this point their growth was unable to exceed the top-down control of grazing.

Species-specific differences in the sensitivity of HNF to CO_2 may lead to significant changes in the composition of the picophytoplankton and prokaryote communities. HNF food webs are complex and successional changes in taxa occur during phytoplankton blooms (Moustaka-Gouni *et al.* 2016). In our study, Hancock *et al.* (2018) observed species-specific differences in the CO_2 tolerances of choanoflagellate species, where *Bicosta antennigera* displayed significant CO_2 sensitivity at levels $\geq$634 µatm while other choanoflagellate species (principally *Diaphanoeca multiannulata*) were unaffected. This change in HNF community composition with increased CO_2 did not affect the total prokaryote abundance but may have implications for the prokaryotic community composition through selective grazing. Changes in prokaryote community composition have been observed in other mesocosm studies (Roy *et al.* 2013; Zhang *et al.* 2013; Bergen *et al.* 2016). There is also evidence that different prokaryote phylogenetic groups have preferences for organic substrates produced by different phytoplankton taxa (Sarmento and Gasol 2012), leading to the possibility that future changes in prokaryote community composition could impact organic matter recycling.

As viral abundance was not determined in our study, we cannot exclude viral lysis as an

explanation for the rapid decline in picophytoplankton and prokaryote abundance. Viral lysis can account to up to 25% of daily production, although grazing by micro- and nanoheterotrophs can be twice as high (Evans *et al.* 2003; Pearce *et al.* 2010). In an Arctic mesocosm study, the decline of a picophytoplankton bloom coincided with a large increase in viral abundance (Brussaard *et al.* 2013). However, later in the study, picophytoplankton were heavily grazed by microzooplankton. Bacteriophages are the dominant viruses in the Prydz Bay area (Pearce *et al.* 2007; Thomson *et al.* 2010; Liang *et al.* 2016), with viral abundance displaying no correlation to picophytoplankton (Liang *et al.* 2016). This suggests that viral lysis was unlikely to be the main cause of the decline in picophytoplankton numbers but may have affected the prokaryotes.

3.5 Conclusions

These result of this study show how ocean acidification can exert both direct and indirect influences on the interactions among trophic levels within the microbial loop. Our study reinforces findings in near shore waters off East Antarctica (Davidson *et al.* 2016; Thomson *et al.* 2016) that HNF abundance is reduced when CO_2 is $\geq$634 µatm, irrespective of temporal changes in the physical and biological environment among seasons and years. This likely resulted in a decline in grazing mortality of picophytoplankton and prokaryotes, allowing these communities to increase in abundance. Such changes in predator-prey interactions with ocean acidification could have significant effects on the food web and biogeochemistry in the Southern Ocean. HNF are an important link in carbon transfer to higher trophic levels as they are grazed upon by microzooplankton and thereafter by higher trophic organisms (Azam *et al.* 1991; Sherr and Sherr 2002). Grazing is also a critical determinant of phytoplankton community composition and standing stocks (Sherr and Sherr 2002).

Our results, together with those of Deppeler *et al.* (2018b) and Hancock *et al.* (2018), indicate it is likely that increasing CO_2 will cause a shift away from blooms dominated by large diatoms towards communities increasingly dominated by prokaryotes, nano- and picophytoplankton. Large phytoplankton cells contribute significantly to deep ocean carbon sequestration (Tréguer *et al.* 2018). They are also the preferred food source for higher trophic organisms, especially the Antarctic krill *Euphausia superba* (Haberman *et al.* 2003; Meyer *et al.* 2003; Schmidt *et al.*

2006). *E. superba* have been found to graze less efficiently on phytoplankton cells $<10\,\mu m$ (Quetin and Ross 1985; Kawaguchi *et al.* 1999; Haberman *et al.* 2003). Therefore, a shift to smaller-celled communities will likely alter the structure of the Antarctic food web. Furthermore, increases in prokaryote abundance will likely intensify the breakdown of organic matter in surface waters, further contributing in a decline in the sequestration of carbon from summer phytoplankton blooms into the deep ocean.

Chapter 4

Effect of ocean acidification on the diatom *Lauderia annulata*: comparison between a culture study and a natural assemblage

4.1 Introduction

Approximately 30% of anthropogenic CO_2 is absorbed into the ocean, altering the chemistry of the surface water and causing a decline in pH (Raven and Falkowski 1999; Sabine 2004; Khatiwala *et al.* 2009). This process, termed 'ocean acidification', has already caused an average decline in the global ocean surface pH of 0.1 units since the industrial revolution (Sabine 2004; Raven *et al.* 2005) and may increase further to 0.6 units with continued anthropogenic CO_2 release (Caldeira and Wickett 2003). High latitude regions are particularly vulnerable to ocean acidification due to the higher solubility of CO_2 in these cold water environments (Orr *et al.* 2005; McNeil and Matear 2008). Antarctic continental shelf waters are highly productive and support the abundance and diversity of life in Antarctica (Arrigo *et al.* 2008a). Any CO_2-induced changes in the marine microbial community, which form the base of the Antarctic food web (Azam *et al.* 1991), is likely to affect higher trophic levels and Southern Ocean biogeochemical cycles.

In Antarctic waters, phytoplankton productivity is highly seasonal and is characterised by large summer blooms, dominated by large diatom species and the primnesiophyte *Phaeocystis antarctica* (Smith and Nelson 1986; Nelson *et al.* 1987; Wright *et al.* 2010). These large diatom blooms can be significant carbon sinks and are also the preferred food source for zooplankton (Azam *et al.* 1991; Longhurst 1991; Kawaguchi *et al.* 1999; Honjo 2004; Kirchman 2008). Some studies suggest that an increase in CO_2 will be beneficial for diatoms, as they are CO_2 limited at current oceanic CO_2 concentrations (Riebesell *et al.* 1993; Tortell *et al.* 2008a; McCarthy *et al.* 2012; Trimborn *et al.* 2013; Qu *et al.* 2017). To counter this limitation in available CO_2 for photosynthesis, many phytoplankton species have carbon concentrating mechanisms (CCMs) that actively uptake HCO_3^- into the cell and convert it to CO_2, increasing the concentration of CO_2 at the site of Rubisco (Badger 1994; Colman *et al.* 2002; Giordano *et al.* 2005; Raven *et al.* 2017). CCMs consume energy, and thus an increase in CO_2 will allow cells to down-regulate their CCMs, freeing up additional energy for other metabolic processes, such as growth (Beardall and Giordano 2002). Increased phytoplankton productivity and abundance with increased CO_2 has been reported at CO_2 levels up to $\sim$1000 µatm (e.g. Sobrino *et al.* 2008; McCarthy *et al.* 2012; Wu *et al.* 2014; Taucher *et al.* 2015). Yet the benefit of elevated CO_2 on growth differs among species, which may be due to preferential use of CO_2 or HCO_3^- uptake

mechanisms (Tortell *et al.* 2008b; Trimborn *et al.* 2013).

The effect of increasing CO_2 (and the subsequent decline in pH) on phytoplankton may not only be due to the individual species' ability to manage the decline in pH but instead depend on the entire community response to increased CO_2. This may be due to CO_2-induced changes in the interactions among species, including different rates of growth, nutrient requirements, and interactions with higher trophic levels, such as preferential grazing or reduction in top-down control (e.g. Suffrian *et al.* 2008; Calbet *et al.* 2014; Ullah *et al.* 2018). Studies on natural communities often report changes in community structure with increased CO_2 (reviewed in Schulz *et al.* 2017). Community studies in Antarctic waters have reported that the phytoplankton community is relatively insensitive to CO_2 levels up to ∼800 µatm. However, one study in the Ross Sea observed an increase in diatom productivity and growth rates with CO_2 ∼800 µatm, although this response may have been induced by an addition of uncharacteristically high iron for the site studied (Tortell *et al.* 2008a). There was no change in *P. antarctica* productivity with increased CO_2, suggesting that diatoms may dominate this region with future increases in CO_2. At CO_2 levels above ∼750 µatm studies on East Antarctic phytoplankton communities reported a decline in large diatom growth rates and an increase in picophytoplankton abundance (Thomson *et al.* 2016; Hancock *et al.* 2018). A change in community size, toward smaller cells, is likely to lead to declines in carbon sequestration and less efficient grazing by higher trophic organisms.

The responses of monospecific phytoplankton isolates are seldom compared to their responses within a natural community. In the one ocean acidification comparison study currently published, differing responses were reported (Wolf *et al.* 2018). In order to test this hypothesis, we isolated the large diatom *Lauderia annulata* from an ocean acidification study on a natural Antarctic marine microbial community (see Deppeler *et al.* 2018b; Hancock *et al.* 2018) and exposed it to fCO_2 levels from 276 to 1063 µatm. Growth rate, abundance, and photosynthetic health were assessed during exponential growth to determine whether *L. annulata* displayed sensitivities to CO_2. This response was then compared to the growth reported in the natural community (Hancock *et al.* 2018) to assess whether community interactions modified its response.

4.2 Methods

A monospecific culture of the Antarctic diatom *Lauderia annulata* was isolated from seawater samples taken from an ocean acidification experiment on a natural marine microbial community at David Station, Antarctica (68° 35′ S 77° 58′ E) in December, 2014 (see Deppeler *et al.* 2018b). Cultures were maintained at 2 °C on a 12:12 h light:dark cycle at 33 μmol photons m^{-2} s^{-1} in L1 medium (Guillard 2003), diluted to 1:10 and with a final macronutrient concentration modified to 88.2 μM NO_3^-, 3.62 μM PO_4^{3-}, and 21.2 μM SiO_3^{2-}. This diatom species was chosen for this study as it was easily identifiable in the natural community study so the data could be directly compared to those reported by (Hancock *et al.* 2018). In addition, this species, at ∼55 μm diameter, was a good representation of large centric diatoms. Large diatoms are an important ecological group in Antarctic waters, significantly contributing to the intense phytoplankton blooms that support the Southern Ocean food web and sequestration of carbon to the deep ocean (Smetacek 1985).

4.2.1 Experimental set up

The experimental system was set up as a modified version of the trace-metal clean incubator system described by Hoffmann *et al.* (2013). As *L. annulata* was isolated from iron-replete waters and subsequently cultured in high nutrient media, this system was not maintained as trace-metal clean. Twelve 2 L polycarbonate bottles (Nalgene) were used as incubation vessels, with an additional four polycarbonate bottles (header tanks) used to replenish the medium in the incubation vessels. The bottle lids were modified with ports for CO_2 delivery, sample removal, media replenishment, and automated pH testing (not used) (Fig. 4.1). Due to technical issues, pH was tested manually (see below) and thus, this port was blocked to avoid external contamination during the experiment. Bottles were washed in 10% HCl (AnalaR, VWR) for 48 h, thoroughly rinsed with MilliQ water, and rinsed with 0.2 μM filtered seawater before use. All tubing and equipment was cleaned with 80% ethanol, rinsed with MilliQ water, and dried in a sterile laminar flow cabinet before use.

The experimental system was set up in a refrigerated cabinet set to 0.5 ± 0.5 °C (see Fig. 4.2).

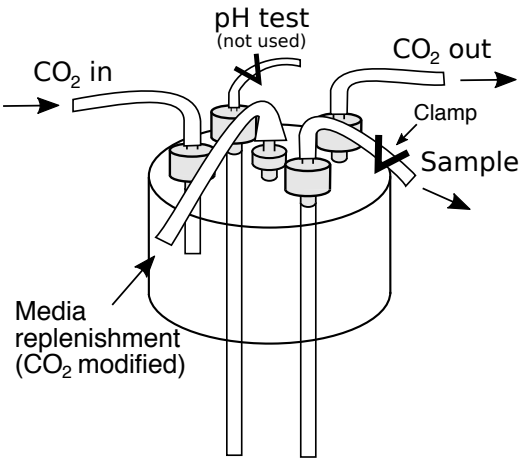

Figure 4.1: Schematic of incubator vessel lids.

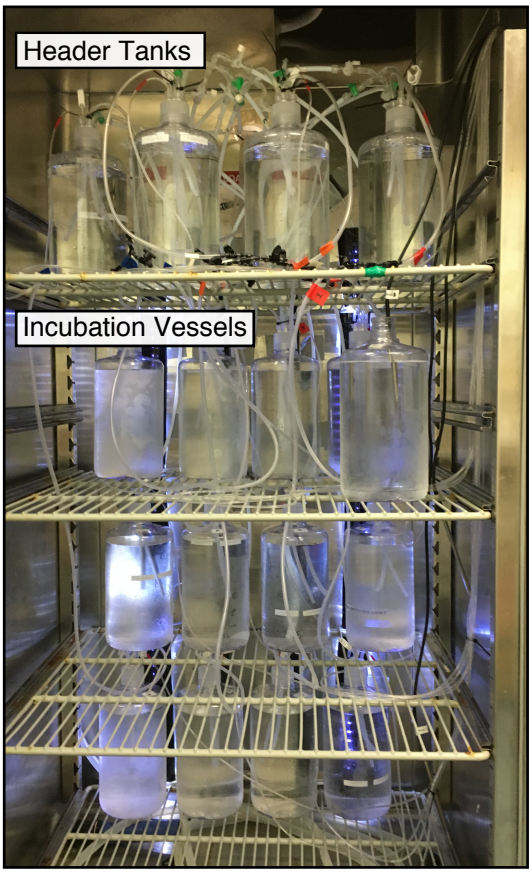

Figure 4.2: Photo of experimental system set up in refrigerated cabinet. Each CO_2 treatment was randomly assigned to one header tank and three incubation vessels. CO_2 treatment designations are shown in Table A5.1. Mixed-CO_2 gas humidification apparatus not shown.

Header tanks for each CO_2 treatment were placed on the top shelf, with incubation vessels placed in rows of four on the remaining shelves. All bottles were filled with 2 L modified 1:10 diluted L1 media (see above) and the 12 incubation vessels inoculated with *L. annulata*, giving a final cell concentration of $1.0 \pm 0.8 \times 10^4$ cells L. Triplicate CO_2 treatments were randomly assigned to incubation vessels using a random number generator (https://www.randomizer.org/) and are detailed in Table A5.1. Incubation vessels were connected to their appropriate CO_2 treatment header tanks with Teflon tubing and media replenishment was controlled by in-line polycarbonate stop-cocks. Lighting was provided by four 1 m waterproof LED light strips (containing 60 5050 SMD cool white LEDs, Jaycar) attached in vertical strips to the back of the cabinet, with light provided on a 19:5 h light:dark cycle. The light output was converted to a daylight spectral distribution by covering with a one

quarter colour temperature blue filter (Arri). Light intensity was measured using a Biospherical Instruments' Laboratory Quantum Scalar Irradiance Meter (QSL-101).

The CO_2 levels were modified by blowing different mixtures of compressed air and CO_2 over the air/water interface in the incubation vessels. The amount of 99.9% CO_2 gas (food grade, BOC) added to the air stream was adjusted to four target CO_2 levels between 400 and 1500 ppm (Table 4.1) using Horiba mass flow control units, with the amount of CO_2 in the mixed gas stream measured using a LICOR LI-820 CO_2 Gas Analyser. CO_2 levels in the mixed gas stream were checked daily and if necessary, adjustments were made to the flow control units to maintain target levels.

After mixing, the CO_2-modified gas was delivered through silicon tubing and entered the incubation vessels through a port in the lid (Fig. 4.1). To minimise condensation in the gas lines, the CO_2-modified gas was cooled and humidified by bubbling through MilliQ water at 0.5 °C and then passed through a condensation trap. The CO_2-modified gas was then passed through a sterile 45 mm GF/F filter (Whatman) to remove airborne contaminants. Inside the bottle the tube was fitted with a length of low-density polyethylene (LDPE) tube positioned ∼1 cm above the surface such that the flow of gas agitated the surface of the media. Even distribution of CO_2 was ensured through gentle manual swirling of the bottles once a day. The four mixed CO_2 gasses were also used to bubble the contents of the header tanks so that the medium used to replenish the experimental bottles was adjusted to the required CO_2 level for each treatment.

4.2.2 Experimental conditions

The experimental conditions for the current study were set up to mimic those of a previous ocean acidification study on a natural Antarctic marine microbial community (see Deppeler *et al.* 2018b; Hancock *et al.* 2018). The CO_2 concentration in each incubation vessel was increased over 5 d under low light intensity, to limit growth during this acclimation period. The light intensity was reduced during this time to $0.4 \pm 0.2\,\mu\text{mol photons}\,\text{m}^{-2}\,\text{s}^{-1}$ by adding two layers of 60% attenuating neutral density filters (Arri) over the LED light strips. After the 5 d acclimation period, the light intensity was increased over 2 d by sequentially removing each of the neutral density filters, resulting in a final light intensity on day 7 of

$23.8 \pm 2.7\,\mu mol\,photons\,m^{-2}\,s^{-1}$ that was maintained for the remainder of the experiment (Table A5.2).

After acclimation, cells were grown for a further 10 d in exponential phase until day 18. Unless otherwise specified, samples for analysis were taken on days 2, 8, 11, 14, 16, and 18. Samples were taken from each incubation vessel with a 60 mL syringe connected to C-flex tubing (Cole-Parmer) that was attached to the sample port on each bottle lid (Fig. 4.1). Inside the lid, a length of LDPE tube was attached that allowed sampling from the middle of the incubation vessel. Before samples were taken for analysis, incubation vessels were mixed by gentle swirling (see above) and 5 mL of the culture was dispensed and discarded from the incubation vessel to flush the internal LDPE sample tubing and syringe. Samples for carbonate chemistry were taken first (see below). Following this, 65 mL of the culture was collected in a 100 mL glass Schott bottle for all other analyses and stored in the dark at 4 °C until use. To avoid external contamination of the bottle contents, the sample tubing was securely clamped shut with a plastic tubing clamp (Dynalon) after sampling.

Incubation vessels were topped up to 2 L with 1:10 diluted L1 media from the appropriate CO_2-modified header tank on days 4, 7, 9, 12, 15, and 16. The volumes required to replenish each incubation vessel were used to calculate the dilution of the culture during the incubation. To avoid significant effects on the diatom culture and carbonate chemistry, the maximum volume removed from the bottle before topping up never exceeded 10% of the culture volume (200 mL) and replenishment was always performed after samples were taken for analysis so as not to influence the results.

4.2.3 Carbonate chemistry

Samples for pH on the total scale (pH_T) analysis were collected daily from the middle of all incubation vessels. Samples were collected in 10 mL glass Exetainer vials (Labco), flushed with sample, capped without headspace to avoid outgassing of CO_2. Samples were stored at room temperature in the dark and analysed within 8 h of collection. pH_T was measured spectrophotometrically (Mettler Toledo UV5) in a 10 mm cuvette using the pH indicator dye m-cresol purple (mCP, Sigma) following Dickson *et al.* (2007). Briefly, sample vials were

warmed to 25 °C in a water bath and transferred to a cuvette with gentle filling from the bottom and flushing with 2x sample volume. Absorbance of the cuvette plus seawater was measured at 434, 578, and 730 nm. Following this, 100 µL of mCP dye was added and the cuvette gently inverted twice to mix. Absorbance of the cuvette plus dyed seawater was measured at 434, 578, and 730 nm and the sample temperature taken with an AA Dailymate digital stick thermometer (±0.1 °C) immediately after analysis. Final absorbance values were corrected for background absorbance (730 nm) and used to calculate the absorbance ratio (A_{578nm}/A_{434nm}). The pH_T of the seawater was calculated following the equations in Dickson *et al.* (2007).

Samples for dissolved inorganic carbon (DIC) analysis were collected from all test containers on all sampling days plus day 4 (see above) in 10 mL glass Exetainer vials, flushed with sample and capped without headspace to avoid CO_2 off-gassing. Samples were poisoned with 5 µL saturated $HgCL_2$ (0.02% v:v final concentration) and stored in the dark at 4 °C until analysis. DIC was analysed by infra-red absorption on an Apollo SciTech AS-C3 analyzer equipped with a LICOR LI-7000 detector. The instrument was calibrated by generating a standard curve from a CRM sample (batch 144) of known DIC concentration (Dickson 2010) at 0.65, 0.75, and 0.85 mL sample volume. For each test sample, the peak area of three 0.75 mL subsamples were analysed to calculate the DIC concentration. Measured DIC was converted to $\mu mol\,kg^{-1}$ using density derived from temperature (25 °C) and salinity (35).

Total carbonate chemistry speciation was calculated and adjusted to the *in situ* temperature (0.5 °C) using CO2calc 1.3.0 (Robbins *et al.* 2010) from measured pH_T, DIC, and *in situ* salinity using carbonic acid dissociation constants from Lueker *et al.* (2000). The mean calculated total alkalinity (TA) for all sample days ($2399\,\mu mol\,kg^{-1}$) was then used for all additional pH_T measurements (all days excluding sample analysis days, see above) to adjust pH_T to *in situ* temperature and calculate fCO_2.

4.2.4 Cell abundance

On each sampling day 10 mL of culture was taken for determination of cell abundance by flow cytometry. Flow cytometry analysis was performed following Marie *et al.* (2005). Samples were stored in the dark at 4 °C, and analysed on a Becton Dickinson FACScan flow cytometer fitted

with a 488 nm laser within 6 h of collection. Samples (1 mL) were prepared from each incubation vessel and run for 5 min at a high flow rate of $\sim$40 µL min^{-1} with MilliQ water was used as sheath fluid. Phytoplankton cells numbers were identified from bivariate scatter plots of red chlorophyll fluorescence (FL3) versus orange fluorescence (FL2). PeakFlow Green 2.5 µm beads (Invitrogen) were added to the sample as an internal fluorescence and size standard. Samples were weighed to $\pm$0.0001 g before and after each run to determine the analyte volume. Final cell counts in cells L^{-1} were calculated using event counts and volume.

4.2.5 Chlorophyll *a*

Samples for Chl *a* concentration were filtered onto 24 mm GF/F filters (Whatman), folded in half, blotted dry, and stored at $-$135 °C until analysis. Chl *a* extractions were performed in 100% methanol following a modified method of Arar and Collins (1997). Chl *a* was extracted from filters by addition of 10 mL of 100% methanol, sonication for $\sim$1 min and incubation at $-$20 °C in the dark for 24 h. Samples were then centrifuged for 15 min at 4000 g in a refrigerated centrifuge at $-$9 °C. The supernatant was transferred to 15 mL polyethylene tubes and 5 mL of the extract was pipetted into a clean 12x100 mm glass tube and allowed to come to room temperature before analysis. Chl *a* concentration of each sample was measured with a Turner 10-AU-005-CE fluorometer, using the acidification technique. The instrument was first standardised against 100% methanol. The fluorescence of the Chl *a* extract was then measured, the sample acidified with 0.15 mL of 0.1 N HCl, thoroughly mixed, incubated in the dark at room temperature for 90 s, and the fluorescence of Chl *a* remeasured. The concentration of Chl *a* was calculated using the equations of Arar and Collins (1997) and an acid ratio of 2.1.

4.2.6 Primary productivity

On each sampling day 25 mL of culture was taken for determination of primary productivity. Incubations were performed following a modified method of Deppeler *et al.* (2018b), based on the small bottle technique of Lewis and Smith (1983). Due to limitations in sample volume, productivity was only measured at high light and in the dark. For all incubation vessels, 50 µL of 0.25 mCi mL^{-1} ^{14}C-sodium bicarbonate (NaH$^{14}CO_3$, PerkinElmer) was added to 25 mL of

sample to make a working solution of 39.2 kBq mL^{-1}. Seven mL aliquots were added to two glass scintillation vials and incubated at 66.5 µmol photons m^{-2} s^{-1} (light) and 0 µmol photons m^{-2} s^{-1} (dark) for 1 h at 0 °C. The reaction was terminated by the addition of 250 µL of 6 N HCl and the vials were shaken for 3 h at 150 rpm to remove dissolved inorganic carbon. A time zero sample was also set up for each incubation vessel to determine background radiation in a similar manner as above, with the immediate addition of 250 µL HCl to quench the reaction without exposure to light. The activity of the working solution was determined by adding 100 µL of working solution to 7 µL 0.1 M NaOH in filtered seawater to capture all added ^{14}C. For all samples, 10 mL Ultima Gold LLT scintillation cocktail (PerkinElmer) was added to each scintillation vial, shaken, and decays per minute were counted in a PerkinElmer Tri-Carb 2910TR Low Activity Liquid Scintillation Analyzer with a maximum counting time set at 5 min. Decays per minute were converted into primary productivity following the equation of Steemann Nielsen (1952), using measured DIC concentrations and normalised to Chl *a* concentration (see above). The linear regression of the primary productivity in the dark and light treatments for each incubation vessel was calculated, and the rate of *in situ* Chl *a*-specific primary productivity ($csGPP_{^{14}C}$) was calculated at the average light irradiance in each incubation vessel (Table A5.2). Gross primary production rates ($GPP_{^{14}C}$) in each incubation vessel were calculated from $csGPP_{^{14}C}$ rates and Chl *a* concentration (see above).

4.2.7 Photophysiology

On sampling days, 20 mL of sample was taken for analysis of photosynthetic efficiency of Chl *a* fluorescence using a Pulse Amplitude Modulated fluorometer (WATER-PAM, Walz). Samples were aliquoted into two 10 mL tubes and placed at 0 °C, with one tube placed at *in situ* experimental light intensity 25 µmol photons m^{-2} s^{-1} (light-adapted) and the other placed in the dark (dark-adapted), for a minimum of 30 min. The photomultiplier gain was adjusted to 15 to ensure an initial fluorescence between 50–1000 during the growth phase of the experiment.

For the dark-adapted samples, a 3 mL aliquot of sample was added to a quartz cuvette and placed in the WATER-PAM. Minimum fluorescence (F_0) was recorded and then maximum fluorescence (F_m) was determined by application of a saturating pulse of light (intensity

8000 μmol photons m^{-2} s^{-1} for 0.8 s). Maximum quantum yield of PSII (F_v/F_m) was then calculated following the equation in (Schreiber 2004). Dark-adapted samples were run on sampling days between day 8 and 18 only.

Rapid light curves (RLCs) were performed on 3 mL aliquots of light-adapted sample at eight increasing actinic light levels (days 2-4: 5, 7, 11, 17, 25, 39, 58, 89, 113 μmol photons m^{-2} s^{-1} and days 8-18: 25, 39, 58, 89, 133, 190, 265, 438 μmol photons m^{-2} s^{-1}). Each light level was applied for 10 s before application of a saturating pulse of light (intensity 8000 μmol photons m^{-2} s^{-1} for 0.8 s). At each actinic light intensity the light-adapted initial flourescence (F) and maximum fluorescence ($F_{m'}$) values were recorded and used to calculate the effective quantum yield of PSII ($\Delta F/F_{m'}$) following the equation in Schreiber (2004). Relative electron transport rates (rETR) were calculated as the product of $\Delta F/F_{m'}$ and actinic irradiance. RLCs were modelled for each treatment following the equation of Platt *et al.* (1980) in the absence of inhibition using the *Phytotools* package in R (Silsbe and Malkin 2015; R Core Team 2016). The photosynthetic parameters of maximum photosynthetic rate ($rETR_{max}$), maximum photosynthetic efficiency (α), and saturating irradiance (E_k) were derived from the curve fit. RLCs were run on days 2 and 4 during the CO_2 acclimation period, and all sampling days between days 8 and 18.

4.2.8 Statistical analysis

Limitations in the available space in the refrigerated cabinet meant that only one CO_2-modified header tank was used to replenish the media in all incubation vessels for each CO_2 treatment. Following Cornwall and Hurd (2016), we acknowledge that the replicates for each CO_2 treatment must be considered as pseudoreplicates. For the purpose of analysis, we treated replicates as independent to assess the differences between treatments, acknowledging that the means and standard error of these pseudoreplicate samples only provide the within-treatment sampling variability for each procedure. For all analyses, either a linear or curved (quadratic) regression model was fitted to the data between days 8 and 18 to assess the trend in each CO_2 treatment over time using the *Stats* package in R (R Core Team 2016). The difference between the trends in all CO_2 treatments over time was assessed by ANOVA with a significance level set

at <0.05. Due to the limitations of the study design we note that these results must be treated as indicative and interpreted conservatively.

4.3 Results

4.3.1 Carbonate chemistry

The carbonate chemistry of the initial 1:10 diluted L1 media at an *in situ* temperature (0.5 °C) was measured to have a pH_T of 8.2 and a DIC of 2193 $\mu mol\,kg^{-1}$, equating to a calculated fCO_2 of 268 µatm and total alkalinity (TA) of 2384 $\mu mol\,kg^{-1}$ (Table A5.3). The fCO_2 in all treatments increased between days 2 and 8, peaking at 378, 430, 717, and 1199 µatm across the four treatment groups (Fig. 4.3). Despite constant delivery of CO_2 gas to the incubation vessels, drawdown of CO_2 by *L. annulata* photosynthesis caused a steady decline in fCO_2 in all treatments between days 8 and 18. The mean fCO_2 levels in each treatment between days 8 and 18 were 276, 381, 668, and 1063 µatm, respectively (Table 4.1). The additional mean carbonate chemistry conditions for all treatments (pH_T, DIC, and TA) are presented in Table 4.1.

Table 4.1: Mean carbonate chemistry conditions in CO_2 treatments between days 8 and 18

Treatment	Target CO_2 (ppm)	fCO_2 (µatm)	pH_T	DIC ($\mu mol\,kg^{-1}$)	TA ($\mu mol\,kg^{-1}$)
1	400	276 ± 35	8.2 ± 0.05	2203 ± 19	2401 ± 5
2	600	381 ± 24	8.1 ± 0.03	2259 ± 7	2399 ± 5
3	900	668 ± 27	7.8 ± 0.02	2342 ± 3	2403 ± 5
4	1500	1063 ± 65	7.7 ± 0.03	2404 ± 4	2407 ± 8

Data are mean ± one standard error of triplicate measurements.

4.3.2 Cell abundance

Abundance remained low during the CO_2 acclimation and increased in all treatments between days 8-18 (Fig. 4.4a). On day 18, abundance of *L. annulata* was $2.3 \pm 0.3 \times 10^5$ cells L in the 276, 381, and 668 µatm treatments, and $3.2 \pm 0.6 \times 10^5$ cells L in the 1063 µatm treatment. Despite this, there were no significant differences in the abundance of *L. annulata* between treatments

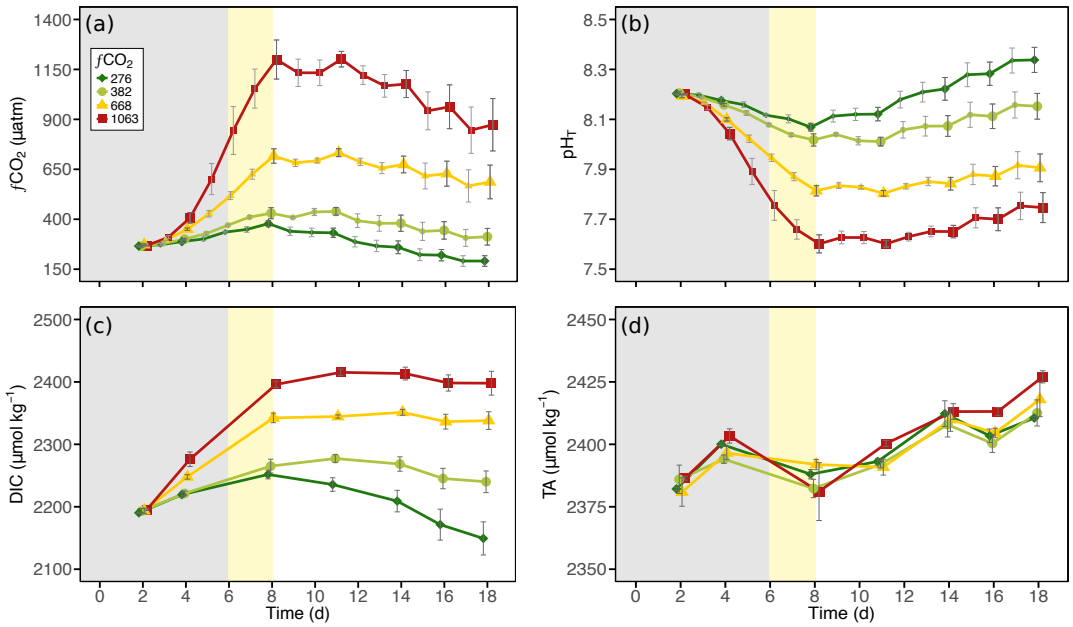

Figure 4.3: The carbonate chemistry conditions for each of the CO_2 treatments over time. (a) Fugacity of CO_2 (fCO_2), (b) pH on the total scale (pH_T), (c) dissolved inorganic carbon (DIC), and (d) total alkalinity (TA). Large points calculated from measured pH_T and DIC. Additional small points calculated from measured pH_T and the mean calculated TA. Error bars display standard error of three pseudoreplicate samples. Shading indicates CO_2 (grey) and light (yellow) acclimation period.

(Table 4.2, A5.4).

4.3.3 Chlorophyll *a*

Chl *a* concentration was low at the beginning of the experiment ($0.29 \pm 0.01\,\mu g\,L^{-1}$) and increased in all treatments after day 8 (Fig. 4.4b). No significant difference was observed in Chl *a* concentration between treatments (Table 4.2, A5.5), with concentrations in all treatments rising to $3.6 \pm 0.4\,\mu g\,L^{-1}$ by day 18.

4.3.4 Primary productivity

At the beginning of the experiment, $csGPP_{^{14}C}$ was similar in all treatments, at $4.2 \pm 0.4\,mg\,C\,(mg\ Chl\ a)^{-1}\,h^{-1}$, and peaked on day 8 (Fig. 4.5a). The 1063 µatm treatment had the highest average $csGPP_{^{14}C}$, reaching $11.7 \pm 1.9\,mg\,C\,(mg\ Chl\ a)^{-1}\,h^{-1}$ on day 8. Between days 8 and 18, $csGPP_{^{14}C}$ declined in all treatments, falling to $3.6 \pm 0.2\,mg\,C\,(mg\ Chl\ a)^{-1}\,h^{-1}$ by

Table 4.2: ANOVA results comparing trends in each CO_2 treatment over time

	F	p
Growth		
Cell abundance	$F_{3,87} = 0.90$	0.44
Chl *a*	$F_{3,62} = 0.65$	0.59
Productivity		
$csGPP^{14}_C$	$F_{3,62} = 0.14$	0.93
GPP^{14}_C	$F_{3,62} = 2.29$	0.09
Photophysiology		
F_v/F_m	$F_{3,51} = 0.81$	0.49
α	$F_{3,51} = 1.95$	0.13
$rETR_{max}$	$F_{3,51} = 0.47$	0.70
E_k	$F_{3,51} = 0.83$	0.48

The data presented is a subset of the full ANOVA tables, which are available in Appendix E.

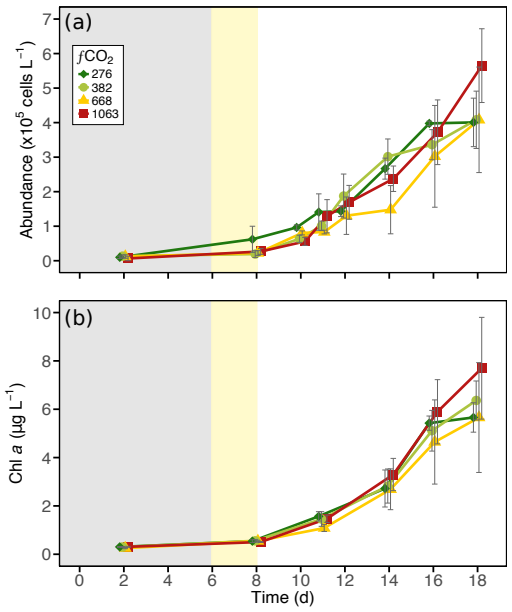

Figure 4.4: The (a) abundance of *Lauderia annulata*, and (b) chlorophyll *a* (Chl *a*) concentration for each of the CO_2 treatments over time. Error bars display standard error of three pseudoreplicate samples. Shading indicates CO_2 (grey) and light (yellow) acclimation period.

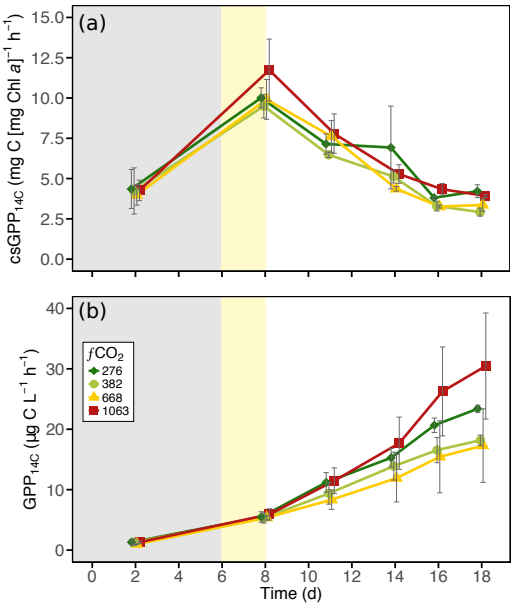

Figure 4.5: The ^{14}C-derived productivity measurements for each of the CO_2 treatments over time. (a) Chl *a*-specific primary productivity ($csGPP^{14}_C$) and (b) gross primary production (GPP^{14}_C). Error bars display standard error of three pseudoreplicate samples. Shading indicates CO_2 (grey) and light (yellow) acclimation period.

day 18.

$GPP_{^{14}C}$ was low in all treatments on day 2 and increased between days 8 and 18 (Fig. 4.5b). The highest average $GPP_{^{14}C}$ was seen in the 1063 µatm treatment on day 18 ($30.5 \pm 15.2\,\mu g\,C\,L^{-1}\,h^{-1}$), although this treatment also showed the highest within-treatment variability. The 668 µatm treatment consistently had the lowest rate of $GPP_{^{14}C}$. This was due to very low productivity in one replicate and as a result, the $csGPP_{^{14}C}$ declined between day 11 and 14, and remained between 3.1–4.2 $mg\,C\,(mg\ Chl\ a)^{-1}\,h^{-1}$ for the rest of the experiment. Despite this, no significant difference was observed between any treatments for both $csGPP_{^{14}C}$ and $GPP_{^{14}C}$ (Table 4.2, A5.6, A5.7).

4.3.5 Photophysiology

The maximum quantum yield of PSII (F_v/F_m) was variable within all treatments on day 8 but stabilised on day 11, with the highest F_v/F_m being in the 276 and 1063 µatm treatments (0.70 ± 0.01 and 0.71 ± 0.03, respectively; Fig. 4.6a). F_v/F_m values declined between days 10-18 but remained above 0.60 in all treatments until day 18. Despite low cell growth and productivity in one 668 µatm replicate (see above), F_v/F_m only declined from 0.71 to 0.57. Again, there was no significant difference between any treatment (Table 4.2, A5.8).

RLCs also demonstrated there was no significant difference in the photosynthetic response among CO_2 treatments (Table 4.2). High variability between days 2-8 in all treatments was likely a result of the low fluorescence values at the beginning of the experiment due to low cell numbers. Maximum photosynthetic efficiency (α) increased between days 2-8, with the 276 µatm treatment the highest on day 8 (0.85 ± 0.05; Fig. 4.6b, A5.9). For the remainder of the experiment, α remained steady at 0.70 ± 0.14 The $rETR_{max}$ declined from 98.7 ± 15.1 on day 8 to 47.0 ± 11.1 on day 18 (Fig. 4.6c, A5.10). Similarly, no significant difference was seen in the saturating irradiance (E_k) among treatments (Table 4.2, A5.11), with the average E_k falling from 134.0 ± 39.7 to 86.1 ± 37.1 µmol photons $m^{-2}\,s^{-1}$ between days 8-18 (Fig. 4.6d).

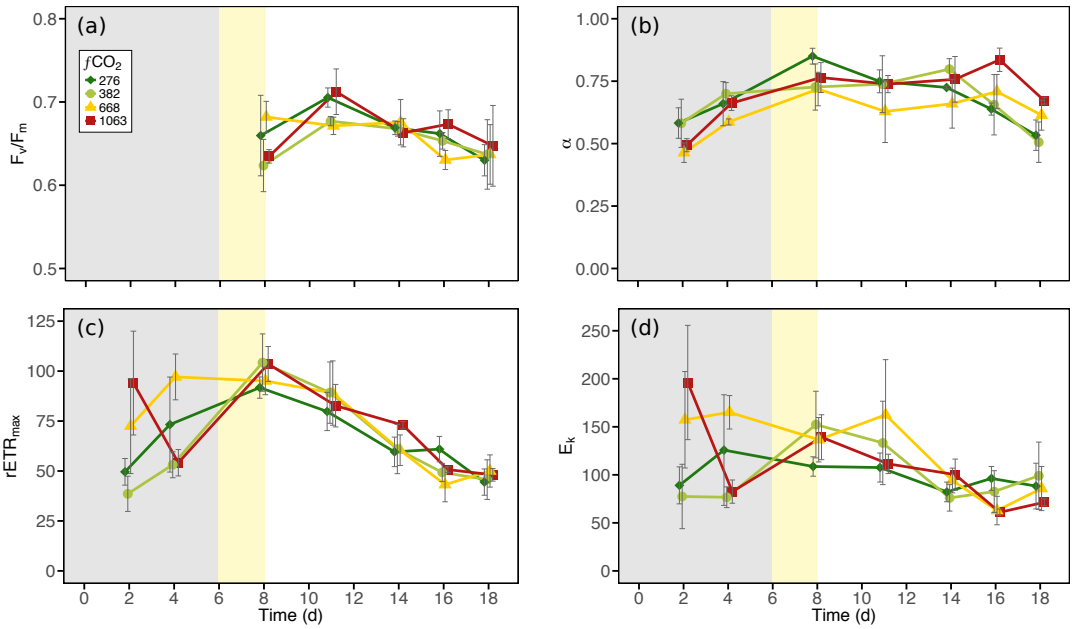

Figure 4.6: The photophysiological measurements for each of the CO_2 treatments over time. (a) Maximum quantum yield of PSII (F_v/F_m), (b) maximum photosynthetic efficiency (α), (c) maximum photosynthetic rate ($rETR_{max}$), and (d) saturating irradiance (E_k). Error bars display standard error of three pseudoreplicate samples. Shading indicates CO_2 (grey) and light (yellow) acclimation period.

4.4 Discussion

This study showed that as a monospecific culture, the large diatom *L. annulata* was insensitive to changes in $f\,CO_2$. Measurements of abundance, primary productivity, and photophysiological health showed no significant difference among $f\,CO_2$ treatments ranging from 276 to 1063 µatm. Tolerance to CO_2 levels up to ~1000 µatm have previously been reported in studies of Antarctic diatoms (e.g Boelen *et al.* 2011; Trimborn *et al.* 2013, 2017) and in natural Antarctic microbial communities (e.g. Tortell *et al.* 2008a; Young *et al.* 2015; Davidson *et al.* 2016). This insensitivity to such a wide range of CO_2 may be, at least in part, due to the large annual range in CO_2 they experience in nature. The *L. annulata* use in this study was isolated from a coastal phytoplankton community in Prydz Bay, Antarctica, a region that experiences high levels of primary productivity during the Austral spring that draws down the $f\,CO_2$ level from ~430 to ~230 µatm (Roden *et al.* 2013), with CO_2 levels as low as 50 µatm recorded (Gibson and Trull 1999). Consequently, the 276 and 381 µatm treatments in this study encompass the natural CO_2 variation that *L. annulata* would be exposed to, demonstrating that it is well adapted to these fluctuations, even when CO_2

is below atmospheric levels.

Tolerance to CO_2 may have been due to down-regulation of CCMs with increasing CO_2. The CO_2 currently available to phytoplankton is below saturating levels for photosynthesis, thus requiring CCMs to increase the concentration of CO_2 in the cell (Riebesell *et al.* 1993; Badger 1994; Giordano *et al.* 2005). CCM activity has been widely demonstrated in phytoplankton at current CO_2 levels (e.g. Burkhardt *et al.* 2001; Colman *et al.* 2002; Tortell *et al.* 2008b; Trimborn *et al.* 2013), including in the community from which *L. annulata* was isolated (Deppeler *et al.* 2018b). It is likely that *L. annulata* operates CCMs, as there was no reduction in growth rate in the CO_2 treatment below current atmospheric concentration (276 µatm). Operation of CCMs requires energy and thus, increasing available CO_2 may allow cells to down-regulate CCM activity and redeploy this energy toward growth or other metabolic processes (Raven 1991). A slight increase in $GPP_{^{14}C}$ was observed in our study at high CO_2 (1063 µatm; Fig 4.5b), which may have been due to down-regulation of CCMs but was not significant and did not affect growth (Fig. 4.4a). For some phytoplankton species, the metabolic cost of operating CCMs is low, so increasing CO_2 has little benefit on growth (Young *et al.* 2015; Goldman *et al.* 2017; Shi *et al.* 2017). Thus, CCM down-regulation may have occurred in *L. annulata* with increasing CO_2 but did not result in increased growth.

It is also possible that CO_2 effects were not observed in our study because *L. annulata* was not exposed to light stress. Light stress can have a synergistic effect with high CO_2, resulting in declines in growth, productivity, and cell health (F_v/F_m) in both monospecific diatom cultures (Li *et al.* 2015; Liu *et al.* 2017; Trimborn *et al.* 2017) and natural phytoplankton communities (Feng *et al.* 2010; Gao *et al.* 2012b; Hoppe *et al.* 2017). The mean saturating light intensity (E_k) we determined for *L. annulata* (102 µmol photons m^{-2} s^{-1}) was over 4-fold higher than the irradiance received during incubation (23.8 ± 2.7 µmol photons m^{-2} s^{-1}). Additionally, minimal change in α and E_k in all treatments over time suggests that *L. annulata* had reached its lower limit for light acclimation. Beardall and Giordano (2002) proposed that at low light intensity, the energy requirement for efficient operation of CCMs may not be met, resulting in a reduction in CO_2 entering the cells. Thus, CCM down-regulation with enhanced CO_2 may stimulate growth under these conditions. Some diatom species have displayed increased growth under low light and high CO_2 conditions (McCarthy *et al.* 2012; Li *et al.* 2017b) but others show no

effect (Liu *et al.* 2017) or reduced growth (Ihnken *et al.* 2011; Passow and Laws 2015) under similar conditions. The growth rate of *L. annulata* did not change across all CO_2 levels, indicating a low energy requirement for CCM operation that was not limited by the experimental light conditions. Alternatively, low light intensity may have reduced the metabolic demands of light stress, such as photoinhibition and PSII repair, which can be exacerbated by increasing CO_2 (Wu *et al.* 2010; McCarthy *et al.* 2012; Li *et al.* 2015).

A lack of persistent mixing in the incubation vessels may have been responsible for the absence of CO_2 effects. Throughout this study, CO_2 modification occurred at the surface of the seawater media, while *L. annulata* would settle on the bottom. However, the passage of mixed-CO_2 air over the surface would have likely elicited some mixing of the CO_2-adjusted surface water within the contents of the incubation vessels. High productivity by *L. annulata* may have increased the pH in the boundary layer around the cells, buffering them from the lower pH media above and relieving them of pH stress (Chrachri *et al.* 2018). In order to avoid establishment of a pH gradient, each vessel was thoroughly mixed daily before samples were taken, thus measurements of primary productivity and photophysiology were always performed at the reported CO_2 levels. There was no difference in the response to CO_2 between these measurements and *in situ* growth and Chl *a* results, indicating that mixing did not change *L. annulata's* response to CO_2. Some studies use CO_2 gas bubbling to both modify the CO_2 and ensure adequate mixing of cultures (Rost *et al.* 2008; Gattuso *et al.* 2010). This method may be detrimental to cells (Shi *et al.* 2009) and as such, was avoided in this study. Space limitations in the cabinet used for this experiment precluded the use of stirring plates or shakers to provide continuous gentle mixing of the culture vessels. However, we acknowledge that using a method that enabled more frequent mixing of the incubation vessel's contents would be recommended.

The response of *L. annulata* in monospecific culture to increasing CO_2 differed when compared the its response in a natural community at Davis Station, Antarctica. *L. annulata* was isolated from the control (343 μatm) treatment of a study investigating the response of a natural Antarctic marine microbial community to ocean acidification (Deppeler *et al.* 2018b). This allowed comparison of the growth response of this species to CO_2 in the natural community to that in the monospecific culture. This comparison showed differences between the monospecific and community-level studies of this taxon. In the community study, *L. annulata* growth was

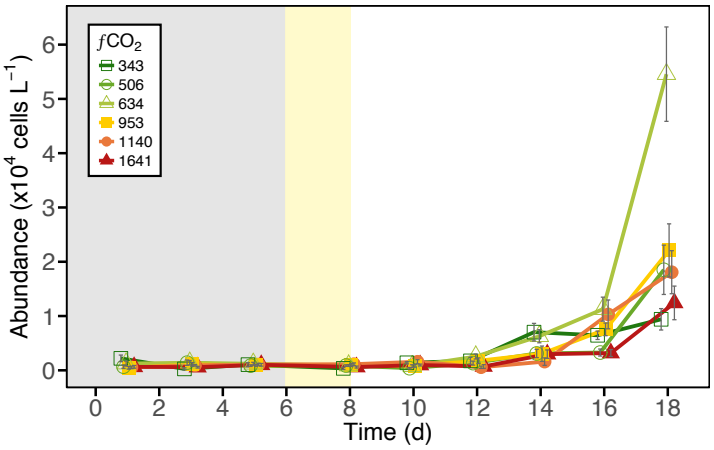

Figure 4.7: The abundance of *Lauderia annulata* in six increasing CO_2 treatments, reported in a community-level ocean acidification study. Error bars display standard error of pseudoreplicate samples. Shading indicates CO_2 (grey) and light (yellow) acclimation period. Modified from Hancock *et al.* (2018).

promoted at CO_2 levels between 506 and 1140 µatm (Fig. 4.7) (Hancock *et al.* 2018). Increasing CO_2 further to 1641 µatm reversed the stimulatory effect of CO_2, with final abundance similar to the control (343 µatm) (Hancock *et al.* 2018). In contrast, there was no effect of increasing CO_2 on *L. annulata* growth in a monospecific culture. The difference in response between the culture and community study suggests that there were factors other than CO_2 that affected the growth of this species. There were differences in light intensity between the two experiments, with a lower mean light intensity in the current study (23.8 ± 2.7 µmol photons m^{-2} s^{-1}), compared to the community study (90.5 ± 22.0 µmol photons m^{-2} s^{-1}) (Deppeler *et al.* 2018b). As discussed above, this difference in light intensity may have led to differing responses between the two studies, where increased light intensity may have stimulated productivity at moderate CO_2 levels but may have had negative effects by increasing stress responses at high CO_2. There is also evidence to suggest that community interactions, such as the starting community composition have a significant effect on the response of individual species to CO_2 (Eggers *et al.* 2014; Sampaio *et al.* 2017) and that competition among some species is dependent upon their initial abundance (Trimborn *et al.* 2013). Community studies are also likely to incorporate additional environmental stressors, such as nutrient limitations and grazing interactions that are absent in controlled culture assays (e.g. Suffrian *et al.* 2008; Rossoll *et al.* 2013; Calbet *et al.* 2014; Bach *et al.* 2016; Ullah *et al.* 2018). Therefore, while culture studies are very useful for evaluating specific

cellular responses to stress, these outcomes are likely to be confounded by environmental variations and community interactions that occur in the real world.

Genetic changes from extended monoclonal culturing may modify the response of phytoplankton to environmental stressors, such as increasing CO_2. Established culture lines may be maintained in the laboratory for many years, even decades, under nutrient, light, and temperature conditions that are different from the ecosystem they were isolated from. Thus, over time these phytoplankton cultures are likely to adapt to the culture conditions they are exposed to (Lakeman *et al.* 2009). A modelling study by Lynch *et al.* (1991) revealed that substantial genetic changes could occur in monoclonal cultures within a few hundred days pushing the fitness of the cultured species away from the natural population. The *L. annulata* used in this study was isolated 3 years previous to this study so it is likely that genetic changes had occurred. In order to minimise adaptation to abnormal conditions, cultures were maintained at low temperature (2 °C), low light intensity on a diel light cycle (33 µmol photons m^{-2} s^{-1} on a 12:12 h dark:light cycle), and in media that contained nutrient concentrations close to those measured in Prydz Bay (see Roden *et al.* 2013; Deppeler *et al.* 2018b). Additionally, *L. annulata* was isolated from the control treatment of the natural ocean acidification study, so it was not previously exposed to artificially elevated levels of CO_2. However, it can not be ruled out that the observed CO_2 response in this study was influenced by genetic changes to the culture over time.

4.5 Conclusions

We chose a large diatom to study because of its ecological relevance in this region. Large phytoplankton support the Southern Ocean food web and can be sources of significant carbon sequestration (Smetacek 1985). A unialgal isolate of *L. annulata* showed that the response of this species was unaffected by exposure to CO_2 levels from present day to those predicted to occur around the end of this century, using the RCP 8.5 scenario (IPCC 2013). Comparison of this study with those of Deppeler *et al.* (2018b) and Hancock *et al.* (2018) show that this insensitivity of *L. annulata* to fCO_2 in culture is replaced by enhanced growth under moderate CO_2 enrichment (506–1140 µatm) when part of a natural community. This indicates that

community-level interactions can influence the response of species to enhanced fCO_2 levels and highlights that monospecific studies are of limited value to predicting future changes in nature as a result of ocean acidification.

Chapter 5

General Discussion

5.1 Discussion

This study suggests that ocean acidification will change the marine microbial community in Antarctic coastal waters, increasing the relative abundance of small diatoms and autotrophic flagellates. Ocean acidification reduced rates of primary productivity, leading to a reduction in phytoplankton biomass and particulate organic matter production. The total abundance of nano-sized (2–20 μm) phytoplankton was not negatively affected by increasing CO_2, suggesting that productivity declines were from larger, micro-sized (20–200 μm) phytoplankton. Similarly, Hancock *et al.* (2018) reported a reduction in micro-sized diatom species at CO_2 levels ≥634 μatm but found that there was a strong species-specific response to elevated CO_2 in the nanophytoplankton community. Increasing CO_2 enhanced the growth of the diatom *Fragilariopsis* spp., while the dominant flagellate, *Phaeocystis antarctica*, was sensitive to CO_2 levels ≥953 μatm (Hancock *et al.* 2018). Despite this significant change in community composition at high CO_2, no reduction in total abundance of nanophytoplankton was observed (Chapter 3). Flow cytometric analyses also showed that the abundance of heterotrophic nanoflagellates (HNFs) was reduced at CO_2 levels ≥634 μatm. This apparently reduced the top-down grazing mortality of picophytoplankton and prokaryotes and allowed their abundance to increase. In contrast, Hancock *et al.* (2018) reported that microzooplankton (ciliates and large heterotrophic dinoflagellates) and autotrophic dinoflagellates appeared to tolerate increased CO_2, although very low abundance of these groups may have concealed any effect. Thus, increasing CO_2 can directly affect microbial growth and physiology, leading to reductions in the abundance of large diatoms and HNF in this region. In addition, it can also indirectly affect the community by altering trophic interactions, favouring increased abundance of picophytoplankton and prokaryotes.

A shift in microbial community structure, favouring the growth of small phytoplankton, will affect biogeochemical cycles in Antarctic coastal waters. Coastal Antarctic waters are areas of high productivity (Arrigo *et al.* 2008a), where summer blooms are dominated by large diatoms and *P. antarctica* (Arrigo *et al.* 1999; Wright and van den Enden 2000; Davidson *et al.* 2010). These blooms draw down the surface CO_2 to as low as ∼50 μatm (Gibson and Trull 1999; Arrigo *et al.* 2008b; Roden *et al.* 2013), making coastal Antarctic regions an important sink for

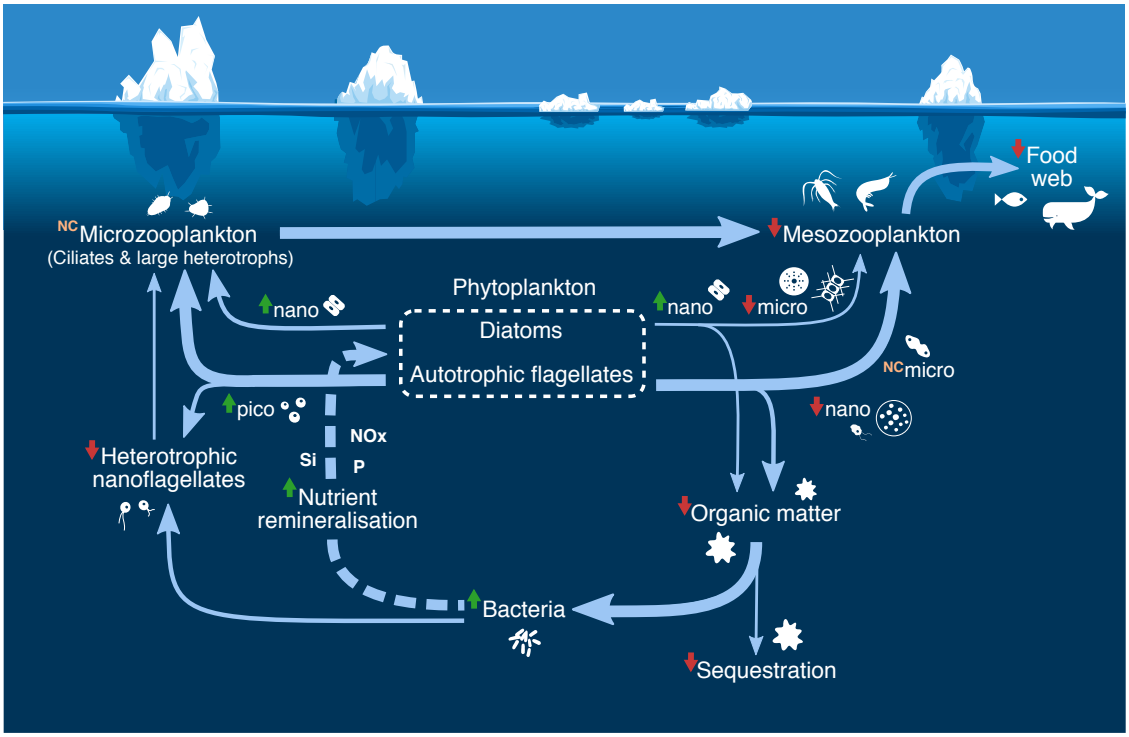

Figure 5.1: Schematic of projected effects of ocean acidification on the microbial loop in Antarctic coastal waters. Blue arrows indicate the predominant interactions and flow of macronutrients and carbon between different protistan groups and biogeochemical cycles in the microbial loop. The thickness of the blue lines indicates the magnitude of these interactions, with the thickest lines signifying the dominant flow. Red and green arrows indicate changes in abundance or concentration of each protistan group and biogeochemical cycle. Red arrows, decreased abundance; green arrows, increased abundance; nc, no change in abundance.

anthropogenic CO_2 (Arrigo *et al.* 2008a,b). Large diatoms contribute substantially to carbon sequestration as they are grazed by the Antarctic krill *Euphausia superba* (krill) (Haberman *et al.* 2003; Meyer *et al.* 2003; Schmidt *et al.* 2006) and reparcelled into large faeces, which rapidly sink to the ocean depths (Smetacek 1985; Schnack-Schiel and Isla 2005). Diatoms that form large chains and have irregular morphology (such as setae) also promote aggregation and entrapment of particles into "marine snow", an essential component of carbon flux (Alldredge and Silver 1988). A reduction in large diatom abundance would therefore reduce the efficiency of the carbon pump (Fig. 5.1). *P. antarctica* blooms can also be responsible for significant carbon export (DiTullio *et al.* 2000), suggesting that a coincident reduction in *P. antarctica* abundance with ocean acidification may further reduce the quantity of carbon sequestered in Antarctic coastal waters. In contrast, small phytoplankton and heterotrophic protists remain in the surface layer and are highly efficient recyclers of carbon and macronutrients, contributing very little to carbon flux (Smetacek *et al.* 1990; Smetacek *et al.* 2004; Tréguer *et al.* 2018). An

increased abundance of smaller-sized phytoplankton would lead to a larger proportion of primary productivity consumed by small grazers, such as microzooplankton and small copepods (Fig. 5.1) (Pearce *et al.* 2010), as krill appear to be more efficient at grazing on phytoplankton >10 μm in size (Quetin and Ross 1985; Kawaguchi *et al.* 1999; Haberman *et al.* 2003). Small grazers produce much smaller faecal pellets that have slower sinking velocities and are more rapidly remineralised by prokaryotes than krill faeces (Smetacek 1985; Turner 2002; Schnack-Schiel and Isla 2005). The increase in prokaryote abundance we observed in high CO_2 treatments due to the inhibition of HNF could increase the rate of remineralisation in the surface layer, although this effect would be mediated by interactions with other bacterivorous protozoa, such as ciliates (Duarte *et al.* 2005). Thus, a shift in community structure toward smaller protists will result in increased cycling of nutrients in surface waters through grazing and remineralisation (Fig. 5.1). Consequently, this will result in a decline in carbon sequestration to the deep ocean, reducing the intensity of the CO_2 sink in coastal Antarctic regions.

Changes in the microbial community toward smaller species will also cause a shift in the dominant flow of energy through less efficient pathways to higher trophic levels. Blooms of diatoms are the preferred food source of krill, a "keystone" species in the Antarctic food web, providing an efficient source of nutrients and fatty acids that are transferred to higher trophic predators, such as penguins, seals, and baleen whales (Murphy *et al.* 1988; Hagen and Auel 2001; Haberman *et al.* 2003; Meyer *et al.* 2003; Schmidt *et al.* 2006; Murphy *et al.* 2007). Nano- and picophytoplankton are more likely to be grazed by HNF, microzooplankton, and small cell grazing mesozooplankton, such as copepods and salps (Fig. 5.1) (Perissinotto and Pakhomov 1998; Atkinson *et al.* 2004; Smetacek *et al.* 2004; Turner 2004). This alternative food web is preyed upon by amphipods, mesopelagic fish and squid, that are an additional food source for Antarctic seabirds, seals, and whales (Murphy *et al.* 2007). Thus, a shift in community composition in this region toward small diatoms and autotrophic flagellates may add extra steps to the trophic chain, resulting in a less efficient transfer of nutrients to higher trophic levels (Fig. 5.1) (Murphy *et al.* 1988). These alternative food webs can support adult marine mammal and bird populations, however they may produce insufficient energy supply to support reproduction (Croxall *et al.* 1988). This has been observed in the Scotia sea, where in

years of low krill abundance, a reliance on a fish-based food web has resulted in large-scale failures in reproductive success for fur seals and penguins (Croxall *et al.* 1988; Reid and Croxall 2001). However, krill are capable of adopting a more varied diet of flagellates, microzooplankton, and occasionally small copepods when diatoms are not abundant (Schmidt *et al.* 2006). Heterotrophic protists can be a good source of nutrition and have been found to benefit krill growth in flagellate-dominated communities (Schmidt *et al.* 2006). Despite this tolerance to changing food supply, krill may be further disadvantaged by ocean acidification, with reports of reduced reproductive success at CO_2 levels near year 2100 projections under the IPCC RCP8.5 (high emission) scenario (Kawaguchi *et al.* 2011; IPCC 2013; Kawaguchi *et al.* 2013). In addition to food web changes, CO_2-induced changes in phytoplankton essential fatty acid content can transfer to higher trophic levels (Bermúdez *et al.* 2016), with unknown effects on the flow of nutrients through the food web. Therefore, ocean acidification effects on the marine microbial community in Antarctic waters is likely to have considerable effects on the entire Antarctic food web.

It is unclear whether the microbial community will be able to adapt to ocean acidification at the rate it is currently changing in Antarctic waters (Orr *et al.* 2005; McNeil and Matear 2008). It is clear that fluctuating environments, like the extreme seasonal fluctuations in fCO_2, light, and macronutrients experienced in coastal Antarctic regions (Gibson and Trull 1999; Roden *et al.* 2013), promotes plasticity and favours evolutionary adaptation (Schaum *et al.* 2012; Schaum and Collins 2014). Acclimation to elevated CO_2 was observed in this study, where an initial CO_2-induced reduction in phytoplankton community health abated over time (see Chapter 2). This acclimation response was likely due to a combination of internal shifts in cellular regulation, along with a change in community structure (Deppeler *et al.* 2018b; Hancock *et al.* 2018). A down-regulation of energy-intensive carbon concentration mechanisms (CCMs) may offset some of the energy constraints for growth (Raven 1991), however the reduction in pH may require the use of proton pumps to maintain pH homeostasis (Taylor *et al.* 2012), negating any energy gained from down-regulation of CCMs (Mackey *et al.* 2015). These physiological responses to increasing CO_2 are likely to drive changes in the community structure by favouring the growth of more CO_2-tolerant taxa and/or strains (Hancock *et al.* 2018). However, adaptation to ocean acidification conditions may eliminate any short-term CO_2-induced

increases in growth rate (Schaum and Collins 2014; Schaum *et al.* 2016). Long-term ocean acidification studies have reported changes in growth rate (Lohbeck *et al.* 2012; Scheinin *et al.* 2015; Torstensson *et al.* 2015; Li *et al.* 2017a; Tong *et al.* 2018), cell size (Schaum *et al.* 2012; Schaum *et al.* 2016), photosynthesis and respiration rates (Schaum *et al.* 2012; Hennon *et al.* 2014), particulate organic matter production (Tong *et al.* 2018), exudation of dissolved organic matter (Torstensson *et al.* 2015), and organic matter stoichiometry (C:N ratio) (Crawfurd *et al.* 2011; Schaum *et al.* 2012; Schaum *et al.* 2016). The magnitude, timing, and direction of these effects differed between species and ecotypes, suggesting that community structure could be dramatically altered over time with as yet unknown consequences on biogeochemical cycles and nutrient transfer through the food web.

5.2 Future Directions

This study provides valuable insights into the effects of ocean acidification on marine microbial communities. This includes the possible mechanisms of effect, tolerance thresholds, effects of increasing CO_2 on community composition, and the utility of monospecific studies in predicting the effects of future changes in CO_2 on Antarctic waters but, inevitably, it also highlights areas where further research is necessary. The following section outlines some of these questions and recommendations for future research.

How does ocean acidification affect flagellates?

Studies predict that with ocean acidification, flagellates will play a much bigger part in the Antarctic ecosystem (Davidson *et al.* 2016; Hancock *et al.* 2018). Yet, little is known about the effects of ocean acidification on Antarctic flagellate species (Wynn-Edwards *et al.* 2014; Hancock *et al.* 2018). Current knowledge suggests that flagellates tolerate the projected reductions in pH that would occur from ocean acidification (pH ∼7.5), with little change in growth rates, cell size, or elemental composition (C:N ratio) (Berge *et al.* 2010; Wynn-Edwards *et al.* 2014). However, Wynn-Edwards *et al.* (2014) reported significant differences in fatty acid content in some species at low pH (*Pyramimonas gelidicola* and *Gymnodinium* sp.) that could result in changed nutrient quality for grazers (see below). There is also some evidence that

reductions in pH can alter flagellate behaviour (Kim *et al.* 2013), flagella motility (Nakajima 2005; Morita *et al.* 2010; Nakamura and Morita 2012), and pH homeostasis (Dason and Colman 2004). Further research into understanding the mechanisms of pH stress and the potential behavioural changes of Antarctic flagellates with ocean acidification will help to clarify the role that flagellates will play in the microbial loop in the future.

Does ocean acidification change the nutritional content of the protistan community?

Fatty acid production by the protistan community is an essential source of nutrients for higher trophic organisms (Schmidt *et al.* 2006). Fatty acid profiles differ among phytoplankton taxa and can be used as indicators for community composition (Dijkman and Kromkamp 2006; Schmidt *et al.* 2006). There is also evidence that differences in protistan community composition can have a direct effect on the fatty acid composition of higher trophic levels, such as the Antarctic krill *Euphausia superba* (Schmidt *et al.* 2006). Little is known about the effect that ocean acidification may have on the fatty acid composition of protistan communities. However, species-specific changes in fatty acid content have been reported (e.g. Rossoll *et al.* 2012; Torstensson *et al.* 2013; Wynn-Edwards *et al.* 2014; King *et al.* 2015; Isari *et al.* 2016; Jacob *et al.* 2016; Bi *et al.* 2017) and thus, the effects are likely to be directly related to CO_2-induced changes in community composition (Bermúdez *et al.* 2016). The effect of ocean acidification on the fatty acid content of the protistan community was not investigated in our study. However, a change in the community composition with elevated CO_2 was observed (Hancock *et al.* 2018). The effect that any change in fatty acid composition will have on the macrozooplankton community is not well understood. In an Arctic mesocosm study, Bermúdez *et al.* (2016) reported a reduction of essential fatty acids in the dominant copepod *Calanus finmarchicus* was related to the essential fatty acid decline in the nanophytoplankton community. Reduced fatty acid concentrations in the diatom *Thalassiosira pseudonana* also caused a reduction in growth and reproduction of the copepod *Acartia tonsa* (Rossoll *et al.* 2012). Therefore, understanding how ocean acidification may affect the fatty acid content of Antarctic phytoplankton species and natural protistan communities is essential to understanding how higher trophic levels may be affected.

How does ocean acidification affect community interactions and grazing?

Grazing interactions are essential for understanding how top-down processes will affect community composition and bloom dynamics. Grazing controls the majority of primary production in the Southern Ocean (Smetacek *et al.* 2004) and can account for ∼50-100% of daily primary and bacterial production in coastal Antarctic waters (Pearce *et al.* 2010). In our study, increased CO_2 slowed HNF growth, reducing the top-down control on the picophytoplankton and prokaryote community. The increased abundance of small diatoms and flagellates in Antarctic waters (see above) favours grazing and proliferation of mesozooplankton, such as copepods and salps, in this region (Atkinson *et al.* 2004; Smetacek *et al.* 2004; Turner 2004), adding additional steps in the trophic chain. Grazing dilution experiments would assist in understanding the effects of ocean acidification on grazing and prey selectivity that are likely under future CO_2 scenarios.

How does ocean acidification affect biogeochemical cycles?

The microbial loop plays an integral part in biogeochemical processes, such as the cycling of nutrients, carbon, and sulfur (Buchan *et al.* 2014). A reduction in diatom size and an increase in flagellate and prokaryote abundance will likely decrease the rate of sinking of organic matter and strengthen remineralisation of particulate matter in the surface ocean (see above) (Smetacek *et al.* 2004). The effects of ocean acidification on carbon flux have been investigated in Northern Hemisphere mesocosm studies (Paul *et al.* 2015; Spilling *et al.* 2016). Utilising a mesocosm design similar to those used in these studies could capture sinking particles and aid our understanding of the effects of ocean acidification on carbon flux and remineralisation of nutrients in Antarctic waters.

Antarctic phytoplankton produce large quantities of dimethylsulfoniopropiothetin (DMSP), which is enzymatically cleaved by prokaryotes into dimethylsulfide (DMS), a volatile compound that contributes to cloud formation when released into the atmosphere (Charlson *et al.* 1987; Curran and Jones 2000). *P. antarctica* is a prolific producer of DMSP in Antarctic waters (DiTullio and Smith 1995; Turner *et al.* 1995; Vance *et al.* 2013) and this species is reportedly sensitive to enhanced CO_2 (Hancock *et al.* 2018). In addition, increased stratification of Antarctic waters may also reduce the abundance of *P. antarctica* in some regions (Arrigo *et al.* 1999; Moisan and

Mitchell 1999). This could have significant effects on the marine sulfur cycle in the Southern Ocean, leading to reductions in cloud formation and global albedo. It is not yet understood how ocean acidification will affect DMSP production in Antarctic marine microbial communities. Yet, the significance of Southern Ocean DMS production to the global sulfur cycle, contributing ∼17% of global DMS emissions (Curran and Jones 2000), makes it imperative to study.

How will changes in iron availability affect the protistan community response to ocean acidification?

Iron is essential for phytoplankton growth (Martin *et al.* 1990; Boyd *et al.* 2007). The Southern Ocean is generally HNLC and therefore a decline in iron availability or the ability of phytoplankton to utilise iron will have a significant effect on their ability to grow in a future ocean. Coastal Antarctic regions are generally considered to be iron-replete (Arrigo *et al.* 2015), however studies have suggested that ocean acidification may affect the bioavailability of iron as well as have physiological effects on phytoplankton, limiting their ability to utilise iron (Shi *et al.* 2010; Hutchins and Boyd 2016; McQuaid *et al.* 2018). Iron limitation may also restrict CO_2-induced changes in productivity and taxonomic shifts (Hoppe *et al.* 2013). Iron limitation may also be more significant in the Southern Ocean in the future as stratification limits the upwelling of iron and sea ice decline reduces the input of iron from sea ice melt (Hutchins and Boyd 2016). Therefore, understanding how coincident ocean acidification and iron limitation affects natural Antarctic marine microbial communities would be essential in understanding how Southern Ocean protistan communities will change in the future.

How will ocean acidification affect microbial communities in other Southern Ocean regions?

The Southern Ocean, south of the Sub-Tropical Front, comprises approximately 20% of the world's ocean surface area and can be divided into five regions, based on the environmental drivers of the phytoplankton community (Sullivan *et al.* 1988; Tréguer and Jacques 1992; Deppeler and Davidson 2017). These comprise of the Sub-Antarctic Zone (SAZ), Permanently Open Ocean Zone (POOZ), Seasonal Sea Ice Zone (SSIZ), Marginal Ice Zone (MIZ), and the Antarctic Continental Shelf Zone (CZ) (Fig. 1.2). The microbial community composition and productivity in each of the different Southern Ocean regions is defined by a number of physical conditions, for example macro- and micronutrients, temperature, sea ice cover, and light. Because of this, it is difficult to extrapolate the results of this thesis to regions where these

physical constraints differ significantly. Boyd *et al.* (2014) demonstrated that the complex permutations of change that occur in different ocean regions make it necessary to perform region-specific studies to fully understand the community responses to change. This is evidenced by ocean acidification studies already performed. McMinn *et al.* (2014) and Coad *et al.* (2016) found that sea ice communities were tolerant of extremely high CO_2 levels (>6000 µatm), while in the SAZ, elevated CO_2 levels increased productivity in sub-Antarctic diatoms through down-regulation of CCMs (Hopkinson *et al.* 2011; Trimborn *et al.* 2013) but may also reduce calcification in some coccolithophores (Müller *et al.* 2015). Larger-scale incubation experiments, such as the one undertaken in this thesis, are necessary in all of the five Southern Ocean regions to observe how ocean acidification and other climate stressors may influence the interactions between trophic levels under region-specific conditions. This is particularly important in the MIZ and POOZ as these regions are relatively unstudied, despite their substantial importance in the Antarctic ecosystem (see Chapter 1).

How will additional climate stressors affect the protistan community?

Climate change models predict that coastal Antarctic regions will experience an increase in freshening, stratification, ocean acidification, warming, and the melting and breakup of glaciers and ice shelves (Gutt *et al.* 2015; Deppeler and Davidson 2017). Whilst ocean acidification alone resulted in a reduction in primary productivity (Deppeler *et al.* 2018b) and change in community composition (Hancock *et al.* 2018), the interactive effects of increased light, decreased salinity, and warming are currently unknown and could exacerbate or diminish these responses (Boyd and Brown 2015). Additional climate stressors, such as increasing temperature, may increase the metabolic demand on grazers, requiring them to consume more nutrients to maintain their growth (Rose *et al.* 2009a). Warming may also reduce the fatty acid content of phytoplankton, leading to reduced nutrition and thus, increasing grazing demand further (Hixson and Arts 2016). However, temperature increases may also alleviate the negative effects of CO_2 on phytoplankton growth in some species (Torstensson *et al.* 2013; Zhu *et al.* 2017). Therefore, it is also important to evaluate the effects of multiple stressors on multiple trophic levels as they may result in further changes to the microbial community composition (Calbet *et al.* 2014). Incorporating multiple stressors into an experimental design can become logistically impossible if all permutations of treatments are included (Boyd *et al.* 2016a). Thus,

some studies have grouped stressors in order to simulate future ocean conditions and assess their interactive effects (e.g. Xu *et al.* 2014; Boyd *et al.* 2016a). However, understanding and evaluating the magnitude and timing of these changes within the region studied is essential in ensuring that the effect of multi-stressors are properly understood (Boyd *et al.* 2014, 2016b).

Can Antarctic phytoplankton adapt to climate change?

Little is known about the ability of Antarctic phytoplankton to adapt to changes in their environment. While microbial communities from Antarctic coastal waters may cope with large variations in CO_2 (Young *et al.* 2015; Davidson *et al.* 2016; Hancock *et al.* 2018, e.g.), their tolerance limits to other environmental factors, such as temperature and salinity, may be very narrow (Moline *et al.* 2004; Montes-Hugo *et al.* 2008). Long-term studies have shown that individual phytoplankton species can adapt to ocean acidification conditions (e.g. Lohbeck *et al.* 2012; Schaum *et al.* 2012; Schaum *et al.* 2016). However, these adaptations may result in physiological changes, such as growth rate or cell size, which may affect their abundance and trophic interactions in the protistan community (Schaum and Collins 2014; Schaum *et al.* 2016). Long-term studies on Antarctic phytoplankton under projected future climate change conditions (both single and multi-stressor) could provide valuable insight into whether key species can adapt to a changing climate and what possible impacts that may have on the protistan community.

Development of bottom-up models to investigate how CO_2-induced changes in the protistan community affect higher trophic levels.

The protistan community is the base of the Southern Ocean food web and supports the wealth of life in Antarctic waters. Therefore, changes in the protistan community, imposed by ocean acidification and other climate stressors, may have a significant effect on the entire food web. Qualitative network models are useful for assessing the response of environmental perturbations on an ecosystem (Melbourne-Thomas *et al.* 2013; Subramaniam *et al.* 2017). However, the predictive power of these models can be diminished when there is insufficient detail in its components (Ratnarajah *et al.* 2016; Goedegebuure *et al.* 2017). Therefore, integrating the results of the ocean acidification studies in this thesis into bottom-up models will help untangle the key community-level interactions that will strengthen predictions of

ecosystem-level changes that may be imposed by ocean acidification.

5.3 Conclusion

The research undertaken in this thesis showed that ocean acidification can alter microbial productivity, trophodynamics, and biogeochemistry in Antarctic coastal waters. While this work uncovered some critical thresholds for tolerance to ocean acidification in the protistan community, there is still much that needs to be done to fully understand the consequences of these results on the entire ecosystem. Shifts in phytoplankton community production and predator-prey interactions with ocean acidification could have a significant effect on the food web and biogeochemistry in the Southern Ocean. Therefore, understanding these effects is critical if we are to predict how climate change may affect the ecosystem services that marine microbes provide in Antarctic waters, such as climate mediation, sustaining biodiversity, and supporting productive fisheries.

Appendix A

Chapter 1 Published Version

frontiers in Marine Science

REVIEW
published: 16 February 2017
doi: 10.3389/fmars.2017.00040

Southern Ocean Phytoplankton in a Changing Climate

Stacy L. Deppeler[1]* *and Andrew T. Davidson*[2, 3]

[1] *Institute for Marine and Antarctic Studies, University of Tasmania, Hobart, TAS, Australia,* [2] *Australian Antarctic Division, Department of the Environment and Energy, Kingston, TAS, Australia,* [3] *Antarctic Climate and Ecosystem Cooperative Research Centre (ACE CRC), University of Tasmania, Hobart, TAS, Australia*

Phytoplankton are the base of the Antarctic food web, sustain the wealth and diversity of life for which Antarctica is renowned, and play a critical role in biogeochemical cycles that mediate global climate. Over the vast expanse of the Southern Ocean (SO), the climate is variously predicted to experience increased warming, strengthening wind, acidification, shallowing mixed layer depths, increased light (and UV), changes in upwelling and nutrient replenishment, declining sea ice, reduced salinity, and the southward migration of ocean fronts. These changes are expected to alter the structure and function of phytoplankton communities in the SO. The diverse environments contained within the vast expanse of the SO will be impacted differently by climate change; causing the identity and the magnitude of environmental factors driving biotic change to vary within and among bioregions. Predicting the net effect of multiple climate-induced stressors over a range of environments is complex. Yet understanding the response of SO phytoplankton to climate change is vital if we are to predict the future state/s of the ecosystem, estimate the impacts on fisheries and endangered species, and accurately predict the effects of physical and biotic change in the SO on global climate. This review looks at the major environmental factors that define the structure and function of phytoplankton communities in the SO, examines the forecast changes in the SO environment, predicts the likely effect of these changes on phytoplankton, and considers the ramifications for trophodynamics and feedbacks to global climate change. Predictions strongly suggest that all regions of the SO will experience changes in phytoplankton productivity and community composition with climate change. The nature, and even the sign, of these changes varies within and among regions and will depend upon the magnitude and sequence in which these environmental changes are imposed. It is likely that predicted changes to phytoplankton communities will affect SO biogeochemistry, carbon export, and nutrition for higher trophic levels.

Keywords: Southern Ocean, phytoplankton, climate change, primary productivity, Antarctica

OPEN ACCESS

Edited by:
Julie Dinasquet, University of California, San Diego, USA

Reviewed by:
Ian Salter, Alfred Wegener Institute for Polar and Marine Research, Germany
Bernard Quéguiner, Aix-Marseille University, France

***Correspondence:**
Stacy L. Deppeler
stacy.deppeler@utas.edu.au

Specialty section:
This article was submitted to Aquatic Microbiology, a section of the journal Frontiers in Marine Science

Received: *30 September 2016*
Accepted: *02 February 2017*
Published: *16 February 2017*

Citation:
Deppeler SL and Davidson AT (2017) Southern Ocean Phytoplankton in a Changing Climate. Front. Mar. Sci. 4:40. doi: 10.3389/fmars.2017.00040

1. INTRODUCTION

Iconic Antarctic wildlife from krill to whales, seals, penguins, and seabirds, ultimately depend on single-celled marine plants (phytoplankton) for their food. More than 500 species of protist have been identified in Antarctic waters, ~350 of which are phytoplankton and ~150 microheterotrophs (Scott and Marchant, 2005, http://taxonomic.aad.gov.au). These organisms coexist with untold numbers of heterotrophic prokaryotes (bacteria and Archaea) and viruses. Together they comprise the microbial food web (**Figure 1**), through which much of the carbon sequestered by phytoplankton is consumed, respired, and/or remineralized (Azam et al., 1983,

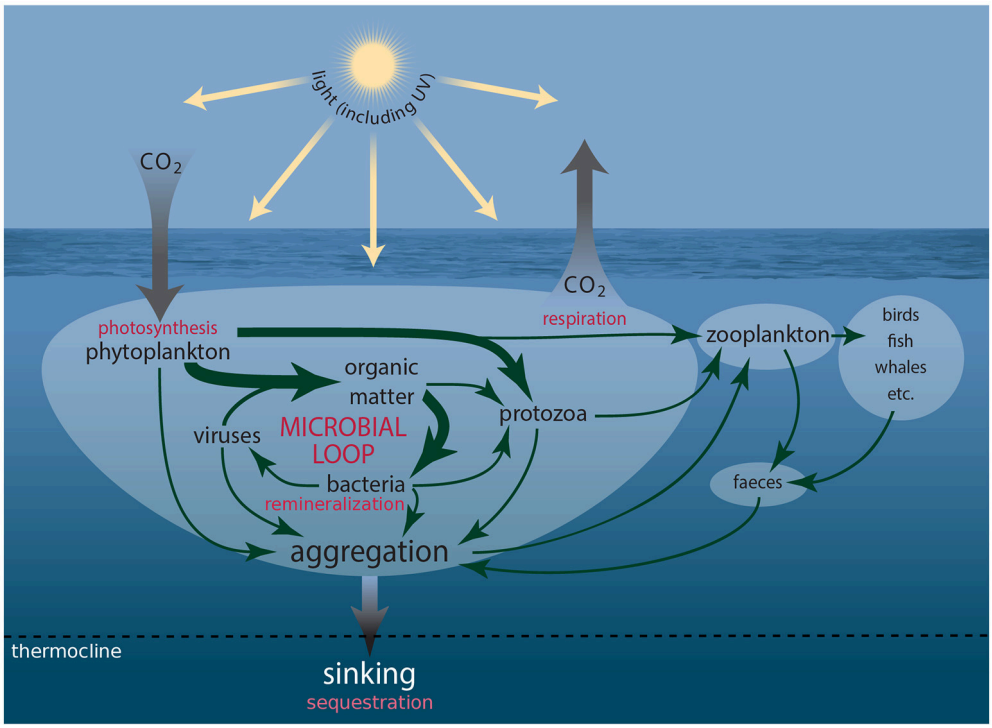

FIGURE 1 | Schematic showing the connections amongst members of the microbial food web and microbial loop and the processes driving carbon transfer to higher trophic levels and flux to the deep ocean.

1991; Fenchel, 2008; Kirchman, 2008). This food web includes the microbial loop in which dissolved carbon substrates fuel the growth of bacteria and Archaea, which are subsequently consumed by protists, returning carbon to the microbial food web that is otherwise lost to the dissolved pool (Azam et al., 1983). Phytoplankton are the base of the Southern Ocean (SO) food web. In nutrient rich Antarctic coastal waters their blooms can reach concentrations approaching 10^8 cells l^{-1}. Chlorophyll *a* (Chl *a*) concentrations as high as 50 μg l^{-1} have been recorded off the West Antarctic Peninsula (WAP), although maximum Chl *a* concentrations off East Antarctica are usually an order of magnitude less (Nelson et al., 1987; Smith and Gordon, 1997; Wright and van den Enden, 2000; Garibotti et al., 2003; Wright et al., 2010; Goldman et al., 2015). The majority of phytoplankton production in the SO is grazed by microheterotrophs or consumed and remineralized by bacteria (Lochte et al., 1997; Christaki et al., 2014). Production that escapes these fates sinks to depth, often in the form of dead cells, aggregates of biogenic material (marine snow), or fecal pellets, sequestering carbon in the deep ocean.

Abbreviations: SO, Southern Ocean; SAZ, sub-Antarctic zone; POOZ, permanently open ocean zone; SSIZ, seasonal sea ice zone; MIZ, marginal ice zone; CZ, Antarctic continental shelf zone; DMSP, dimethylsulfoniopropiothetin; DMS, dimethylsulfide; Chl *a*, Chlorophyll *a*; HNLC, high nutrient, low chlorophyll; UCDW, upper circumpolar deep water; SAM, Southern Annular Mode; WAP, west Antarctic peninsula; ASL, Amundsen Sea Low; ENSO, El Niño-Southern Oscillation; SIE, sea ice extent; CCM, carbon concentrating mechanism; PAR, photosynthetically active radiation; UV, ultraviolet.

Some phytoplankton, such as prymnesiophytes and dinoflagellates, also synthesize substantial quantities of dimethylsulfoniopropiothetin (DMSP), which when enzymatically cleaved, forms dimethylsulfide (DMS). Oxidation of DMS in the atmosphere forms sulfate aerosols, which nucleate cloud formation and increase the reflectance of solar radiation (Charlson et al., 1987). The microbial food web plays a vital role in metabolizing these sulfur compounds (Kiene et al., 2000; Simó, 2004). The active involvement of phytoplankton in the sequestration and synthesis of climate-active gases (CO_2) and biogenic sulfur compounds (DMSP and DMS), plus the mediation of the fate of these compounds by protozoa and bacteria means that microbes are a crucial determinant of future global climate (**Figure 1**).

The SO plays a substantial role in mediating global climate. The world's oceans have taken up between 25 and 30% of the anthropogenic CO_2 released to the atmosphere, with ~40% of this uptake occurring in the SO (Raven and Falkowski, 1999; Sabine et al., 2004; Khatiwala et al., 2009; Takahashi et al., 2009; Frölicher et al., 2015). Without this, the atmospheric CO_2 concentration would be ~50% higher than it is today. Drawdown of CO_2 by phytoplankton photosynthesis and vertical transport of this biologically sequestered carbon to the deep ocean (the biological pump) is responsible for around 10% this uptake (Cox et al., 2000; Siegel et al., 2014). Any climate-induced change in the structure or function of phytoplankton communities is likely to alter the efficiency of the biological pump, with feedbacks to the rate of

climate change (Matear and Hirst, 1999; Le Quéré et al., 2007).

The SO is a region of seasonal extremes in productivity that reflect the large fluctuations in the SO environment. In summer, the development of large blooms of phytoplankton support a profusion of Antarctic life. Their metabolic activity also affects biogeochemical cycles in the SO, which in turn can influence the global climate. Whilst their effect on global climate is substantial, their microscopic size means they are intimately exposed to changes in their environment and are also likely to be affected by climate change. Already, climate change is causing the southward migration of ocean fronts, increasing sea surface temperatures, and changes in sea ice cover (Constable et al., 2014). Further changes in temperature, salinity, wind strength, mixed layer depth, sea ice thickness, duration and extent, and glacial ice melt are predicted. These changes are likely to affect the composition, abundance, and productivity of phytoplankton in the SO and feed back to threaten the ecosystem services they provide, namely sustaining biodiversity, fueling the food web and fisheries, and mediating global climate (Moline et al., 2004).

The SO is a vast and diverse environment, and hence the effect of climate change on the phytoplankton community is likely to be complex. For the purposes of this review we define the SO as waters south of the Sub-Tropical Front, thereby comprising ∼20% of the world's ocean surface area. We subdivide these waters into five regions that group waters according to the environmental drivers of the phytoplankton community in a similar manner as Tréguer and Jacques (1992) and Sullivan et al. (1988), namely the Sub-Antarctic Zone (SAZ), Permanently Open Ocean Zone (POOZ), Seasonal Sea Ice Zone (SSIZ), Marginal Ice Zone (MIZ), and the Antarctic Continental Shelf Zone (CZ) (**Figure 2**). Differences in environmental factors (physical, chemical, and biological) and processes (e.g., stratification, mixing, grazing) define the composition, abundance, and productivity of the phytoplankton community, both within and between these regions. Climate change is expected to elicit widespread changes in oceanography in each region, such as the displacement of oceanographic fronts (Sokolov and Rintoul, 2009b), as well as different permutations of climate-induced stressors that may interact synergistically or antagonistically, with either beneficial or detrimental effects on the phytoplankton community (Boyd and Brown, 2015; Boyd et al., 2016).

Here we identify the factors and processes that critically affect phytoplankton communities in each region of the SO, consider the impacts of climate change on each of these regions, examine the likely effect of these changes on the phytoplankton inhabiting these waters, and predict the possible repercussions for the Antarctic ecosystem.

2. SUB-ANTARCTIC ZONE

The Sub-Antarctic Zone (SAZ) comprises more than half the total area of the SO and incorporates three important frontal regions; the Sub-Tropical Front, the Sub-Antarctic Front, and the Polar Front (**Figure 2**) (Orsi et al., 1995). Within this region, the waters between the Sub-Antarctic Front and the Polar Front are also referred to as the Polar Frontal Zone (e.g., Tréguer and Jacques, 1992). This region forms an important transitional boundary within the SO between the dominance of coccolithophores that construct carbonate shells to the north and diatoms with silicate frustules to the south (**Figures 2**, **3**) (Trull et al., 2001a,b; Honjo, 2004). Macro- and micronutrients are more abundant at the Polar Frontal Zone where nutrients are entrained across the bottom of the mixed layer, supporting deep chlorophyll maxima at depths up to 90 m. These deep chlorophyll maxima support blooms of large diatoms, such as *Rhizosolenia* sp. and *Thalassiothrix* sp., which can grow to high abundance and contribute significantly to carbon and silica flux (Tréguer and Van Bennekom, 1991; Kopczyńska et al., 2001; Kemp et al., 2006; Assmy et al., 2013). For the purpose of this review we are combining all waters between the Sub-Tropical Front to the north and the Polar Front to the south as the SAZ, as the physical and biological characteristics of these regions are similar.

This region of the SO is a major contributor to the uptake of CO_2 by the ocean (Metzl et al., 1999; Sabine et al., 2004; Frölicher et al., 2015). The westerly winds that circulate Antarctica carry water from the Antarctic Slope Front north across the SAZ by Ekman transport (**Figure 3**). This water has a partial pressure of carbon dioxide (pCO_2) below that of the atmosphere, allowing CO_2 to dissolve into the ocean (the solubility pump). North of the Sub-Antarctic Front, surface water is convected to hundreds of meters, forming Antarctic Intermediate Water and Sub-Antarctic Mode Water (**Figure 3**) (Wong et al., 1999; Matear et al., 2000; Rintoul and Trull, 2001; Lumpkin and Speer, 2007). In doing so, it carries an estimated ∼1 Gt C yr^{-1} to the ocean's interior and connects the upper and lower components of the global overturning circulation (Metzl et al., 1999; Sloyan and Rintoul, 2001a,b).

The SAZ is the largest high nutrient, low chlorophyll (HNLC) province in the world's ocean. Over the year phytoplankton productivity in this region is limited by a variety of bottom-up (silicic acid, iron, and light) and top-down (grazing) factors (**Figure 4A**) (e.g., Banse, 1996; Boyd et al., 2001; Hiscock et al., 2003; Doblin et al., 2011). Iron is the main factor limiting phytoplankton growth in the SAZ, despite inputs from dust, shelf sediments, and hydrothermal vents (Boyd et al., 2004; Blain et al., 2007; Cassar et al., 2007; Pollard et al., 2009; Boyd and Ellwood, 2010; Tagliabue et al., 2010). Silica is replete in these waters in spring but it is drawn down by silicifying plankton, such as diatoms, silicoflagellates, and radiolarians, to limiting concentrations by autumn (Trull et al., 2001a; Salter et al., 2007; Pollard et al., 2009). In iron-limited regions of the SAZ, Si:C ratios are high, resulting in low carbon export (Salter et al., 2007, 2012; Assmy et al., 2013). In addition, light levels experienced by phytoplankton can be very low due to cloudiness and mixed layer depths ranging from 70 to 100 m in summer to as deep as 600 m in winter (Bishop and Rossow, 1991; Rintoul and Trull, 2001). In regions of shallow or complex bathymetry, such as sea mounts, or in waters downstream of sub-Antarctic islands, resuspension of iron-rich sediments naturally fertilizes the SAZ waters creating areas of high productivity (Salter et al., 2007; Pollard et al., 2009). Large, heavily-silicified diatoms, such as *Eucampia antarctica* and *Fragilariopsis kerguelensis*, are responsible for high levels of export in these naturally fertilized regions (Salter et al., 2007, 2012; Assmy et al., 2013; Rembauville

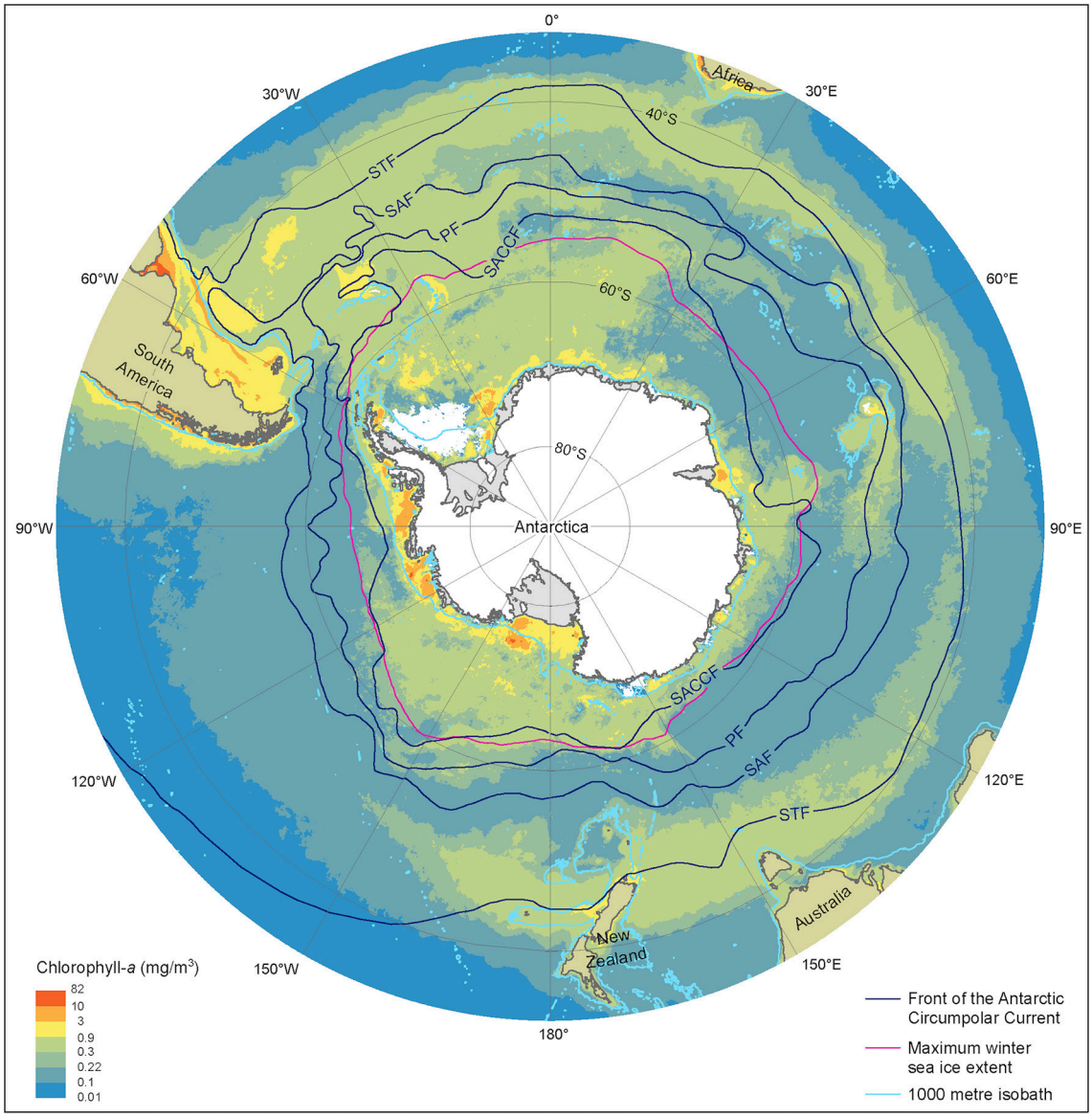

FIGURE 2 | Summer near-surface Chlorophyll *a* concentration, frontal locations and sea ice extent in the Southern Ocean. Chlorophyll *a* is determined from MODerate-resolution Imaging Spectroradiometer, Aqua satellite estimates from austral summer season between 2002/03 and 2015/16 at 9 km resolution. Black lines represent, frontal positions from Orsi et al. (1995). The red line denotes the maximum extent of sea ice averaged over the 1979/80 to 2007/08 winter seasons, derived from Scanning Multichannel Microwave Radiometer and Special Sensor Microwave/Image satellite data. Light blue lines depict the 1000 m depth isobath, derived using the General Bathymetric Chart of the Oceans, version 20150318. STF, Sub-Tropical Front; SAF, Sub-Antarctic Front; PF Polar Front; SACCF, Southern Antarctic Circumpolar Current Front.

et al., 2016b,c). This export is aided by silica limitation, the exhaustion of which ceases diatom growth and accelerates rates of sinking. Nutrient limitation also causes a succession in the phytoplankton community to picoeukaryotes, such as *Phaeocystis* sp. and coccolithophorids (Salter et al., 2007; Quéguiner, 2013; Balch et al., 2016).

Small taxa, including nanoflagellates, cyanobacteria, dinoflagellates, coccolithophores, and small or lightly silicified diatoms, dominate the protistan community in the SAZ (Odate and Fukuchi, 1995; Kopczyńska et al., 2001, 2007; de Salas et al., 2011). Copepods and mesopelagic fish, particularly myctophids, are important primary and secondary consumers of the phytoplankton in these waters and form an alternative food web for squid, predatory mesopelagic fish, and penguins (Kozlov, 1995; Cherel et al., 2010; Murphy et al., 2016). Measured rates of microzooplankton grazing (Jones et al., 1998; Griffiths et al., 1999; Safi et al., 2007; Pearce et al., 2011), together with high grazer biomass (Kopczyńska et al., 2001) suggest that grazers consume much of the primary productivity in this region. As a result of the physical and biological factors limiting primary

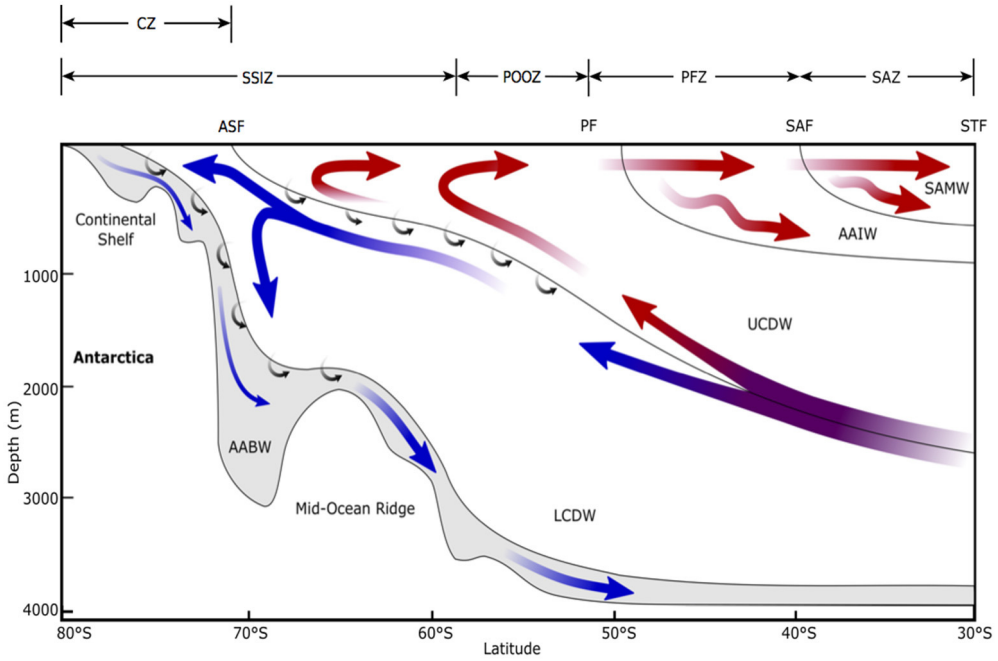

FIGURE 3 | Schematic view of the meridional overturning circulation of the Southern Ocean, modified from Figure 3 in Post et al. (2014). STF, Sub-Tropical Front; SAF, Sub-Antarctic Front; PF, Polar Front; ASF, Antarctic Slope Front; SAMW, Sub-Antarctic Mode Water; AAIW, Antarctic Intermediate Water; UCDW, Upper Circumpolar Deep Water; LCDW, Lower Circumpolar Deep Water; AABW, Antarctic Bottom Water; SAZ, Sub-Antarctic Zone; PFZ, Polar Frontal Zone; POOZ, Permanently Open Ocean Zone; SSIZ, Seasonal Sea Ice Zone; CZ, Continental Zone. Arrows indicate mean flow direction. Red arrows show the upper cell and blue shows the deep cell. Small arrows indicate diabatic transport due to interior mixing. Note that this is an averaged view of the emergent residual flow due to complex, time-varying, three-dimensional processes and does not reflect the current directions of any given section across the Antarctic Circumpolar Current.

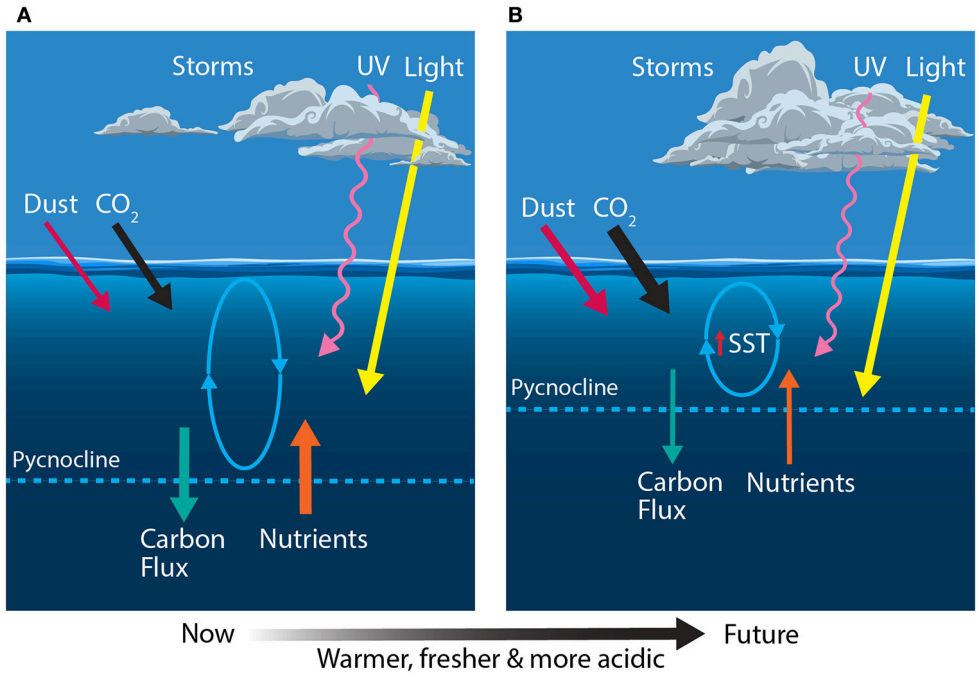

FIGURE 4 | Schematic showing the primary physical constraints on phytoplankton in the Sub-Antarctic Zone (SAZ) (A) before and **(B)** after climate change, modified from Boyd and Law (2011). Ovals represent the depth of mixing and arrow thickness reflects relative rates of flux. SST, sea surface temperature.

productivity in the SAZ, phytoplankton abundance is moderately low and varies little among seasons (Banse, 1996). The SAZ is more productive in the Atlantic sector and around 170°W where iron concentrations are higher due to the proximity of land (**Figure 2**) (Comiso et al., 1993; de Baar et al., 1995; Moore and Abbott, 2000). Despite the low levels of primary productivity, export efficiency is high in HNLC waters of the SAZ, suggesting that small taxa contribute to a high proportion of carbon export (Trull et al., 2001b; Lam and Bishop, 2007; Cassar et al., 2015; Laurenceau-Cornec et al., 2015).

Climate predictions suggest that waters of the SAZ will become warmer, fresher and more acidic; the frequency of storms will increase, bringing more wind-blown dust to the region; and phytoplankton will experience increased irradiances of photosynthetically active radiation (PAR) and ultraviolet (UV) radiation (**Figure 4B**) (Matear and Hirst, 1999; Caldeira and Wickett, 2003; Orr et al., 2005; Marinov et al., 2010; Boyd and Law, 2011; Boyd et al., 2016). Together, these changes may have profound consequences for phytoplankton in the SAZ and the role of this region in mediating global climate.

Models suggest that global warming is likely to reduce the efficiency of both the solubility and biological pumps (Sarmiento and Le Quéré, 1996; Matear and Hirst, 1999). For phytoplankton, increased precipitation and warming increases the buoyancy of surface waters, enhancing stratification and reducing mixed layer depths over much of the SAZ. This reduces the delivery of nutrients to surface water, thereby reducing phytoplankton production and the vertical flux of biogenic carbon to the deep ocean via the biological pump (Matear and Hirst, 1999 and references therein; Boyd and Law, 2011; Petrou et al., 2016). The declining efficiency of the biological pump means it would be unable to compensate for any decline in the solubility of CO_2 as the ocean warms (Matear and Hirst, 1999). Recent studies also indicate that rising temperatures cause rates of grazing to increase more rapidly than rates of phytoplankton growth (Sarmento et al., 2010; Evans et al., 2011; Caron and Hutchins, 2013; Behrenfeld, 2014; Biermann et al., 2015; Cael and Follows, 2016). Thus, phytoplankton standing stocks are likely to decline and the proportion of primary production respired in near-surface waters by prokaryotes and grazers will increase. The nutritional quality of phytoplankton may also decline at higher temperatures (Finkel et al., 2010 and references therein; Hixson and Arts, 2016), suggesting grazers will also need to consume more phytoplankton to obtain the nutrition they require. Together, these factors are predicted to reduce phytoplankton productivity and the uptake of CO_2 by the ocean in the SAZ region.

The absence of iron is regarded as the primary cause of HNLC waters of the SO having the world's highest inventory of unused surface macronutrients (Martin et al., 1990; Boyd et al., 2007). As the largest HNLC region in the ocean, low rates of iron supply to the SAZ restrict primary production, alter phytoplankton species composition, increase Si:C export ratios, and constrain the biological pump (Ridgwell, 2002; Salter et al., 2012; Assmy et al., 2013; Salter et al., 2014). Aeolian dust makes a significant contribution to iron supply in the SAZ in areas downwind of landmasses and any increase in storm activity as a result of climate change may enhance delivery of iron-rich dust to these areas, enhancing productivity and carbon drawdown in this region (Cassar et al., 2007; Boyd and Law, 2011; Boyd et al., 2012, 2016). Investigations into sediment cores taken in the sub-Antarctic South Atlantic have correlated increased aeolian iron supply to the SAZ with increased productivity during ice ages, strengthening the biological pump and causing significant declines in atmospheric CO_2 (Anderson et al., 2014; Martínez-García et al., 2014). Increased desertification through climate change-related vegetation loss may result in a 10-fold increase in dust over the Southern Hemisphere (Woodward et al., 2005). However, the increase in dust will depend on both climate change and anthropogenic changes in land-use and re-vegetation, the net effects of which are currently uncertain (Ridgwell, 2002; Hutchins and Boyd, 2016).

While oceanic uptake of CO_2 ameliorates the accumulation of this gas in the atmosphere, it also alters the carbonate chemistry of the ocean. Absorption of CO_2 by the ocean reduces its pH (termed ocean acidification) and increases the solubility of calcium carbonate by reducing its saturation state (Ω) (Caldeira and Wickett, 2003; Orr et al., 2005). Coccolithophorids are the only calcifying phytoplankton in the SO and are most abundant in naturally iron-fertilized regions in the SAZ, such as fronts and downstream of sub-Antarctic islands (Salter et al., 2014; Balch et al., 2016). Calcification releases CO_2 (the carbonate counter-pump), resulting in the elevation of pCO_2 concentrations in SAZ waters where coccolithophores are highly abundant, particularly around the Sub-Antarctic Front (Patil et al., 2014; Saavedra-Pellitero et al., 2014; Balch et al., 2016). Studies of the dominant coccolithophore, *Emiliania huxleyi*, found morphological variations in calcification that closely followed the southerly decline in calcite saturation state but were strain-specific rather than caused by acidification (Cubillos et al., 2007; Patil et al., 2014; Saavedra-Pellitero et al., 2014; Malinverno et al., 2015). However, culture studies by Müller et al. (2015) reported that calcification by *E. huxleyi* decreased at pCO_2 concentrations >1000 μatm. This suggests that calcifying phytoplankton in the SAZ will be vulnerable to predicted increases in pCO_2. A decrease in calcification is anticipated to have a greater negative impact on the carbonate counter-pump than cell growth, leading to greater surface water pCO_2 uptake but potentially reducing vertical carbon flux through a decline in the ballasting effect of calcification (Riebesell et al., 2009; Müller et al., 2015; Balch et al., 2016).

Minimal research has been performed on the effect of ocean acidification on non-calcifying phytoplankton in the SAZ. Boyd et al. (2016) included ocean acidification in their multi-stressor study on a sub-Antarctic diatom and whilst their experimental design did not allow for full analysis of each individual stressor, they found that ocean acidification was not likely to be a primary controller in diatom physiology. Studies on other sub-Antarctic diatom species have reported an increase in productivity with increased CO_2 concentration, likely due to reduced energetic costs associated with the down-regulation of carbon concentrating mechanisms (CCMs) (Hopkinson et al., 2011; Trimborn et al., 2013). Most SO phytoplankton use CCMs to increase the intracellular concentration of CO_2 for fixation by RubisCO (Hopkinson et al., 2011). This process requires

substantial energy consumption and the down-regulation of CCMs is thought to decrease the energy cost of carbon acquisition for phytoplankton photosynthesis (e.g., Raven, 1991; Rost et al., 2008; Hopkinson et al., 2011). However, iron and light limitation in these waters is likely to inhibit any positive effects of increased CO_2 supply (Hoppe et al., 2013, 2015).

Stratification of the water column is predicted to increase in the SAZ region, trapping phytoplankton in a shallowing mixed layer where they are exposed to higher irradiances of PAR and UV radiation (280–400 nm) (Davidson, 2006; Gao et al., 2012; Häder et al., 2015). Light wavelengths are differentially attenuated by sea water. Blue wavelengths (~500 nm) can reach depths exceeding 250 m in clear oceanic water but the penetration rapidly decreases as radiation tends toward infrared (longer) and ultraviolet (shorter) wavelengths (**Figure 5**) (Davidson, 2006). Thus, red and infrared wavelengths only warm the very surface of the ocean, while damaging irradiances of UV-B penetrate to ≤30 m depth (Karentz and Lutze, 1990; Buma et al., 2001; Davidson, 2006). Rates of phytoplankton productivity in the SAZ are commonly limited by light availability due to cloudiness and deep mixing. Increased stratification could mitigate this limitation by keeping cells in sunlit near-surface waters. Overall, productivity would still be constrained by the availability of key nutrients (iron and silicate), which already limit phytoplankton production in the SAZ despite the low light. Thus, increased rates of productivity are unlikely to result in higher biomass or carbon export in this region without a coincident increase in nutrient supply (see above).

Exposing phytoplankton in the SAZ to higher irradiances of PAR, Ultraviolet-A (UV-A, 315–400 nm), and Ultraviolet-B (UV-B, 280–315 nm) is also likely to increase photodamage. The damage to intracellular molecules or structures become progressively less repairable as wavelengths decline below 350 nm, reducing phytoplankton productivity, growth and survival, and changing the species composition, with implications for ecosystem structure and function (e.g., Karentz, 1991; Marchant and Davidson, 1991; Davidson, 2006). The amount of damage sustained by cells is a function of the dose and dose rate of UV exposure; the frequency and duration of exposure to low irradiances to allow repair; and species-specific differences in the UV-tolerance of component species in natural phytoplankton communities (e.g., Cullen and Lesser, 1991; Davidson, 2006; Häder et al., 2015). It is hard to assess the additional risk UV exposure may have to phytoplankton in the SAZ as such details are currently unavailable. Studies by Helbling et al. (1994) and Neale et al. (1998a,b) showed that increasing the rate of change in the light climate altered the balance between damage and repair and greatly increased the biological impact of a specific UV dose. Thus, trapping cells in a shallow mixed zone where they receive repeated exposure to high PAR and UV irradiances over short time scales (see above, **Figure 5**) may have a far greater impact on the growth, production, and survival of phytoplankton than ozone depletion (Davidson, 2006).

The SAZ region is being increasingly penetrated by both sub-tropical and polar waters. The climate-induced increase in the positive phase of the Southern Annular Mode (SAM) has caused the westerly wind belt to intensify and move south

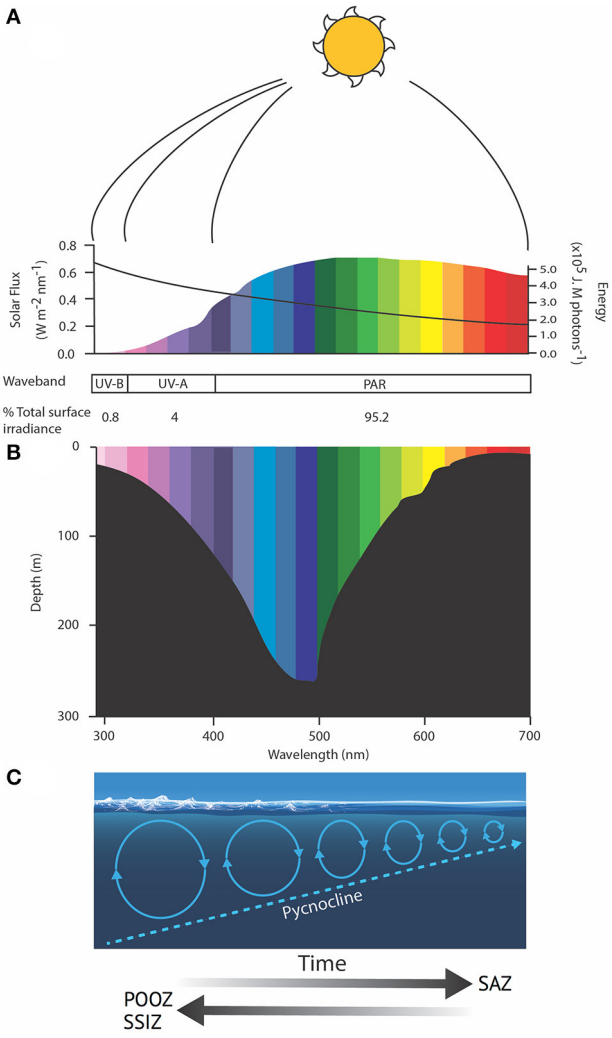

FIGURE 5 | Schematic showing (A) the spectral flux (colored bars) and molar photon energy (black line) of solar radiation, **(B)** the wavelength-dependent penetration of light in the ocean and **(C)** the role of wind in deepening the mixed layer depth, modified from Davidson (2006). Solar spectral flux was calculated from the UVSpec model for noon at the summer solstice at Davis Station, Antarctica, an albedo of 0.5 and a column Ozone of 300 Dobson units. Photon energy was calculated after Kirk (1994). SAZ, Sub-Antarctic Zone; POOZ, Permanently Open Ocean Zone; SSIZ, Seasonal Sea Ice Zone; PAR, photosynthetically active radiation.

(see POOZ below). This increase in the velocity of westerly winds to the south of the SAZ has enhanced upwelling at the Antarctic Slope Front and increased its Ekman transport into the SAZ from the south, increasing phytoplankton growth in the cool, nutrient-rich water (Lovenduski and Gruber, 2005; DiFiore et al., 2006). A 37 year dataset of surface Chl *a* measurements south of Australia from vessels of the Japanese Antarctic Research Expeditions show as similar trend of increasing Chl *a* spreading northward from these northern limits of the POOZ (55°S) into the Polar Frontal Zone (40°S) (Hirawake et al., 2005). The southward movement of the westerly wind belt has also increased the penetration of sub-tropical waters into

the SAZ; supplementing iron supply, exacerbating warming, and intensifying climate-induced stratification (Lovenduski and Gruber, 2005; Poloczanska et al., 2007; Ridgway, 2007). Warmer waters also allow the incursion of sub-tropical phytoplankton and grazers into SAZ waters, causing additional grazing competition and unknown effects on the SO food web (McLeod et al., 2012).

Not all of the SAZ is expected to experience shallowing mixed layer depth as a result of climate change. At the sub-Antarctic convergence, increased wind will deepen the mixed layer, causing declines in phytoplankton productivity through light limitation (Lovenduski and Gruber, 2005). In addition, there are zonal differences in the effect of the increasingly positive SAM on mixed layer depth in the SAZ region, with deepening over the eastern Indian Ocean and central Pacific Ocean, and shallowing over the western Pacific Ocean (Sallée et al., 2010). Resulting in a mosaic of changing factors that limit phytoplankton productivity, from nutrient limitation in shallower regions to light limitation in deeply mixed waters.

Clearly, phytoplankton occupying the SAZ region are likely to experience a range of environmental stressors as a result of climate change. The net effect of these changes is uncertain. Most studies investigate the physiological effects of change on phytoplankton by imposing single stressors (e.g., Boyd et al., 2013; Trimborn et al., 2013) but research shows interaction among stressors alter their response. A multi-stressor study by Boyd et al. (2016) using a sub-Antarctic diatom showed that its response to environmental change was governed by the range of stresses to which it was exposed. Negative responses to several stressors (CO_2, nutrients, and light) were offset by positive responses to others (temperature and iron). Thus, the response of an organism is determined by the interactive effect of all the stresses they experience (Boyd et al., 2016). Equally, responses of single species (e.g., Boelen et al., 2011; Trimborn et al., 2014; Müller et al., 2015) provide valuable insights into the mechanisms of sensitivity and tolerance but avoid interactions among species and trophic levels that can alter the responses or sensitivity of a community to a stressor (Davidson et al., 2016; Thomson et al., 2016). Yet gaining maximum predictive strength by simultaneously performing multi-stressor and multi-trophic level studies is often logistically so demanding as to be impractical.

Predicted responses by phytoplankton in the SAZ to climate change differ. Many propose that the stratification-induced decline in nutrient supply to surface waters will reduce their productivity and favor small flagellates (e.g., Matear and Hirst, 1999; Marinov et al., 2010; Petrou et al., 2016), heightening the role of the microbial food web and reducing carbon export. While Boyd et al. (2016) indicates that increases in iron and temperature may double growth rates and favor diatoms; scenarios which have major and opposing influences on regional productivity and biogeochemistry. It is likely that the effect of climate change on phytoplankton in the SAZ is going to be determined by the timing, rate, and magnitude of change in each stressor. Stochastic inputs of iron, wind, and storms disrupt stratification; influencing productivity, species composition, and export production through changes in nutrients and light climate. Changes in community composition from diatoms to flagellates also affect particulate matter stoichiometry in this region, causing a decline in nutritional quality for grazing zooplankton (Martiny et al., 2013; Rembauville et al., 2016a) and subsequent flow on effects throughout the food web (Finkel et al., 2010). Ocean acidification will also cause declines in carbonate saturation, affecting coccolithophore calcification, resulting in greater surface pCO_2 uptake and decreased carbon export. Overall, our synthesis suggests that productivity will decline in the SAZ due to the net response of nutrient limitation and increased grazing, especially in silicate-limited waters.

3. PERMANENTLY OPEN OCEAN ZONE

The Permanently Open Ocean Zone (POOZ) lies between the Polar Front and the northern limit of the winter sea ice, covering approximately 14 million km^2 (**Figure 2**). The Polar Front at the northern extent of the POOZ forms a natural barrier between the warm SAZ water (5–10°C) and the cold Antarctic water (<2°C) (Pollard et al., 2002; Sokolov and Rintoul, 2009a). These waters are predominantly HNLC with a phytoplankton community dominated by nano- and picoflagellates but characteristically contain even less Chl *a* than the SAZ (Becquevort et al., 2000; Moore and Abbott, 2000; Kopczyńska et al., 2001; Olguín and Alder, 2011). The exception to this is where iron concentrations in surface waters are enhanced by upwelling and/or sediment input/resuspension from sea floor bathymetry and sub-Antarctic islands (**Figure 2**) (e.g., Pollard et al., 2002; Ardelan et al., 2010; Rembauville et al., 2015b). This pattern differs from that of macronutrients, which decline northwards across the POOZ region, nitrate falling from ∼25–20 $\mu mol\ l^{-1}$ and silicate from ∼60–10 $\mu mol\ l^{-1}$. These nutrients are upwelled at the Antarctic Slope Front and are progressively drawn down by phytoplankton as they are transported northward across the POOZ by Ekman drift (Tréguer and Jacques, 1992; Pollard et al., 2002).

The POOZ displays a strong seasonality in biological production (Abbott et al., 2000). Strong winds in winter deepen the mixed layer, bringing nutrient-rich water to the surface. These nutrients fuel phytoplankton growth in spring when sunlight increases, conditions are calmer, and phytoplankton are confined to shallower mixed depths by stratification (**Figure 6A**) (Abbott et al., 2000; Pollard et al., 2002; Constable et al., 2014). Whilst the POOZ is considered to be an iron-limited environment, silicate limitation and grazing by micro- and metazooplankton also limit the duration of the diatom-dominated bloom in this region (Abbott et al., 2000; Becquevort et al., 2000; Timmermans et al., 2001; Strzepek et al., 2011; Christaki et al., 2014). Like the SAZ, large, heavily silicified diatoms contribute significantly to carbon export (Rembauville et al., 2015a,b, 2016b; Rigual-Hernández et al., 2015). In regions of natural iron fertilization (e.g., the Kerguelen Plateau), phytoplankton production appears to be strongly linked to higher trophic levels rather than making a substantial contribution to carbon export (Obernosterer et al., 2008; Christaki et al., 2014; Laurenceau-Cornec et al., 2015; Rembauville et al., 2015b).

Modeling studies predict the POOZ region will experience a poleward shift and strengthening of the westerly winds; deepening of the summertime mixed layer depth; increasing cloud cover; warming and freshening of surface waters; and decreasing pH (**Figure 6B**) (Orr et al., 2005; McNeil and Matear,

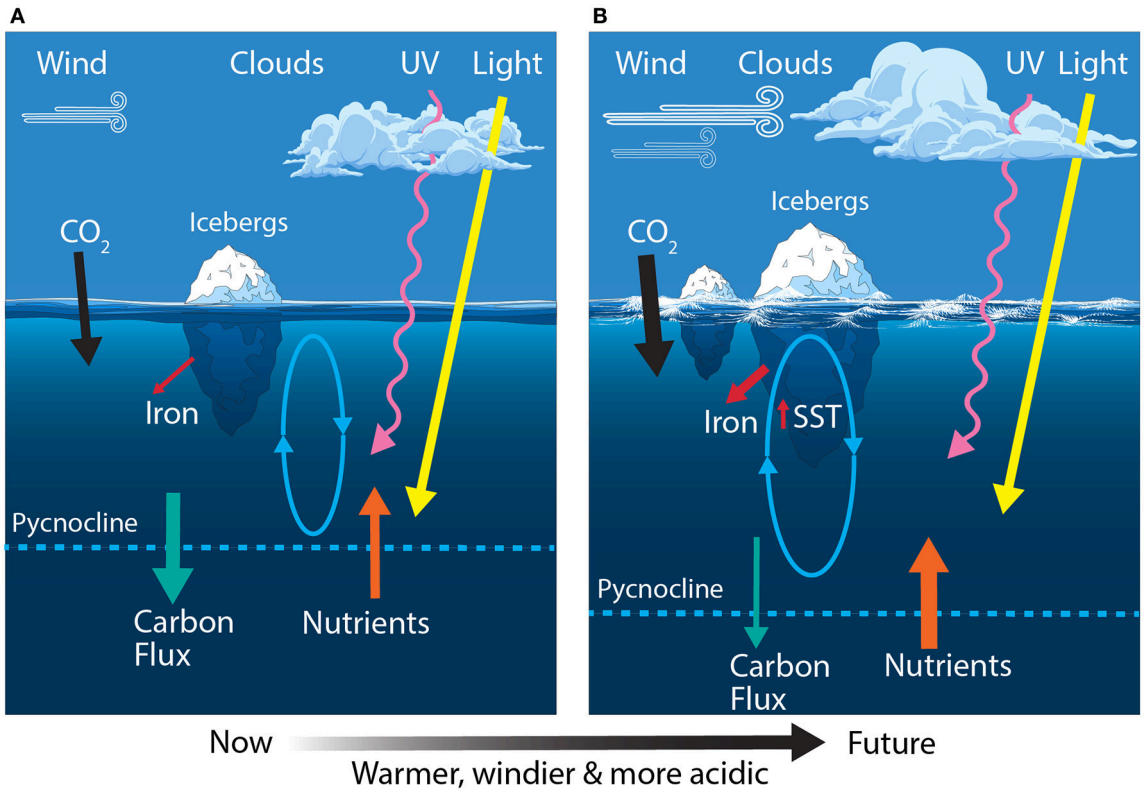

FIGURE 6 | Schematic showing the primary physical constraints on phytoplankton in the Permanently Open Ocean Zone (POOZ) (A) before and **(B)** after climate change. Ovals represent the depth of mixing and arrow thickness reflects relative rates of flux. SST, sea surface temperature.

2008; Meijers, 2014; Leung et al., 2015; Armour et al., 2016; Haumann et al., 2016). Thus far, sea surface warming in the POOZ of only 0.02°C per decade has been slower than the global average of 0.08°C per decade, since 1950 (Armour et al., 2016). This is due to heat taken up by surface water in the POOZ being transported northward by Ekman drift into the SAZ (**Figure 3**). Despite this, it has been proposed that rising temperatures may be contributing to an observed range extension of *E. huxleyi* below 60°S (Cubillos et al., 2007; Winter et al., 2014).

Whilst warming is expected to increase phytoplankton productivity (Sarmiento et al., 2004; Behrenfeld et al., 2006; Steinacher et al., 2010), this effect is offset against the increasingly positive phase of SAM, which is causing an intensification and southerly shift of westerly winds in summer (Lenton and Matear, 2007; Lovenduski et al., 2007). The SAM controls the north-south shift of the circumpolar westerly winds and is the dominant climate-induced environmental change in Antarctic waters, substantially affecting SO circulation and CO_2 uptake (Thompson and Solomon, 2002; Lenton and Matear, 2007; Lovenduski et al., 2007; Swart et al., 2014). In the last 50 years there has been an observed increase in the positive phase of SAM, strongly related to the depletion of ozone in the atmosphere above Antarctica (Son et al., 2008; Polvani et al., 2011). Leung et al. (2015) predict that the positive SAM will continue to deepen the summer mixed layer and increase cloud cover in the POOZ, resulting in decreasing light availability and causing a decline in phytoplankton biomass and productivity. Observed trends in summertime mixed layer depth, cloud cover, and Chl *a* (since 1950, 1980, and 1997, respectively) correspond well to the modeled projections (Leung et al., 2015).

Conversely, some predict the increase in positive SAM may enhance phytoplankton productivity in the POOZ. Deepening of the mixed layer can increase the upwelling of nutrients, which some models predict will promote phytoplankton productivity and export production south of 60°S (Lovenduski and Gruber, 2005; Hauck et al., 2013, 2015; Laufkötter et al., 2015). It is hard to assess the validity of such predictions for the POOZ region as these models combine all waters south of the Polar Front, including the SSIZ. Using satellite and Argo data, Carranza and Gille (2015) reported a correlation of increased Chl *a* in the SO with increased mixed layer depth. A positive SAM also increases eddy formation and transports SAZ water across the Polar Front (Meredith and Hogg, 2006; Kahru et al., 2007; Hogg et al., 2008). These cyclonic eddies trap warm water at their core, enhance stratification, and upwell nutrients and iron, creating ideal conditions for phytoplankton productivity (Kahru et al., 2007) and may also contribute significantly to ocean warming in the POOZ (Hogg et al., 2008).

Increased nutrient input from melting icebergs may also increase productivity in the POOZ. Climate warming and the breakup of Antarctic ice shelves (Scambos et al., 2000) could increase the number of icebergs in the POOZ (see CZ

below). Melting icebergs enrich the surrounding water with iron, enhancing phytoplankton growth and productivity (Cefarelli et al., 2011; Lin et al., 2011; Shaw et al., 2011; Vernet et al., 2011, 2012), and increasing export of carbon from surface waters (Smith et al., 2011). This heightened productivity also attracts large grazing populations that increase food availability to higher trophic levels and facilitates the sequestration of carbon to the deep ocean through fecal pellet production (Vernet et al., 2011).

Climate change is expected to change the location and area of the POOZ. The Polar Front, which denotes the northern limit of the POOZ has already shifted 60 km south since 1992 and this southward migration is expected to continue as the climate warms (Sokolov and Rintoul, 2009b). To the south, the northernmost extent of sea ice coverage is also predicted to retreat with ocean warming. Overall, this would result in a net increase in the area of the POOZ in the future (Bracegirdle et al., 2008; McNeil and Matear, 2008; Boyd et al., 2014). Some studies suggest that an increase in open ocean habitat will increase production in this region (Bopp et al., 2001; Behrenfeld et al., 2006). However, it is not yet understood how the multi-stressor effects of the accompanying environmental changes, such as ocean warming, decreased pH, light availability, and nutrient supply will affect the phytoplankton community.

The effect of climate change on phytoplankton productivity in the POOZ will strongly depend on the changes in light limitation and nutrient supply. Deepening of the summertime mixed layer depth due to increases in the strength of westerly winds are likely to further reduce the light available to phytoplankton, reducing their productivity over much of the POOZ (see above). However, increased nutrient concentrations as a result of increased mixing and melting icebergs, together with the incursions of warm-core eddies from the Polar Front may promote localized phytoplankton blooms when light is not limiting. Furthermore, increased nutrient concentrations might promote the growth of large diatoms (Timmermans et al., 2001), as well as increased abundance of phytoplankton in near surface waters rather than forming deep chlorophyll maxima. This increase in abundance is likely to increase the functioning of the microbial loop and promote grazing, as has been observed in naturally iron-fertilized regions of the POOZ (Christaki et al., 2014). It is also likely that with a future southward shift in SSIZ extent (see SSIZ below) the brief but substantial blooms of *Phaeocystis* sp. and large diatoms of the MIZ will be replaced by a prolonged but subdued bloom of phytoplankton over summer in waters that are now part of the POOZ (see MIZ below, Behrenfeld et al., 2006).

4. SEASONAL SEA ICE ZONE

In the following sections we divide the region of the SO covered by sea ice into two distinct zones. First we consider the effects of climate change on the extent, advance and retreat of ice over the entire Seasonal Sea Ice Zone (SSIZ) and examine the implications for phytoplankton. Then we consider the processes occurring at the northern margin of the sea ice (the marginal ice zone, MIZ), and how these are predicted to respond to a changing climate.

The SSIZ encompasses the region of the SO between the winter maximum and summer minimum of sea ice cover (**Figure 2**). The sea ice is one of the largest and most dynamic ecosystems on earth, extending to over 19 million km^2 in winter and retreating to ∼3 million km^2 over summer (Brierley and Thomas, 2002; Comiso and Nishio, 2008; Convey et al., 2009). Total productivity within the SSIZ has been estimated at ∼140–180 Tg C yr^{-1} (Arrigo et al., 1997, 2008b). Sea ice cover plays an important role in the regulation of climate by controlling heat and gas exchange between the atmosphere and the ocean (Massom and Stammerjohn, 2010). Snow covered sea ice creates a high albedo surface that reflects most of the sun's energy back into space, thereby reducing warming of the polar oceans (Perovich, 1990). Conversely, in winter the ice cover insulates the ocean from direct exposure to the cold atmosphere (Stroeve et al., 2016 and references therein). Not only is sea ice itself an important regulator of global climate, it also provides a vital environment for Antarctic life.

Sea ice supports a diverse community of algae that possess some of the most extreme adaptations to environmental stress recorded. They inhabit a range of environments throughout the ice; from surface ponds to brine channels in the sea ice interior and at the bottom ice-water interface (Knox, 2007; Arrigo, 2014). Here they can experience extremely low temperatures (<-20°C), light irradiances (<1 μmol m^{-2} s^{-1}), CO_2 concentrations (<100 μatm), and salinities up to ∼200 PSU (Thomas and Dieckmann, 2002 and references therein). Primary production by sea ice algae contributes between 24-70 Tg C yr^{-1} (Legendre et al., 1992; Arrigo et al., 1997; Saenz and Arrigo, 2014) and phytoplankton biomass averages between 1 and 100 mg Chl *a* m^{-2}, although it can exceed 1000 mg Chl *a* m^{-2} in some regions (Lizotte, 2001; Arrigo et al., 2010). Ice algal biomass and productivity varies greatly at small spatial and temporal scales, primarily due to changes in snow cover, ice thickness, surface flooding, and ice rafting (McMinn et al., 2007; Meiners et al., 2012; Arrigo, 2014 and references within). Thus, ice algae are able to thrive in this harsh physical environment.

Ice algal productivity is essential to the nutrition of higher trophic levels in Antarctic waters. Productivity and algal biomass within the sea ice is generally low during the winter (Arrigo et al., 1998a). Conditions are most favorable at the ice-water interface, where warmer temperature (-1.8°C), lower salinity (∼35 PSU), and high nutrients maintain higher productivity rates than the sea ice interior (Lizotte, 2001). These bottom ice algal communities are an essential food source for zooplankton over winter (Brierley and Thomas, 2002 and references therein, Jia et al., 2016), when phytoplankton biomass in the waters beneath the sea ice are very low due to light limitation (Perrin et al., 1987; Legendre et al., 1992; Robins et al., 1995). For example, the phenology of the Antarctic krill, *Euphausia superba*, a keystone organism in SO food webs, is integrally liked to sea ice and seasonality, largely due to its being a refuge and source of algal nutrition over winter (Kawaguchi and Satake, 1994; Daly, 1998; Atkinson et al., 2004; Smetacek and Nicol, 2005; Quetin and Ross, 2009) and is associated with the ice at all stages of its life cycle (Flores et al., 2012 and references therein). Thus, changes in the timing and/or extent of sea ice cover are likely to have major implications for the Antarctic food web (see below, Quetin and Ross, 2009).

Changes in the extent, duration, thickness, and transparency of sea ice will have major implications for the algae that inhabit

the ice and processes that drive phytoplankton productivity during sea ice retreat. In stark contrast to the decline currently observed in the Arctic (Stroeve et al., 2012 and references therein), the overall sea ice extent (SIE) around Antarctica has experienced a modest increase of between 0.9 and 1.5% since 1979 (Comiso and Nishio, 2008; Turner et al., 2009; Parkinson and Cavalieri, 2012; Simmonds, 2015), and modeled increases in sea ice volume of ∼0.4% yr^{-1} between 1992 and 2010 due to approximately equal increases in both SIE and thickness (Holland et al., 2014). This culminated in the National Snow and Ice Data Center (NSIDC) reporting a maximum recorded SIE >20 million km^2 in September 2014, 1.54 million km^2 above the 1981 to 2010 average (Fetterer et al., 2016a). However, the SIE around Antarctica in November 2016 was only 14.54 million km^2, 1.81 million km^2 below the 1981 to 2010 average (Fetterer et al., 2016b), demonstrating substantial interannual variability. Furthermore, the long term trend in increasing SIE is not uniform around Antarctica, with a significant decrease in the Amundsen and Bellingshausen Seas of between −5.1 and −6.6% per decade but a large increase in the Ross Sea of between 4.2 and 5.2% per decade due to the Amundsen Sea Low (ASL) (see below, Comiso and Nishio, 2008; Massom and Stammerjohn, 2010; Parkinson and Cavalieri, 2012).

Dramatic changes in SIE in some regions around Antarctica have altered the timing of sea ice growth and retreat. The large changes in SIE between the Ross Sea and the WAP are driven by the combined influence of the El Niño-Southern Oscillation (ENSO), the SAM, and their interaction with the ASL, the deepest low pressure cell around Antarctica (Arrigo and Thomas, 2004; Liu et al., 2004; Massom et al., 2008; Stammerjohn et al., 2008; Pezza et al., 2012; Raphael et al., 2016). The positive SAM phase and the La Niña phase of the ENSO have deepened the ASL. Increasing greenhouse gasses and stratospheric ozone recovery may also exacerbate the current SIE trends in these regions by further deepening the ASL (Raphael et al., 2016). The resultant strengthening of winds associated with the ASL lead to the compression of the sea ice in the Amundsen and Bellingshausen Seas and expansion in the Ross Sea. As a result, sea ice extent around the West Antarctic Peninsula (WAP) has declined by up to 40% over the past 26 years (Smith and Stammerjohn, 2001; Ducklow et al., 2007; Parkinson and Cavalieri, 2012). Modeling studies predict that continued global warming will eventually override the SAM and ENSO effects, increasing warming to the atmosphere and ocean, and resulting in significant declines in SIE around Antarctica (Bracegirdle et al., 2008; Ferreira et al., 2015).

Changes in sea ice concentration, extent, and seasonality critically affect the timing and productivity of phytoplankton blooms. In the western Ross Sea, sea ice retreats later and advances earlier, reducing the ice-free season by ∼2.6 months (Stammerjohn et al., 2012). The delay in ice retreat has delayed the onset of the summer bloom and decreased its duration, thereby reducing total seasonal productivity (Arrigo and van Dijken, 2004). Conversely, earlier retreat and delayed advance of sea ice has resulted in a 3 month lengthening of the summer ice-free season in the Amundsen and Bellingshausen Seas (Stammerjohn et al., 2012). While this extension of the ice-free period was expected to increase annual phytoplankton production and growth (Sarmiento et al., 2004; Moreau et al., 2015), no such trend has yet been observed (Smith et al., 2008; Montes-Hugo et al., 2008). This may be due to constraints imposed by nutrient and light limitation that are also key drivers of phytoplankton growth in the SSIZ (Pearce et al., 2010; Westwood et al., 2010).

The observed increase in SIE is contrary to modeling studies that predict a decline in SIE with global warming (Maksym et al., 2012 and references therein), reflecting the complex interaction of factors influencing the distribution and concentration of sea ice around Antarctica (Sen Gupta et al., 2009; Parkinson and Cavalieri, 2012 and references therein, Turner et al., 2013). Models indicate that the continued warming of the Earth's climate will result in a 33% decline in Antarctic SIE by 2100 (Bracegirdle et al., 2008). Historical records (whaling records, ice charts, and direct observations) and concentrations of methane sulfonic acid in ice cores suggest SIE has declined at least 20% since the 1950s (Curran et al., 2003; de la Mare, 2009).

The seasonal southward retreat of the sea ice initiates the phytoplankton bloom (see MIZ below) and changes in the timing of sea ice growth and retreat will alter the timing of these blooms. Such changes can impose temporal asynchronies and spatial separations between grazers and their food, reducing grazer abundance, reproductive success, and altering the distributions of higher trophic levels (Moline et al., 2008). SO zooplankton use the sea ice as a refuge and food source in the winter (Daly, 1998; Murphy et al., 2007; Jia et al., 2016). MIZ phytoplankton blooms supply the essential fatty acids required for reproduction and over-wintering strategies (Schnack-Schiel et al., 1998; Hagen, 1999). It is not yet known how changes in sea ice retreat will affect higher trophic levels in SSIZ but a delay in the summer bloom may restrict the availability of an essential food source during vulnerable life-stages, resulting in significant grazer mortality and less food availability to higher trophic organisms.

A decline in SIE is likely to decrease overall ice algal abundance, reducing carbon flux to the deep ocean. Decaying sea ice releases plumes of ice algal aggregates that can sink from surface waters at rates ≤200 m d^{-1} (Thomas et al., 1998; Wright and van den Enden, 2000; Wright et al., 2010). Given that sea ice algae contribute to ∼12% of annual productivity in the SSIZ (Saenz and Arrigo, 2014); the large accumulations of algal biomass amongst the sea ice (see above); and the fact that the rate of sedimentation would largely preclude remineralization of these algal aggregates; it is likely that declining ice algal abundance would reduce this region's contribution to vertical carbon flux.

A reduction in SIE extent, and therefore sea ice algal biomass, is also likely to reduce the contribution of Antarctic sea ice algae to the global biogenic sulfur budget via synthesis of DMSP and subsequent release of DMS. Many intracellular roles have been proposed for DMSP and DMS, including cryoprotectant, antioxidant, metabolic overflow product, and even a compound that mediates grazer interactions (Kirst et al., 1991; Malin, 2006 and references therein). DMS is oxidized in the atmosphere to sulfate aerosols which nucleate cloud condensation, altering global albedo (Charlson et al., 1987, 1992). Estimates suggest that the Antarctic region contributes 17% of

the global DMS emissions (Curran and Jones, 2000), with the highest concentrations of these DMSP and DMS compounds often found amongst sea ice (e.g., Kirst et al., 1991; Turner et al., 1995; Trevena and Jones, 2006; Jones et al., 2010; Vance et al., 2013). Any climate-induced decline in SIE and/or duration (see above) could reduce the magnitude of DMS production in the SSIZ, feeding back to global climate by reducing cloud-induced albedo.

Thinning of sea ice could substantially contribute to the loss of sea ice volume within the SSIZ, impacting ice algal communities. Observations of ice thickness in the SSIZ are sparse and difficult to obtain, displaying large variability within regions and among seasons (Worby et al., 2008). As a result, current trends in Antarctic sea ice thickness are not well understood (Kwok, 2010; Hobbs et al., 2016 and references therein) and based upon model estimates (Holland et al., 2014). The majority of the sea ice in the SSIZ is first-year ice, with ice thickness seldom exceeding 2 m (Worby et al., 2008; Meiners et al., 2012). Ice algal biomass is often concentrated in the bottom 20 cm of the ice (Palmisano and Sullivan, 1983; McMinn et al., 2007; Meiners et al., 2012), with thicker ice (>1.0 m) supporting higher algal biomass than thin ice (<0.4 m), due to longer time for colonization and growth of the bottom ice algal community, along with development of internal communities from the rafting of ice floes (McMinn et al., 2007; Meiners et al., 2012). Thus, a decline in sea ice thickness may result in a reduction in bottom community biomass, which is an important food source for zooplankton (Brierley and Thomas, 2002; Jia et al., 2016), thereby causing a shift in the diet of Antarctic birds and mammals toward less efficient pathways (Murphy et al., 2007; Moline et al., 2008; Flores et al., 2012; Ballerini et al., 2014).

A warming atmosphere is predicted to result in more precipitation that could cause an increase in snow deposits on the surface of the sea ice (Bracegirdle et al., 2008; Massom et al., 2008). Increased snow load depresses ice floes, flooding the ice surface and fostering phytoplankton blooms in the high light, high nutrient environment at the snow-ice interface (Arrigo et al., 1997; Massom et al., 2006). Surface communities are most often associated with thin ice (<0.4 m) (Meiners et al., 2012) and as such, could become more prominent in the future. Increased albedo caused by greater snow cover on the ice would also limit light transmission through the ice, reducing ice algal productivity in internal and bottom communities (Grossi et al., 1987; Palmisano et al., 1987).

Sea ice is a substantial sink for CO_2 over winter. Air-ice exchange at the ice surface over-saturates the CO_2 in sea ice brine and contributes as much as 58% of the annual atmospheric CO_2 uptake in the SO (Delille et al., 2014). Ice cover provides a barrier between the atmosphere and the surface water, slowing atmospheric CO_2 uptake (Boyd et al., 2008) and limiting predicted pCO_2 levels by 2100 to 500–580 μatm. Furthermore, it prohibits outgassing of upwelled water supersaturated in CO_2 over winter (Gibson and Trull, 1999; Roden et al., 2013). The few studies investigating the effect of ocean acidification on sea ice algal communities suggest they can tolerate CO_2 concentrations up to 10,000 μatm (McMinn et al., 2014; Coad et al., 2016).

The increasingly positive SAM (see SAZ above) exposes the SSIZ is to stronger winds. However, future recovery of the ozone hole will reduce the SAM favoring increasing warming and stratification (see Conclusion), with consequent declines in the SIE extent, thickness and duration of ice cover. This is likely to have a strong negative effect on sea ice algal abundance, through a loss of habitat. Whilst ice algae are not major contributors to overall SO primary productivity, they are essential in the life cycles of many zooplankton species. Thus, declines in ice algal abundance will likely have a significant negative effect on critical links in the SO food web, especially krill, and promote different and less energy efficient trophic pathways such as consumption of phytoplankton by salps or via copepods to myctophids. Such changes would reduce the capacity of the SO to support the current abundance of iconic, krill-dependent Antarctic wildlife (Murphy et al., 2007, 2016).

The development of the phytoplankton bloom and succession of the pelagic phytoplankton community is initiated by the seasonal retreat of the sea ice across the SSIZ. Here we consider the effects of climate-induced changes on processes in the MIZ.

5. MARGINAL ICE ZONE

The region where the dense sea ice pack transitions to open ocean is known as the marginal ice zone (MIZ). It is an area of high productivity that accounts for the majority of the spring-summer phytoplankton blooms (**Figure 2**) (Arrigo et al., 2008b). The area of the MIZ varies greatly over spring and summer, ranging from 6 million km^2 in December to ∼0.2 million km^2 by March (Fitch and Moore, 2007). Sea ice formation in the winter scavenges phytoplankton cells into the ice and concentrates iron from the surface water (de Baar et al., 1995; Boyd, 2002; Lannuzel et al., 2010, 2016). In the spring, low salinity, high iron melt water is released from the sea ice, creating a buoyant layer of fresher water that traps phytoplankton in an environment where conditions are ideal for growth (high light, and high macro- and micronutrients). This fosters large phytoplankton blooms (**Figure 7A**) (Smith and Nelson, 1986; Sullivan et al., 1988), which can reach biomasses of over 200 mg Chl *a* m^{-2} (e.g., Smith and Nelson, 1986; Nelson et al., 1987; Wright et al., 2010). The region was thought to house very high rates of productivity (∼400 Tg C yr^{-1}) (Smith et al., 1988; Arrigo et al., 1998b) and contribute 40-50% of the productivity of the entire SO (Smith and Nelson, 1986; Sakshaug, 1994). Advances in satellite technology and modeling algorithms provide more conservative results (Arrigo et al., 2008b; Taylor et al., 2013), suggesting the MIZ contributes ∼114 Tg C yr^{-1}. This equates to a total annual productivity of 54–68 g C m^{-2} yr^{-1}, which is ∼5 times that in the sea ice (∼24 Tg C yr^{-1}) but is similar to that in the POOZ (∼62 g C m^{-2} yr^{-1}) (Moore and Abbott, 2000; Arrigo et al., 2008b; Saenz and Arrigo, 2014).

A diverse array of phytoplankton inhabit the MIZ, undergoing successional change due to ice retreat, warming, nutrient depletion, and grazing (Davidson et al., 2010; Wright et al., 2010). Phytoplankton blooms in East Antarctica and the Weddell Sea, are commonly co-dominated by the colonial life-stage of *Phaeocystis* sp. and diatoms, with increasing diatom abundance

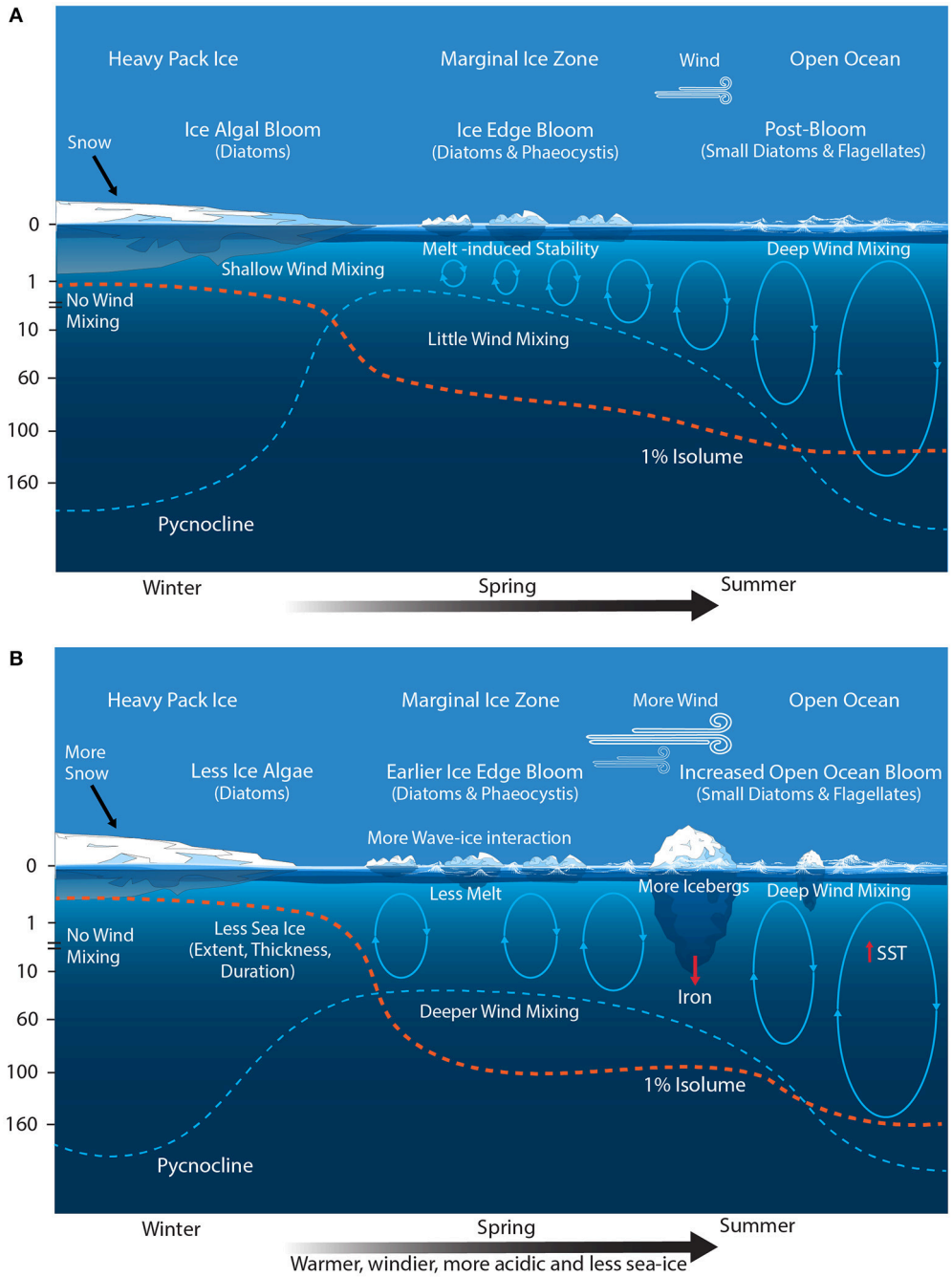

FIGURE 7 | Schematic showing the primary physical constraints on phytoplankton in the Seasonal Sea Ice and Marginal Ice Zones (SSIZ and MIZ) (A) before and **(B)** after climate change. Modified from Sullivan et al. (1988) and Petrou et al. (2016). Ovals represent the depth of mixing and arrow thickness reflect relative rates. Blue dashed line denotes the location of the pycnocline; and the red dashed line depicts the approximated depth for 1% surface irradiance. SST, sea surface temperature.

over time and the appearance of dinoflagellates, silicoflagellates, and heterotrophic protists later in the season (Waters et al., 2000; Kang et al., 2001; Davidson et al., 2010). Once the available iron has been exhausted, the community shifts to one more typical of the POOZ, consisting of small diatoms and flagellates (Pearce et al., 2010; Wright et al., 2010). In the WAP, diatom-dominated blooms in the spring shift to flagellate communities as melting sea ice and glacial run-off reduce the salinity of surface waters (Kang et al., 2001). However, icebergs released by the breakup of ice shelves will increase nutrient input, as in the POOZ (see above, Duprat et al., 2016), promoting additional blooms of large diatoms.

Phytoplankton in the MIZ can contribute directly or indirectly to vertical flux. During large blooms phytoplankton aggregate

to form marine snow, which fall rapidly through the water column, contributing to carbon sequestration into the deep ocean (Alldredge and Silver, 1988). High algal biomass within decaying sea ice in summer is also a rich source of nutrition and a site of reproduction for grazers (Schnack-Schiel et al., 1998; Thomas et al., 1998). This grazing transfers carbon to higher trophic levels but can also contribute to vertical carbon flux by reparceling cells into rapidly sinking fecal pellets (Cadée et al., 1992; Burkill et al., 1995; Perissinotto and Pakhomov, 1998; Pearce et al., 2010).

Climate change is predicted to decrease SIE, increase icebergs, and cause SAM-induced increases in wind and wave action (**Figure 7B**). The effect of decreased SIE on total annual productivity in the SO may not be large. Reduced SIE would shift the latitudinal range of the MIZ southward, resulting in an increase in the area of the POOZ (Smetacek and Nicol, 2005). However, the restriction of intense primary productivity in the MIZ to the spring-summer season results in area-normalized annual primary production similar to that of the POOZ (see above, Moore and Abbott, 2000; Arrigo et al., 2008b), suggesting that an increase in the size of the POOZ may not significantly affect total SO productivity (Arrigo et al., 2008b). Admittedly, this does not take into account other potential effects of climate change on the POOZ (see above), nor does it consider the effect of the absence of ice on the timing and magnitude of the phytoplankton bloom. It is likely that blooms would start earlier due to the higher light climate but may develop slower due to greater mixed depths (see below) and the lack of iron fertilization from the ice melt (Behrenfeld et al., 2006).

The most profound change in the MIZ may be caused by the increasingly positive phase of SAM. The poleward shift and intensification of wind strength and storms is predicted to deepen the mixed layer and reduce phytoplankton production in the MIZ (**Figure 7B**) (Lovenduski and Gruber, 2005; Yin, 2005; Hemer et al., 2010; Massom and Stammerjohn, 2010; Young et al., 2011; Dobrynin et al., 2012). Phytoplankton blooms in the MIZ are patchy in space and time (Smith and Nelson, 1986). They generally occur in shallow mixed layers where wind speeds are <5 m s^{-1} (Fitch and Moore, 2007). Storms, wind mixing, and waves deepen mixed depths in the MIZ, reducing the light availability and inhibiting bloom development (**Figure 7B**) (Venables and Meredith, 2014). As a result, blooms only cover 17–24% of the MIZ over summer with maximum coverage of only 0.36 million km^2 in December (Savidge et al., 1996; Fitch and Moore, 2007). Evidence from culture studies and blooms in the Ross Sea indicate that *Phaeocystis* sp. is more tolerant of deeply mixed, low light environments than diatoms (Arrigo et al., 1999; Moisan and Mitchell, 1999). Therefore, a more deeply mixed MIZ could cause a shift toward *Phaeocystis* sp. dominated blooms.

Large, early season blooms of *Phaeocystis* sp. can be responsible for substantial carbon export, rapidly sinking from surface waters and avoiding grazing pressure. *Phaeocystis* sp. colonies are encased in a tough outer coating, providing an effective defense against grazing protozoa and small zooplankton (Smetacek et al., 2004). In combination with their ability to draw down larger amounts of CO_2 than diatoms (Arrigo et al., 2000), it is likely that an increase in blooms dominated by *Phaeocystis* sp. may enhance carbon export in the MIZ (DiTullio et al., 2000). *Phaeocystis* sp. are also responsible for generating large amounts of DMSP (DiTullio and Smith, 1995; Turner et al., 1995; Vance et al., 2013). If increased mixing favors *Phaeocystis* sp. growth, it may counteract some of the loss of DMSP from decreased SIE in the SSIZ (see SSIZ above).

An increase in wind and wave action could also potentially increase the area of the MIZ by increasing the breakup and dispersal of sea ice by waves (Yin, 2005; Hemer et al., 2010; Young et al., 2011; Dobrynin et al., 2012; Stroeve et al., 2016). In spring and summer, large waves propagate through the sea ice up to 200 km, breaking up ice floes and accelerating ice retreat (Kohout et al., 2014; Horvat et al., 2016). Some satellite derived estimates of the MIZ region suggest a positive trend in MIZ area over time during spring (Stroeve et al., 2016), although not all models agree due to difficulties in accurately mapping the MIZ from satellite images (Ackley et al., 2003). However, changes in MIZ area are not likely to be uniform within the SSIZ, with Massom et al. (2006) reporting a contraction of the MIZ in the WAP due to strong northerly winds from the ASL (see SSIZ above). Interestingly, intense phytoplankton blooms still occurred amongst in the slurry of frazil ice between floes in this region (Massom et al., 2006), suggesting MIZ size is not necessarily a good indicator of its productivity.

Bloom formation within the MIZ is reliant on the coincidence of optimal conditions for phytoplankton growth. Increases in turbulent mixing by wind and waves would decrease light availability through a deepened mixed layer, with likely reductions in productivity and changes in the phytoplankton community structure within MIZ blooms. Additional nutrient inputs from melting icebergs are likely to cause localized increases in productivity but the extent of this effect would be felt most in the SSIZ, where growth of phytoplankton has drawn down nutrient concentrations. The net effect of future increases in MIZ area and decline in overall SIE remain uncertain.

6. ANTARCTIC CONTINENTAL SHELF ZONE

Antarctic Continental Shelf Zone (CZ) waters make up the smallest area of the SO (1.28 million km^2) but they are also highly productive, contributing 66.1 Tg C yr^{-1} or an average of 460 mg C m^{-2} d^{-1} (Arrigo et al., 2008b). The high productivity in this region is due to high surface nutrient concentrations; iron enrichment from coastal sediments and basal shelf melt; and upwelled upper circumpolar deep water (UCDW, **Figure 3**) onto the continental shelf from the easterly-flowing Antarctic Slope Current, which approximately follows the 1,000 m isobath (**Figure 2**) (Jacobs, 1991; Smetacek and Nicol, 2005; Westwood et al., 2010; Williams et al., 2010). Blooms in CZ waters make a vital contribution to supporting the abundance and diversity of life in Antarctica. They attract large numbers of grazers that consume phytoplankton, that in turn feed higher tropic levels, while also producing fecal pellets, that are either remineralized into nutrients by heterotrophic microbes or sink rapidly into deep water, supporting the biological pump (Cadée et al., 1992; Turner, 2002; Honjo, 2004; Schnack-Schiel and Isla, 2005). Open

water regions over the CZ are important foraging areas for many Antarctic species, especially during the summer breeding season (Arrigo and van Dijken, 2003; Smith et al., 2007; Stroeve et al., 2016). For example, DMS released from grazed phytoplankton acts as an olfactory foraging cue for white-chinned petrels (Nevitt et al., 1995) and Adélie penguin breeding success has been related to the proximity of colonies to open water (Ainley et al., 1998). The CZ is also a significant CO_2 sink over the summer as high rates of primary productivity cause surface CO_2 undersaturation (Hoppema et al., 1995; Gibson and Trull, 1999; Ducklow et al., 2007; Arrigo et al., 2008a; Roden et al., 2013).

Polynyas contribute to high productivity over the CZ with average annual primary production rates up to 105.4 g C m^{-2} yr^{-1} (Arrigo and van Dijken, 2003; Arrigo et al., 2015). Strong, cold katabatic winds freeze the surface water of the polynya, creating ice that is pushed north, adding to the seasonal sea ice extent and contributing to the generation of Antarctic Bottom Water through exclusion of high salinity brine by sea ice as it forms (Orsi et al., 1999). The Ross Sea polynya is the largest and the most productive polynya in Antarctica, contributing on average, 22.2 Tg C yr^{-1} (Arrigo et al., 2015), with daily production as high as 6 g C m^{-2} d^{-1} (Smith and Gordon, 1997). These high productivity rates are likely due to substantial iron input from upwelling of underlying sediments and basal melt of nearby ice shelves (Arrigo et al., 2015). Future increases in sea surface temperature are likely to accelerate the melting of ice shelves, increasing the input of fresh, stratified, iron-rich water to polynyas. increasing productivity in these regions (Feng et al., 2010).

Spatial differences in the factors controlling phytoplankton production have been observed within CZ waters. Consequently, the cause and rate of climate-induced change in these waters differs with location. Substantial differences have already been observed between East and West Antarctica (Turner et al., 2014 and references therein) and as such, we separately address the effects climate change on the phytoplankton communities in each of these two regions.

6.1. West Antarctica

The West Antarctic CZ spans from the Amundsen and Bellingshausen Seas in the west to the Weddell Sea in the east and is dominated by the Antarctic Peninsula. Productivity is highest along the WAP and the Weddell Sea with rates of over 600 mg C m^{-2} d^{-1} during the peak of summer (El-Sayed and Taguchi, 1981; Arrigo et al., 2008b; Vernet et al., 2008). The flow of warm, nutrient-rich UCDW onto the continental shelf (**Figure 3**) in the WAP accelerates sea ice retreat and enhances phytoplankton productivity (Kavanaugh et al., 2015), fostering diatom blooms as in the MIZ (see above). These are replaced by small flagellate and cryptophyte communities in the fresher, more stratified surface water later in the season (Moline et al., 2004; Ducklow et al., 2007). High production in the WAP and Scotia Sea support abundant krill populations, which are in turn food for a wealth of higher predators (Ducklow et al., 2007 and references therein).

Climate change threats to the West Antarctic CZ include warming, freshening, increased stratification, the melting and break up of glaciers and ice shelves, and ocean acidification (**Figure 8B**). The WAP is one of the fastest warming regions on Earth with an increase in the mean atmospheric temperature of 2°C (6°C in the winter) since 1950 (Meredith and King, 2005; Ducklow et al., 2007). No similar warming event has occurred on Earth in the last 1,800 years (Vaughan et al., 2003). Along with atmospheric warming in the WAP, increased heat delivery of UCDW from the Antarctic Circumpolar Current onto the shelf has caused a 0.6°C increase in temperature of the upper 300 m of the water column (Meredith and King, 2005; Turner et al., 2014). This warming trend has resulted in increased glacial melt, with 87% of glaciers in the Antarctic Peninsula showing signs of retreat since 1950 (Cook et al., 2005; Peck et al., 2010). Glacial melt has resulted in an influx of fresh water to coastal regions of the WAP, freshening and increasing the stratification of surface waters over the summer. While phytoplankton productivity is expected to increase with increasing sea surface temperature (Rose et al., 2009), the phytoplankton community is likely to be more affected by resultant changes in SIE and freshwater inputs to the CZ (Arrigo et al., 2015; Moreau et al., 2015).

Freshening of surface waters from glacial melt has led to a documented change in the phytoplankton community in the WAP from diatom-dominated assemblages to cryptophytes and small flagellates (Moline et al., 2004; Montes-Hugo et al., 2008). The resultant shift in size distribution from large to small phytoplankton cells has had a significant flow on effect to zooplankton grazers, particularly krill and salps (Moline et al., 2004). This region is historically an area of high krill abundance, which is the preferred food source for the many Antarctic birds and mammals that live in the WAP (Atkinson et al., 2004). Changes to the phytoplankton community structure, favoring small cells, negatively affects krill grazing as they feed most efficiently on cells >10 μm and are unable to capture particles <6 μm in size (Kawaguchi et al., 1999). This has caused a shift in dominance to salps, mucoid feeders that are unaffected by the particle size of their prey (Moline et al., 2004), and a shift toward a less efficient fish-based food web (Murphy et al., 2007). Reductions in the krill population in the WAP are expected have a significant negative effect on the food chain in this region (Ballerini et al., 2014).

Surface water freshening causes a concurrent stratification of the water column, elevating phytoplankton into shallow mixed layers with higher light intensity. Phytoplankton productivity is enhanced through increased light, however, excessive light and elevated UV-A and UV-B exposure can lead to photoinhibition and cell damage (see SAZ above, Moreau et al., 2015). In order to limit the damage of these conditions, phytoplankton can channel metabolic reserves into photoprotection and tolerance mechanisms (Davidson, 2006). A lengthening of the open water season in the WAP, caused by earlier sea ice retreat (see SSIZ above), has increased productivity in the CZ, whilst also increasing photoinhibition rates (Moreau et al., 2015). Thus far, the increase in production is much greater than the loss due to photoinhibition so it is expected that increased stratification will lead to a net increase in primary productivity in the future (Moreau et al., 2015).

Stronger westerly winds, as a result of a positive SAM, are bringing warmer air across the Antarctic Peninsula, increasing

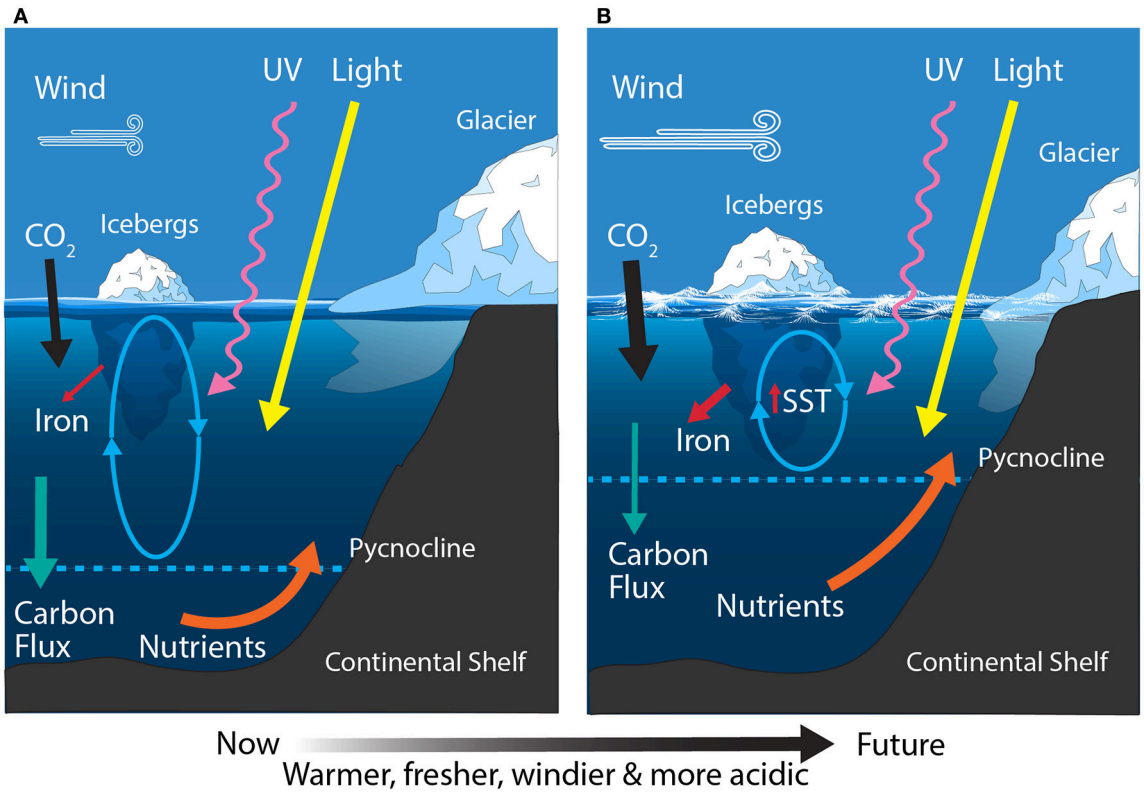

FIGURE 8 | Schematic showing the primary physical constraints on phytoplankton in the Antarctic Continental Shelf Zone (CZ) (A) before and **(B)** after climate change. Ovals represent the depth of mixing and arrow thickness reflects relative rates of flux. SST, sea surface temperature.

snowfall and causing a break up of large ice shelves (e.g., Scambos et al., 2000; Rack and Rott, 2004; Turner et al., 2014). The break up of the Larsen A ice shelf created new areas of high nutrient open water, stimulating phytoplankton blooms and increasing productivity in a previously ice-covered pelagic habitat (Bertolin and Schloss, 2009). The continued retreat of glaciers and breaking up of ice shelves has led to the creation of new carbon sinks around the Antarctic Peninsula that have increased productivity up to 3.5 Tg C m^{-2} yr^{-1} (Peck et al., 2010). The continued break up of ice shelves will also lead to an increase in icebergs over the CZ. Melting icebergs have been found to provide a significant amount of iron and nutrients to surface waters, leading to increased phytoplankton productivity (Lin et al., 2011; Vernet et al., 2011; Duprat et al., 2016). Increased iceberg numbers will also contribute to increased productivity throughout the SSIZ and POOZ as they are propelled by ocean currents around Antarctica (see above).

Little work has investigated the effect of ocean acidification on phytoplankton in West Antarctic waters. The CO_2 concentration in waters over the West Antarctic CZ vary seasonally from ~176 to 503 µatm through to the uptake of CO_2 by phytoplankton in the summer and return to super-saturated levels in winter under the sea ice (Moreau et al., 2012). Coastal phytoplankton communities from the WAP (both diatom-dominated and mixed diatom-flagellate communities) displayed no significant change in community composition, cell size, or growth rate when exposed to 800 µatm CO_2 (Young et al., 2015). Yet, results of this study did demonstrate the differences in physiological carbon uptake among phytoplankton species as production by diatoms may be enhanced by down-regulation of CCMs at high pCO_2, while a slight decline in production by *Phaeocystis* sp. was attributed to the alternative bicarbonate transport pathway used by this species.

6.2. East Antarctica

The East Antarctic CZ ranges from the Ross Sea in the east to the eastern edge of the Weddell Sea in the west. The Ross Sea is the most productive region in the CZ, contributing ~24 Tg C m^{-2} yr^{-1} and accounting for ~30% of the total annual production in shelf waters (Sweeney et al., 2000; Arrigo et al., 2008b). Iron and light availability are the dominant factors controlling growth of phytoplankton in the Ross Sea (**Figure 8A**) (Smith et al., 2000b; Feng et al., 2010; Sedwick et al., 2011). In addition, the relative abundances of the dominant phytoplankton (diatoms and *Phaeocystis* sp.) are linked to mixed layer depth, with diatoms dominant in highly stratified water and *Phaeocystis* sp. where it is deeply mixed (Arrigo et al., 1999). These phytoplankton blooms support a unique food web in the Ross Sea, structured around the crystal krill, *Euphausia crystallorophias*, and the Antarctic silverfish, *Pleuragramma antarcticum* (Smith et al., 2007). Elsewhere around East Antarctica the CZ is relatively narrow and contributes ~12 Tg C m^{-2} yr^{-1} (Arrigo et al.,

2008b) and like the West Antarctic CZ, the Antarctic krill, *E. superba*, is a keystone species (Nicol et al., 2000, 2010). Here the phytoplankton community is dominated by blooms of diatoms and *Phaeocystis* sp. during the summer and shifts to small flagellates once nutrients have been exhausted (Waters et al., 2000; Wright and van den Enden, 2000; Davidson et al., 2010).

The East Antarctic CZ is expected to experience increased freshening, stratification, the melting and break up of glaciers and ice shelves, ocean acidification, and modest warming (**Figure 8B**). In contrast to the warming trend around West Antarctica, there has been a measured cooling over East Antarctica for the same period (1969–2000) (Thompson and Solomon, 2002). Despite this, most recent model projections for the Ross Sea by the end of the century predict a 0.15–0.4°C increase in SST, with decreases in the mixed layer depth (∼50–70 m), sea ice concentration (2–11%), and macronutrient concentrations (Rickard and Behrens, 2016). Freshening has already been reported in the Ross Sea and has been attributed to changes in precipitation, sea ice production, and melting of the West Antarctic ice sheet (Jacobs et al., 2002). Projected changes to the remaining area of East Antarctica are not well understood but similar trends are anticipated (Watanabe et al., 2003; Convey et al., 2009; Gutt et al., 2015).

Ocean acidification is anticipated to affect polar waters sooner than the rest of the world, due to the increased solubility of CO_2 in cold water (Orr et al., 2005; McNeil and Matear, 2008). Phytoplankton communities in Antarctic shelf waters are already exposed to strong annual variations in pCO_2 (Gibson and Trull, 1999; Sweeney et al., 2000; Roden et al., 2013; Shadwick et al., 2013; Kapsenberg et al., 2015). Sea ice cover during the winter restricts air-sea gas transfer, allowing for CO_2 oversaturation of the water column (up to 450 μatm) through upwelling of high CO_2 UCDW water from the Antarctic Slope Current (**Figure 3**). Photosynthetic drawdown over the summer can result in CO_2 levels falling below 100 μatm. This large seasonal variation seems to favor species that tolerate large fluctuations in pH. Phytoplankton communities have been observed to show little change in composition when grown at CO_2 concentrations similar to those already experienced in coastal environments (84–643 μatm) (Davidson et al., 2016). However, superimposing anthropogenic pCO_2 increase upon the large natural fluctuation already occurring in the natural environment may push some species past their limit sooner than anticipated (McNeil and Matear, 2008), causing changes in phytoplankton productivity, growth and community composition. Concentrations of CO_2 exceeding 1,000 μatm induced a change in phytoplankton community composition in Prydz Bay, increasing the abundance of small phytoplankton species (Davidson et al., 2016; Thomson et al., 2016). Studies on Ross Sea phytoplankton communities also suggest that high CO_2 concentrations (760–800 μatm) may cause a shift in dominance in this region from *Phaeocystis* sp. to large chain-forming diatom communities (Tortell et al., 2008; Feng et al., 2010). Investigation into the physiological reasons for changes in growth rates link increased growth and carbon fixation to the energy saved through the down-regulation of CCMs (Rost et al., 2008; Tortell et al., 2008), while inhibition of growth and productivity may be related to the metabolic costs of proton pumps to exclude hydrogen ions (Gao et al., 2012; McMinn et al., 2014).

A change in phytoplankton community composition will likely have significant effects on carbon export in the CZ. A shift toward smaller cell communities will allow for increased remineralization of cells through the microbial consumption, decreasing the downward flux of carbon into the deep ocean (Finkel et al., 2010 and references therein). These cells are also likely to be less efficiently grazed by zooplankton, resulting in less carbon transfer to higher trophic organisms. Any CO_2-induced increase in the dominance of diatoms in the Ross Sea may cause a decline in net carbon export as blooms of *Phaeocystis* sp. are capable of exporting more carbon than diatoms (Arrigo et al., 2000). However, diatom-dominated communities are likely to be grazed more than *Phaeocystis* sp., providing better nutrition for the Antarctic food web and also producing negatively buoyant feces that can assist in the sinking of diatoms (Schnack-Schiel and Isla, 2005).

Whilst most studies have focused on individual factors predicted to alter as a result of climate change, phytoplankton in the SO will be simultaneously exposed to multiple climate change stressors (Gutt et al., 2015). Recent work has focused on the interaction of multiple stressors on phytoplankton growth in the Ross Sea, highlighting the complex interaction between environmental changes and the phytoplankton community (Rose et al., 2009; Feng et al., 2010; Xu et al., 2014; Zhu et al., 2016). Iron promotes phytoplankton growth, whereas interactive effects between iron, warming, increased CO_2, and light favor the dominance of diatoms over *Phaeocystis* sp. (Rose et al., 2009; Xu et al., 2014; Zhu et al., 2016). In contrast, high pCO_2 only affected diatoms, favoring the growth of large centric species (Feng et al., 2010). As well as causing shifts in phytoplankton taxa, changes in temperature and iron supply caused modifications to microzooplankton abundance, suggesting possible changes in predator/prey interactions (Rose et al., 2009). No multi-stressor experiments have yet been performed on other East Antarctic phytoplankton communities, though it appears likely that climate-induced change will alter the competitive interactions among dominant phytoplankton taxa and change trophodynamics throughout continental waters.

Freshening, increased stratification, ocean acidification, and the melting and break up of glaciers and ice shelves are all occurring across the Antarctic CZ due to climate change. Phytoplankton growth is promoted by freshening, increased stratification, and the break-up of ice shelves by establishing conditions that are optimal for growth, most notably an increase in iron supply and light availability. However, freshening and ocean acidification also appear to be responsible for shifts in community composition that could result in a decrease in food quality and availability for grazers. This could have a significant negative effect on the structure and function of the Antarctic food web as well as reducing carbon export. In contrast, the proposed CO_2-induced increase in abundance of large diatoms in the Ross Sea may benefit the food web in this region but may still result in a decline in carbon export.

Temperature trends currently differ between East and West Antarctica, with significant warming in West Antarctica and

a slight cooling trend over East Antarctica. Increases in temperature appear to promote phytoplankton growth and may accelerate sea ice retreat, changing the timing and magnitude of bloom onset in this highly productive region. However, the interactive effects that this combination of climate stressors will have on phytoplankton communities in this region is not well understood. Further work will be required before we can fully understand how phytoplankton over the CZ will be affected by a changing climate.

7. CONCLUSION

The SO comprises a vast expanse of ocean containing a diverse array of environments, each of which exposing phytoplankton to environmental factors that limit their production, growth, survival, and composition. Despite these stressors, phytoplankton thrive in some of the most extreme conditions on earth. Climate-induced changes in the physical characteristics of the SO and the responses by phytoplankton differ substantially among environments. No long-term trends in satellite-derived Chl *a* or primary productivity are yet detectable due to the large background of interannual/decadal variability (Henson et al., 2010; Gregg and Rousseaux, 2014). It is unlikely that unambiguous trends due to climate change will be seen until approximately 2055 (Henson et al., 2010). However, some longer time series of underway Chl *a* measurements exist that could indicate climate-induced trends (see below).

Given the competing influences on phytoplankton within each region of the SO, predictions are bound to be tentative and contentious. Our assessment of the available information suggest the responses of phytoplankton in various regions of the SO are:

- In the SAZ, the stratification-induced decline in nutrient supply to surface waters (**Figure 4**) will reduce productivity and favor small flagellates (e.g., Matear and Hirst, 1999; Marinov et al., 2010; Petrou et al., 2016). Boyd et al. (2016) indicates that increases in iron and temperature may double growth rates and favor diatoms but such events depend on the frequency and magnitude of storms to deposit dust in the SAZ and the proximity to land.
- In the POOZ, productivity may increase due to enhanced mixing, eddy activity, and nutrient supply from upwelling and melting icebergs (**Figure 6**). Yet, light limitation imposed by a deepened mixed layer and increased cloud cover may limit this potential increase (Armour et al., 2016).
- In the SSIZ, ice algal abundance is likely to decrease through a decline in SIE, thickness, and duration (**Figure 7**). The absence of sea ice will preclude ice algae providing an essential food source over winter for some zooplankton species. This has the potential to cause significant changes throughout the Antarctic food web. The decline of sea ice as a result of ocean warming may not markedly alter the annual SO productivity but the expansion of the POOZ into the SSIZ is likely to alter the timing, magnitude, and duration of the phytoplankton blooms in these waters.
- In the MIZ, increased wind and wave action is likely to accelerate sea ice retreat, increasing the mixed layer depth and destabilizing the seasonal progression of phytoplankton blooms (**Figure 7**). Such changes would reduce the frequency of ice edge blooms and cause taxonomic shifts in the phytoplankton community toward small diatoms and flagellates.
- In the CZ, the few available studies suggest that warming, freshening, and ocean acidification are likely to elicit changes to community composition (**Figure 8**), with reports of a shift toward communities composed of smaller cells and flagellates (Moline et al., 2004; Davidson et al., 2016). Increased nutrients and stratification from melting glaciers and icebergs are likely to increase productivity (**Figure 8**). Localized shifts in community composition in the Ross Sea toward diatom-dominated communities will potentially decrease carbon export but may provide better nutrition for higher trophic levels.

These changes are likely to have a significant effect on the biogeochemical processes in the SO, affecting the biological pump, microbial loop, and nutrition for higher trophic levels. It is likely that the effect of climate change on phytoplankton in each of these regions is going to be determined by the timing, rate, and magnitude of change in each stressor; as well as the sequence in which these stressors are imposed. Climate change models of the SO still contain large uncertainties, in part due to knowledge gaps in biogeochemical processes and carbon uptake (Frölicher et al., 2016). The vast majority of phytoplankton research in the SO have been observational studies, providing essential data on phytoplankton communities, seasonal community succession, nutrient utilization, primary and export production, and food web interactions (e.g., El-Sayed, 1994; Nicol et al., 2000, 2010; Smith et al., 2000a; Olguín and Alder, 2011; Quéguiner, 2013). These studies are essential for our understanding of the current and potential future state of SO phytoplankton. Relatively few studies have focused on the manipulation of climate stressors on SO phytoplankton species/communities (e.g., Tortell et al., 2008; Rose et al., 2009; Hoppe et al., 2013; Müller et al., 2015; Boyd et al., 2016; Coad et al., 2016; Davidson et al., 2016). More of these studies are necessary in all of the regions of the SO to determine the thresholds for climate-induced stressors on phytoplankton communities. It is also important to perform multi-stressor experiments, incorporating a range of environmental factors affected by climate change, if we are to understand the interactive effects (from synergistic to antagonistic) of future stressors on phytoplankton species and communities (e.g., Feng et al., 2010; Xu et al., 2014; Boyd et al., 2016; Zhu et al., 2016).

The vastness and environmental diversity of the SO; the inherent spatial and temporal variability in phytoplankton communities; and the logistical costs and difficulty in obtaining data from the SO, especially year-round observations, means the effect of climate change on phytoplankton in this region is poorly understood. In some instances, advances in remote sensing technology and computer modeling have allowed access to data sets that can assist in understanding trends. However, they are still limited in their ability to detect some physical changes, such as sea ice thickness and Chl *a* concentration in waters covered by ice (Massom et al., 2006; Hobbs et al., 2016). There are very

few places that have long-term monitoring programs to detect changes in the physical and biological environment (such as the Palmer-Long Term Ecological Research program, Smith et al., 1995) and few of these have collected data for a sufficient duration to detect trends in phytoplankton against the background of natural variation. Decades long monitoring programs should be established as a matter of urgency to detect changes in SO phytoplankton abundance, production, and composition.

Stratospheric ozone concentrations exert a pervasive effect on atmospheric circulation in the Southern Hemisphere and recovery of the ozone hole will change the trajectory of climate. Concern over ozone depletion and the consequent rise in short wave UV radiation reaching the Earth's surface, galvanized the international community, culminating in the Montreal protocol, which banned the use of ozone depleting substances, such as chlorofluorocarbons (CFCs) and halons. Unrecognized at the time, ozone depletion was also the primary cause of increases in the positive phase of the SAM, resulting in the acceleration and poleward shift of westerly winds over the SO (see POOZ above, Polvani et al., 2011; Thompson et al., 2011). This proved to be the most obvious and persistent characteristic of Southern Hemisphere climate change in the last half century (Thompson and Wallace, 2000; Polvani et al., 2011). Modeling studies indicate that recovery of the ozone hole will decelerate the westerly winds (Son et al., 2008) and result in a more rapid rise in Antarctic temperatures than elsewhere in the Southern Hemisphere (Shindell and Schmidt, 2004). Nearly 30 years after the Montreal protocol came into effect, the first signs are emerging that the ozone hole is beginning to heal (Solomon et al., 2016). Projections suggest that ozone concentrations in the stratosphere are likely to return to pre-ozone hole values around 2065 (Son et al., 2008; Schiermeier, 2009). Thus, the main factor presently driving climate change and phytoplankton responses over much of the SO will decline over the next half century. Ozone depletion and positive SAM cause increases in wind and wave action, deeper mixing, and increased nutrient entrainment into surface waters (see POOZ, SSIZ, MIZ above). Replenishment of ozone is likely to reverse these climate-induced drivers of phytoplankton dynamics in Antarctic waters, moving to a scenario reminiscent of the SAZ region and dominated by increased warming, stratification, and declining nutrient availability in surface waters. The effect of this reversal in climate fortunes is unknown but the rate of change (∼50 years) may prove too fast for some species to adapt and/or evolve to the changing environment.

The response of phytoplankton to anticipated future environmental conditions in the SO will eventually depend upon their capacity to adapt and evolve (Boyd et al., 2016 and references therein). Phytoplankton communities have short generation times and high genetic diversity, which allow for adaptation to changing environmental conditions through natural selection (Collins et al., 2014). Some SO phytoplankton communities are already exposed to large variations in their environment, such as sea ice and coastal communities. Phytoplankton that are already exposed to large variations in their environment are considered inherently more tolerant and capable of adapting to future changes (Sackett et al., 2013; Schaum and Collins, 2014). Davidson et al. (2016) showed that exposing natural microbial communities to the large range in CO_2 concentrations they encounter in nature over a year had little effect. Concentrations above this reduced productivity and changed the composition of the phytoplankton community, suggesting that their tolerance to variability outside of those normally encountered was low. Furthermore, current experiments, which determine the tolerance limits of phytoplankton over short time scales, may not be a good indicator of long-term resilience as the metabolic costs of climate-induced stress may not be sustainable over numerous generations (Schaum and Collins, 2014; Torstensson et al., 2015). It is currently unknown whether the rate of environmental change will outpace the ability of SO phytoplankton to adapt and/or evolve. It is, however, inevitable that changes at the base of the SO will influence trophodynamics, biogeochemistry, and climate change.

AUTHOR CONTRIBUTIONS

SD and AD both wrote, edited and produced the figures for the manuscript.

FUNDING

This review was funded by the Australian Government, Department of Environment and Energy as part of Australian Antarctic Science Project 4026 at the Australian Antarctic Division and an Elite Research Scholarship awarded by the Institute for Marine and Antarctic Studies, University of Tasmania.

ACKNOWLEDGMENTS

We would like to thank Indiah Hodgson-Johnston and the staff at the Australian Antarctic Division Data Centre for assistance with the production of our figures.

REFERENCES

Abbott, M. R., Richman, J. G., Letelier, R. M., and Bartlett, J. S. (2000). The spring bloom in the Antarctic Polar Frontal Zone as observed from a mesoscale array of bio-optical sensors. *Deep Sea Res. Part II Top. Stud. Oceanogr.* 47, 3285–3314. doi: 10.1016/S0967-0645(00)00069-2

Ackley, S., Wadhams, P., Comiso, J. C., and Worby, A. P. (2003). Decadal decrease of Antarctic sea ice extent inferred from whaling records revisited on the basis of historical and modern sea ice records. *Polar Res.* 22, 19–25. doi: 10.3402/polar.v22i1.6439

Ainley, D. G., Wilson, P. R., Barton, K. J., Ballard, G., Nur, N., and Karl, B. (1998). Diet and foraging effort of Adélie penguins in relation to pack-ice conditions in the southern Ross Sea. *Polar Biol.* 20, 311–319. doi: 10.1007/s003000050308

Alldredge, A. L., and Silver, M. W. (1988). Characteristics, dynamics and significance of marine snow. *Prog. Oceanogr.* 20, 41–82. doi: 10.1016/0079-6611(88)90053-5

Anderson, R. F., Barker, S., Fleisher, M., Gersonde, R., Goldstein, S. L., Kuhn, G., et al. (2014). Biological response to millennial variability of dust and nutrient supply in the Subantarctic South Atlantic Ocean. *Philos. Trans. R. Soc. A Math. Phys. Eng. Sci.* 372:20130054. doi: 10.1098/rsta.2013.0054

Ardelan, M. V., Holm-Hansen, O., Hewes, C. D., Reiss, C. S., Silva, N. S., Dulaiova, H., et al. (2010). Natural iron enrichment around the Antarctic Peninsula in the Southern Ocean. *Biogeosciences* 7, 11–25. doi: 10.5194/bg-7-11-2010

Armour, K. C., Marshall, J., Scott, J. R., Donohoe, A., and Newsom, E. R. (2016). Southern Ocean warming delayed by circumpolar upwelling and equatorward transport. *Nat. Geosci.* 9, 549–554. doi: 10.1038/ngeo2731

Arrigo, K., Worthen, D., Dixon, P., and Lizotte, M. P. (1998a). "Primary productivity of near surface communities within antarctic pack ice," in *Antarctic Sea Ice: Biological Processes, Interactions and Variability*, eds M. P. Lizotte and K. R. Arrigo (Washington, DC: American Geophysical Union), 23–43.

Arrigo, K. R. (2014). Sea ice ecosystems. *Ann. Rev. Mar. Sci.* 6, 439–467. doi: 10.1146/annurev-marine-010213-135103

Arrigo, K. R., DiTullio, G. R., Dunbar, R. B., Robinson, D. H., VanWoert, M., Worthen, D. L., et al. (2000). Phytoplankton taxonomic variability in nutrient utilization and primary production in the Ross Sea. *J. Geophys. Res. Oceans* 105, 8827–8846. doi: 10.1029/1998JC000289

Arrigo, K. R., Mock, T., and Lizotte, M. P. (2010). "Primary Producers and Sea Ice," in *Sea Ice, 2 Edn.*, Chap. 8, eds D. N. Thomas and G. Dieckmann (Ames, IA: Blackwell Publishing Ltd.), 283–326.

Arrigo, K. R., Robinson, D. H., Worthen, D. L., Dunbar, R. B., DiTullio, G. R., VanWoert, M., et al. (1999). Phytoplankton community structure and the drawdown of nutrients and CO_2 in the Southern Ocean. *Science* 283, 365–367. doi: 10.1126/science.283.5400.365

Arrigo, K. R., and Thomas, D. N. (2004). Large scale importance of sea ice biology in the Southern Ocean. *Antarct. Sci.* 16, 471–486. doi: 10.1017/S0954102004002263

Arrigo, K. R., van Dijken, G., and Long, M. (2008a). Coastal Southern Ocean: a strong anthropogenic CO_2 sink. *Geophys. Res. Lett.* 35:L21602. doi: 10.1029/2008GL035624

Arrigo, K. R., and van Dijken, G. L. (2003). Phytoplankton dynamics within 37 Antarctic coastal polynya systems. *J. Geophys. Res. Oceans* 108:3271. doi: 10.1029/2002jc001739

Arrigo, K. R., and van Dijken, G. L. (2004). Annual changes in sea-ice, chlorophyll *a*, and primary production in the Ross Sea, Antarctica. *Deep Sea Res. Part II Top. Stud. Oceanogr.* 51, 117–138. doi: 10.1016/j.dsr2.2003.04.003

Arrigo, K. R., van Dijken, G. L., and Bushinsky, S. (2008b). Primary production in the Southern Ocean, 1997–2006. *J. Geophys. Res. Oceans* 113:C08004. doi: 10.1029/2007JC004551

Arrigo, K. R., van Dijken, G. L., and Strong, A. L. (2015). Environmental controls of marine productivity hot spots around Antarctica. *J. Geophys. Res. Oceans* 120, 5545–5565. doi: 10.1002/2015JC010888

Arrigo, K. R., Worthen, D., Schnell, A., and Lizotte, M. P. (1998b). Primary production in Southern Ocean waters. *J. Geophys. Res. Oceans* 103, 15587–15600. doi: 10.1029/98JC00930

Arrigo, K. R., Worthen, D. L., Lizotte, M. P., Dixon, P., and Dieckmann, G. (1997). Primary production in Antarctic Sea Ice. *Science* 276, 394–397. doi: 10.1126/science.276.5311.394

Assmy, P., Smetacek, V., Montresor, M., Klaas, C., Henjes, J., Strass, V. H., et al. (2013). Thick-shelled, grazer-protected diatoms decouple ocean carbon and silicon cycles in the iron-limited Antarctic Circumpolar Current. *Proc. Natl. Acad. Sci. U.S.A.* 110, 20633–20638. doi: 10.1073/pnas.1309345110

Atkinson, A., Siegel, V., Pakhomov, E., and Rothery, P. (2004). Long-term decline in krill stock and increase in salps within the Southern Ocean. *Nature* 432, 100–103. doi: 10.1038/nature02996

Azam, F., Fenchel, T., Field, J. G., Gray, J. C., Meyer-Reil, L. A., and Thingstad, F. (1983). The ecological role of water-column microbes in the sea. *Mar. Ecol. Prog. Ser.* 10, 257–264. doi: 10.3354/meps010257

Azam, F., Smith, D. C., and Hollibaugh, J. T. (1991). The role of the microbial loop in Antarctic pelagic ecosystems. *Polar Res.* 10, 239–243. doi: 10.3402/polar.v10i1.6742

Balch, W. M., Bates, N. R., Lam, P. J., Twining, B. S., Rosengard, S. Z., Bowler, B. C., et al. (2016). Factors regulating the Great Calcite Belt in the Southern Ocean and its biogeochemical significance. *Global Biogeochem. Cycles* 30, 1124–1144. doi: 10.1002/2016GB005414

Ballerini, T., Hofmann, E. E., Ainley, D. G., Daly, K., Marrari, M., Ribic, C. A., et al. (2014). Productivity and linkages of the food web of the southern region of the western Antarctic Peninsula continental shelf. *Prog. Oceanogr.* 122, 10–29. doi: 10.1016/j.pocean.2013.11.007

Banse, K. (1996). Low seasonality of low concentrations of surface chlorophyll in the Subantarctic water ring: underwater irradiance, iron, or grazing? *Prog. Oceanogr.* 37, 241–291. doi: 10.1016/s0079-6611(96)00006-7

Becquevort, S., Menon, P., and Lancelot, C. (2000). Differences of the protozoan biomass and grazing during spring and summer in the Indian sector of the Southern Ocean. *Polar Biol.* 23, 309–320. doi: 10.1007/s003000050450

Behrenfeld, M. J. (2014). Climate-mediated dance of the plankton. *Nat. Clim. Change* 4, 880–887. doi: 10.1038/nclimate2349

Behrenfeld, M. J., O'Malley, R. T., Siegel, D. A., McClain, C. R., Sarmiento, J. L., Feldman, G. C., et al. (2006). Climate-driven trends in contemporary ocean productivity. *Nature* 444, 752–755. doi: 10.1038/nature05317

Bertolin, M. L., and Schloss, I. R. (2009). Phytoplankton production after the collapse of the Larsen A Ice Shelf, Antarctica. *Polar Biol.* 32, 1435–1446. doi: 10.1007/s00300-009-0638-x

Biermann, A., Lewandowska, A., Engel, A., and Riebesell, U. (2015). Organic matter partitioning and stoichiometry in response to rising water temperature and copepod grazing. *Mar. Ecol. Prog. Ser.* 522, 49–65. doi: 10.3354/meps11148

Bishop, J. K. B., and Rossow, W. B. (1991). Spatial and temporal variability of global surface solar irradiance. *J. Geophys. Res. Oceans* 96, 16839–16858. doi: 10.1029/91JC01754

Blain, S., Quéguiner, B., Armand, L., Belviso, S., Bombled, B., Bopp, L., et al. (2007). Effect of natural iron fertilization on carbon sequestration in the Southern Ocean. *Nature* 446, 1070–1074. doi: 10.1038/nature05700

Boelen, P., van de Poll, W. H., van der Strate, H. J., Neven, I. A., Beardall, J., and Buma, A. G. J. (2011). Neither elevated nor reduced CO_2 affects the photophysiological performance of the marine Antarctic diatom *Chaetoceros brevis*. *J. Exp. Mar. Biol. Ecol.* 406, 38–45. doi: 10.1016/j.jembe.2011.06.012

Bopp, L., Monfray, P., Aumont, O., Dufresne, J.-L., Le Treut, H., Madec, G., et al. (2001). Potential impact of climate change on marine export production. *Global Biogeochem. Cycles* 15, 81–99. doi: 10.1029/1999GB001256

Boyd, P. W. (2002). Environmental factors controlling phytoplankton processes in the Southern Ocean. *J. Phycol.* 38, 844–861. doi: 10.1046/j.1529-8817.2002.t01-1-01203.x

Boyd, P. W., Arrigo, K. R., Strzepek, R., and van Dijken, G. L. (2012). Mapping phytoplankton iron utilization: insights into Southern Ocean supply mechanisms. *J. Geophys. Res. Oceans* 117:C06009. doi: 10.1029/2011JC007726

Boyd, P. W., and Brown, C. J. (2015). Modes of interactions between environmental drivers and marine biota. *Front. Mar. Sci.* 2:9. doi: 10.3389/fmars.2015.00009

Boyd, P. W., Crossley, A. C., DiTullio, G. R., Griffiths, F. B., Hutchins, D. A., Queguiner, B., et al. (2001). Control of phytoplankton growth by iron supply and irradiance in the subantarctic Southern Ocean: experimental results from the SAZ Project. *J. Geophys. Res. Oceans* 106, 31573–31583. doi: 10.1029/2000JC000348

Boyd, P. W., Dillingham, P. W., McGraw, C. M., Armstrong, E. A., Cornwall, C. E., Feng, Y.-Y., et al. (2016). Physiological responses of a Southern Ocean diatom to complex future ocean conditions. *Nat. Clim. Change* 6, 207–213. doi: 10.1038/nclimate2811

Boyd, P. W., Doney, S. C., Strzepek, R., Dusenberry, J., Lindsay, K., and Fung, I. (2008). Climate-mediated changes to mixed-layer properties in the Southern Ocean: assessing the phytoplankton response. *Biogeosciences* 5, 847–864. doi: 10.5194/bg-5-847-2008

Boyd, P. W., and Ellwood, M. J. (2010). The biogeochemical cycle of iron in the ocean. *Nat. Geosci.* 3, 675–682. doi: 10.1038/ngeo964

Boyd, P. W., Jickells, T., Law, C. S., Blain, S., Boyle, E. A., Buesseler, K. O., et al. (2007). Mesoscale iron enrichment experiments 1993-2005: synthesis and future directions. *Science* 315, 612–617. doi: 10.1126/science.1131669

Boyd, P. W., and Law, C. S. (2011). *An Ocean Climate Change Atlas for New Zealand Waters*. Technical Report 79, Wellington: NIWA.

Boyd, P. W., Lennartz, S. T., Glover, D. M., and Doney, S. C. (2014). Biological ramifications of climate-change-mediated oceanic multi-stressors. *Nat. Clim. Change* 5, 71–79. doi: 10.1038/nclimate2441

Boyd, P. W., McTainsh, G., Sherlock, V., Richardson, K., Nichol, S., Ellwood, M., et al. (2004). Episodic enhancement of phytoplankton stocks in New Zealand subantarctic waters: contribution of atmospheric and oceanic iron supply. *Global Biogeochem. Cycles* 18:GB1029. doi: 10.1029/2002GB002020

Boyd, P. W., Rynearson, T. A., Armstrong, E. A., Fu, F., Hayashi, K., Hu, Z., et al. (2013). Marine phytoplankton temperature versus growth responses from polar to tropical waters - outcome of a scientific community-wide study. *PLoS ONE* 8:e63091. doi: 10.1371/journal.pone.0063091

Bracegirdle, T. J., Connolley, W. M., and Turner, J. (2008). Antarctic climate change over the twenty first century. *J. Geophys. Res. Atmospher.* 113:D03103. doi: 10.1029/2007JD008933

Brierley, A. S., and Thomas, D. N. (2002). "Ecology of Southern Ocean pack ice," in *Advances in Marine Biology, Vol. 43*, eds A. Southward, C. Young, and L. Fuiman (Cambridge, MA: Academic Press), 171–276.

Buma, A. G. J., De Boer, M. K., and Boelen, P. (2001). Depth distributions of DNA damage in antarctic marine phyto and bacterioplankton exposed to summertime UV radiation. *J. Phycol.* 37, 200–208. doi: 10.1046/j.1529-8817.2001.037002200.x

Burkill, P., Edwards, E., and Sleight, M. (1995). Microzooplankton and their role in controlling phytoplankton growth in the marginal ice zone of the Bellingshausen Sea. *Deep Sea Res. Part II Top. Stud. Oceanogr.* 42, 1277–1290. doi: 10.1016/0967-0645(95)00060-4

Cadée, G., González, H., and Schnack-Schiel, S. (1992). Krill diet affects faecal string settling. *Polar Biol.* 12, 75–80. doi: 10.1007/978-3-642-77595-6_8

Cael, B. B., and Follows, M. J. (2016). On the temperature dependence of oceanic export efficiency. *Geophys. Res. Lett.* 43, 5170–5175. doi: 10.1002/2016GL068877

Caldeira, K., and Wickett, M. E. (2003). Oceanography: anthropogenic carbon and ocean pH. *Nature* 425, 365–365. doi: 10.1038/425365a

Caron, D. A., and Hutchins, D. A. (2013). The effects of changing climate on microzooplankton grazing and community structure: drivers, predictions and knowledge gaps. *J. Plank. Res.* 35, 235–252. doi: 10.1093/plankt/fbs091

Carranza, M. M., and Gille, S. T. (2015). Southern Ocean wind-driven entrainment enhances satellite chlorophyll-a through the summer. *J. Geophys. Res. Oceans* 120, 304–323. doi: 10.1002/2014JC010203

Cassar, N., Bender, M. L., Barnett, B. A., Fan, S., Moxim, W. J., Levy, H., et al. (2007). The Southern Ocean biological response to Aeolian iron deposition. *Science* 317, 1067–1070. doi: 10.1126/science.1144602

Cassar, N., Wright, S. W., Thomson, P. G., Trull, T. W., Westwood, K. J., de Salas, M., et al. (2015). The relation of mixed-layer net community production to phytoplankton community composition in the Southern Ocean. *Global Biogeochem. Cycles* 29, 446–462. doi: 10.1002/2014GB004936

Cefarelli, A. O., Vernet, M., and Ferrario, M. E. (2011). Phytoplankton composition and abundance in relation to free-floating Antarctic icebergs. *Deep Sea Res. II Top. Stud. Oceanogr.* 58, 1436–1450. doi: 10.1016/j.dsr2.2010.11.023

Charlson, R. J., Lovelock, J. E., Andreae, M. O., and Warren, S. G. (1987). Oceanic phytoplankton, atmospheric sulphur, cloud albedo and climate. *Nature* 326, 655–661. doi: 10.1038/326655a0

Charlson, R. J., Schwartz, S. E., Hales, J. M., Cess, R. D., Coakley, J. A., Hansen, J. E., et al. (1992). Climate forcing by anthropogenic aerosols. *Science* 255, 423–430. doi: 10.1126/science.255.5043.423

Cherel, Y., Fontaine, C., Richard, P., and Labatc, J.-P. (2010). Isotopic niches and trophic levels of myctophid fishes and their predators in the Southern Ocean. *Limnol. Oceanogr.* 55, 324–332. doi: 10.4319/lo.2010.55.1.0324

Christaki, U., Lefèvre, D., Georges, C., Colombet, J., Catala, P., Courties, C., et al. (2014). Microbial food web dynamics during spring phytoplankton blooms in the naturally iron-fertilized Kerguelen area (Southern Ocean). *Biogeosciences* 11, 6739–6753. doi: 10.5194/bg-11-6739-2014

Coad, T., McMinn, A., Nomura, D., and Martin, A. (2016). Effect of elevated CO_2 concentration on microalgal communities in Antarctic pack ice. *Deep Sea Res. Part II Top. Stud. Oceanogr.* 131, 160–169. doi: 10.1016/j.dsr2.2016.01.005

Collins, S., Rost, B., and Rynearson, T. A. (2014). Evolutionary potential of marine phytoplankton under ocean acidification. *Evol. Appl.* 7, 140–155. doi: 10.1111/eva.12120

Comiso, J. C., McClain, C. R., Sullivan, C. W., Ryan, J. P., and Leonard, C. L. (1993). Coastal zone color scanner pigment concentrations in the Southern Ocean and relationships to geophysical surface features. *J. Geophys. Res. Oceans* 98, 2419–2451. doi: 10.1029/92JC02505

Comiso, J. C., and Nishio, F. (2008). Trends in the sea ice cover using enhanced and compatible AMSR-E, SSM/I, and SMMR data. *J. Geophys. Res. Oceans* 113:C02S07. doi: 10.1029/2007JC004257

Constable, A. J., Melbourne-Thomas, J., Corney, S. P., Arrigo, K. R., Barbraud, C., Barnes, D. K. A., et al. (2014). Climate change and Southern Ocean ecosystems I: how changes in physical habitats directly affect marine biota. *Global Change Biol.* 20, 3004–3025. doi: 10.1111/gcb.12623

Convey, P., Bindschadler, R., di Prisco, G., Fahrbach, E., Gutt, J., Hodgson, D., et al. (2009). Antarctic climate change and the environment. *Antarct. Sci.* 21:541. doi: 10.1017/S0954102009990642

Cook, A. J., Fox, A. J., Vaughan, D. G., and Ferrigno, J. G. (2005). Retreating Glacier fronts on the Antarctic Peninsula over the past half-century. *Science* 308, 541–544. doi: 10.1126/science.1104235

Cox, P. M., Betts, R. A., Jones, C. D., Spall, S. A., and Totterdell, I. J. (2000). Acceleration of global warming due to carbon-cycle feedbacks in a coupled climate model. *Nature* 408, 184–187. doi: 10.1038/35041539

Cubillos, J., Wright, S., Nash, G., de Salas, M., Griffiths, B., Tilbrook, B., et al. (2007). Calcification morphotypes of the coccolithophorid *Emiliania huxleyi* in the Southern Ocean: changes in 2001 to 2006 compared to historical data. *Mar. Ecol. Prog. Ser.* 348, 47–54. doi: 10.3354/meps07058

Cullen, J. J., and Lesser, M. P. (1991). Inhibition of photosynthesis by ultraviolet radiation as a function of dose and dosage rate: results for a marine diatom. *Mar. Biol.* 111, 183–190. doi: 10.1007/BF01319699

Curran, M. A. J., and Jones, G. B. (2000). Dimethyl sulfide in the Southern Ocean: seasonality and flux. *J. Geophys. Res. Atmospheres* 105, 20451–20459. doi: 10.1029/2000JD900176

Curran, M. A. J., van Ommen, T. D., Morgan, V. I., Phillips, K. L., and Palmer, A. S. (2003). Ice core evidence for Antarctic Sea ice decline since the 1950s. *Science* 302, 1203–1206. doi: 10.1126/science.1087888

Daly, K. L. (1998). "Physioecology of Juvenile Antarctic Krill (*Euphausia superba*) during spring in ice-covered seas," in *Antarctic Sea Ice: Biological Processes, Interactions and Variability*, eds M. P. Lizotte and K. R. Arrigo (Washington, DC: American Geophysical Union), 183–198.

Davidson, A., McKinlay, J., Westwood, K., Thomson, P., van den Enden, R., de Salas, M., et al. (2016). Enhanced CO_2 concentrations change the structure of Antarctic marine microbial communities. *Mar. Ecol. Prog. Ser.* 552, 93–113. doi: 10.3354/meps11742

Davidson, A. T. (2006). "Effects of ultraviolet radiation on microalgal growth," in *Algal Culture, Analogues of Blooms and Applications*, Vol. 2, ed D. V. Subba Rao (Enfield, NH: Science Publishers), 715–768.

Davidson, A. T., Scott, F. J., Nash, G. V., Wright, S. W., and Raymond, B. (2010). Physical and biological control of protistan community composition, distribution and abundance in the seasonal ice zone of the Southern Ocean between 30 and 80°E. *Deep Sea Res. Part II Top. Stud. Oceanogr.* 57, 828–848. doi: 10.1016/j.dsr2.2009.02.011

de Baar, H. J. W., de Jong, J. T. M., Bakker, D. C. E., Löscher, B. M., Veth, C., Bathmann, U., et al. (1995). Importance of iron for plankton blooms and carbon dioxide drawdown in the Southern Ocean. *Nature* 373, 412–415. doi: 10.1038/373412a0

de la Mare, W. K. (2009). Changes in Antarctic sea-ice extent from direct historical observations and whaling records. *Clim. Change* 92, 461–493. doi: 10.1007/s10584-008-9473-2

de Salas, M. F., Eriksen, R., Davidson, A. T., and Wright, S. W. (2011). Protistan communities in the Australian sector of the Sub-Antarctic Zone during SAZ-Sense. *Deep Sea Res. Part II Top. Stud. Oceanogr.* 58, 2135–2149. doi: 10.1016/j.dsr2.2011.05.032

Delille, B., Vancoppenolle, M., Geilfus, N.-X., Tilbrook, B., Lannuzel, D., Schoemann, V., et al. (2014). Southern ocean CO_2 sink: the contribution of the sea ice. *J. Geophys. Res. Oceans* 119, 6340–6355. doi: 10.1002/2014JC009941

DiFiore, P. J., Sigman, D. M., Trull, T. W., Lourey, M. J., Karsh, K., Cane, G., et al. (2006). Nitrogen isotope constraints on subantarctic biogeochemistry. *J. Geophys. Res. Oceans* 111:C08016. doi: 10.1029/2005JC003216

DiTullio, G. R., Grebmeier, J. M., Arrigo, K. R., Lizotte, M. P., Robinson, D. H., Leventer, A., et al. (2000). Rapid and early export of *Phaeocystis*

antarctica blooms in the Ross Sea, Antarctica. *Nature* 404, 595–598. doi: 10.1038/35007061

DiTullio, G. R., and Smith, W. O. (1995). Relationship between dimethylsulfide and phytoplankton pigment concentrations in the Ross Sea, Antarctica. *Deep Sea Res. Part I Oceanogr. Res. Papers* 42, 873–892. doi: 10.1016/0967-0637(95)00051-7

Doblin, M. A., Petrou, K. L., Shelly, K., Westwood, K., van den Enden, R., Wright, S., et al. (2011). Diel variation of chlorophyll-*a* fluorescence, phytoplankton pigments and productivity in the Sub-Antarctic and Polar Front Zones south of Tasmania, Australia. *Deep Sea Res. Part II Top. Stud. Oceanogr.* 58, 2189–2199. doi: 10.1016/j.dsr2.2011.05.021

Dobrynin, M., Murawsky, J., and Yang, S. (2012). Evolution of the global wind wave climate in CMIP5 experiments. *Geophys. Res. Lett.* 39:L18606. doi: 10.1029/2012gl052843

Ducklow, H. W., Baker, K., Martinson, D. G., Quetin, L. B., Ross, R. M., Smith, R. C., et al. (2007). Marine pelagic ecosystems: the West Antarctic Peninsula. *Philos. Trans. R. Soc. B Biol. Sci.* 362, 67–94. doi: 10.1098/rstb.2006.1955

Duprat, L. P. A. M., Bigg, G. R., and Wilton, D. J. (2016). Enhanced Southern Ocean marine productivity due to fertilization by giant icebergs. *Nat. Geosci.* 9, 219–221. doi: 10.1038/ngeo2633

El-Sayed, S. Z. (ed.). (1994). *Southern Ocean Ecology: The BIOMASS Perspective*. Cambridge: Cambridge University Press.

El-Sayed, S. Z., and Taguchi, S. (1981). Primary production and standing crop of phytoplankton along the ice-edge in the Weddell Sea. *Deep Sea Res. A Oceanogr. Res. Papers* 28, 1017–1032. doi: 10.1016/0198-0149(81)90015-7

Evans, C., Thomson, P. G., Davidson, A. T., Bowie, A. R., van den Enden, R., Witte, H., et al. (2011). Potential climate change impacts on microbial distribution and carbon cycling in the Australian Southern Ocean. *Deep Sea Res. II Top. Stud. Oceanogr.* 58, 2150–2161. doi: 10.1016/j.dsr2.2011.05.019

Fenchel, T. (2008). The microbial loop - 25 years later. *J. Exp. Mar. Biol. Ecol.* 366, 99–103. doi: 10.1016/j.jembe.2008.07.013

Feng, Y., Hare, C., Rose, J., Handy, S., DiTullio, G., Lee, P., et al. (2010). Interactive effects of iron, irradiance and CO_2 on Ross Sea phytoplankton. *Deep Sea Res. I Oceanogr. Res. Papers* 57, 368–383. doi: 10.1016/j.dsr.2009.10.013

Ferreira, D., Marshall, J., Bitz, C. M., Solomon, S., and Plumb, A. (2015). Antarctic ocean and sea ice response to ozone depletion: A two-time-scale problem. *Journal of Climate*, 28(3):1206–1226. doi: 10.1175/JCLI-D-14-00313.1

Fetterer, F., Knowles, K., Meier, W., and Savoie, M. (2016a). *Sea Ice Index, Version 2*. Boulder, CO: NSIDC: National Snow and Ice Data Center, September 2014 extent.

Fetterer, F., Knowles, K., Meier, W., and Savoie, M. (2016b). *Sea Ice Index, Version 2*. Boulder, CO: NSIDC: National Snow and Ice Data Center, November 2016 extent.

Finkel, Z. V., Beardall, J., Flynn, K. J., Quigg, A., Rees, T. A. V., and Raven, J. A. (2010). Phytoplankton in a changing world: cell size and elemental stoichiometry. *J. Plank. Res.* 32, 119–137. doi: 10.1093/plankt/fbp098

Fitch, D. T., and Moore, J. K. (2007). Wind speed influence on phytoplankton bloom dynamics in the Southern Ocean Marginal Ice Zone. *J. Geophys. Res. Oceans* 112:C08006.

Flores, H., Atkinson, A., Kawaguchi, S., Krafft, B., Milinevsky, G., Nicol, S., et al. (2012). Impact of climate change on Antarctic krill. *Mar. Ecol. Prog. Ser.* 458, 1–19. doi: 10.3354/meps09831

Frölicher, T. L., Rodgers, K. B., Stock, C. A., and Cheung, W. W. L. (2016). Sources of uncertainties in 21st century projections of potential ocean ecosystem stressors. *Global Biogeochem. Cycles* 30, 1224–1243. doi: 10.1002/2015GB005338

Frölicher, T. L., Sarmiento, J. L., Paynter, D. J., Dunne, J. P., Krasting, J. P., and Winton, M. (2015). Dominance of the Southern Ocean in anthropogenic carbon and heat uptake in CMIP5 models. *J. Climate* 28, 862–886. doi: 10.1175/JCLI-D-14-00117.1

Gao, K., Helbling, E., Häder, D., and Hutchins, D. (2012). Responses of marine primary producers to interactions between ocean acidification, solar radiation, and warming. *Mar. Ecol. Prog. Ser.* 470, 167–189. doi: 10.3354/meps10043

Garibotti, I., Vernet, M., Ferrario, M., Smith, R., Ross, R., and Quetin, L. (2003). Phytoplankton spatial distribution patterns along the western Antarctic Peninsula (Southern Ocean). *Mar. Ecol. Prog. Ser.* 261, 21–39. doi: 10.3354/meps261021

Gibson, J. A., and Trull, T. W. (1999). Annual cycle of fCO_2 under sea-ice and in open water in Prydz Bay, East Antarctica. *Mar. Chem.* 66, 187–200. doi: 10.1016/S0304-4203(99)00040-7

Goldman, J. A. L., Kranz, S. A., Young, J. N., Tortell, P. D., Stanley, R. H. R., Bender, M. L., et al. (2015). Gross and net production during the spring bloom along the Western Antarctic Peninsula. *New Phytol.* 205, 182–191. doi: 10.1111/nph.13125

Gregg, W. W., and Rousseaux, C. S. (2014). Decadal trends in global pelagic ocean chlorophyll: a new assessment integrating multiple satellites, *in situ* data, and models. *J. Geophys. Res. Oceans* 119, 5921–5933. doi: 10.1002/2014JC010158

Griffiths, F. B., Bates, T. S., Quinn, P. K., Clementson, L. A., and Parslow, J. S. (1999). Oceanographic context of the first aerosol characterization experiment (ACE 1): a physical, chemical, and biological overview. *J. Geophys. Res. Atmospheres* 104, 21649–21671. doi: 10.1029/1999JD900386

Grossi, S., Kottmeier, S., Moe, R., Taylor, G., and Sullivan, C. (1987). Sea ice microbial communities. VI. Growth and primary production in bottom ice under graded snow cover. *Mar. Ecol. Prog. Ser.* 35, 153–164. doi: 10.3354/meps035153

Gutt, J., Bertler, N., Bracegirdle, T. J., Buschmann, A., Comiso, J., Hosie, G., et al. (2015). The Southern Ocean ecosystem under multiple climate change stresses - an integrated circumpolar assessment. *Global Change Biol.* 21, 1434–1453. doi: 10.1111/gcb.12794

Häder, D.-P., Williamson, C. E., Wängberg, S.-Å., Rautio, M., Rose, K. C., Gao, K., et al. (2015). Effects of UV radiation on aquatic ecosystems and interactions with other environmental factors. *Photochem. Photobiol. Sci.* 14, 108–126. doi: 10.1039/C4PP90035A

Hagen, W. (1999). Reproductive strategies and energetic adaptations of polar zooplankton. *Invert. Reproduct. Dev.* 36, 25–34. doi: 10.1080/07924259.1999.9652674

Hauck, J., Völker, C., Wang, T., Hoppema, M., Losch, M., and Wolf-Gladrow, D. A. (2013). Seasonally different carbon flux changes in the Southern Ocean in response to the southern annular mode. *Global Biogeochem. Cycles* 27, 1236–1245. doi: 10.1002/2013GB004600

Hauck, J., Völker, C., Wolf-Gladrow, D. A., Laufkötter, C., Vogt, M., Aumont, O., et al. (2015). On the Southern Ocean CO_2 uptake and the role of the biological carbon pump in the 21st century. *Global Biogeochem. Cycles* 29, 1451–1470. doi: 10.1002/2015GB005140

Haumann, F. A., Gruber, N., Münnich, M., Frenger, I., and Kern, S. (2016). Sea-ice transport driving Southern Ocean salinity and its recent trends. *Nature* 537, 89–92. doi: 10.1038/nature19101

Helbling, E. W., Villafañe, V., and Holm-Hansen, O. (1994). "Effects of ultraviolet radiation on Antarctic marine phytoplankton photosynthesis with particular attention to the influence of mixing," in *Ultraviolet Radiation in Antarctica: Measurements and Biological Effects*, eds C. S. Weiler and P. A. Penhale (Washington, DC: American Geophysical Union), 207–227.

Hemer, M. A., Church, J. A., and Hunter, J. R. (2010). Variability and trends in the directional wave climate of the Southern Hemisphere. *Int. J. Climatol.* 30, 475–491. doi: 10.1002/joc.1900

Henson, S. A., Sarmiento, J. L., Dunne, J. P., Bopp, L., Lima, I., Doney, S. C., et al. (2010). Detection of anthropogenic climate change in satellite records of ocean chlorophyll and productivity. *Biogeosciences* 7, 621–640. doi: 10.5194/bg-7-621-2010

Hirawake, T., Odate, T., and Fukuchi, M. (2005). Long-term variation of surface phytoplankton chlorophyll *a* in the Southern Ocean during the 1965–2002. *Geophys. Res. Lett.* 32:L05606. doi: 10.1029/2004GL021394

Hiscock, M. R., Marra, J., Smith, W. O. J., Goericke, R., Measures, C., Vink, S., et al. (2003). Primary productivity and its regulation in the Pacific Sector of the Southern Ocean. *Deep Sea Res. II Top. Stud. Oceanogr.* 50, 533–558. doi: 10.1016/S0967-0645(02)00583-0

Hixson, S. M., and Arts, M. T. (2016). Climate warming is predicted to reduce omega-3, long-chain, polyunsaturated fatty acid production in phytoplankton. *Global Change Biol.* 22, 2744–2755. doi: 10.1111/gcb.13295

Hobbs, W. R., Massom, R., Stammerjohn, S., Reid, P., Williams, G., and Meier, W. (2016). A review of recent changes in Southern Ocean sea ice, their drivers and forcings. *Global Planet. Change* 143, 228–250. doi: 10.1016/j.gloplacha.2016.06.008

Hogg, A. M. C., Meredith, M. P., Blundell, J. R., and Wilson, C. (2008). Eddy heat flux in the Southern Ocean: response to variable wind forcing. *J. Climate* 21, 608–620. doi: 10.1175/2007JCLI1925.1

Holland, P. R., Bruneau, N., Enright, C., Losch, M., Kurtz, N. T., and Kwok, R. (2014). Modeled trends in Antarctic Sea ice thickness. *J. Clim.* 27, 3784–3801. doi: 10.1175/JCLI-D-13-00301.1

Honjo, S. (2004). Particle export and the biological pump in the Southern Ocean. *Antarct. Sci.* 16, 501–516. doi: 10.1017/S0954102004002287

Hopkinson, B. M., Dupont, C. L., Allen, A. E., and Morel, F. M. M. (2011). Efficiency of the CO_2-concentrating mechanism of diatoms. *Proc. Natl. Acad. Sci. U.S.A.* 108, 3830–3837. doi: 10.1073/pnas.1018062108

Hoppe, C. J. M., Hassler, C. S., Payne, C. D., Tortell, P. D., Rost, B., and Trimborn, S. (2013). Iron limitation modulates ocean acidification effects on Southern Ocean phytoplankton communities. *PLoS ONE* 8:e79890. doi: 10.1371/journal.pone.0079890

Hoppe, C. J. M., Holtz, L.-M., Trimborn, S., and Rost, B. (2015). Ocean acidification decreases the light-use efficiency in an Antarctic diatom under dynamic but not constant light. *New Phytol.* 207, 159–171. doi: 10.1111/nph.13334

Hoppema, M., Fahrbach, E., Schröder, M., Wisotzki, A., and de Baar, H. J. (1995). Winter-summer differences of carbon dioxide and oxygen in the Weddell Sea surface layer. *Mar. Chem.* 51, 177–192. doi: 10.1016/0304-4203(95)00065-8

Horvat, C., Tziperman, E., and Campin, J.-M. (2016). Interaction of sea ice floe size, ocean eddies, and sea ice melting. *Geophys. Res. Lett.* 43, 8083–8090. doi: 10.1002/2016GL069742

Hutchins, D. A., and Boyd, P. W. (2016). Marine phytoplankton and the changing ocean iron cycle. *Nat. Clim. Change* 6, 1072–1079. doi: 10.1038/nclimate3147

Jacobs, S. S. (1991). On the nature and significance of the Antarctic Slope Front. *Mar. Chem.* 35, 9–24. doi: 10.1016/S0304-4203(09)90005-6

Jacobs, S. S., Giulivi, C. F., and Mele, P. A. (2002). Freshening of the ross Sea during the late 20th century. *Science* 297, 386–389. doi: 10.1126/science.1069574

Jia, Z., Swadling, K. M., Meiners, K. M., Kawaguchi, S., and Virtue, P. (2016). The zooplankton food web under East Antarctic pack ice - A stable isotope study. *Deep Sea Res. II Top. Stud. Oceanogr.* 131, 189–202. doi: 10.1016/j.dsr2.2015.10.010

Jones, G., Fortescue, D., King, S., Williams, G., and Wright, S. (2010). Dimethylsulphide and dimethylsulphoniopropionate in the South-West Indian Ocean sector of East Antarctica from 30° to 80°E during BROKE-West. *Deep Sea Res. II Top. Stud. Oceanogr.* 57, 863–876. doi: 10.1016/j.dsr2.2009.01.003

Jones, G. B., Curran, M. A. J., Swan, H. B., Greene, R. M., Griffiths, F. B., and Clementson, L. A. (1998). Influence of different water masses and biological activity on dimethylsulphide and dimethylsulphoniopropionate in the subantarctic zone of the Southern Ocean during ACE 1. *J. Geophys. Res. Atmospheres* 103, 16691–16701. doi: 10.1029/98JD01200

Kahru, M., Mitchell, B. G., Gille, S. T., Hewes, C. D., and Holm-Hansen, O. (2007). Eddies enhance biological production in the Weddell-Scotia Confluence of the Southern Ocean. *Geophys. Res. Lett.* 34:L14603. doi: 10.1029/2007GL030430

Kang, S.-H., Kang, J.-S., Lee, S., Chung, K. H., Kim, D., and Park, M. G. (2001). Antarctic phytoplankton assemblages in the marginal ice zone of the Northwestern Weddell Sea. *J. Plank. Res.* 23, 333–352. doi: 10.1093/plankt/23.4.333

Kapsenberg, L., Kelley, A. L., Shaw, E. C., Martz, T. R., and Hofmann, G. E. (2015). Near-shore Antarctic pH variability has implications for the design of ocean acidification experiments. *Sci. Rep.* 5:9638. doi: 10.1038/srep10497

Karentz, D. (1991). Ecological considerations of Antarctic ozone depletion. *Antarct. Sci.* 3, 3–11. doi: 10.1017/S0954102091000032

Karentz, D., and Lutze, L. H. (1990). Evaluation of biologically harmful ultraviolet radiation in Antarctica with a biological dosimeter designed for aquatic environments. *Limnol. Oceanogr.* 35, 549–561. doi: 10.4319/lo.1990.35.3.0549

Kavanaugh, M., Abdala, F., Ducklow, H., Glover, D., Fraser, W., Martinson, D., et al. (2015). Effect of continental shelf canyons on phytoplankton biomass and community composition along the western Antarctic Peninsula. *Mar. Ecol. Prog. Ser.* 524, 11–26. doi: 10.3354/meps11189

Kawaguchi, S., Ichii, T., and Naganobu, M. (1999). Green krill, the indicator of micro- and nano-size phytoplankton availability to krill. *Polar Biol.* 22, 133–136. doi: 10.1007/s003000050400

Kawaguchi, S., and Satake, M. (1994). Relationship between recruitment near the South Shetland Islands of the Antarctic krill and the degree of ice cover. *Fish. Sci.* 60, 123–124.

Kemp, A. E. S., Pearce, R. B., Grigorov, I., Rance, J., Lange, C. B., Quilty, P., et al. (2006). Production of giant marine diatoms and their export at oceanic frontal zones: implications for Si and C flux from stratified oceans. *Global Biogeochem. Cycles* 20:GB4S04. doi: 10.1029/2006GB002698

Khatiwala, S., Primeau, F., and Hall, T. (2009). Reconstruction of the history of anthropogenic CO_2 concentrations in the ocean. *Nature* 462, 346–349. doi: 10.1038/nature08526

Kiene, R., Linn, L., and Bruton, J. (2000). New and important roles for DMSP in marine microbial communities. *J. Sea Res.* 43, 209–224. doi: 10.1016/S1385-1101(00)00023-X

Kirchman, D. L. (2008). *Microbial Ecology of the Oceans, 2 Edn.* Hoboken, NJ: Wiley-Blackwell. doi: 10.1002/9780470281840

Kirk, J. T. O. (1994). *Light and Photosynthesis in Aquatic Ecosystems*. Cambridge: Cambridge University Press.

Kirst, G., Thiel, C., Wolff, H., Nothnagel, J., Wanzek, M., and Ulmke, R. (1991). Dimethylsulfoniopropionate (DMSP) in icealgae and its possible biological role. *Mar. Chem.* 35, 381–388. doi: 10.1016/S0304-4203(09)90030-5

Knox, G. A. (2007). "Sea-ice microbial communities," in *Biology of the Southern Ocean, 2 Edn.*, Chap. 3 (Boca Raton, FL: CRC Press), 59–96.

Kohout, A. L., Williams, M. J. M., Dean, S. M., and Meylan, M. H. (2014). Storm-induced sea-ice breakup and the implications for ice extent. *Nature* 509, 604–607. doi: 10.1038/nature13262

Kopczyńska, E. E., Dehairs, F., Elskens, M., and Wright, S. (2001). Phytoplankton and microzooplankton variability between the Subtropical and Polar Fronts south of Australia: thriving under regenerative and new production in late summer. *J. Geophys. Res. Oceans* 106, 31597–31609. doi: 10.1029/2000JC000278

Kopczyńska, E. E., Savoye, N., Dehairs, F., Cardinal, D., and Elskens, M. (2007). Spring phytoplankton assemblages in the Southern Ocean between Australia and Antarctica. *Polar Biol.* 31, 77–88. doi: 10.1007/s00300-007-0335-6

Kozlov, A. N. (1995). A review of the trophic role of mesopelagic fish of the family Myctophidae in the Southern Ocean ecosystem. *CCAMLR Sci.* 2, 71–77.

Kwok, R. (2010). Satellite remote sensing of sea-ice thickness and kinematics: a review. *J. Glaciol.* 56, 1129–1140. doi: 10.3189/002214311796406167

Lam, P. J., and Bishop, J. K. (2007). High biomass, low export regimes in the Southern Ocean. *Deep Sea Res. Part II Topic. Stud. Oceanogr.* 54, 601–638. doi: 10.1016/j.dsr2.2007.01.013

Lannuzel, D., Chever, F., van der Merwe, P. C., Janssens, J., Roukaerts, A., Cavagna, A.-J., et al. (2016). Iron biogeochemistry in Antarctic pack ice during SIPEX-2. *Deep Sea Res. Part II Topic. Stud. Oceanogr.* 131, 111–122. doi: 10.1016/j.dsr2.2014.12.003

Lannuzel, D., Schoemann, V., de Jong, J., Pasquer, B., van der Merwe, P., Masson, F., et al. (2010). Distribution of dissolved iron in Antarctic sea ice: Spatial, seasonal, and inter-annual variability. *J. Geophys. Res. Biogeosci.* 115:G03022. doi: 10.1029/2009JG001031

Laufkötter, C., Vogt, M., Gruber, N., Aita-Noguchi, M., Aumont, O., Bopp, L., et al. (2015). Drivers and uncertainties of future global marine primary production in marine ecosystem models. *Biogeosciences* 12, 6955–6984. doi: 10.5194/bg-12-6955-2015

Laurenceau-Cornec, E. C., Trull, T. W., Davies, D. M., Bray, S. G., Doran, J., Planchon, F., et al. (2015). The relative importance of phytoplankton aggregates and zooplankton fecal pellets to carbon export: insights from free-drifting sediment trap deployments in naturally iron-fertilised waters near the Kerguelen Plateau. *Biogeosciences* 12, 1007–1027. doi: 10.5194/bg-12-1007-2015

Le Quéré, C., Rodenbeck, C., Buitenhuis, E. T., Conway, T. J., Langenfelds, R., Gomez, A., et al. (2007). Saturation of the Southern Ocean CO_2 Sink Due to Recent Climate Change. *Science* 316, 1735–1738. doi: 10.1126/science.1136188

Legendre, L., Ackley, S. F., Dieckmann, G. S., Gulliksen, B., Horner, R., Hoshiai, T., et al., (1992). Ecology of sea ice biota - 2. Global significance. *Polar Biol.* 12, 429–444. doi: 10.1007/bf00243114

Lenton, A., and Matear, R. J. (2007). Role of the southern annular mode (SAM) in southern ocean CO_2 uptake. *Glob. Biogeochem. Cycles* 21:GB2016. doi: 10.1029/2006GB002714

Leung, S., Cabré, A., and Marinov, I. (2015). A latitudinally banded phytoplankton response to 21st century climate change in the Southern

Ocean across the CMIP5 model suite. *Biogeosciences* 12, 5715–5734. doi: 10.5194/bg-12-5715-2015

Lin, H., Rauschenberg, S., Hexel, C. R., Shaw, T. J., and Twining, B. S. (2011). Free-drifting icebergs as sources of iron to the Weddell Sea. *Deep Sea Res. Part II Topic. Stud. Oceanogr.* 58, 1392–1406. doi: 10.1016/j.dsr2.2010.11.020

Liu, J., Curry, J. A., and Martinson, D. G. (2004). Interpretation of recent Antarctic sea ice variability. *Geophys. Res. Lett.* 31, 2000–2003. doi: 10.1029/2003GL018732

Lizotte, M. P. (2001). The contributions of Sea Ice Algae to Antarctic marine primary production. *Am. Zool.* 41, 57–73. doi: 10.1093/icb/41.1.57

Lochte, K., Bjørnsen, P. K., Giesenhagen, H., and Weber, A. (1997). Bacterial standing stock and production and their relation to phytoplankton in the Southern Ocean. *Deep Sea Res. Part II Topic. Stud. Oceanogr.* 44, 321–340. doi: 10.1016/S0967-0645(96)00081-1

Lovenduski, N. S., and Gruber, N. (2005). Impact of the Southern Annular mode on Southern Ocean circulation and biology. *Geophys. Res. Lett.* 32:L11603. doi: 10.1029/2005gl022727

Lovenduski, N. S., Gruber, N., Doney, S. C., and Lima, I. D. (2007). Enhanced CO_2 outgassing in the Southern Ocean from a positive phase of the Southern Annular Mode. *Glob. Biogeochem. Cycles* 21:GB2026. doi: 10.1029/2006GB002900

Lumpkin, R., and Speer, K. (2007). Global ocean meridional overturning. *J. Phys. Oceanogr.* 37, 2550–2562. doi: 10.1175/JPO3130.1

Maksym, T., Stammerjohn, S., Ackley, S., and Massom, R. (2012). Antarctic Sea Ice-A Polar Opposite? *Oceanography* 25, 140–151. doi: 10.5670/oceanog.2012.88

Malin, G. (2006). OCEANS: New pieces for the marine sulfur cycle jigsaw. *Science* 314, 607–608. doi: 10.1126/science.1133279

Malinverno, E., Triantaphyllou, M. V., and Dimiza, M. D. (2015). Coccolithophore assemblage distribution along a temperate to polar gradient in the West Pacific sector of the Southern Ocean (January 2005). *Micropaleontology* 61, 489–506.

Marchant, H. J., and Davidson, A. (1991). "Possible impacts of ozone depletion on trophic interactions and biogenic vertical carbon flux in the Southern Ocean," in *Proceedings of the International Conference on the Role of the Polar Regions in Global Change Held in Fairbanks, Alaska Volume 2*, eds G. Weller, C. L. Wilson, and B. A. B. Severin (Fairbanks, AK: Geophysical Institute, University of Alaska Fairbanks, Geophysical Institute, University of Alaska Fairbanks), 397–400.

Marinov, I., Doney, S. C., and Lima, I. D. (2010). Response of ocean phytoplankton community structure to climate change over the 21st century: partitioning the effects of nutrients, temperature and light. *Biogeosciences* 7, 3941–3959. doi: 10.5194/bg-7-3941-2010

Martin, J. H., Gordon, R. M., and Fitzwater, S. E. (1990). Iron in Antarctic waters. *Nature* 345, 156–158. doi: 10.1038/345156a0

Martínez-García, A., Sigman, D. M., Ren, H., Anderson, R. F., Straub, M., Hodell, D. A., et al. (2014). Iron fertilization of the Subantarctic ocean during the last ice age. *Science* 343, 1347–1350. doi: 10.1126/science.1246848

Martiny, A. C., Pham, C. T. A., Primeau, F. W., Vrugt, J. A., Moore, J. K., Levin, S. A., et al. (2013). Strong latitudinal patterns in the elemental ratios of marine plankton and organic matter. *Nat. Geosci.* 6, 279–283. doi: 10.1038/ngeo1757

Massom, R. A., and Stammerjohn, S. E. (2010). Antarctic sea ice change and variability - physical and ecological implications. *Polar Sci.* 4, 149–186. doi: 10.1016/j.polar.2010.05.001

Massom, R. A., Stammerjohn, S. E., Lefebvre, W., Harangozo, S. A., Adams, N., Scambos, T. A., et al. (2008). West Antarctic Peninsula sea ice in 2005: extreme ice compaction and ice edge retreat due to strong anomaly with respect to climate. *J. Geophys. Res. Oceans* 113, C02S20. doi: 10.1029/2007jc004239

Massom, R. A., Stammerjohn, S. E., Smith, R. C., Pook, M. J., Iannuzzi, R. A., Adams, N., et al. (2006). Extreme anomalous atmospheric circulation in the West Antarctic Peninsula region in Austral Spring and Summer 2001/02, and Its Profound Impact on Sea Ice and Biota. *J. Clim.* 19, 3544–3571. doi: 10.1175/JCLI3805.1

Matear, R. J., and Hirst, A. C. (1999). Climate change feedback on the future oceanic CO_2 uptake. *Tellus B* 51, 722–733. doi: 10.3402/tellusb.v51i3.16472

Matear, R. J., Hirst, A. C., and McNeil, B. I. (2000). Changes in dissolved oxygen in the Southern Ocean with climate change. *Geochem. Geophys. Geosyst.* 1:2000GC000086. doi: 10.1029/2000gc000086

McLeod, D. J., Hallegraeff, G. M., Hosie, G. W., and Richardson, A. J. (2012). Climate-driven range expansion of the red-tide dinoflagellate *Noctiluca scintillans* into the Southern Ocean. *J. Plankton Res.* 34, 332–337. doi: 10.1093/plankt/fbr112

McMinn, A., Müller, M. N., Martin, A., and Ryan, K. G. (2014). The response of Antarctic Sea Ice Algae to changes in pH and CO_2. *PLoS ONE* 9:e86984. doi: 10.1371/journal.pone.0086984

McMinn, A., Ryan, K. G., Ralph, P. J., and Pankowski, A. (2007). Spring sea ice photosynthesis, primary productivity and biomass distribution in eastern Antarctica, 2002–2004. *Mar. Biol.* 151, 985–995. doi: 10.1007/s00227-006-0533-8

McNeil, B. I., and Matear, R. J. (2008). Southern Ocean acidification: a tipping point at 450-ppm atmospheric CO_2. *Proc. Natl. Acad. Sci. U.S.A.* 105, 18860–18864. doi: 10.1073/pnas.0806318105

Meijers, A. J. S. (2014). The Southern Ocean in the Coupled Model Intercomparison Project phase 5. *Philos. Trans. R. Soc. A Math. Phys. Eng. Sci.* 372:20130296. doi: 10.1098/rsta.2013.0296

Meiners, K. M., Vancoppenolle, M., Thanassekos, S., Dieckmann, G. S., Thomas, D. N., Tison, J. L., et al. (2012). Chlorophyll *a* in Antarctic sea ice from historical ice core data. *Geophys. Res. Lett.* 39:L21602. doi: 10.1029/2012GL053478

Meredith, M. P., and Hogg, A. M. (2006). Circumpolar response of Southern Ocean eddy activity to a change in the Southern Annular Mode. *Geophys. Res. Lett.* 33, L16608. doi: 10.1029/2006GL026499

Meredith, M. P., and King, J. C. (2005). Rapid climate change in the ocean west of the Antarctic Peninsula during the second half of the 20th century. *Geophys. Res. Lett.* 32:L19604. doi: 10.1029/2005gl024042

Metzl, N., Tilbrook, B., and Poisson, A. (1999). The annual fCO_2 cycle and the air-sea CO_2 flux in the sub-Antarctic Ocean. *Tellus B* 51, 849–861. doi: 10.3402/tellusb.v51i4.16495

Moisan, T. A., and Mitchell, B. G. (1999). Photophysiological acclimation of *Phaeocystis antarctica* Karsten under light limitation. *Limnol. Oceanogr.* 44, 247–258. doi: 10.4319/lo.1999.44.2.0247

Moline, M. A., Claustre, H., Frazer, T. K., Schofield, O., and Vernet, M. (2004). Alteration of the food web along the Antarctic Peninsula in response to a regional warming trend. *Global Change Biol.* 10, 1973–1980. doi: 10.1111/j.1365-2486.2004.00825.x

Moline, M. A., Karnovsky, N. J., Brown, Z., Divoky, G. J., Frazer, T. K., Jacoby, C. A., et al. (2008). High latitude changes in ice dynamics and their impact on polar marine ecosystems. *Ann. N.Y. Acad. Sci.* 1134, 267–319. doi: 10.1196/annals.1439.010

Montes-Hugo, M., Vernet, M., Martinson, D., Smith, R., and Iannuzzi, R. (2008). Variability on phytoplankton size structure in the western Antarctic Peninsula (1997–2006). *Deep Sea Res. Part II Topic. Stud. Oceanogr.* 55, 2106–2117. doi: 10.1016/j.dsr2.2008.04.036

Moore, J. K., and Abbott, M. R. (2000). Phytoplankton chlorophyll distributions and primary production in the Southern Ocean. *J. Geophys. Res. Oceans* 105, 28709–28722. doi: 10.1029/1999JC000043

Moreau, S., Mostajir, B., Bélanger, S., Schloss, I. R., Vancoppenolle, M., Demers, S., et al. (2015). Climate change enhances primary production in the western Antarctic Peninsula. *Glob. Change Biol.* 21, 2191–2205. doi: 10.1111/gcb.12878

Moreau, S., Schloss, I., Mostajir, B., Demers, S., Almandoz, G., Ferrario, M., et al. (2012). Influence of microbial community composition and metabolism on air-sea ΔpCO_2 variation off the western Antarctic Peninsula. *Mar. Ecol. Prog. Ser.* 446, 45–59. doi: 10.3354/meps09466

Müller, M., Trull, T., and Hallegraeff, G. (2015). Differing responses of three Southern Ocean *Emiliania huxleyi* ecotypes to changing seawater carbonate chemistry. *Mar. Ecol. Prog. Ser.* 531, 81–90. doi: 10.3354/meps11309

Murphy, E., Watkins, J., Trathan, P., Reid, K., Meredith, M., Thorpe, S., et al. (2007). Spatial and temporal operation of the Scotia Sea ecosystem: a review of large-scale links in a krill centred food web. *Philos. Trans. R. Soc. B Biol. Sci.* 362, 113–148. doi: 10.1098/rstb.2006.1957

Murphy, E. J., Cavanagh, R. D., Drinkwater, K. F., Grant, S. M., Heymans, J. J., Hofmann, E. E., et al. (2016). Understanding the structure and functioning of polar pelagic ecosystems to predict the impacts of change. *Proc. R. Soc. B Biol. Sci.* 283, 20161646. doi: 10.1098/rspb.2016.1646

Neale, P. J., Cullen, J. J., and Davis, R. F. (1998a). Inhibition of marine photosynthesis by ultraviolet radiation: Variable sensitivity of phytoplankton

in the Weddell-Scotia Confluence during the austral spring. *Limnol. Oceanogr.* 43, 433–448. doi: 10.4319/lo.1998.43.3.0433

Neale, P. J., Davis, R. F., and Cullen, J. J. (1998b). Interactive effects of ozone depletion and vertical mixing on photosynthesis of Antarctic phytoplankton. *Nature* 392, 585–589. doi: 10.1038/33374

Nelson, D. M., Smith, W. O. J., Gordon, L. I., and Huber, B. A. (1987). Spring distributions of density, nutrients, and phytoplankton biomass in the ice edge zone of the Weddell-Scotia Sea. *J. Geophys. Res. Oceans* 92:7181. doi: 10.1029/jc092ic07p07181

Nevitt, G. A., Veit, R. R., and Kareiva, P. (1995). Dimethyl sulphide as a foraging cue for Antarctic Procellariiform seabirds. *Nature* 376, 680–682. doi: 10.1038/376680ao

Nicol, S., Meiners, K., and Raymond, B. (2010). BROKE-West, a large ecosystem survey of the South West Indian Ocean sector of the Southern Ocean, 30°E–80°E (CCAMLR Division 58.4.2). *Deep Sea Res. Part II Topic. Stud. Oceanogr.* 57, 693–700. doi: 10.1016/j.dsr2.2009.11.002

Nicol, S., Pauly, T., Bindoff, N., and Strutton, P. (2000). "BROKE" a biological/oceanographic survey off the coast of East Antarctica (80–150°E) carried out in January-March 1996. *Deep Sea Res. Part II Topic. Stud. Oceanogr.* 47, 2281–2297. doi: 10.1016/S0967-0645(00)00026-6

Obernosterer, I., Christaki, U., Lefèvre, D., Catala, P., Van Wambeke, F., and Lebaron, P. (2008). Rapid bacterial mineralization of organic carbon produced during a phytoplankton bloom induced by natural iron fertilization in the Southern Ocean. *Deep Sea Res. II Topic. Stud. Oceanogr.* 55, 777–789. doi: 10.1016/j.dsr2.2007.12.005

Odate, T., and Fukuchi, M. (1995). Distribution and community structure of picoplankton in the Southern Ocean during the late austral summer of 1992. *Proc. NIPR Symp. Polar Biol.* 8, 86–100.

Olguín, H. F., and Alder, V. A. (2011). Species composition and biogeography of diatoms in antarctic and subantarctic (Argentine shelf) waters (37–76°S). *Deep Sea Res. Part II Topic. Stud. Oceanogr.* 58, 139–152. doi: 10.1016/j.dsr2.2010.09.031

Orr, J. C., Fabry, V. J., Aumont, O., Bopp, L., Doney, S. C., Feely, R. A., et al. (2005). Anthropogenic ocean acidification over the twenty-first century and its impact on calcifying organisms. *Nature* 437, 681–686. doi: 10.1038/nature04095

Orsi, A., Johnson, G., and Bullister, J. (1999). Circulation, mixing, and production of Antarctic Bottom Water. *Prog. Oceanogr.* 43, 55–109. doi: 10.1016/S0079-6611(99)00004-X

Orsi, A. H., Whitworth, T., and Nowlin, W. D. (1995). On the meridional extent and fronts of the Antarctic Circumpolar Current. *Deep Sea Res. I Oceanogr. Res. Papers* 42, 641–673. doi: 10.1016/0967-0637(95)00021-W

Palmisano, A., SooHoo, J., Moe, R., and Sullivan, C. (1987). Sea ice microbial communities. VII. Changes in under-ice spectral irradiance during the development of Antarctic sea ice microalgal communities. *Mar. Ecol. Prog. Ser.* 35, 165–173. doi: 10.3354/meps035165

Palmisano, A. C., and Sullivan, C. W. (1983). Sea ice microbial communities (SIMCO) 1. Distribution, abundance, and primary production of ice microalgae in McMurdo Sound, Antarctica in 1980. *Polar Biol.* 2, 171–177. doi: 10.1007/BF00448967

Parkinson, C. L., and Cavalieri, D. J. (2012). Antarctic sea ice variability and trends, 1979-2010. *Cryosphere* 6, 871–880. doi: 10.5194/tc-6-871-2012

Patil, S. M., Mohan, R., Shetye, S., Gazi, S., and Jafar, S. (2014). Morphological variability of *Emiliania huxleyi* in the Indian sector of the Southern Ocean during the austral summer of 2010. *Mar. Micropaleontol.* 107, 44–58. doi: 10.1016/j.marmicro.2014.01.005

Pearce, I., Davidson, A. T., Thomson, P. G., Wright, S., and van den Enden, R. (2010). Marine microbial ecology off East Antarctica (30–80°E): Rates of bacterial and phytoplankton growth and grazing by heterotrophic protists. *Deep Sea Res. Part II Topic. Stud. Oceanogr.* 57, 849–862. doi: 10.1016/j.dsr2.2008.04.039

Pearce, I., Davidson, A. T., Thomson, P. G., Wright, S., and van den Enden, R. (2011). Marine microbial ecology in the sub-Antarctic Zone: Rates of bacterial and phytoplankton growth and grazing by heterotrophic protists. *Deep Sea Res. Part II Topic. Stud. Oceanogr.* 58, 2248–2259. doi: 10.1016/j.dsr2.2011.05.030

Peck, L. S., Barnes, D. K. A., Cook, A. J., Fleming, A. H., and Clarke, A. (2010). Negative feedback in the cold: Ice retreat produces new carbon sinks in Antarctica. *Glob. Change Biol.* 16, 2614–2623. doi: 10.1111/j.1365-2486.2009.02071.x

Perissinotto, R., and Pakhomov, E. A. (1998). Contribution of salps to carbon flux of marginal ice zone of the Lazarev Sea, southern ocean. *Mar. Biol.* 131, 25–32. doi: 10.1007/s002270050292

Perovich, D. K. (1990). Theoretical estimates of light reflection and transmission by spatially complex and temporally varying sea ice covers. *J. Geophys. Res. Oceans* 95:9557. doi: 10.1029/jc095ic06p09557

Perrin, R. A., Lu, P., and Marchant, H. J. (1987). Seasonal variation in marine phytoplankton and ice algae at a shallow antarctic coastal site. *Hydrobiologia* 146, 33–46. doi: 10.1007/BF00007575

Petrou, K., Kranz, S. A., Trimborn, S., Hassler, C. S., Ameijeiras, S. B., Sackett, O., et al. (2016). Southern Ocean phytoplankton physiology in a changing climate. *J. Plant Physiol.* 203, 135–150. doi: 10.1016/j.jplph.2016.05.004

Pezza, A. B., Rashid, H. A., and Simmonds, I. (2012). Climate links and recent extremes in Antarctic sea ice, high-latitude cyclones, Southern Annular Mode and ENSO. *Clim. Dyn.* 38, 57–73. doi: 10.1007/s00382-011-1044-y

Pollard, R., Lucas, M., and Read, J. (2002). Physical controls on biogeochemical zonation in the Southern Ocean. *Deep Sea Res. Part II Topic. Stud. Oceanogr.* 49, 3289–3305. doi: 10.1016/S0967-0645(02)00084-X

Pollard, R. T., Salter, I., Sanders, R. J., Lucas, M. I., Moore, C. M., Mills, R. A., et al. (2009). Southern Ocean deep-water carbon export enhanced by natural iron fertilization. *Nature* 457, 577–580. doi: 10.1038/nature07716

Poloczanska, E., Babcock, R., Butler, A., Hobday, A., Hoegh-Guldberg, O., Kunz, T., et al. (2007). "Climate change and Australian marine life," in *Oceanography and Marine Biology. Vol. 45*, eds R. N. Gibson, R. J. A. Atkinson, and J. D. M. Gordon (Boca Raton, FL: CRC Press), 407–78.

Polvani, L. M., Waugh, D. W., Correa, G. J. P., and Son, S.-W. (2011). Stratospheric ozone depletion: the main driver of twentieth-century atmospheric circulation changes in the southern hemisphere. *J. Clim.* 24, 795–812. doi: 10.1175/2010JCLI3772.1

Post, A., L., Meijers, A., Fraser, A., Meiners, K., Ayers, J., Bindoff, N., et al. (2014). "Environmental setting," in *Biogeographic Atlas of the Southern Ocean*, eds C. De Broyer, P. Koubbi, H. J. Griffiths, B. Raymond, C. D'Udekem d'Acoz (Cambridge, UK: Scientific Committee on Antarctic Research), 46–64.

Quéguiner, B. (2013). Iron fertilization and the structure of planktonic communities in high nutrient regions of the Southern Ocean. *Deep Sea Res. Part II Topic. Stud. Oceanogr.* 90, 43–54. doi: 10.1016/j.dsr2.2012.07.024

Quetin, L. B., and Ross, R. M. (2009). "Life under Antarctic pack ice: a krill perspective," in *Smithsonian at the Poles: Contributions to International Polar Year Science*, eds I. Krupnik, M. Lang, and S. Miller (Washington, DC: Smithsonian Institute), 285–298. doi: 10.5479/si.097884601X.21

Rack, W., and Rott, H. (2004). Pattern of retreat and disintegration of the Larsen B ice shelf, Antarctic Peninsula. *Ann. Glaciol.* 39, 505–510. doi: 10.3189/172756404781814005

Raphael, M. N., Marshall, G. J., Turner, J., Fogt, R. L., Schneider, D., Dixon, D. A., et al. (2016). The Amundsen Sea low: variability, change, and impact on Antarctic Climate. *Bull. Am. Meteorol. Soc.* 97, 111–121. doi: 10.1175/BAMS-D-14-00018.1

Raven, J. A. (1991). Physiology of inorganic C acquisition and implications for resource use efficiency by marine phytoplankton: relation to increased CO_2 and temperature. *Plant Cell Environ.* 14, 779–794. doi: 10.1111/j.1365-3040.1991.tb01442.x

Raven, J. A., and Falkowski, P. G. (1999). Oceanic sinks for atmospheric CO_2. *Plant Cell Environ.* 22, 741–755. doi: 10.1046/j.1365-3040.1999.00419.x

Rembauville, M., Blain, S., Armand, L., Quéguiner, B., and Salter, I. (2015a). Export fluxes in a naturally iron-fertilized area of the Southern Ocean - Part 2: Importance of diatom resting spores and faecal pellets for export. *Biogeosciences* 12, 3171–3195. doi: 10.5194/bg-12-3171-2015

Rembauville, M., Blain, S., Caparros, J., and Salter, I. (2016a). Particulate matter stoichiometry driven by microplankton community structure in summer in the Indian sector of the Southern Ocean. *Limnol. Oceanogr.* 61, 1301–1321. doi: 10.1002/lno.10291

Rembauville, M., Manno, C., Tarling, G., Blain, S., and Salter, I. (2016b). Strong contribution of diatom resting spores to deep-sea carbon transfer in naturally iron-fertilized waters downstream of South Georgia. *Deep Sea Res. I Oceanogr. Res. Papers* 115, 22–35. doi: 10.1016/j.dsr.2016.05.002

Rembauville, M., Meilland, J., Ziveri, P., Schiebel, R., Blain, S., and Salter, I. (2016c). Planktic foraminifer and coccolith contribution to carbonate export fluxes

over the central Kerguelen Plateau. *Deep Sea Res. I Oceanogr. Res. Papers* 111, 91–101. doi: 10.1016/j.dsr.2016.02.017

Rembauville, M., Salter, I., Leblond, N., Gueneugues, A., and Blain, S. (2015b). Export fluxes in a naturally iron-fertilized area of the Southern Ocean - Part 1: Seasonal dynamics of particulate organic carbon export from a moored sediment trap. *Biogeosciences* 12, 3153–3170. doi: 10.5194/bg-12-3153-2015

Rickard, G., and Behrens, E. (2016). CMIP5 Earth System Models with biogeochemistry: A Ross Sea assessment. *Antarct. Sci.* 28, 327–346. doi: 10.1017/S0954102016000122

Ridgway, K. R. (2007). Long-term trend and decadal variability of the southward penetration of the East Australian Current. *Geophys. Res. Lett.* 34:L13613. doi: 10.1029/2007gl030393

Ridgwell, A. J. (2002). Dust in the Earth system: the biogeochemical linking of land, air and sea. *Philos. Trans. R. Soc. A Math. Phys. Eng. Sci.* 360, 2905–2924. doi: 10.1098/rsta.2002.1096

Riebesell, U., Körtzinger, A., and Oschlies, A. (2009). Sensitivities of marine carbon fluxes to ocean change. *Proc. Natl. Acad. Sci. U.S.A.* 106, 20602–20609. doi: 10.1073/pnas.0813291106

Rigual-Hernández, A. S., Trull, T. W., Bray, S. G., Closset, I., and Armand, L. K. (2015). Seasonal dynamics in diatom and particulate export fluxes to the deep sea in the Australian sector of the southern Antarctic Zone. *J. Mar. Syst.* 142, 62–74. doi: 10.1016/j.jmarsys.2014.10.002

Rintoul, S. R., and Trull, T. W. (2001). Seasonal evolution of the mixed layer in the Subantarctic zone south of Australia. *J. Geophys. Res. Oceans* 106, 31447–31462. doi: 10.1029/2000JC000329

Robins, D., Harris, R., Bedo, A., Fernandez, E., Fileman, T., Harbour, D., et al. (1995). The relationship between suspended particulate material, phytoplankton and zooplankton during the retreat of the marginal ice zone in the Bellingshausen Sea. *Deep Sea Res. Part II Topic. Stud. Oceanogr.* 42, 1137–1158. doi: 10.1029/2000JC000329

Roden, N. P., Shadwick, E. H., Tilbrook, B., and Trull, T. W. (2013). Annual cycle of carbonate chemistry and decadal change in coastal Prydz Bay, East Antarctica. *Mar. Chem.* 155, 135–147. doi: 10.1016/j.marchem.2013.06.006

Rose, J. M., Feng, Y., DiTullio, G. R., Dunbar, R. B., Hare, C. E., Lee, P. A., et al. (2009). Synergistic effects of iron and temperature on Antarctic phytoplankton and microzooplankton assemblages. *Biogeosciences* 6, 3131–3147. doi: 10.5194/bg-6-3131-2009

Rost, B., Zondervan, I., and Wolf-Gladrow, D. (2008). Sensitivity of phytoplankton to future changes in ocean carbonate chemistry: current knowledge, contradictions and research directions. *Mar. Ecol. Prog. Ser.* 373, 227–237. doi: 10.3354/meps07776

Saavedra-Pellitero, M., Baumann, K.-H., Flores, J.-A., and Gersonde, R. (2014). Biogeographic distribution of living coccolithophores in the Pacific sector of the Southern Ocean. *Mar. Micropaleontol.* 109, 1–20. doi: 10.1016/j.marmicro.2014.03.003

Sabine, C. L., Feely, R. A., Gruber, N., Key, R. M., Lee, K., Bullister, J. L., et al. (2004). The Oceanic Sink for Anthropogenic CO_2. *Science* 305, 367–371. doi: 10.1126/science.1097403

Sackett, O., Petrou, K., Reedy, B., De Grazia, A., Hill, R., Doblin, M., et al. (2013). Phenotypic Plasticity of Southern Ocean Diatoms: Key to Success in the Sea Ice Habitat? *PLoS ONE* 8:e81185. doi: 10.1371/journal.pone.0081185

Saenz, B. T., and Arrigo, K. R. (2014). Annual primary production in Antarctic sea ice during 2005-2006 from a sea ice state estimate. *J. Geophys. Res. Oceans* 119, 3645–3678. doi: 10.1002/2013JC009677

Safi, K. A., Brian Griffiths, F., and Hall, J. A. (2007). Microzooplankton composition, biomass and grazing rates along the WOCE SR3 line between Tasmania and Antarctica. *Deep Sea Res. I Oceanogr. Res. Papers* 54, 1025–1041. doi: 10.1016/j.dsr.2007.05.003

Sakshaug, E. (1994). "Discussant's report: primary production in the Antarctic pelagial - a view from the north," in *Southern Ocean Ecology: The BIOMASS Perspective*, ed S. Z. El-Sayed (Cambridge, UK: Cambridge University Press), 125–126.

Sallée, J.-B., Speer, K. G., and Rintoul, S. R. (2010). Zonally asymmetric response of the Southern Ocean mixed-layer depth to the Southern Annular Mode. *Nat. Geosci.* 3, 273–279. doi: 10.1038/ngeo812

Salter, I., Kemp, A. E. S., Moore, C. M., Lampitt, R. S., Wolff, G. A., and Holtvoeth, J. (2012). Diatom resting spore ecology drives enhanced carbon export from a naturally iron-fertilized bloom in the Southern Ocean. *Glob. Biogeochem. Cycles* 26:GB1014. doi: 10.1029/2010GB003977

Salter, I., Lampitt, R. S., Sanders, R., Poulton, A., Kemp, A. E., Boorman, B., et al. (2007). Estimating carbon, silica and diatom export from a naturally fertilised phytoplankton bloom in the Southern Ocean using PELAGRA: a novel drifting sediment trap. *Deep Sea Res. Part II Topic. Stud. Oceanogr.* 54, 2233–2259. doi: 10.1016/j.dsr2.2007.06.008

Salter, I., Schiebel, R., Ziveri, P., Movellan, A., Lampitt, R., and Wol, G. A. (2014). Carbonate counter pump stimulated by natural iron fertilization in the Polar Frontal Zone. *Nat. Geosci.* 7, 885–889. doi: 10.1038/ngeo2285

Sarmento, H., Montoya, J. M., Vazquez-Dominguez, E., Vaque, D., and Gasol, J. M. (2010). Warming effects on marine microbial food web processes: how far can we go when it comes to predictions? *Philos. Trans. R. Soc. B Biol. Sci.* 365, 2137–2149. doi: 10.1098/rstb.2010.0045

Sarmiento, J. L., and Le Quéré, C. (1996). Oceanic carbon dioxide uptake in a model of century-scale global warming. *Science* 274, 1346–1350. doi: 10.1126/science.274.5291.1346

Sarmiento, J. L., Slater, R., Barber, R., Bopp, L., Doney, S. C., Hirst, A. C., et al. (2004). Response of ocean ecosystems to climate warming. *Glob. Biogeochem. Cycles* 18:GB3003. doi: 10.1029/2003gb002134

Savidge, G., Priddle, J., Gilpin, L., Bathmann, U., Murphy, E., Owens, N., et al. (1996). An assessment of the role of the marginal ice zone in the carbon cycle of the Southern Ocean. *Antarct. Sci.* 8, 349–358. doi: 10.1017/S0954102096000521

Scambos, T. A., Hulbe, C., Fahnestock, M., and Bohlander, J. (2000). The link between climate warming and break-up of ice shelves in the Antarctic Peninsula. *J. Glaciol.* 46, 516–530. doi: 10.3189/172756500781833043

Schaum, C. E., and Collins, S. (2014). Plasticity predicts evolution in a marine alga. *Proc. R. Soc. B Biol. Sci.* 281:20141486. doi: 10.1098/rspb.2014.1486

Schiermeier, Q. (2009). Atmospheric science: Fixing the sky. *Nature* 460, 792–795. doi: 10.1038/460792a

Schnack-Schiel, S. B., and Isla, E. (2005). The role of zooplankton in the pelagic-benthic coupling of the Southern Ocean. *Sci. Mar.* 69, 39–55. doi: 10.3989/scimar.2005.69s239

Schnack-Schiel, S. B., Thomas, D., Dahms, H.-U., Haas, C., and Mizdalski, E. (1998). "Copepods in Antarctic Sea Ice," in *Antarctic Sea Ice: Biological Processes, Interactions and Variability*, eds M. P. Lizotte and K. R. Arrigo (Washington, DC: American Geophysical Union), 173–182.

Scott, F. J., and Marchant, H. J. (2005). *Antarctic Marine Protists*. Canberra: Australian Biological Resources Study.

Sedwick, P. N., Marsay, C. M., Sohst, B. M., Aguilar-Islas, A. M., Lohan, M. C., Long, M. C., et al. (2011). Early season depletion of dissolved iron in the Ross Sea polynya: implications for iron dynamics on the Antarctic continental shelf. *J. Geophys. Res. Oceans* 116, 1–19. doi: 10.1029/2010JC006553

Sen Gupta, A., Santoso, A., Taschetto, A. S., Ummenhofer, C. C., Trevena, J., and England, M. H. (2009). Projected Changes to the Southern Hemisphere Ocean and Sea Ice in the IPCC AR4 Climate Models. *J. Clim.* 22, 3047–3078. doi: 10.1175/2008JCLI2827.1

Shadwick, E. H., Trull, T. W., Thomas, H., and Gibson, J. A. E. (2013). Vulnerability of polar oceans to anthropogenic acidification: comparison of Arctic and Antarctic seasonal cycles. *Sci. Rep.* 3:2339. doi: 10.1038/srep02339

Shaw, T., Raiswell, R., Hexel, C., Vu, H., Moore, W., Dudgeon, R., et al. (2011). Input, composition, and potential impact of terrigenous material from free-drifting icebergs in the Weddell Sea. *Deep Sea Res. Part II Topic. Stud. Oceanogr.* 58, 1376–1383. doi: 10.1016/j.dsr2.2010.11.012

Shindell, D. T., and Schmidt, G. A. (2004). Southern Hemisphere climate response to ozone changes and greenhouse gas increases. *Geophys. Res. Lett.* 31:L18209. doi: 10.1029/2004gl020724

Siegel, D. A., Buesseler, K. O., Doney, S. C., Sailley, S. F., Behrenfeld, M. J., and Boyd, P. W. (2014). Global assessment of ocean carbon export by combining satellite observations and food-web models. *Glob. Biogeochem. Cycles* 28, 181–196. doi: 10.1002/2013GB004743

Simmonds, I. (2015). Comparing and contrasting the behaviour of Arctic and Antarctic sea ice over the 35 year period 1979-2013. *Ann,. Glaciol.* 56, 18–28. doi: 10.3189/2015AoG69A909

Simó, R. (2004). From cells to globe: approaching the dynamics of DMS(P) in the ocean at multiple scales. *Can. J. Fish. Aquat. Sci.* 61, 673–684. doi: 10.1139/f04-030

Sloyan, B. M., and Rintoul, S. R. (2001a). Circulation, renewal, and modification of antarctic mode and intermediate water. *J. Phys. Oceanogr.* 31, 1005–1030. doi: 10.1175/1520-0485(2001)031<1005:CRAMOA>2.0.CO;2

Sloyan, B. M., and Rintoul, S. R. (2001b). The Southern Ocean Limb of the Global Deep Overturning Circulation. *J. Phys. Oceanogr.* 31, 143–173. doi: 10.1175/1520-0485(2001)031<0143:TSOLOT>2.0.CO;2

Smetacek, V., Assmy, P., and Henjes, J. (2004). The role of grazing in structuring Southern Ocean pelagic ecosystems and biogeochemical cycles. *Antarct. Sci.* 16, 541–558. doi: 10.1017/S0954102004002317

Smetacek, V., and Nicol, S. (2005). Polar ocean ecosystems in a changing world. *Nature* 437, 362–368. doi: 10.1038/nature04161

Smith, K., Sherman, A., Shaw, T., Murray, A., Vernet, M., and Cefarelli, A. (2011). Carbon export associated with free-drifting icebergs in the Southern Ocean. *Deep Sea Res. Part II Topic. Stud. Oceanogr.* 58, 1485–1496. doi: 10.1016/j.dsr2.2010.11.027

Smith, R., Baker, K., Fraser, W., Hofmann, E., Karl, D., Klink, J., et al. (1995). The palmer LTER: a long-term ecological research program at palmer station, Antarctica. *Oceanography* 8, 77–86. doi: 10.5670/oceanog.1995.01

Smith, R. C., Martinson, D. G., Stammerjohn, S. E., Iannuzzi, R. A., and Ireson, K. (2008). Bellingshausen and western Antarctic Peninsula region: pigment biomass and sea-ice spatial/temporal distributions and interannual variabilty. *Deep Sea Res. Part II Topic. Stud. Oceanogr.* 55, 1949–1963. doi: 10.1016/j.dsr2.2008.04.027

Smith, R. C., and Stammerjohn, S. E. (2001). Variations of surface air temperature and sea-ice extent in the western Antarctic Peninsula region. *Ann. Glaciol.* 33, 493–500. doi: 10.3189/172756401781818662

Smith, W. O. J., Ainley, D. G., and Cattaneo-Vietti, R. (2007). Trophic interactions within the Ross Sea continental shelf ecosystem. *Philos. Trans. R. Soc. B Biol. Sci.* 362, 95–111. doi: 10.1098/rstb.2006.1956

Smith, W. O. J., Anderson, R. F., Keith Moore, J., Codispoti, L. A., and Morrison, J. M. (2000a). The US Southern Ocean Joint Global Ocean Flux Study: an introduction to AESOPS. *Deep Sea Res. Part II Topic. Stud. Oceanogr.* 47, 3073–3093. doi: 10.1016/S0967-0645(00)00059-X

Smith, W. O. J., and Gordon, L. I. (1997). Hyperproductivity of the Ross Sea (Antarctica) polynya during austral spring. *Geophys. Res. Lett.* 24, 233–236. doi: 10.1029/96GL03926

Smith, W. O. J., Keene, N. K., and Comiso, J. C. (1988). "Interannual variability in estimated primary productivity of the Antarctic Marginal Ice Zone," in *Antarctic Ocean and Resources Variability*, ed D. Sahrhage (Berlin; Heidelberg: Springer), 131–139. doi: 10.1007/978-3-642-73724-4_10

Smith, W. O. J., Marra, J., Hiscock, M. R., and Barber, R. T. (2000b). The seasonal cycle of phytoplankton biomass and primary productivity in the Ross Sea, Antarctica. *Deep Sea Res. Part II Topic. Stud. Oceanogr.* 47, 3119–3140. doi: 10.1016/S0967-0645(00)00061-8

Smith, W. O. J., and Nelson, D. M. (1986). Importance of Ice Edge Phytoplankton Production in the Southern Ocean. *BioScience* 36, 251–257. doi: 10.2307/1310215

Sokolov, S., and Rintoul, S. R. (2009a). Circumpolar structure and distribution of the Antarctic Circumpolar Current fronts: 1. Mean circumpolar paths. *J. Geophys. Res. Oceans* 114, C11018. doi: 10.1029/2008JC005108

Sokolov, S., and Rintoul, S. R. (2009b). Circumpolar structure and distribution of the Antarctic Circumpolar Current fronts: 2. Variability and relationship to sea surface height. *J. Geophys. Res. Oceans* 114, 1–15. doi: 10.1029/2008JC005248

Solomon, S., Ivy, D. J., Kinnison, D., Mills, M. J., Neely, R. R., and Schmidt, A. (2016). Emergence of healing in the Antarctic ozone layer. *Science* 353, 269–274. doi: 10.1126/science.aae0061

Son, S.-W., Polvani, L. M., Waugh, D. W., Akiyoshi, H., Garcia, R., Kinnison, D., et al. (2008). The Impact of Stratospheric Ozone Recovery on the Southern Hemisphere Westerly Jet. *Science* 320, 1486–1489. doi: 10.1126/science.1155939

Stammerjohn, S., Massom, R., Rind, D., and Martinson, D. (2012). Regions of rapid sea ice change: an inter-hemispheric seasonal comparison. *Geophys. Res. Lett.* 39:L06501. doi: 10.1029/2012gl050874

Stammerjohn, S. E., Martinson, D. G., Smith, R. C., and Iannuzzi, R. A. (2008). Sea ice in the western Antarctic Peninsula region: Spatio-temporal variability from ecological and climate change perspectives. *Deep Sea Res. Part II Topic. Stud. Oceanogr.* 55, 2041–2058. doi: 10.1016/j.dsr2.2008.04.026

Steinacher, M., Joos, F., Frölicher, T. L., Bopp, L., Cadule, P., Cocco, V., et al. (2010). Projected 21st century decrease in marine productivity: a multi-model analysis. *Biogeosciences* 7, 979–1005. doi: 10.5194/bg-7-979-2010

Stroeve, J. C., Jenouvrier, S., Campbell, G. G., Barbraud, C., and Delord, K. (2016). Mapping and assessing variability in the Antarctic marginal ice zone, pack ice and coastal polynyas in two sea ice algorithms with implications on breeding success of snow petrels. *Cryosphere* 10, 1823–1843. doi: 10.5194/tc-10-1823-2016

Stroeve, J. C., Kattsov, V., Barrett, A., Serreze, M., Pavlova, T., Holland, M., et al. (2012). Trends in Arctic sea ice extent from CMIP5, CMIP3 and observations. *Geophys. Res. Lett.* 39:L16502. doi: 10.1029/2012gl052676

Strzepek, R. F., Maldonado, M. T., Hunter, K. A., Frew, R. D., and Boyd, P. W. (2011). Adaptive strategies by Southern Ocean phytoplankton to lessen iron limitation: uptake of organically complexed iron and reduced cellular iron requirements. *Limnol. Oceanogr.* 56, 1983–2002. doi: 10.4319/lo.2011.56.6.1983

Sullivan, C. W., McClain, C. R., Comiso, J. C., and Smith, W. O. (1988). Phytoplankton standing crops within an Antarctic ice edge assessed by satellite remote sensing. *J. Geophys. Res.* 93, 12487. doi: 10.1029/JC093iC10p12487

Swart, N. C., Fyfe, J. C., Saenko, O. A., and Eby, M. (2014). Wind-driven changes in the ocean carbon sink. *Biogeosciences* 11, 6107–6117. doi: 10.5194/bg-11-6107-2014

Sweeney, C., Hansell, D. A., Carlson, C. A., Codispoti, L., Gordon, L. I., Marra, J., et al. (2000). Biogeochemical regimes, net community production and carbon export in the Ross Sea, Antarctica. *Deep Sea Res. Part II Topic. Stud. Oceanogr.* 47, 3369–3394. doi: 10.1016/S0967-0645(00)00072-2

Tagliabue, A., Bopp, L., Dutay, J.-C., Bowie, A. R., Chever, F., Jean-Baptiste, P., et al. (2010). Hydrothermal contribution to the oceanic dissolved iron inventory. *Nat. Geosci.* 3, 252–256. doi: 10.1038/ngeo818

Takahashi, T., Sutherland, S. C., Wanninkhof, R., Sweeney, C., Feely, R. A., Chipman, D. W., et al. (2009). Climatological mean and decadal change in surface ocean pCO_2, and net sea-air CO_2 flux over the global oceans. *Deep Sea Res. Part II Topic. Stud. Oceanogr.* 56, 554–577. doi: 10.1016/j.dsr2.2008.12.009

Taylor, M. H., Losch, M., and Bracher, A. (2013). On the drivers of phytoplankton blooms in the Antarctic marginal ice zone: a modeling approach. *J. Geophys. Res. Oceans*, 118, 63–75. doi: 10.1029/2012JC008418

Thomas, D. N., and Dieckmann, G. S. (2002). Antarctic Sea Ice–a Habitat for Extremophiles. *Science* 295, 641–644. doi: 10.1126/science.1063391

Thomas, D. N., Lara, R. J., Haas, C., Schnack-Schiel, S. B., Dieckmann, G. S., Kattner, G., et al. (1998). "Biological Soup Within Decaying Summer Sea Ice in the Amundsen Sea, Antarctica," in *Antarctic Sea Ice: Biological Processes, Interactions and Variability*, eds M. P. Lizotte and K. R. Arrigo (Washington, DC: American Geophysical Union), 161–171.

Thompson, D. W. J., and Solomon, S. (2002). Interpretation of recent southern hemisphere climate change. *Science* 296, 895–899. doi: 10.1126/science.1069270

Thompson, D. W. J., Solomon, S., Kushner, P. J., England, M. H., Grise, K. M., and Karoly, D. J. (2011). Signatures of the Antarctic ozone hole in Southern Hemisphere surface climate change. *Nat. Geosci.* 4, 741–749. doi: 10.1038/ngeo1296

Thompson, D. W. J., and Wallace, J. M. (2000). Annular modes in the extratropical circulation. part I: month-to-month variability. *J. Clim.* 13, 1000–1016. doi: 10.1175/1520-0442(2000)013<1000:AMITEC>2.0.CO;2

Thomson, P., Davidson, A., and Maher, L. (2016). Increasing CO_2 changes community composition of pico- and nano-sized protists and prokaryotes at a coastal Antarctic site. *Mar. Ecol. Prog. Ser.* 554, 51–69. doi: 10.3354/meps11803

Timmermans, K. R., Gerringa, L. J. A., de Baar, H. J. W., van der Wagt, B., Veldhuis, M. J. W., de Jong, J. T. M., et al. (2001). Growth rates of large and small Southern Ocean diatoms in relation to availability of iron in natural seawater. *Limnol. Oceanogr.* 46, 260–266. doi: 10.4319/lo.2001.46.2.0260

Torstensson, A., Hedblom, M., Mattsdotter Björk, M., Chierici, M., and Wulff, A. (2015). Long-term acclimation to elevated pCO_2 alters carbon metabolism and reduces growth in the Antarctic diatom *Nitzschia lecointei*. *Proc. R. Soc. B Biol. Sci.* 282:20151513. doi: 10.1098/rspb.2015.1513

Tortell, P. D., Payne, C. D., Li, Y., Trimborn, S., Rost, B., Smith, W. O. J., et al. (2008). CO_2 sensitivity of Southern Ocean phytoplankton. *Geophys. Res. Lett.* 35, L04605. doi: 10.1029/2007GL032583

Tréguer, P., and Jacques, G. (1992). Dynamics of nutrients and phytoplankton, and fluxes of carbon, nitrogen and silicon in the Antarctic Ocean. *Polar Biol.* 12, 149–162. doi: 10.1007/978-3-642-77595-6_17

Tréguer, P., and Van Bennekom, A. (1991). The annual production of biogenic silica in the Antarctic Ocean. *Mar. Chem.* 35, 477–487. doi: 10.1016/S0304-4203(09)90038-X

Trevena, A. J., and Jones, G. B. (2006). Dimethylsulphide and dimethylsulphoniopropionate in Antarctic sea ice and their release during sea ice melting. *Mar. Chem.* 98, 210–222. doi: 10.1016/j.marchem.2005.09.005

Trimborn, S., Brenneis, T., Sweet, E., and Rost, B. (2013). Sensitivity of Antarctic phytoplankton species to ocean acidification: Growth, carbon acquisition, and species interaction. *Limnol. Oceanogr.* 58, 997–1007. doi: 10.4319/lo.2013.58.3.0997

Trimborn, S., Thoms, S., Petrou, K., Kranz, S. A., and Rost, B. (2014). Photophysiological responses of Southern Ocean phytoplankton to changes in CO_2 concentrations: short-term versus acclimation effects. *J. Exp. Mar. Biol. Ecol.* 451, 44–54. doi: 10.1016/j.jembe.2013.11.001

Trull, T. W., Bray, S. G., Manganini, S. J., Honjo, S., and François, R. (2001b). Moored sediment trap measurements of carbon export in the Subantarctic and Polar Frontal Zones of the Southern Ocean, south of Australia. *J. Geophys.* 106, 31489–31509. doi: 10.1029/2000JC000308

Trull, T. W., Rintoul, S. R., Hadfield, M., and Abraham, E. R. (2001a). Circulation and seasonal evolution of polar waters south of Australia: implications for iron fertilization of the Southern Ocean. *Deep Sea Res. Part II Topic. Stud. Oceanogr.* 48, 2439–2466. doi: 10.1016/S0967-0645(01)00003-0

Turner, J. (2002). Zooplankton fecal pellets, marine snow and sinking phytoplankton blooms. *Aquat. Microb. Ecol.* 27, 57–102. doi: 10.3354/ame027057

Turner, J., Barrand, N. E., Bracegirdle, T. J., Convey, P., Hodgson, D. A., Jarvis, M., et al. (2014). Antarctic climate change and the environment: an update. *Polar Record* 50, 237–259. doi: 10.1017/S0032247413000296

Turner, J., Bracegirdle, T. J., Phillips, T., Marshall, G. J., and Hosking, J. S. (2013). An initial assessment of Antarctic Sea Ice Extent in the CMIP5 Models. *J. Clim.* 26, 1473–1484. doi: 10.1175/JCLI-D-12-00068.1

Turner, J., Comiso, J. C., Marshall, G. J., Lachlan-Cope, T. A., Bracegirdle, T., Maksym, T., et al. (2009). Non-annular atmospheric circulation change induced by stratospheric ozone depletion and its role in the recent increase of Antarctic sea ice extent. *Geophys. Res. Lett.* 36, L08502. doi: 10.1029/2009GL037524

Turner, S., Nightingale, P., Broadgate, W., and Liss, P. (1995). The distribution of dimethyl sulphide and dimethylsulphoniopropionate in Antarctic waters and sea ice. *Deep Sea Res. Part II Topic. Stud. Oceanogr.* 42, 1059–1080. doi: 10.1016/0967-0645(95)00066-Y

Vance, T., Davidson, A., Thomson, P., Levasseur, M., Lizotte, M., Curran, M., et al. (2013). Rapid DMSP production by an Antarctic phytoplankton community exposed to natural surface irradiances in late spring. *Aquat. Microb. Ecol.* 71, 117–129. doi: 10.3354/ame01670

Vaughan, D. G., Marshall, G. J., Connolley, W. M., Parkinson, C., Mulvaney, R., Hodgson, D. A., et al. (2003). Recent rapid regional climate warming on the Antarctic Peninsula. *Clim. Change* 60, 243–274. doi: 10.1023/A:1026021217991

Venables, H. J., and Meredith, M. P. (2014). Feedbacks between ice cover, ocean stratification, and heat content in Ryder Bay, western Antarctic Peninsula. *J. Geophys. Res. Oceans* 119, 5323–5336. doi: 10.1002/2013JC009669

Vernet, M., Martinson, D., Iannuzzi, R., Stammerjohn, S., Kozlowski, W., Sines, K., et al. (2008). Primary production within the sea-ice zone west of the Antarctic Peninsula: I-Sea ice, summer mixed layer, and irradiance. *Deep Sea Res. Part II Topic. Stud. Oceanogr.* 55, 2068–2085. doi: 10.1016/j.dsr2.2008.05.021

Vernet, M., Sines, K., Chakos, D., Cefarelli, A., and Ekern, L. (2011). Impacts on phytoplankton dynamics by free-drifting icebergs in the NW Weddell Sea. *Deep Sea Res. Part II Topic. Stud. Oceanogr.* 58, 1422–1435. doi: 10.1016/j.dsr2.2010.11.022

Vernet, M., Smith, K., Cefarelli, A., Helly, J., Kaufmann, R., Lin, H., et al. (2012). Islands of Ice: Influence of Free-Drifting Antarctic Icebergs on Pelagic Marine Ecosystems. *Oceanography* 25, 38–39. doi: 10.5670/oceanog.2012.72

Watanabe, O., Jouzel, J., Johnsen, S., Parrenin, F., Shoji, H., and Yoshida, N. (2003). Homogeneous climate variability across East Antarctica over the past three glacial cycles. *Nature* 422, 509–512. doi: 10.1038/nature01525

Waters, R., van den Enden, R., and Marchant, H. (2000). Summer microbial ecology off East Antarctica (80–150°E): protistan community structure and bacterial abundance. *Deep Sea Res. Part II Topic. Stud. Oceanogr.* 47, 2401–2435. doi: 10.1016/S0967-0645(00)00030-8

Westwood, K. J., Brian Griffiths, F., Meiners, K. M., and Williams, G. D. (2010). Primary productivity off the Antarctic coast from 30°–80°E; BROKE-West survey, 2006. *Deep Sea Res. Part II Topic. Stud. Oceanogr.* 57, 794–814. doi: 10.1016/j.dsr2.2008.08.020

Williams, G., Nicol, S., Aoki, S., Meijers, A., Bindoff, N., Iijima, Y., et al. (2010). Surface oceanography of BROKE-West, along the Antarctic margin of the south-west Indian Ocean (30–80°E). *Deep Sea Res. Part II Topic. Stud. Oceanogr.* 57, 738–757. doi: 10.1016/j.dsr2.2009.04.020

Winter, A., Henderiks, J., Beaufort, L., Rickaby, R. E. M., and Brown, C. W. (2014). Poleward expansion of the coccolithophore *Emiliania huxleyi*. *J. Plankton Res.* 36, 316–325. doi: 10.1093/plankt/fbt110

Wong, A. P. S., Bindoff, N. L., and Church, J. a. (1999). Large-scale freshening of intermediate waters in the Pacific and Indian oceans. *Nature* 400, 440–443. doi: 10.1038/22733

Woodward, S., Roberts, D. L., and Betts, R. A. (2005). A simulation of the effect of climate change-induced desertification on mineral dust aerosol. *Geophys. Res. Lett.* 32, 2–5. doi: 10.1029/2005GL023482

Worby, A. P., Geiger, C. A., Paget, M. J., Van Woert, M. L., Ackley, S. F., and DeLiberty, T. L. (2008). Thickness distribution of Antarctic sea ice. *J. Geophys. Res. Oceans* 113, C05S92. doi: 10.1029/2007jc004254

Wright, S. W., and van den Enden, R. L. (2000). Phytoplankton community structure and stocks in the East Antarctic marginal ice zone (BROKE survey, January-March 1996) determined by CHEMTAX analysis of HPLC pigment signatures. *Deep Sea Res. Part II Topic. Stud. Oceanogr.* 47, 2363–2400. doi: 10.1016/S0967-0645(00)00029-1

Wright, S. W., van den Enden, R. L., Pearce, I., Davidson, A. T., Scott, F. J., and Westwood, K. J. (2010). Phytoplankton community structure and stocks in the Southern Ocean (30–80 °E) determined by CHEMTAX analysis of HPLC pigment signatures. *Deep Sea Res. Part II Topic. Stud. Oceanogr.* 57, 758–778. doi: 10.1016/j.dsr2.2009.06.015

Xu, K., Fu, F.-X., and Hutchins, D. A. (2014). Comparative responses of two dominant Antarctic phytoplankton taxa to interactions between ocean acidification, warming, irradiance, and iron availability. *Limnol. Oceanogr.* 59, 1919–1931. doi: 10.4319/lo.2014.59.6.1919

Yin, J. H. (2005). A consistent poleward shift of the storm tracks in simulations of 21st century climate. *Geophys. Res. Lett.* 32:L18701. doi: 10.1029/2005gl023684

Young, I. R., Zieger, S., and Babanin, A. V. (2011). Global trends in Wind Speed and Wave Height. *Science* 332, 451–455. doi: 10.1126/science.1197219

Young, J., Kranz, S., Goldman, J., Tortell, P., and Morel, F. (2015). Antarctic phytoplankton down-regulate their carbon-concentrating mechanisms under high CO_2 with no change in growth rates. *Mar. Ecol. Prog. Ser.* 532, 13–28. doi: 10.3354/meps11336

Zhu, Z., Xu, K., Fu, F., Spackeen, J., Bronk, D., and Hutchins, D. (2016). A comparative study of iron and temperature interactive effects on diatoms and *Phaeocystis antarctica* from the Ross Sea, Antarctica. *Mar. Ecol. Prog. Ser.* 550, 39–51. doi: 10.3354/meps11732

Conflict of Interest Statement: The authors declare that the research was conducted in the absence of any commercial or financial relationships that could be construed as a potential conflict of interest.

Copyright © 2017 Deppeler and Davidson. This is an open-access article distributed under the terms of the Creative Commons Attribution License (CC BY). The use, distribution or reproduction in other forums is permitted, provided the original author(s) or licensor are credited and that the original publication in this journal is cited, in accordance with accepted academic practice. No use, distribution or reproduction is permitted which does not comply with these terms.

Appendix B

Chapter 2 Published Version

Biogeosciences, 15, 209–231, 2018
https://doi.org/10.5194/bg-15-209-2018
© Author(s) 2018. This work is distributed under
the Creative Commons Attribution 3.0 License.

Biogeosciences Open Access EGU

Ocean acidification of a coastal Antarctic marine microbial community reveals a critical threshold for CO_2 tolerance in phytoplankton productivity

Stacy Deppeler[1], Katherina Petrou[2], Kai G. Schulz[3], Karen Westwood[4,5], Imojen Pearce[4], John McKinlay[4], and Andrew Davidson[4,5]

[1]Institute for Marine and Antarctic Studies, University of Tasmania, Private Bag 129, Hobart, Tasmania 7001, Australia
[2]School of Life Sciences, University of Technology Sydney, 15 Broadway, Ultimo, New South Wales 2007, Australia
[3]Centre for Coastal Biogeochemistry, Southern Cross University, Military Rd, East Lismore, NSW 2480, Australia
[4]Australian Antarctic Division, Department of the Environment and Energy, 203 Channel Highway, Kingston, Tasmania 7050, Australia
[5]Antarctic Climate and Ecosystems Cooperative Research Centre, Private Bag 80, Hobart, Tasmania 7001, Australia

Correspondence: Stacy Deppeler (stacy.deppeler@utas.edu.au)

Received: 1 June 2017 – Discussion started: 29 June 2017
Revised: 10 October 2017 – Accepted: 6 November 2017 – Published: 11 January 2018

Abstract. High-latitude oceans are anticipated to be some of the first regions affected by ocean acidification. Despite this, the effect of ocean acidification on natural communities of Antarctic marine microbes is still not well understood. In this study we exposed an early spring, coastal marine microbial community in Prydz Bay to CO_2 levels ranging from ambient (343 µatm) to 1641 µatm in six 650 L minicosms. Productivity assays were performed to identify whether a CO_2 threshold existed that led to a change in primary productivity, bacterial productivity, and the accumulation of chlorophyll *a* (Chl *a*) and particulate organic matter (POM) in the minicosms. In addition, photophysiological measurements were performed to identify possible mechanisms driving changes in the phytoplankton community. A critical threshold for tolerance to ocean acidification was identified in the phytoplankton community between 953 and 1140 µatm. CO_2 levels $\geq$ 1140 µatm negatively affected photosynthetic performance and Chl *a*-normalised primary productivity ($csGPP_{^{14}C}$), causing significant reductions in gross primary production ($GPP_{^{14}C}$), Chl *a* accumulation, nutrient uptake, and POM production. However, there was no effect of CO_2 on C : N ratios. Over time, the phytoplankton community acclimated to high CO_2 conditions, showing a down-regulation of carbon concentrating mechanisms (CCMs) and likely adjusting other intracellular processes. Bacterial abundance initially increased in CO_2 treatments $\geq$ 953 µatm (days 3–5), yet gross bacterial production ($GBP_{^{14}C}$) remained unchanged and cell-specific bacterial productivity ($csBP_{^{14}C}$) was reduced. Towards the end of the experiment, $GBP_{^{14}C}$ and $csBP_{^{14}C}$ markedly increased across all treatments regardless of CO_2 availability. This coincided with increased organic matter availability (POC and PON) combined with improved efficiency of carbon uptake. Changes in phytoplankton community production could have negative effects on the Antarctic food web and the biological pump, resulting in negative feedbacks on anthropogenic CO_2 uptake. Increases in bacterial abundance under high CO_2 conditions may also increase the efficiency of the microbial loop, resulting in increased organic matter remineralisation and further declines in carbon sequestration.

1 Introduction

The Southern Ocean (SO) is a significant sink for anthropogenic CO_2 (Metzl et al., 1999; Sabine et al., 2004; Frölicher et al., 2015). Approximately 30 % of anthropogenic CO_2 emissions have been absorbed by the world's oceans,

of which 40 % has been via the SO (Raven and Falkowski, 1999; Sabine et al., 2004; Khatiwala et al., 2009; Takahashi et al., 2009, 2012; Frölicher et al., 2015). While ameliorating CO_2 accumulation in the atmosphere, increasing oceanic CO_2 uptake alters the chemical balance of surface waters, with the average pH having already decreased by 0.1 units since pre-industrial times (Sabine et al., 2004; Raven et al., 2005). If anthropogenic emissions continue unabated, future concentrations of CO_2 in the atmosphere are projected to reach $\sim$ 930 µatm by 2100 and peak at $\sim$ 2000 µatm by 2250 (Meinshausen et al., 2011; IPCC, 2013). This will result in a further reduction of the surface ocean pH by up to 0.6 pH units, with unknown consequences for the marine microbial community (Caldeira and Wickett, 2003). High-latitude oceans have been identified as amongst the first regions to experience the negative effects of ocean acidification, causing potentially harmful reductions in the aragonite saturation state and a decline in the ocean's capacity for future CO_2 uptake (Sabine et al., 2004; Orr et al., 2005; McNeil and Matear, 2008; Fabry et al., 2009; Hauck and Völker, 2015). Marine microbes play a pivotal role in the uptake and storage of CO_2 in the ocean through phytoplankton photosynthesis and the vertical transport of biological carbon to the deep ocean (Longhurst, 1991; Honjo, 2004). As the buffering capacity of the SO decreases over time, the biological contribution to total CO_2 uptake is expected to increase in importance (Hauck et al., 2015; Hauck and Völker, 2015). Thus, it is necessary to understand the effects of high CO_2 on the productivity of the marine microbial community if we are to predict how they may affect ocean biogeochemistry in the future.

Phytoplankton primary production provides the food source for higher trophic levels and plays a critical role in the sequestration of carbon from the atmosphere into the deep ocean (Azam et al., 1983, 1991; Longhurst, 1991; Honjo, 2004; Fenchel, 2008; Kirchman, 2008). In Antarctic waters it is restricted to a short summer season and is characterised by intense phytoplankton blooms that can reach over 200 mg Chl a m^{-2} (Smith and Nelson, 1986; Nelson et al., 1987; Wright et al., 2010). Relative to elsewhere in the SO, the continental shelf around Antarctica accounts for a disproportionately high percentage of annual primary productivity (Arrigo et al., 2008a). In coastal Antarctic waters, seasonal CO_2 variability can be up to 450 µatm over a year (Gibson and Trull, 1999; Boyd et al., 2008; Moreau et al., 2012; Roden et al., 2013; Tortell et al., 2014). Sea ice forms a barrier to the outgassing of CO_2 in winter, causing supersaturation of the surface water to $\sim$ 500 µatm. Intense primary productivity in summer rapidly draws down CO_2 to $<$100 µatm, making this region a significant CO_2 sink during summer months (Hoppema et al., 1995; Ducklow et al., 2007; Arrigo et al., 2008b).

Ocean acidification studies on individual phytoplankton species have reported differing trends in primary productivity and growth rates. Increased CO_2 enhanced rates of primary productivity (Wu et al., 2010; Trimborn et al., 2013) and growth (Sobrino et al., 2008; Tew et al., 2014; Baragi et al., 2015; Chen et al., 2015; King et al., 2015) in some diatom species, while others were unaffected (Chen and Durbin, 1994; Sobrino et al., 2008; Berge et al., 2010; Trimborn et al., 2013; Chen et al., 2015; Hoppe et al., 2015; King et al., 2015; Bi et al., 2017). In contrast, CO_2-related declines in primary productivity and growth rate have also been observed (Barcelos e Ramos et al., 2014; Hoppe et al., 2015; King et al., 2015; Shi et al., 2017), suggesting that responses to ocean acidification are largely species specific. These differing responses among phytoplankton species may also cause changes in the composition of phytoplankton communities (Trimborn et al., 2013). It is difficult to extrapolate the response of individual species to natural communities, as monospecific studies exclude interactions among species and trophic levels. Estimates of CO_2 tolerance under laboratory conditions may also be influenced by experimental acclimation periods (Trimborn et al., 2014; Hennon et al., 2015; Torstensson et al., 2015; Li et al., 2017a), differences in experimental conditions (e.g. nutrients, light climate) (Hoppe et al., 2015; Hong et al., 2017; Li et al., 2017b), methods of CO_2 manipulation (Shi et al., 2009; Gattuso et al., 2010), and region-specific environmental adaptations (Schaum et al., 2012). Thus, investigations on natural communities are essential in order to better understand the outcome of these complex interactions.

The effects of ocean acidification on natural Antarctic phytoplankton communities is currently not well understood (Petrou et al., 2016; Deppeler and Davidson, 2017). Tolerance to CO_2 levels up to $\sim$ 800 µatm have been reported for natural coastal communities in the West Antarctic Peninsula and Prydz Bay, East Antarctica (Young et al., 2015; Davidson et al., 2016). Although in Prydz Bay, when CO_2 levels exceeded 780 µatm, primary productivity declined and community composition shifted toward smaller picoeukaryotes (Davidson et al., 2016; Thomson et al., 2016; Westwood et al., 2018). In contrast, Ross Sea phytoplankton communities responded to CO_2 levels $\geq$ 750 µatm with an increase in primary productivity and abundance of large chain-forming diatoms, suggesting that as CO_2 increases in this region, diatoms may increase in dominance over the prymnesiophyte *Phaeocystis antarctica* (Tortell et al., 2008b; Feng et al., 2010). The paucity of information regarding the ocean acidification response of these Antarctic coastal phytoplankton communities highlights the need for further research to determine region-specific tolerances and potential tipping points in community productivity and composition in Antarctica.

Bacteria play an essential role in the microbial food web through the remineralisation of nutrients from sinking particles (Azam et al., 1991) and as a food source for heterotrophic nanoflagellates (Pearce et al., 2010). Bacterial populations respond to increases in phytoplankton primary productivity by increasing their productivity and abundance, with maximum abundance often occurring after the peak of

the phytoplankton bloom (Pearce et al., 2007). High CO_2 levels have been observed to have either no effect on abundance and productivity (Grossart et al., 2006; Allgaier et al., 2008; Paulino et al., 2008; Baragi et al., 2015; Wang et al., 2016) or increase growth rate and production only during the post-bloom phase of an experiment (Grossart et al., 2006; Sperling et al., 2013; Westwood et al., 2018). Thus, bacterial communities appear to be relatively tolerant to ocean acidification, with bacterial growth indirectly affected by the ocean acidification responses of the phytoplankton community (Grossart et al., 2006; Allgaier et al., 2008; Engel et al., 2013; Piontek et al., 2013; Sperling et al., 2013; Bergen et al., 2016).

Mesocosm experiments are an effective way of monitoring the community response of microbial assemblages to environmental changes. Experiments examining multiple species and trophic levels can provide responses that differ significantly from monospecific studies. Numerous mesocosm studies have now been performed to assess the effect of ocean acidification on natural marine microbial communities around the world (e.g. Kim et al., 2006; Hopkinson et al., 2010; Riebesell et al., 2013; Paul et al., 2015; Bach et al., 2016; Bunse et al., 2016). Studies in the Arctic reported increases in phytoplankton primary productivity, growth, and organic matter concentration at CO_2 levels ≥ 800 µatm under nutrient-replete conditions (Bellerby et al., 2008; Egge et al., 2009; Engel et al., 2013; Schulz et al., 2013), whilst the bacterial community was unaffected (Grossart et al., 2006; Allgaier et al., 2008; Paulino et al., 2008; Baragi et al., 2015). These studies also highlight the importance of nutrient availability in the community response to elevated CO_2, with substantial differences in primary and bacterial productivity, chlorophyll *a* (Chl *a*), and elemental stoichiometry observed between nutrient-replete and nutrient-limited conditions (Riebesell et al., 2013; Schulz et al., 2013; Sperling et al., 2013; Bach et al., 2016).

Previous community-level studies investigating the effects of ocean acidification on natural coastal marine microbial communities in East Antarctica reported declines in primary and bacterial productivity when CO_2 levels exceeded 780 µatm (Westwood et al., 2018). To build upon the results of Westwood et al. (2018), a similar experimental design was utilised, with a natural marine microbial community from the same region exposed to CO_2 levels ranging from 343 to 1641 µatm in 650 L minicosms. The methods were refined in our study to include an acclimation period to the CO_2 treatment under low light. Rates of primary productivity, bacterial productivity, and the accumulation of particulate organic matter (POM) were examined to ascertain whether the threshold for tolerance to CO_2 was similar to that reported by Westwood et al. (2018) or if acclimation affected the community response to high CO_2. Photophysiological measurements were also undertaken to assess underlying mechanisms that caused shifts in phytoplankton community productivity.

Figure 1. Minicosm tanks filled with seawater in a temperature-controlled shipping container.

2 Methods

2.1 Minicosm set-up

Natural microbial assemblages were incubated in six 650 L polythene tanks (minicosms) housed in a temperature-controlled shipping container (Fig. 1). All minicosms were acid washed with 10 % vol : vol AR HCl, thoroughly rinsed with MilliQ water, and given a final rinse with seawater from the sampling site before use. The minicosms were filled with seawater taken amongst decomposing fast ice in Prydz Bay at Davis Station, Antarctica (68°35′ S, 77°58′ E) on 19 November 2014. Water was transferred by helicopter in multiple collections using a 720 L Bambi Bucket to fill a 7000 L polypropylene holding tank. Seawater was gravity fed into the minicosm tanks through Teflon-lined hosing fitted with an in-line 200 µm Arkal filter to exclude metazooplankton. All minicosms were filled simultaneously to ensure uniform distribution of microbes in all tanks.

The ambient water temperature at the time of sampling in Prydz Bay was −1.0 °C. Tanks were temperature controlled to an average temperature of 0.0 °C, with a maximum range of ±0.5 °C, through the cooling of the shipping container and warming with two 300 W aquarium heaters (Fluval) that were connected to a temperature control program via Carel temperature controllers. The contents of each tank were gently mixed by a shielded high-density polyethylene auger rotating at 15 rpm, and each tank was covered with a sealed acrylic lid.

Each tank was illuminated on a 19 : 5 h light : dark cycle by two 150 W HQI-TS/NDL (Osram) metal halide lamps (transmission spectra; Deppeler et al., 2017a). The light output was filtered by a light-scattering filter and a one-quarter colour temperature (CT) blue filter (Arri) to convert the tungsten lighting to a daylight spectral distribution; attenuating wavelengths were < 500 nm by ~ 20 % and > 550 nm by ~ 40 % (Davidson et al., 2016).

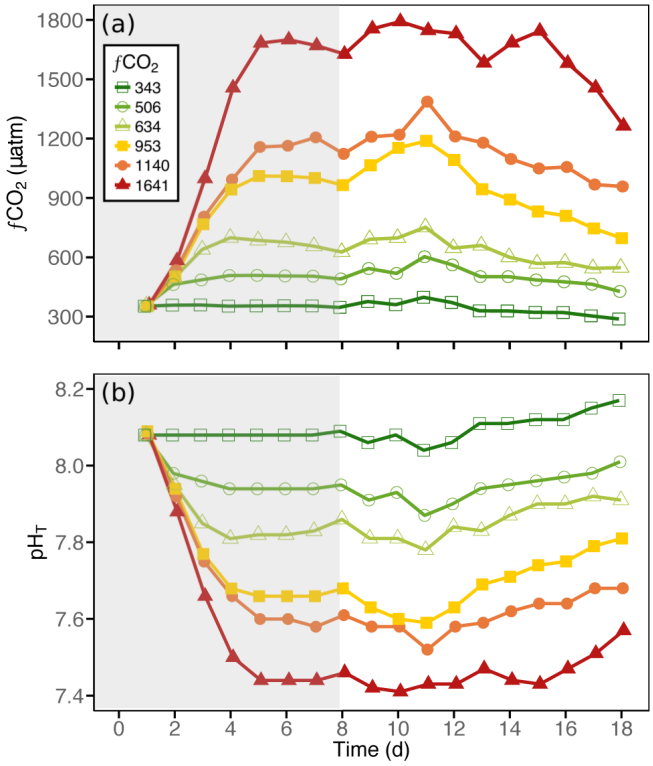

Figure 2. The **(a)** fCO_2 and **(b)** pH_T conditions within each of the minicosm treatments over time. Grey shading indicates CO_2 and light acclimation period.

Similar to Schulz et al. (2017), the fugacity of carbon dioxide (fCO_2) in each tank was raised to the target concentration in a stepwise manner over the first 5 days of the incubation (Fig. 2, see below). During this acclimation, phytoplankton growth in the tanks was slowed by attenuating the light intensity to 0.9 ± 0.2 µmol photons m^{-2} s^{-1} using two 90 % neutral density (ND) filters (Arri).

At the conclusion of this CO_2 acclimation period, the light intensity was increased for 24 h through the replacement of the two 90 % ND filters with one 60 % ND filter. The final light intensity was achieved on day 7 with a one-quarter CT blue and a light-scattering filter, which proved to be saturating for photosynthesis (see below).

Unless otherwise specified, samples were taken for analyses on days 1, 3, and 5 during the CO_2 acclimation period and every 2 days from day 8 to 18.

2.2 Carbonate chemistry measurements and calculations

Samples for carbonate chemistry measurements were collected daily from each minicosm in 500 mL glass-stoppered bottles (Schott Duran) following the guidelines of Dickson et al. (2007). Subsamples for dissolved inorganic carbon (DIC; 50 mL glass-stoppered bottles) and pH on the total scale (pH_T; 100 mL glass-stoppered bottles) measurements were gently pressure filtered (0.2 µm) with a peristaltic pump at a flow rate of ~30 mL min^{-1}, similar to Bockmon and Dickson (2014).

DIC was measured by infrared absorption on an Apollo SciTech AS-C3 analyser equipped with a Li-cor LI-7000 detector using triplicate 1.5 mL samples. The instrument was calibrated (and checked for linearity) within the expected DIC concentration range with five sodium carbonate standards (Merck Suprapur) that were dried for 2 h at 230 °C and prepared gravimetrically in MilliQ water (18.2 MΩ cm^{-1}) at 25 °C. Furthermore, daily measurements of certified reference material batch CRM127 (Dickson, 2010) were used for improved accuracy. Volumetrically measured DIC was converted to µmol kg^{-1} using calculated density derived from known temperature and salinity. The typical precision among triplicate measurements was < 2 µmol kg^{-1}.

The pH_T was measured spectrophotometrically (GBC UV–vis 916) in a 10 cm thermostated (25 °C) cuvette using the pH indicator dye m-cresol purple (Acros Organics; 62625-31-4, lot A0321770) following the approach described in Dickson et al. (2007), which included changes in sample pH due to dye addition. Contact with air was minimised by sample delivery, dye addition, and mixing via a syringe pump (Tecan; Cavro XLP 6000). Dye impurities and instrument performance were accounted for by applying a constant off-set (+0.003 pH units), determined by the comparison of the measured and calculated pH_T (from known DIC and total alkalinity (TA), including silicate and phosphate) of CRM127. Typical measurement precision for triplicates was 0.001 for higher and 0.003 for lower pH treatments. For further details see Schulz et al. (2017).

Carbonate chemistry speciation was calculated from measured DIC and pH_T. In a first step at salinities measured in situ (WTW197 conductivity meter), practical alkalinity (PA) was calculated at 25 °C using the dissociation constants for carbonic acid determined by Mehrbach et al. (1973) as refitted by Lueker et al. (2000). Then, total carbonate chemistry speciation was calculated from measured DIC and calculated PA for in situ temperature conditions.

2.3 Carbonate chemistry manipulation

The fCO_2 in the minicosms was adjusted by additions of 0.22 µm filtered natural seawater that was saturated by bubbling with AR-grade CO_2 for ≥ 30 min. In order to keep fCO_2 as constant as possible throughout the experiment, pH in each minicosm was measured with a portable NBS-calibrated probe (Mettler Toledo) in the morning before sampling and in the afternoon to estimate the necessary amount of DIC to be added. The required volume of CO_2-enriched seawater was then transferred into 1000 mL infusion bags and added to the individual minicosms at a rate of about 50 mL min^{-1}. After reaching target levels, the mean fCO_2 levels in the minicosms were 343, 506, 634, 953, 1140, and 1641 µatm (Table S1 in the Supplement).

2.4 Light irradiance

The average light intensity in each minicosm tank was calculated by measuring light intensity in the empty tanks at three depths (top, middle, and near-bottom) and across each tank (left, middle, and right) using a Biospherical Instruments Laboratory Quantum Scalar Irradiance Meter (QSL-101). The average light irradiance received by the phytoplankton within each tank was calculated following the equation of Riley (1957) (Table 1). Incoming irradiance ($\overline{I_o}$) was calculated as the average light intensity across the top of the tank. The average vertical light attenuation (K_d) was calculated as the slope from the regression of the natural log of light intensity at all three depths, and mixed depth (Z_m) was the depth of the minicosm tanks (1.14 m).

Changes in vertical light attenuation due to increases in Chl *a* concentration throughout the experimental period were calculated from the equation in Westwood et al. (2018); $K_{d(\text{biomass})} = 0.0451157 \times \text{Chl } a\ (\text{mg m}^{-3})$. Total light attenuation $K_{d(\text{total})}$ in each tank at each sampling day was calculated by addition of K_d and $K_{d(\text{biomass})}$.

2.5 Nutrient analysis

No nutrients were added to the minicosms during the experiment. Macronutrient samples were obtained from each minicosm following the protocol of Davidson et al. (2016). Seawater was filtered through 0.45 µm Sartorius filters into 50 mL Falcon tubes and frozen at −20 °C for analysis in Australia. Concentrations of ammonia, nitrate plus nitrite (NO_x), soluble reactive phosphorus (SRP), and molybdate reactive silica (Silica) were determined using flow injection analysis by Analytical Services Tasmania following Davidson et al. (2016).

2.6 Elemental analysis

Samples for POM analysis, particulate organic carbon (POC), and particulate organic nitrogen (PON) were collected following the method of Pearce et al. (2007). Equipment for sample preparation was soaked in Decon 90 (Decon Laboratories) for > 2 days and thoroughly rinsed in MilliQ water before use. Forceps and cutting blades were rinsed in 100 % acetone between samples. Seawater was filtered through muffled 25 mm Sartorius quartz microfibre filters until clogged. The filters were folded in half and frozen at −80 °C for analysis in Australia. Filters were thawed and opposite 1/8 subsamples were cut and transferred into a silver POC cup (Elemental Analysis Ltd). Inorganic carbon was removed from each sample through the addition of 20 µL of 2N HCl to each cup and drying at 60 °C for 36 h. When dry, each cup was folded shut, compressed into a pellet, and stored in desiccant until analysed at the Central Science Laboratory, University of Tasmania using a Thermo Finnigan EA 1112 Series Flash Elemental Analyzer.

2.7 Chlorophyll *a*

Seawater was collected from each minicosm and a measured volume was filtered through 13 mm Whatman GF/F filters (maximum filtration time of 20 min). Filters were folded in half, blotted dry, and immediately frozen in liquid nitrogen for analysis in Australia. Chlorophyll *a* (Chl *a*) pigments were extracted, analysed by HPLC, and quantified following the methods of Wright et al. (2010). Chl *a* was extracted from filters with 300 µL of dimethylformamide plus 50 µL of methanol, containing 140 ng apo-8′-carotenal (Fluka) internal standard, followed by bead beating and centrifugation to separate the extract from particulate matter. Extracts (125 µL) were diluted to 80 % with water and analysed on a Waters HPLC using a Waters Symmetry C8 column and a Waters 996 photodiode array detector. Chl *a* was identified by its retention time and absorption spectra compared to a mixed standard sample from known cultures (Jeffrey and Wright, 1997), which was run daily before samples. Peak integrations were performed using Waters Empower software, checked manually for corrections, and quantified using the internal standard method (Mantoura and Repeta, 1997).

2.8 ^{14}C primary productivity

Primary productivity incubations were performed following the method of Westwood et al. (2010) based on the technique of Lewis and Smith (1983). This method incubated phytoplankton for 1 h, minimising respiratory losses of photoassimilated ^{14}C so that the uptake nearly approximated gross primary productivity (e.g. Dring and Jewson, 1982; González et al., 2008; Regaudie-de Gioux et al., 2014). Samples were analysed for total organic carbon (TO^{14}C) content, thereby including any ^{14}C-labelled photosynthate leaked to the dissolved organic carbon (DO^{14}C) pool (Regaudie-de Gioux et al., 2014).

For all samples, 5.92 MBq (0.16 mCi) of ^{14}C-sodium bicarbonate ($NaH^{14}CO_3$; PerkinElmer) was added to 162 mL of seawater from each minicosm, creating a working solution of 37 kBq mL^{-1}. Aliquots of this working solution (7 mL) were then added to glass scintillation vials and incubated for 1 h at 21 light intensities ranging from 0–1412 µmol photons m^{-2} s^{-1}. The temperature within each of the vials was maintained at -1.0 ± 0.3 °C through water cooling of the incubation chamber. The reaction was terminated with the addition of 250 µL of 6N HCl and the vials were shaken for 3 h at 200 rpm to remove dissolved inorganic carbon. Duplicate time zero (T_0) samples were set up in a similar manner to determine background radiation, with 250 µL of 6N HCl added immediately to quench the reaction without exposure to light. Duplicate 100 % samples were also performed to determine the activity of the working solution for each minicosm. For each 100 % sample, 100 µL of working solution was added to 7 mL 0.1 M NaOH in filtered seawater to bind all ^{14}C. For radioactive

counts, 10 mL of Ultima Gold LLT scintillation cocktail (PerkinElmer) was added to each scintillation vial, shaken, and decays per minute (DPM) were counted in a PerkinElmer Tri-Carb 2910TR Low Activity Liquid Scintillation Analyzer with a maximum counting time set at 3 min.

DPM counts were converted into primary productivity following the equation of Steemann Nielsen (1952) (Table 1) using measured DIC concentrations (varying between $\sim$2075 and 2400 µmol kg^{-1}) and normalised to Chl *a* using minicosm Chl *a* concentration (see above). Photosynthesis versus irradiance (PE) curves were modelled for each treatment following the equation of Platt et al. (1980) using the phytotools package in R (Silsbe and Malkin, 2015; R Core Team, 2016). Photosynthetic parameter estimates included the light-saturated photosynthetic rate (P_{max}), maximum photosynthetic efficiency (α), photoinhibition rate (β), and saturating irradiance (E_k).

Chl *a*-specific primary productivity ($csGPP_{^{14}C}$) was calculated following the equation of Platt et al. (1980) using average minicosm light irradiance ($\overline{I}$). Gross primary production rates ($GPP_{^{14}C}$) in each tank were calculated from modelled $csGPP_{^{14}C}$ and Chl *a* concentration (see above). Calculations and units for each parameter are presented in Table 1.

2.9 Gross community productivity

Community photosynthesis and respiration rates were measured using custom-made mini-chambers. The system consisted of four 5.1 mL glass vials with oxygen sensor spots (Pyro Science) attached on the inside of the vials with non-toxic silicon glue. The vials were sealed, ensuring that any oxygen bubbles were omitted, and all vials were stirred continuously using small Teflon magnetic fleas to allow homogenous mixing of gases within the system during measurements. To improve the signal-to-noise ratio, seawater from each minicosm was concentrated above a 0.8 µm, 47 mm diameter polycarbonate membrane filter (Poretics) with gentle vacuum filtration and resuspended in seawater from each minicosm CO_2 treatment. Each chamber was filled with the cell suspension and placed in a temperature-controlled incubator (0.0 $\pm$ 0.5 °C). Light was supplied via fluorescent bulbs above each chamber and light intensity was calibrated using a 4π sensor. Oxygen optode spots were connected to a FireSting O_2 logger and data were acquired using FireSting software (Pyro Science). The optode was calibrated according to the manufacturer's protocol immediately prior to measurements using a freshly prepared sodium thiosulfate solution (10 % *w* / *w*) and agitated filtered seawater (0.2 µm) at experimental temperature for 0 and 100 % air saturation values, respectively. Oxygen concentration was recorded until a linear change in rate was established for each pseudoreplicate ($n = 4$).

Measurements were first recorded in the light (188 µmol photons m^{-2} s^{-1}) and subsequently in the dark, with the initial steeper portion of the slope used for a linear regression analysis to determine the post-illumination (PI) respiration rate. Gross community production (GCP_{O_2}) was then calculated from dark PI respiration ($Resp_{O_2}$) and net community production (NCP_{O_2}) rates and normalised to Chl *a* concentration ($csGCP_{O_2}$, Table 1). Chl *a* content for each concentrated sample was determined by extracting pigments in 90 % chilled acetone and incubating in the dark at 4 °C for 24 h. Chl *a* concentrations were determined using a spectrophotometer (Cary 50; Varian) and calculated according to the equations of Jeffrey and Humphrey (1975), modified by Ritchie (2006).

2.10 Chlorophyll *a* fluorescence

The photosynthetic efficiency of the microalgal community was measured via Chl *a* fluorescence using a pulse-amplitude-modulated fluorometer (WATER-PAM; Walz). A 3 mL aliquot from each minicosm was transferred into a quartz cuvette with continuous stirring to prevent cells from settling. To establish an appropriate dark adaptation period, several replicates were measured after 5, 10, 15, 20, and 30 min of dark adaptation, with the latter having the highest maximum quantum yield of PSII (F_v / F_m). Following dark adaptation, minimum fluorescence (F_0) was recorded before the application of a high-intensity saturating pulse of light (saturating pulse width = 0.8 s; saturating pulse intensity >3000 µmol photons m^{-2} s^{-1}), and maximum fluorescence (F_m) was determined. The maximum quantum yield of PSII was calculated from these two parameters (Schreiber, 2004). Following F_v / F_m, a five-step steady-state light curve (SSLC) was conducted with each light level (130, 307, 600, 973, 1450 µmol photons m^{-2} s^{-1}) applied for 5 min before recording the light-adapted minimum (F_t) and maximum fluorescence ($F_{m'}$) values. Each light step was spaced by a 30 s dark "recovery" period before the next light level was applied. Three pseudoreplicate measurements were conducted on each minicosm sample at 0.1 °C. Non-photochemical quenching (NPQ) of Chl *a* fluorescence was calculated from F_m and $F_{m'}$ measurements. Relative electron transport rates (rETRs) were calculated as the product of effective quantum yield (ΔF / $F_{m'}$) and actinic irradiance (I_a). Calculations and units for each parameter are presented in Table 1.

2.11 Community carbon concentrating mechanism activity

To investigate the effects of CO_2 on carbon uptake, two inhibitors for carbonic anhydrase (CA) were applied to the 343 and 1641 µatm treatments on day 15: ethoxzolamide (EZA; Sigma), which inhibits both intracellular carbonic anhydrase (iCA) and extracellular carbonic anhydrase (eCA), and acetazolamide (AZA; Sigma), which blocks eCA only. Stock solutions of EZA (20 mM) and AZA (5 mM) were prepared in MilliQ water, and the pH was adjusted using NaOH to

Table 1. Definitions, measurements, and calculations for productivity data.

Name	Definition	Units	Measurements and calculations
Primary productivity			
Carbon incorporation	Total ^{14}C-sodium bicarbonate incorporation	mg C (mg Chl a)$^{-1}$ L^{-1} h^{-1}	Equation from Steemann Nielsen (1952)= $\frac{(\mathrm{DPM}_s - \mathrm{DPM}_{T_0})}{\mathrm{DPM}_{100\,\%}} \times \mathrm{DIC} \times 1.05$ / time / Chl a
α	Maximum photosynthetic efficiency	mg C (mg Chl a)$^{-1}$ (µmol photons m^{-2} s^{-1})$^{-1}$ h^{-1}	Modelled from PE curve of 21 light intensities 0–1411 µmol photons m^{-2} s^{-1}
β	Photoinhibition rate	mg C (mg Chl a)$^{-1}$ (µmol photons m^{-2} s^{-1})$^{-1}$ h^{-1}	Modelled from PE curve of 21 light intensities 0–1411 µmol photons m^{-2} s^{-1}
$P_{\max}$	Maximum photosynthetic rate	mg C (mg Chl a)$^{-1}$ h^{-1}	Equation from Platt et al. (1980) = $P_s \times \frac{\alpha}{(\alpha+\beta)} \times \frac{\beta}{(\alpha+\beta)}^{\frac{\beta}{\alpha}}$
E_k	Saturating irradiance	µmol photons m^{-2} s^{-1}	Equation from Platt et al. (1980) = $P_{\max}/\alpha$
$\overline{I}$	Average irradiance received by phytoplankton cells	µmol photons m^{-2} s^{-1}	Equation from Riley (1957)= $\overline{I}_o(1 - e^{(-K_d \times Z_m)})/(K_d \times Z_m)$
csGPP$_{^{14}C}$	^{14}C Chl a-specific primary productivity	mg C (mg Chl a)$^{-1}$ h^{-1}	Equation from Platt et al. (1980)= $P_s \times e^{\frac{-\alpha\overline{I}}{P_s}} \times e^{\frac{-\beta\overline{I}}{P_s}}$
GPP$_{^{14}C}$	^{14}C gross primary production	µg C L^{-1} h^{-1}	= csGPP$_{^{14}C}$ × Chl a
csGCP$_{O_2}$	O_2 Chl a-specific gross community productivity	mg O_2 (mg Chl a)$^{-1}$ h^{-1}	= (NCP$_{O_2}$ + Resp$_{O_2}$) / Chl a
GCP$_{O_2}$	O_2 gross community production	mg O_2 L^{-1} h^{-1}	= csGCP$_{O_2}$ × Chl a
Photophysiology			
F_v / F_m	Maximum quantum yield of PSII	(arbitrary units)	= $(F_m - F_O)/F_m$
ΔF / $F_{m'}$	Effective quantum yield of PSII	(arbitrary units)	= $(F_{m'} - F)/F_{m'}$
rETR	Relative electron transport rate	(arbitrary units)	= $\Delta F_v/F_{m'} \times I_a$
NPQ	Non-photochemical quenching	(arbitrary units)	= $(F_m - F_{m'})/F_{m'}$
Bacterial productivity			
nmol leucine$_{inc}$	Moles of exogenous ^{14}C-leucine incorporated	nmol L^{-1} h^{-1}	Equation from Kirchman (2001) = (DPM$_s$ − DPM$_{t_0}$) / time / 2.22×10^6 × SA (nmol µCi^{-1}) / sample vol (L)
GBP$_{^{14}C}$	^{14}C gross bacterial production	µg C L^{-1} h^{-1}	Equation from Simon and Azam (1989) = (nmol leucine$_{inc}$ / 10^3) ×131.2 / 0.073 × 0.86 × 2
csBP$_{^{14}C}$	^{14}C cell-specific bacterial productivity	fg C cell^{-1} L^{-1} h^{-1}	= GBP$_{^{14}C}$ / cells L^{-1}

P_s : maximum photosynthetic output with no photoinhibition, from Platt et al. (1980); DPM$_S$: sample DPM; SA: specific activity of ^{14}C-leucine isotope. All other abbreviations are defined in the "Methods" section.

minimise pH changes when added to the samples. Before fluorometric measurements were made, water samples from the 343 and 1641 µatm CO_2 treatments were filtered into ≥ 10 and <10 µm fractions and aliquots were inoculated either with 50 µL of MilliQ water adjusted with NaOH (control) or a 50 µM final concentration of chemical inhibitor (EZA and AZA). Fluorescence measurements of size-fractionated control- and inhibitor-exposed cells were performed using the WATER-PAM. A 3 mL aliquot of sample was transferred into a quartz cuvette with stirring and left in the dark for 30 min before the maximum quantum yield of PSII (F_v / F_m) was determined (as described above). Actinic light was then applied at 1450 µmol photons m^{-2} s^{-1} for 5 min before the effective quantum yield of PSII (ΔF / $F_{m'}$) was recorded. Three pseudoreplicate measurements were conducted on each minicosm sample at 0.1 °C.

2.12 Bacterial abundance

Bacterial abundance was determined daily using a Becton Dickinson FACScan or FACSCalibur flow cytometer fitted with a 488 nm laser following the protocol of Thomson et al. (2016). Samples were pre-filtered through a 50 µm mesh (Nitex), stored at 4 °C in the dark, and analysed within 6 h of collection. Samples were stained for 20 min with 1 : 10 000 dilution SYBR Green I (Invitrogen) (Marie et al., 2005), and PeakFlow Green 2.5 µm beads (Invitrogen) were added to the sample as an internal fluorescence standard. Three pseudoreplicate samples were prepared from each minicosm seawater sample. Samples were run for 3 min at a low flow rate (~ 12 µL min^{-1}) and bacterial abundance was determined from side scatter (SSC) versus green (FL1) fluorescence bivariate scatter plots. The analysed volume was calibrated to the sample run time and each sample was run for precisely 3 min, resulting in an analysed volume of 0.0491 and 0.02604 mL on the FACSCalibur and FACScan, respectively. The volume analysed was then used to calculate final cell concentrations.

2.13 Bacterial productivity

Bacterial productivity measurements were performed following the leucine incorporation by microcentrifuge method of Kirchman (2001). Briefly, 70 nM ^{14}C-leucine (PerkinElmer) was added to 1.7 mL of seawater from each minicosm in 2 mL polyethylene Eppendorf tubes and incubated for 2 h in the dark at 4 °C. Three pseudoreplicate samples were prepared from each minicosm seawater sample. The reaction was terminated by the addition of 90 µL of 100 % trichloroacetic acid (TCA; Sigma) to each tube. Duplicate background controls were also performed following the same method, with 100 % TCA added immediately before incubation. After incubation, samples were spun for 15 min at 12 500 rpm and the supernatant was removed. The cell pellet was resuspended into 1.7 mL of ice-cold 5 % TCA and spun again for 15 min at 12 500 rpm and the supernatant was removed. The cell pellet was then resuspended into 1.7 mL of ice-cold 80 % ethanol, spun for a further 15 min at 12 500 rpm, and the supernatant was removed. The cell pellet was allowed to dry completely before addition of 1 mL of Ultima Gold scintillation cocktail (PerkinElmer). The Eppendorf tubes were placed into glass scintillation vials and DPMs were counted in a PerkinElmer Tri-Carb 2910TR Low Activity Liquid Scintillation Analyzer with a maximum counting time of 3 min.

DPM counts were converted to ^{14}C-leucine incorporation rates following the equation in Kirchman (2001) and used to calculate gross bacterial production ($GBP_{^{14}C}$) following Simon and Azam (1989). Bacterial production was divided by total bacterial abundance to determine the cell-specific bacterial productivity within each treatment ($csBP_{^{14}C}$). Calculations and units for each parameter are presented in Table 1.

2.14 Statistical analysis

The minicosm experimental design measured the microbial community growth in six unreplicated fCO_2 treatments. Therefore, subsamples from each minicosm were within-treatment pseudoreplicates and thus only provide a measure of the variability of the within-treatment sampling and measurement procedures. We use pseudoreplicates as true replicates in order to provide an informal assessment of differences among treatments, noting that results must be treated as indicative and interpreted conservatively.

For all analyses, a linear or curved (quadratic) regression model was fitted to each CO_2 treatment over time using the stats package in R (R Core Team, 2016), and an omnibus test of differences between the trends among CO_2 treatments over time was assessed by ANOVA. This analysis ignored the repeated measures nature of the data set, which could not be modelled due to the low number of time points and an absence of replication at each time. For the CCM activity measurements, differences between treatments were tested by one-way ANOVA followed by a post-hoc Tukey's test to determine which treatments differed. The significance level for all tests was set at < 0.05.

3 Results

3.1 Carbonate chemistry

The fCO_2 of each treatment was modified in a stepwise fashion over 5 days to allow for acclimation of the microbial community to the changed conditions. Target treatment conditions were reached in all tanks by day 5 and ranged from 343 to 1641 µatm, equating to an average pH_T of 8.10 to 7.45 (Fig. 2, Table S1), respectively. The initial seawater was calculated to have an fCO_2 of 356 µatm and a PA of 2317 µmol kg^{-1}, from a measured pH_T of 8.08 and DIC of 2187 µmol kg^{-1} (Fig. S1 and Table S2 in the Supple-

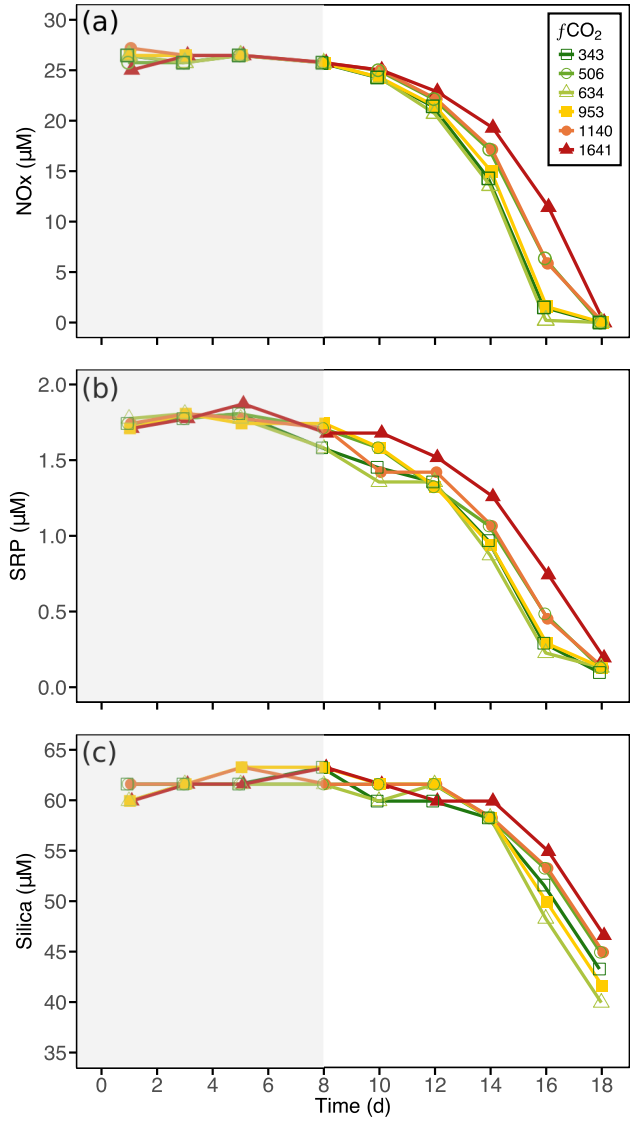

Figure 3. Nutrient concentration in each of the minicosm treatments over time. **(a)** Nitrate + nitrite (NO_x), **(b)** soluble reactive phosphorus (SRP), and **(c)** molybdate reactive silica (silica). Grey shading indicates CO_2 and light acclimation period.

ment). One minicosm was maintained close to these conditions (343 µatm) throughout the experiment as a control treatment.

3.2 Light climate

The average light irradiance for all CO_2 treatments is presented in Table S3. During the CO_2 acclimation period (days 1–5) the average light irradiance was 0.9 ± 0.2 µmol photons m^{-2} s^{-1} and was increased to 90.5 ± 21.5 µmol photons m^{-2} s^{-1} by day 8. The average vertical light attenuation (K_d) across all minicosm tanks was 0.92 ± 0.2. Increasing Chl *a* concentration over time in all CO_2 treatments increased $K_{d(total)}$ from 0.96 ± 0.01 on day 1 to 3.53 ± 0.28 on day 18, resulting in a decline in average light irradiance within the minicosms from 86.61 ± 20.5 to 35.97 ± 9.3 µmol photons m^{-2} s^{-1} between days 8 and 18.

3.3 Nutrients

Nutrient concentrations were similar across all treatments at the beginning of the experiment (Table S2 in the Supplement) and did not change during the acclimation period (days 1–5). Ammonia concentrations were initially low (0.95 ± 0.18 µM) and fell rapidly to concentrations below the limits of detection beyond day 12 in all treatments (Fig. S2 in the Supplement). No differences in drawdown between CO_2 treatments were observed, and thus it was excluded from further analysis. NO_x fell from 26.2 ± 0.74 µM on day 8 to concentrations below detection limits on day 18 (Fig. 3a), with the slowest drawdown in the 1641 µatm treatment. SRP concentrations were initially 1.74 ± 0.02 µM and all CO_2 treatments followed a similar drawdown sequence to NO_x, reaching very low concentrations (0.13 ± 0.03 µM) on day 18 in all treatments (Fig. 3b). In contrast, silica was replete in all treatments throughout the experiment falling from 60.0 ± 0.91 µM to 43.6 ± 2.45 µM (Fig. 3c). The drawdown of silica was exponential from day 8 onwards and followed a similar pattern to NO_x and SRP, with the highest silica drawdown in the 634 µatm and the least in the 1641 µatm treatment.

3.4 Particulate organic matter

Particulate organic carbon (POC) and nitrogen (PON) concentrations were initially low at 4.7 ± 0.15 and 0.5 ± 0.98 µM, respectively, and increased after day 8 in all treatments (Fig. 4a, b). The accumulation of POC and PON was effectively the reciprocal of the drawdown of nutrients (see above), being lowest in the high CO_2 treatments (≥ 1140 µatm) and highest in the 343 and 643 µatm treatments. Rates of POC and PON accumulation were both affected by nutrient exhaustion, with declines in the 343 and 634 µatm treatments between days 16 and 18. POC and PON concentrations on day 18 were highest in the 953 µatm treatment. The ratio of POC to PON (C : N) was similar for all treatments, declining from 8.0 ± 0.38 on day 8 to 5.7 ± 0.28 on day 16 (Fig. 4c). The slowest initial decline in the C : N ratio occurred in the 1641 µatm treatment, displaying a prolonged lag until day 10, after which it decreased to values similar to all other treatments. Nutrient exhaustion on day 18 coincided with an increase in the C : N ratio in all treatments, with C : N ratios >10 in the 343, 634, and 953 µatm treatments and lower C : N ratios (8.6–6.7) in the 506, 1140, and 1641 µatm treatments.

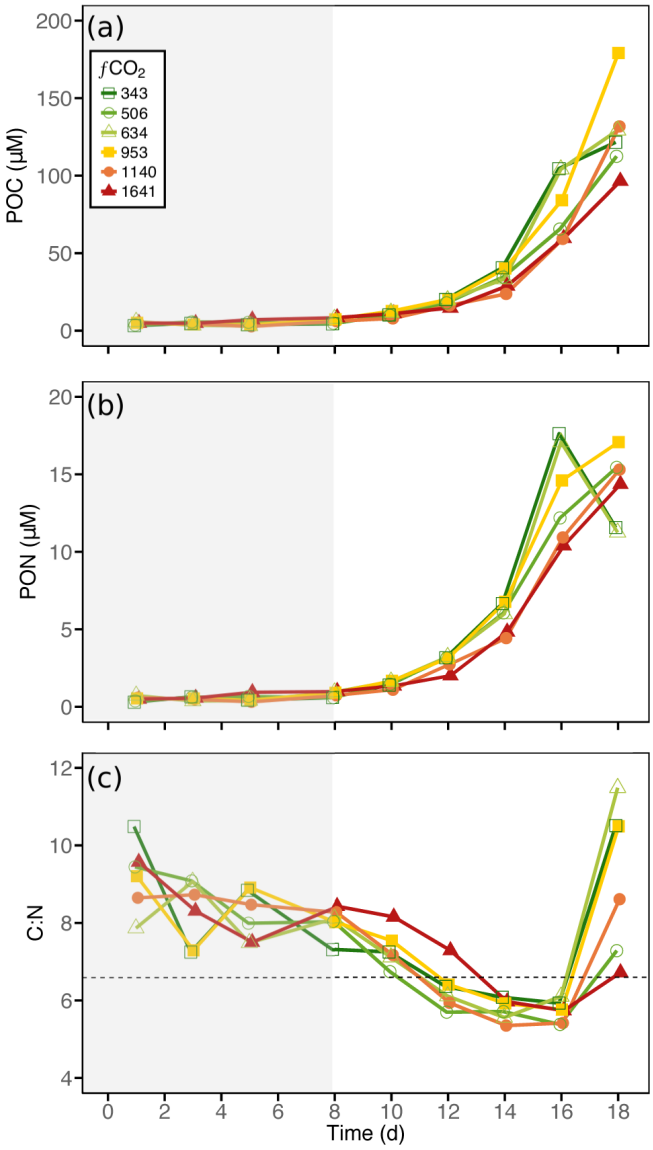

Figure 4. Particulate organic matter concentration and C : N ratio of each of the minicosm treatments over time. **(a)** Particulate organic carbon (POC), **(b)** particulate organic nitrogen (PON), and **(c)** carbon : nitrogen (C : N) ratio. The dashed line indicates C : N Redfield ratio of 6.6. Grey shading indicates CO_2 and light acclimation period.

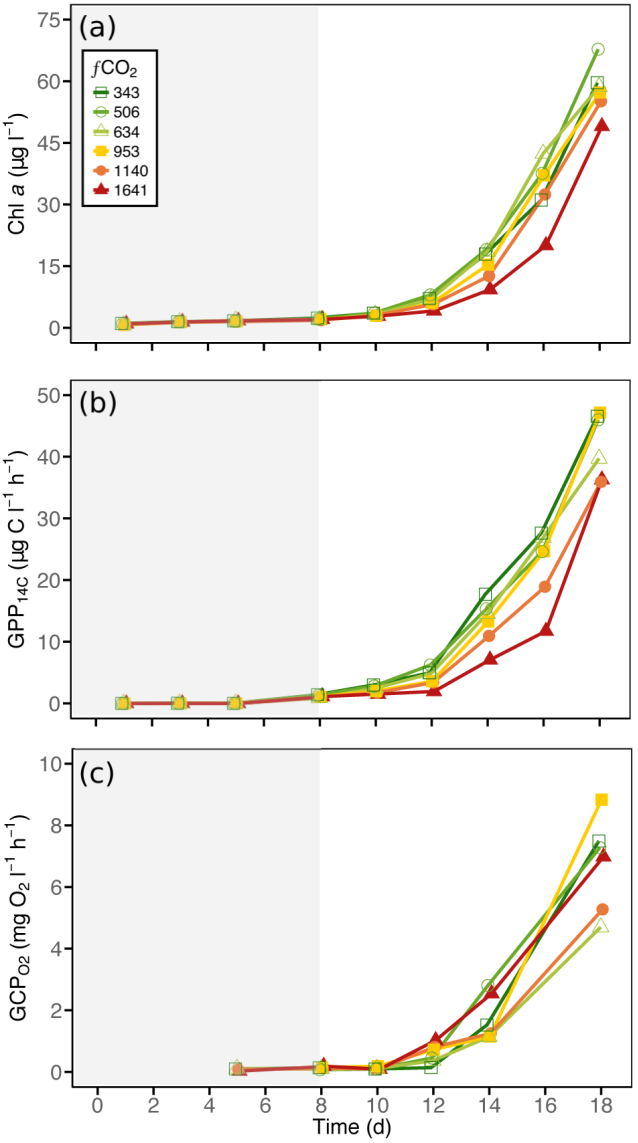

Figure 5. Phytoplankton biomass accumulation and community primary production in each of the minicosm treatments over time. **(a)** Chlorophyll *a* (Chl *a*) concentration, **(b)** ^{14}C-derived gross primary production ($GPP_{^{14}C}$), and **(c)** O_2-derived gross community production (GCP_{O_2}). Grey shading indicates CO_2 and light acclimation period.

3.5 Chlorophyll *a*

Chl *a* concentrations were low at the beginning of the experiment at $0.91 \pm 0.16\,\mu g\,L^{-1}$ and increased in all treatments after day 8 (Fig. 5a). Chl *a* accumulation rates were similar amongst treatments $\leq 634\,\mu atm$ until day 14, with a slightly higher Chl *a* concentration in the 506 and 634 µatm treatments on day 16 compared to the control treatment. By day 18, only the 506 µatm treatment remained higher than the control. Chl *a* accumulation rates in the 953 and 1140 µatm treatments were initially slow but increased after day 14, with Chl *a* concentrations similar to the control on days 16–18. The highest CO_2 treatment (1641 µatm) had the slowest rates of Chl *a* accumulation, displaying a lag in growth between days 8 and 12, after which the Chl *a* concentration increased but remained lower than the control. Rates of Chl *a* accumulation slowed between days 16 and 18 in all treatments except 1641 µatm, coinciding with nutrient limitation. At day 18, the highest Chl *a* concentration was in the 506 µatm exposed treatment and lowest at 1641 µatm.

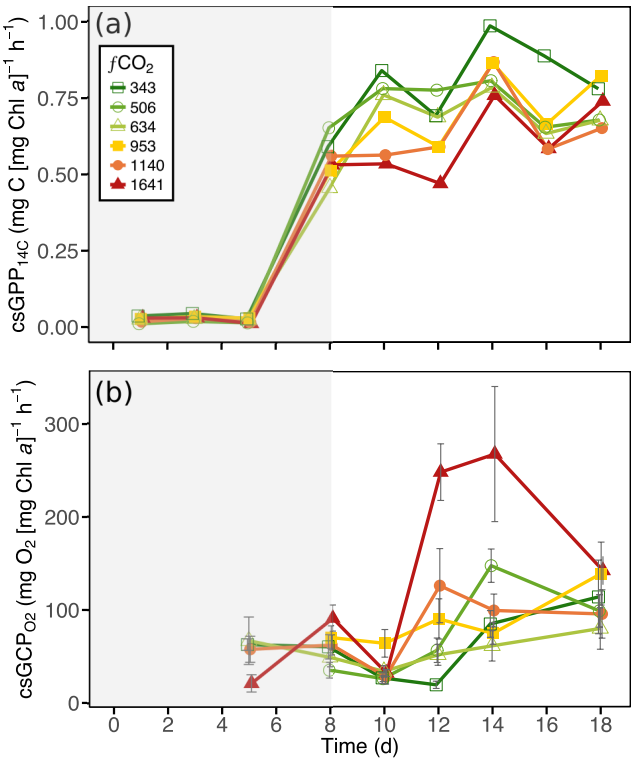

Figure 6. **(a)** ^{14}C-derived Chl *a*-specific primary productivity ($csGPP_{^{14}C}$) and **(b)** O_2-derived Chl *a*-specific community productivity ($csGCP_{O_2}$) in each of the minicosm treatments over time. Error bars display 1 standard deviation of pseudoreplicate samples. Grey shading indicates CO_2 and light acclimation period.

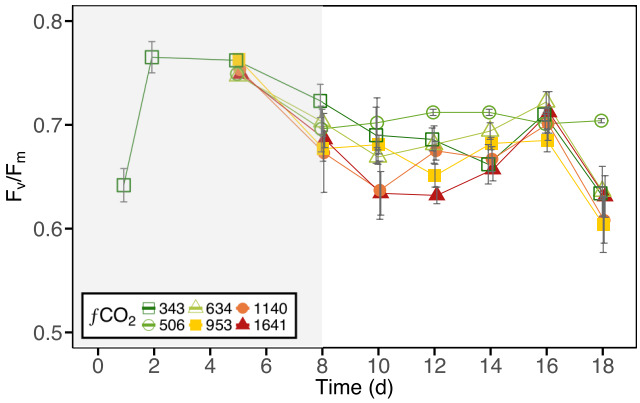

Figure 7. Maximum quantum yield of PSII (F_v / F_m) in each of the minicosm treatments over time. Error bars display 1 standard deviation of pseudoreplicate samples. Grey shading indicates CO_2 and light acclimation period.

The omnibus test among CO_2 treatments of trends in Chl *a* over time indicated that the accumulation of Chl *a* in at least one treatment differed significantly from that of the control ($F_{5,23} = 5.5$, $p = 0.002$; Table S4). Examination of individual coefficients from the model revealed that only the highest CO_2 treatment, 1641 µatm, was significantly different from the control at the 5 % level.

3.6 ^{14}C primary productivity

During the CO_2 and light acclimation phase of the experiment (days 1–8), all treatments displayed a steady decline in the maximum photosynthetic rate (P_{max}) and the maximum photosynthetic efficiency (α) until the levels on day 8 were approximately half of those at the beginning of the experiment, suggesting cellular acclimation to the light conditions (Fig. S3a, b in the Supplement). Thereafter, relative to the control, P_{max} and α were lowest in CO_2 levels ≥ 953 µatm and ≥ 634 µatm, respectively. Rates of photoinhibition (β) and saturating irradiance (E_k) were variable and did not differ among treatments (Fig. S3c, d). The average E_k across all treatments was 28.7 ± 8.6 µmol photons $m^{-2}\,s^{-1}$, indicating that the light intensity in the minicosms was saturating for photosynthesis (see above) and not inhibiting ($\beta < 0.002$ mg C (mg Chl *a*)$^{-1}$ (µmol photons $m^{-2}\,s^{-1}$)$^{-1}$ h^{-1}).

Chl *a*-specific primary productivity ($csGPP_{^{14}C}$) and gross primary production ($GPP_{^{14}C}$) were low during the CO_2 acclimation (days 1–5) and increased with increasing light climate after day 5. Rates of $csGPP_{^{14}C}$ in treatments ≥ 634 µatm CO_2 were consistently lower than the control between days 8 and 16, with the lowest rates in the highest CO_2 treatment (1641 µatm; Fig. 6a). Rates of $GPP_{^{14}C}$ in treatments ≤ 953 were similar between days 8 and 16, with the 343 (control), 506, and 953 µatm treatments increasing to 46.7 ± 0.34 µg C L^{-1} h^{-1} by day 18 (Fig. 5b). Compared to these treatments, $GPP_{^{14}C}$ in the 634 µatm treatment was lower on day 18, only reaching 39.7 µg C L^{-1} h^{-1}, possibly due to the concurrent limitation of NO_x in this treatment on day 16 (see above).

The omnibus test among tanks of the trends in CO_2 treatments over time indicated that $GPP_{^{14}C}$ in at least one treatment differed significantly from the control ($F_{5,23} = 4.9$, $p = 0.003$; Table S5 in the Supplement). Examination of the significance of individual curve terms revealed that this manifested as differences between the 1140 and 1641 µatm treatments and the control group at the 5 % level. No other curves were different from the control. In particular, $GPP_{^{14}C}$ in the 1641 µatm treatment was much lower until day 12, after which it increased steadily until day 16. Between days 16 and 18, a substantial increase in $GPP_{^{14}C}$ was observed in this treatment, subsequently resulting in a rate on day 18 that was similar to the 1140 µatm treatment (36.3 ± 0.08 µg C L^{-1} h^{-1}) although these treatments never reached rates of $GPP_{^{14}C}$ as high as the control.

3.7 Gross community productivity

The productivity of the phytoplankton community increased over time in all CO_2 treatments; however, there were

clear differences in the timing and magnitude of this increase between treatments (Fig. 6b). A CO_2 effect was evident on day 12 when Chl *a*-normalised gross O_2 productivity rates ($csGCP_{O_2}$) increased with increasing CO_2 level, ranging from 19.5–248 mg O_2 (mg Chl *a*)$^{-1}$ h^{-1}. After day 12, the communities in CO_2 treatments $\leq$ 634 µatm continued to increase their rates of $csGCP_{O_2}$ until day 18 (97.7 ± 17.0 mg O_2 (mg Chl *a*)$^{-1}$ h^{-1}). The 953 and 1140 µatm CO_2 treatments peaked on day 12 (90.4 and 126 mg O_2 (mg Chl *a*)$^{-1}$ h^{-1}, respectively) and then declined on day 14 to rates similar to the control treatment. In contrast, the 1641 µatm treatment maintained high rates of $csGCP_{O_2}$ from days 12–14 (258 ± 13.8 mg O_2 (mg Chl *a*)$^{-1}$ h^{-1}), coinciding with the recovery of photosynthetic health (F_v / F_m; see below) and the initiation of growth in this treatment (see above). After this time, rates of $csGCP_{O_2}$ declined in this treatment to rates similar to the control. Despite these differences in $csGCP_{O_2}$, there was no significant difference in the gross community production (GCP_{O_2}) among CO_2 treatments (Fig. 5c).

3.8 Community photosynthetic efficiency

The community maximum quantum yield of PSII (F_v / F_m) showed a dynamic response over the duration of the experiment (Fig. 7). Values initially increased during the low-light CO_2 adjustment period but declined by day 8 when irradiance levels had increased. Between days 8 and 14, differences were evident in the photosynthetic health of the phytoplankton community across the CO_2 treatments, although by day 16 these differences had disappeared. Steady-state light curves revealed that the community photosynthetic response did not change with increasing CO_2. The effective quantum yield of PSII (ΔF / $F_{m'}$) and NPQ showed no variability with CO_2 treatment (Figs. S5 and S6 in the Supplement). There was, however, a notable decline in overall NPQ in all tanks with time, indicating an adjustment to the higher light conditions. Relative electron transport rates (rETR) showed differentiation with respect to CO_2 at high light (1450 µmol photons m^{-2} s^{-1}) on days 10–12. However, as seen with the F_v / F_m response, this difference was diminished by day 18 (Fig. S7 in the Supplement).

3.9 Community CCM activity

There was a significant decline in the effective quantum yield of PSII (ΔF / $F_{m'}$) with the addition of the iCA and eCA inhibitor EZA to both the large ($\geq$ 10 µm, $p = 0.02$) and small (<10 µm, $p < 0.001$) size fractions of the phytoplankton community exposed to the control (343 µatm) CO_2 treatment (Fig. 8). The addition of EZA to cells under high CO_2 (1641 µatm) had no effect on ΔF / $F_{m'}$ for either size fraction. However, in the case of the small cells under high CO_2 (Fig. 8b), ΔF / $F_{m'}$ was the same as that measured in the control CO_2 in the presence of EZA. The addition of AZA, which inhibits eCA only, had no effect for either CO_2 treatment in the large-celled community. In contrast, there was a significant decline in ΔF / $F_{m'}$ in the smaller fraction in the control CO_2 treatment ($p < 0.001$), but no effect of AZA addition under high CO_2. Again, the high CO_2 cells exhibited the same ΔF / $F_{m'}$ as those measured under the control CO_2 in the presence of AZA.

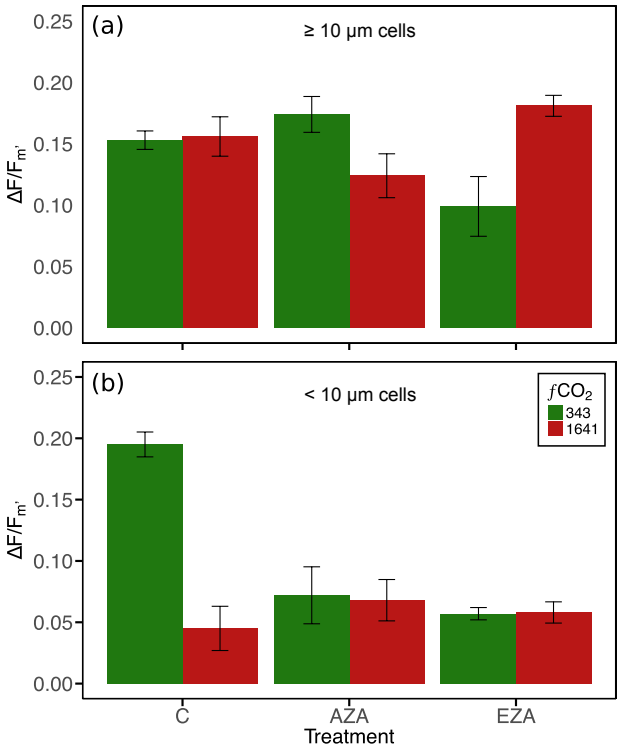

Figure 8. Effective quantum yield of PSII (ΔF / $F_{m'}$) of **(a)** large ($\geq$ 10 µm) and **(b)** small (<10 µm) phytoplankton in the control (343 µatm) and high (1641 µatm) CO_2 treatments treated with carbonic anhydrase (CA) inhibitors. A decline in ΔF / $F_{m'}$ with the application of inhibitor indicates CCM activity. C denotes the control treatment, which received no CA inhibitor; AZA is the acetazolamide treatment, which blocks extracellular carbonic anhydrase; EZA is the ethoxzolamide treatment, which blocks intracellular and extracellular carbonic anhydrase. Error bars display 1 standard deviation of pseudoreplicate samples.

3.10 Bacterial abundance

During the 8-day acclimation period, bacterial abundance in treatments $\geq$ 634 µatm increased with increasing CO_2, reaching 26.0–32.4 $\times$ 10^7 cells L^{-1} and remaining high until day 13 (Fig. 9a). Between days 7 and 13, bacterial abundances in CO_2 treatments $\geq$ 953 were higher than the control. In contrast, abundance remained constant in treatments $\leq$ 506 µatm ($20.6 \pm 1.4 \times 10^7$ cells L^{-1}) until day 11. Cell numbers rapidly declined in all treatments after day 12, finally stabilising at $0.5 \pm 0.2 \times 10^7$ cells L^{-1}. An omnibus test

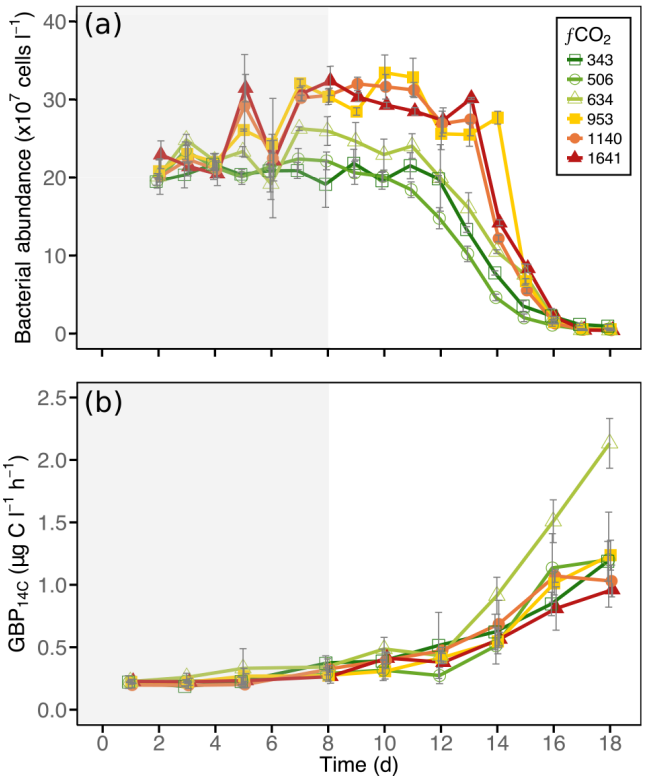

Figure 9. Bacterial abundance and community production in each of the minicosm treatments over time. **(a)** Bacterial cell abundance and **(b)** ^{14}C-derived gross bacterial production (GBP$_{14C}$). Error bars display 1 standard deviation of pseudoreplicate samples. Grey shading indicates CO_2 and light acclimation period.

among CO_2 treatments of the trends in bacterial abundance over time showed that changes in abundance in at least one treatment differed significantly from the control ($F_{5,185} = 9.8$, $p < 0.001$; Table S6 in the Supplement). Examination of individual coefficients from the model revealed that CO_2 treatments ≥ 953 µatm were significantly different from the control at the 5 % level.

3.11 Bacterial productivity

Gross bacterial production (GBP$_{14C}$) was low in all CO_2 treatments (0.2 ± 0.03 µg C L^{-1} h^{-1}) and changed little during the first 5 days of incubation (Fig. 9b). Thereafter it increased, coinciding with exponential growth in the phytoplankton community. The most rapid increase in GBP$_{14C}$ was observed in the 634 µatm treatment, resulting in a rate twice that of all other treatments by day 18 (2.1 µg C L^{-1} h^{-1}). No difference was observed among other treatments, all of which increased to an average rate of 1.1 ± 0.1 µg C L^{-1} h^{-1} by day 18. Cell-specific bacterial productivity (csBP$_{14C}$) was low in all treatments (1.2 ± 0.5 fg C L^{-1} h^{-1}) until day 14, with slower rates in treatments ≥ 953 µatm, likely due to high cell abundances observed in these treatments (Fig. S8 in the Supplement). It then increased from day 14, coinciding with a decline in bacterial abundance. Rates of csBP$_{14C}$ did not differ among treatments until day 18, when the rate in the 634 µatm treatment was higher than all other treatments (0.5 pg C cell^{-1} L^{-1} h^{-1}).

4 Discussion

Our study of a natural Antarctic phytoplankton community identified a critical threshold for tolerance of CO_2 between 953 and 1140 µatm, above which photosynthetic health was negatively affected and rates of carbon fixation and Chl *a* accumulation declined. Low rates of primary productivity also led to declines in nutrient uptake rates and POM production, although there was no effect of CO_2 on C : N ratios, indicating that ocean acidification effects on the phytoplankton community did not modify POM stoichiometry. Assessing the temporal trends of Chl *a*, GPP$_{14C}$, and PON against CO_2 treatment revealed that the downturn in these parameters occurred between 634 and 953 µatm fCO_2 and could be discerned following ≥ 12 days incubation (Fig. 10). On the final day of the experiment (day 18), this CO_2 threshold was less clear and likely confounded by the effects of nutrient limitation (Westwood et al., 2018). In contrast, bacterial productivity was unaffected by increased CO_2. Instead, production coincided with increased organic matter supply from phytoplankton primary productivity. In the following sections these effects will be investigated further, with suggestions for possible mechanisms that may be driving the responses observed.

4.1 Ocean acidification effects on phytoplankton productivity

The results of this study suggest that exposing phytoplankton to high CO_2 levels can decouple the two stages of photosynthesis (see also the discussion below). At CO_2 levels ≥ 1140 µatm, Chl *a*-specific oxygen production (csGCP$_{O_2}$) increased strongly yet displayed the lowest rates of Chl *a*-specific carbon fixation (csGPP$_{14C}$; Fig. 6). This mismatch in oxygen production and carbon fixation is likely due to the two-stage process in the photosynthetic fixation of carbon (reviewed in Behrenfeld et al., 2004). In the first stage, light-dependent reactions occur within the chloroplast, converting light energy (photons) into the cellular energy products, adenosine triphosphate (ATP), and nicotinamide adenine dinucleotide phosphate (NADPH), producing O_2 as a by-product. This cellular energy is then utilised in a second, light-independent pathway, which uses the carbon-fixing enzyme RuBisCO to convert CO_2 into sugars through the Calvin cycle. However, under certain circumstances the relative pool of energy may also be consumed in alternative pathways, such as respiration and photoprotection (Behrenfeld et al., 2004; Gao and Campbell, 2014). Increases in en-

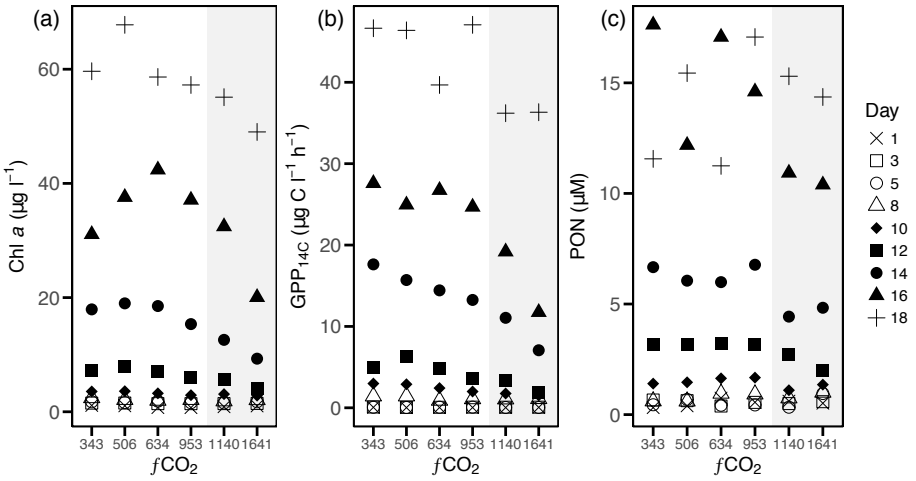

Figure 10. Temporal trends of **(a)** Chl *a*, **(b)** ^{14}C-derived gross primary production (GPP_{14C}), and **(c)** particulate organic nitrogen (PON) against CO_2 treatment. Grey shading indicates CO_2 treatments $\geq$ 1140 µatm.

ergy requirements for these alternate pathways have been demonstrated, where measurements of maximum photosynthetic rates (P_{max}) and photosynthetic efficiency (α) display changes that result in no change to saturating irradiance levels (E_k) (Behrenfeld et al., 2004, 2008; Halsey et al., 2010). This "E_k-independent variability" was evident in our study, in which decreases in P_{max} and α were observed in the high CO_2 treatments, while E_k remained unaffected (Fig. S3 in the Supplement).

This highlights an important tipping point in the phytoplankton community's ability to cope with the energetic requirements of maintaining efficient productivity under high CO_2. While studies on individual phytoplankton species have reported decoupling of the photosynthetic pathway under conditions of stress, no studies to date on natural phytoplankton communities have reported this response. Under laboratory conditions, stresses such as nutrient limitations (Halsey et al., 2010) or a combination of high CO_2 and light climate (Hoppe et al., 2015; Liu et al., 2017) have been shown to induce such a response in which isolated phytoplankton species possess higher energy requirements for carbon fixation. In our study, the phytoplankton community experienced a dynamic light climate due to continuous gentle mixing of the minicosm contents, and although nutrients were not limiting, the phytoplankton in the higher CO_2 treatments did show lower $csGPP_{14C}$ rates (Fig. 6a), which could be linked to higher energy demand for light-independent processes. Since nutrients were replete and not a likely source of stress, it follows that CO_2 and light were likely the only sources of stress on this community.

Increased respiration rates could account for the decreased carbon fixation rates measured. Thus far, respiration rates are commonly reported as either unaffected or lower under increasing CO_2 (Hennon et al., 2014; Trimborn et al., 2014; Spilling et al., 2016). This effect is generally attributed to declines in cellular energy requirements via processes such as the down-regulation of CCMs, which can result in observed increased rates of production (Spilling et al., 2016). Despite this, decreased growth rates have been linked to enhanced respiratory carbon loss at high CO_2 levels (800–1000 µatm) (Gao et al., 2012b). The contribution of community respiration rates to $csGCP_{O_2}$ was high and increased with increasing CO_2 (Fig. S4 in the Supplement). However, respiration rates were generally proportional to the increase in O_2 production (i.e. the ratio of production to respiration remained constant across CO_2 conditions), making it unlikely to be a significant contributor to the decline in carbon fixation. Instead, high respiration rates were possibly a result of heterotrophic activity.

It has been suggested that the negative effects of ocean acidification are predominantly due to the decline in pH and not the increase in CO_2 concentration (e.g. McMinn et al., 2014; Coad et al., 2016). A decline in pH with ocean acidification increases the hydrogen ion (H^+) concentration in the seawater and is likely to make it increasingly difficult for phytoplankton cells to maintain cellular homeostasis. Metabolic processes, such as photosynthesis and respiration, impact cellular H^+ fluxes between compartments, making it necessary to temporarily balance internal H^+ concentrations through H^+ channels (Taylor et al., 2012). Under normal oceanic conditions (pH $\sim$8.1), when the extracellular environment is above pH 7.8, excess H^+ ions generated within the cell are able to passively diffuse out of the cell through these H^+ channels. However, a lowering of the oceanic pH below 7.8 is likely to halt this passive removal of internal H^+, requiring the utilisation of energy-intensive proton pumps (Taylor et al., 2012) and thus potentially reducing the energy pool available for carbon fixation. While not well understood, these H^+ channels may also perform important cellular functions, such as nutrient uptake, cellular signalling,

and defense (Taylor et al., 2012). Our results are consistent with this idea of a critical pH threshold, as significant declines in $GPP_{^{14}C}$ were observed in treatments $\geq 1140\,\mu atm$ (Fig. 10), which are the CO_2 treatments for which the pH ranged from 7.69–7.45 (Fig. 2).

Despite the initial stress of high CO_2 between days 8 and 12, the phytoplankton community displayed a strong ability to adapt to these conditions. The CO_2-induced reduction in F_v / F_m showed a steady recovery between days 12 and 16, with all treatments displaying similarly high F_v / F_m at day 16 (0.68–0.71; Fig. 7). This recovery in photosynthetic health suggests that the phytoplankton community was able to acclimate to the high CO_2 conditions, possibly through cellular acclimation, changes in community structure, or most likely, a combination of both. Cellular acclimations were observed in our study. A lowering of NPQ and a minimisation of the CO_2-related response to photoinhibition (rETR) at high light intensity suggested that PSII was being down-regulated to adjust to a higher light climate (Figs. S6 and S7 in the Supplement). Decreased energy requirements for carbon fixation were also observed in the photosynthetic pathway, resulting in increases in $GPP_{^{14}C}$ and Chl *a* accumulation rates (Fig. 5). Acclimation to increased CO_2 has been reported in a number of studies, resulting in shifts in carbon and energy utilisation (Sobrino et al., 2008; Hopkinson et al., 2010; Hennon et al., 2014; Trimborn et al., 2014; Zheng et al., 2015). Numerous photophysiological investigations on individual phytoplankton species also report species-specific tolerances to increased CO_2 (Gao et al., 2012a; Gao and Campbell, 2014; Trimborn et al., 2013, 2014), and a general trend toward smaller-celled communities with increased CO_2 has been reported in ocean acidification studies globally (Schulz et al., 2017). Changes in community structure were observed with increasing CO_2, with taxon-specific thresholds of CO_2 tolerance (Hancock et al., 2017). Within the diatom community, the response was also related to size, leading to an increase in abundance of small ($< 20\,\mu m$) diatoms in the higher CO_2 treatments ($\geq 953\,\mu atm$). Therefore, the community acclimation observed is likely driven by an increase in the growth of more tolerant species.

It is often suggested that the down-regulation of CCMs helps to moderate the sensitivity of phytoplankton communities to increasing CO_2. The carbon-fixing enzyme RuBisCO has a low affinity for CO_2 that is compensated for through CCMs that actively increase the intracellular CO_2 (Raven, 1991; Badger, 1994; Badger et al., 1998; Hopkinson et al., 2011). This process requires additional cellular energy (Raven, 1991) and numerous studies have suggested that the energy savings from down-regulation of CCMs in phytoplankton could explain increases in rates of primary productivity at elevated CO_2 levels (e.g. Cassar et al., 2004; Tortell et al., 2008b, 2010; Trimborn et al., 2013; Young et al., 2015). In Antarctic phytoplankton communities, Young et al. (2015) showed that the energetic costs of CCMs are low and any down-regulation at increased CO_2 would provide little benefit. We found that the CCM component carbonic anhydrase (CA) was utilised by the phytoplankton community at our control CO_2 level (343 µatm) and was down-regulated at high CO_2 (1641 µatm; Fig. 8). Yet we saw no promotion of primary productivity that coincided with this down-regulation. Thus, our data support the previous studies showing that increased CO_2 may alleviate energy supply constraints but does not necessarily lead to increased rates of carbon fixation (Rost et al., 2003; Cassar et al., 2004; Riebesell, 2004).

Furthermore, size-specific differences in phytoplankton CCM utilisation were observed. The absence of eCA activity in the large phytoplankton ($\geq 10\,\mu m$; Fig. 8a) suggests that bicarbonate (HCO_3^-) was the dominant carbon source used by this fraction of the phytoplankton community (Burkhardt et al., 2001; Tortell et al., 2008a). This is not surprising as direct HCO_3^- uptake has been commonly reported among Antarctic phytoplankton communities (Cassar et al., 2004; Tortell et al., 2008a, 2010). On the other hand, the small phytoplankton ($<10\,\mu m$; Fig. 8b) seem to have used both iCA and eCA, implying that carbon for photosynthesis was sourced through both the extracellular conversion of HCO_3^- to CO_2 and direct HCO_3^- uptake (Rost et al., 2003). Despite these patterns, CCM activity in this study was only determined via Chl *a* fluorescence and therefore direct measurement of light-dependent reactions in photosynthesis. This imposes limitations to the interpretability of this particular data set, as CA is involved primarily in carbon acquisition, which occurs during photosynthetic reactions that are independent of light.

The presence of iCA has also been proposed as a possible mechanism for increased sensitivity of phytoplankton to decreased pH conditions. Satoh et al. (2001) found that the presence of iCA caused strong intracellular acidification and inhibition of carbon fixation when a CO_2-tolerant iCA-expressing algal species was transferred from ambient conditions to very high CO_2 (40 %). Down-regulation of iCA through acclimation in a 5 % CO_2 treatment eliminated this response, with similar tolerance observed in an algal species with low ambient iCA activity. Thus, the down-regulation of iCA activity at high CO_2, as was seen in our study, may not only decrease cellular energy demands but may also be operating as a cellular protection mechanism, allowing the cell to maintain intracellular homeostasis.

Contrary to the high CO_2 treatments, the phytoplankton community appeared to tolerate CO_2 levels up to 953 µatm, which identified a CO_2 threshold. Between days 8 and 14 we observed a small and insignificant CO_2-related decline in F_v / F_m, $GPP_{^{14}C}$, and Chl *a* accumulation among the 343–953 µatm treatments (Figs. 7 and 10). Tolerance of CO_2 levels up to $\sim 1000\,\mu atm$ has often been observed in natural phytoplankton communities in regions exposed to fluctuating CO_2 levels. In these communities, increasing CO_2 often had no effect on primary productivity (Tortell et al., 2000; Tortell and Morel, 2002; Tortell et al., 2008b; Hopkinson

et al., 2010; Tanaka et al., 2013; Sommer et al., 2015; Young et al., 2015; Spilling et al., 2016) or growth (Tortell et al., 2008b; Schulz et al., 2013), although an increase in primary production has been observed in some instances (Riebesell, 2004; Tortell et al., 2008b; Egge et al., 2009; Tortell et al., 2010; Hoppe et al., 2013; Holding et al., 2015). These differing responses may be due to differences in community composition, nutrient supply, or ecological adaptations of the phytoplankton community in the region studied. They may also be due to differences in the experimental methods, especially the range of CO_2 concentrations employed (Hancock et al., 2017), the mechanism used to manipulate CO_2 concentrations, the duration of the acclimation and incubation, the nature and volume of the mesocosms used, and the extent to which higher trophic levels are screened from the mesocosm contents (see Davidson et al., 2016).

Previous studies in Prydz Bay report a tolerance of the phytoplankton community to CO_2 levels up to 750 µatm (Davidson et al., 2016; Thomson et al., 2016; Westwood et al., 2018). Although these experiments differed in nutrient concentration, community composition, and CO_2 manipulation from ours, when taken together, these studies demonstrate consistent CO_2 effects throughout the Antarctic summer season and across years in this location. The most likely reason for this high tolerance is that these communities are already exposed to highly variable CO_2 conditions. CO_2 naturally builds beneath the sea ice in winter when primary productivity is low (Perrin et al., 1987; Legendre et al., 1992), and is rapidly depleted during spring and summer by phytoplankton blooms, resulting in annual fCO_2 fluctuations between $\sim$50 and 500 µatm (Gibson and Trull, 1999; Roden et al., 2013). Thus, variable CO_2 environments appear to promote adaptations within the phytoplankton community to manage the stress imposed by fluctuating CO_2.

Changes in POM production and the C : N ratio in phytoplankton communities can have significant effects on carbon sequestration and change their nutritional value for higher trophic levels (Finkel et al., 2010; van de Waal et al., 2010; Polimene et al., 2016). We observed a decline in particulate organic matter production (POM) at CO_2 levels $\geq$ 1140 µatm (Fig. 10), while changes in organic matter stoichiometry (C : N ratio) appeared to be predominantly controlled by nutrient consumption (Fig. 4). Increases in POM production were similar to Chl *a* accumulation, with declines in high CO_2 treatments ($\geq$ 1140 µatm) due to low rates of primary productivity. Carbon overconsumption has been reported in some natural phytoplankton communities exposed to increased CO_2, resulting in observed or inferred increases in the particulate C : N ratio (Riebesell et al., 2007; Engel et al., 2014). While in our study the C : N ratio did decline to below the Redfield ratio during exponential growth, it remained within previously reported C : N ratios of coastal phytoplankton communities in this region (Gibson and Trull, 1999; Pasquer et al., 2010). However, as we did not analyse the elemental composition of dissolved inorganic matter, carbon overconsumption cannot be completely ruled out (Kähler and Koeve, 2001). Therefore, it is difficult to say whether or not changes in primary productivity will affect organic matter stoichiometry in this region, particularly as any resultant long-term changes in community composition to more CO_2-tolerant taxa may also have an effect (Finkel et al., 2010).

4.2 Ocean acidification effects on bacterial productivity

In contrast to the phytoplankton community, bacteria were tolerant of high CO_2 levels. The low bacterial productivity and abundance of the initial community is characteristic of the post-winter bacterial community in Prydz Bay where growth is limited by organic nutrient availability (Pearce et al., 2007). Whilst an increase in cell abundance was observed at CO_2 levels $\geq$ 634 µatm (Fig. 9a), it was possible that this response was driven by a decline in grazing by heterotrophs (Thomson et al., 2016; Westwood et al., 2018) instead of a direct CO_2-related promotion of bacterial growth. The subsequent decline in abundance was likely due to top-down control from the heterotrophic nanoflagellate community, which displayed an increase in abundance at this time (Hancock et al., 2017). Bacterial tolerance to high CO_2 has been reported previously in this region (Thomson et al., 2016; Westwood et al., 2018) and has also been reported in numerous studies in the Arctic (Grossart et al., 2006; Allgaier et al., 2008; Paulino et al., 2008; Baragi et al., 2015; Wang et al., 2016), suggesting that the marine bacterial community will be resilient to increasing CO_2.

While we detected an increase in bacterial productivity, this response appeared to be correlated with an increase in Chl *a* concentration and available POM rather than CO_2. Bacterial productivity was similar among all CO_2 treatments, except for a final promotion of productivity at 634 µatm on day 18 (Fig. 9b). This promotion of growth may be linked to an increase in diatom abundance observed in this treatment (Hancock et al., 2017). The coupling of bacterial growth with phytoplankton productivity has been reported by numerous studies on natural marine microbial communities (Allgaier et al., 2008; Grossart et al., 2006; Engel et al., 2013; Piontek et al., 2013; Sperling et al., 2013; Bergen et al., 2016). Thus, it is likely that the bacterial community was controlled more by grazing and nutrient availability than by CO_2 level.

5 Conclusions

These results support the identification of a tipping point in the marine microbial community response to CO_2 between 953 and 1140 µatm. When exposed to $CO_2 \geq$ 634 µatm, declines in growth rates, primary productivity, and organic matter production were observed in the phytoplankton community and became significantly different at $\geq$ 1140 µatm. Despite this, the community displayed the ability to adapt to these high CO_2 conditions by down-regulating CCMs and

likely adjusting other intracellular mechanisms to cope with the added stress of low pH. However, the lag in growth and subsequent acclimation to high CO_2 conditions allowed for more tolerant species to thrive (Hancock et al., 2017).

Conditions in Antarctic coastal regions fluctuate throughout the seasons and the marine microbial community is already tolerant to changes in CO_2 level, light availability, and nutrients (Gibson and Trull, 1999; Roden et al., 2013). It is possible that phytoplankton communities already exposed to highly variable conditions will be more capable of adapting to the projected changes in CO_2 (Schaum and Collins, 2014; Boyd et al., 2016). This will likely also include adaptation at the community level, causing a shift in dominance to more tolerant species. This has been observed in numerous ocean acidification experiments, with a trend in community composition favouring picophytoplankton and away from large diatoms (Davidson et al., 2016; reviewed in Schulz et al., 2017). Such a change in phytoplankton community composition may have flow-on effects to higher trophic levels that feed on Antarctic phytoplankton blooms. It could also have a significant effect on the biological pump, with decreased carbon drawdown at high CO_2, causing a negative feedback on anthropogenic CO_2 uptake. Coincident increases in bacterial abundance under high CO_2 conditions may also increase the efficiency of the microbial loop, resulting in increased organic matter remineralisation and further declines in carbon sequestration.

Data availability. Experimental data used for analysis are available via the Australian Antarctic Data Centre.

Environmental data: Australian Antarctic Data Centre, http://dx.doi.org/10.4225/15/599a7dfe9470a (Deppeler et al., 2017a).

Productivity data: Australian Antarctic Data Centre, http://dx.doi.org/10.4225/15/599a7cc747c61 (Deppeler et al., 2017b).

The Supplement related to this article is available online at https://doi.org/10.5194/bg-15-209-2018-supplement.

Author contributions. AD, KW, and KP conceived and designed the experiments. AD led and oversaw the minicosm experiment. SD and KP performed the experiments and data analysis. KS performed the carbonate system measurements and manipulation. IP performed pigment extraction and analysis. JM provided statistical guidance. SD wrote the paper with significant input from KP, KS, and AD. All authors provided contributions and a critical review of the paper.

Competing interests. The authors declare that they have no conflict of interest.

Acknowledgements. This study was funded by the Australian Government, Department of Environment and Energy as part of the Australian Antarctic Science Project 4026 at the Australian Antarctic Division and an Elite Research Scholarship awarded by the Institute for Marine and Antarctic Studies, University of Tasmania. We would like to thank Andrew McMinn for valuable comments on our paper, Penelope Pascoe for the flow cytometric analyses, Cristin Sheehan for photosynthesis and respiration data, and Thomas Rodemann from the Central Science Laboratory, University of Tasmania for elemental analysis of our POM samples. We gratefully acknowledge the assistance of AAD technical support in designing and equipping the minicosms and Davis Station expeditioners in the summer of 2014–2015 for their support and assistance.

Edited by: Richard Matear
Reviewed by: two anonymous referees

References

Allgaier, M., Riebesell, U., Vogt, M., Thyrhaug, R., and Grossart, H.-P.: Coupling of heterotrophic bacteria to phytoplankton bloom development at different pCO_2 levels: a mesocosm study, Biogeosciences, 5, 1007–1022, https://doi.org/10.5194/bg-5-1007-2008, 2008.

Arrigo, K. R., van Dijken, G. L., and Bushinsky, S.: Primary production in the Southern Ocean, 1997–2006, J. Geophys. Res.-Ocean., 113, C08004, https://doi.org/10.1029/2007JC004551, 2008a.

Arrigo, K. R., van Dijken, G. L., and Long, M.: Coastal Southern Ocean: A strong anthropogenic CO_2 sink, Geophys. Res. Lett., 35, L21602, https://doi.org/10.1029/2008GL035624, 2008b.

Azam, F., Fenchel, T., Field, J. G., Gray, J. C., Meyer-Reil, L. A., and Thingstad, F.: The ecological role of water-column microbes in the sea, Mar. Ecol. Prog. Ser., 10, 257–264, https://doi.org/10.3354/meps010257, 1983.

Azam, F., Smith, D. C., and Hollibaugh, J. T.: The role of the microbial loop in Antarctic pelagic ecosystems, Polar Res., 10, 239–243, https://doi.org/10.1111/j.1751-8369.1991.tb00649.x, 1991.

Bach, L. T., Taucher, J., Boxhammer, T., Ludwig, A., Achterberg, E. P., Algueró-Muñiz, M., Anderson, L. G., Bellworthy, J., Büdenbender, J., Czerny, J., Ericson, Y., Esposito, M., Fischer, M., Haunost, M., Hellemann, D., Horn, H. G., Hornick, T., Meyer, J., Sswat, M., Zark, M., and Riebesell, U.: Influence of ocean acidification on a natural winter-to-summer plankton succession first insights from a long-term mesocosm study draw attention to periods of low nutrient concentrations, PLoS One, 11, e0159068, https://doi.org/10.1371/journal.pone.0159068, 2016.

Badger, M.: The Role of Carbonic Anhydrase in Photosynthesis, Annu. Rev. Plant Physiol. Plant Mol. Biol., 45, 369–392, https://doi.org/10.1146/annurev.arplant.45.1.369, 1994.

Badger, M. R., Andrews, T. J., Whitney, S., Ludwig, M., Yellowlees, D. C., Leggat, W., and Price, G. D.: The diversity and coevolution of Rubisco, plastids, pyrenoids, and chloroplast-based CO_2-concentrating mechanisms in algae, Can. J. Bot., 76, 1052–1071, https://doi.org/10.1139/cjb-76-6-1052, 1998.

Baragi, L. V., Khandeparker, L., and Anil, A. C.: Influence of elevated temperature and pCO_2 on the marine periphytic diatom

Navicula distans and its associated organisms in culture, Hydrobiologia, 762, 127–142, https://doi.org/10.1007/s10750-015-2343-9, 2015.

Barcelos e Ramos, J., Schulz, K. G., Brownlee, C., Sett, S., and Azevedo, E. B.: Effects of Increasing Seawater Carbon Dioxide Concentrations on Chain Formation of the Diatom *Asterionellopsis glacialis*, PLoS One, 9, e90749, https://doi.org/10.1371/journal.pone.0090749, 2014.

Behrenfeld, M. J., Prasil, O., Babin, M., and Bruyant, F.: In Search of a Physiological Basis for Covariations in Light-Limited and Light-Saturated Photosynthesis, J. Phycol., 40, 4–25, https://doi.org/10.1046/j.1529-8817.2004.03083.x, 2004.

Behrenfeld, M. J., Halsey, K. H., and Milligan, A. J.: Evolved physiological responses of phytoplankton to their integrated growth environment., Philos. T. R. Soc. B, 363, 2687–2703, https://doi.org/10.1098/rstb.2008.0019, 2008.

Bellerby, R. G. J., Schulz, K. G., Riebesell, U., Neill, C., Nondal, G., Heegaard, E., Johannessen, T., and Brown, K. R.: Marine ecosystem community carbon and nutrient uptake stoichiometry under varying ocean acidification during the PeECE III experiment, Biogeosciences, 5, 1517–1527, https://doi.org/10.5194/bg-5-1517-2008, 2008.

Berge, T., Daugbjerg, N., Balling Andersen, B., and Hansen, P.: Effect of lowered pH on marine phytoplankton growth rates, Mar. Ecol. Prog. Ser., 416, 79–91, https://doi.org/10.3354/meps08780, 2010.

Bergen, B., Endres, S., Engel, A., Zark, M., Dittmar, T., Sommer, U., and Jürgens, K.: Acidification and warming affect prominent bacteria in two seasonal phytoplankton bloom mesocosms, Environ. Microbiol., 18, 4579–4595, https://doi.org/10.1111/1462-2920.13549, 2016.

Bi, R., Ismar, S., Sommer, U., and Zhao, M.: Environmental dependence of the correlations between stoichiometric and fatty acid-based indicators of phytoplankton nutritional quality, Limnol. Oceanogr., 62, 334–347, https://doi.org/10.1002/lno.10429, 2017.

Bockmon, E. E. and Dickson, A. G.: A seawater filtration method suitable for total dissolved inorganic carbon and pH analyses, Limnol. Oceanogr. Methods, 12, 191–195, https://doi.org/10.4319/lom.2014.12.191, 2014.

Boyd, P. W., Doney, S. C., Strzepek, R., Dusenberry, J., Lindsay, K., and Fung, I.: Climate-mediated changes to mixed-layer properties in the Southern Ocean: assessing the phytoplankton response, Biogeosciences, 5, 847–864, https://doi.org/10.5194/bg-5-847-2008, 2008.

Boyd, P. W., Cornwall, C. E., Davidson, A., Doney, S. C., Fourquez, M., Hurd, C. L., Lima, I. D., and McMinn, A.: Biological responses to environmental heterogeneity under future ocean conditions, Global Change Biol., 22, 2633–2650, https://doi.org/10.1111/gcb.13287, 2016.

Bunse, C., Lundin, D., Karlsson, C. M. G., Vila-Costa, M., Palovaara, J., Akram, N., Svensson, L., Holmfeldt, K., González, J. M., Calvo, E., Pelejero, C., Marrasé, C., Dopson, M., Gasol, J. M., and Pinhassi, J.: Response of marine bacterioplankton pH homeostasis gene expression to elevated CO_2, Nat. Clim. Change, 1, 1–7, https://doi.org/10.1038/nclimate2914, 2016.

Burkhardt, S., Amoroso, G., Riebesell, U., and Sültemeyer, D.: CO_2 and HCO_3^- uptake in marine diatoms acclimated to different CO_2 concentrations, Limnol. Oceanogr., 46, 1378–1391, https://doi.org/10.4319/lo.2001.46.6.1378, 2001.

Caldeira, K. and Wickett, M. E.: Oceanography: Anthropogenic carbon and ocean pH, Nature, 425, 365–365, https://doi.org/10.1038/425365a, 2003.

Cassar, N., Laws, E. A., Bidigare, R. R., and Popp, B. N.: Bicarbonate uptake by Southern Ocean phytoplankton, Global Biogeochem. Cy., 18, 1–10, https://doi.org/10.1029/2003GB002116, 2004.

Chen, C. and Durbin, E.: Effects of pH on the growth and carbon uptake of marine phytoplankton, Mar. Ecol. Prog. Ser., 109, 83–94, https://doi.org/10.3354/meps109083, 1994.

Chen, H., Guan, W., Zeng, G., Li, P., and Chen, S.: Alleviation of solar ultraviolet radiation (UVR)-induced photoinhibition in diatom *Chaetoceros curvisetus* by ocean acidification, J. Mar. Biol. Assoc. UK, 95, 661–667, https://doi.org/10.1017/S0025315414001568, 2015.

Coad, T., McMinn, A., Nomura, D., and Martin, A.: Effect of elevated CO_2 concentration on microalgal communities in Antarctic pack ice, Deep-Sea Res. Part II, 131, 160–169, https://doi.org/10.1016/j.dsr2.2016.01.005, 2016.

Davidson, A., McKinlay, J., Westwood, K., Thomson, P., van den Enden, R., de Salas, M., Wright, S., Johnson, R., and Berry, K.: Enhanced CO_2 concentrations change the structure of Antarctic marine microbial communities, Mar. Ecol. Prog. Ser., 552, 93–113, https://doi.org/10.3354/meps11742, 2016.

Deppeler, S. L. and Davidson, A. T.: Southern Ocean Phytoplankton in a Changing Climate, Front. Mar. Sci., 4, 1–28, https://doi.org/10.3389/fmars.2017.00040, 2017.

Deppeler, S. L., Davidson, A. T., and Schulz, K.: Environmental data for Davis 14/15 ocean acidification minicosm experiment, Australian Antarctic Data Centre, https://doi.org/10.4225/15/599a7dfe9470a, 2017a (updated 2017).

Deppeler, S. L., Petrou, K., Schulz, K., Davidson, A. T., Mckinlay, J., Pearce, I., and Westwood, K. J.: Data for manuscript "Ocean acidification of a coastal Antarctic marine microbial community reveals a critical threshold for CO_2 tolerance in phytoplankton productivity", Australian Antarctic Data Centre, https://doi.org/10.4225/15/599a7cc747c61, 2017b (updated 2017).

Dickson, A.: Standards for Ocean Measurements, Oceanography, 23, 34–47, https://doi.org/10.5670/oceanog.2010.22, 2010.

Dickson, A., Sabine, C., and Christian, J., eds.: Guide to Best Practices for Ocean CO_2 Measurements, North Pacific Marine Science Organization, Sidney, British Columbia, 191 pp., 2007.

Dring, M. J. and Jewson, D. H.: What Does 14C Uptake by Phytoplankton Really Measure? A Theoretical Modelling Approach, Proc. R. Soc. B, 214, 351–368, https://doi.org/10.1098/rspb.1982.0016, 1982.

Ducklow, H. W., Baker, K., Martinson, D. G., Quetin, L. B., Ross, R. M., Smith, R. C., Stammerjohn, S. E., Vernet, M., and Fraser, W.: Marine pelagic ecosystems: the West Antarctic Peninsula, Philos. T. R. Soc. B, 362, 67–94, https://doi.org/10.1098/rstb.2006.1955, 2007.

Egge, J. K., Thingstad, T. F., Larsen, A., Engel, A., Wohlers, J., Bellerby, R. G. J., and Riebesell, U.: Primary production during nutrient-induced blooms at elevated CO_2 concentrations,

Biogeosciences, 6, 877–885, https://doi.org/10.5194/bg-6-877-2009, 2009.

Engel, A., Borchard, C., Piontek, J., Schulz, K. G., Riebesell, U., and Bellerby, R.: CO_2 increases ^{14}C primary production in an Arctic plankton community, Biogeosciences, 10, 1291–1308, https://doi.org/10.5194/bg-10-1291-2013, 2013.

Engel, A., Piontek, J., Grossart, H.-P., Riebesell, U., Schulz, K. G., and Sperling, M.: Impact of CO_2 enrichment on organic matter dynamics during nutrient induced coastal phytoplankton blooms, J. Plankton Res., 36, 641–657, https://doi.org/10.1093/plankt/fbt125, 2014.

Fabry, V., McClintock, J., Mathis, J., and Grebmeier, J.: Ocean Acidification at High Latitudes: The Bellwether, Oceanography, 22, 160–171, https://doi.org/10.5670/oceanog.2009.105, 2009.

Fenchel, T.: The microbial loop – 25 years later, J. Exp. Mar. Bio. Ecol., 366, 99–103, https://doi.org/10.1016/j.jembe.2008.07.013, 2008.

Feng, Y., Hare, C., Rose, J., Handy, S., DiTullio, G., Lee, P., Smith, W. J., Peloquin, J., Tozzi, S., Sun, J., Zhang, Y., Dunbar, R., Long, M., Sohst, B., Lohan, M., and Hutchins, D.: Interactive effects of iron, irradiance and CO_2 on Ross Sea phytoplankton, Deep-Sea Res. Part I, 57, 368–383, https://doi.org/10.1016/j.dsr.2009.10.013, 2010.

Finkel, Z. V., Beardall, J., Flynn, K. J., Quigg, A., Rees, T. A. V., and Raven, J. A.: Phytoplankton in a changing world: cell size and elemental stoichiometry, J. Plankton Res., 32, 119–137, https://doi.org/10.1093/plankt/fbp098, 2010.

Frölicher, T. L., Sarmiento, J. L., Paynter, D. J., Dunne, J. P., Krasting, J. P., and Winton, M.: Dominance of the Southern Ocean in Anthropogenic Carbon and Heat Uptake in CMIP5 Models, J. Clim., 28, 862–886, https://doi.org/10.1175/JCLI-D-14-00117.1, 2015.

Gao, K. and Campbell, D. A.: Photophysiological responses of marine diatoms to elevated CO_2 and decreased pH: a review, Funct. Plant Biol., 41, 449–459, https://doi.org/10.1071/FP13247, 2014.

Gao, K., Helbling, E., Häder, D., and Hutchins, D.: Responses of marine primary producers to interactions between ocean acidification, solar radiation, and warming, Mar. Ecol. Prog. Ser., 470, 167–189, https://doi.org/10.3354/meps10043, 2012a.

Gao, K., Xu, J., Gao, G., Li, Y., Hutchins, D. A., Huang, B., Wang, L., Zheng, Y., Jin, P., Cai, X., Häder, D.-p., Li, W., Xu, K., Liu, N., and Riebesell, U.: Rising CO_2 and increased light exposure synergistically reduce marine primary productivity, Nat. Clim. Change, 2, 519–523, https://doi.org/10.1038/nclimate1507, 2012b.

Gattuso, J.-P., Gao, K., Lee, K., Rost, B., and Schulz, K. G.: Approaches and tools to manipulate the carbonate chemistry, in: Guide to best practices for ocean acidification research and data reporting, edited by Riebesell, U., Fabry, V. J., Hansson, L., and Gattuso, J.-P., chap. 2, 41–52, Publications Office of the European Union, Luxembourg, https://doi.org/10.2777/66906, 2010.

Gibson, J. A. and Trull, T. W.: Annual cycle of fCO_2 under sea-ice and in open water in Prydz Bay, East Antarctica, Mar. Chem., 66, 187–200, https://doi.org/10.1016/S0304-4203(99)00040-7, 1999.

González, N., Gattuso, J. P., and Middelburg, J. J.: Oxygen production and carbon fixation in oligotrophic coastal bays and the relationship with gross and net primary production, Aquat. Microb. Ecol., 52, 119–130, https://doi.org/10.3354/ame01208, 2008.

Grossart, H.-P., Allgaier, M., Passow, U., and Riebesell, U.: Testing the effect of CO_2 concentration on the dynamics of marine heterotrophic bacterioplankton, Limnol. Oceanogr., 51, 1–11, https://doi.org/10.4319/lo.2006.51.1.0001, 2006.

Halsey, K. H., Milligan, A. J., and Behrenfeld, M. J.: Physiological optimization underlies growth rate-independent chlorophyll-specific gross and net primary production, Photosynth. Res., 103, 125–137, https://doi.org/10.1007/s11120-009-9526-z, 2010.

Hancock, A. M., Davidson, A. T., McKinlay, J., McMinn, A., Schulz, K., and van den Enden, R. L.: Ocean acidification changes the structure of an Antarctic coastal protistan community, Biogeosciences Discuss., https://doi.org/10.5194/bg-2017-224, in review, 2017.

Hauck, J. and Völker, C.: Rising atmospheric CO_2 leads to large impact of biology on Southern Ocean CO_2 uptake via changes of the Revelle factor, Geophys. Res. Lett., 42, 1459–1464, https://doi.org/10.1002/2015GL063070, 2015.

Hauck, J., Völker, C., Wolf-Gladrow, D. A., Laufkötter, C., Vogt, M., Aumont, O., Bopp, L., Buitenhuis, E. T., Doney, S. C., Dunne, J., Gruber, N., Hashioka, T., John, J., Quéré, C. L., Lima, I. D., Nakano, H., Séférian, R., and Totterdell, I.: On the Southern Ocean CO_2 uptake and the role of the biological carbon pump in the 21st century, Global Biogeochem. Cy., 29, 1451–1470, https://doi.org/10.1002/2015GB005140, 2015.

Hennon, G. M. M., Quay, P., Morales, R. L., Swanson, L. M., and Virginia Armbrust, E.: Acclimation conditions modify physiological response of the diatom *Thalassiosira pseudonana* to elevated CO_2 concentrations in a nitrate-limited chemostat, J. Phycol., 50, 243–253, https://doi.org/10.1111/jpy.12156, 2014.

Hennon, G. M. M., Ashworth, J., Groussman, R. D., Berthiaume, C., Morales, R. L., Baliga, N. S., Orellana, M. V., and Armbrust, E. V.: Diatom acclimation to elevated CO_2 via cAMP signalling and coordinated gene expression, Nat. Clim. Change, 5, 761–765, https://doi.org/10.1038/nclimate2683, 2015.

Holding, J. M., Duarte, C. M., Sanz-Martín, M., Mesa, E., Arrieta, J. M., Chierici, M., Hendriks, I. E., García-Corral, L. S., Regaudie-de Gioux, A., Delgado, A., Reigstad, M., Wassmann, P., and Agustí, S.: Temperature dependence of CO_2-enhanced primary production in the European Arctic Ocean, Nat. Clim. Change, 5, 1079–1082, https://doi.org/10.1038/nclimate2768, 2015.

Hong, H., Li, D., Lin, W., Li, W., and Shi, D.: Nitrogen nutritional condition affects the response of energy metabolism in diatoms to elevated carbon dioxide, Mar. Ecol. Prog. Ser., 567, 41–56, https://doi.org/10.3354/meps12033, 2017.

Honjo, S.: Particle export and the biological pump in the Southern Ocean, Antarct. Sci., 16, 501–516, https://doi.org/10.1017/S0954102004002287, 2004.

Hopkinson, B. M., Xu, Y., Shi, D., McGinn, P. J., and Morel, F. M. M.: The effect of CO_2 on the photosynthetic physiology of phytoplankton in the Gulf of Alaska, Limnol. Oceanogr., 55, 2011–2024, https://doi.org/10.4319/lo.2010.55.5.2011, 2010.

Hopkinson, B. M., Dupont, C. L., Allen, A. E., and Morel, F. M. M.: Efficiency of the CO_2-concentrating mechanism of diatoms, P. Natl. Acad. Sci., 108, 3830–3837, https://doi.org/10.1073/pnas.1018062108, 2011.

Hoppe, C. J. M., Hassler, C. S., Payne, C. D., Tortell, P. D., Rost, B., and Trimborn, S.: Iron Limitation Modulates Ocean Acidification Effects on Southern Ocean Phytoplankton Communities, PLoS One, 8, e79890, https://doi.org/10.1371/journal.pone.0079890, 2013.

Hoppe, C. J. M., Holtz, L.-M., Trimborn, S., and Rost, B.: Ocean acidification decreases the light-use efficiency in an Antarctic diatom under dynamic but not constant light, New Phytol., 207, 159–171, https://doi.org/10.1111/nph.13334, 2015.

Hoppema, M., Fahrbach, E., Schröder, M., Wisotzki, A., and de Baar, H. J.: Winter-summer differences of carbon dioxide and oxygen in the Weddell Sea surface layer, Mar. Chem., 51, 177–192, https://doi.org/10.1016/0304-4203(95)00065-8, 1995.

IPCC: Climate Change 2013: The Physical Science Basis. Contribution of Working Group I to the Fifth Assessment Report of the Intergovernmental Panel on Climate Change, Cambridge University Press, Cambridge, UK and New York, NY, USA, https://doi.org/10.1017/CBO9781107415324, 2013.

Jeffrey, S. and Humphrey, G.: New spectrophotometric equations for determining chlorophylls *a*, *b*, c_1 and c_2 in higher plants, algae and natural phytoplankton, Biochem. Physiol. Pflanz., 167, 191–194, https://doi.org/10.1016/S0015-3796(17)30778-3, 1975.

Jeffrey, S. W. and Wright, S. W.: Qualitative and quantitative HPLC analysis of SCOR reference algal cultures, in: Phytoplankton Pigments in Oceanography: Guidelines to Modern Methods, edited by: Jeffrey, S., Mantoura, R., and Wright, S., 343–360, UNESCO, Paris, 1997.

Kähler, P. and Koeve, W.: Marine dissolved organic matter: Can its C:N ratio explain carbon overconsumption?, Deep-Sea Res. Part I, 48, 49–62, https://doi.org/10.1016/S0967-0637(00)00034-0, 2001.

Khatiwala, S., Primeau, F., and Hall, T.: Reconstruction of the history of anthropogenic CO_2 concentrations in the ocean, Nature, 462, 346–349, https://doi.org/10.1038/nature08526, 2009.

Kim, J.-M., Lee, K., Shin, K., Kang, J.-H., Lee, H.-W., Kim, M., Jang, P.-G., and Jang, M.-C.: The effect of seawater CO_2 concentration on growth of a natural phytoplankton assemblage in a controlled mesocosm experiment, Limnol. Oceanogr., 51, 1629–1636, https://doi.org/10.4319/lo.2006.51.4.1629, 2006.

King, A., Jenkins, B., Wallace, J., Liu, Y., Wikfors, G., Milke, L., and Meseck, S.: Effects of CO_2 on growth rate, C:N:P, and fatty acid composition of seven marine phytoplankton species, Mar. Ecol. Prog. Ser., 537, 59–69, https://doi.org/10.3354/meps11458, 2015.

Kirchman, D. L.: Measuring Bacterial Biomass Production and Growth Rates from Leucine Incorporation in Natural Aquatic Environments, in: Methods in Microbiology, edited by: Paul, J., vol. 30, chap. 12, 227–237, Academic Press, St. Petersburg, FL, https://doi.org/10.1016/S0580-9517(01)30047-8, 2001.

Kirchman, D. L.: Microbial ecology of the oceans, Wiley-Blackwell, Hoboken, NJ, 2 edn., 620 pp., 2008.

Legendre, L., Ackley, S. F., Dieckmann, G. S., Gulliksen, B., Horner, R., Hoshiai, T., Melnikov, I. A., Reeburgh, W. S., Spindler, M., and Sullivan, C. W.: Ecology of sea ice biota – 2. Global significance, Polar Biol., 12, 429–444, https://doi.org/10.1007/BF00243114, 1992.

Lewis, M. and Smith, J.: A small volume, short-incubation-time method for measurement of photosynthesis as a function of incident irradiance, Mar. Ecol. Prog. Ser., 13, 99–102, https://doi.org/10.3354/meps013099, 1983.

Li, F., Beardall, J., Collins, S., and Gao, K.: Decreased photosynthesis and growth with reduced respiration in the model diatom *Phaeodactylum tricornutum* grown under elevated CO_2 over 1800 generations, Global Change Biol., 23, 127–137, https://doi.org/10.1111/gcb.13501, 2017a.

Li, W., Yang, Y., Li, Z., Xu, J., and Gao, K.: Effects of seawater acidification on the growth rates of the diatom *Thalassiosira (Conticribra) weissflogii* under different nutrient, light, and UV radiation regimes, J. Appl. Phycol., 29, 133–142, https://doi.org/10.1007/s10811-016-0944-y, 2017b.

Liu, N., Beardall, J., and Gao, K.: Elevated CO_2 and associated seawater chemistry do not benefit a model diatom grown with increased availability of light, Aquat. Microb. Ecol., 79, 137–147, https://doi.org/10.3354/ame01820, 2017.

Longhurst, A. R.: Role of the marine biosphere in the global carbon cycle, Limnol. Oceanogr., 36, 1507–1526, https://doi.org/10.4319/lo.1991.36.8.1507, 1991.

Lueker, T. J., Dickson, A. G., and Keeling, C. D.: Ocean pCO_2 calculated from dissolved inorganic carbon, alkalinity, and equations for K_1 and K_2: validation based on laboratory measurements of CO_2 in gas and seawater at equilibrium, Mar. Chem., 70, 105–119, https://doi.org/10.1016/S0304-4203(00)00022-0, 2000.

Mantoura, R. and Repeta, D.: Calibration methods for HPLC, in: Phytoplankton Pigments in Oceanography: Guidelines to Modern Methods, edited by: Jeffrey, S., Mantoura, R., and Wright, S., 407–428, UNESCO, Paris, 1997.

Marie, D., Simon, N., and Vaulot, D.: Phytoplankton cell counting by flow cytometry, in: Algal Culturing Techniques, edited by: Anderson, R. A., chap. 17, 253–267, Academic Press, San Diego, CA, USA, https://doi.org/10.1016/B978-012088426-1/50018-4, 2005.

McMinn, A., Müller, M. N., Martin, A., and Ryan, K. G.: The Response of Antarctic Sea Ice Algae to Changes in pH and CO_2, PLoS One, 9, e86 984, https://doi.org/10.1371/journal.pone.0086984, 2014.

McNeil, B. I. and Matear, R. J.: Southern Ocean acidification: A tipping point at 450-ppm atmospheric CO_2, P. Natl. Acad. Sci., 105, 18860–18864, https://doi.org/10.1073/pnas.0806318105, 2008.

Mehrbach, C., Culberson, C. H., Hawley, J. E., and Pytkowicx, R. M.: Measurement of the Apparent Dissociation Constants of Carbonic Acid in Seawater At Atmospheric Pressure, Limnol. Oceanogr., 18, 897–907, https://doi.org/10.4319/lo.1973.18.6.0897, 1973.

Meinshausen, M., Smith, S. J., Calvin, K., Daniel, J. S., Kainuma, M. L. T., Lamarque, J., Matsumoto, K., Montzka, S. A., Raper, S. C. B., Riahi, K., Thomson, A., Velders, G. J. M., and van Vuuren, D. P. P.: The RCP greenhouse gas concentrations and their extensions from 1765 to 2300, Clim. Change, 109, 213–241, https://doi.org/10.1007/s10584-011-0156-z, 2011.

Metzl, N., Tilbrook, B., and Poisson, A.: The annual fCO_2 cycle and the air-sea CO_2 flux in the sub-Antarctic Ocean, Tellus B, 51, 849–861, https://doi.org/10.1034/j.1600-0889.1999.t01-3-00008.x, 1999.

Moreau, S., Schloss, I., Mostajir, B., Demers, S., Almandoz, G., Ferrario, M., and Ferreyra, G.: Influence of microbial community composition and metabolism on air-sea ΔpCO_2 variation off the

western Antarctic Peninsula, Mar. Ecol. Prog. Ser., 446, 45–59, https://doi.org/10.3354/meps09466, 2012.

Nelson, D. M., Smith, W. O. J., Gordon, L. I., and Huber, B. A.: Spring distributions of density, nutrients, and phytoplankton biomass in the ice edge zone of the Weddell-Scotia Sea, J. Geophys. Res.-Ocean., 92, 7181, https://doi.org/10.1029/JC092iC07p07181, 1987.

Orr, J. C., Fabry, V. J., Aumont, O., Bopp, L., Doney, S. C., Feely, R. A., Gnanadesikan, A., Gruber, N., Ishida, A., Joos, F., Key, R. M., Lindsay, K., Maier-Reimer, E., Matear, R., Monfray, P., Mouchet, A., Najjar, R. G., Plattner, G.-K., Rodgers, K. B., Sabine, C. L., Sarmiento, J. L., Schlitzer, R., Slater, R. D., Totterdell, I. J., Weirig, M.-F., Yamanaka, Y., and Yool, A.: Anthropogenic ocean acidification over the twenty-first century and its impact on calcifying organisms, Nature, 437, 681–686, https://doi.org/10.1038/nature04095, 2005.

Pasquer, B., Mongin, M., Johnston, N., and Wright, S.: Distribution of particulate organic matter (POM) in the Southern Ocean during BROKE-West (30°E - 80°E), Deep-Sea Res. Part II, 57, 779–793, https://doi.org/10.1016/j.dsr2.2008.12.040, 2010.

Paul, C., Matthiessen, B., and Sommer, U.: Warming, but not enhanced CO_2 concentration, quantitatively and qualitatively affects phytoplankton biomass, Mar. Ecol. Prog. Ser., 528, 39–51, https://doi.org/10.3354/meps11264, 2015.

Paulino, A. I., Egge, J. K., and Larsen, A.: Effects of increased atmospheric CO_2 on small and intermediate sized osmotrophs during a nutrient induced phytoplankton bloom, Biogeosciences, 5, 739–748, https://doi.org/10.5194/bg-5-739-2008, 2008.

Pearce, I., Davidson, A., Bell, E., and Wright, S.: Seasonal changes in the concentration and metabolic activity of bacteria and viruses at an Antarctic coastal site, Aquat. Microb. Ecol., 47, 11–23, https://doi.org/10.3354/ame047011, 2007.

Pearce, I., Davidson, A. T., Thomson, P. G., Wright, S., and van den Enden, R.: Marine microbial ecology off East Antarctica (30–80° E): Rates of bacterial and phytoplankton growth and grazing by heterotrophic protists, Deep-Sea Res. Part II, 57, 849–862, https://doi.org/10.1016/j.dsr2.2008.04.039, 2010.

Perrin, R. A., Lu, P., and Marchant, H. J.: Seasonal variation in marine phytoplankton and ice algae at a shallow Antarctic coastal site, Hydrobiologia, 146, 33–46, https://doi.org/10.1007/BF00007575, 1987.

Petrou, K., Kranz, S. A., Trimborn, S., Hassler, C. S., Ameijeiras, S. B., Sackett, O., Ralph, P. J., and Davidson, A. T.: Southern Ocean phytoplankton physiology in a changing climate, J. Plant Physiol., 203, 135–150, https://doi.org/10.1016/j.jplph.2016.05.004, 2016.

Piontek, J., Borchard, C., Sperling, M., Schulz, K. G., Riebesell, U., and Engel, A.: Response of bacterioplankton activity in an Arctic fjord system to elevated pCO_2: results from a mesocosm perturbation study, Biogeosciences, 10, 297–314, https://doi.org/10.5194/bg-10-297-2013, 2013.

Platt, T., Gallegos, C. L., and Harrison, W. G.: Photoinibition of photosynthesis in natural assemblages of marine phytoplankton, J. Mar. Res., 38, 687–701, 1980.

Polimene, L., Sailley, S., Clark, D., Mitra, A., and Allen, J. I.: Biological or microbial carbon pump? The role of phytoplankton stoichiometry in ocean carbon sequestration, J. Plankton Res., 39, 180–186, https://doi.org/10.1093/plankt/fbw091, 2016.

R Core Team: R: A Language and Environment for Statistical Computing, R Foundation for Statistical Computing, Vienna, Austria, https://www.R-project.org/ (last access: 11 December 2017), 2016.

Raven, J. A.: Physiology of inorganic C acquisition and implications for resource use efficiency by marine phytoplankton: relation to increased CO_2 and temperature, Plant, Cell Environ., 14, 779–794, https://doi.org/10.1111/j.1365-3040.1991.tb01442.x, 1991.

Raven, J. A. and Falkowski, P. G.: Oceanic sinks for atmospheric CO_2, Plant, Cell Environ., 22, 741–755, https://doi.org/10.1046/j.1365-3040.1999.00419.x, 1999.

Raven, J. A., Caldeira, K., Elderfield, H., Hoegh-Guldberg, O., Liss, P., Riebesell, U., Shepherd, J., Turley, C., and Watson, A.: Ocean acidification due to increasing atmospheric carbon dioxide, Tech. Rep. June, The Royal Society, 2005.

Regaudie-de Gioux, A., Lasternas, S., Agustí, S., Duarte, C. M., and Benitez, N. G.: Comparing marine primary production estimates through different methods and development of conversion equations, Front. Mar. Sci., 1, 1–14, https://doi.org/10.3389/fmars.2014.00019, 2014.

Riebesell, U.: Effects of CO_2 Enrichment on Marine Phytoplankton, J. Oceanogr., 60, 719–729, https://doi.org/10.1007/s10872-004-5764-z, 2004.

Riebesell, U., Schulz, K. G., Bellerby, R. G. J., Botros, M., Fritsche, P., Meyerhöfer, M., Neill, C., Nondal, G., Oschlies, A., Wohlers, J., and Zöllner, E.: Enhanced biological carbon consumption in a high CO_2 ocean, Nature, 450, 545–548, https://doi.org/10.1038/nature06267, 2007.

Riebesell, U., Gattuso, J.-P., Thingstad, T. F., and Middelburg, J. J.: Preface "Arctic ocean acidification: pelagic ecosystem and biogeochemical responses during a mesocosm study", Biogeosciences, 10, 5619–5626, https://doi.org/10.5194/bg-10-5619-2013, 2013.

Riley, G. A.: Phytoplankton of the North Central Sargasso Sea, 1950-521, Limnol. Oceanogr., 2, 252–270, https://doi.org/10.1002/lno.1957.2.3.0252, 1957.

Ritchie, R. J.: Consistent sets of spectrophotometric chlorophyll equations for acetone, methanol and ethanol solvents, Photosynth. Res., 89, 27–41, https://doi.org/10.1007/s11120-006-9065-9, 2006.

Roden, N. P., Shadwick, E. H., Tilbrook, B., and Trull, T. W.: Annual cycle of carbonate chemistry and decadal change in coastal Prydz Bay, East Antarctica, Mar. Chem., 155, 135–147, https://doi.org/10.1016/j.marchem.2013.06.006, 2013.

Rost, B., Riebesell, U., Burkhardt, S., and Sültemeyer, D.: Carbon acquisition of bloom-forming marine phytoplankton, Limnol. Oceanogr., 48, 55–67, https://doi.org/10.4319/lo.2003.48.1.0055, 2003.

Sabine, C. L., Feely, R. A., Gruber, N., Key, R. M., Lee, K., Bullister, J. L., Wanninkhof, R., Wong, C. S., Wallace, D. W. R., Tilbrook, B., Millero, F. J., Peng, T.-H., Kozyr, A., Ono, T., and Rios, A. F.: The Oceanic Sink for Anthropogenic CO_2, Science, 305, 367–371, https://doi.org/10.1126/science.1097403, 2004.

Satoh, A., Kurano, N., and Miyachi, S.: Inhibition of photosynthesis by intracellular carbonic anhydrase in microalgae under excess concentrations of CO_2, Photosynth. Res., 68, 215–224, https://doi.org/10.1023/A:1012980223847, 2001.

Schaum, C. E. and Collins, S.: Plasticity predicts evolution in a marine alga, P. R. Soc. B Biol. Sci., 281, 1793, https://doi.org/10.1098/rspb.2014.1486, 2014.

Schaum, E., Rost, B., Millar, A. J., and Collins, S.: Variation in plastic responses of a globally distributed picoplankton species to ocean acidification, Nat. Clim. Change, 3, 298–302, https://doi.org/10.1038/nclimate1774, 2012.

Schreiber, U.: Pulse-Amplitude-Modulation (PAM) Fluorometry and Saturation Pulse Method: An Overview, in: Chlorophyll a Fluorescence, edited by: Papageorgiou, G. C. and Govindjee, 279–319, Springer Netherlands, Dordrecht, https://doi.org/10.1007/978-1-4020-3218-9_11, 2004.

Schulz, K. G., Bellerby, R. G. J., Brussaard, C. P. D., Büdenbender, J., Czerny, J., Engel, A., Fischer, M., Koch-Klavsen, S., Krug, S. A., Lischka, S., Ludwig, A., Meyerhöfer, M., Nondal, G., Silyakova, A., Stuhr, A., and Riebesell, U.: Temporal biomass dynamics of an Arctic plankton bloom in response to increasing levels of atmospheric carbon dioxide, Biogeosciences, 10, 161–180, https://doi.org/10.5194/bg-10-161-2013, 2013.

Schulz, K. G., Bach, L. T., Bellerby, R. G. J., Bermúdez, R., Büdenbender, J., Boxhammer, T., Czerny, J., Engel, A., Ludwig, A., Meyerhöfer, M., Larsen, A., Paul, A. J., Sswat, M., and Riebesell, U.: Phytoplankton Blooms at Increasing Levels of Atmospheric Carbon Dioxide: Experimental Evidence for Negative Effects on Prymnesiophytes and Positive on Small Picoeukaryotes, Front. Mar. Sci., 4, 1–18, https://doi.org/10.3389/fmars.2017.00064, 2017.

Shi, D., Xu, Y., and Morel, F. M. M.: Effects of the pH/pCO_2 control method on medium chemistry and phytoplankton growth, Biogeosciences, 6, 1199–1207, https://doi.org/10.5194/bg-6-1199-2009, 2009.

Shi, Q., Xiahou, W., and Wu, H.: Photosynthetic responses of the marine diatom *Thalassiosira pseudonana* to CO_2-induced seawater acidification, Hydrobiologia, 788, 361–369, https://doi.org/10.1007/s10750-016-3014-1, 2017.

Silsbe, G. M. and Malkin, S. Y.: phytotools: Phytoplankton Production Tools, https://CRAN.R-project.org/package=phytotools (last access: 11 December 2017), R package version 1.0, 2015.

Simon, M. and Azam, F.: Protein content and protein synthesis rates of planktonic marine bacteria, Mar. Ecol. Prog. Ser., 51, 201–213, https://doi.org/10.3354/meps051201, 1989.

Smith, W. O. and Nelson, D. M.: Importance of Ice Edge Phytoplankton Production in the Southern Ocean, BioScience, 36, 251–257, https://doi.org/10.2307/1310215, 1986.

Sobrino, C., Ward, M. L., and Neale, P. J.: Acclimation to elevated carbon dioxide and ultraviolet radiation in the diatom *Thalassiosira pseudonana*: Effects on growth, photosynthesis, and spectral sensitivity of photoinhibition, Limnol. Oceanogr., 53, 494–505, https://doi.org/10.4319/lo.2008.53.2.0494, 2008.

Sommer, U., Paul, C., and Moustaka-Gouni, M.: Warming and Ocean Acidification Effects on Phytoplankton—From Species Shifts to Size Shifts within Species in a Mesocosm Experiment, PLoS One, 10, e0125239, https://doi.org/10.1371/journal.pone.0125239, 2015.

Sperling, M., Piontek, J., Gerdts, G., Wichels, A., Schunck, H., Roy, A.-S., La Roche, J., Gilbert, J., Nissimov, J. I., Bittner, L., Romac, S., Riebesell, U., and Engel, A.: Effect of elevated CO_2 on the dynamics of particle-attached and free-living bacterioplankton communities in an Arctic fjord, Biogeosciences, 10, 181–191, https://doi.org/10.5194/bg-10-181-2013, 2013.

Spilling, K., Paul, A. J., Virkkala, N., Hastings, T., Lischka, S., Stuhr, A., Bermúdez, R., Czerny, J., Boxhammer, T., Schulz, K. G., Ludwig, A., and Riebesell, U.: Ocean acidification decreases plankton respiration: evidence from a mesocosm experiment, Biogeosciences, 13, 4707–4719, https://doi.org/10.5194/bg-13-4707-2016, 2016.

Steemann Nielsen, E.: The Use of Radio-active Carbon (C^{14}) for Measuring Organic Production in the Sea, ICES J. Mar. Sci., 18, 117–140, https://doi.org/10.1093/icesjms/18.2.117, 1952.

Takahashi, T., Sutherland, S. C., Wanninkhof, R., Sweeney, C., Feely, R. A., Chipman, D. W., Hales, B., Friederich, G., Chavez, F., Sabine, C., Watson, A., Bakker, D. C., Schuster, U., Metzl, N., Yoshikawa-Inoue, H., Ishii, M., Midorikawa, T., Nojiri, Y., Körtzinger, A., Steinhoff, T., Hoppema, M., Olafsson, J., Arnarson, T. S., Tilbrook, B., Johannessen, T., Olsen, A., Bellerby, R., Wong, C., Delille, B., Bates, N., and de Baar, H. J.: Climatological mean and decadal change in surface ocean pCO_2, and net sea–air CO_2 flux over the global oceans, Deep-Sea Res. Part II, 56, 554–577, https://doi.org/10.1016/j.dsr2.2008.12.009, 2009.

Takahashi, T., Sweeney, C., Hales, B., Chipman, D., Newberger, T., Goddard, J., Iannuzzi, R., and Sutherland, S.: The Changing Carbon Cycle in the Southern Ocean, Oceanography, 25, 26–37, https://doi.org/10.5670/oceanog.2012.71, 2012.

Tanaka, T., Alliouane, S., Bellerby, R. G. B., Czerny, J., de Kluijver, A., Riebesell, U., Schulz, K. G., Silyakova, A., and Gattuso, J.-P.: Effect of increased pCO_2 on the planktonic metabolic balance during a mesocosm experiment in an Arctic fjord, Biogeosciences, 10, 315–325, https://doi.org/10.5194/bg-10-315-2013, 2013.

Taylor, A. R., Brownlee, C., and Wheeler, G. L.: Proton channels in algae: reasons to be excited, Trends Plant Sci., 17, 675–684, https://doi.org/10.1016/j.tplants.2012.06.009, 2012.

Tew, K. S., Kao, Y.-C., Ko, F.-C., Kuo, J., Meng, P.-J., Liu, P.-J., and Glover, D. C.: Effects of elevated CO_2 and temperature on the growth, elemental composition, and cell size of two marine diatoms: potential implications of global climate change, Hydrobiologia, 741, 79–87, https://doi.org/10.1007/s10750-014-1856-y, 2014.

Thomson, P., Davidson, A., and Maher, L.: Increasing CO_2 changes community composition of pico- and nano-sized protists and prokaryotes at a coastal Antarctic site, Mar. Ecol. Prog. Ser., 554, 51–69, https://doi.org/10.3354/meps11803, 2016.

Torstensson, A., Hedblom, M., Mattsdotter Björk, M., Chierici, M., and Wulff, A.: Long-term acclimation to elevated pCO_2 alters carbon metabolism and reduces growth in the Antarctic diatom *Nitzschia lecointei*, P. R. Soc. B, 282, 20151513, https://doi.org/10.1098/rspb.2015.1513, 2015.

Tortell, P. D. and Morel, F. M. M.: Sources of inorganic carbon for phytoplankton in the eastern Subtropical and Equatorial Pacific Ocean, Limnol. Oceanogr., 47, 1012–1022, https://doi.org/10.4319/lo.2002.47.4.1012, 2002.

Tortell, P. D., Rau, G. H., and Morel, F. M. M.: Inorganic carbon acquisition in coastal Pacific phytoplankton communities, Limnol. Oceanogr., 45, 1485–1500, https://doi.org/10.4319/lo.2000.45.7.1485, 2000.

Tortell, P. D., Payne, C., Gueguen, C., Strzepek, R. F., Boyd, P. W., and Rost, B.: Inorganic carbon uptake by South-

ern Ocean phytoplankton, Limnol. Oceanogr., 53, 1266–1278, https://doi.org/10.4319/lo.2008.53.4.1266, 2008a.

Tortell, P. D., Payne, C. D., Li, Y., Trimborn, S., Rost, B., Smith, W. O. J., Riesselman, C., Dunbar, R. B., Sedwick, P., and DiTullio, G. R.: CO_2 sensitivity of Southern Ocean phytoplankton, Geophys. Res. Lett., 35, L04605, https://doi.org/10.1029/2007GL032583, 2008b.

Tortell, P. D., Trimborn, S., Li, Y., Rost, B., and Payne, C. D.: Inorganic carbon utilization by Ross Sea phytoplankton across natural and experimental CO_2 gradients, J. Phycol., 46, 433–443, https://doi.org/10.1111/j.1529-8817.2010.00839.x, 2010.

Tortell, P. D., Asher, E. C., Ducklow, H. W., Goldman, J. A. L., Dacey, J. W. H., Grzymski, J. J., Young, J. N., Kranz, S. A., Bernard, K. S., and Morel, F. M. M.: Metabolic balance of coastal Antarctic waters revealed by autonomous pCO_2 and ΔO_2/Ar measurements, Geophys. Res. Lett., 41, 6803–6810, https://doi.org/10.1002/2014GL061266, 2014.

Trimborn, S., Brenneis, T., Sweet, E., and Rost, B.: Sensitivity of Antarctic phytoplankton species to ocean acidification: Growth, carbon acquisition, and species interaction, Limnol. Oceanogr., 58, 997–1007, https://doi.org/10.4319/lo.2013.58.3.0997, 2013.

Trimborn, S., Thoms, S., Petrou, K., Kranz, S. A., and Rost, B.: Photophysiological responses of Southern Ocean phytoplankton to changes in CO_2 concentrations: Short-term versus acclimation effects, J. Exp. Mar. Bio. Ecol., 451, 44–54, https://doi.org/10.1016/j.jembe.2013.11.001, 2014.

van de Waal, D. B., Verschoor, A. M., Verspagen, J. M., van Donk, E., and Huisman, J.: Climate-driven changes in the ecological stoichiometry of aquatic ecosystems, Front. Ecol. Environ., 8, 145–152, https://doi.org/10.1890/080178, 2010.

Wang, Y., Zhang, R., Zheng, Q., Deng, Y., Van Nostrand, J. D., Zhou, J., and Jiao, N.: Bacterioplankton community resilience to ocean acidification: evidence from microbial network analysis, ICES J. Mar. Sci. J. du Cons., 73, 865–875, https://doi.org/10.1093/icesjms/fsv187, 2016.

Westwood, K., Thomson, P., van den Enden, R., Maher, L., Wright, S., and Davidson, A.: Ocean acidification impacts primary and bacterial production in Antarctic coastal waters during austral summer, J. Exp. Mar. Bio. Ecol., 498, 46–60, https://doi.org/10.1016/j.jembe.2017.11.003, 2018.

Westwood, K. J., Brian Griffiths, F., Meiners, K. M., and Williams, G. D.: Primary productivity off the Antarctic coast from 30°–80° E; BROKE-West survey, 2006, Deep-Sea Res. Part II, 57, 794–814, https://doi.org/10.1016/j.dsr2.2008.08.020, 2010.

Wright, S. W., van den Enden, R. L., Pearce, I., Davidson, A. T., Scott, F. J., and Westwood, K. J.: Phytoplankton community structure and stocks in the South ern Ocean (30–80° E) determined by CHEMTAX analysis of HPLC pigment signatures, Deep-Sea Res. Part II, 57, 758–778, https://doi.org/10.1016/j.dsr2.2009.06.015, 2010.

Wu, Y., Gao, K., and Riebesell, U.: CO_2-induced seawater acidification affects physiological performance of the marine diatom *Phaeodactylum tricornutum*, Biogeosciences, 7, 2915–2923, https://doi.org/10.5194/bg-7-2915-2010, 2010.

Young, J., Kranz, S., Goldman, J., Tortell, P., and Morel, F.: Antarctic phytoplankton down-regulate their carbon-concentrating mechanisms under high CO_2 with no change in growth rates, Mar. Ecol. Prog. Ser., 532, 13–28, https://doi.org/10.3354/meps11336, 2015.

Zheng, Y., Giordano, M., and Gao, K.: Photochemical responses of the diatom *Skeletonema costatum* grown under elevated CO_2 concentrations to short-term changes in pH, Aquat. Biol., 23, 109–118, https://doi.org/10.3354/ab00619, 2015.

Appendix C

Supplementary data for Chapter 2

Table A3.1: Mean carbonate chemistry conditions in minicosms

Tank	fCO_2 (µatm)	pH_T	DIC (µmol kg^{-1})	PA (µmol kg^{-1}
1	343 ± 30	8.10 ± 0.04	2188 ± 6	2324 ± 11
2	506 ± 43	7.94 ± 0.03	2243 ± 8	2325 ± 10
3	634 ± 63	7.85 ± 0.04	2270 ± 5	2325 ± 12
4	953 ± 148	7.69 ± 0.07	2314 ± 11	2321 ± 11
5	1140 ± 112	7.61 ± 0.04	2337 ± 5	2320 ± 10
6	1641 ± 140	7.45 ± 0.04	2377 ± 8	2312 ± 10

Data are mean ± one standard deviation of triplicate pseudoreplicate measurements

Table A3.2: Initial conditions of seawater sampled from Prydz Bay, Antarctica

Condition	Value
fCO_2, µatm	356 ± 6
pH_T	8.08
DIC, µmol kg^{-1}	2187 ± 6
PA, µmol kg^{-1}	2317 ± 6
Temperature, °C	-1.03 ± 0.17
Salinity	34.3
NOx, µM	26.19 ± 0.74
SRP, µM	1.74 ± 0.02
Silicate, µM	60.75 ± 0.91

Data are mean ± one standard deviation of all six minicosm measurements

Table A3.3: Average light irradiance (µmol photons m^{-2} s^{-1}) in minicosms

Tank	fCO_2 (µatm)	Low light	Medium light	High light
1	343	0.94	22.02	97.41
2	506	0.60	15.95	59.68
3	634	1.04	26.41	103.24
4	953	1.19	22.53	118.33
5	1140	0.71	21.44	71.51
6	1641	0.90	22.02	92.95

Low light: quarter CT blue filter, two 90% ND filters, light-scattering filter
Medium light: quarter CT blue filter, one 60% ND filter, light-scattering filter
High light: one quarter CT blue filter, light-scattering filter

Table A3.4: ANOVA table for trends in CO_2 treatments over time for Chl *a*

	Df	Sum Sq	Mean Sq	F value	Pr(>F)
Day	1	12304.2	12304.2	1802.5	**<0.01**
I(Day^2)	1	2214.5	2214.5	324.4	**<0.01**
$f\,CO_2$	5	267.0	53.4	7.8	**<0.01**
Day:$f\,CO_2$	5	186.0	37.2	5.5	**<0.01**
Residuals	23	157.0	6.8		

Bold text denotes significant p-values (<0.05)

Table A3.5: ANOVA table for trends in CO_2 treatments over time for $GPP_{^{14}C}$

	Df	Sum Sq	Mean Sq	F value	Pr(>F)
Day	1	6405.2	6405.2	1271.6	**<0.01**
I(Day^2)	1	1056.1	1056.1	209.7	**<0.01**
$f\,CO_2$	5	211.9	42.4	8.4	**<0.01**
Day:$f\,CO_2$	5	124.6	24.9	4.9	**<0.01**
Residuals	23	115.9	5.0		

Bold text denotes significant p-values (<0.05)

Table A3.6: ANOVA table for trends in CO_2 treatments over time for bacterial abundance

	Df	Sum Sq	Mean Sq	F value	Pr(>F)
Day	1	2.1×10^{18}	2.1×10^{18}	1470.6	**<0.01**
I(Day^2)	1	4.3×10^{16}	4.3×10^{16}	30.1	**<0.01**
$f\,CO_2$	5	2.0×10^{17}	4.1×10^{16}	28.1	**<0.01**
Day:$f\,CO_2$	5	7.1×10^{16}	1.4×10^{16}	9.8	**<0.01**
Residuals	185	2.7×10^{17}	1.5×10^{15}		

Bold text denotes significant p-values (<0.05)

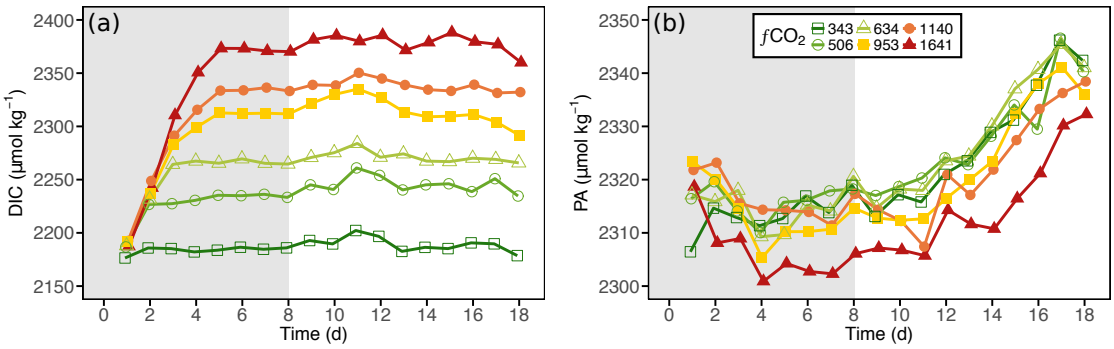

Figure A3.1: (a) Dissolved inorganic carbon (DIC) and (b) practical alkalinity (PA) conditions within each of the minicosm treatments over time. Grey shading indicates CO_2 and light acclimation period.

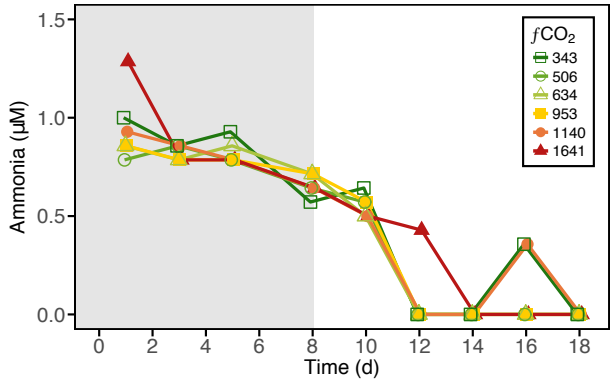

Figure A3.2: Ammonia concentration in each of the minicosm treatments over time. Grey shading indicates CO_2 and light acclimation period.

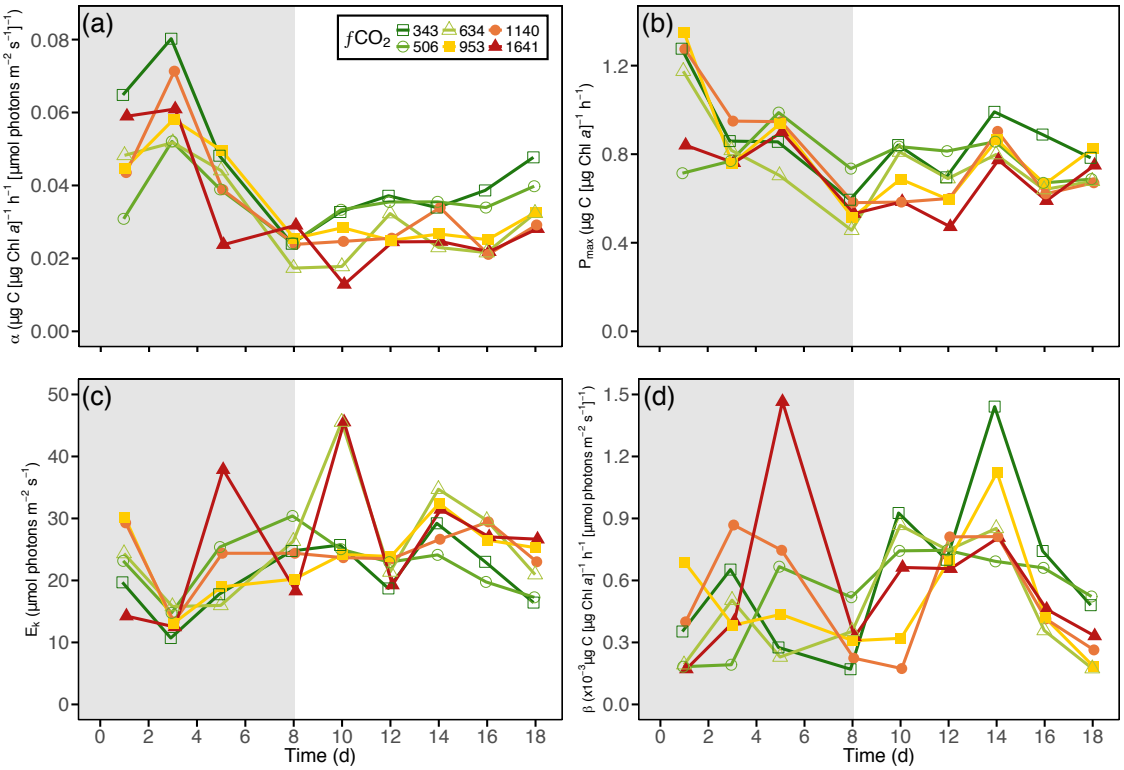

Figure A3.3: Photosynthetic parameters from ^{14}C-derived photosynthesis versus irradiance (PE) curves from each of the minicosm treatments over time. (a) Maximum photosynthetic efficiency (α), (b) maximum photosynthetic rate (P_{max}), (c) saturating irradiance (E_k) and (d) photoinhibition rate (β). Grey shading indicates CO_2 and light acclimation period.

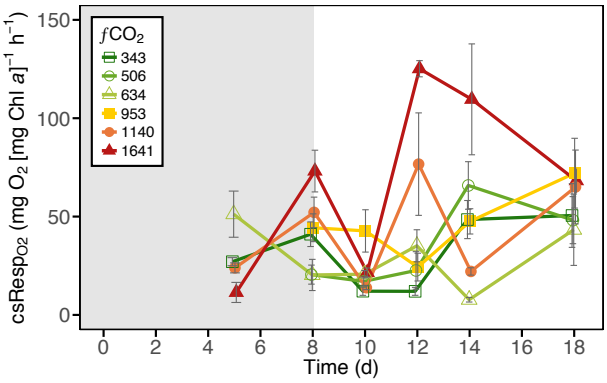

Figure A3.4: O_2-derived Chl *a*-specific community respiration ($csResp_{O_2}$) within each of the minicosm treatments over time. Error bars display one standard deviation of pseudoreplicate samples. Grey shading indicates CO_2 and light acclimation period.

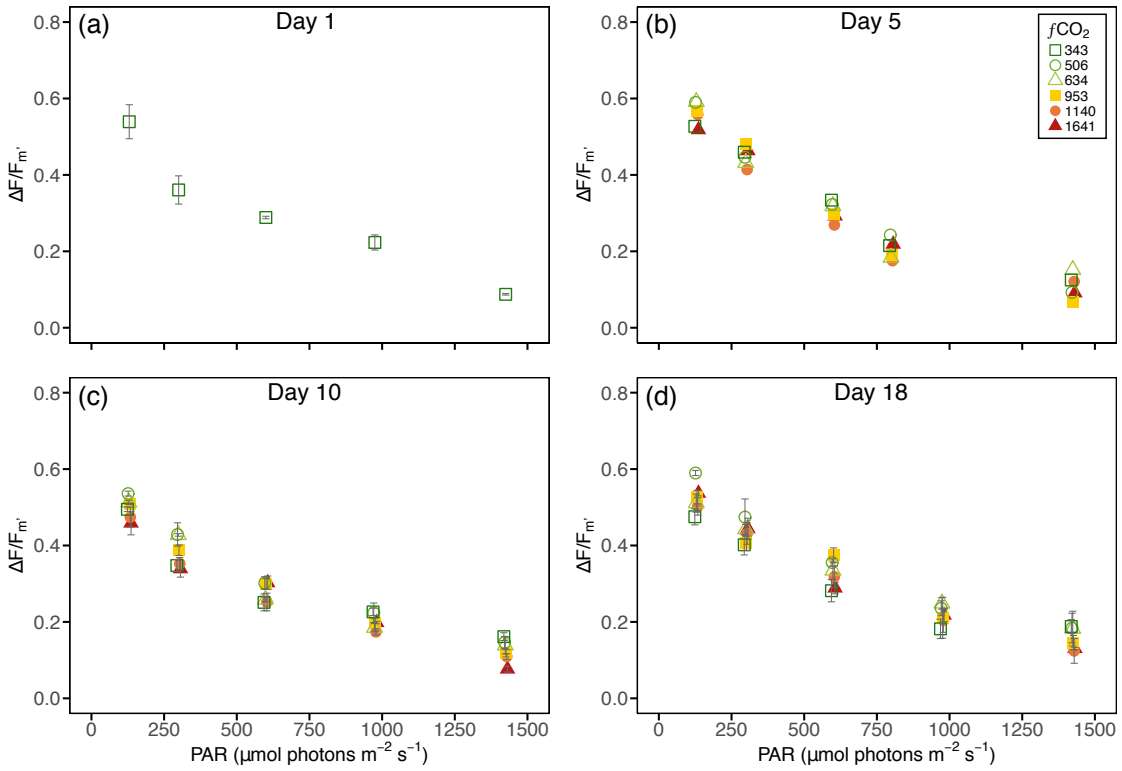

Figure A3.5: Effective quantum yield ($\Delta F_v/F_m$) within minicosm treatments on days 1, 5, 10, and 18. Error bars display one standard deviation of pseudoreplicate samples.

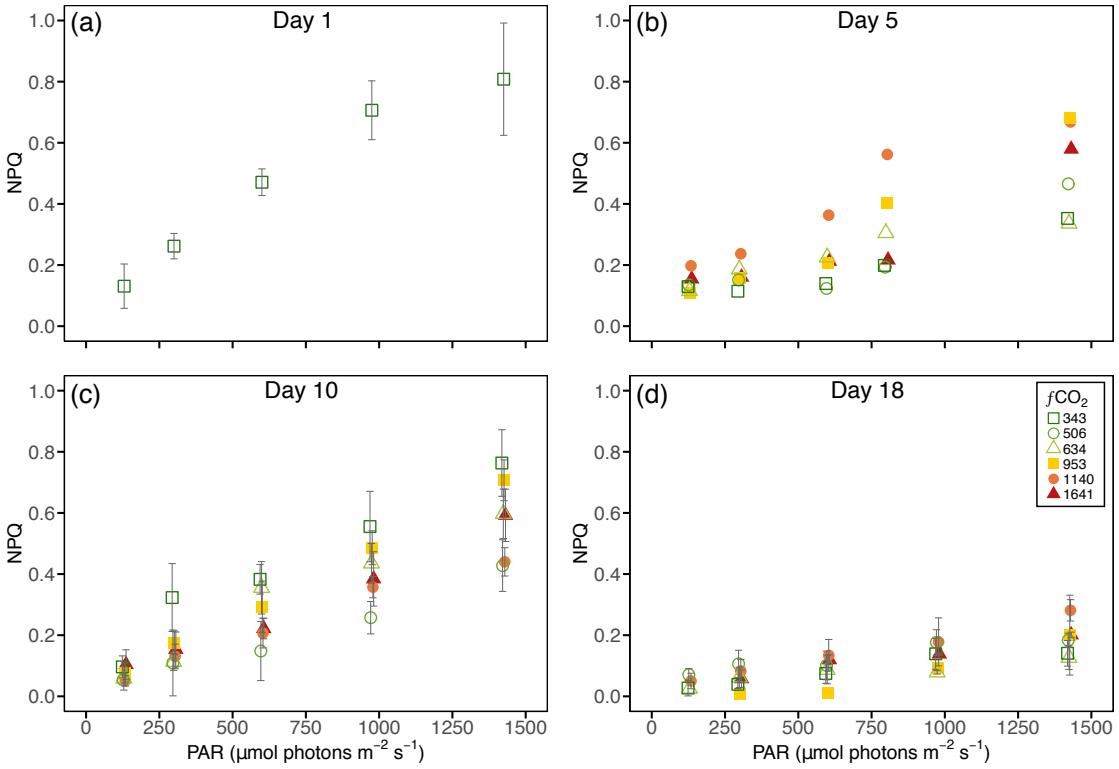

Figure A3.6: Non-photochemical quenching (NPQ) within minicosm treatments on days 1, 5, 10, and 18. Error bars display one standard deviation of pseudoreplicate samples.

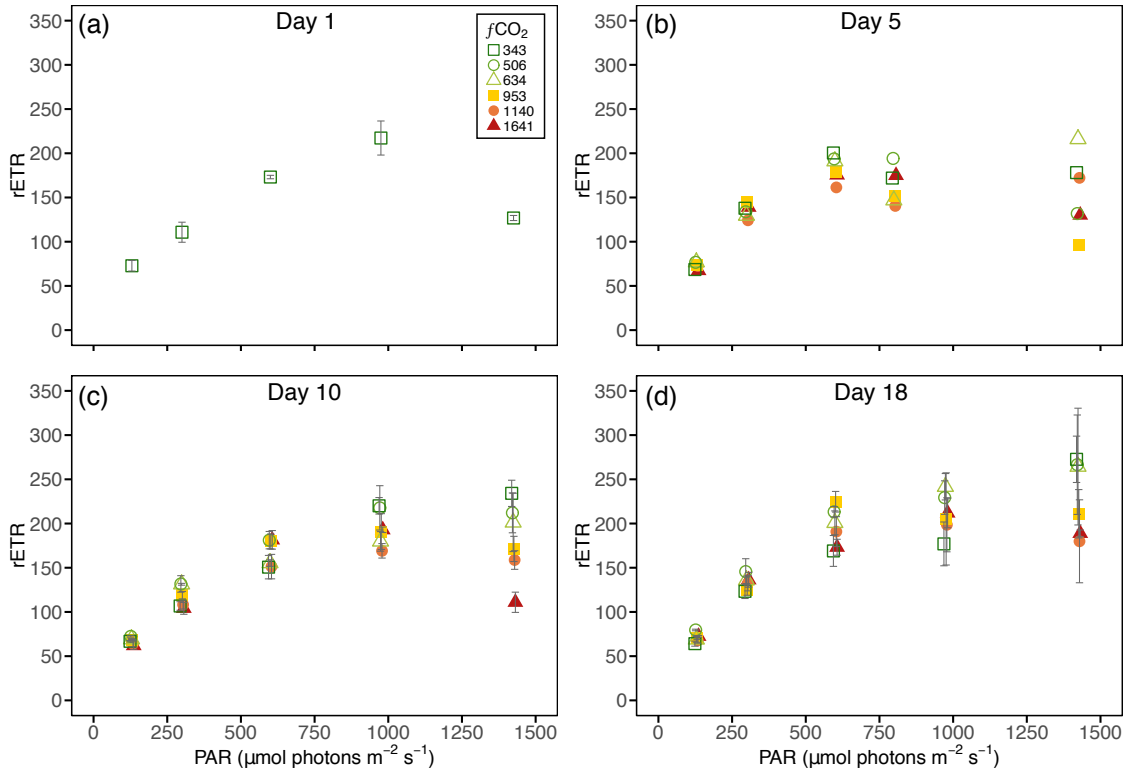

Figure A3.7: Relative electron transport rate (rETR) within minicosm treatments on days 1, 5, 10, and 18. Error bars display one standard deviation of pseudoreplicate samples.

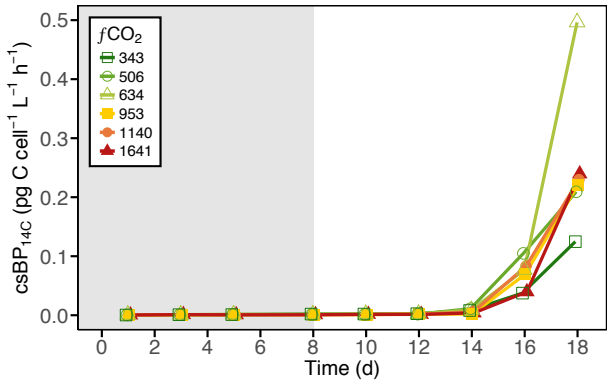

Figure A3.8: ^{14}C-derived cell-specific bacterial productivity (csBP$_{^{14}C}$) within each of the minicosm treatments over time. Grey shading indicates CO_2 and light acclimation period.

Appendix D

Supplementary data for Chapter 3

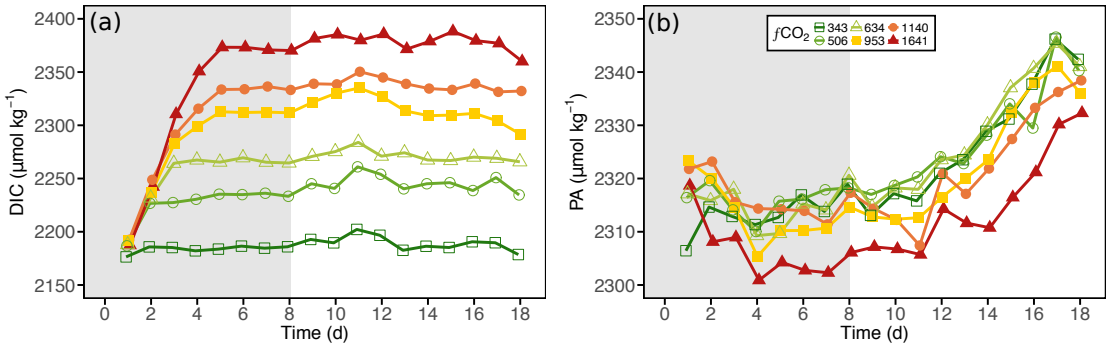

Figure A4.1: The (a) dissolved inorganic carbon (DIC), and (b) practical alkalinity (PA) carbonate chemistry conditions in each of the minicosm treatments over time. Grey shading indicates CO_2 and light acclimation period.

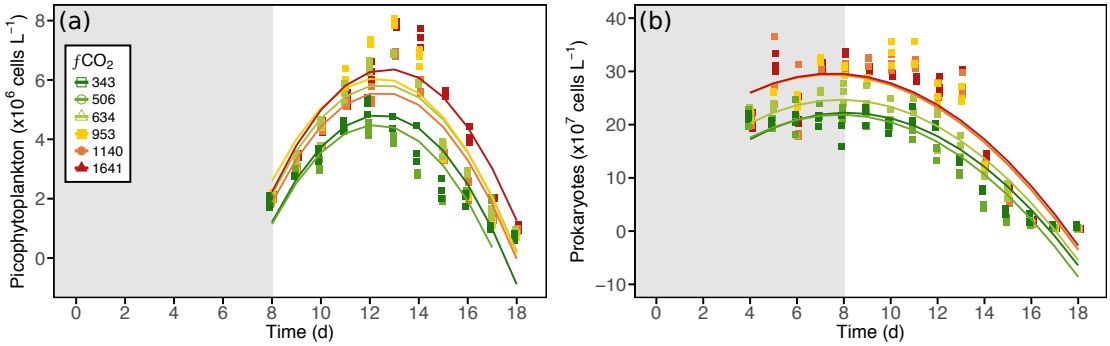

Figure A4.2: Model fit for (a) picophytoplankton and (b) prokaryote abundance in each of the minicosm treatments over time.

Table A4.1: Initial conditions of seawater sampled from Prydz Bay, Antarctica

Condition	Value
$f\,CO_2$, µatm	356 ± 6
pH_T	8.08
DIC, µmol kg^{-1}	2187 ± 6
PA, µmol kg^{-1}	2317 ± 6
Temperature, °C	-1.03 ± 0.17
Salinity	34.3
NOx, µM	26.19 ± 0.74
SRP, µM	1.74 ± 0.02
Silicate, µM	60.75 ± 0.91

Data are mean ± one standard deviation of all six minicosm measurements

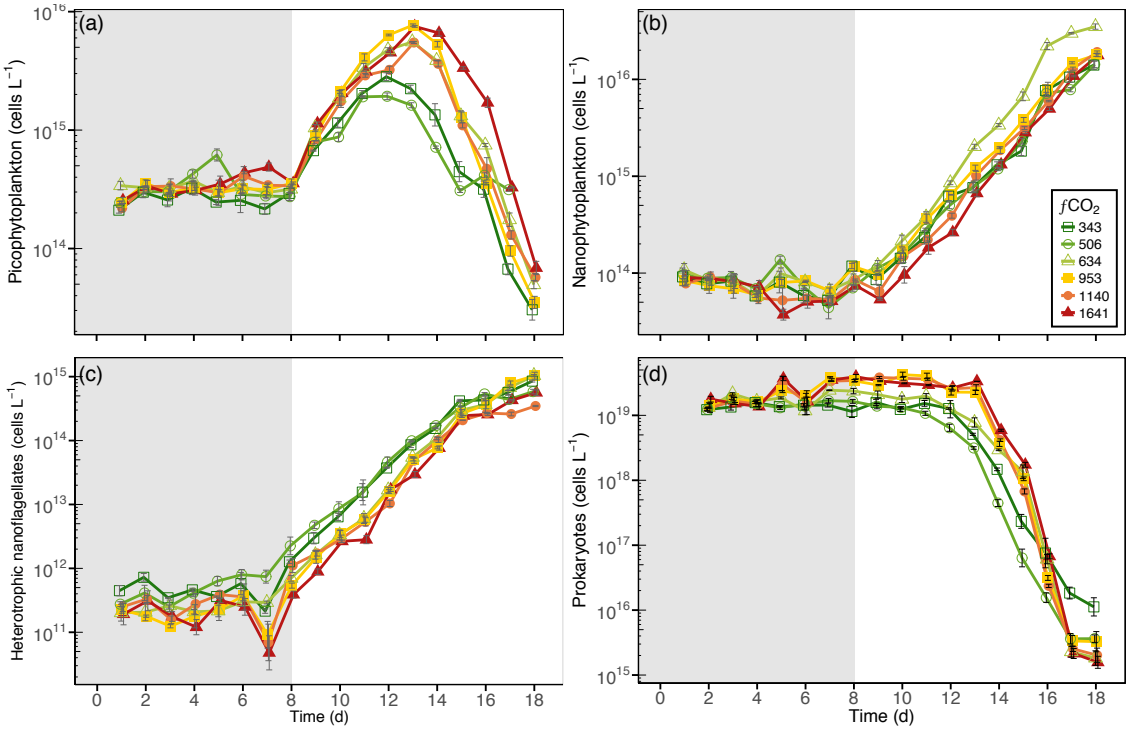

Figure A4.3: Log-transformed abundance of (a) picophytoplankton, (b) nanophytoplankton, (c) heterotrophic nanoflagellates, and (d) prokaryotes in each of the minicosm treatments over time. Error bars display standard error of pseudoreplicate samples. Grey shading indicates CO_2 and light acclimation period.

Table A4.2: ANOVA table for trends in CO_2 treatment over time for picophytoplankton abundance

	Df	Sum Sq	Mean Sq	F value	Pr(>F)
Day	1	5.4×10^{13}	5.4×10^{13}	77.3	**<0.01**
I(Day^2)	1	4.8×10^{14}	4.8×10^{14}	686.1	**<0.01**
fCO$_2$	5	8.6×10^{13}	1.7×10^{13}	24.8	**<0.01**
Day:fCO$_2$	5	5.5×10^{12}	1.1×10^{12}	1.6	0.16
Residuals	182	1.3×10^{14}	6.9×10^{11}		

Bold text denotes significant p-values (<0.05).

Table A4.3: ANOVA table for trends in CO_2 treatment over time for nanophytoplankton abundance

	Df	Sum Sq	Mean Sq	F value	Pr(>F)
Day	1	2.5×10^{15}	2.5×10^{15}	3850.4	**<0.01**
I(Day^2)	1	1.0×10^{15}	1.0×10^{15}	1627.9	**<0.01**
fCO$_2$	5	7.2×10^{13}	1.4×10^{13}	22.4	**<0.01**
Day:fCO$_2$	5	9.9×10^{13}	2.0×10^{13}	31.0	**<0.01**
Residuals	311	2.0×10^{14}	6.3×10^{11}		

Bold text denotes significant p-values (<0.05).

Table A4.4: ANOVA table for trends in CO_2 treatment over time for heterotrophic nanoflagellate abundance

	Df	Sum Sq	Mean Sq	F value	Pr(>F)
Day	1	2.0×10^{14}	2.0×10^{14}	5832.7	**<0.01**
I(Day^2)	1	5.6×10^{13}	5.6×10^{13}	1630.0	**<0.01**
$f\,CO_2$	5	2.4×10^{12}	4.8×10^{11}	13.9	**<0.01**
Day:$f\,CO_2$	5	2.7×10^{12}	5.4×10^{11}	15.8	**<0.01**
Residuals	307	1.0×10^{13}	3.4×10^{10}		

Bold text denotes significant p-values (<0.05).

Table A4.5: ANOVA table for trends in CO_2 treatment over time for prokaryote abundance

	Df	Sum Sq	Mean Sq	F value	Pr(>F)
Day	1	1.9×10^{18}	1.9×10^{18}	1076.7	**<0.01**
I(Day^2)	1	6.4×10^{17}	6.4×10^{17}	363.5	**<0.01**
$f\,CO_2$	5	2.3×10^{17}	4.6×10^{16}	26.2	**<0.01**
Day:$f\,CO_2$	5	1.2×10^{16}	2.4×10^{15}	1.4	0.24
Residuals	256	4.5×10^{17}	1.7×10^{15}		

Bold text denotes significant p-values (<0.05).

Table A4.6: ANOVA table comparing trends of picophytoplankton growth rates with heterotrophic nanoflagellate abundance on day 13

	Estimate	Std. Error	t value	Pr(>t)
(Intercept)	2.7×10^{-1}	4.2×10^{-2}	6.5	**<0.01**
HNF	-9.1×10^{-3}	1.4×10^{-2}	-0.2	0.84

Residual standard error: 0.03 on 16 degrees of freedom
Multiple R-squared: 0.003, Adjusted R-squared: -0.06
F-statistic: 0.04 on 1 and 16 DF, p-value: 0.84

Bold text denotes significant p-values (<0.05). HNF; heterotrophic nanoflagellate.

Table A4.7: ANOVA table comparing trends of prokryote growth rates with heterotrophic nanoflagellate abundance on day 8

	Estimate	Std. Error	t value	Pr(>t)
(Intercept)	9.4×10^{-2}	2.1×10^{-2}	4.5	**<0.01**
HNF	-3.4×10^{-7}	1.3×10^{-7}	-2.7	**0.01**
Residual standard error: 0.03 on 16 degrees of freedom Multiple R-squared: 0.32, Adjusted R-squared: 0.28 F-statistic: 7.46 on 1 and 16 DF, p-value: **0.01**				

Bold text denotes significant p-values (<0.05). HNF; heterotrophic nanoflagellates.

Appendix E

Supplementary data for Chapter 4

Table A5.1: Randomised assignment of CO_2 treatments in cabinet

Position	1	2	3	4
Holding Tanks	3	2	4	1
Shelf 1	2	3	4	4
Shelf 2	3	4	1	1
Shelf 3	1	2	3	2

1: 276 µatm, 2: 381 µatm,
3: 668 µatm, 4: 1063 µatm.

Table A5.2: Average light irradiance received by each incubation vessel in µmol photons m^{-2} s^{-1}

Position	1	2	3	4
Shelf 1	24.92	23.26	24.92	27.41
Shelf 2	24.09	19.10	24.09	27.41
Shelf 3	21.59	19.10	25.75	24.09

Table A5.3: Initial conditions of 1:10 diluted L1 medium used in experiment

Condition	Value
fCO_2, µatm	278
pH_T	8.2
DIC, µmol kg^{-1}	2193
TA, µmol kg^{-1}	2384
Temperature, °C	0.5
Salinity	35
NO_3, µM	88.2
PO_4, µM	3.62
SiO_3, µM	21.2

Table A5.4: ANOVA table for trends in CO_2 treatment over time for cell abundance

	Df	Sum Sq	Mean Sq	F value	Pr(>F)
Day	1	5.90×10^{11}	5.90×10^{11}	164.12	**<0.01**
I(Day^2)	1	6.36×10^{10}	6.36×10^{10}	17.70	**<0.01**
$f\,CO_2$	3	1.46×10^{10}	4.86×10^{9}	1.35	0.26
Day:$f\,CO_2$	3	9.74×10^{9}	3.25×10^{9}	0.90	0.44
Residuals	87	3.13×10^{11}	3.59×10^{9}		

Bold text denotes significant p-values (<0.05).

Table A5.5: ANOVA table for trends in CO_2 treatment over time for chlorophyll *a*

	Df	Sum Sq	Mean Sq	F value	Pr(>F)
Day	1	102.31	102.31	139.82	**<0.01**
I(Day^2)	1	14.62	14.62	19.99	**<0.01**
$f\,CO_2$	3	1.91	0.64	0.87	0.46
Day:$f\,CO_2$	3	1.43	0.48	0.65	0.59
Residuals	62	45.37	0.73		

Bold text denotes significant p-values (<0.05).

Table A5.6: ANOVA table for trends in CO_2 treatment over time for Chl *a*-specific primary productivity

	Df	Sum Sq	Mean Sq	F value	Pr(>F)
Day	1	54.58	54.58	14.13	**<0.01**
I(Day^2)	1	249.47	249.47	64.60	**<0.01**
$f\,CO_2$	3	12.02	4.01	1.04	0.38
Day:$f\,CO_2$	3	1.67	0.56	0.14	0.93
Residuals	62	239.43	3.86		

Bold text denotes significant p-values (<0.05).

Table A5.7: ANOVA table for trends in CO_2 treatment over time for gross primary productivity

	Df	Sum Sq	Mean Sq	F value	Pr(>F)
Day	1	1175.37	1175.37	107.342	**<0.01**
I(Day^2)	1	0.05	0.05	0.004	0.95
$f\,CO_2$	3	140.94	46.98	4.291	**0.01**
Day:$f\,CO_2$	3	75.31	25.10	2.293	0.09
Residuals	62	678.89	10.95		

Bold text denotes significant p-values (<0.05).

Table A5.8: ANOVA table for trends in CO_2 treatment over time for F_v/F_m

	Df	Sum Sq	Mean Sq	F value	Pr(>F)
Day	1	0.003	0.003	1.90	0.17
I(Day^2)	1	0.013	0.013	7.67	**0.01**
$f\,CO_2$	3	0.002	0.001	0.38	0.77
Day:$f\,CO_2$	3	0.004	0.001	0.81	0.49
Residuals	51	0.089	0.002		

Bold text denotes significant p-values (<0.05).

Table A5.9: ANOVA table for trends in CO_2 treatment over time for α

	Df	Sum Sq	Mean Sq	F value	Pr(>F)
Day	1	0.15	0.15	10.11	**<0.01**
I(Day^2)	1	0.04	0.04	2.63	0.11
$f\,CO_2$	3	0.06	0.02	1.45	0.24
Day:$f\,CO_2$	3	0.09	0.03	1.95	0.13
Residuals	51	0.75	0.01		

Bold text denotes significant p-values (<0.05).

Table A5.10: ANOVA table for trends in CO_2 treatment over time for $rETR_{max}$

	Df	Sum Sq	Mean Sq	F value	Pr(>F)
Day	1	23268.1	23268.1	103.91	**<0.01**
I(Day^2)	1	66.7	66.7	0.30	0.59
$f\,CO_2$	3	189.0	63.0	0.28	0.84
Day:$f\,CO_2$	3	316.6	105.5	0.47	0.70
Residuals	51	11420.7	223.9		

Bold text denotes significant p-values (<0.05).

Table A5.11: ANOVA table for trends in CO_2 treatment over time for E_k

	Df	Sum Sq	Mean Sq	F value	Pr(>F)
Day	1	28519	28518.7	17.42	**<0.01**
I(Day^2)	1	850	850.4	0.52	0.47
$f\,CO_2$	3	2113	704.2	0.43	0.73
Day:$f\,CO_2$	3	4078	1359.3	0.83	0.48
Residuals	51	83476	1636.8		

Bold text denotes significant p-values (<0.05).

REFERENCES

Abbott, MR, Richman, JG, Letelier, RM, and Bartlett, JS (2000). The spring bloom in the Antarctic Polar Frontal Zone as observed from a mesoscale array of bio-optical sensors. *Deep Sea Research Part II: Topical Studies in Oceanography*, 47 (15-16):3285–3314. doi: 10.1016/S0967-0645(00)00069-2.

Aberle, N, Schulz, KG, Stuhr, A, Malzahn, AM, Ludwig, A, and Riebesell, U (2013). High tolerance of microzooplankton to ocean acidification in an Arctic coastal plankton community. *Biogeosciences*, 10 (3):1471–1481. doi: 10.5194/bg-10-1471-2013.

Ackley, S, Wadhams, P, Comiso, JC, and Worby, AP (2003). Decadal decrease of Antarctic sea ice extent inferred from whaling records revisited on the basis of historical and modern sea ice records. *Polar Research*, 22 (1):19–25. doi: 10.1111/j.1751-8369.2003.tb00091.x.

Ainley, DG, Wilson, PR, Barton, KJ, Ballard, G, Nur, N, and Karl, B (1998). Diet and foraging effort of Adélie penguins in relation to pack-ice conditions in the southern Ross Sea. *Polar Biology*, 20 (5):311–319. doi: 10.1007/s003000050308.

Alldredge, AL and Silver, MW (1988). Characteristics, dynamics and significance of marine snow. *Progress in Oceanography*, 20 (1):41–82. doi: 10.1016/0079-6611(88)90053-5.

Allgaier, M, Riebesell, U, Vogt, M, Thyrhaug, R, and Grossart, HP (2008). Coupling of heterotrophic bacteria to phytoplankton bloom development at different pCO_2 levels: a mesocosm study. *Biogeosciences*, 5 (4):1007–1022. doi: 10.5194/bg-5-1007-2008.

Anderson, RF, Barker, S, Fleisher, M, Gersonde, R, Goldstein, SL, Kuhn, G, *et al.* (2014). Biological response to millennial variability of dust and nutrient supply in the Subantarctic South Atlantic Ocean. *Philosophical Transactions of the Royal Society A: Mathematical, Physical and Engineering Sciences*, 372 (2019):20130054–20130054. doi: 10.1098/rsta.2013.0054.

Arar, EJ and Collins, GB (1997). Method 445.0: In Vitro Determination of Chlorophyll *a* and Pheophytin a in Marine and Freshwater Algae by Fluorescence. Tech. rep. Cincinnati: United

States Environmental Protection Agency, Office of Research and Development, National Exposure Research Laboratory, pp. 1–22.

Archer, SD, Leakey, RJG, Burkill, PH, and Sleigh, MA (1996). Microbial dynamics in coastal waters of East Antarctica: Herbivory by heterotrophic dinoflagellates. *Marine Ecology Progress Series*, 139 (1-3):239–255. doi: 10.3354/meps139239.

Ardelan, MV, Holm-Hansen, O, Hewes, CD, Reiss, CS, Silva, NS, Dulaiova, H, *et al.* (2010). Natural iron enrichment around the Antarctic Peninsula in the Southern Ocean. *Biogeosciences*, 7 (1):11–25. doi: 10.5194/bg-7-11-2010.

Armour, KC, Marshall, J, Scott, JR, Donohoe, A, and Newsom, ER (2016). Southern Ocean warming delayed by circumpolar upwelling and equatorward transport. *Nature Geoscience*, 9 (7):549–554. doi: 10.1038/ngeo2731.

Arrigo, KR, Robinson, DH, Worthen, DL, Dunbar, RB, DiTullio, GR, VanWoert, M, *et al.* (1999). Phytoplankton Community Structure and the Drawdown of Nutrients and CO_2 in the Southern Ocean. *Science*, 283 (5400):365–367. doi: 10.1126/science.283.5400.365.

Arrigo, KR, Worthen, DL, Lizotte, MP, Dixon, P, and Dieckmann, G (1997). Primary Production in Antarctic Sea Ice. *Science*, 276 (5311):394–7. doi: 10.1126/science.276.5311.394.

Arrigo, KR (2014). Sea Ice Ecosystems. *Annual Review of Marine Science*, 6 (1):439–467. doi: 10.1146/annurev-marine-010213-135103.

Arrigo, KR, DiTullio, GR, Dunbar, RB, Robinson, DH, VanWoert, M, Worthen, DL, *et al.* (2000). Phytoplankton taxonomic variability in nutrient utilization and primary production in the Ross Sea. *Journal of Geophysical Research: Oceans*, 105 (C4):8827–8846. doi: 10.1029/1998JC000289.

Arrigo, KR, van Dijken, GL, and Bushinsky, S (2008a). Primary production in the Southern Ocean, 1997-2006. *Journal of Geophysical Research: Oceans*, 113 (8):C08004. doi: 10.1029/2007JC004551.

Arrigo, KR, van Dijken, GL, and Strong, AL (2015). Environmental controls of marine productivity hot spots around Antarctica. *Journal of Geophysical Research: Oceans*, 120 (8):5545–5565. doi: 10.1002/2015JC010888.

Arrigo, KR, van Dijken, G, and Long, M (2008b). Coastal Southern Ocean: A strong anthropogenic CO_2 sink. *Geophysical Research Letters*, 35 (21):L21602. doi: 10.1029/2008GL035624.

Arrigo, KR, Worthen, D, Schnell, A, and Lizotte, MP (1998a). Primary production in Southern Ocean waters. *Journal of Geophysical Research: Oceans*, 103 (C8):15587–15600. doi: 10.1029/98JC00930.

Arrigo, KR, Mock, T, and Lizotte, MP (2010). Primary Producers and Sea Ice. *Sea Ice*. Ed. by DN Thomas and G Dieckmann. 2nd ed. Ames, Iowa: Blackwell Publishing Ltd. Chap. 8, p 283–326.

Arrigo, KR and Thomas, DN (2004). Large scale importance of sea ice biology in the Southern Ocean. *Antarctic Science*, 16 (4):471–486. doi: 10.1017/S0954102004002263.

Arrigo, KR and van Dijken, GL (2003). Phytoplankton dynamics within 37 Antarctic coastal polynya systems. *Journal of Geophysical Research: Oceans*, 108 (C8):27-1–27-18. doi: 10.1029/2002JC001739.

Arrigo, KR and van Dijken, GL (2004). Annual changes in sea-ice, chlorophyll *a*, and primary production in the Ross Sea, Antarctica. *Deep Sea Research Part II: Topical Studies in Oceanography*, 51 (1-3):117–138. doi: 10.1016/j.dsr2.2003.04.003.

Arrigo, K, Worthen, D, Dixon, P, and Lizotte, MP (1998b). Primary Productivity of Near Surface Communities Within Antarctic Pack Ice. *Antarctic Sea Ice: Biological Processes, Interactions and Variability*. Ed. by MP Lizotte and KR Arrigo. Washington, D.C.: American Geophysical Union, p 23–43.

Assmy, P, Smetacek, V, Montresor, M, Klaas, C, Henjes, J, Strass, VH, *et al.* (2013). Thick-shelled, grazer-protected diatoms decouple ocean carbon and silicon cycles in the iron-limited Antarctic Circumpolar Current. *Proceedings of the National Academy of Sciences of the United States of America*, 110 (51):20633–20638. doi: 10.1073/pnas.1309345110.

Atkinson, A, Siegel, V, Pakhomov, E, and Rothery, P (2004). Long-term decline in krill stock and increase in salps within the Southern Ocean. *Nature*, 432 (7013):100–103. doi: 10.1038/nature02996.

Azam, F, Smith, DC, and Hollibaugh, JT (1991). The role of the microbial loop in Antarctic pelagic ecosystems. *Polar Research*, 10 (1):239–243. doi: 10.1111/j.1751-8369.1991.tb00649.x.

Azam, F, Fenchel, T, Field, JG, Gray, JC, Meyer-Reil, LA, and Thingstad, F (1983). The ecological role of water-column microbes in the sea. *Marine Ecology Progress Series*, 10 (3):257–264. doi: 10.3354/meps010257.

Azam, F and Malfatti, F (2007). Microbial structuring of marine ecosystems. *Nature Reviews Microbiology*, 5 (10):782–791. doi: 10.1038/nrmicro1747.

Bach, LT, Taucher, J, Boxhammer, T, Ludwig, A, Achterberg, EP, Algueró-Muñiz, M, *et al.* (2016). Influence of Ocean Acidification on a Natural Winter-to-Summer Plankton Succession: First Insights from a Long-Term Mesocosm Study Draw Attention to Periods of Low Nutrient Concentrations. *PLOS ONE*, 11 (8):e0159068. doi: 10.1371/journal.pone.0159068.

Badger, M (1994). The Role of Carbonic Anhydrase in Photosynthesis. *Annual Review of Plant Physiology and Plant Molecular Biology*, 45 (1):369–392. doi: 10.1146/annurev.arplant.45.1.369.

Badger, MR, Andrews, TJ, Whitney, S, Ludwig, M, Yellowlees, DC, Leggat, W, *et al.* (1998). The diversity and coevolution of Rubisco, plastids, pyrenoids, and chloroplast-based CO_2-concentrating mechanisms in algae. *Canadian Journal of Botany*, 76 (6):1052–1071. doi: 10.1139/cjb-76-6-1052.

Balch, WM, Bates, NR, Lam, PJ, Twining, BS, Rosengard, SZ, Bowler, BC, *et al.* (2016). Factors regulating the Great Calcite Belt in the Southern Ocean and its biogeochemical significance. *Global Biogeochemical Cycles*, 30 (8):1124–1144. doi: 10.1002/2016GB005414.

Ballerini, T, Hofmann, EE, Ainley, DG, Daly, K, Marrari, M, Ribic, CA, *et al.* (2014). Productivity and linkages of the food web of the southern region of the western Antarctic Peninsula continental shelf. *Progress in Oceanography*, 122:10–29. doi: 10.1016/j.pocean.2013.11.007.

Banse, K (1996). Low seasonality of low concentrations of surface chlorophyll in the Subantarctic water ring: underwater irradiance, iron, or grazing? *Progress in Oceanography*, 37 (3-4):241–291. doi: 10.1016/S0079-6611(96)00006-7.

Baragi, LV, Khandeparker, L, and Anil, AC (2015). Influence of elevated temperature and pCO_2 on the marine periphytic diatom *Navicula distans* and its associated organisms in culture. *Hydrobiologia*, 762 (1):127–142. doi: 10.1007/s10750-015-2343-9.

Barcelos e Ramos, J, Schulz, KG, Brownlee, C, Sett, S, and Azevedo, EB (2014). Effects of Increasing Seawater Carbon Dioxide Concentrations on Chain Formation of the Diatom *Asterionellopsis glacialis*. *PLoS ONE*, 9 (3):e90749. doi: 10.1371/journal.pone.0090749.

Beardall, J and Giordano, M (2002). Ecological implications of microalgal and cyanobacterial CO_2 concentrating mechanisms, and their regulation. *Functional Plant Biology*, 29 (3):335. doi: 10.1071/pp01195.

Becquevort, S, Menon, P, and Lancelot, C (2000). Differences of the protozoan biomass and grazing during spring and summer in the Indian sector of the Southern Ocean. *Polar Biology*, 23 (5):309–320. doi: 10.1007/s003000050450.

Behrenfeld, MJ (2014). Climate-mediated dance of the plankton. *Nature Climate Change*, 4 (10):880–887. doi: 10.1038/nclimate2349.

Behrenfeld, MJ, Prasil, O, Babin, M, and Bruyant, F (2004). In Search of a Physiological Basis for Covariations in Light-Limited and Light-Saturated Photosynthesis. *Journal of Phycology*, 40 (1):4–25. doi: 10.1046/j.1529-8817.2004.03083.x.

Behrenfeld, MJ, Halsey, KH, and Milligan, AJ (2008). Evolved physiological responses of phytoplankton to their integrated growth environment. *Philosophical Transactions of the Royal Society B*, 363 (1504):2687–2703. doi: 10.1098/rstb.2008.0019.

Behrenfeld, MJ, O'Malley, RT, Siegel, DA, McClain, CR, Sarmiento, JL, Feldman, GC, *et al.* (2006). Climate-driven trends in contemporary ocean productivity. *Nature*, 444 (7120):752–755. doi: 10.1038/nature05317.

Bellerby, RGJ, Schulz, KG, Riebesell, U, Neill, C, Nondal, G, Heegaard, E, *et al.* (2008). Marine ecosystem community carbon and nutrient uptake stoichiometry under varying ocean acidification during the PeECE III experiment. *Biogeosciences*, 5 (6):1517–1527. doi: 10.5194/bg-5-1517-2008.

Berge, T, Daugbjerg, N, Balling Andersen, B, and Hansen, P (2010). Effect of lowered pH on marine phytoplankton growth rates. *Marine Ecology Progress Series*, 416:79–91. doi: 10.3354/meps08780.

Bergen, B, Endres, S, Engel, A, Zark, M, Dittmar, T, Sommer, U, *et al.* (2016). Acidification and warming affect prominent bacteria in two seasonal phytoplankton bloom mesocosms. *Environmental Microbiology*, 18 (12):4579–4595. doi: 10.1111/1462-2920.13549.

Bermúdez, JR, Riebesell, U, Larsen, A, and Winder, M (2016). Ocean acidification reduces transfer of essential biomolecules in a natural plankton community. *Scientific Reports*, 6:27749. doi: 10.1038/srep27749.

Bertolin, ML and Schloss, IR (2009). Phytoplankton production after the collapse of the Larsen A Ice Shelf, Antarctica. *Polar Biology*, 32 (10):1435–1446. doi: 10.1007/s00300-009-0638-x.

Bertrand, EM, McCrow, JP, Moustafa, A, Zheng, H, McQuaid, JB, Delmont, TO, *et al.* (2015). Phytoplankton–bacterial interactions mediate micronutrient colimitation at the coastal

Antarctic sea ice edge. *Proceedings of the National Academy of Sciences*, 112:9938–9943. doi: 10.1073/pnas.1501615112.

Bi, R, Ismar, S, Sommer, U, and Zhao, M (2017). Environmental dependence of the correlations between stoichiometric and fatty acid-based indicators of phytoplankton nutritional quality. *Limnology and Oceanography*, 62 (1):334–347. doi: 10.1002/lno.10429.

Biermann, A, Lewandowska, A, Engel, A, and Riebesell, U (2015). Organic matter partitioning and stoichiometry in response to rising water temperature and copepod grazing. *Marine Ecology Progress Series*, 522:49–65. doi: 10.3354/meps11148.

Bishop, JKB and Rossow, WB (1991). Spatial and temporal variability of global surface solar irradiance. *Journal of Geophysical Research: Oceans*, 96 (C9):16839. doi: 10.1029/91JC01754.

Biswas, H, Jie, J, Li, Y, Zhang, G, Zhu, ZY, Wu, Y, *et al.* (2015). Response of a natural phytoplankton community from the Qingdao coast (Yellow Sea, China) to variable CO_2 levels over a short-term incubation experiment. *Current Science*, 108 (10):1901–1909.

Bjørnsen, PK and Kuparinen, J (1991). Growth and herbivory by heterotrophic dinoflagellates in the Southern Ocean, studied by microcosm experiments. *Marine Biology*, 109 (3):397–405. doi: 10.1007/BF01313505.

Blain, S, Quéguiner, B, Armand, L, Belviso, S, Bombled, B, Bopp, L, *et al.* (2007). Effect of natural iron fertilization on carbon sequestration in the Southern Ocean. *Nature*, 446 (7139):1070–1074. doi: 10.1038/nature05700.

Bockmon, EE and Dickson, AG (2014). A seawater filtration method suitable for total dissolved inorganic carbon and pH analyses. *Limnology and Oceanography: Methods*, 12 (4):191–195. doi: 10.4319/lom.2014.12.191.

Boelen, P, van de Poll, WH, van der Strate, HJ, Neven, IA, Beardall, J, and Buma, AGJ (2011). Neither elevated nor reduced CO_2 affects the photophysiological performance of the marine Antarctic diatom *Chaetoceros brevis*. *Journal of Experimental Marine Biology and Ecology*, 406 (1-2):38–45. doi: 10.1016/j.jembe.2011.06.012.

Bopp, L, Monfray, P, Aumont, O, Dufresne, JL, Le Treut, H, Madec, G, *et al.* (2001). Potential impact of climate change on marine export production. *Global Biogeochemical Cycles*, 15 (1):81–99. doi: 10.1029/1999GB001256.

Boyd, PW, Jickells, T, Law, CS, Blain, S, Boyle, EA, Buesseler, KO, *et al.* (2007). Mesoscale Iron Enrichment Experiments 1993-2005: Synthesis and Future Directions. *Science*, 315 (5812):612–617. doi: 10.1126/science.1131669.

Boyd, PW, Arrigo, KR, Strzepek, R, and Van Dijken, GL (2012). Mapping phytoplankton iron utilization: Insights into Southern Ocean supply mechanisms. *Journal of Geophysical Research: Oceans*, 117 (6):doi: 10.1029/2011JC007726.

Boyd, PW, Crossley, AC, DiTullio, GR, Griffiths, FB, Hutchins, DA, Queguiner, B, *et al.* (2001). Control of phytoplankton growth by iron supply and irradiance in the subantarctic Southern Ocean: Experimental results from the SAZ Project. *Journal of Geophysical Research: Oceans*, 106 (C12):31573–31583. doi: 10.1029/2000JC000348.

Boyd, PW, Dillingham, PW, McGraw, CM, Armstrong, EA, Cornwall, CE, Feng, Yy, *et al.* (2016a). Physiological responses of a Southern Ocean diatom to complex future ocean conditions. *Nature Climate Change*, 6 (2):207–213. doi: 10.1038/nclimate2811.

Boyd, PW and Ellwood, MJ (2010). The biogeochemical cycle of iron in the ocean. *Nature Geoscience*, 3 (10):675–682. doi: 10.1038/ngeo964.

Boyd, PW, McTainsh, G, Sherlock, V, Richardson, K, Nichol, S, Ellwood, M, *et al.* (2004). Episodic enhancement of phytoplankton stocks in New Zealand subantarctic waters: Contribution of atmospheric and oceanic iron supply. *Global Biogeochemical Cycles*, 18 (1):GB1029. doi: 10.1029/2002GB002020.

Boyd, PW (2002). Environmental factors controlling phytoplankton processes in the Southern Ocean. *Journal of Phycology*, 38 (5):844–861. doi: 10.1046/j.1529-8817.2002.t01-1-01203.x.

Boyd, PW, Cornwall, CE, Davison, A, Doney, SC, Fourquez, M, Hurd, CL, *et al.* (2016b). Biological responses to environmental heterogeneity under future ocean conditions. *Global Change Biology*, 22 (8):2633–2650. doi: 10.1111/gcb.13287.

Boyd, PW, Doney, SC, Strzepek, R, Dusenberry, J, Lindsay, K, and Fung, I (2008). Climate-mediated changes to mixed-layer properties in the Southern Ocean: assessing the phytoplankton response. *Biogeosciences*, 5 (3):847–864. doi: 10.5194/bg-5-847-2008.

Boyd, PW, Lennartz, ST, Glover, DM, and Doney, SC (2014). Biological ramifications of climate-change-mediated oceanic multi-stressors. *Nature Climate Change*, 5 (1):71–79. doi: 10.1038/nclimate2441.

Boyd, PW, Rynearson, TA, Armstrong, EA, Fu, F, Hayashi, K, Hu, Z, *et al.* (2013). Marine Phytoplankton Temperature versus Growth Responses from Polar to Tropical Waters – Outcome of a Scientific Community-Wide Study. *PLoS ONE*, 8 (5):e63091. doi: 10.1371/journal.pone.0063091.

Boyd, PW and Brown, CJ (2015). Modes of interactions between environmental drivers and marine biota. *Frontiers in Marine Science*, 2 (February):1–9. doi: 10.3389/fmars.2015.00009.

Boyd, PW and Law, CS (2011). An Ocean Climate Change Atlas for New Zealand waters. Tech. rep. (79). Wellington, NZ: NIWA, pp. 1–20.

Bracegirdle, TJ, Connolley, WM, and Turner, J (2008). Antarctic climate change over the twenty first century. *Journal of Geophysical Research: Atmospheres*, 113 (D3):D03103. doi: 10.1029/2007JD008933.

Brierley, AS and Thomas, DN (2002). Ecology of Southern Ocean pack ice. *Advances in Marine Biology*. Vol. 43. Elsevier Science Ltd, p 171–276. doi: 10.1016/S0065-2881(02)43005-2.

Brussaard, CPD, Noordeloos, AAM, Witte, H, Collenteur, MCJ, Schulz, K, Ludwig, A, *et al.* (2013). Arctic microbial community dynamics influenced by elevated CO_2 levels. *Biogeosciences*, 10 (2):719–731. doi: 10.5194/bg-10-719-2013.

Buchan, A, LeCleir, GR, Gulvik, CA, and González, JM (2014). Master recyclers: features and functions of bacteria associated with phytoplankton blooms. *Nature Reviews Microbiology*, 12 (10):686–698. doi: 10.1038/nrmicro3326.

Buma, AGJ, De Boer, MK, and Boelen, P (2001). Depth distributions of DNA damage in Antarctic marine phyto- and bacterioplankton exposed to summertime UV radiation. *Journal of Phycology*, 37 (2):200–208. doi: 10.1046/j.1529-8817.2001.037002200.x.

Bunse, C, Lundin, D, Karlsson, CMG, Vila-Costa, M, Palovaara, J, Akram, N, *et al.* (2016). Response of marine bacterioplankton pH homeostasis gene expression to elevated CO_2. *Nature Climate Change*, 1 (January):1–7. doi: 10.1038/nclimate2914.

Burkhardt, S, Amoroso, G, Riebesell, U, and Sültemeyer, D (2001). CO_2 and HCO_3^- uptake in marine diatoms acclimated to different CO_2 concentrations. *Limnology and Oceanography*, 46 (6):1378–1391. doi: 10.4319/lo.2001.46.6.1378.

Burkill, P, Edwards, E, and Sleight, M (1995). Microzooplankton and their role in controlling phytoplankton growth in the marginal ice zone of the Bellingshausen Sea. *Deep Sea Research*

Part II: Topical Studies in Oceanography, 42 (4-5):1277–1290. doi: 10.1016/0967-0645(95)00060-4.

Cadée, G, González, H, and Schnack-Schiel, S (1992). Krill diet affects faecal string settling. *Polar Biology*, 12 (1):75–80. doi: 10.1007/BF00239967.

Cael, BB and Follows, MJ (2016). On the temperature dependence of oceanic export efficiency. *Geophysical Research Letters*, 43 (10):5170–5175. doi: 10.1002/2016GL068877.

Calbet, A, Sazhin, AF, Nejstgaard, JC, Berger, SA, Tait, ZS, Olmos, L, *et al.* (2014). Future Climate Scenarios for a Coastal Productive Planktonic Food Web Resulting in Microplankton Phenology Changes and Decreased Trophic Transfer Efficiency. *PLoS ONE*, 9 (4):e94388. doi: 10.1371/journal.pone.0094388.

Caldeira, K and Wickett, ME (2003). Oceanography: Anthropogenic carbon and ocean pH. *Nature*, 425 (6956):365–365. doi: 10.1038/425365a.

Caron, DA and Hutchins, DA (2013). The effects of changing climate on microzooplankton grazing and community structure: Drivers, predictions and knowledge gaps. *Journal of Plankton Research*, 35 (2):235–252. doi: 10.1093/plankt/fbs091.

Carranza, MM and Gille, ST (2015). Southern Ocean wind-driven entrainment enhances satellite chlorophyll-*a* through the summer. *Journal of Geophysical Research: Oceans*, 120 (1):304–323. doi: 10.1002/2014JC010203.

Cassar, N, Bender, ML, Barnett, BA, Fan, S, Moxim, WJ, Levy, H, *et al.* (2007). The Southern Ocean Biological Response to Aeolian Iron Deposition. *Science*, 317 (5841):1067–1070. doi: 10.1126/science.1144602.

Cassar, N, Laws, EA, Bidigare, RR, and Popp, BN (2004). Bicarbonate uptake by Southern Ocean phytoplankton. *Global Biogeochemical Cycles*, 18 (2):1–10. doi: 10.1029/2003GB002116.

Cassar, N, Wright, SW, Thomson, PG, Trull, TW, Westwood, KJ, de Salas, M, *et al.* (2015). The relation of mixed-layer net community production to phytoplankton community composition in the Southern Ocean. *Global Biogeochemical Cycles*, 29 (4):446–462. doi: 10.1002/2014GB004936.

Cefarelli, AO, Vernet, M, and Ferrario, ME (2011). Phytoplankton composition and abundance in relation to free-floating Antarctic icebergs. *Deep Sea Research Part II: Topical Studies in Oceanography*, 58 (11-12):1436–1450. doi: 10.1016/j.dsr2.2010.11.023.

Charlson, RJ, Schwartz, SE, Hales, JM, Cess, RD, Coakley, JA, Hansen, JE, *et al.* (1992). Climate Forcing by Anthropogenic Aerosols. *Science*, 255 (5043):423–30. doi: 10.1126/science.255.5043.423.

Charlson, RJ, Lovelock, JE, Andreae, MO, and Warren, SG (1987). Oceanic phytoplankton, atmospheric sulphur, cloud albedo and climate. *Nature*, 326 (6114):655–661. doi: 10.1038/326655a0.

Chen, C and Durbin, E (1994). Effects of pH on the growth and carbon uptake of marine phytoplankton. *Marine Ecology Progress Series*, 109:83–94. doi: 10.3354/meps109083.

Chen, H, Guan, W, Zeng, G, Li, P, and Chen, S (2015). Alleviation of solar ultraviolet radiation (UVR)-induced photoinhibition in diatom *Chaetoceros curvisetus* by ocean acidification. *Journal of the Marine Biological Association of the United Kingdom*, 95 (04):661–667. doi: 10.1017/S0025315414001568.

Cherel, Y, Fontaine, C, Richard, P, and Labatc, JP (2010). Isotopic niches and trophic levels of myctophid fishes and their predators in the Southern Ocean. *Limnology and Oceanography*, 55 (1):324–332. doi: 10.4319/lo.2010.55.1.0324.

Chrachri, A, Hopkinson, BM, Flynn, K, Brownlee, C, and Wheeler, GL (2018). Dynamic changes in carbonate chemistry in the microenvironment around single marine phytoplankton cells. *Nature Communications*, 9 (1):74. doi: 10.1038/s41467-017-02426-y.

Christaki, U, Lefèvre, D, Georges, C, Colombet, J, Catala, P, Courties, C, *et al.* (2014). Microbial food web dynamics during spring phytoplankton blooms in the naturally iron-fertilized Kerguelen area (Southern Ocean). *Biogeosciences*, 11 (23):6739–6753. doi: 10.5194/bg-11-6739-2014.

Coad, T, McMinn, A, Nomura, D, and Martin, A (2016). Effect of elevated CO_2 concentration on microalgal communities in Antarctic pack ice. *Deep Sea Research Part II: Topical Studies in Oceanography*, 131:160–169. doi: 10.1016/j.dsr2.2016.01.005.

Collins, S, Rost, B, and Rynearson, TA (2014). Evolutionary potential of marine phytoplankton under ocean acidification. *Evolutionary Applications*, 7 (1):140–155. doi: 10.1111/eva.12120.

Colman, B, Huertas, IE, Bhatti, S, and Dason, JS (2002). The diversity of inorganic carbon acquisition mechanisms in eukaryotic microalgae. *Functional Plant Biology*, 29 (3):261–270. doi: 10.1071/PP01184.

Comiso, JC, McClain, CR, Sullivan, CW, Ryan, JP, and Leonard, CL (1993). Coastal zone color scanner pigment concentrations in the Southern Ocean and relationships to geophysical surface features. *Journal of Geophysical Research: Oceans*, 98 (C2):2419–2451. doi: 10.1029/92JC02505.

Comiso, JC and Nishio, F (2008). Trends in the sea ice cover using enhanced and compatible AMSR-E, SSM/I, and SMMR data. *Journal of Geophysical Research: Oceans*, 113 (2):C02S07. doi: 10.1029/2007JC004257.

Constable, AJ, Melbourne-Thomas, J, Corney, SP, Arrigo, KR, Barbraud, C, Barnes, DKA, *et al.* (2014). Climate change and Southern Ocean ecosystems I: how changes in physical habitats directly affect marine biota. *Global Change Biology*, 20 (10):3004–3025. doi: 10.1111/gcb.12623.

Convey, P, Bindschadler, R, di Prisco, G, Fahrbach, E, Gutt, J, Hodgson, D, *et al.* (2009). Antarctic climate change and the environment. *Antarctic Science*, 21 (06):541. doi: 10.1017/S0954102009990642.

Cook, AJ, Fox, AJ, Vaughan, DG, and Ferrigno, JG (2005). Retreating Glacier Fronts on the Antarctic Peninsula over the Past Half-Century. *Science*, 308 (5721):541–544. doi: 10.1126/science.1104235.

Cornwall, CE and Hurd, CL (2016). Experimental design in ocean acidification research: problems and solutions. *ICES Journal of Marine Science*, 73 (3):572–581. doi: 10.1093/icesjms/fsv118.

Cox, PM, Betts, RA, Jones, CD, Spall, SA, and Totterdell, IJ (2000). Acceleration of global warming due to carbon-cycle feedbacks in a coupled climate model. *Nature*, 408 (6809):184–187. doi: 10.1038/35041539.

Crawfurd, KJ, Raven, JA, Wheeler, GL, Baxter, EJ, and Joint, I (2011). The Response of *Thalassiosira pseudonana* to Long-Term Exposure to Increased CO_2 and Decreased pH. *PLoS ONE*, 6 (10):e26695. doi: 10.1371/journal.pone.0026695.

Crawfurd, KJ, Alvarez-Fernandez, S, Mojica, KDA, Riebesell, U, and Brussaard, CPD (2017). Alterations in microbial community composition with increasing fCO_2: a mesocosm study in the eastern Baltic Sea. *Biogeosciences*, 14 (16):3831–3849. doi: 10.5194/bg-14-3831-2017.

Croxall, JP, McCann, TS, Prince, PA, and Rothery, P (1988). Reproductive Performance of Seabirds and Seals at South Georgia and Signy Island, South Orkney Islands, 1976–1987:

Implications for Southern Ocean Monitoring Studies. *Antarctic Ocean and Resources Variability*. Ed. by D Sahrhage. Berlin, Heidelberg: Springer Berlin Heidelberg, p 261–285. doi: 10.1007/978-3-642-73724-4_23.

Cubillos, J, Wright, S, Nash, G, de Salas, M, Griffiths, B, Tilbrook, B, *et al.* (2007). Calcification morphotypes of the coccolithophorid *Emiliania huxleyi* in the Southern Ocean: changes in 2001 to 2006 compared to historical data. *Marine Ecology Progress Series*, 348:47–54. doi: 10.3354/meps07058.

Cullen, JJ and Lesser, MP (1991). Inhibition of photosynthesis by ultraviolet radiation as a function of dose and dosage rate: Results for a marine diatom. *Marine Biology*, 111 (2):183–190. doi: 10.1007/BF01319699.

Curran, MAJ, van Ommen, TD, Morgan, VI, Phillips, KL, and Palmer, AS (2003). Ice Core Evidence for Antarctic Sea Ice Decline Since the 1950s. *Science*, 302 (5648):1203–1206. doi: 10.1126/science.1087888.

Curran, MAJ and Jones, GB (2000). Dimethyl sulfide in the Southern Ocean: Seasonality and flux. *Journal of Geophysical Research: Atmospheres*, 105 (D16):20451–20459. doi: 10.1029/2000JD900176.

Daly, KL (1998). Physioecology of Juvenile Antarctic Krill (*Euphausia superba*) During Spring in Ice-Covered Seas. *Antarctic Sea Ice: Biological Processes, Interactions and Variability*. Ed. by MP Lizotte and KR Arrigo. Washington, D.C.: American Geophysical Union, p 183–198.

Dason, JS and Colman, B (2004). Inhibition of growth in two dinoflagellates by rapid changes in external pH. *Canadian Journal of Botany*, 82 (4):515–520. doi: 10.1139/b04-023.

Davidson, AT (2006). Effects of ultraviolet radiation on microalgal growth. *Algal Culture, Analogues of Blooms and Applications. Volume 2.* Ed. by DV Subba Rao. Enfield, NH: Science Publishers, p 715–768.

Davidson, AT, Scott, FJ, Nash, GV, Wright, SW, and Raymond, B (2010). Physical and biological control of protistan community composition, distribution and abundance in the seasonal ice zone of the Southern Ocean between 30 and 80°E. *Deep Sea Research Part II: Topical Studies in Oceanography*, 57 (9-10):828–848. doi: 10.1016/j.dsr2.2009.02.011.

Davidson, A, McKinlay, J, Westwood, K, Thomson, P, van den Enden, R, de Salas, M, *et al.* (2016). Enhanced CO_2 concentrations change the structure of Antarctic marine microbial communities. *Marine Ecology Progress Series*, 552:93–113. doi: 10.3354/meps11742.

De la Mare, WK (2009). Changes in Antarctic sea-ice extent from direct historical observations and whaling records. *Climatic Change*, 92 (3-4):461–493. doi: 10.1007/s10584-008-9473-2.

De Baar, HJW, de Jong, JTM, Bakker, DCE, Löscher, BM, Veth, C, Bathmann, U, *et al.* (1995). Importance of iron for plankton blooms and carbon dioxide drawdown in the Southern Ocean. *Nature*, 373 (6513):412–415. doi: 10.1038/373412a0.

De Salas, MF, Eriksen, R, Davidson, AT, and Wright, SW (2011). Protistan communities in the Australian sector of the Sub-Antarctic Zone during SAZ-Sense. *Deep Sea Research Part II: Topical Studies in Oceanography*, 58 (21-22):2135–2149. doi: 10.1016/j.dsr2.2011.05.032.

Delille, B, Vancoppenolle, M, Geilfus, NX, Tilbrook, B, Lannuzel, D, Schoemann, V, *et al.* (2014). Southern Ocean CO_2 sink: The contribution of the sea ice. *Journal of Geophysical Research: Oceans*, 119 (9):6340–6355. doi: 10.1002/2014JC009941.

Deppeler, SL, Davidson, AT, and Schulz, KG (2018a). Environmental data for Davis 14/15 ocean acidification minicosm experiment. Tech. rep. Australian Antarctic Data Centre. doi: 10.4225/15/599a7dfe9470a.

Deppeler, SL and Davidson, AT (2017). Southern Ocean Phytoplankton in a Changing Climate. *Frontiers in Marine Science*, 4 (40):1–18. doi: 10.3389/fmars.2017.00040.

Deppeler, S, Petrou, K, Schulz, KG, Westwood, K, Pearce, I, McKinlay, J, *et al.* (2018b). Ocean acidification of a coastal Antarctic marine microbial community reveals a critical threshold for CO_2 tolerance in phytoplankton productivity. *Biogeosciences*, 15 (1):209–231. doi: 10.5194/bg-15-209-2018.

Dickson, A, Sabine, C, and Christian, J, eds. (2007). Guide to Best Practices for Ocean CO_2 Measurements. Sidney, British Columbia: North Pacific Marine Science Organization, p 191.

Dickson, A (2010). Standards for Ocean Measurements. *Oceanography*, 23 (3):34–47. doi: 10.5670/oceanog.2010.22.

DiFiore, PJ, Sigman, DM, Trull, TW, Lourey, MJ, Karsh, K, Cane, G, *et al.* (2006). Nitrogen isotope constraints on subantarctic biogeochemistry. *Journal of Geophysical Research: Oceans*, 111 (8):C08016. doi: 10.1029/2005JC003216.

Dijkman, NA and Kromkamp, JC (2006). Phospholipid-derived fatty acids as chemotaxonomic markers for phytoplankton: Application for inferring phytoplankton composition. *Marine Ecology Progress Series*, 324:113–125. doi: 10.3354/meps324113.

DiTullio, GR, Grebmeier, JM, Arrigo, KR, Lizotte, MP, Robinson, DH, Leventer, A, *et al.* (2000). Rapid and early export of *Phaeocystis antarctica* blooms in the Ross Sea, Antarctica. *Nature*, 404 (6778):595–598. doi: 10.1038/35007061.

DiTullio, GR and Smith, WO (1995). Relationship between dimethylsulfide and phytoplankton pigment concentrations in the Ross Sea, Antarctica. *Deep Sea Research Part I: Oceanographic Research Papers*, 42 (6):873–892. doi: 10.1016/0967-0637(95)00051-7.

Doblin, MA, Petrou, KL, Shelly, K, Westwood, K, van den Enden, R, Wright, S, *et al.* (2011). Diel variation of chlorophyll-*a* fluorescence, phytoplankton pigments and productivity in the Sub-Antarctic and Polar Front Zones south of Tasmania, Australia. *Deep Sea Research Part II: Topical Studies in Oceanography*, 58 (21-22):2189–2199. doi: 10.1016/j.dsr2.2011.05.021.

Dobrynin, M, Murawsky, J, and Yang, S (2012). Evolution of the global wind wave climate in CMIP5 experiments. *Geophysical Research Letters*, 39 (18):L18606. doi: 10.1029/2012GL052843.

Dring, MJ and Jewson, DH (1982). What Does ^{14}C Uptake by Phytoplankton Really Measure? A Theoretical Modelling Approach. *Proceedings of the Royal Society B: Biological Sciences*, 214 (1196):351–368. doi: 10.1098/rspb.1982.0016.

Duarte, CM, Agustí, S, Vaqué, D, Agawin, NSR, Felipe, J, Casamayor, EO, *et al.* (2005). Experimental test of bacteria-phytoplankton coupling in the Southern Ocean. *Limnology and Oceanography*, 50 (6):1844–1854. doi: 10.4319/lo.2005.50.6.1844.

Ducklow, HW, Baker, K, Martinson, DG, Quetin, LB, Ross, RM, Smith, RC, *et al.* (2007). Marine pelagic ecosystems: the West Antarctic Peninsula. *Philosophical Transactions of the Royal Society B: Biological Sciences*, 362 (1477):67–94. doi: 10.1098/rstb.2006.1955.

Duprat, LPAM, Bigg, GR, and Wilton, DJ (2016). Enhanced Southern Ocean marine productivity due to fertilization by giant icebergs. *Nature Geoscience*, 9 (3):219–221. doi: 10.1038/ngeo2633.

Egge, JK, Thingstad, TF, Larsen, A, Engel, A, Wohlers, J, Bellerby, RGJ, *et al.* (2009). Primary production during nutrient-induced blooms at elevated CO_2 concentrations. *Biogeosciences*, 6 (5):877–885. doi: 10.5194/bg-6-877-2009.

Eggers, SL, Lewandowska, AM, Barcelos e Ramos, J, Blanco-Ameijeiras, S, Gallo, F, and Matthiessen, B (2014). Community composition has greater impact on the functioning of

marine phytoplankton communities than ocean acidification. *Global Change Biology*, 20 (3):713–723. doi: 10.1111/gcb.12421.

Endres, S, Galgani, L, Riebesell, U, Schulz, KG, and Engel, A (2014). Stimulated Bacterial Growth under Elevated pCO_2: Results from an Off-Shore Mesocosm Study. *PLoS ONE*, 9 (6):e99228. doi: 10.1371/journal.pone.0099228.

Engel, A, Borchard, C, Piontek, J, Schulz, KG, Riebesell, U, and Bellerby, R (2013). CO_2 increases ^{14}C primary production in an Arctic plankton community. *Biogeosciences*, 10 (3):1291–1308. doi: 10.5194/bg-10-1291-2013.

Engel, A, Piontek, J, Grossart, HP, Riebesell, U, Schulz, KG, and Sperling, M (2014). Impact of CO_2 enrichment on organic matter dynamics during nutrient induced coastal phytoplankton blooms. *Journal of Plankton Research*, 36 (3):641–657. doi: 10.1093/plankt/fbt125.

Evans, C, Archer, SD, Jacquet, S, and Wilson, WH (2003). Direct estimates of the contribution of viral lysis and microzooplankton grazing to the decline of a *Micromonas* spp. population. *Aquatic Microbial Ecology*, 30 (3):207–219. doi: 10.3354/ame030207.

Evans, C, Thomson, PG, Davidson, AT, Bowie, AR, van den Enden, R, Witte, H, *et al.* (2011). Potential climate change impacts on microbial distribution and carbon cycling in the Australian Southern Ocean. *Deep Sea Research Part II: Topical Studies in Oceanography*, 58 (21-22):2150–2161. doi: 10.1016/j.dsr2.2011.05.019.

Fabry, V, McClintock, J, Mathis, J, and Grebmeier, J (2009). Ocean Acidification at High Latitudes: The Bellwether. *Oceanography*, 22 (4):160–171. doi: 10.5670/oceanog.2009.105.

Fenchel, T (2008). The microbial loop - 25 years later. *Journal of Experimental Marine Biology and Ecology*, 366 (1-2):99–103. doi: 10.1016/j.jembe.2008.07.013.

Feng, Y, Hare, C, Rose, J, Handy, S, DiTullio, G, Lee, P, *et al.* (2010). Interactive effects of iron, irradiance and CO_2 on Ross Sea phytoplankton. *Deep Sea Research Part I: Oceanographic Research Papers*, 57 (3):368–383. doi: 10.1016/j.dsr.2009.10.013.

Ferreira, D, Marshall, J, Bitz, CM, Solomon, S, and Plumb, A (2015). Antarctic ocean and sea ice response to ozone depletion: A two-time-scale problem. *Journal of Climate*, 28 (3):1206–1226. doi: 10.1175/JCLI-D-14-00313.1.

Fetterer, F, Knowles, K, Meier, W, and Savoie, M (2016a). Sea Ice Index, Version 2. Boulder, Colorado USA: NSIDC: National Snow and Ice Data Center. Chap. S_201409_extn_v2. doi: 10.7265/N5736NV7.

Fetterer, F, Knowles, K, Meier, W, and Savoie, M (2016b). Sea Ice Index, Version 2. Boulder, Colorado USA: NSIDC: National Snow and Ice Data Center. Chap. S_201611_e. doi: 10.7265/N5736NV7.

Finkel, ZV, Beardall, J, Flynn, KJ, Quigg, A, Rees, TAV, and Raven, JA (2010). Phytoplankton in a changing world: cell size and elemental stoichiometry. *Journal of Plankton Research*, 32 (1):119–137. doi: 10.1093/plankt/fbp098.

Fitch, DT and Moore, JK (2007). Wind speed influence on phytoplankton bloom dynamics in the Southern Ocean Marginal Ice Zone. *Journal of Geophysical Research: Oceans*, 112 (C8):C08006. doi: 10.1029/2006JC004061.

Flombaum, P, Gallegos, JL, Gordillo, Ra, Rincon, J, Zabala, LL, Jiao, N, *et al.* (2013). Present and future global distributions of the marine Cyanobacteria *Prochlorococcus* and *Synechococcus*. *Proceedings of the National Academy of Sciences*, 110 (24):9824–9829. doi: 10.1073/pnas.1307701110.

Flores, H, Atkinson, A, Kawaguchi, S, Krafft, B, Milinevsky, G, Nicol, S, *et al.* (2012). Impact of climate change on Antarctic krill. *Marine Ecology Progress Series*, 458:1–19. doi: 10.3354/meps09831.

Flynn, KJ, Blackford, JC, Baird, ME, Raven, JA, Clark, DR, Beardall, J, *et al.* (2012). Changes in pH at the exterior surface of plankton with ocean acidification. *Nature Climate Change*, 2 (7):510–513. doi: 10.1038/nclimate1489.

Frölicher, TL, Rodgers, KB, Stock, CA, and Cheung, WWL (2016). Sources of uncertainties in 21st century projections of potential ocean ecosystem stressors. *Global Biogeochemical Cycles*, 30 (8):1224–1243. doi: 10.1002/2015GB005338.

Frölicher, TL, Sarmiento, JL, Paynter, DJ, Dunne, JP, Krasting, JP, and Winton, M (2015). Dominance of the Southern Ocean in Anthropogenic Carbon and Heat Uptake in CMIP5 Models. *Journal of Climate*, 28 (2):862–886. doi: 10.1175/JCLI-D-14-00117.1.

Gao, K and Campbell, DA (2014). Photophysiological responses of marine diatoms to elevated CO_2 and decreased pH: a review. *Functional Plant Biology*, 41 (5):449–459. doi: 10.1071/FP13247.

Gao, K, Helbling, E, Häder, D, and Hutchins, D (2012a). Responses of marine primary producers to interactions between ocean acidification, solar radiation, and warming. *Marine Ecology Progress Series*, 470:167–189. doi: 10.3354/meps10043.

Gao, K, Xu, J, Gao, G, Li, Y, Hutchins, DA, Huang, B, *et al.* (2012b). Rising CO_2 and increased light exposure synergistically reduce marine primary productivity. *Nature Climate Change*, 2 (7):519–523. doi: 10.1038/nclimate1507.

Garibotti, I, Vernet, M, Ferrario, M, Smith, R, Ross, R, and Quetin, L (2003). Phytoplankton spatial distribution patterns along the western Antarctic Peninsula (Southern Ocean). *Marine Ecology Progress Series*, 261:21–39. doi: 10.3354/meps261021.

Gast, RJ, Fay, SA, and Sanders, RW (2018). Mixotrophic Activity and Diversity of Antarctic Marine Protists in Austral Summer. *Frontiers in Marine Science*, 5:1–12. doi: 10.3389/fmars.2018.00013.

Gattuso, JP, Gao, K, Lee, K, Rost, B, and Schulz, KG (2010). Approaches and tools to manipulate the carbonate chemistry. *Guide to best practices for ocean acidification research and data reporting*. Ed. by U Riebesell, VJ Fabry, L Hansson, and JP Gattuso. Luxembourg: Publications Office of the European Union. Chap. 2, p 41–52. doi: 10.2777/66906.

Gibson, JA and Trull, TW (1999). Annual cycle of $f\,CO_2$ under sea-ice and in open water in Prydz Bay, East Antarctica. *Marine Chemistry*, 66 (3-4):187–200. doi: 10.1016/S0304-4203(99)00040-7.

Giordano, M, Beardall, J, and Raven, JA (2005). CO_2 Concentrating Mechanisms in Algae: Mechanisms, Environmental Modulation, and Evolution. *Annual Review of Plant Biology*, 56 (1):99–131. doi: 10.1146/annurev.arplant.56.032604.144052.

Goedegebuure, M, Melbourne-Thomas, J, Corney, SP, Hindell, MA, and Constable, AJ (2017). Beyond big fish: The case for more detailed representations of top predators in marine ecosystem models. *Ecological Modelling*, 359:182–192. doi: 10.1016/j.ecolmodel.2017.04.004.

Goldman, JAL, Kranz, SA, Young, JN, Tortell, PD, Stanley, RHR, Bender, ML, *et al.* (2015). Gross and net production during the spring bloom along the Western Antarctic Peninsula. *New Phytologist*, 205 (1):182–191. doi: 10.1111/nph.13125.

Goldman, JAL, Bender, ML, and Morel, FMM (2017). The effects of pH and pCO_2 on photosynthesis and respiration in the diatom Thalassiosira weissflogii. *Photosynthesis Research*, 132 (1):83–93. doi: 10.1007/s11120-016-0330-2.

González, N, Gattuso, JP, and Middelburg, JJ (2008). Oxygen production and carbon fixation in oligotrophic coastal bays and the relationship with gross and net primary production. *Aquatic Microbial Ecology*, 52 (2):119–130. doi: 10.3354/ame01208.

Gregg, WW and Rousseaux, CS (2014). Decadal trends in global pelagic ocean chlorophyll: A new assessment integrating multiple satellites, in situ data, and models. *Journal of Geophysical Research: Oceans*, 119 (9):5921–5933. doi: 10.1002/2014JC010158.

Griffiths, FB, Bates, TS, Quinn, PK, Clementson, LA, and Parslow, JS (1999). Oceanographic context of the First Aerosol Characterization Experiment (ACE 1): A physical, chemical, and biological overview. *Journal of Geophysical Research: Atmospheres*, 104 (D17):21649–21671. doi: 10.1029/1999JD900386.

Grossart, Hp, Allgaier, M, Passow, U, and Riebesell, U (2006). Testing the effect of CO_2 concentration on the dynamics of marine heterotrophic bacterioplankton. *Limnology and Oceanography*, 51 (1):1–11. doi: 10.4319/lo.2006.51.1.0001.

Grossi, S, Kottmeier, S, Moe, R, Taylor, G, and Sullivan, C (1987). Sea ice microbial communities. VI. Growth and primary production in bottom ice under graded snow cover. *Marine Ecology Progress Series*, 35 (January):153–164. doi: 10.3354/meps035153.

Guillard, RRL (2003). Culture Methods. *Manual on harmful marine microalgae*. Ed. by GM Hallegraeff, DM Anderson, and AD Cembella. Paris: UNESCO. Chap. 3, p 45–62.

Gutt, J, Bertler, N, Bracegirdle, TJ, Buschmann, A, Comiso, J, Hosie, G, *et al.* (2015). The Southern Ocean ecosystem under multiple climate change stresses - an integrated circumpolar assessment. *Global Change Biology*, 21 (4):1434–1453. doi: 10.1111/gcb.12794.

Haberman, KL, Quetin, LB, and Ross, RM (2003). Diet of the Antarctic krill (Euphausia superba Dana). *Journal of Experimental Marine Biology and Ecology*, 283 (1-2):79–95. doi: 10.1016/S0022-0981(02)00466-5.

Häder, DP, Williamson, CE, Wängberg, SÅ, Rautio, M, Rose, KC, Gao, K, *et al.* (2015). Effects of UV radiation on aquatic ecosystems and interactions with other environmental factors. *Photochemical & Photobiological Sciences*, 14 (1):108–126. doi: 10.1039/C4PP90035A.

Hagen, W (1999). Reproductive strategies and energetic adaptations of polar zooplankton. *Invertebrate Reproduction & Development*, 36 (1-3):25–34. doi: 10.1080/07924259.1999.9652674.

Hagen, W and Auel, H (2001). Seasonal adaptations and the role of lipids in oceanic zooplankton. *Zoology*, 104 (3-4):313–326. doi: 10.1078/0944-2006-00037.

Halsey, KH, Milligan, AJ, and Behrenfeld, MJ (2010). Physiological optimization underlies growth rate-independent chlorophyll-specific gross and net primary production. *Photosynthesis Research*, 103 (2):125–137. doi: 10.1007/s11120-009-9526-z.

Hancock, AM, Davidson, AT, McKinlay, J, McMinn, A, Schulz, K, and van den Enden, RL (2018). Ocean acidification changes the structure of an Antarctic coastal protistan community. *Biogeosciences*, 15 (1):1–32. doi: 10.5194/bg-2017-224.

Hauck, J and Völker, C (2015). Rising atmospheric CO_2 leads to large impact of biology on Southern Ocean CO_2 uptake via changes of the Revelle factor. *Geophysical Research Letters*, 42 (5):1459–1464. doi: 10.1002/2015GL063070.

Hauck, J, Völker, C, Wang, T, Hoppema, M, Losch, M, and Wolf-Gladrow, DA (2013). Seasonally different carbon flux changes in the Southern Ocean in response to the southern annular mode. *Global Biogeochemical Cycles*, 27 (4):1236–1245. doi: 10.1002/2013GB004600.

Hauck, J, Völker, C, Wolf-Gladrow, DA, Laufkötter, C, Vogt, M, Aumont, O, *et al.* (2015). On the Southern Ocean CO_2 uptake and the role of the biological carbon pump in the 21st century. *Global Biogeochemical Cycles*, 29 (9):1451–1470. doi: 10.1002/2015GB005140.

Haumann, FA, Gruber, N, Münnich, M, Frenger, I, and Kern, S (2016). Sea-ice transport driving Southern Ocean salinity and its recent trends. *Nature*, 537 (7618):89–92. doi: 10.1038/nature19101.

Helbling, EW, Villafañe, V, and Holm-Hansen, O (1994). Effects of ultraviolet radiation on Antarctic marine phytoplankton photosynthesis with particular attention to the influence of mixing. *Ultraviolet Radiation in Antarctica: Measurements and Biological Effects*. Ed. by CS Weiler and PA Penhale. Vol. 62. Washington, D.C.: American Geophysical Union, p 207–227. doi: 10.1029/AR062p0207.

Hemer, MA, Church, JA, and Hunter, JR (2010). Variability and trends in the directional wave climate of the Southern Hemisphere. *International Journal of Climatology*, 30 (4):475–491. doi: 10.1002/joc.1900.

Hennon, GMM, Quay, P, Morales, RL, Swanson, LM, and Virginia Armbrust, E (2014). Acclimation conditions modify physiological response of the diatom *Thalassiosira pseudonana*

to elevated CO_2 concentrations in a nitrate-limited chemostat. *Journal of Phycology*, 50 (2):243–253. doi: 10.1111/jpy.12156.

Hennon, GMM, Ashworth, J, Groussman, RD, Berthiaume, C, Morales, RL, Baliga, NS, *et al.* (2015). Diatom acclimation to elevated CO_2 via cAMP signalling and coordinated gene expression. *Nature Climate Change*, 5 (8):761–765. doi: 10.1038/nclimate2683.

Henson, SA, Sarmiento, JL, Dunne, JP, Bopp, L, Lima, I, Doney, SC, *et al.* (2010). Detection of anthropogenic climate change in satellite records of ocean chlorophyll and productivity. *Biogeosciences*, 7 (2):621–640. doi: 10.5194/bg-7-621-2010.

Hirawake, T, Odate, T, and Fukuchi, M (2005). Long-term variation of surface phytoplankton chlorophyll *a* in the Southern Ocean during the 1965-2002. *Geophysical Research Letters*, 32 (5):L05606. doi: 10.1029/2004GL021394.

Hiscock, MR, Marra, J, Smith, WOJ, Goericke, R, Measures, C, Vink, S, *et al.* (2003). Primary productivity and its regulation in the Pacific Sector of the Southern Ocean. *Deep Sea Research Part II: Topical Studies in Oceanography*, 50 (3-4):533–558. doi: 10.1016/S0967-0645(02)00583-0.

Hixson, SM and Arts, MT (2016). Climate warming is predicted to reduce omega-3, long-chain, polyunsaturated fatty acid production in phytoplankton. *Global Change Biology*, 22 (8):2744–2755. doi: 10.1111/gcb.13295.

Hobbs, WR, Massom, R, Stammerjohn, S, Reid, P, Williams, G, and Meier, W (2016). A review of recent changes in Southern Ocean sea ice, their drivers and forcings. *Global and Planetary Change*, 143:228–250. doi: 10.1016/j.gloplacha.2016.06.008.

Hoffmann, LJ, Breitbarth, E, McGraw, CM, Law, CS, Currie, KI, and Hunter, KA (2013). A trace-metal clean, pH-controlled incubator system for ocean acidification incubation studies. *Limnology and Oceanography: Methods*, 11 (1):53–61. doi: 10.4319/lom.2013.11.53.

Hogg, AMC, Meredith, MP, Blundell, JR, and Wilson, C (2008). Eddy Heat Flux in the Southern Ocean: Response to Variable Wind Forcing. *Journal of Climate*, 21 (4):608–620. doi: 10.1175/2007JCLI1925.1.

Holding, JM, Duarte, CM, Sanz-Martín, M, Mesa, E, Arrieta, JM, Chierici, M, *et al.* (2015). Temperature dependence of CO_2-enhanced primary production in the European Arctic Ocean. *Nature Climate Change*, 5 (12):1079–1082. doi: 10.1038/nclimate2768.

Holland, PR, Bruneau, N, Enright, C, Losch, M, Kurtz, NT, and Kwok, R (2014). Modeled Trends in Antarctic Sea Ice Thickness. *Journal of Climate*, 27 (10):3784–3801. doi: 10.1175/JCLI-D-13-00301.1.

Hong, H, Li, D, Lin, W, Li, W, and Shi, D (2017). Nitrogen nutritional condition affects the response of energy metabolism in diatoms to elevated carbon dioxide. *Marine Ecology Progress Series*, 567:41–56. doi: 10.3354/meps12033.

Honjo, S (2004). Particle export and the biological pump in the Southern Ocean. *Antarctic Science*, 16 (4):501–516. doi: 10.1017/S0954102004002287.

Hopkinson, BM, Xu, Y, Shi, D, McGinn, PJ, and Morel, FMM (2010). The effect of CO_2 on the photosynthetic physiology of phytoplankton in the Gulf of Alaska. *Limnology and Oceanography*, 55 (5):2011–2024. doi: 10.4319/lo.2010.55.5.2011.

Hopkinson, BM, Dupont, CL, Allen, AE, and Morel, FMM (2011). Efficiency of the CO_2-concentrating mechanism of diatoms. *Proceedings of the National Academy of Sciences*, 108 (10):3830–3837. doi: 10.1073/pnas.1018062108.

Hoppe, CJM, Schuback, N, Semeniuk, D, Giesbrecht, K, Mol, J, Thomas, H, *et al.* (2017). Resistance of Arctic phytoplankton to ocean acidification and enhanced irradiance. *Polar Biology*,1–15. doi: 10.1007/s00300-017-2186-0.

Hoppe, CJM, Hassler, CS, Payne, CD, Tortell, PD, Rost, B, and Trimborn, S (2013). Iron Limitation Modulates Ocean Acidification Effects on Southern Ocean Phytoplankton Communities. *PLoS ONE*, 8 (11):e79890. doi: 10.1371/journal.pone.0079890.

Hoppe, CJ, Holtz, LM, Trimborn, S, and Rost, B (2015). Ocean acidification decreases the light-use efficiency in an Antarctic diatom under dynamic but not constant light. *New Phytologist*, 207 (1):159–171. doi: 10.1111/nph.13334.

Hoppema, M, Fahrbach, E, Schröder, M, Wisotzki, A, and de Baar, HJ (1995). Winter-summer differences of carbon dioxide and oxygen in the Weddell Sea surface layer. *Marine Chemistry*, 51 (3):177–192. doi: 10.1016/0304-4203(95)00065-8.

Horvat, C, Tziperman, E, and Campin, Jm (2016). Interaction of sea ice floe size, ocean eddies, and sea ice melting. *Geophysical Research Letters*, 43 (15):8083–8090. doi: 10.1002/2016GL069742.

Hutchins, DA and Boyd, PW (2016). Marine phytoplankton and the changing ocean iron cycle. *Nature Climate Change*, 6 (12):1072–1079. doi: 10.1038/nclimate3147.

Hutchins, DA and Fu, F (2017). Microorganisms and ocean global change. *Nature Microbiology*, 2:1–11. doi: 10.1038/nmicrobiol.2017.58.

Ihnken, S, Roberts, S, and Beardall, J (2011). Differential responses of growth and photosynthesis in the marine diatom *Chaetoceros muelleri* to CO_2 and light availability. *Phycologia*, 50 (2):182–193. doi: 10.2216/10-11.1.

IPCC (2013). Climate Change 2013: The Physical Science Basis. Contribution of Working Group I to the Fifth Assessment Report of the Intergovernmental Panel on Climate Change. Ed. by T Stocker, D Qin, GK Plattner, M Tignor, S Allen, J Boschung, *et al.* Cambridge, United Kingdom and New York, NY, USA: Cambridge University Press, p 1535. doi: 10.1017/CBO9781107415324.

Isari, S, Zervoudaki, S, Peters, J, Papantoniou, G, Pelejero, C, and Saiz, E (2016). Lack of evidence for elevated CO_2-induced bottom-up effects on marine copepods: a dinoflagellate–calanoid prey–predator pair. *ICES Journal of Marine Science: Journal du Conseil*, 73 (3):650–658. doi: 10.1093/icesjms/fsv078.

Jacob, BG, von Dassow, P, Salisbury, JE, Navarro, JM, and Vargas, CA (2016). Impact of low pH/high pCO_2 on the physiological response and fatty acid content in diatom *Skeletonema pseudocostatum*. *Journal of the Marine Biological Association of the United Kingdom*, 97 (2):1–9. doi: 10.1017/S0025315416001570.

Jacobs, SS, Giulivi, CF, and Mele, PA (2002). Freshening of the Ross Sea During the Late 20th Century. *Science*, 297 (5580):386–389. doi: 10.1126/science.1069574.

Jacobs, SS (1991). On the nature and significance of the Antarctic Slope Front. *Marine Chemistry*, 35 (1-4):9–24. doi: 10.1016/S0304-4203(09)90005-6.

Jeffrey, SW and Wright, SW (1997). Qualitative and quantitative HPLC analysis of SCOR reference algal cultures. *Phytoplankton Pigments in Oceanography: Guidelines to Modern Methods*. Ed. by S Jeffrey, R Mantoura, and S Wright. Paris: UNESCO, p 343–360.

Jeffrey, S and Humphrey, G (1975). New spectrophotometric equations for determining chlorophylls a, b, c_1 and c_2 in higher plants, algae and natural phytoplankton. *Biochemie und Physiologie der Pflanzen*, 167 (2):191–194. doi: 10.1016/S0015-3796(17)30778-3.

Jia, Z, Swadling, KM, Meiners, KM, Kawaguchi, S, and Virtue, P (2016). The zooplankton food web under East Antarctic pack ice – A stable isotope study. *Deep Sea Research Part II: Topical Studies in Oceanography*, 131:189–202. doi: 10.1016/j.dsr2.2015.10.010.

Jones, GB, Curran, MAJ, Swan, HB, Greene, RM, Griffiths, FB, and Clementson, LA (1998). Influence of different water masses and biological activity on dimethylsulphide and dimethylsulphoniopropionate in the subantarctic zone of the Southern Ocean during ACE 1. *Journal of Geophysical Research: Atmospheres*, 103 (D13):16691–16701. doi: 10.1029/98JD01200.

Jones, G, Fortescue, D, King, S, Williams, G, and Wright, S (2010). Dimethylsulphide and dimethylsulphoniopropionate in the South-West Indian Ocean sector of East Antarctica from 30° to 80°E during BROKE-West. *Deep Sea Research Part II: Topical Studies in Oceanography*, 57 (9-10):863–876. doi: 10.1016/j.dsr2.2009.01.003.

Kähler, P and Koeve, W (2001). Marine dissolved organic matter: Can its C:N ratio explain carbon overconsumption? *Deep-Sea Research Part I: Oceanographic Research Papers*, 48 (1):49–62. doi: 10.1016/S0967-0637(00)00034-0.

Kahru, M, Mitchell, BG, Gille, ST, Hewes, CD, and Holm-Hansen, O (2007). Eddies enhance biological production in the Weddell-Scotia Confluence of the Southern Ocean. *Geophysical Research Letters*, 34 (14):L14603. doi: 10.1029/2007GL030430.

Kang, SH, Kang, JS, Lee, S, Chung, KH, Kim, D, and Park, MG (2001). Antarctic Phytoplankton Assemblages in the Marginal Ice Zone of the Northwestern Weddell Sea. *Journal of Plankton Research*, 23 (4):333–352. doi: 10.1093/plankt/23.4.333.

Kapsenberg, L, Kelley, AL, Shaw, EC, Martz, TR, and Hofmann, GE (2015). Near-shore Antarctic pH variability has implications for the design of ocean acidification experiments. *Scientific Reports*, 5:9638. doi: 10.1038/srep09638.

Karentz, D (1991). Ecological considerations of Antarctic ozone depletion. *Antarctic Science*, 3 (01):3–11. doi: 10.1017/S0954102091000032.

Karentz, D and Lutze, LH (1990). Evaluation of biologically harmful ultraviolet radiation in Antarctica with a biological dosimeter designed for aquatic environments. *Limnology and Oceanography*, 35 (3):549–561. doi: 10.4319/lo.1990.35.3.0549.

Kavanaugh, M, Abdala, F, Ducklow, H, Glover, D, Fraser, W, Martinson, D, *et al.* (2015). Effect of continental shelf canyons on phytoplankton biomass and community composition along the western Antarctic Peninsula. *Marine Ecology Progress Series*, 524:11–26. doi: 10.3354/meps11189.

Kawaguchi, S, Ishida, A, King, R, Raymond, B, Waller, N, Constable, A, *et al.* (2013). Risk maps for Antarctic krill under projected Southern Ocean acidification. *Nature Climate Change*, 3 (9):843–847. doi: 10.1038/nclimate1937.

Kawaguchi, S, Ichii, T, and Naganobu, M (1999). Green krill, the indicator of micro- and nano-size phytoplankton availability to krill. *Polar Biology*, 22 (2):133–136. doi: 10.1007/s003000050400.

Kawaguchi, S, Kurihara, H, King, RA, Hale, L, Berli, T, Robinson, JP, *et al.* (2011). Will krill fare well under Southern Ocean acidification? *Biology letters*, 7 (2):288–291. doi: 10.1098/rsbl.2010.0777.

Kawaguchi, S and Satake, M (1994). Relationship between Recruitment near the South Shetland Islands of the Antarctic Krill and the Degree of Ice Cover. *Fisheries Science*, 60 (1):123–124.

Kemp, AES, Pearce, RB, Grigorov, I, Rance, J, Lange, CB, Quilty, P, *et al.* (2006). Production of giant marine diatoms and their export at oceanic frontal zones: Implications for Si and C flux from stratified oceans. *Global Biogeochemical Cycles*, 20 (4):GB4S04. doi: 10.1029/2006GB002698.

Khatiwala, S, Primeau, F, and Hall, T (2009). Reconstruction of the history of anthropogenic CO_2 concentrations in the ocean. *Nature*, 462 (7271):346–349. doi: 10.1038/nature08526.

Kiene, R, Linn, L, and Bruton, J (2000). New and important roles for DMSP in marine microbial communities. *Journal of Sea Research*, 43 (3-4):209–224. doi: 10.1016/S1385-1101(00)00023-X.

Kim, H, Spivack, AJ, and Menden-Deuer, S (2013). pH alters the swimming behaviors of the raphidophyte *Heterosigma akashiwo*: Implications for bloom formation in an acidified ocean. *Harmful Algae*, 26:1–11. doi: 10.1016/j.hal.2013.03.004.

Kim, JM, Lee, K, Shin, K, Kang, JH, Lee, HW, Kim, M, *et al.* (2006). The effect of seawater CO_2 concentration on growth of a natural phytoplankton assemblage in a controlled mesocosm experiment. *Limnology and Oceanography*, 51 (4):1629–1636. doi: 10.4319/lo.2006.51.4.1629.

King, A, Jenkins, B, Wallace, J, Liu, Y, Wikfors, G, Milke, L, *et al.* (2015). Effects of CO_2 on growth rate, C:N:P, and fatty acid composition of seven marine phytoplankton species. *Marine Ecology Progress Series*, 537:59–69. doi: 10.3354/meps11458.

Kirchman, DL (2001). Measuring Bacterial Biomass Production and Growth Rates from Leucine Incorporation in Natural Aquatic Environments. *Methods in Microbiology*. Ed. by J Paul. Vol. 30. St Petersburg, FL: Academic Press. Chap. 12, p 227–237. doi: 10.1016/S0580-9517(01)30047-8.

Kirchman, DL (2008). Microbial ecology of the oceans. 2nd ed. Hoboken, N.J.: Wiley-Blackwell, p 620.

Kirk, JTO (1994). Light and photosynthesis in aquatic ecosystems. Cambridge, UK: Cambridge University Press, p 509.

Kirst, G, Thiel, C, Wolff, H, Nothnagel, J, Wanzek, M, and Ulmke, R (1991). Dimethylsulfoniopropionate (DMSP) in icealgae and its possible biological role. *Marine Chemistry*, 35 (1-4):381–388. doi: 10.1016/S0304-4203(09)90030-5.

Knox, GA (2007). Se-Ice Microbial Communities. *Biology of the Southern Ocean*. 2nd ed. Boca Raton, FL: CRC Press. Chap. 3, p 59–96.

Kohout, AL, Williams, MJM, Dean, SM, and Meylan, MH (2014). Storm-induced sea-ice breakup and the implications for ice extent. *Nature*, 509 (7502):604–607. doi: 10.1038/nature13262.

Kopczyńska, EE, Dehairs, F, Elskens, M, and Wright, S (2001). Phytoplankton and microzooplankton variability between the Subtropical and Polar Fronts south of Australia: Thriving under regenerative and new production in late summer. *Journal of Geophysical Research: Oceans*, 106 (C12):31597–31609. doi: 10.1029/2000JC000278.

Kopczyńska, EE, Savoye, N, Dehairs, F, Cardinal, D, and Elskens, M (2007). Spring phytoplankton assemblages in the Southern Ocean between Australia and Antarctica. *Polar Biology*, 31 (1):77–88. doi: 10.1007/s00300-007-0335-6.

Kozlov, AN (1995). A review of the trophic role of mesopelagic fish of the family Myctophidae in the Southern Ocean ecosystem. *CCAMLR Science*, 2:71–77.

Krause, E, Wichels, A, Giménez, L, Lunau, M, Schilhabel, MB, and Gerdts, G (2012). Small Changes in pH Have Direct Effects on Marine Bacterial Community Composition: A Microcosm Approach. *PLoS ONE*, 7 (10):e47035. doi: 10.1371/journal.pone.0047035.

Kwok, R (2010). Satellite remote sensing of sea-ice thickness and kinematics: a review. *Journal of Glaciology*, 56 (200):1129–1140. doi: 10.3189/002214311796406167.

Lakeman, MB, von Dassow, P, and Cattolico, RA (2009). The strain concept in phytoplankton ecology. *Harmful Algae*, 8 (5):746–758. doi: 10.1016/j.hal.2008.11.011.

Lam, PJ and Bishop, JK (2007). High biomass, low export regimes in the Southern Ocean. *Deep Sea Research Part II: Topical Studies in Oceanography*, 54 (5-7):601–638. doi: 10.1016/j.dsr2.2007.01.013.

Landry, MR and Calbet, A (2004). Microzooplankton production in the oceans. *ICES Journal of Marine Science*, 61 (4):501–507. doi: 10.1016/j.icesjms.2004.03.011.

Lannuzel, D, Chever, F, van der Merwe, PC, Janssens, J, Roukaerts, A, Cavagna, AJ, *et al.* (2016). Iron biogeochemistry in Antarctic pack ice during SIPEX-2. *Deep Sea Research Part II: Topical Studies in Oceanography*, 131:111–122. doi: 10.1016/j.dsr2.2014.12.003.

Lannuzel, D, Schoemann, V, de Jong, J, Pasquer, B, van der Merwe, P, Masson, F, *et al.* (2010). Distribution of dissolved iron in Antarctic sea ice: Spatial, seasonal, and inter-annual variability. *Journal of Geophysical Research: Biogeosciences*, 115 (G3):G03022. doi: 10.1029/2009JG001031.

Laufkötter, C, Vogt, M, Gruber, N, Aita-Noguchi, M, Aumont, O, Bopp, L, *et al.* (2015). Drivers and uncertainties of future global marine primary production in marine ecosystem models. *Biogeosciences*, 12 (23):6955–6984. doi: 10.5194/bg-12-6955-2015.

Laurenceau-Cornec, EC, Trull, TW, Davies, DM, Bray, SG, Doran, J, Planchon, F, *et al.* (2015). The relative importance of phytoplankton aggregates and zooplankton fecal pellets to carbon export: Insights from free-drifting sediment trap deployments in naturally iron-fertilised waters near the Kerguelen Plateau. *Biogeosciences*, 12 (4):1007–1027. doi: 10.5194/bg-12-1007-2015.

Le Quéré, C, Rodenbeck, C, Buitenhuis, ET, Conway, TJ, Langenfelds, R, Gomez, A, *et al.* (2007). Saturation of the Southern Ocean CO_2 Sink Due to Recent Climate Change. *Science*, 316 (5832):1735–1738. doi: 10.1126/science.1136188.

Legendre, L, Ackley, SF, Dieckmann, GS, Gulliksen, B, Horner, R, Hoshiai, T, *et al.* (1992). Ecology of sea ice biota - 2. Global significance. *Polar Biology*, 12 (3-4):429–444. doi: 10.1007/BF00243114.

Lenton, A and Matear, RJ (2007). Role of the Southern Annular Mode (SAM) in Southern Ocean CO_2 uptake. *Global Biogeochemical Cycles*, 21 (2):GB2016. doi: 10.1029/2006GB002714.

Leung, S, Cabré, A, and Marinov, I (2015). A latitudinally banded phytoplankton response to 21st century climate change in the Southern Ocean across the CMIP5 model suite. *Biogeosciences*, 12 (19):5715–5734. doi: 10.5194/bg-12-5715-2015.

Lewis, M and Smith, J (1983). A small volume, short-incubation-time method for measurement of photosynthesis as a function of incident irradiance. *Marine Ecology Progress Series*, 13 (1):99–102. doi: 10.3354/meps013099.

Li, F, Beardall, J, Collins, S, and Gao, K (2017a). Decreased photosynthesis and growth with reduced respiration in the model diatom *Phaeodactylum tricornutum* grown under elevated CO_2 over 1800 generations. *Global Change Biology*, 23 (1):127–137. doi: 10.1111/gcb.13501.

Li, G, Brown, CM, Jeans, JA, Donaher, NA, McCarthy, A, and Campbell, DA (2015). The nitrogen costs of photosynthesis in a diatom under current and future pCO_2. *New Phytologist*, 205 (2):533–543. doi: 10.1111/nph.13037.

Li, W, Yang, Y, Li, Z, Xu, J, and Gao, K (2017b). Effects of seawater acidification on the growth rates of the diatom *Thalassiosira (Conticribra) weissflogii* under different nutrient, light, and UV radiation regimes. *Journal of Applied Phycology*, 29 (1):133–142. doi: 10.1007/s10811-016-0944-y.

Liang, Y, Bai, X, Jiang, Y, Wang, M, He, J, and McMinn, A (2016). Distribution of marine viruses and their potential hosts in Prydz Bay and adjacent Southern Ocean, Antarctic. *Polar Biology*, 39 (2):365–378. doi: 10.1007/s00300-015-1787-8.

Lin, H, Rauschenberg, S, Hexel, CR, Shaw, TJ, and Twining, BS (2011). Free-drifting icebergs as sources of iron to the Weddell Sea. *Deep Sea Research Part II: Topical Studies in Oceanography*, 58 (11-12):1392–1406. doi: 10.1016/j.dsr2.2010.11.020.

Lin, L, He, J, Zhao, Y, Zhang, F, and Cai, M (2012). Flow cytometry investigation of picoplankton across latitudes and along the circum Antarctic Ocean. *Acta Oceanologica Sinica*, 31 (1):134–142. doi: 10.1007/s13131-012-0185-0.

Liu, J, Curry, JA, and Martinson, DG (2004). Interpretation of recent Antarctic sea ice variability. *Geophysical Research Letters*, 31 (2):2000–2003. doi: 10.1029/2003GL018732.

Liu, N, Beardall, J, and Gao, K (2017). Elevated CO_2 and associated seawater chemistry do not benefit a model diatom grown with increased availability of light. *Aquatic Microbial Ecology*, 79 (2):137–147. doi: 10.3354/ame01820.

Lizotte, MP (2001). The Contributions of Sea Ice Algae to Antarctic Marine Primary Production. *American Zoologist*, 41 (1):57–73. doi: 10.1668/0003-1569(2001)041[0057:TCOSIA]2.0.CO;2.

Lochte, K, Bjørnsen, PK, Giesenhagen, H, and Weber, A (1997). Bacterial standing stock and production and their relation to phytoplankton in the Southern Ocean. *Deep Sea Research Part II: Topical Studies in Oceanography*, 44 (1-2):321–340. doi: 10.1016/S0967-0645(96)00081-1.

Lohbeck, KT, Riebesell, U, and Reusch, TBH (2012). Adaptive evolution of a key phytoplankton species to ocean acidification. *Nature Geoscience*, 5 (5):346–351. doi: 10.1038/ngeo1441.

Longhurst, AR (1991). Role of the marine biosphere in the global carbon cycle. *Limnology and Oceanography*, 36 (8):1507–1526. doi: 10.4319/lo.1991.36.8.1507.

Lovenduski, NS and Gruber, N (2005). Impact of the Southern Annular Mode on Southern Ocean circulation and biology. *Geophysical Research Letters*, 32 (11):doi: 10.1029/2005GL022727.

Lovenduski, NS, Gruber, N, Doney, SC, and Lima, ID (2007). Enhanced CO_2 outgassing in the Southern Ocean from a positive phase of the Southern Annular Mode. *Global Biogeochemical Cycles*, 21 (2):GB2026. doi: 10.1029/2006GB002900.

Lueker, TJ, Dickson, AG, and Keeling, CD (2000). Ocean pCO_2 calculated from dissolved inorganic carbon, alkalinity, and equations for K_1 and K_2: validation based on laboratory measurements of CO_2 in gas and seawater at equilibrium. *Marine Chemistry*, 70 (1-3):105–119. doi: 10.1016/S0304-4203(00)00022-0.

Lumpkin, R and Speer, K (2007). Global Ocean Meridional Overturning. *Journal of Physical Oceanography*, 37 (10):2550–2562. doi: 10.1175/JPO3130.1.

Lynch, M, Gabriel, W, and Wood, AM (1991). Adaptive and demographic responses of plankton populations to environmental change. *Limnology and Oceanography*, 36 (7):1301–1312. doi: 10.4319/lo.1991.36.7.1301.

Mackey, K, Morris, JJ, Morel, F, and Kranz, S (2015). Response of Photosynthesis to Ocean Acidification. *Oceanography*, 25 (2):74–91. doi: 10.5670/oceanog.2015.33.

Maksym, T, Stammerjohn, S, Ackley, S, and Massom, R (2012). Antarctic Sea Ice–A Polar Opposite? *Oceanography*, 25 (3):140–151. doi: 10.5670/oceanog.2012.88.

Malin, G (2006). OCEANS: New Pieces for the Marine Sulfur Cycle Jigsaw. *Science*, 314 (5799):607–608. doi: 10.1126/science.1133279.

Malinverno, E, Triantaphyllou, MV, and Dimiza, MD (2015). Coccolithophore assemblage distribution along a temperate to polar gradient in the West Pacific sector of the Southern Ocean (January 2005). *Micropaleontology*, 61 (6):489–506.

Mantoura, R and Repeta, D (1997). Calibration methods for HPLC. *Phytoplankton Pigments in Oceanography: Guidelines to Modern Methods*. Ed. by S Jeffrey, R Mantoura, and S Wright. Paris: UNESCO, p 407–428.

Marchant, HJ and Davidson, A (1991). Possible impacts of ozone depletion on trophic interactions and biogenic vertical carbon flux in the Southern Ocean. *Proceedings of the International Conference on the Role of the Polar Regions in Global Change Held in Fairbanks, Alaska on 11-15 June 1990. Volume 2*. Ed. by G Weller, CL Wilson, and BAB Severin. Geophysical Institute, University of Alaska Fairbanks. Fairbanks, AK: Geophysical Institute, University of Alaska Fairbanks, pp. 397–400.

Marie, D, Simon, N, and Vaulot, D (2005). Phytoplankton Cell Counting by Flow Cytometry. *Algal Culturing Techniques*. Ed. by RA Anderson. San Diego, CA, USA: Academic Press. Chap. 17, p 253–267. doi: 10.1016/B978-012088426-1/50018-4.

Marinov, I, Doney, SC, and Lima, ID (2010). Response of ocean phytoplankton community structure to climate change over the 21st century: partitioning the effects of nutrients, temperature and light. *Biogeosciences*, 7 (12):3941–3959. doi: 10.5194/bg-7-3941-2010.

Martin, JH, Gordon, RM, and Fitzwater, SE (1990). Iron in Antarctic waters. *Nature*, 345 (6271):156–158. doi: 10.1038/345156a0.

Martínez-García, A, Sigman, DM, Ren, H, Anderson, RF, Straub, M, Hodell, DA, *et al.* (2014). Iron fertilization of the Subantarctic ocean during the last ice age. *Science*, 343 (6177):1347–50. doi: 10.1126/science.1246848.

Martiny, AC, Pham, CTA, Primeau, FW, Vrugt, JA, Moore, JK, Levin, SA, *et al.* (2013). Strong latitudinal patterns in the elemental ratios of marine plankton and organic matter. *Nature Geoscience*, 6 (4):279–283. doi: 10.1038/ngeo1757.

Massom, RA and Stammerjohn, SE (2010). Antarctic sea ice change and variability – Physical and ecological implications. *Polar Science*, 4 (2):149–186. doi: 10.1016/j.polar.2010.05.001.

Massom, RA, Stammerjohn, SE, Lefebvre, W, Harangozo, SA, Adams, N, Scambos, TA, *et al.* (2008). West Antarctic Peninsula sea ice in 2005: Extreme ice compaction and ice edge

retreat due to strong anomaly with respect to climate. *Journal of Geophysical Research: Oceans*, 113 (2):C02S20. doi: 10.1029/2007JC004239.

Massom, RA, Stammerjohn, SE, Smith, RC, Pook, MJ, Iannuzzi, RA, Adams, N, *et al.* (2006). Extreme Anomalous Atmospheric Circulation in the West Antarctic Peninsula Region in Austral Spring and Summer 2001/02, and Its Profound Impact on Sea Ice and Biota. *Journal of Climate*, 19 (15):3544–3571. doi: 10.1175/JCLI3805.1.

Matear, RJ, Hirst, AC, and McNeil, BI (2000). Changes in dissolved oxygen in the Southern Ocean with climate change. *Geochemistry, Geophysics, Geosystems*, 1 (11):2000GC000086. doi: 10.1029/2000GC000086.

Matear, RJ and Hirst, AC (1999). Climate change feedback on the future oceanic CO_2 uptake. *Tellus B*, 51 (3):722–733. doi: 10.1034/j.1600-0889.1999.t01-1-00012.x.

McCarthy, A, Rogers, SP, Duffy, SJ, and Campbell, DA (2012). Elevated carbon dioxide differentially alters the photophysiology of *Thalassiosira pseudonana* (bacillariophyceae) and *Emiliania huxleyi* (haptophyta). *Journal of Phycology*, 48 (3):635–646. doi: 10.1111/j.1529-8817.2012.01171.x.

McLeod, DJ, Hallegraeff, GM, Hosie, GW, and Richardson, AJ (2012). Climate-driven range expansion of the red-tide dinoflagellate *Noctiluca scintillans* into the Southern Ocean. *Journal of Plankton Research*, 34 (4):332–337. doi: 10.1093/plankt/fbr112.

McMinn, A, Ryan, KG, Ralph, PJ, and Pankowski, A (2007). Spring sea ice photosynthesis, primary productivity and biomass distribution in eastern Antarctica, 2002-2004. *Marine Biology*, 151 (3):985–995. doi: 10.1007/s00227-006-0533-8.

McMinn, A, Müller, MN, Martin, A, and Ryan, KG (2014). The Response of Antarctic Sea Ice Algae to Changes in pH and CO_2. *PLoS ONE*, 9 (1):e86984. doi: 10.1371/journal.pone.0086984.

McNeil, BI and Matear, RJ (2008). Southern Ocean acidification: A tipping point at 450-ppm atmospheric CO_2. *Proceedings of the National Academy of Sciences*, 105 (48):18860–18864. doi: 10.1073/pnas.0806318105.

McQuaid, JB, Kustka, AB, Oborník, M, Horák, A, McCrow, JP, Karas, BJ, *et al.* (2018). Carbonate-sensitive phytotransferrin controls high-affinity iron uptake in diatoms. *Nature*, 555 (7697):534–537. doi: 10.1038/nature25982.

Meakin, NG and Wyman, M (2011). Rapid shifts in picoeukaryote community structure in response to ocean acidification. *The ISME Journal*, 5 (9):1397–1405. doi: 10.1038/ismej.2011.18.

Mehrbach, C, Culberson, CH, Hawley, JE, and Pytkowicx, RM (1973). Measurement of the Apparent Dissociation Constants of Carbonic Acid in Seawater At Atmospheric Pressure. *Limnology and Oceanography*, 18 (6):897–907. doi: 10.4319/lo.1973.18.6.0897.

Meijers, AJS (2014). The Southern Ocean in the Coupled Model Intercomparison Project phase 5. *Philosophical Transactions of the Royal Society A: Mathematical, Physical and Engineering Sciences*, 372 (2019):20130296–20130296. doi: 10.1098/rsta.2013.0296.

Meiners, KM, Vancoppenolle, M, Thanassekos, S, Dieckmann, GS, Thomas, DN, Tison, JL, *et al.* (2012). Chlorophyll *a* in Antarctic sea ice from historical ice core data. *Geophysical Research Letters*, 39 (21):L21602. doi: 10.1029/2012GL053478.

Meinshausen, M, Smith, SJ, Calvin, K, Daniel, JS, Kainuma, MLT, Lamarque, J, *et al.* (2011). The RCP greenhouse gas concentrations and their extensions from 1765 to 2300. *Climatic Change*, 109 (1):213–241. doi: 10.1007/s10584-011-0156-z.

Melbourne-Thomas, J, Constable, A, Wotherspoon, S, and Raymond, B (2013). Testing Paradigms of Ecosystem Change under Climate Warming in Antarctica. *PLoS ONE*, 8 (2):e55093. doi: 10.1371/journal.pone.0055093.

Meredith, MP and Hogg, AM (2006). Circumpolar response of Southern Ocean eddy activity to a change in the Southern Annular Mode. *Geophysical Research Letters*, 33 (16):L16608. doi: 10.1029/2006GL026499.

Meredith, MP and King, JC (2005). Rapid climate change in the ocean west of the Antarctic Peninsula during the second half of the 20th century. *Geophysical Research Letters*, 32 (19):L19604. doi: 10.1029/2005GL024042.

Metzl, N, Tilbrook, B, and Poisson, A (1999). The annual fCO_2 cycle and the air-sea CO_2 flux in the sub-Antarctic Ocean. *Tellus B*, 51 (4):849–861. doi: 10.1034/j.1600-0889.1999.t01-3-00008.x.

Meyer, B, Atkinson, A, Blume, B, and Bathmann, UV (2003). Feeding and energy budgets of larval antarctic krill *Euphausia superba* in summer. *Marine Ecology Progress Series*, 257:167–177. doi: 10.3354/meps257167.

Mitra, A, Flynn, KJ, Burkholder, JM, Berge, T, Calbet, A, Raven, JA, *et al.* (2014). The role of mixotrophic protists in the biological carbon pump. *Biogeosciences*, 11 (4):995–1005. doi: 10.5194/bg-11-995-2014.

Moisan, TA and Mitchell, BG (1999). Photophysiological acclimation of *Phaeocystis antarctica* Karsten under light limitation. *Limnology and oceanography*, 44 (2):247–258. doi: 10.4319/lo.1999.44.2.0247.

Moline, MA, Claustre, H, Frazer, TK, Schofield, O, and Vernet, M (2004). Alteration of the food web along the Antarctic Peninsula in response to a regional warming trend. *Global Change Biology*, 10 (12):1973–1980. doi: 10.1111/j.1365-2486.2004.00825.x.

Moline, MA, Karnovsky, NJ, Brown, Z, Divoky, GJ, Frazer, TK, Jacoby, CA, *et al.* (2008). High Latitude Changes in Ice Dynamics and Their Impact on Polar Marine Ecosystems. *Annals of the New York Academy of Sciences*, 1134 (1):267–319. doi: 10.1196/annals.1439.010.

Montes-Hugo, M, Vernet, M, Martinson, D, Smith, R, and Iannuzzi, R (2008). Variability on phytoplankton size structure in the western Antarctic Peninsula (1997–2006). *Deep Sea Research Part II: Topical Studies in Oceanography*, 55 (18-19):2106–2117. doi: 10.1016/j.dsr2.2008.04.036.

Moore, JK and Abbott, MR (2000). Phytoplankton chlorophyll distributions and primary production in the Southern Ocean. *Journal of Geophysical Research: Oceans*, 105 (C12):28709–28722. doi: 10.1029/1999JC000043.

Moreau, S, Schloss, I, Mostajir, B, Demers, S, Almandoz, G, Ferrario, M, *et al.* (2012). Influence of microbial community composition and metabolism on air-sea ΔpCO_2 variation off the western Antarctic Peninsula. *Marine Ecology Progress Series*, 446 (2009):45–59. doi: 10.3354/meps09466.

Moreau, S, Mostajir, B, Bélanger, S, Schloss, IR, Vancoppenolle, M, Demers, S, *et al.* (2015). Climate change enhances primary production in the western Antarctic Peninsula. *Global Change Biology*, 21 (6):2191–2205. doi: 10.1111/gcb.12878.

Morita, M, Suwa, R, Iguchi, A, Nakamura, M, Shimada, K, Sakai, K, *et al.* (2010). Ocean acidification reduces sperm flagellar motility in broadcast spawning reef invertebrates. *Zygote*, 18 (02):103–107. doi: 10.1017/S0967199409990177.

Moustaka-Gouni, M, Kormas, KA, Scotti, M, Vardaka, E, and Sommer, U (2016). Warming and Acidification Effects on Planktonic Heterotrophic Pico- and Nanoflagellates in a Mesocosm Experiment. *Protist*, 167 (4):389–410. doi: 10.1016/j.protis.2016.06.004.

Müller, M, Trull, T, and Hallegraeff, G (2015). Differing responses of three Southern Ocean *Emiliania huxleyi* ecotypes to changing seawater carbonate chemistry. *Marine Ecology Progress Series*, 531:81–90. doi: 10.3354/meps11309.

Murphy, EJ, Cavanagh, RD, Drinkwater, KF, Grant, SM, Heymans, JJ, Hofmann, EE, *et al.* (2016). Understanding the structure and functioning of polar pelagic ecosystems to predict the impacts of change. *Proceedings of the Royal Society B: Biological Sciences*, 283 (1844):20161646. doi: 10.1098/rspb.2016.1646.

Murphy, EJ, Morris, DJ, Watkins, JL, and Priddle, J (1988). Scales of interaction between Antarctic krill and the environment. *Antarctic Ocean and Resources Variability*,120–130. doi: 10.1007/978-3-642-73724-4_9.

Murphy, E, Watkins, J, Trathan, P, Reid, K, Meredith, M, Thorpe, S, *et al.* (2007). Spatial and temporal operation of the Scotia Sea ecosystem: a review of large-scale links in a krill centred food web. *Philosophical Transactions of the Royal Society B: Biological Sciences*, 362 (1477):113–148. doi: 10.1098/rstb.2006.1957.

Nakajima, A (2005). Increase in intracellular pH induces phosphorylation of axonemal proteins for activation of flagellar motility in starfish sperm. *Journal of Experimental Biology*, 208 (23):4411–4418. doi: 10.1242/jeb.01906.

Nakamura, M and Morita, M (2012). Sperm motility of the scleractinian coral *Acropora digitifera* under preindustrial, current, and predicted ocean acidification regimes. *Aquatic Biology*, 15 (3):299–302. doi: 10.3354/ab00436.

Neale, PJ, Cullen, JJ, and Davis, RF (1998a). Inhibition of marine photosynthesis by ultraviolet radiation: Variable sensitivity of phytoplankton in the Weddell-Scotia Confluence during the austral spring. *Limnology and Oceanography*, 43:433–448. doi: 10.4319/lo.1998.43.3.0433.

Neale, PJ, Davis, RF, and Cullen, JJ (1998b). Interactive effects of ozone depletion and vertical mixing on photosynthesis of Antarctic phytoplankton. *Nature*, 392 (6676):585–589. doi: 10.1038/33374.

Nelson, DM, Smith, WOJ, Gordon, LI, and Huber, BA (1987). Spring distributions of density, nutrients, and phytoplankton biomass in the ice edge zone of the Weddell-Scotia Sea. *Journal of Geophysical Research: Oceans*, 92 (C7):7181. doi: 10.1029/JC092iC07p07181.

Nevitt, GA, Veit, RR, and Kareiva, P (1995). Dimethyl sulphide as a foraging cue for Antarctic Procellariiform seabirds. *Nature*, 376 (6542):680–682. doi: 10.1038/376680a0.

Newbold, LK, Oliver, AE, Booth, T, Tiwari, B, DeSantis, T, Maguire, M, *et al.* (2012). The response of marine picoplankton to ocean acidification. *Environmental Microbiology*, 14 (9):2293–2307. doi: 10.1111/j.1462-2920.2012.02762.x.

Nicol, S, Pauly, T, Bindoff, N, and Strutton, P (2000). "BROKE" a biological/oceanographic survey off the coast of East Antarctica (80–150° E) carried out in January-March 1996. *Deep Sea Research Part II: Topical Studies in Oceanography*, 47 (12-13):2281–2297. doi: 10.1016/S0967-0645(00)00026-6.

Nicol, S, Meiners, K, and Raymond, B (2010). BROKE-West, a large ecosystem survey of the South West Indian Ocean sector of the Southern Ocean, 30° E–80° E (CCAMLR Division 58.4.2). *Deep Sea Research Part II: Topical Studies in Oceanography*, 57 (9-10):693–700. doi: 10.1016/j.dsr2.2009.11.002.

Obernosterer, I, Christaki, U, Lefèvre, D, Catala, P, Van Wambeke, F, and Lebaron, P (2008). Rapid bacterial mineralization of organic carbon produced during a phytoplankton bloom induced by natural iron fertilization in the Southern Ocean. *Deep-Sea Research Part II: Topical Studies in Oceanography*, 55 (5-7):777–789. doi: 10.1016/j.dsr2.2007.12.005.

Odate, T and Fukuchi, M (1995). Distribution and community structure of picoplankton in the Southern Ocean during the late austral summer of 1992. *Proceedings of the NIPR Symposium on Polar Biology*, 8:86–100.

Olguín, HF and Alder, VA (2011). Species composition and biogeography of diatoms in antarctic and subantarctic (Argentine shelf) waters (37-76° S). *Deep Sea Research Part II: Topical Studies in Oceanography*, 58 (1-2):139–152. doi: 10.1016/j.dsr2.2010.09.031.

Orr, JC, Fabry, VJ, Aumont, O, Bopp, L, Doney, SC, Feely, RA, *et al.* (2005). Anthropogenic ocean acidification over the twenty-first century and its impact on calcifying organisms. *Nature*, 437 (7059):681–6. doi: 10.1038/nature04095.

Orsi, A, Johnson, G, and Bullister, J (1999). Circulation, mixing, and production of Antarctic Bottom Water. *Progress in Oceanography*, 43 (1):55–109. doi: 10.1016/S0079-6611(99)00004-X.

Orsi, AH, Whitworth, T, and Nowlin, WD (1995). On the meridional extent and fronts of the Antarctic Circumpolar Current. *Deep Sea Research Part I: Oceanographic Research Papers*, 42 (5):641–673. doi: 10.1016/0967-0637(95)00021-W.

Padan, E, Bibi, E, Ito, M, and Krulwich, TA (2005). Alkaline pH homeostasis in bacteria: New insights. *Biochimica et Biophysica Acta - Biomembranes*, 1717 (2):67–88. doi: 10.1016/j.bbamem.2005.09.010.

Palmisano, AC and Sullivan, CW (1983). Sea ice microbial communities (SIMCO) 1. Distribution, abundance, and primary production of ice microalgae in McMurdo Sound, Antarctica in 1980. *Polar Biology*, 2 (3):171–177. doi: 10.1007/BF00448967.

Palmisano, A, SooHoo, J, Moe, R, and Sullivan, C (1987). Sea ice microbial communities. VII. Changes in under-ice spectral irradiance during the development of Antarctic sea ice microalgal communities. *Marine Ecology Progress Series*, 35:165–173. doi: 10.3354/meps035165.

Parkinson, CL and Cavalieri, DJ (2012). Antarctic sea ice variability and trends, 1979-2010. *The Cryosphere*, 6 (4):871–880. doi: 10.5194/tc-6-871-2012.

Pasquer, B, Mongin, M, Johnston, N, and Wright, S (2010). Distribution of particulate organic matter (POM) in the Southern Ocean during BROKE-West (30°E - 80°E). *Deep Sea Research Part II: Topical Studies in Oceanography*, 57 (9-10):779–793. doi: 10.1016/j.dsr2.2008.12.040.

Passow, U and Laws, EEA (2015). Ocean acidification as one of multiple stressors: Growth response of *Thalassiosira weissflogii* (diatom) under temperature and light stress. *Marine Ecology Progress Series*, 541:75–90. doi: 10.3354/meps11541.

Patil, SM, Mohan, R, Shetye, S, Gazi, S, and Jafar, S (2014). Morphological variability of *Emiliania huxleyi* in the Indian sector of the Southern Ocean during the austral summer of 2010. *Marine Micropaleontology*, 107:44–58. doi: 10.1016/j.marmicro.2014.01.005.

Paul, C, Matthiessen, B, and Sommer, U (2015). Warming, but not enhanced CO_2 concentration, quantitatively and qualitatively affects phytoplankton biomass. *Marine Ecology Progress Series*, 528:39–51. doi: 10.3354/meps11264.

Paulino, AI, Egge, JK, and Larsen, A (2008). Effects of increased atmospheric CO_2 on small and intermediate sized osmotrophs during a nutrient induced phytoplankton bloom. *Biogeosciences*, 5 (3):739–748. doi: 10.5194/bg-5-739-2008.

Pearce, I, Davidson, A, Bell, E, and Wright, S (2007). Seasonal changes in the concentration and metabolic activity of bacteria and viruses at an Antarctic coastal site. *Aquatic Microbial Ecology*, 47 (1):11–23. doi: 10.3354/ame047011.

Pearce, I, Davidson, AT, Thomson, PG, Wright, S, and van den Enden, R (2010). Marine microbial ecology off East Antarctica (30 - 80°E): Rates of bacterial and phytoplankton growth and grazing by heterotrophic protists. *Deep Sea Research Part II: Topical Studies in Oceanography*, 57 (9-10):849–862. doi: 10.1016/j.dsr2.2008.04.039.

Pearce, I, Davidson, AT, Thomson, PG, Wright, S, and van den Enden, R (2011). Marine microbial ecology in the sub-Antarctic Zone: Rates of bacterial and phytoplankton growth and grazing by heterotrophic protists. *Deep Sea Research Part II: Topical Studies in Oceanography*, 58 (21-22):2248–2259. doi: 10.1016/j.dsr2.2011.05.030.

Peck, LS, Barnes, DKA, Cook, AJ, Fleming, AH, and Clarke, A (2010). Negative feedback in the cold: Ice retreat produces new carbon sinks in Antarctica. *Global Change Biology*, 16 (9):2614–2623. doi: 10.1111/j.1365-2486.2009.02071.x.

Perissinotto, R and Pakhomov, EA (1998). Contribution of salps to carbon flux of marginal ice zone of the Lazarev Sea, southern ocean. *Marine Biology*, 131 (1):25–32. doi: 10.1007/s002270050292.

Perovich, DK (1990). Theoretical estimates of light reflection and transmission by spatially complex and temporally varying sea ice covers. *Journal of Geophysical Research: Oceans*, 95 (C6):9557. doi: 10.1029/JC095iC06p09557.

Perrin, RA, Lu, P, and Marchant, HJ (1987). Seasonal variation in marine phytoplankton and ice algae at a shallow antarctic coastal site. *Hydrobiologia*, 146 (1):33–46. doi: 10.1007/BF00007575.

Petrou, K, Kranz, SA, Trimborn, S, Hassler, CS, Ameijeiras, SB, Sackett, O, *et al.* (2016). Southern Ocean phytoplankton physiology in a changing climate. *Journal of Plant Physiology*, 203:135–150. doi: 10.1016/j.jplph.2016.05.004.

Pezza, AB, Rashid, HA, and Simmonds, I (2012). Climate links and recent extremes in antarctic sea ice, high-latitude cyclones, Southern Annular Mode and ENSO. *Climate Dynamics*, 38 (1-2):57–73. doi: 10.1007/s00382-011-1044-y.

Piontek, J, Borchard, C, Sperling, M, Schulz, KG, Riebesell, U, and Engel, A (2013). Response of bacterioplankton activity in an Arctic fjord system to elevated pCO_2: results from a mesocosm perturbation study. *Biogeosciences*, 10 (1):297–314. doi: 10.5194/bg-10-297-2013.

Platt, T, Gallegos, CL, and Harrison, WG (1980). Photoinibition of photosynthesis in natural assemblages of marine phytoplankton. *Journal of Marine Research*, 38 (4):687–701.

Polimene, L, Sailley, S, Clark, D, Mitra, A, and Allen, JI (2016). Biological or microbial carbon pump? The role of phytoplankton stoichiometry in ocean carbon sequestration. *Journal of Plankton Research*, 39 (2):180–186. doi: 10.1093/plankt/fbw091.

Pollard, R, Lucas, M, and Read, J (2002). Physical controls on biogeochemical zonation in the Southern Ocean. *Deep Sea Research Part II: Topical Studies in Oceanography*, 49 (16):3289–3305. doi: 10.1016/S0967-0645(02)00084-X.

Pollard, RT, Salter, I, Sanders, RJ, Lucas, MI, Moore, CM, Mills, RA, *et al.* (2009). Southern Ocean deep-water carbon export enhanced by natural iron fertilization. *Nature*, 457 (7229):577–580. doi: 10.1038/nature07716.

Poloczanska, E, Babcock, R, Butler, A, Hobday, A, Hoegh-Guldberg, O, Kunz, T, *et al.* (2007). Climate change and Australian marine life. *Oceanography and marine biology. Volume 45*. Ed. by RN Gibson, RJA Atkinson, and JDM Gordon. Boca Raton, FL: CRC Press, p 407–78.

Polvani, LM, Waugh, DW, Correa, GJP, and Son, SW (2011). Stratospheric Ozone Depletion: The Main Driver of Twentieth-Century Atmospheric Circulation Changes in the Southern Hemisphere. *Journal of Climate*, 24 (3):795–812. doi: 10.1175/2010JCLI3772.1.

Pörtner, HO (2008). Ecosystem effects of ocean acidification in times of ocean warming: A physiologist's view. *Marine Ecology Progress Series*, 373:203–217. doi: 10.3354/meps07768.

Post, A, Meijers, A, Fraser, A, Meiners, K, Ayers, J, Bindoff, N, *et al.* (2014). Environmental setting. *Biogeographic Atlas of the Southern Ocean*. Ed. by C De Broyer, P Koubbi, HJ Griffiths, B Raymond, C D'Udekem d'Acoz, AP Van de Putte, *et al.* Cambridge UK: Scientific Committee on Antarctic Research. Chap. 4, p 46–64.

Qu, CF, Liu, FM, Zheng, Z, Wang, YB, Li, XG, Yuan, HM, *et al.* (2017). Effects of ocean acidification on the physiological performance and carbon production of the Antarctic sea ice

diatom *Nitzschia* sp. ICE-H. *Marine Pollution Bulletin*, 120 (1-2):184–191. doi: 10.1016/j.marpolbul.2017.05.018.

Quéguiner, B (2013). Iron fertilization and the structure of planktonic communities in high nutrient regions of the Southern Ocean. *Deep Sea Research Part II: Topical Studies in Oceanography*, 90:43–54. doi: 10.1016/j.dsr2.2012.07.024.

Quetin, LB and Ross, RM (1985). Feeding by Antarctic Krill, *Euphausia superba*: Does Size Matter? *Antarctic Nutrient Cycles and Food Webs*. Ed. by W Siegfried, P Condy, and R Laws. Berlin, Heidelberg: Springer Berlin Heidelberg, p 372–377. doi: 10.1007/978-3-642-82275-9_52.

Quetin, LB and Ross, RM (2009). Life under Antarctic pack ice: a krill perspective. *Smithsonian at the Poles: Contributions to International Polar Year Science*. Ed. by I Krupnik, M Lang, and S Miller. Washington, D.C.: Smithsonian Institute, p 285–298.

R Core Team (2016). R: A Language and Environment for Statistical Computing. Vienna, Austria.

Rack, W and Rott, H (2004). Pattern of retreat and disintegration of the Larsen B ice shelf, Antarctic Peninsula. *Annals of Glaciology*, 39 (1):505–510. doi: 10.3189/172756404781814005.

Raphael, MN, Marshall, GJ, Turner, J, Fogt, RL, Schneider, D, Dixon, DA, *et al.* (2016). The Amundsen Sea Low: Variability, Change, and Impact on Antarctic Climate. *Bulletin of the American Meteorological Society*, 97 (1):111–121. doi: 10.1175/BAMS-D-14-00018.1.

Ratnarajah, L, Melbourne-Thomas, J, Marzloff, MP, Lannuzel, D, Meiners, KM, Chever, F, *et al.* (2016). A preliminary model of iron fertilisation by baleen whales and Antarctic krill in the Southern Ocean: Sensitivity of primary productivity estimates to parameter uncertainty. *Ecological Modelling*, 320:203–212. doi: 10.1016/j.ecolmodel.2015.10.007.

Raven, JA (1991). Physiology of inorganic C acquisition and implications for resource use efficiency by marine phytoplankton: relation to increased CO_2 and temperature. *Plant, Cell and Environment*, 14 (8):779–794. doi: 10.1111/j.1365-3040.1991.tb01442.x.

Raven, JA and Falkowski, PG (1999). Oceanic sinks for atmospheric CO_2. *Plant, Cell and Environment*, 22 (6):741–755. doi: 10.1046/j.1365-3040.1999.00419.x.

Raven, JA, Beardall, J, and Sánchez-Baracaldo, P (2017). The possible evolution and future of CO_2-concentrating mechanisms. *Journal of Experimental Botany*, 68 (14):3701–3716. doi: 10.1093/jxb/erx110.

Raven, J, Caldeira, K, Elderfield, H, Hoegh-Guldberg, O, Liss, P, Riebesell, U, *et al.* (2005). Ocean acidification due to increasing atmospheric carbon dioxide. Tech. rep. (June). The Royal Society, p. 68.

Regaudie-de-gioux, A, Lasternas, S, Agustí, S, Duarte, CM, and Benitez, NG (2014). Comparing marine primary production estimates through different methods and development of conversion equations. *Frontiers in Marine Science*, 1 (July):1–14. doi: 10.3389/fmars.2014.00019.

Reid, K and Croxall, JP (2001). Environmental response of upper trophic-level predators reveals a system change in an Antarctic marine ecosystem. *Proceedings of the Royal Society B: Biological Sciences*, 268 (1465):377–384. doi: 10.1098/rspb.2000.1371.

Rembauville, M, Blain, S, Caparros, J, and Salter, I (2016a). Particulate matter stoichiometry driven by microplankton community structure in summer in the Indian sector of the Southern Ocean. *Limnology and Oceanography*, 61 (4):1301–1321. doi: 10.1002/lno.10291.

Rembauville, M, Manno, C, Tarling, G, Blain, S, and Salter, I (2016b). Strong contribution of diatom resting spores to deep-sea carbon transfer in naturally iron-fertilized waters downstream of South Georgia. *Deep Sea Research Part I: Oceanographic Research Papers*, 115:22–35. doi: 10.1016/j.dsr.2016.05.002.

Rembauville, M, Meilland, J, Ziveri, P, Schiebel, R, Blain, S, and Salter, I (2016c). Planktic foraminifer and coccolith contribution to carbonate export fluxes over the central Kerguelen Plateau. *Deep Sea Research Part I: Oceanographic Research Papers*, 111:91–101. doi: 10.1016/j.dsr.2016.02.017.

Rembauville, M, Salter, I, Leblond, N, Gueneugues, A, and Blain, S (2015a). Export fluxes in a naturally iron-fertilized area of the Southern Ocean – Part 1: Seasonal dynamics of particulate organic carbon export from a moored sediment trap. *Biogeosciences*, 12 (11):3153–3170. doi: 10.5194/bg-12-3153-2015.

Rembauville, M, Blain, S, Armand, L, Quéguiner, B, and Salter, I (2015b). Export fluxes in a naturally iron-fertilized area of the Southern Ocean – Part 2: Importance of diatom resting

spores and faecal pellets for export. *Biogeosciences*, 12 (11):3171–3195. doi: 10.5194/bg-12-3171-2015.

Rickard, G and Behrens, E (2016). CMIP5 Earth System Models with biogeochemistry: a Ross Sea assessment. *Antarctic Science*, 28 (05):327–346. doi: 10.1017/S0954102016000122.

Ridgway, KR (2007). Long-term trend and decadal variability of the southward penetration of the East Australian Current. *Geophysical Research Letters*, 34 (13):doi: 10.1029/2007GL030393.

Ridgwell, AJ (2002). Dust in the Earth system: the biogeochemical linking of land, air and sea. *Philosophical Transactions of the Royal Society A: Mathematical, Physical and Engineering Sciences*, 360 (1801):2905–2924. doi: 10.1098/rsta.2002.1096.

Riebesell, U, Bellerby, RGJ, Grossart, HP, and Thingstad, F (2008). Mesocosm CO_2 perturbation studies: from organism to community level. *Biogeosciences*, 5 (4):1157–1164. doi: 10.5194/bg-5-1157-2008.

Riebesell, U, Gattuso, JP, Thingstad, TF, and Middelburg, JJ (2013). Preface "Arctic ocean acidification: pelagic ecosystem and biogeochemical responses during a mesocosm study". *Biogeosciences*, 10 (8):5619–5626. doi: 10.5194/bg-10-5619-2013.

Riebesell, U, Wolf-Gladrow, DA, and Smetacek, V (1993). Carbon dioxide limitation of marine phytoplankton growth rates. *Nature*, 361 (6409):249–251. doi: 10.1038/361249a0.

Riebesell, U, Schulz, KG, Bellerby, RGJ, Botros, M, Fritsche, P, Meyerhöfer, M, *et al.* (2007). Enhanced biological carbon consumption in a high CO_2 ocean. *Nature*, 450 (7169):545–548. doi: 10.1038/nature06267.

Riebesell, U (2004). Effects of CO_2 Enrichment on Marine Phytoplankton. *Journal of Oceanography*, 60 (4):719–729. doi: 10.1007/s10872-004-5764-z.

Riebesell, U, Körtzinger, A, and Oschlies, A (2009). Sensitivities of marine carbon fluxes to ocean change. *Proceedings of the National Academy of Sciences of the United States of America*, 106 (49):20602–20609. doi: 10.1073/pnas.0813291106.

Rigual-Hernández, AS, Trull, TW, Bray, SG, Closset, I, and Armand, LK (2015). Seasonal dynamics in diatom and particulate export fluxes to the deep sea in the Australian sector of the southern Antarctic Zone. *Journal of Marine Systems*, 142:62–74. doi: 10.1016/j.jmarsys.2014.10.002.

Riley, GA (1957). Phytoplankton of the North Central Sargasso Sea, 1950-52. *Limnology and Oceanography*, 2 (3):252–270. doi: 10.1002/lno.1957.2.3.0252.

Rintoul, SR and Trull, TW (2001). Seasonal evolution of the mixed layer in the Subantarctic zone south of Australia. *Journal of Geophysical Research: Oceans*, 106 (C12):31447–31462. doi: 10.1029/2000JC000329.

Ritchie, RJ (2006). Consistent sets of spectrophotometric chlorophyll equations for acetone, methanol and ethanol solvents. *Photosynthesis Research*, 89 (1):27–41. doi: 10.1007/s11120-006-9065-9.

Robbins, L, Hansen, M, Kleypas, J, and Meylan, S (2010). CO_2calc: A User-Friendly Seawater Carbon Calculator for Windows, Mac OS X, and iOS (iPhone). Tech. rep. U.S. Geological Survey Open-File Report 2010–1280, p. 17.

Robins, D, Harris, R, Bedo, A, Fernandez, E, Fileman, T, Harbour, D, *et al.* (1995). The relationship between suspended particulate material, phytoplankton and zooplankton during the retreat of the marginal ice zone in the Bellingshausen Sea. *Deep Sea Research Part II: Topical Studies in Oceanography*, 42 (4-5):1137–1158. doi: 10.1016/0967-0645(95)00058-X.

Roden, NP, Shadwick, EH, Tilbrook, B, and Trull, TW (2013). Annual cycle of carbonate chemistry and decadal change in coastal Prydz Bay, East Antarctica. *Marine Chemistry*, 155 (0):135–147. doi: 10.1016/j.marchem.2013.06.006.

Rose, JM, Feng, Y, DiTullio, GR, Dunbar, RB, Hare, CE, Lee, PA, *et al.* (2009a). Synergistic effects of iron and temperature on Antarctic phytoplankton and microzooplankton assemblages. *Biogeosciences*, 6 (12):3131–3147. doi: 10.5194/bg-6-3131-2009.

Rose, J, Feng, Y, Gobler, C, Gutierrez, R, Hare, C, Leblanc, K, *et al.* (2009b). Effects of increased pCO_2 and temperature on the North Atlantic spring bloom. II. Microzooplankton abundance and grazing. *Marine Ecology Progress Series*, 388:27–40. doi: 10.3354/meps08134.

Rose, JM, Caron, DA, Sieracki, ME, and Poulton, N (2004). Counting heterotrophic nanoplanktonic protists in cultures and aquatic communities by flow cytometry. *Aquatic Microbial Ecology*, 34 (3):263–277. doi: 10.3354/ame034263.

Rossoll, D, Sommer, U, and Winder, M (2013). Community interactions dampen acidification effects in a coastal plankton system. *Marine Ecology Progress Series*, 486:37–46. doi: 10.3354/meps10352.

Rossoll, D, Bermúdez, R, Hauss, H, Schulz, KG, Riebesell, U, Sommer, U, *et al.* (2012). Ocean Acidification-Induced Food Quality Deterioration Constrains Trophic Transfer. *PLoS ONE*, 7 (4):e34737. doi: 10.1371/journal.pone.0034737.

Rost, B, Riebesell, U, Burkhardt, S, and Sültemeyer, D (2003). Carbon acquisition of bloom-forming marine phytoplankton. *Limnology and Oceanography*, 48 (1):55–67. doi: 10.4319/lo.2003.48.1.0055.

Rost, B, Zondervan, I, and Wolf-Gladrow, D (2008). Sensitivity of phytoplankton to future changes in ocean carbonate chemistry: current knowledge, contradictions and research directions. *Marine Ecology Progress Series*, 373:227–237. doi: 10.3354/meps07776.

Roy, AS, Gibbons, SM, Schunck, H, Owens, S, Caporaso, JG, Sperling, M, *et al.* (2013). Ocean acidification shows negligible impacts on high-latitude bacterial community structure in coastal pelagic mesocosms. *Biogeosciences*, 10 (1):555–566. doi: 10.5194/bg-10-555-2013.

Saavedra-Pellitero, M, Baumann, KH, Flores, JA, and Gersonde, R (2014). Biogeographic distribution of living coccolithophores in the Pacific sector of the Southern Ocean. *Marine Micropaleontology*, 109:1–20. doi: 10.1016/j.marmicro.2014.03.003.

Sabine, CL (2004). The Oceanic Sink for Anthropogenic CO_2. *Science*, 305 (5682):367–371. doi: 10.1126/science.1097403.

Sackett, O, Petrou, K, Reedy, B, De Grazia, A, Hill, R, Doblin, M, *et al.* (2013). Phenotypic Plasticity of Southern Ocean Diatoms: Key to Success in the Sea Ice Habitat? *PLoS ONE*, 8 (11):e81185. doi: 10.1371/journal.pone.0081185.

Saenz, BT and Arrigo, KR (2014). Annual primary production in Antarctic sea ice during 2005-2006 from a sea ice state estimate. *Journal of Geophysical Research: Oceans*, 119 (6):3645–3678. doi: 10.1002/2013JC009677.

Safi, KA, Griffiths, FB, and Hall, JA (2007). Microzooplankton composition, biomass and grazing rates along the WOCE SR3 line between Tasmania and Antarctica. *Deep Sea Research Part I: Oceanographic Research Papers*, 54 (7):1025–1041. doi: 10.1016/j.dsr.2007.05.003.

Sakshaug, E (1994). Discussant's report: primary production in the Antarctic pelagial - a view from the north. *Southern Ocean Ecology: The BIOMASS Perspective*. Ed. by SZ El-Sayed. Cambridge, UK: Cambridge University Press, p 399.

Sallée, JB, Speer, KG, and Rintoul, SR (2010). Zonally asymmetric response of the Southern Ocean mixed-layer depth to the Southern Annular Mode. *Nature Geoscience*, 3 (4):273–279. doi: 10.1038/ngeo812.

Salter, I, Kemp, AES, Moore, CM, Lampitt, RS, Wolff, GA, and Holtvoeth, J (2012). Diatom resting spore ecology drives enhanced carbon export from a naturally iron-fertilized bloom in the Southern Ocean. *Global Biogeochemical Cycles*, 26 (1):GB1014. doi: 10.1029/2010GB003977.

Salter, I, Lampitt, RS, Sanders, R, Poulton, A, Kemp, AE, Boorman, B, *et al.* (2007). Estimating carbon, silica and diatom export from a naturally fertilised phytoplankton bloom in the Southern Ocean using PELAGRA: A novel drifting sediment trap. *Deep Sea Research Part II: Topical Studies in Oceanography*, 54 (18-20):2233–2259. doi: 10.1016/j.dsr2.2007.06.008.

Salter, I, Schiebel, R, Ziveri, P, Movellan, A, Lampitt, R, and Wol, GA (2014). Carbonate counter pump stimulated by natural iron fertilization in the Polar Frontal Zone. *Nature Geoscience*, 7 (December):885–889. doi: 10.1038/NGEO2285.

Sampaio, E, Gallo, F, Schulz, K, Azevedo, E, and Barcelos e Ramos, J (2017). Phytoplankton interactions can alter species response to present and future CO_2 concentrations. *Marine Ecology Progress Series*, 575:31–42. doi: 10.3354/meps12197.

Sarmento, H and Gasol, JM (2012). Use of phytoplankton-derived dissolved organic carbon by different types of bacterioplankton. *Environmental Microbiology*, 14 (9):2348–2360. doi: 10.1111/j.1462-2920.2012.02787.x.

Sarmento, H, Montoya, JM, Vazquez-Dominguez, E, Vaque, D, and Gasol, JM (2010). Warming effects on marine microbial food web processes: how far can we go when it comes to predictions? *Philosophical Transactions of the Royal Society B: Biological Sciences*, 365 (1549):2137–2149. doi: 10.1098/rstb.2010.0045.

Sarmiento, JL, Slater, R, Barber, R, Bopp, L, Doney, SC, Hirst, AC, *et al.* (2004). Response of ocean ecosystems to climate warming. *Global Biogeochemical Cycles*, 18 (3):GB3003. doi: 10.1029/2003GB002134.

Sarmiento, JL and Le Quéré, C (1996). Oceanic Carbon Dioxide Uptake in a Model of Century-Scale Global Warming. *Science*, 274 (5291):1346–1350. doi: 10.1126/science.274.5291.1346.

Satoh, A, Kurano, N, and Miyachi, S (2001). Inhibition of photosynthesis by intracellular carbonic anhydrase in microalgae under excess concentrations of CO_2. *Photosynthesis Research*, 68 (3):215–224. doi: 10.1023/A:1012980223847.

Savidge, G, Priddle, J, Gilpin, L, Bathmann, U, Murphy, E, Owens, N, *et al.* (1996). An assessment of the role of the marginal ice zone in the carbon cycle of the Southern Ocean. *Antarctic Science*, 8 (04):349–358. doi: 10.1017/S0954102096000521.

El-Sayed, SZ, ed. (1994). Souther Ocean Ecology: The BIOMASS Perspective. Cambridge, UK: Cambridge University Press, p 399.

El-Sayed, SZ and Taguchi, S (1981). Primary production and standing crop of phytoplankton along the ice-edge in the Weddell Sea. *Deep Sea Research Part A. Oceanographic Research Papers*, 28 (9):1017–1032. doi: 10.1016/0198-0149(81)90015-7.

Scambos, TA, Hulbe, C, Fahnestock, M, and Bohlander, J (2000). The link between climate warming and break-up of ice shelves in the Antarctic Peninsula. *Journal of Glaciology*, 46 (154):516–530. doi: 10.3189/172756500781833043.

Schaum, CE, Rost, B, and Collins, S (2016). Environmental stability affects phenotypic evolution in a globally distributed marine picoplankton. *The ISME Journal*, 10 (1):75–84. doi: 10.1038/ismej.2015.102.

Schaum, CE and Collins, S (2014). Plasticity predicts evolution in a marine alga. *Proceedings of the Royal Society B: Biological Sciences*, 281 (1793):20141486–20141486. doi: 10.1098/rspb.2014.1486.

Schaum, E, Rost, B, Millar, AJ, and Collins, S (2012). Variation in plastic responses of a globally distributed picoplankton species to ocean acidification. *Nature Climate Change*, 3 (3):298–302. doi: 10.1038/nclimate1774.

Scheinin, M, Riebesell, U, Rynearson, TA, Lohbeck, KT, and Collins, S (2015). Experimental evolution gone wild. *Journal of The Royal Society Interface*, 12 (106):20150056–20150056. doi: 10.1098/rsif.2015.0056.

Schiermeier, Q (2009). Atmospheric science: Fixing the sky. *Nature*, 460 (7257):792–795. doi: 10.1038/460792a.

Schmidt, K, Atkinson, A, Petzke, KJ, Voss, M, and Pond, DW (2006). Protozoans as a food source for Antarctic krill, *Euphausia superba*: Complementary insights from stomach content, fatty

acids, and stable isotopes. *Limnology and Oceanography*, 51 (5):2409–2427. doi: 10.4319/lo.2006.51.5.2409.

Schnack-Schiel, SB and Isla, E (2005). The role of zooplankton in the pelagic-benthic coupling of the Southern Ocean. *Scientia Marina*, 69 (S2):39–55. doi: 10.3989/scimar.2005.69s239.

Schnack-Schiel, SB, Thomas, D, Dahms, HU, Haas, C, and Mizdalski, E (1998). Copepods in Antarctic Sea Ice. *Antarctic Sea Ice: Biological Processes, Interactions and Variability*. Ed. by MP Lizotte and KR Arrigo. Washington, D.C.: American Geophysical Union, p 173–182.

Schreiber, U (2004). Pulse-Amplitude-Modulation (PAM) Fluorometry and Saturation Pulse Method: An Overview. *Chlorophyll a Fluorescence*. Ed. by GC Papageorgiou and Govindjee. Dordrecht: Springer Netherlands, p 279–319. doi: 10.1007/978-1-4020-3218-9_11.

Schulz, KG, Bellerby, RGJ, Brussaard, CPD, Büdenbender, J, Czerny, J, Engel, A, *et al.* (2013). Temporal biomass dynamics of an Arctic plankton bloom in response to increasing levels of atmospheric carbon dioxide. *Biogeosciences*, 10 (1):161–180. doi: 10.5194/bg-10-161-2013.

Schulz, KG, Bach, LT, Bellerby, RGJ, Bermúdez, R, Büdenbender, J, Boxhammer, T, *et al.* (2017). Phytoplankton Blooms at Increasing Levels of Atmospheric Carbon Dioxide: Experimental Evidence for Negative Effects on Prymnesiophytes and Positive on Small Picoeukaryotes. *Frontiers in Marine Science*, 4 (64):1–18. doi: 10.3389/fmars.2017.00064.

Scott, FJ and Marchant, HJ (2005). Antarctic Marine Protists. Ed. by FJ Scott and HJ Marchant. Canberra: Australian Biological Resources Study, p 536.

Sedwick, PN, Marsay, CM, Sohst, BM, Aguilar-Islas, AM, Lohan, MC, Long, MC, *et al.* (2011). Early season depletion of dissolved iron in the Ross Sea polynya: Implications for iron dynamics on the Antarctic continental shelf. *Journal of Geophysical Research: Oceans*, 116 (12):1–19. doi: 10.1029/2010JC006553.

Sen Gupta, A, Santoso, A, Taschetto, AS, Ummenhofer, CC, Trevena, J, and England, MH (2009). Projected Changes to the Southern Hemisphere Ocean and Sea Ice in the IPCC AR4 Climate Models. *Journal of Climate*, 22 (11):3047–3078. doi: 10.1175/2008JCLI2827.1.

Shadwick, EH, Trull, TW, Thomas, H, and Gibson, JAE (2013). Vulnerability of Polar Oceans to Anthropogenic Acidification: Comparison of Arctic and Antarctic Seasonal Cycles. *Scientific Reports*, 3:2339. doi: 10.1038/srep02339.

Shaw, T, Raiswell, R, Hexel, C, Vu, H, Moore, W, Dudgeon, R, *et al.* (2011). Input, composition, and potential impact of terrigenous material from free-drifting icebergs in the Weddell Sea.

Deep Sea Research Part II: Topical Studies in Oceanography, 58 (11-12):1376–1383. doi: 10.1016/j.dsr2.2010.11.012.

Sherr, EB, Caron, DA, and Sherr, BF (1993). Staining of Heterotrophic Protists for Visualization via Epifluorescence Microscopy. *Handbook of Methods in Aquatic Microbial Ecology*. Ed. by PF Kemp, BF Sherr, EB Sherr, and JJ Cole. Boca Raton, FL: CRC Press. Chap. 26, p 213–227.

Sherr, EB and Sherr, BF (1993). Preservation and Storage of Samples for Enumeration of Heterotrophic Protists. *Handbook of Methods in Aquatic Microbial Ecology*. Ed. by PF Kemp, BF Sherr, EB Sherr, and JJ Cole. Boca Raton, FL: CRC Press. Chap. 25, p 207–212.

Sherr, EB and Sherr, BF (2002). Significance of predation by protists. *Antonie van Leeuwenhoek*, 81:293–308. doi: 10.1023/A:1020591307260.

Shi, D, Xu, Y, and Morel, FMM (2009). Effects of the pH/pCO_2 control method on medium chemistry and phytoplankton growth. *Biogeosciences*, 6 (7):1199–1207. doi: 10.5194/bg-6-1199-2009.

Shi, D, Xu, Y, Hopkinson, BM, and Morel, FMM (2010). Effect of Ocean Acidification on Iron Availability to Marine Phytoplankton. *Science*, 327 (5966):676–679. doi: 10.1126/science.1183517.

Shi, Q, Xiahou, W, and Wu, H (2017). Photosynthetic responses of the marine diatom *Thalassiosira pseudonana* to CO_2-induced seawater acidification. *Hydrobiologia*, 788 (1):361–369. doi: 10.1007/s10750-016-3014-1.

Shindell, DT and Schmidt, GA (2004). Southern Hemisphere climate response to ozone changes and greenhouse gas increases. *Geophysical Research Letters*, 31 (18):L18209. doi: 10.1029/2004GL020724.

Siegel, DA, Buesseler, KO, Doney, SC, Sailley, SF, Behrenfeld, MJ, and Boyd, PW (2014). Global assessment of ocean carbon export by combining satellite observations and food-web models. *Global Biogeochemical Cycles*, 28 (3):181–196. doi: 10.1002/2013GB004743.

Silsbe, GM and Malkin, SY (2015). phytotools: Phytoplankton Production Tools.

Simmonds, I (2015). Comparing and contrasting the behaviour of Arctic and Antarctic sea ice over the 35 year period 1979–2013. *Annals of Glaciology*, 56 (69):18–28. doi: 10.3189/2015AoG69A909.

Simó, R (2004). From cells to globe: approaching the dynamics of DMS(P) in the ocean at multiple scales. *Canadian Journal of Fisheries and Aquatic Sciences*, 61 (5):673–684. doi: 10.1139/f04-030.

Simon, M and Azam, F (1989). Protein content and protein synthesis rates of planktonic marine bacteria. *Marine Ecology Progress Series*, 51 (3):201–213. doi: 10.3354/meps051201.

Sloyan, BM and Rintoul, SR (2001a). Circulation, Renewal, and Modification of Antarctic Mode and Intermediate Water. *Journal of Physical Oceanography*, 31 (4):1005–1030. doi: 10.1175/1520-0485(2001)031<1005:CRAMOA>2.0.CO;2.

Sloyan, BM and Rintoul, SR (2001b). The Southern Ocean Limb of the Global Deep Overturning Circulation*. *Journal of Physical Oceanography*, 31 (1):143–173. doi: 10.1175/1520-0485(2001)031<0143:TSOLOT>2.0.CO;2.

Smetacek, V, Scharek, R, and Nöthig, EM (1990). Seasonal and Regional Variation in the Pelagial and its Relationship to the Life History Cycle of Krill. *Antarctic Ecosystems*. Ed. by KR Kerry and G Hempel. Berlin, Heidelberg: Springer Berlin Heidelberg, p 103–114. doi: 10.1007/978-3-642-84074-6_10.

Smetacek, VS (1985). Role of sinking in diatom life-hystory: ecological, evolutionary and geological significance. *Marine Biology*, 84:239–251. doi: 10.1007/BF00392493.

Smetacek, V, Assmy, P, and Henjes, J (2004). The role of grazing in structuring Southern Ocean pelagic ecosystems and biogeochemical cycles. *Antarctic Science*, 16 (4):541–558. doi: 10.1017/S0954102004002317.

Smetacek, V and Nicol, S (2005). Polar ocean ecosystems in a changing world. *Nature*, 437 (7057):362–368. doi: 10.1038/nature04161.

Smith, K, Sherman, A, Shaw, T, Murray, A, Vernet, M, and Cefarelli, A (2011). Carbon export associated with free-drifting icebergs in the Southern Ocean. *Deep Sea Research Part II: Topical Studies in Oceanography*, 58 (11-12):1485–1496. doi: 10.1016/j.dsr2.2010.11.027.

Smith, RC, Martinson, DG, Stammerjohn, SE, Iannuzzi, RA, and Ireson, K (2008). Bellingshausen and western Antarctic Peninsula region: Pigment biomass and sea-ice spatial/temporal distributions and interannual variabilty. *Deep Sea Research Part II: Topical Studies in Oceanography*, 55 (18-19):1949–1963. doi: 10.1016/j.dsr2.2008.04.027.

Smith, RC and Stammerjohn, SE (2001). Variations of surface air temperature and sea-ice extent in the western Antarctic Peninsula region. *Annals of Glaciology*, 33 (1):493–500. doi: 10.3189/172756401781818662.

Smith, R, Baker, K, Fraser, W, Hofmann, E, Karl, D, Klink, J, *et al.* (1995). The Palmer LTER: A Long-Term Ecological Research Program at Palmer Station, Antarctica. *Oceanography*, 8 (3):77–86. doi: 10.5670/oceanog.1995.01.

Smith, WO, Keene, NK, and Comiso, JC (1988). Interannual Variability in Estimated Primary Productivity of the Antarctic Marginal Ice Zone. *Antarctic Ocean and Resources Variability*. Ed. by D Sahrhage. Berlin, Heidelberg: Springer Berlin Heidelberg, p 131–139. doi: 10.1007/978-3-642-73724-4_10.

Smith, WO, Anderson, RF, Moore, JK, Codispoti, LA, and Morrison, JM (2000a). The US Southern Ocean Joint Global Ocean Flux Study: An introduction to AESOPS. *Deep-Sea Research Part II: Topical Studies in Oceanography*, 47 (15-16):3073–3093. doi: 10.1016/S0967-0645(00)00059-X.

Smith, WO and Gordon, LI (1997). Hyperproductivity of the Ross Sea (Antarctica) polynya during austral spring. *Geophysical Research Letters*, 24 (3):233–236. doi: 10.1029/96GL03926.

Smith, WO and Nelson, DM (1986). Importance of Ice Edge Phytoplankton Production in the Southern Ocean. *BioScience*, 36 (4):251–257. doi: 10.2307/1310215.

Smith, WO, Ainley, DG, and Cattaneo-Vietti, R (2007). Trophic interactions within the Ross Sea continental shelf ecosystem. *Philosophical Transactions of the Royal Society B: Biological Sciences*, 362 (1477):95–111. doi: 10.1098/rstb.2006.1956.

Smith, WO, Marra, J, Hiscock, MR, and Barber, RT (2000b). The seasonal cycle of phytoplankton biomass and primary productivity in the Ross Sea, Antarctica. *Deep Sea Research Part II: Topical Studies in Oceanography*, 47 (15-16):3119–3140. doi: 10.1016/S0967-0645(00)00061-8.

Sobrino, C, Ward, ML, and Neale, PJ (2008). Acclimation to elevated carbon dioxide and ultraviolet radiation in the diatom *Thalassiosira pseudonana*: Effects on growth, photosynthesis, and spectral sensitivity of photoinhibition. *Limonology And Oceanography*, 53 (2):494–505. doi: 10.4319/lo.2008.53.2.0494.

Sokolov, S and Rintoul, SR (2009a). Circumpolar structure and distribution of the Antarctic Circumpolar Current fronts: 1. Mean circumpolar paths. *Journal of Geophysical Research: Oceans*, 114 (C11):C11018. doi: 10.1029/2008JC005108.

Sokolov, S and Rintoul, SR (2009b). Circumpolar structure and distribution of the Antarctic Circumpolar Current fronts: 2. Variability and relationship to sea surface height. *Journal of Geophysical Research: Oceans*, 114 (11):1–15. doi: 10.1029/2008JC005248.

Solomon, S, Ivy, DJ, Kinnison, D, Mills, MJ, Neely, RR, and Schmidt, A (2016). Emergence of healing in the Antarctic ozone layer. *Science*, 353 (6296):269–274. doi: 10.1126/science.aae0061.

Sommer, U, Paul, C, and Moustaka-Gouni, M (2015). Warming and Ocean Acidification Effects on Phytoplankton–From Species Shifts to Size Shifts within Species in a Mesocosm Experiment. *PLOS ONE*, 10 (5):e0125239. doi: 10.1371/journal.pone.0125239.

Son, SW, Polvani, LM, Waugh, DW, Akiyoshi, H, Garcia, R, Kinnison, D, *et al.* (2008). The Impact of Stratospheric Ozone Recovery on the Southern Hemisphere Westerly Jet. *Science*, 320 (5882):1486–1489. doi: 10.1126/science.1155939.

Sperling, M, Piontek, J, Gerdts, G, Wichels, A, Schunck, H, Roy, AS, *et al.* (2013). Effect of elevated CO_2 on the dynamics of particle-attached and free-living bacterioplankton communities in an Arctic fjord. *Biogeosciences*, 10 (1):181–191. doi: 10.5194/bg-10-181-2013.

Spilling, K, Paul, AJ, Virkkala, N, Hastings, T, Lischka, S, Stuhr, A, *et al.* (2016). Ocean acidification decreases plankton respiration: evidence from a mesocosm experiment. *Biogeosciences*, 13 (16):4707–4719. doi: 10.5194/bg-13-4707-2016.

Stammerjohn, SE, Martinson, DG, Smith, RC, and Iannuzzi, RA (2008). Sea ice in the western Antarctic Peninsula region: Spatio-temporal variability from ecological and climate change perspectives. *Deep Sea Research Part II: Topical Studies in Oceanography*, 55 (18-19):2041–2058. doi: 10.1016/j.dsr2.2008.04.026.

Stammerjohn, S, Massom, R, Rind, D, and Martinson, D (2012). Regions of rapid sea ice change: An inter-hemispheric seasonal comparison. *Geophysical Research Letters*, 39 (6):L06501. doi: 10.1029/2012GL050874.

Steemann Nielsen, E (1952). The Use of Radio-active Carbon (C14) for Measuring Organic Production in the Sea. *ICES Journal of Marine Science*, 18 (2):117–140. doi: 10.1093/icesjms/18.2.117.

Steinacher, M, Joos, F, Frölicher, TL, Bopp, L, Cadule, P, Cocco, V, *et al.* (2010). Projected 21st century decrease in marine productivity: a multi-model analysis. *Biogeosciences*, 7 (3):979–1005. doi: 10.5194/bg-7-979-2010.

Stoecker, DK, Hansen, PJ, Caron, DA, and Mitra, A (2017). Mixotrophy in the Marine Plankton. *Annual Review of Marine Science*, 9 (1):311–335. doi: 10.1146/annurev-marine-010816-060617.

Stroeve, JC, Kattsov, V, Barrett, A, Serreze, M, Pavlova, T, Holland, M, *et al.* (2012). Trends in Arctic sea ice extent from CMIP5, CMIP3 and observations. *Geophysical Research Letters*, 39 (16):L16502. doi: 10.1029/2012GL052676.

Stroeve, JC, Jenouvrier, S, Campbell, GG, Barbraud, C, and Delord, K (2016). Mapping and assessing variability in the Antarctic marginal ice zone, pack ice and coastal polynyas in two sea ice algorithms with implications on breeding success of snow petrels. *The Cryosphere*, 10 (4):1823–1843. doi: 10.5194/tc-10-1823-2016.

Strzepek, RF, Maldonado, MT, Hunter, KA, Frew, RD, and Boyd, PW (2011). Adaptive strategies by Southern Ocean phytoplankton to lessen iron limitation: Uptake of organically complexed iron and reduced cellular iron requirements. *Limnology and Oceanography*, 56 (6):1983–2002. doi: 10.4319/lo.2011.56.6.1983.

Subramaniam, RC, Melbourne-Thomas, J, Davidson, AT, and Corney, SP (2017). Mechanisms driving Antarctic microbial community responses to ocean acidification: a network modelling approach. *Polar Biology*, 40 (3):727–734. doi: 10.1007/s00300-016-1989-8.

Suffrian, K, Simonelli, P, Nejstgaard, JC, Putzeys, S, Carotenuto, Y, and Antia, AN (2008). Microzooplankton grazing and phytoplankton growth in marine mesocosms with increased CO_2 levels. *Biogeosciences*, 5 (4):1145–1156. doi: 10.5194/bg-5-1145-2008.

Sullivan, CW, McClain, CR, Comiso, JC, and Smith, WO (1988). Phytoplankton standing crops within an Antarctic ice edge assessed by satellite remote sensing. *Journal of Geophysical Research*, 93 (C10):12487. doi: 10.1029/JC093iC10p12487.

Swart, NC, Fyfe, JC, Saenko, OA, and Eby, M (2014). Wind-driven changes in the ocean carbon sink. *Biogeosciences*, 11 (21):6107–6117. doi: 10.5194/bg-11-6107-2014.

Sweeney, C, Hansell, DA, Carlson, CA, Codispoti, L, Gordon, LI, Marra, J, *et al.* (2000). Biogeochemical regimes, net community production and carbon export in the Ross Sea, Antarctica. *Deep Sea Research Part II: Topical Studies in Oceanography*, 47 (15-16):3369–3394. doi: 10.1016/S0967-0645(00)00072-2.

Tagliabue, A, Bopp, L, Dutay, JC, Bowie, AR, Chever, F, Jean-Baptiste, P, *et al.* (2010). Hydrothermal contribution to the oceanic dissolved iron inventory. *Nature Geoscience*, 3 (4):252–256. doi: 10.1038/ngeo818.

Takahashi, T, Sutherland, SC, Wanninkhof, R, Sweeney, C, Feely, RA, Chipman, DW, *et al.* (2009). Climatological mean and decadal change in surface ocean pCO_2, and net sea–air CO_2 flux over the global oceans. *Deep Sea Research Part II: Topical Studies in Oceanography*, 56 (8-10):554–577. doi: 10.1016/j.dsr2.2008.12.009.

Takahashi, T, Sweeney, C, Hales, B, Chipman, D, Newberger, T, Goddard, J, *et al.* (2012). The Changing Carbon Cycle in the Southern Ocean. *Oceanography*, 25 (3):26–37. doi: 10.5670/oceanog.2012.71.

Tanaka, T, Alliouane, S, Bellerby, RGB, Czerny, J, de Kluijver, A, Riebesell, U, *et al.* (2013). Effect of increased pCO_2 on the planktonic metabolic balance during a mesocosm experiment in an Arctic fjord. *Biogeosciences*, 10 (1):315–325. doi: 10.5194/bg-10-315-2013.

Taucher, J, Jones, J, James, A, Brzezinski, MA, Carlson, CA, Riebesell, U, *et al.* (2015). Combined effects of CO_2 and temperature on carbon uptake and partitioning by the marine diatoms *Thalassiosira weissflogii* and *Dactyliosolen fragilissimus*. *Limnology and Oceanography*, 60 (3):901–919. doi: 10.1002/lno.10063.

Taylor, AR, Brownlee, C, and Wheeler, GL (2012). Proton channels in algae: Reasons to be excited. *Trends in Plant Science*, 17 (11):675–684. doi: 10.1016/j.tplants.2012.06.009.

Taylor, MH, Losch, M, and Bracher, A (2013). On the drivers of phytoplankton blooms in the Antarctic marginal ice zone: A modeling approach. *Journal of Geophysical Research: Oceans*, 118 (1):63–75. doi: 10.1029/2012JC008418.

Teira, E, Fernández, A, Álvarez-Salgado, XA, García-Martín, EE, Serret, P, and Sobrino, C (2012). Response of two marine bacterial isolates to high CO_2 concentration. *Marine Ecology Progress Series*, 453:27–36. doi: 10.3354/meps09644.

Tew, KS, Kao, YC, Ko, FC, Kuo, J, Meng, PJ, Liu, PJ, *et al.* (2014). Effects of elevated CO_2 and temperature on the growth, elemental composition, and cell size of two marine diatoms:

potential implications of global climate change. *Hydrobiologia*, 741 (1):79–87. doi: 10.1007/s10750-014-1856-y.

Thomas, DN and Dieckmann, GS (2002). Antarctic Sea Ice–a Habitat for Extremophiles. *Science*, 295 (5555):641–644. doi: 10.1126/science.1063391.

Thomas, DN, Lara, RJ, Haas, C, Schnack-Schiel, SB, Dieckmann, GS, Kattner, G, *et al.* (1998). Biological Soup Within Decaying Summer Sea Ice in the Amundsen Sea, Antarctica. *Antarctic Sea Ice: Biological Processes, Interactions and Variability*. Ed. by MP Lizotte and KR Arrigo. Washington, D.C.: American Geophysical Union, p 161–171.

Thompson, DWJ and Solomon, S (2002). Interpretation of Recent Southern Hemisphere Climate Change. *Science*, 296 (5569):895–899. doi: 10.1126/science.1069270.

Thompson, DWJ, Solomon, S, Kushner, PJ, England, MH, Grise, KM, and Karoly, DJ (2011). Signatures of the Antarctic ozone hole in Southern Hemisphere surface climate change. *Nature Geoscience*, 4 (11):741–749. doi: 10.1038/ngeo1296.

Thompson, DWJ and Wallace, JM (2000). Annular Modes in the Extratropical Circulation. Part I: Month-to-Month Variability. *Journal of Climate*, 13 (5):1000–1016. doi: 10.1175/1520-0442(2000)013<1000:AMITEC>2.0.CO;2.

Thomson, PG, Davidson, AT, van den Enden, R, Pearce, I, Seuront, L, Paterson, JS, *et al.* (2010). Distribution and abundance of marine microbes in the Southern Ocean between 30 and 80 °E. *Deep Sea Research Part II: Topical Studies in Oceanography*, 57 (9-10):815–827. doi: 10.1016/j.dsr2.2008.10.040.

Thomson, P, Davidson, A, and Maher, L (2016). Increasing CO_2 changes community composition of pico- and nano-sized protists and prokaryotes at a coastal Antarctic site. *Marine Ecology Progress Series*, 554:51–69. doi: 10.3354/meps11803.

Timmermans, KR, Gerringa, LJA, de Baar, HJW, van der Wagt, B, Veldhuis, MJW, de Jong, JTM, *et al.* (2001). Growth rates of large and small Southern Ocean diatoms in relation to availability of iron in natural seawater. *Limnology and Oceanography*, 46 (2):260–266. doi: 10.4319/lo.2001.46.2.0260.

Tong, S, Gao, K, and Hutchins, DA (2018). Adaptive evolution in the coccolithophore *Gephyrocapsa oceanica* following 1,000 generations of selection under elevated CO_2. *Global Change Biology*, 12 (10):3218–3221. doi: 10.1111/gcb.14065.

Torstensson, A, Hedblom, M, Andersson, J, Andersson, MX, and Wulff, A (2013). Synergism between elevated pCO_2 and temperature on the Antarctic sea ice diatom *Nitzschia lecointei*. *Biogeosciences*, 10:6391–6401. doi: 10.5194/bg-10-6391-2013.

Torstensson, A, Hedblom, M, Mattsdotter Björk, M, Chierici, M, and Wulff, A (2015). Long-term acclimation to elevated pCO_2 alters carbon metabolism and reduces growth in the Antarctic diatom *Nitzschia lecointei*. *Proceedings of the Royal Society B: Biological Sciences*, 282 (1815):20151513. doi: 10.1098/rspb.2015.1513.

Tortell, PD, Asher, EC, Ducklow, HW, Goldman, JAL, Dacey, JWH, Grzymski, JJ, *et al.* (2014). Metabolic balance of coastal Antarctic waters revealed by autonomous pCO_2 and $\Delta O_2/Ar$ measurements. *Geophysical Research Letters*, 41 (19):6803–6810. doi: 10.1002/2014GL061266.

Tortell, PD and Morel, FMM (2002). Sources of inorganic carbon for phytoplankton in the eastern Subtropical and Equatorial Pacific Ocean. *Limnology and Oceanography*, 47 (4):1012–1022. doi: 10.4319/lo.2002.47.4.1012.

Tortell, PD, Payne, CD, Li, Y, Trimborn, S, Rost, B, Smith, WO, *et al.* (2008a). CO_2 sensitivity of Southern Ocean phytoplankton. *Geophysical Research Letters*, 35 (4):L04605. doi: 10.1029/2007GL032583.

Tortell, PD, Payne, C, Gueguen, C, Strzepek, RF, Boyd, PW, and Rost, B (2008b). Inorganic carbon uptake by Southern Ocean phytoplankton. *Limnology and Oceanography*, 53 (4):1266–1278. doi: 10.4319/lo.2008.53.4.1266.

Tortell, PD, Trimborn, S, Li, Y, Rost, B, and Payne, CD (2010). Inorganic carbon utilization by Ross Sea phytoplankton across natural and experimental CO_2 gradients. *Journal of Phycology*, 46 (3):433–443. doi: 10.1111/j.1529-8817.2010.00839.x.

Tortell, PD, Rau, GH, and Morel, FMM (2000). Inorganic carbon acquisition in coastal Pacific phytoplankton communities. *Limnology and Oceanography*, 45 (7):1485–1500. doi: 10.4319/lo.2000.45.7.1485.

Tréguer, P and Van Bennekom, A (1991). The annual production of biogenic silica in the Antarctic Ocean. *Marine Chemistry*, 35 (1-4):477–487. doi: 10.1016/S0304-4203(09)90038-X.

Tréguer, P, Bowler, C, Moriceau, B, Dutkiewicz, S, Gehlen, M, Aumont, O, *et al.* (2018). Influence of diatom diversity on the ocean biological carbon pump. *Nature Geoscience*, 11 (1):27–37. doi: 10.1038/s41561-017-0028-x.

Tréguer, P and Jacques, G (1992). Dynamics of nutrients and phytoplankton, and fluxes of carbon, nitrogen and silicon in the Antarctic Ocean. *Polar Biology*, 12 (2):149–162. doi: 10.1007/BF00238255.

Trevena, AJ and Jones, GB (2006). Dimethylsulphide and dimethylsulphoniopropionate in Antarctic sea ice and their release during sea ice melting. *Marine Chemistry*, 98 (2-4):210–222. doi: 10.1016/j.marchem.2005.09.005.

Trimborn, S, Brenneis, T, Sweet, E, and Rost, B (2013). Sensitivity of Antarctic phytoplankton species to ocean acidification: Growth, carbon acquisition, and species interaction. *Limnology and Oceanography*, 58 (3):997–1007. doi: 10.4319/lo.2013.58.3.0997.

Trimborn, S, Thoms, S, Brenneis, T, Heiden, JP, Beszteri, S, and Bischof, K (2017). Two Southern Ocean diatoms are more sensitive to ocean acidification and changes in irradiance than the prymnesiophyte *Phaeocystis antarctica*. *Physiologia Plantarum*, 160 (2):155–170. doi: 10.1111/ppl.12539.

Trimborn, S, Thoms, S, Petrou, K, Kranz, SA, and Rost, B (2014). Photophysiological responses of Southern Ocean phytoplankton to changes in CO_2 concentrations: Short-term versus acclimation effects. *Journal of Experimental Marine Biology and Ecology*, 451:44–54. doi: 10.1016/j.jembe.2013.11.001.

Trull, TW, Bray, SG, Manganini, SJ, Honjo, S, and François, R (2001a). Moored sediment trap measurements of carbon export in the Subantarctic and Polar Frontal Zones of the Southern Ocean, south of Australia. *Journal of Geophysical Research: Oceans*, 106 (C12):31489–31509. doi: 10.1029/2000JC000308.

Trull, T, Rintoul, SR, Hadfield, M, and Abraham, ER (2001b). Circulation and seasonal evolution of polar waters south of Australia: implications for iron fertilization of the Southern Ocean. *Deep Sea Research Part II: Topical Studies in Oceanography*, 48 (11-12):2439–2466. doi: 10.1016/S0967-0645(01)00003-0.

Turner, JT (2004). The Importance of Small Pelagic Planktonic Copepods and Their Role in Pelagic Marine Food Webs. *Zoological Studies*, 43 (2):255–266.

Turner, J, Barrand, NE, Bracegirdle, TJ, Convey, P, Hodgson, DA, Jarvis, M, *et al.* (2014). Antarctic climate change and the environment: an update. *Polar Record*, 50 (03):237–259. doi: 10.1017/S0032247413000296.

Turner, J, Bracegirdle, TJ, Phillips, T, Marshall, GJ, and Hosking, JS (2013). An Initial Assessment of Antarctic Sea Ice Extent in the CMIP5 Models. *Journal of Climate*, 26 (5):1473–1484. doi: 10.1175/JCLI-D-12-00068.1.

Turner, J, Comiso, JC, Marshall, GJ, Lachlan-Cope, TA, Bracegirdle, T, Maksym, T, *et al.* (2009). Non-annular atmospheric circulation change induced by stratospheric ozone depletion and its role in the recent increase of Antarctic sea ice extent. *Geophysical Research Letters*, 36 (8):L08502. doi: 10.1029/2009GL037524.

Turner, J (2002). Zooplankton fecal pellets, marine snow and sinking phytoplankton blooms. *Aquatic Microbial Ecology*, 27 (1):57–102. doi: 10.3354/ame027057.

Turner, S, Nightingale, P, Broadgate, W, and Liss, P (1995). The distribution of dimethyl sulphide and dimethylsulphoniopropionate in Antarctic waters and sea ice. *Deep Sea Research Part II: Topical Studies in Oceanography*, 42 (4-5):1059–1080. doi: 10.1016/0967-0645(95)00066-Y.

Ullah, H, Nagelkerken, I, Goldenberg, SU, and Fordham, DA (2018). Climate change could drive marine food web collapse through altered trophic flows and cyanobacterial proliferation. *PLOS Biology*, 16 (1):e2003446. doi: 10.1371/journal.pbio.2003446.

Van de Waal, DB, Verschoor, AM, Verspagen, JM, van Donk, E, and Huisman, J (2010). Climate-driven changes in the ecological stoichiometry of aquatic ecosystems. *Frontiers in Ecology and the Environment*, 8 (3):145–152. doi: 10.1890/080178.

Vance, T, Davidson, A, Thomson, P, Levasseur, M, Lizotte, M, Curran, M, *et al.* (2013). Rapid DMSP production by an Antarctic phytoplankton community exposed to natural surface irradiances in late spring. *Aquatic Microbial Ecology*, 71 (2):117–129. doi: 10.3354/ame01670.

Vaughan, DG, Marshall, GJ, Connolley, WM, Parkinson, C, Mulvaney, R, Hodgson, DA, *et al.* (2003). Recent rapid regional climate warming on the Antarctic Peninsula. *Climatic Change*, 60 (3):243–274. doi: 10.1023/A:1026021217991.

Venables, HJ and Meredith, MP (2014). Feedbacks between ice cover, ocean stratification, and heat content in Ryder Bay, western Antarctic Peninsula. *Journal of Geophysical Research: Oceans*, 119 (8):5323–5336. doi: 10.1002/2013JC009669.

Vernet, M, Sines, K, Chakos, D, Cefarelli, A, and Ekern, L (2011). Impacts on phytoplankton dynamics by free-drifting icebergs in the NW Weddell Sea. *Deep Sea Research Part II: Topical Studies in Oceanography*, 58 (11-12):1422–1435. doi: 10.1016/j.dsr2.2010.11.022.

Vernet, M, Martinson, D, Iannuzzi, R, Stammerjohn, S, Kozlowski, W, Sines, K, *et al.* (2008). Primary production within the sea-ice zone west of the Antarctic Peninsula: I–Sea ice, summer mixed layer, and irradiance. *Deep Sea Research Part II: Topical Studies in Oceanography*, 55 (18-19):2068–2085. doi: 10.1016/j.dsr2.2008.05.021.

Vernet, M, Smith, K, Cefarelli, A, Helly, J, Kaufmann, R, Lin, H, *et al.* (2012). Islands of Ice: Influence of Free-Drifting Antarctic Icebergs on Pelagic Marine Ecosystems. *Oceanography*, 25 (3):38–39. doi: 10.5670/oceanog.2012.72.

Wang, Y, Zhang, R, Zheng, Q, Deng, Y, Van Nostrand, JD, Zhou, J, *et al.* (2016). Bacterioplankton community resilience to ocean acidification: evidence from microbial network analysis. *ICES Journal of Marine Science: Journal du Conseil*, 73 (3):865–875. doi: 10.1093/icesjms/fsv187.

Watanabe, O, Jouzel, J, Johnsen, S, Parrenin, F, Shoji, H, and Yoshida, N (2003). Homogeneous climate variability across East Antarctica over the past three glacial cycles. *Nature*, 422 (6931):509–512. doi: 10.1038/nature01525.

Waters, R, van den Enden, R, and Marchant, H (2000). Summer microbial ecology off East Antarctica (80–150°E): protistan community structure and bacterial abundance. *Deep Sea Research Part II: Topical Studies in Oceanography*, 47 (12-13):2401–2435. doi: 10.1016/S0967-0645(00)00030-8.

Westwood, KJ, Thomson, PG, van den Enden, RL, Maher, LE, Wright, SW, and Davidson, AT (2018). Ocean acidification impacts primary and bacterial production in Antarctic coastal waters during austral summer. *Journal of Experimental Marine Biology and Ecology*, 498 (January 2018):46–60. doi: 10.1016/j.jembe.2017.11.003.

Westwood, KJ, Griffiths, FB, Meiners, KM, and Williams, GD (2010). Primary productivity off the Antarctic coast from 30°–80°E; BROKE-West survey, 2006. *Deep Sea Research Part II: Topical Studies in Oceanography*, 57 (9-10):794–814. doi: 10.1016/j.dsr2.2008.08.020.

Williams, G, Nicol, S, Aoki, S, Meijers, A, Bindoff, N, Iijima, Y, *et al.* (2010). Surface oceanography of BROKE-West, along the Antarctic margin of the south-west Indian Ocean (30–80°E). *Deep Sea Research Part II: Topical Studies in Oceanography*, 57 (9-10):738–757. doi: 10.1016/j.dsr2.2009.04.020.

Winter, A, Henderiks, J, Beaufort, L, Rickaby, REM, and Brown, CW (2014). Poleward expansion of the coccolithophore *Emiliania huxleyi*. *Journal of Plankton Research*, 36 (2):316–325. doi: 10.1093/plankt/fbt110.

Wolf, KKE, Hoppe, CJM, and Rost, B (2018). Resilience by diversity: Large intraspecific differences in climate change responses of an Arctic diatom. *Limnology and Oceanography*, 63 (1):397–411. doi: 10.1002/lno.10639.

Wong, APS, Bindoff, NL, and Church, JA (1999). Large-scale freshening of intermediate waters in the Pacific and Indian oceans. *Nature*, 400 (29 July 1999):440–443. doi: doi:10.1038/22733.

Woodward, S, Roberts, DL, and Betts, RA (2005). A simulation of the effect of climate change-induced desertification on mineral dust aerosol. *Geophysical Research Letters*, 32 (18):2–5. doi: 10.1029/2005GL023482.

Worby, AP, Geiger, CA, Paget, MJ, Van Woert, ML, Ackley, SF, and DeLiberty, TL (2008). Thickness distribution of Antarctic sea ice. *Journal of Geophysical Research: Oceans*, 113 (5):C05S92. doi: 10.1029/2007JC004254.

Wright, SW, Ishikawa, A, Marchant, HJ, Davidson, AT, van den Enden, RL, and Nash, GV (2009). Composition and significance of picophytoplankton in Antarctic waters. *Polar Biology*, 32 (5):797–808. doi: 10.1007/s00300-009-0582-9.

Wright, SW and van den Enden, RL (2000). Phytoplankton community structure and stocks in the East Antarctic marginal ice zone (BROKE survey, January-March 1996) determined by CHEMTAX analysis of HPLC pigment signatures. *Deep Sea Research Part II: Topical Studies in Oceanography*, 47 (12-13):2363–2400. doi: 10.1016/S0967-0645(00)00029-1.

Wright, SW, van den Enden, RL, Pearce, I, Davidson, AT, Scott, FJ, and Westwood, KJ (2010). Phytoplankton community structure and stocks in the Southern Ocean (30-80°E) determined by CHEMTAX analysis of HPLC pigment signatures. *Deep Sea Research Part II: Topical Studies in Oceanography*, 57 (9-10):758–778. doi: 10.1016/j.dsr2.2009.06.015.

Wu, Y, Gao, K, and Riebesell, U (2010). CO_2-induced seawater acidification affects physiological performance of the marine diatom *Phaeodactylum tricornutum*. *Biogeosciences*, 7 (9):2915–2923. doi: 10.5194/bg-7-2915-2010.

Wu, Y, Campbell, DA, Irwin, AJ, Suggett, DJ, and Finkel, ZV (2014). Ocean acidification enhances the growth rate of larger diatoms. *Limnology and Oceanography*, 59 (3):1027–1034. doi: 10.4319/lo.2014.59.3.1027.

Wynn-Edwards, C, King, R, Davidson, A, Wright, S, Nichols, P, Wotherspoon, S, *et al.* (2014). Species-Specific Variations in the Nutritional Quality of Southern Ocean Phytoplankton in Response to Elevated pCO_2. *Water*, 6 (12):1840–1859. doi: 10.3390/w6061840.

Xu, K, Fu, FX, and Hutchins, DA (2014). Comparative responses of two dominant Antarctic phytoplankton taxa to interactions between ocean acidification, warming, irradiance, and iron availability. *Limnology and Oceanography*, 59 (6):1919–1931. doi: 10.4319/lo.2014.59.6.1919.

Yin, JH (2005). A consistent poleward shift of the storm tracks in simulations of 21st century climate. *Geophysical Research Letters*, 32 (18):L18701. doi: 10.1029/2005GL023684.

Young, IR, Zieger, S, and Babanin, AV (2011). Global Trends in Wind Speed and Wave Height. *Science*, 332 (6028):451–455. doi: 10.1126/science.1197219.

Young, J, Kranz, S, Goldman, J, Tortell, P, and Morel, F (2015). Antarctic phytoplankton down-regulate their carbon-concentrating mechanisms under high CO_2 with no change in growth rates. *Marine Ecology Progress Series*, 532:13–28. doi: 10.3354/meps11336.

Zhang, R, Xia, X, Lau, SCK, Motegi, C, Weinbauer, MG, and Jiao, N (2013). Response of bacterioplankton community structure to an artificial gradient of pCO_2 in the Arctic Ocean. *Biogeosciences*, 10 (6):3679–3689. doi: 10.5194/bg-10-3679-2013.

Zheng, Y, Giordano, M, and Gao, K (2015). Photochemical responses of the diatom *Skeletonema costatum* grown under elevated CO_2 concentrations to short-term changes in pH. *Aquatic Biology*, 23 (2):109–118. doi: 10.3354/ab00619.

Zhu, Z, Qu, P, Gale, J, Fu, F, and Hutchins, DA (2017). Individual and interactive effects of warming and CO_2 on *Pseudo-nitzschia subcurvata* and *Phaeocystis antarctica*, two dominant phytoplankton from the Ross Sea, Antarctica. *Biogeosciences*, 14:(23), 5281–5295. doi: 10.5194/bg-14-5281-2017.

Zhu, Z, Xu, K, Fu, F, Spackeen, J, Bronk, D, and Hutchins, D (2016). A comparative study of iron and temperature interactive effects on diatoms and *Phaeocystis antarctica* from the Ross Sea, Antarctica. *Marine Ecology Progress Series*, 550:39–51. doi: 10.3354/meps11732.